frontiers | Research Topics

# Biomarkers in autoimmune diseases of the central nervous system

**Edited by**
Mei-Ping Ding, Long-Jun Wu, Shougang Guo and Honghao Wang

**Coordinated by**
Yin-Xi Zhang

**Published in**
Frontiers in Immunology
Frontiers in Neurology

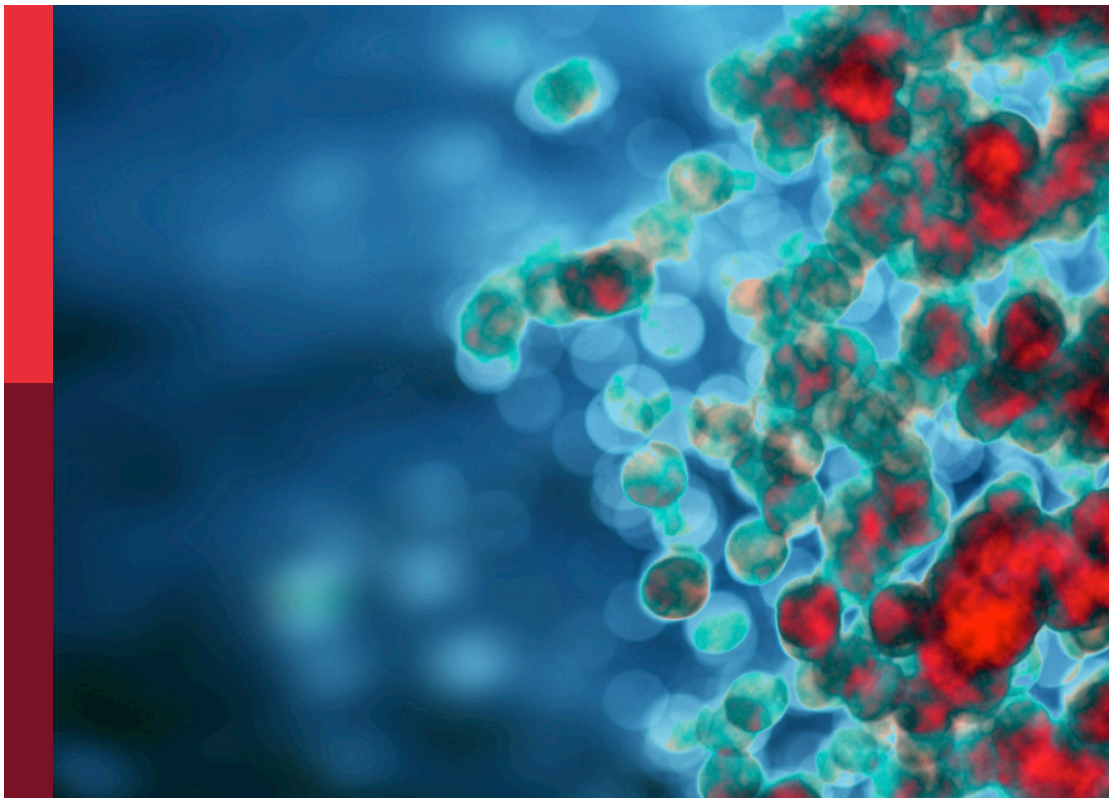

ISSN 1664-8714
ISBN 978-2-8325-3409-0
DOI 10.3389/978-2-8325-3409-0

## About Frontiers

Frontiers is more than just an open access publisher of scholarly articles: it is a pioneering approach to the world of academia, radically improving the way scholarly research is managed. The grand vision of Frontiers is a world where all people have an equal opportunity to seek, share and generate knowledge. Frontiers provides immediate and permanent online open access to all its publications, but this alone is not enough to realize our grand goals.

## Frontiers journal series

The Frontiers journal series is a multi-tier and interdisciplinary set of open-access, online journals, promising a paradigm shift from the current review, selection and dissemination processes in academic publishing. All Frontiers journals are driven by researchers for researchers; therefore, they constitute a service to the scholarly community. At the same time, the *Frontiers journal series* operates on a revolutionary invention, the tiered publishing system, initially addressing specific communities of scholars, and gradually climbing up to broader public understanding, thus serving the interests of the lay society, too.

## Dedication to quality

Each Frontiers article is a landmark of the highest quality, thanks to genuinely collaborative interactions between authors and review editors, who include some of the world's best academicians. Research must be certified by peers before entering a stream of knowledge that may eventually reach the public - and shape society; therefore, Frontiers only applies the most rigorous and unbiased reviews. Frontiers revolutionizes research publishing by freely delivering the most outstanding research, evaluated with no bias from both the academic and social point of view. By applying the most advanced information technologies, Frontiers is catapulting scholarly publishing into a new generation.

## What are Frontiers Research Topics?

Frontiers Research Topics are very popular trademarks of the *Frontiers journals series*: they are collections of at least ten articles, all centered on a particular subject. With their unique mix of varied contributions from Original Research to Review Articles, Frontiers Research Topics unify the most influential researchers, the latest key findings and historical advances in a hot research area.

Find out more on how to host your own Frontiers Research Topic or contribute to one as an author by contacting the Frontiers editorial office: frontiersin.org/about/contact

# Biomarkers in autoimmune diseases of the central nervous system

**Topic editors**

Mei-Ping Ding — Zhejiang University, China

Long-Jun Wu — Mayo Clinic, United States

Shougang Guo — Department of Neurology, Shandong Provincial Hospital, China

Honghao Wang — Department of Neurology, Guangzhou First People's Hospital, China

**Topic coordinator**

Yin-Xi Zhang — Zhejiang University, China

**Citation**

Ding, M.-P., Wu, L.-J., Guo, S., Wang, H., Zhang, Y.-X., eds. (2023). *Biomarkers in autoimmune diseases of the central nervous system*. Lausanne: Frontiers Media SA. doi: 10.3389/978-2-8325-3409-0

# Table of contents

frontiers | Frontiers in Immunology

TYPE Editorial
PUBLISHED 18 August 2023
DOI 10.3389/fimmu.2023.1266953



OPEN ACCESS

EDITED AND REVIEWED BY
Hans-Peter Hartung,
Heinrich Heine University of Düsseldorf, Germany

*CORRESPONDENCE
Hong-Hao Wang
wang_whh@163.com
Shou-Gang Guo
guoshougang1124@163.com
Long-Jun Wu
wu.longjun@mayo.edu
Mei-Ping Ding
dmp-neurology@zju.edu.cn

RECEIVED 25 July 2023
ACCEPTED 31 July 2023
PUBLISHED 18 August 2023

CITATION
Zhang Y-X, Wang H-H, Guo S-G, Wu L-J and Ding M-P (2023) Editorial: Biomarkers in autoimmune diseases of the central nervous system.
*Front. Immunol.* 14:1266953.
doi: 10.3389/fimmu.2023.1266953



# Editorial: Biomarkers in autoimmune diseases of the central nervous system

Yin-Xi Zhang[1], Hong-Hao Wang[2*], Shou-Gang Guo[3*], Long-Jun Wu[4*] and Mei-Ping Ding[1*]

[1]Department of Neurology, Second Affiliated Hospital, School of Medicine, Zhejiang University, Hangzhou, China, [2]Department of Neurology, Guangzhou First People's Hospital, School of Medicine, Southern China University of Technology, Guangzhou, China, [3]Department of Neurology, Shandong Provincial Hospital Affiliated to Shandong First Medical University, Shandong Academy of Medical Sciences, Jinan, China, [4]Department of Neurology, Mayo Clinic, Rochester, MN, United States

KEYWORDS

**biomarker, autoimmune disease, central nervous system, inflammatory demyelinating disease, autoimmune encephalitis**

Editorial on the Research Topic
Biomarkers in autoimmune diseases of the central nervous system

Autoimmune diseases of the central nervous system (CNS) represent a group of complex and disabling disorders characterized by the immune system mistakenly targeting the brain and spinal cord. This results in structure damage and functional impairment. The pathogenesis of these diseases involves immune cells, autoantibodies and immune molecules directly or indirectly attacking the CNS, leading to neuronal or axonal injury, myelin loss and other neuropathological changes. Although CNS autoimmune diseases account for a small portion of neurological disorders, patients may exhibit extensive involvement and various manifestations, posing significant challenges in diagnosis and treatment. In the past two decades, there has been a rapid expansion in the understanding of CNS autoimmune diseases, particularly CNS inflammatory demyelinating diseases and autoimmune encephalitis. While notable discoveries have shed light on the autoimmune basis of these conditions, the exact pathogenesis remains unclear, and further in-depth research is needed.

Biomarkers are of great value in our understanding and management of CNS autoimmune diseases. They reflect the presence, nature, and intensity of certain immune responses triggered by both genetic and environmental factors. Biomarkers are of great importance in clinical diagnosis, estimating disease risk or prognosis, evaluating disease severity, and monitoring treatment response and disease progression (1). For instance, the detection of disease-specific antibodies aids in accurate diagnosis and precise treatment. Furthermore, the identification of diverse biomarkers holds the potential to advance personalized medicine.

To provide a platform for sharing the latest research advances in this field, we have organized this Research Topic. The Research Topic comprises 21 manuscripts, including 13 original research articles, 4 brief research reports, 1 review, 1 meta-analysis and systematic review and 2 case reports. These papers have broadened the contemporary knowledge and understanding of biomarkers of autoimmune CNS disorders. In this Editorial, we highlight

the representative articles contributing to this Research topic and summarize their main findings.

CNS inflammatory demyelinating diseases are a category of autoimmune-mediated disorders sharing the basic pathological hallmark of myelin loss and neuroinflammation. These diseases occur throughout the world and preferentially affect young adults, with multiple sclerosis (MS), neuromyelitis optica spectrum disorder (NMOSD), and myelin oligodendrocyte glycoprotein (MOG) antibody-associated disease (MOGAD) being the main representatives (2, 3). CNS inflammatory demyelinating diseases have distinct clinical characteristics, and involve biomarkers with important clinical implication. Liu et al. analyzed circulating antigen-specific memory T cell subsets, to explore their association with disease activity of MS. Their findings revealed positive regulatory roles for CD8 + memory T cell populations in MS, which established a valuable foundation for identifying potential serological biomarkers and exploring novel treatment approaches. A study by Karimi et al. focused on the regulatory transcriptional gene network underlying MS. The results demonstrated that the LASP1, S100A6 and TUBA1C genes were most likely to play a biological role in the development of MS and might serve as potential diagnostic and therapeutic biomarkers. Yadav et al. conducted the study using a humanized spontaneous experimental autoimmune encephalomyelitis model to investigate the underlying biology of MS-associated gut inflammation. They observed that gut infiltration of Th17 cells and recruitment of neutrophils were linked with the development of gut dysbiosis and intestinal inflammation, and suggested that fecal Lcn-2 level was a sensitive biological indicator for gut dysbiosis in MS. In addition, Zhou et al. recruited 30 Eastern patients with MS and comprehensively evaluated the cerebral blood flow (CBF) features using the arterial spin labeling technique and their relationship with multiple clinical parameters for the first time. The authors concluded that CBF could be a potential quantitative neuroimaging marker associated with disease severity. Miyamoto et al. performed a retrospective analysis of serum complement factors in 21 patients with NMOSD and 25 patients with Guillain-Barré syndrome. The study revealed that complement biomarkers (e.g., Ba, sC5b-9, and complement factor H) in peripheral blood could contribute to the pathogenesis and pathological status of NMOSD. Shi et al. collected 90 blood samples from 59 patients with NMOSD and 31 healthy controls, aiming to assess the correlation between granzyme B (GzmB) levels in CD8+T cells and clinical characteristics. They found the involvement of GzmB-expressing CD8+ T cells in the inflammatory response in NMOSD, which could be considered a possible biomarker for therapeutic effectiveness and disability progression. Chen et al. compared the different immunological mechanisms between aquaporin 4 antibody-positive optic neuritis (ON) and MOG antibody-positive ON based on transcriptomics analysis of patients' whole blood, providing novel insights into the pathogenesis of these two diseases. Moreover, Sun C. et al. retrospectively examined the neuroimaging and clinicopathological differences between tumefactive demyelinating lesions and sentinel lesions of primary central nervous system lymphoma, designing to determine relevant biomarkers and improve early accurate diagnosis.

Compared with CNS inflammatory demyelinating diseases, autoimmune encephalitis is a relatively new field of research but recently becomes an active research hotspot in CNS neuroimmunology. Autoimmune encephalitis is an umbrella term for the non-infectious, immune-mediated inflammation of the brain parenchyma, in which neural antibodies can be found in a large proportion of patients (4). Neuronal surface antibody-associated autoimmune encephalitis is the most common subgroup, mainly including anti-N-methyl-D-aspartate receptor (NMDAR) encephalitis and anti-leucine-rich glioma-inactivated 1 (LGI1) encephalitis (5). Shao et al. explored the coagulation function in patients with anti-NMDAR encephalitis, identifying serum D-dimer and neutrophil levels as effective predictors of disease severity for anti-NMDAR encephalitis. Ma et al. conducted a meta-analysis and systematic review, analyzing the concentrations of cytokines/chemokines in the unstimulated cerebrospinal fluid (CSF) or serum of patients with anti-NMDAR encephalitis. Their findings highlighted the involvement of multiple immune cell interactions mediated by cytokines/chemokines in the central immune response, with T cells playing a pivotal role in the immunopathogenesis of anti-NMDAR encephalitis. Li J. et al. examined chitinase-3 likeprotein-1 (CHI3L1) and its correlation with modified Rankin Scale score. They concluded that CHI3L1 level in CSF was associated with the severity and outcome of anti-LGI1 encephalitis. Another study by Zhao-Fleming et al. characterized the cardiac arrythmias among patients with anti-LGI1 encephalitis, emphasizing the importance of identifying this phenomenon despite the rarity and generally favorable prognosis. Hara et al. investigated lymphocyte subset analyses of B cells and circulating T follicular helper cells (cTfh) in patients with autoimmune encephalitis with seizures. The results revealed that elevated frequency of plasmablasts and inducible T-cell co-stimulator-expressing cTfh17 shift in peripheral blood mononuclear cells might provide a new indicator for the presence of antibodies in patients with autoimmune encephalitis. Additionally, Sun Y. et al. enrolled 10 patients with anti-amphiphysin encephalitis and described the clinical and paraclinical characteristics, treatment, and prognostic predictors. Zhu et al. reported a case of anti-neurexin-3α-associated autoimmune encephalitis secondary to contrast-induced encephalopathy. Li Y. et al. presented a patient with the dual positivity of anti-NMDAR antibody and anti-metabotropic glutamate receptor 5 antibody, along with bilateral ovarian teratomas and reversible splenial lesion syndrome. As the most important diagnostic biomarker for autoimmune encephalitis, precise antibody test and comprehensive result interpretation are crucial. Muñoz-Sánchez et al. assessed the clinical performance of two indirect immunofluorescent cell-based assays (IIF-CBA) using paired serum/CSF in a large cohort of patients with anti-LGI1 encephalitis. They pointed out that both serum and CSF samples should be examined if using a commercial IIF-CBA for antibody confirmation to reduce false negative results in suspected anti-LGI1 encephalitis. Zong et al. evaluated the anti-glutamate decarboxylase 65 (GAD65) antibody levels measuring by different detection methods and reconfirmed that GAD65 antibody levels were significantly higher in patients with neuropsychiatric disease than in patients with diabetes. Furthermore, Nagata et al. addressed the clinical relevance of currently available commercial rat brain

immunohistochemistry and the immunostaining patterns of neuronal surface antigens. The authors stated that tissue-based assay is clinically helpful for screening neuronal surface antibody and glial fibrillary acidic protein antibody, and neuronal surface antigen specific immunoreactivity can be regarded as a useful biomarker of autoimmune encephalitis.

Finally, the well-rounded review of this Research Topic by Zhang et al. summarized the biomarkers in autoimmune diseases of the CNS and their potential clinical significance and application prospects. These biomarkers were usually classified into diagnostic, drug monitoring and safety and outcome predictive purpose based on clinical need, containing CNS injury markers, humoral markers, cytokines and cell markers in serum or CSF. They concluded that promising biomarkers had a significant impact on early intervention and prevention of future disability.

In summary, the collection of articles in this Research Topic expands the current knowledge regarding biomarkers in autoimmune diseases of the CNS. These studies provide novel scientific evidence and highlight recent progress in this continually evolving field.

## Author contributions

Y-XZ: Conceptualization, Data curation, Formal Analysis, Investigation, Writing – original draft, Writing – review & editing. H-HW: Conceptualization, Data curation, Formal Analysis, Investigation, Supervision, Validation, Writing – review & editing. S-GG: Conceptualization, Data curation, Formal Analysis, Investigation, Supervision, Validation, Writing – review & editing. L-JW: Conceptualization, Data curation, Formal Analysis, Investigation, Supervision, Validation, Writing – review & editing. M-PD: Conceptualization, Data curation, Formal Analysis, Investigation, Supervision, Validation, Writing – review & editing.

## Acknowledgments

We thank all the authors for contributing their valuable work to this Research Topic and we thank all the reviewers for their constructive comments and thoughtful suggestions. We are also grateful to the editorial board for approving this topic and we hope these Research Topic of papers will advance the state of research on biomarkers in autoimmune diseases of the central nervous system.

## Conflict of interest

The authors declare that the research was conducted in the absence of any commercial or financial relationships that could be construed as a potential conflict of interest.

The authors declared that they were an editorial board member of Frontiers, at the time of submission. This had no impact on the peer review process and the final decision.

## Publisher's note



## References

1. Lleó A. Biomarkers in neurological disorders: a fast-growing market. *Brain Commun* (2021) 3(2):fcab086. doi: 10.1093/braincomms/fcab086

2. Hu W, Lucchinetti CF. The pathological spectrum of CNS inflammatory demyelinating diseases. *Semin Immunopathol* (2009) 31(4):439–53. doi: 10.1007/s00281-009-0178-z

3. Li EC, Zheng Y, Cai MT, Lai QL, Fang GL, Du BQ, et al. Seizures and epilepsy in multiple sclerosis, aquaporin 4 antibody-positive neuromyelitis optica spectrum disorder, and myelin oligodendrocyte glycoprotein antibody-associated disease. *Epilepsia* (2022) 63(9):2173–91. doi: 10.1111/epi.17315

4. Abbatemarco JR, Yan C, Kunchok A, Rae-Grant A. Antibody-mediated autoimmune encephalitis: A practical approach. *Cleve Clin J Med* (2021) 88(8):459–71. doi: 10.3949/ccjm.88a.20122

5. Lai QL, Cai MT, Zheng Y, Fang GL, Du BQ, Shen CH, et al. Evaluation of CSF albumin quotient in neuronal surface antibody-associated autoimmune encephalitis. *Fluids Barriers CNS* (2022) 19(1):93. doi: 10.1186/s12987-022-00392-2

frontiers | Frontiers in Immunology

TYPE Original Research
PUBLISHED 18 August 2022
DOI 10.3389/fimmu.2022.986473



OPEN ACCESS

EDITED BY
Shougang Guo,
Shandong Provincial Hospital, China

REVIEWED BY
Juan Yang,
Mayo Clinic, United States
Jiawei Wang,
Beijing Tongren Hospital, Capital Medical University, China
Abhijit Chakraborty,
Baylor College of Medicine, United States

*CORRESPONDENCE
Feng Qiu
qiufengnet@hotmail.com
Jianguo Liu
doctorljg@sina.com

†These authors share first authorship

SPECIALTY SECTION
This article was submitted to Multiple Sclerosis and Neuroimmunology, a section of the journal Frontiers in Immunology

RECEIVED 05 July 2022
ACCEPTED 29 July 2022
PUBLISHED 18 August 2022

CITATION
Sun C, Han J, Lin Y, Qi X, Li C, Liu J and Qiu F (2022) Neuroimaging and clinicopathological differences between tumefactive demyelinating lesions and sentinel lesions of primary central nervous system lymphoma. *Front. Immunol.* 13:986473. doi: 10.3389/fimmu.2022.986473



# Neuroimaging and clinicopathological differences between tumefactive demyelinating lesions and sentinel lesions of primary central nervous system lymphoma

Chenjing Sun[1†], Jinming Han[2†], Ye Lin[1†], Xiaokun Qi[1], Changqing Li[3], Jianguo Liu[1*] and Feng Qiu[1*]

[1]Senior Department of Neurology, The First Medical Center of PLA General Hospital, Beijing, China, [2]Department of Neurology, Xuanwu Hospital, Capital Medical University, Beijing, China, [3]Department of Neurology, Beijing Chaoyang Hospital, Capital Medical University, Beijing, China

**Objective:** It is still a challenge to distinguish sentinel lesions of primary central nervous system lymphoma (PCNSL) from atypical tumefactive demyelinating lesions (TDLs) in clinical practice. We aimed to investigate potential differences of clinical features, neuroimaging findings and pathological characteristics between PCNSL and TDLs, improving early accurate diagnosis.

**Methods:** It was a retrospective study involving 116 patients with TDLs and 150 patients with PCNSLs. All cases were pathologically confirmed. Clinical features, neuroimaging findings and pathological characteristics between two groups were analyzed.

**Results:** The onset age was 37 ± 14 years in TDLs and 58 ± 13 years in PCNSL (p=0.000). Main onset symptom was headache in TDLs, while cognitive impairment was frequently noted in PCNSL. CT brain scan image showed hypodense lesions in most cases of TDL (110/116, 94.8%), while approximately 80% patients (120/150) with PCNSL had hyperdense lesions. Furthermore, we found that the presence of Creutzfeldt-Peters cells (might be misdiagnosed as tumor cells) may serve as an important feature in TDLs.

**Conclusions:** Onset age of patients with TDLs was younger than PCNSL. Neuroimaging features on brain CT scan might provide clues to make a differential diagnosis. Pathological features of PCNSL with sentinel lesions or following steroids therapy might mimic TDLs. Dynamic neuroimaging pathological and follow-up information were essential for an accurate diagnosis.

KEYWORDS

tumefactive demyelinating lesions, primary central nervous system lymphoma, sentinel lesions, pathology, neuroimaging, diagnosis

# Introduction

Tumefactive demyelinating lesions (TDLs), also called demyelinating pseudotumor (DPT), was first described by van der Velden and colleagues (1). TDLs are special inflammatory demyelinating lesions (> 20 mm in diameter) in the central nervous system (CNS), causing a variety of clinical manifestations. During an early disease stage, some patients only presented with cognitive impairment and TDLs (with surrounding edema or/and enhanced lesions) can be detected incidentally on magnetic resonance imaging (MRI) even. So TDLs are easily made as a suspected diagnosis of tumor (such as primary central nervous system lymphoma (PCNSL) or high-grade glioma) (2–4). PCNSL is a rare disease condition representing 6% of intracranial neoplasms and 1-2% of systemic lymphoma, with the plaques usually being involved the midline structure and white matter areas (5),. Main therapeutic approaches for PCNSL and TDLs are different. Shrinking PCNSL lesions can be noted following corticosteroids and TDLs can be easily misdiagnosed as PCNSL causing unreasonable treatment. Some PCNSL lesions can be appeared as demyelinating lesions during an early disease stage, described as a 'sentinel lesion' (6–8). Brain lesions following corticosteroids in PCNSL and sentinel lesions share similar pathological features and the final diagnosis is still challenging even after multiple times of biopsies. Previous studies regarding sentinel lesions of PCNSL and atypical TDLs were limited in reviews, case reports or small sample sizes (9–12). Therefore, investigating potential differences of clinical features, neuroimaging findings and pathological characteristics between PCNSL and TDLs is of importance.

# Methods

## Ethics statement

This study was conducted at the Sixth Medical Center of PLA General Hospital, Beijing, China. The patients/participants provided their written informed consent to participate in this study. This study was reviewed and approved by The Six Medical Center of PLA General Hospital, China.

## Patient information

A total of 116 patients with TDLs and 150 patients with PCNSL who were treated in the Sixth Medical Center of PLA General Hospital between January 1$^{st}$, 2010 and January 1$^{st}$ 2022 were included in this study. Detailed history including sex, onset age, onset neurological symptoms and treatment regimens were retrospectively reviewed and analyzed.

## Neuroimaging information

All patients were examined with a GE lightspeed 16-slince CT and GE Signa 1.5 or 3. 0 T MRI (General Electric, Milwaukee, WI, USA). The CT scan ranged from the canthomeatal line to calvarium. Brain window (window level: 35Hu, window width: 80hu) and bone window (window level: 450Hu, window width: 1500Hu). Scan parameters included tube voltage 130Kv, tube current:270mAs, 4.8mm slice thickness, andcontinuous scan 16 layers. The matrix was 512 * 512. Imaging slice thickness and interslice gap were same in all participants. Conventional imaging techniques were used: turbo spin-echo sequences for $T_2$ _Weighted imaging ($T_2$WI) (TR 4,660 ms; TE 110 ms; 6-mm slice thickness with a 2-mm interslice gap), FLAIR imaging (TR 9,000 ms; TE 120 ms; TI 2,200 ms, matrix 256 × 192, field of view (FOV) 240 mm; 6-mm slice thickness with a 2-mm interslice gap), $T_1$-weighted ($T_1$WI) T1-weighted imaging (TR 2415 ms; TE 13.9 ms; TI 750 ms; 6-mm slice thickness with a 2-mm interslice gap) and diffusion-weighted imaging (DWI) (TR 7000ms; TE 83.7 ms, b = 1,000 sec/mm$^2$, 6-mm slice thickness with a 2-mm interslice gap). Contrast $T_1$WI (TR 400-600 ms; TE 6-10 ms; matrix 256 × 224, field of view (FOV) 240 mm; 6-mm slice thickness with a 2-mm interslice gap). A bolus of gadolinium diethylenetriamine pentaacetic acid (Gd-DTPA 0.1 mmol/kg) was used.

## Immunohistochemistry

Immunohistochemical staining was performed using the EnVision™Systems (Dako, Glostrup, Denmark) according to the manufacturer's instructions. In brief, primary antibodies (mouse anti-human LCA (M 0701), CD34 (Kit-0004), CD20 (M 0755) and CD68 (IS 609); rabbit anti-human S-100 (GA 504), CD3(Kit-0003), PAX 5(312R-1) and GFAP (Z 0334)) were incubated with brain sections followed by incubation with secondary antibodies. The sections of staining were photographed under an optical microscope (BX51, Olympus, Tokyo, Japan) and photos were captured by the software DP2-BSW(Olympus). All antibodies were purchased from Dako except that anti-CD3 and CD34 were purchased from Maixin Biotechnology Corp. Ltd (Fuzhou, China), PAX 5 was purchased from Sigma-Aldrich (Shanghai) Trading Co. Ltd.

## Evaluation of immunohistochemical staining

Immunohistochemical staining was evaluated by two experienced pathologists. Both the distribution (the percentage of positive cells) and the intensity of staining were assessed in a semi-quantitative manner. The following score system was used for recording positive cells: none (not stained) =0, focal (less than one-third of cells stained) =1, multifocal (less than two-thirds of cells stained) =2, and diffuse (most cells stained) =3. The intensity of staining was graded as follows: none (not stained) =0, mild (between 0 and 2) =1, and strong (clearly identified under scale bar 50μm) = 2. The scores for distribution and intensity were added and graded as follows: 0–2 = (-, negative), 3–5 = (+, positive).

## Statistical analysis

SPSS 22.0 software was used for statistical analysis of the data:

1. Kollomogorov-Smirnoff test was used and all measurement conformed to normal distribution. Data characteristics were described by $\bar{x} \pm s$.
2. Pearson Chi-Sqrare test was used for enumeration data: ① Four-table table, if the theoretical frequency of more than 20% cells was between 1 and 5($1 \leq T < 5$), correction for continuity of chi-square test was used. And if the theoretical frequency of more than 1 cell was less than 1 ($T < 1$), Fisher's test was used. ②R×C table, if $T < 1$ or more than 20% of the cells had $T < 5$, the likelihood ratio was used.
3. $P < 0.05$ mean statistically significant.

# Results

## Clinical profiles of the patients with TDL and PCNSL

We summaried the distinguishment between TDLs and PCNSL in Table 1. The onset age in the TDL group was 37 ± 14 years old (Table 2). One of patients with TDLs was initially diagnosed as PCNSL or metastatic tumor and then treated with the gamma knife and glucocorticoid. However, a relapse occurred eight years later and demyelinating lesions complicated with radiation encephalopathy were confirmed by the brain biopsy.

The onset age in the PCNSL group was 58 ± 13years, older than age in the TDLs group (p=0.000, Table 2). Multiple biopsies were performed in a total of 4 cases for the definite diagnosis, and 15 cases received glucocorticoid treatment before biopsy, which might change histopathological features and lead to the misdiagnosis.

There was no significantly statistical difference in onsets of TDL and PCNSL (P=0.094) (Table 2), suggesting that tumor was not the only diagnosis if onsets of patients with intracranial space-occupying lesions were headache, limb weakness, numbness, or reduced vision.

## Neuroimaging of TDL and PCNSL

The lesions of TDLs and PCNSL mainly involved in the white matter, such as lateral ventricles and centrum ovale. Upon brain CT scans, 110 cases of TDLs had hypointense lesions, and 6 cases of TDLs showed isodense lesions. Approximately 80% patients (120/150) with PCNSL had hyperdense lesions, while 12 cases had hypointense lesions with central lesion enhancement (Figure 1). Regarding MRI, all brain lesions of TDLs and PCNSL showed hyperintense on $T_2$WI and fluid attenuated inversion recovery (FLAIR) sequences. On diffusion-weighted imaging (DWI) sequence, brain lesions in TDLs showed hyperintense, while lesions in PCNSL appeared slightly hyperintense. Brain lesions in TDLs showed flake, 'comb sign'(Figure 2D), ring or 'C' like enhancement (Figures 2A, B) and the 'C' opening toward grey matter which differentiated from PCNSL (Figures 2B, 3C). Acute lesions of TDLs (Figure 2C) could be easily misdiagnosed as PCNSL since its lesions showed the patchy, clump or ball-like enhancement (Figure 3). Furthermore, shrinking lesions following corticosteroids in PCNSL might lead to misdiagnose as TDLs, and brain lesions in TDLs with a mass effect and obvious enhancement could be easily misdiagnosed as PCNSL.

TABLE 1 The distinguishment between TDLs and PCNSL.

| | TDLs | PCNSL |
|---|---|---|
| clinical identification | | |
| Onset age | Average age is 36 | Older age |
| Onset time | 1/4-1/3 acute onset, mostly chronic onset | insidious onset or slow progressive, rarely acute onset |
| Clinical features | mild symptoms in the initial stage, but more obvious than tumors, and the movement disorder is more obvious if the pyramidal tract is involved | Relatively mild, slow progressive motor involvement, even if the pyramidal tract is involved, the onset symptoms are mostly epilepsy |
| Onset symptoms | Mainly apathy, headache, partial limb weakness and vision loss | Mainly cognitive impairment and memory loss, but also headache and vision loss |
| Involved location | common white matter involvement, but cortical and subcortical white matter can also be involved; lesions can be single or multiple, most lesions are not connected, and the corpus callosum is generally not thickened | It is more likely to involve midline structures such as the thalamus, brainstem, corpus callosum, and lateral ventricle triangle, and bilateral hemisphere involvement is common |
| CSF | The pressure is common normal<br>the protein is normal or increased, and MBP is positive. | The pressure is normal<br>the protein is normal<br>MBP is negative or slightly positive<br>and the IL-6 and IL-10 are increased, especially the ratio. |
| Glucocorticoid | The lesions gradually reduced or disappeared<br>the symptoms continued improved | Temporarily significantly reduced or disappeared (ghost cells), but new lesions may appear in other intracranial locations. |
| neuroimaging | | |
| CT | Hypointense or isodense lesions and finally hypointense lesions in the increasing stage but no enhancement | Hypointense or isointense at the beginning of the onset, and develop into hyperintensity as the disease progresses, and spheroid enhancement |
| MRI | T1WI hypointense and T2WI hyperintense;<br>clear lesion boundary;<br>ring-like or C-like enhancement in acute or subacute phase, and a few clump-like enhancement; enhancement becomes less and less obvious with time flies;<br>after 3 months goes spinal cord lesions become more obvious enhancement, TDLs are not considered;<br>DWI in acute or subacute phase is mostly hyperintensity, and the hyperintensity gradually decreases with time flies; SWI generally has no microbleeds; the perfusion of the lesion shows hypoperfusion. | Lymphoma cells have obvious enhancement, and the enhancement becomes more pronounced over time, manifesting as “clenched fist” and “notch sign”, rarely “ring” or “semi-ring” enhancement, sometimes involving subcortical “U”-shaped fibers, along the cortical infiltrating, and “semi-ring” enhancement may appear. Sometimes necrotic cyst may appear “ring” on DWI but the enhancement is often homogeneous or mixed significant solid; in the early stage, it is mostly hypointense or isointense on DWI, and gradually become hyperintense over time; microbleeds are rarely seen on SWI; the perfusion scan shows hyperperfusion. |
| Pathology | | |
| | inflammatory demyelination with relative preservation of axons. Creutzfeldt-Peters cells are key features but easily as tumor cells | Intracerebral demyelinating lesions appear at the beginning of the onset or after glucocorticoid treatment called “sentinel lesions” and then tumor cells slowly grow. |

TABLE 2 Statistical between TDL and PCNSL.

| | TDLs | PCNSL | P |
|---|---|---|---|
| **Number of subjects** | 116 | 150 | |
| **Age(years)** | 37 ± 14 | 58 ± 13 | 0.000 |
| **Gender** | | | 0.661 |
| **Male** | 55 | 90 | |
| **Famale** | 61 | 60 | |
| **onset** | | | 0.094 |
| **headache** | 42 (36.2%) | 35 (23.3%) | |
| **weakness** | 18 (15.5%) | 25 (16.7%) | |
| **numbness** | 18 (15.5%) | 10 (6.7%) | |
| **reduced vision** | 11 (9.5%) | 10 (6.7%) | |

## Pathological features of TDL and PCNSL

Telangiectasia with hemorrhage and perivascular infiltrates were observed in patients with TDL (Figure 4A). The presence of Creutzfeldt-Peters cells was another key feature in the TDL group (Figure 4B), with reactive astrocytes being seen in active inflammatory diseases. LCA-, CD20- and CD3-positive cells were detected in areas around the blood vessels (Figures 4C–F). Marked perivascular lymphocytic infiltrates were detected in TDLs. A few scattered atypical lymphocytes were observed in one case of TDLs and clinical symptoms were aggravated following corticosteroids, which made PCNSL as a possible diagnosis. However, widely depigmented myelin and positive LCA, CD20 and CD3 staining suggested a diagnosis of TDL.

Tumor cells were absent in sentinel lesions of PCNSL which were easily misdiagnosed. Multiple biopsies were performed in some cases of PCNSL due to atypical pathological features. Hypercellular plaques of PCNSL were characterized by axonal damaged associated with perivascular lymphocytic cuffing, perilesional edema and focal degeneration. However, demyelination and tumor cells were absent. The diagnosis of TDLs was challenging. For example, a 68-year-old man in our study was received three times of biopsies. Pathological profiles of previous two biopsies showed tissue edema, focal spongiform degeneration, profound perivascular and parenchymal infiltration composed mainly of lymphocytes with

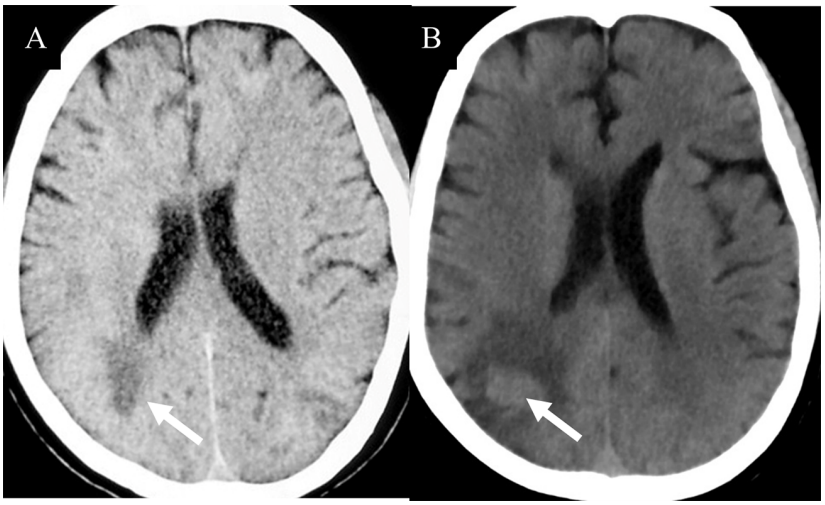


FIGURE 1
**(A)** Isodense lesion (white arrow) were detected on CT during an early disease. **(B)** One months later, brain lesions appeared hyperintense (white arrow). Pathological examinations indicated a diagnosis of PCNSL.

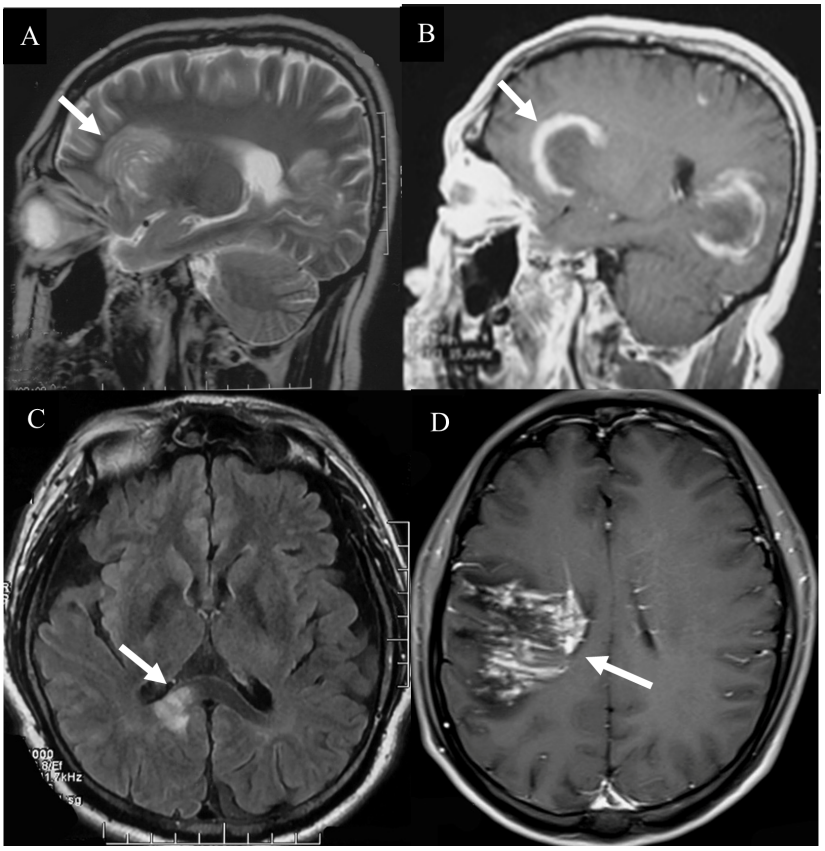


FIGURE 2
Hyperintense lesions in TDLs. **(A)** A Balo-like lesion (white arrow). **(B)** The 'C' like enhancement lesion (white arrow). **(C)** The lesions of TDLs without thickened corpus callosum (white arrow). **(D)** "comb sign" enhancement (white arrow).

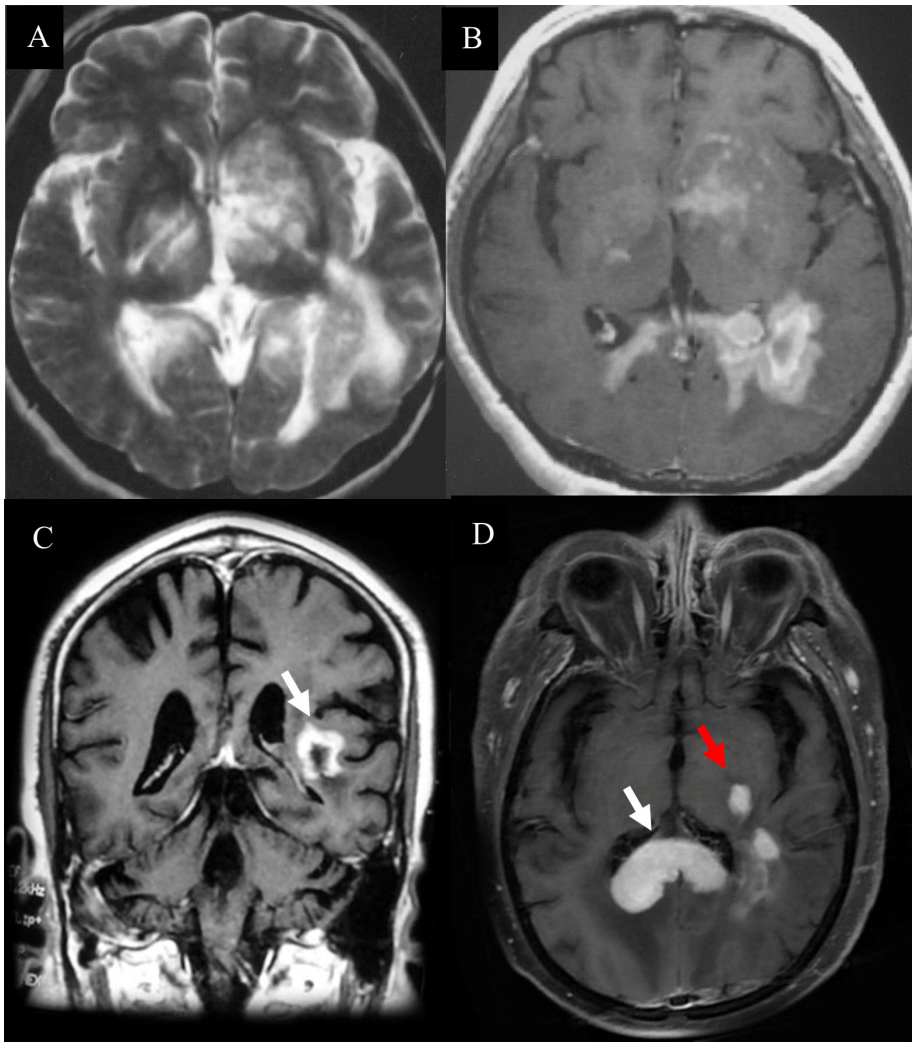


FIGURE 3
Hyperintense lesions in PCNSL. **(A)**The diffuse infiltrating lesions on T2 sequences. **(B)**The clump lesions with a ring-like enhancement. **(C)** The 'C' opening was not toward grey matter which differentiated from TDLs. **(D)** "kidney type"(White arrow) and "raindrop"-like (Red arrow) enhancement with thickened corpus callosum, while the lesions of TDLs without thickened corpus callosum.

the nuclear division. Immunohistochemical staining showed CD20-positive cells around the blood vessels. The patient was treated based on the diagnosis of TDL, which was not effective. The patient's symptoms gradually deteriorated, and he thus received the third biopsy. The pathology showed that atypical lymphocytes were infiltrated around blood vessels (Figure 5A) and CD20-positive cells (Figure 5B). Furthermore, the cells were CD3-negative, indicating a diagnosis of PCNSL.

## Discussion

In our study, we disclosed neuroimaging and clinicopathological differences between TDLs and sentinel lesions of PCNSL. Onset age of patients with TDLs was younger than PCNSL. Neuroimaging features on brain CT might provide clues to make a differential diagnosis. Pathological features of PCNSL with sentinel lesions or following steroids therapy might mimic TDLs. We found that the presence of Creutzfeldt-Peters cells (could be misdiagnosed as tumor cells) may serve as an important feature in TDLs. Dynamic neuroimaging pathological and follow-up information are essential for an accurate diagnosis.

Recent studies have suggested that TDLs may be a group of relatively independent diseases, or an early manifestation of demyelinating diseases, such as multiple sclerosis (MS), neuromyelitis optica spectrum disorder (NMOSD), acute disseminated encephalomyelitis (ADEM), myelin oligodendrocyte glycoprotein antibody-associated disease (MOGAD) and clinically

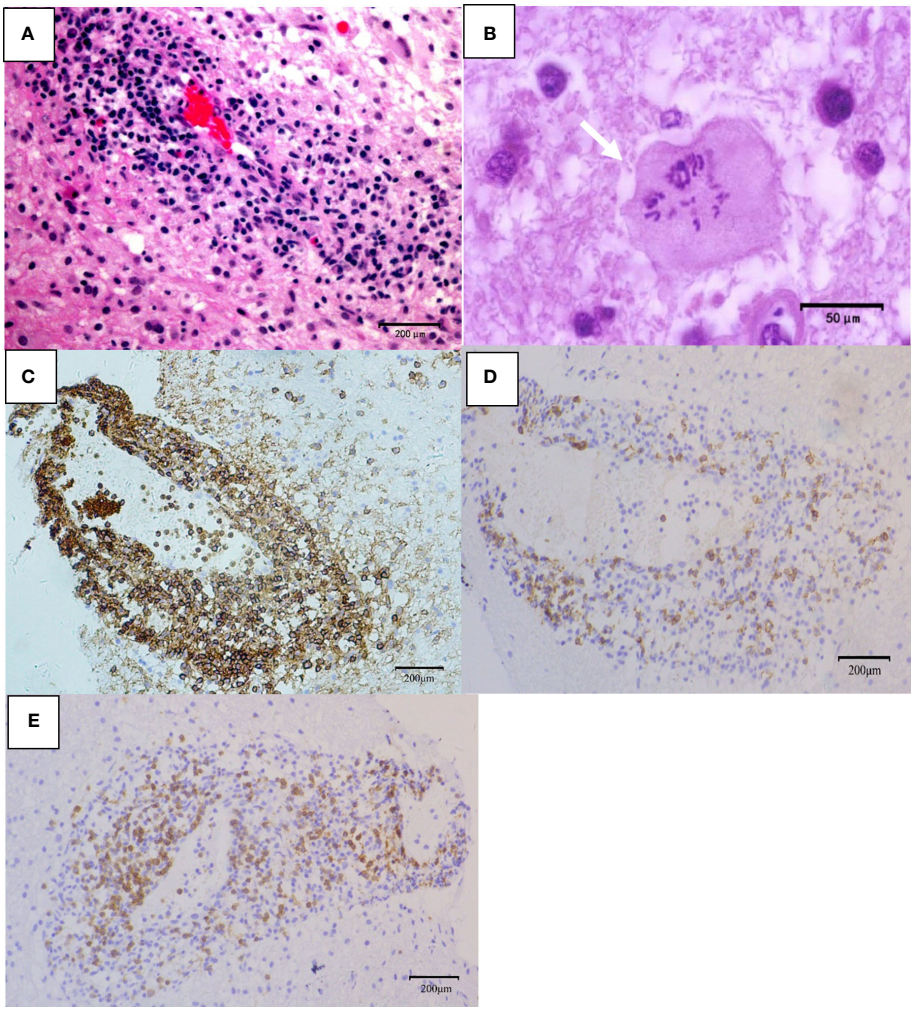


FIGURE 4
Pathological features of TDL. **(A)** Telangiectasia with hemorrhage and perivascular inflammatory cuff (hematoxylin and eosin, scale bar =200μm); **(B)** Creutzfeldt-Peters cells (white arrow, hematoxylin and eosin, scale bar =50μm);**(C)** $LCA^+$ lymphocytes around the blood vessels (LCA, scale bar =200μm); **(D)** $CD20^+$ B lymphocytes around the blood vessels (CD20, scale bar =200μm); **(E)** $CD3^+$ T lymphocytes around the blood vessels (CD3, scale bar =200μm).

isolated syndrome (CIS) (13–15). Clinical manifestations mainly depend on the location and scope of the lesions. Symptoms may gradually increase or aggravate during active phase, but rarely only show epileptic seizures. Onsets of headache, slurred speech, and weakness are more common (16). In early stage, some patients may only present mental and cognitive impairment such as memory loss, unresponsiveness, apathy, which are ignored and inadvertently take MRI to find large intracranial lesions, even accompanied by peripheral edema and mass or/and enhanced lesions (17). Mass-occupying lesions are easily diagnosed as a tumor, such as PCNSL or high-grade glioma (9, 14, 18, 19). During the phase of TDLs is progressing, symptoms may gradually increase or worsen, and reduced vision may also present. When TDLs lesions are diffuse or multiple, cognitive impairment and voiding dysfunction appear, and some can occur. Although TDLs is a rare type of CNS inflammatory demyelinating disease, many different diseases need to be differentially diagnosed. Therefore, a detailed understanding of clinical imaging characteristics of TDLs will be helpful to distinguish them from tumors, avoiding unnecessary traumatic surgery and radiation therapy. Ultimately, pathological diagnosis is also the key point.

Our study included 116 patients with TDLs and 150 patients with PCNSL. All of them were pathologically confirmed in our hospital. These valuable resources might help us to further understand the characteristics of TDLs and PCNSL, especially distinguishing sentinel lesions of PCNSL from TDLs. The onset

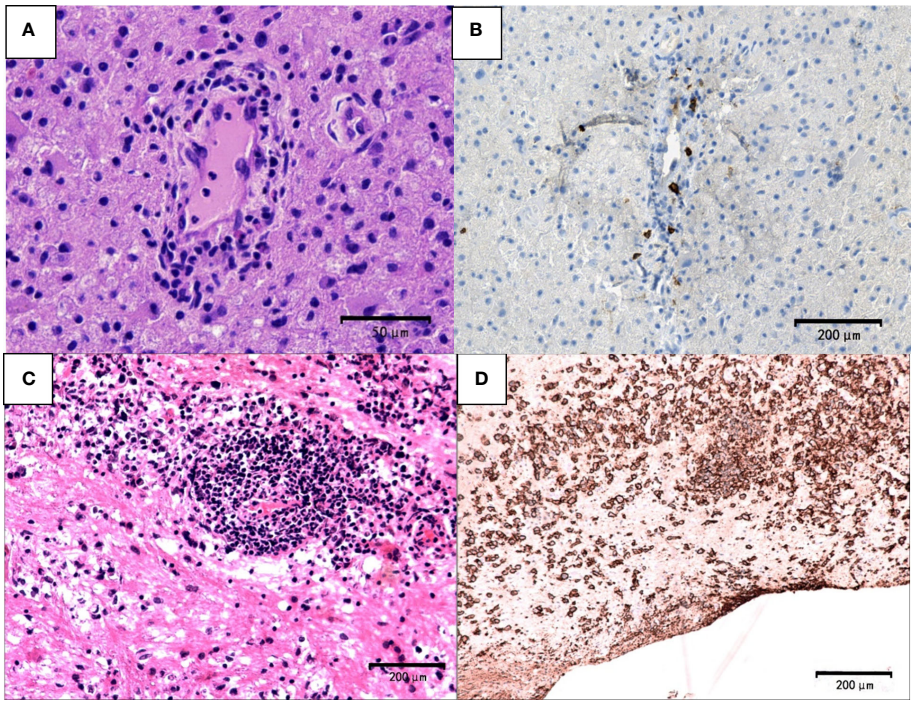


FIGURE 5
Pathological features of PCNSL. The first biopsy **(A, B)**. **(A)** demyelinated lesions as well as perivascular and parenchymal infiltration mainly composed lymphocytes (hematoxylin and eosin, scale bar =50μm). **(B)** CD20-negative cells (CD20, scale bar =200μm). The third biopsy **(C)** atypical lymphocyte infiltration around blood vessels (hematoxylin and eosin; scale bar=200μm) **(D)** $CD20^{+}$ B lymphocytes and typical tumor cells (CD20; scale bar =200μm).

age of PCNSL was older than that of TDLs. PCNSL with isodense lesions on brain CT scans need to be differentiated from TDLs. Atypical pathological features in PCNSL might be related to the use of corticosteroids.

It was worth noting that hyperdensity in CT and boundary definition of lesions in T1 and T2 in the differences between TDLs and PCNSL. The characteristic "comb-tooth sign", C-type or ring enhancement, double-layer enhancement, and density of DWI changes in MRI should be useful to diagnose TDLs. On the contrary, relatively uniform and significant sheet-like or spherical enhancement, "notch sign", "pointy angle sign", "kidney type", and "raindrop"-like enhancement implied PCNSL.

## Conclusion

Distinguishing sentinel lesions of PCNSL and TDLs during an early disease stage remains a challenge. Due to pathological features of PCNSL are dynamic and can be associated with disease evolution, corticosteroid is not recommended for PCNSL before a definite diagnosis being made. Furthermore, repeated biopsies may be needed in some patients with PCNSL and TDLs for a definitive diagnosis.

## Limitation

Although the large sample was analyzed in our research, a single-center design should be stated as a limitation. Limited clinical profiles, imaging profiles, laboratory, and pathological findings in patients with TDL and PCNSL prevented further analysis. In future, we will continue to collect patients from multiple centers for further analysis.

## Data availability statement

The original contributions presented in the study are included in the article/supplementary material. Further inquiries can be directed to the corresponding authors.

## Author contributions

CS, JH and YL acquired the clinical data, reviewed the literature, and drafted the article. FQ and JL designed the study, supervised the initial drafting, and critically revised the article. XQ and CL collected and analyzed the clinical data.

All authors contributed to the article and approved the submitted version.

## Conflict of interest

The authors declare that the research was conducted in the absence of any commercial or financial relationships that could be construed as a potential conflict of interest.

## Publisher's note



## References

1. van der Velden M, Bots GT, Endtz LJ. Cranial CT in multiple sclerosis showing a mass effect. *Surg Neurol* (1979) 12(4):307–10.

2. Ohe Y, Hayashi T, Mishima K, Nishikawa R, Sasaki A, Matsuda H, et al. Central nervous system lymphoma initially diagnosed as tumefactive multiple sclerosis after brain biopsy. *Intern Med* (2013) 52(4):483–8. doi: 10.2169/internalmedicine.52.8531

3. Liu J, Qiao W, Zheng K, Zhao H, Qian H, Yao S, et al. [Comparison of tumefactive demyelinating lesions and glioma by clinical presentations and neuroimaging studies]. *Zhonghua Yi Xue Za Zhi* (2014) 94(39):3047–51. Available at: https://europepmc.org/article/MED/25549675

4. Lu SS, Kim SJ, Kim HS, Choi CG, Lim YM, Kim EJ, et al. Utility of proton MR spectroscopy for differentiating typical and atypical primary central nervous system lymphomas from tumefactive demyelinating lesions. *AJNR Am J Neuroradiol* (2014) 35(2):270–7. doi: 10.3174/ajnr.A3677

5. Chiavazza C, Pellerino A, Ferrio F, Cistaro A, Soffietti R, Rudà R, et al. Primary CNS lymphomas: Challenges in diagnosis and monitoring. *BioMed Res Int* (2018) 2018:3606970. doi: 10.1155/2018/3606970

6. Bajagain M, Oyoshi T, Hanada T, Higa N, Hiraki T, Kamimura K, et al. Histopathological variation in the demyelinating sentinel lesion of primary central nervous system lymphoma. *Surg Neurol Int* (2020) 11:342. doi: 10.25259/SNI_531_2020

7. Kalus S, Di Muzio B, Gaillard F. Demyelination preceding a diagnosis of central nervous system lymphoma. *J Clin Neurosci* (2016) 24:146–8. doi: 10.1016/j.jocn.2015.07.013

8. Kvarta MD, Sharma D, Castellani RJ, Morales RE, Reich SG Kimball AS, et al. Demyelination as a harbinger of lymphoma: a case report and review of primary central nervous system lymphoma preceded by multifocal sentinel demyelination. *BMC Neurol* (2016) 16:72. doi: 10.1186/s12883-016-0596-1

9. Suh CH, Kim HS, Jung SC, Choi CG, Kim SJ. MRI Findings in tumefactive demyelinating lesions: A systematic review and meta-analysis. *AJNR Am J Neuroradiol* (2018) 39(9):1643–9. doi: 10.3174/ajnr.A5775

10. Yasuda S, Yano H, Kimura A, Suzui N, Nakayama N, Shinoda J, et al. Frontal tumefactive demyelinating lesion mimicking glioblastoma differentiated by methionine positron emission tomography. *World Neurosurg* (2018) 119:244–8. doi: 10.1016/j.wneu.2018.08.027

11. Ekmekci O, Eraslan C. Silent tumefactive demyelinating lesions and radiologically isolated syndrome. *Case Rep Neurol Med* (2018) 2018:8409247. doi: 10.1155/2018/8409247

12. Naeem SB, Niazi F, Baig A, Sadiq H, Sattar M. Primary CNS lymphoma vs. tumefactive multiple sclerosis: A diagnostic challenge. *J Coll Physicians Surg Pak* (2018) 28(1):66–8. doi: 10.1016/j.wneu.2018.08.027

13. Plowman RS, Varma H. Prognostic factors in tumefactive demyelinating lesions: A retrospective study. *J Neurol Sci* (2021) 428:117591. doi: 10.1016/j.jns.2021.117591

14. Sánchez P, Chan F, Hardy TA. Tumefactive demyelination: updated perspectives on diagnosis and management. *Expert Rev Neurother* (2021) 21(9):1005–17. doi: 10.1080/14737175.2021.1971077

15. Garg RK, Malhotra HS, Kumar N, Pandey S, Patil MR, Uniyal R, et al. Tumefactive demyelinating brain lesion developing after administration of adenovector-based COVID-19 vaccine: A case report. *Neurol India* (2022) 70(1):409–11. doi: 10.4103/0028-3886.338642

16. Neuroimmunology Branch of Chinese Society for Immunology, Neuroimmunology Group of PLA Neurology Professional Committee of Science and Technology CommitteeChinese Guidelines for the diagnosis and management of tumefactive demyelinating lesions of central nervous system. *Chin Med J (Engl)* (2017) 130(15):1838–50. doi: 10.4103/0366-6999.211547

17. Lebrun C. Radiologically isolated syndrome should be treated with disease-modifying therapy - commentary. *Mult Scler* (2017) 23(14):1821–3. doi: 10.1177/1352458517727149

18. French HD. Tumefactive multiple sclerosis versus high-grade glioma: A diagnostic dilemma. *Surg Neurol Int* (2021) 12:199. doi: 10.25259/SNI_901_2020

19. Nakayama M, Naganawa S, Ouyang M, Jones KA, Kim J, Capizzano AA, et al. A review of clinical and imaging findings in tumefactive demyelination. *AJR Am J Roentgenol* (2021) 5(19):1–12. doi: 10.2214/AJR.20.23226

frontiers | Frontiers in Immunology

TYPE Brief Research Report
PUBLISHED 11 October 2022
DOI 10.3389/fimmu.2022.948479



OPEN ACCESS

EDITED BY
Carlo Di Bonaventura,
Department of Human Neurosciences,
Sapienza University of Rome, Italy

REVIEWED BY
Alessandra Morano,
Department of Neurology
and Psychiatry, Sapienza
University of Rome, Italy
Nicolás Lundahl Ciano-Petersen,
Instituto de Investigación Biomédica
de Málaga - IBIMA, Spain

*CORRESPONDENCE
Divyanshu Dubey
Dubey.divyanshu@mayo.edu

SPECIALTY SECTION
This article was submitted to
Autoimmune and Autoinflammatory
Disorders,
a section of the journal
Frontiers in Immunology

RECEIVED 19 May 2022
ACCEPTED 27 September 2022
PUBLISHED 11 October 2022

CITATION
Zhao-Fleming HH, Zahid A,
Lu T, Sun X, Pittock SJ,
Lee H-C and Dubey D (2022)
Characterization of cardiac
bradyarrhythmia associated with
LGI1-IgG autoimmune encephalitis.
*Front. Immunol.* 13:948479.
doi: 10.3389/fimmu.2022.948479



# Characterization of cardiac bradyarrhythmia associated with LGI1-IgG autoimmune encephalitis

Hannah H. Zhao-Fleming[1], Anza Zahid[1], Tong Lu[2], Xiaojing Sun[2], Sean J. Pittock[1,3], Hon-Chi Lee[2] and Divyanshu Dubey[1,3]*

[1]Department of Neurology, Mayo Clinic, Rochester, MN, United States, [2]Department of Cardiovascular Medicine, Mayo Clinic, Rochester, MN, United States, [3]Department of Laboratory Medicine and Pathology, Mayo Clinic, Rochester, MN, United States

**Objective:** To evaluate and characterize cardiac arrythmias associated with LGI1-IgG (Leucine-rich glioma inactivated 1–IgG) autoimmune encephalitis (AE).

**Patients and methods:** In this retrospective descriptive study, we identified Mayo Clinic patients (May 1, 2008 – December 31, 2020) with LGI1-IgG AE who had electrocardiogram proven bradyarrhythmias during the initial presentation. Inclusion criteria were 1) LGI1-IgG positivity with a consistent clinical syndrome; 2) electrocardiographic evidence of bradyarrhythmia; and 3) sufficient clinical details. We excluded patients who were taking negative ionotropic agents at the time of their bradyarrhythmias. We collected demographic/clinical data including details of bradyarrhythmia (severity, duration, treatments), and neurologic and cardiac outcomes.

**Results:** We found that patients with LGI1-IgG AE had bradyarrhythmia at a frequency of 8% during the initial presentation. The bradyarrhythmia was often asymptomatic (6/11, 55%); however, the episode was severe with one patient requiring a pacemaker. Outcome was also generally favorable with the majority (8/11, 73%) having full resolution without further cardiac intervention. Lastly, we found that mouse and human cardiac tissues express LGI1 (mRNA and protein).

**Conclusion:** LGI1-IgG AE can be rarely associated with bradyarrhythmias. Although the disease course is mostly favorable, some cases may require pacemaker placement to avoid devastating outcomes.

KEYWORDS

**LGI1-IgG, autoimmune encephalitis, cardiac bradyarrhythmia, outcomes, seizures**

# Introduction

A population-based epidemiology study based in Olmsted County demonstrated that autoimmune encephalitis is as common as infectious encephalitis. (1) Furthermore, over the last few decades recognition of this potentially treatable conditions has exponentially increased, primarily because of widespread utilization of neural autoantibody evaluation as diagnostic markers. Leucine-rich glioma inactivated 1 (LGI1) IgG is one of the most common pathogenic neural specific autoantibodies associated with autoimmune encephalitis in adults. (2) Few cases of bradyarrhythmia in association with LGI1 autoimmune encephalitis have been reported. (3, 4) However, larger cohort studies analyzing cardiac rhythm dysfunction are lacking, suggesting that this may be an under reported phenomenon. In this study, we characterize the episodes of bradyarrhythmias among LGI1 encephalitis patients and evaluate LGI1 expression in cardiac tissue.

# Methods

## Study approval and patient consents

The Mayo Clinic Institutional Review Board approved this study and all patients consented to the use of their medical records for research purposes.

## Patient identification

We retrospectively identified Mayo Clinic patients from May 1, 2008 to December 31, 2020 through Advanced Cohort Explorer, an electronic retrieval system that interrogates the electronic medical record, and this was cross referenced with our prior studies on LGI1 antibody encephalitis. The inclusion criteria included: (1) LGI1 antibody positivity in serum and/or CSF; (2) patient evaluated at Mayo Clinic (Minnesota, Florida, Arizona); (3) clinical syndrome consistent with LGI1 IgG autoimmunity; and (4) electrocardiographic (ECG) documentation of bradycardia (defined as heart rate less than 60 beats per minute). Our exclusion criteria was 1) when bradycardia was not a part of the LGI1 antibody encephalitis presentation and 2) cases where there was concurrent negative ionotropic agents used. These medications include diltiazem, amiodaron, propranolol, metoprolol, midazolam and carvedilol. Mayo Clinic medical records of all included cases were reviewed by three physicians (H.H.Z., A.Z., and D.D.) independently. Detailed cohort identification process is outlined in Figure 1. Demographic and clinical data along with MRI brain, electrocardiography findings and clinical outcomes were collected.

## LGI1-IgG assay

LGI1 autoantibodies were detected by transfected cell-based immunofluorescence assay (CBA; EUROIMMUN, Lubeck, Germany) in Mayo Neuroimmunology Laboratory, as previously described (5).

## Quantitative real-time PCR

mRNA was extracted from isolated C57BL/6 (The Jackson Laboratory) mouse cardiomyocytes with the RNeasy Plus Mini Kit (Qiagen, Cat. No: 74134). The mRNA was then reverse transcribed to cDNA using SuperScript™ III First-Strand Synthesis SuperMix (Invitrogen, Cat. No: 18080-400). This cDNA is then amplified using taq polymerase (Denville Scientific, Cat. No: 1091201), and PCR primer: LGI-1 primers: 5' TCC TCG AAG GAT TTC GAT TG 3'(forward), 5' ACA TGG TCC CAT TCA AGG AA 3'(reverse). GAPDH primers: 5′-TGCCAAGGCTGTGGGCAAGG-3′ (forward) and 5′-TGGGCCCTCAGATGCCTGCT-3′ (reverse). Thermocycling was done as follows: initial denaturation at 94°C for 5 minutes, 35 cycles of denaturation at 94°C for 30 seconds, primer annealing at 58°C for 30 seconds, and extension at 72° C for 30 seconds, followed by final extension at 72°C for 5 minutes.

## Immunoprecipitation

Human heart tissue from an organ donor was ground into powder with mortar and pestle in liquid nitrogen. This was made into a solution with RIPA buffer (in mM): Tris 50, NaCl 150, NaF 2, EDTA 1, EGTA 1, NaVO4 1, and 1% Triton X-100 containing protease inhibitor cocktail (Complete Mini, EDTAfree; Roche Diagnostics GmbH, Germany) and placed on ice for 1 hour. Then, the homogenate was centrifuged at 8700 rpm at 4°C for 10 min. The supernatant (200 µg in 200 µl) was pre-cleared with Protein G Plus-agarose beads (Santa Cruz Biotechnology, Santa Cruz, CA) at 4°C for 1 hour, and the pre-cleared supernatant was incubated with mouse anti-LGI1 antibodies (2 µg/200 µg protein, Invitrogen, S283-7) at 4°C overnight. The next day, the samples were incubated with 30 µl Protein G Plus-agarose at 4°C for 3 h with rotation. After washing the beads with RIPA/protease inhibitor buffer, the immunoprecipitates were collected and eluted with 30 µl SDS-PAGE loading buffer per tube. The immunoprecipitates were resolved by SDS-PAGE (4–15% gel) and blotted against anti-LGI1 antibody with 1:1000 dilution.

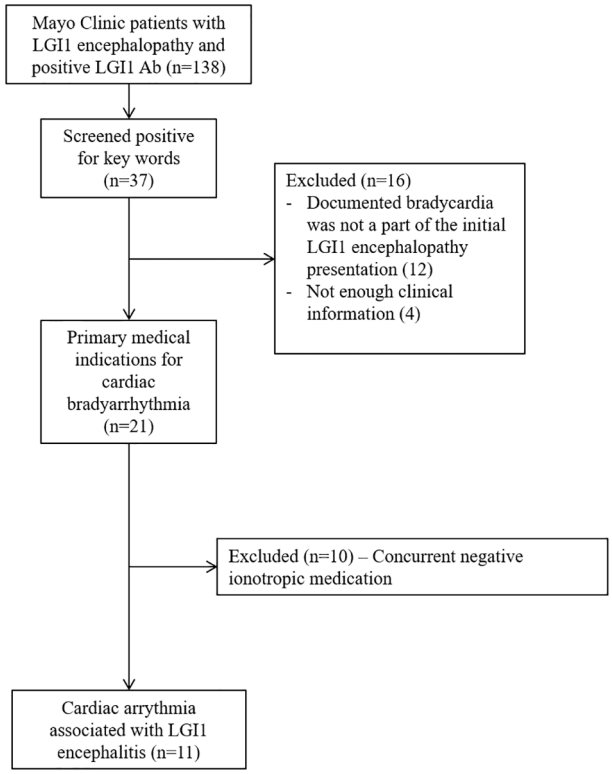


FIGURE 1
Flowchart depicting search strategy for identification of patients cardiac arrythmia within 6 months of LGI1 neurological autoimmunity.

# Results

## Patient cohort and frequency of cardiac arrythmia

Among 137 cases we found 11 cases with LGI1 IgG seropositivity to have a cardiac bradyarrhythmia that is not otherwise explained by medical co-morbidities, representing a frequency of 8%. The median age of our cohort was 64 years old (range 18-82 years), and 8/11 (73%) of our cohort was male. In our cohort, (121/137, 88%) had cardiac rhythm measured by ECG, (71/121, 59%) with 12-lead ECG, and (50/121, 41%) with 1-2 lead ECG within an electroencephalogram (EEG) evaluation. Of the 50 patients whose cardiac rhythm was monitored only within the EEG, only 8 (16%) had EEG reports that commented on the heart rate specifically. Only two of these 11 patients had history of structural heart disease (one had coronary artery disease and the other had mitral regurgitation). Other medical comorbidities included hypertension (n=7), hyperlipidemia (n=6), diabetes mellitus (n=3) and obstructive sleep apnea (n=2). Four patients had inhouse echocardiograms done after the bradycardia event, none of which demonstrated any ischemic cardiac changes. Two patients had neurology notes mention outside echocardiogram performed and was unremarkable. Five patients did not have internal or external echocardiograms. Three of our patients had a history of autoimmunity (Hashimoto thyroiditis, prior acute inflammatory demyelinating polyneuropathy, and interstitial lung disease). Three of our patients had a history of cancers, none of which were active at the time of LGI1 encephalitis (prostate cancer and melanoma, prostate cancer and basal cell carcinoma of the skin, and squamous cell carcinoma of the skin). Further details of our patient population, as well as certain details of their cardiac episode are described in Table 1.

## Clinical information of the cardiac arrythmia event

In all 11 patients, cardiac arrhythmia was a part of their initial presentation. Although hyponatremia was common during the encephalitic episode (64%), it was not common at the time of bradycardia capture (10%, Table 1). When available, other electrolytes were also within normal levels (potassium levels available in 10/11 patients and magnesium levels available in 3/11 patients). Neurological presentation was most commonly seizures (6/11, 55%), followed by encephalopathy (2/11, 18%) and both seizures and encephalopathy (2/11, 18%), and one patient presented with neuropathic pain involving the lower

10.3389/fimmu.2022.948479

TABLE 1 Demographics, co-morbidities, details of cardiac episode, treatments and outcomes of symptomatic bradycardiac associated with LGI1 encephalopathy.

| LGI1-IgG positive patients with bradycardia | (n = 11) |
|---|---|
| **Demographics** | |
| Age at onset – Median (range, years) | 64 (18-82) |
| - Sex, male (%) | 8/11 (73%) |
| - Ethnicity, Caucasian (%) | 11/11 (100%) |
| **Sodium levels** | |
| - Hyponatremia[a] anytime during episode | 7/11 (64%) |
| - Lowest sodium level during episode – Median (range, mmol/L) | 131 (114-138) |
| - Hyponatremia at time of bradycardia capture[b] | 1/10 (10%) |
| **ECG findings** | |
| - Sinus bradycardia (%) | 7/11 (64%) |
| - Sinus bradycardia with PVCs (%) | 2/11 (18%) |
| - Bradycardia with 1st degree AV block (%) | 1/11 (9%) |
| **EEG findings[c]** | |
| - Ictal discharges (%) | 5/10 (50%) |
| - Interictal discharges/slowing (%) | 2/10 (20%) |
| - Normal (%) | 3/10 (30%) |
| **Bradycardia onset/detection** | |
| - After onset of seizures | 5/11 (45%) |
| - Preceding onset of seizures | 3/11 (27%) |
| - During same presentation | 3/11 (27%) |
| **MRI findings** | |
| - Medial temporal T2 hyperintensity, n (%) | 5/11 (36%) |
| - Other abnormalities | 2/11 (18%) |
| - Unremarkable findings (%) | 4/11 (36%) |
| **Immunotherapies** | |
| - Corticosteroids | 6/11 (55%) |
| - PLEX | 0/11 (0%) |
| - IVIG | 2/11 (18%) |
| **Cardiac Outcome** | |
| - No evidence of continued bradycardia | 8/11 (73%) |
| - Continued bradycardia | 1/11 (9%) |
| - Pacemaker placement | 1/11 (9%) |
| **Neurologic outcome at last follow-up** | |
| - Seizure free on antiepileptic | 3/11 (27%) |
| - Seizure free on immunomodulation | 4/11 (36%) |
| - Residual cognitive deficits | 3/11 (27%) |
| - Persistent seizures and cognitive decline | 1/11 (9%) |
| - Unknown | 2/11 (18%) |

[a]Hyponatremia defined as serum sodium levels less than 135 mmol/L, [b]One patient did not have sodium documented at bradycardia capture, [c]One patient without EEG documented.
AV, atrial ventricular; ECG, electrocardiogram; EEG, electroencephalogram; IVIG, intravenous immunoglobulins; PLEX, plasma exchange; PVC, premature ventricular contraction.

extremities. All the cardiac episodes were associated with seizures within 8 months. Seizure semiology was most commonly focal sensory aware (4/11, 36%), followed by focal sensory with impaired awareness (2/11, 18%), focal motor aware (2/11, 18%), focal motor/sensory with impaired awareness (2/11, 18%), and focal motor/sensory aware (1/11, 9%). In 6/11 (55%) of our patients, faciobrachial dystonic seizures were additionally noted. EEG showed interictal discharges or slowing in 2/10 patients (one patient had bi-hemispheric slowing and the other had epileptiform changes in the right temporal head region) and temporal lobe ictal discharges in 5/10 patients. Three patients had other documented evidence of autonomic dysfunction (all orthostatic dysfunction), with one patient having objective evidence of orthostatic intolerance on autonomic reflex testing. Notably, at the time of the bradycardia capture, 6 patients were taking antiseizure medications, 5 of whom were taking sodium channel blockers, specifically lacosamide, valproic acid, phenytoin, and oxcarbazepine. The one patient in our cohort who had persistent bradycardia was on phenytoin during initial bradycardia episode.

ECG findings of bradyarrhythmia were most commonly asymptomatic (6/11, 55%), median heart rate on initial ECG was 55 (range 37-59). In our patients who were symptomatic in association with their bradyarrhythmia, symptoms were either mild (generalized tremulousness) or more severe (presyncope, syncope, and exercise intolerance). In one of our patients, the bradycardia led to sinus arrest, requiring placement of a pacemaker, 2 months prior to the development of encephalopathy and subsequent LGI1-IgG evaluation. One patient was noted to have bradycardia during routine EEG without associated ictal discharges.

Most patients had favorable outcomes from neurological perspective. All patients achieved seizure freedom (Table 1). Three of our patients had continued cognitive deficits, including memory deficits and word finding difficulties. Two patients were still on a corticosteroid taper at last follow-up with cognitive deficits thought to be secondary to the active autoimmune encephalitis, while one patient had persistent cognitive deficit, thought to be the sequelae of prior encephalitis and immunomodulation was not offered.

From a cardiac perspective, one patient required pacemaker placement and another patient had persistent asymptomatic bradycardia at last follow-up 9 months after initial presentation, but she did not require additional management. Lastly, another LGI1 encephalitis patient who had arrythmia at the time of initial presentation, presented to the emergency department at an outside hospital with syncopal episodes, followed by unexpected sudden death three days later.

## LGI1 expression *in vivo*

We found that LGI1 mRNA is expressed in wild type mouse cardiomyocytes by RT-PCR (Figure 2A). We also found that LGI1 protein is expressed in human cardiomyocytes *via* immunoprecipitation and western blotting (Figure 2B).

## Discussion

In this study, we described a cohort of LGI1-IgG seropositive patients who had bradycardia at presentation. Few cases had bradycardia preceding the onset of encephalopathy. The outcomes of the bradycardia were generally positive, with 73% recovering completely. One patient had continued bradycardia without the need for further intervention, and another patient required pacemaker placement. The general demographics, including age, sex, and ethnicity of the cases included in this study are like prior studies, (6) suggesting that this is not a sub-specific group pre-disposed to cardiac arrythmias. The incidence of sinus bradycardia in our cohort is 8% and appears to be higher than that of the general population which is estimated to be 0.8 per 1000 person-year, although the true incidence of sinus node dysfunction in the general population is unknown. (7, 8)

Several mechanisms for cardiac arrythmias associated with seizure disorders have been proposed in the past, such as temporal lobe seizures causing ictal bradycardia (9) and involvement of the insular cortex contributing to bradyarrhythmias (10). Even among the cases included in this study we cannot exclude effect of temporal or insular discharges on cardiac arrythmias. However, as all cardiac dysrhythmias in our study were not temporally related to the seizures an alternative pathophysiology such as a potential direct role of LGI1 IgG on cardiac myocytes is possible. LGI1, an extracellular component of the voltage-gated potassium channel (VGKC) complex, is tightly complexed with Kv1 channels and LGI1 antibodies are thought to bind to LGI1 and alter neuronal excitability and synaptic transmission. (11) LGI1 has been reported to co-assemble with Kv1.4 and KVβ1, slowing channel inactivation through inhibition of the effects of Kvβ1. (12) It is intriguing that Kv1.4 is known to be present in the heart. (13) Whether LGI1 antibodies would affect the function of Kv1.4 in the heart is unknown. Our finding that LGI1 is expressed in cardiac tissue raises the possibility of direct cardiac effect of the LGI1-IgG as a potential etiology for these cardiac manifestations.

Patients with asymptomatic sinus bradycardia in the general population are not associated with incident cardiovascular diseases or mortality. (14) Although most of our patients had favorable cardiac outcomes, one patient with focal motor seizures presented to the emergency department with a syncopal episode while corticosteroids were being tapered. Due to lack of access to outside facility records presence of persistent cardiac arrythmia could not be confirmed at/around the time of syncope. He unfortunately died suddenly three days later without a clear cause.

Sudden cardiac death has also been previously reported in LGI1 encephalitis. (15) In the reported case, no arrythmia was documented because the event happened outside the hospital setting. Pathology showed no significant coronary disease or evidence of myocardial ischemia, further highlighting the importance of understanding the rare but potential fatal cardiac dysfunction in LGI1 AE. Furthermore, in a large study on sudden death in epilepsy, the authors found that heart rate variability derangement is significantly more pronounced in epilepsy patients prior to their sudden death when compared with the surviving epileptic controls, suggesting a strong cardiac rhythm component in sudden death in epilepsy. (16)

Studies have demonstrated that the anti-seizure medications (ASMs) working primarily through sodium channel blockade may be more efficacious than other ASMs with other mechanisms of action for managing seizures associated with LGI1 AE. (17) However, some sodium channel blocking medications, such as lacosamide, can cause or potentially worsen bradyarrhythmias. (18, 19) Sodium channel blocking drugs are known to be proarrhythmic in patients with history of coronary artery disease and structural heart disease. (20) Indeed, five of our patients were taking sodium channel blockers during

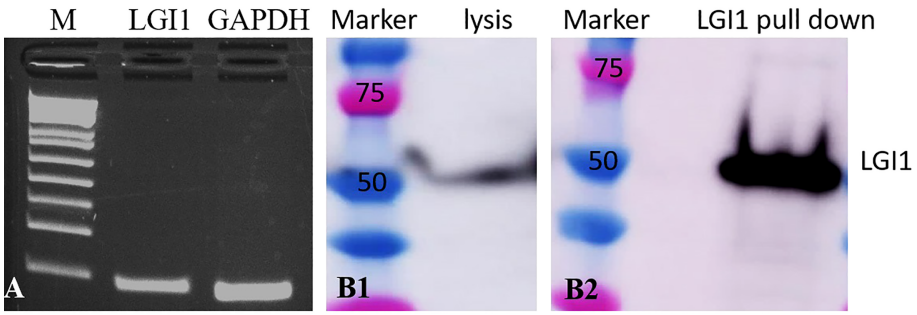


FIGURE 2
Cardiomyocytes express LGI1 mRNA and protein. **(A)** qt-PCR showing LGI1 and GAPDH (control) mRNA expression in mouse cardiomyocytes; **(B)** western blot of human heart ventricle lysate demonstrates binding of commercial LGI1 commercial antibodies to ~50 kD protein (B1); immunoprecipitation and western blot screening of human heart ventricle lysates with LGI1 commercial antibody also demonstrates a ~50 kD molecular weight band (B2).

their bradycardia episode, therefore among these cases adverse effect of anti-seizure medications cannot be completely excluded. Pre-screening LGI1 AE patients with an electrocardiogram may help identify patients with bradyarrhythmias, which will aid in the ASM selection.

Our study has some potential limitations including its retrospective design. There is likely under detection of cardiac arrythmias if the patient did not exhibit overt cardiac symptoms such as syncope prompting an ECG. Indeed, only 71/137 (52%) of our cohort had their cardiac rhythms accessed by a 12-lead ECG at the time of their initial presentation. Although more of our cohort did have heart rate monitoring as a part of their EEG study, only 16% of the EEG reports commented on heart rates in particular. Lastly, our cohort was 73% male with a median age of 64 years, which is the demographic prone to cardiovascular comorbidities. (21) Although we excluded patients with known alternate cardiac causes for arrhythmias, we cannot exclude the possibility that our patients had preclinical or undiagnosed cardiac comorbidities. Indeed, five of our patients did not have any cardiac echocardiogram documented after their bradycardiac episode. However, temporal association of detection of arrythmias with onset of neurological dysfunction and demonstration of LGI1 protein expression in the cardiac tissue supports the presence of this rare but potentially fatal cardiac manifestation of LGI1 autoimmunity.

## Data availability statement

The raw data supporting the conclusions of this article will be made available by the authors, without undue reservation.

## Ethics statement

The studies involving human participants were reviewed and approved by Mayo Clinic Institutional Review Board. The patients/participants provided their written informed consent to participate in this study.

## Author contributions

HHZ designed and conceptualized study; drafted the manuscript and figures; analyzed and interpreted the data. AZ analyzed and interpreted the data; revised the manuscript for intellectual content. TL performed RT-PCR and immunoprecipitation experiments; Interpreted the data; revised the manuscript for intellectual content. XS performed RT-PCR and immunoprecipitation experiments; Interpreted the data; revised the manuscript for intellectual content. SP interpreted the data; revised the manuscript for intellectual content. H-CL designed and conceptualized study; interpreted the data; revised the manuscript for intellectual content. DD designed and conceptualized study; analyzed and interpreted the data; Revised the manuscript for intellectual content; study supervision. All authors contributed to the article and approved the submitted version.

## Conflict of interest

SP reports grants, personal fees and non-financial support from Alexion Pharmaceuticals, Inc.; grants, personal fees, non-financial support and other support from MedImmune, Inc/Viela Bio.; personal fees for consulting from Genentech/Roche. He has a patent, Patent# 8,889,102 (Application#12-678350, Neuromyelitis Optica Autoantibodies as a Marker for Neoplasia) – issued; a patent, Patent# 9,891,219B2 (Application#12-573942, Methods for Treating Neuromyelitis Optica [NMO] by Administration of Eculizumab to an individual that is Aquaporin-4 (AQP4)-IgG Autoantibody positive) – issued. DD has consulted for UCB, Immunovant and Astellas pharmaceuticals. All compensation for consulting activities is paid directly to Mayo Clinic. DD has patents pending for KLHL11 and LUZP4 as markers of neurological autoimmunity.

The remaining authors declare that the research was conducted in the absence of any commercial or financial relationships that could be construed as a potential conflict of interest

## Publisher's note

All claims expressed in this article are solely those of the authors and do not necessarily represent those of their affiliated organizations, or those of the publisher, the editors and the reviewers. Any product that may be evaluated in this article, or claim that may be made by its manufacturer, is not guaranteed or endorsed by the publisher.

## References

1. Dubey D, Pittock SJ, Kelly CR, Mckeon A, Lopez-Chiriboga AS, Lennon VA, et al. Autoimmune encephalitis epidemiology and a comparison to infectious encephalitis. *Ann Neurol* (2018) 83:166–77. doi: 10.1002/ana.25131

2. Binks SNM, Klein CJ, Waters P, Pittock SJ, Irani SR. LGI1, CASPR2 and related antibodies: a molecular evolution of the phenotypes. *J Neurol Neurosurg Psychiatry* (2018) 89:526–34. doi: 10.1136/jnnp-2017-315720

3. Naasan G, Irani SR, Bettcher BM, Geschwind MD, Gelfand JM. Episodic bradycardia as neurocardiac prodrome to voltage-gated potassium channel complex/leucine-rich, glioma inactivated 1 antibody encephalitis. *JAMA Neurol* (2014) 71:1300–4. doi: 10.1001/jamaneurol.2014.1234

4. Nilsson AC, Blaabjerg M. More evidence of a neurocardiac prodrome in anti-LGI1 encephalitis. *J Neurol Sci* (2015) 357:310–1. doi: 10.1016/j.jns.2015.07.015

5. Klein CJ, Lennon VA, Aston PA, Mckeon A, O'toole O, Quek A, et al. Insights from LGI1 and CASPR2 potassium channel complex autoantibody subtyping. *JAMA Neurol* (2013) 70:229–34. doi: 10.1001/jamaneurol.2013.592

6. Dubey D, Britton J, Mckeon A, Gadoth A, Zekeridou A, Lopez Chiriboga SA, et al. Randomized placebo-controlled trial of intravenous immunoglobulin in autoimmune LGI1/CASPR2 epilepsy. *Ann Neurol* (2020) 87:313–23. doi: 10.1002/ana.25655

7. Tsao CW, Aday AW, Almarzooq ZI, Alonso A, Beaton AZ, Bittencourt MS, et al. Heart disease and stroke statistics-2022 update: A report from the American heart association. *Circulation* (2022) 145:e153–639. doi: 10.1161/CIR.0000000000001052

8. Jensen PN, Gronroos NN, Chen LY, Folsom AR, Defilippi C, heckbert SR, et al. Incidence of and risk factors for sick sinus syndrome in the general population. *J Am Coll Cardiol* (2014) 64:531–8. doi: 10.1016/j.jacc.2014.03.056

9. Britton JW, Ghearing GR, Benarroch EE, Cascino GD. The ictal bradycardia syndrome: localization and lateralization. *Epilepsia* (2006) 47:737–44. doi: 10.1111/j.1528-1167.2006.00509.x

10. Oppenheimer SM, Gelb A, Girvin JP, Hachinski VC. Cardiovascular effects of human insular cortex stimulation. *Neurology* (1992) 42:1727–32. doi: 10.1212/WNL.42.9.1727

11. van Sonderen A, Petit-Pedrol M, Dalmau J, Titulaer MJ. The value of LGI1, Caspr2 and voltage-gated potassium channel antibodies in encephalitis. *Nat Rev Neurol* (2017) 13:290–301. doi: 10.1038/nrneurol.2017.43

12. Schulte U, Thumfart JO, Klöcker N, Sailer CA, Bildl W, Biniossek M, et al. The epilepsy-linked Lgi1 protein assembles into presynaptic Kv1 channels and inhibits inactivation by Kvbeta1. *Neuron* (2006) 49:697–706. doi: 10.1016/j.neuron.2006.01.033

13. Grandi E, Sanguinetti MC, Bartos DC, Bers DM, Chen-Izu Y, Chiamvimonvat N, et al. Potassium channels in the heart: structure, function and regulation. *J Physiol* (2017) 595:2209–28. doi: 10.1113/JP272864

14. Dharod A, Soliman EZ, Dawood F, Chen H, Shea S, Nazarian S, et al. Association of asymptomatic bradycardia with incident cardiovascular disease and mortality: The multi-ethnic study of atherosclerosis (MESA). *JAMA Intern Med* (2016) 176:219–27. doi: 10.1001/jamainternmed.2015.7655

15. Rizzi R, Fisicaro F, Zangrandi A, Ghidoni E, Baiardi S, Ragazzi M, et al. Sudden cardiac death in a patient with LGI1 antibody-associated encephalitis. *Seizure* (2019) 65:148–50. doi: 10.1016/j.seizure.2019.01.013

16. Sivathamboo S, Friedman D, Laze J, Nightscales R, Chen Z, Kuhlmann L, et al. Association of short-term heart rate variability and sudden unexpected death in epilepsy. *Neurology* (2021) 97:e2357–67. doi: 10.1212/WNL.0000000000012946

17. Feyissa AM, López-Chiriboga AS, Britton J. W. Antiepileptic drug therapy in patients with autoimmune epilepsy. *Neurol Neuroimmunol Neuroinflamm* (2017) 4:e353. doi: 10.1212/NXI.0000000000000353

18. Nizam A, Mylavarapu K, Thomas D, Briskin K, Wu B, Saluja D, et al. Lacosamide-induced second-degree atrioventricular block in a patient with partial epilepsy. *Epilepsia* (2011) 52:e153–5. doi: 10.1111/j.1528-1167.2011.03212.x

19. Yang C, Peng Y, Zhang L, Zhao L. Safety and tolerability of lacosamide in patients with epilepsy: A systematic review and meta-analysis. *Front Pharmacol* (2021) 12:694381. doi: 10.3389/fphar.2021.694381

20. Roden DM. Pharmacology and toxicology of Nav1.5-class 1 anti-arrhythmic drugs. *Card Electrophysiol Clin* (2014) 6:695–704. doi: 10.1016/j.ccep.2014.07.003

21. Khurshid S, Choi SH, Weng L-C, Wang EY, Trinquart L, Benjamin EJ, et al. Frequency of cardiac rhythm abnormalities in a half million adults. *Circulation: Arrhythmia Electrophysiology* (2018) 11:e006273. doi: 10.1161/CIRCEP.118.006273

frontiers | Frontiers in Immunology

TYPE Original Research
PUBLISHED 17 October 2022
DOI 10.3389/fimmu.2022.1025908



OPEN ACCESS

EDITED BY
Honghao Wang,
Guangzhou First People's Hospital, China

REVIEWED BY
Jinzhou Feng,
First Affiliated Hospital of Chongqing Medical University, China
Yaqing Shu,
Third Affiliated Hospital of Sun Yat-sen University, China

*CORRESPONDENCE
Sheng Chen
mztcs@163.com
Min Zhang
zm11518@rjh.com.cn

†These authors have contributed equally to this work and share first authorship

SPECIALTY SECTION
This article was submitted to Multiple Sclerosis and Neuroimmunology, a section of the journal Frontiers in Immunology

RECEIVED 23 August 2022
ACCEPTED 22 September 2022
PUBLISHED 17 October 2022

CITATION
Zhou Q, Zhang T, Meng H, Shen D, Li Y, He L, Gao Y, Zhang Y, Huang X, Meng H, Li B, Zhang M and Chen S (2022) Characteristics of cerebral blood flow in an Eastern sample of multiple sclerosis patients: A potential quantitative imaging marker associated with disease severity.
*Front. Immunol.* 13:1025908.
doi: 10.3389/fimmu.2022.1025908



# Characteristics of cerebral blood flow in an Eastern sample of multiple sclerosis patients: A potential quantitative imaging marker associated with disease severity

Qinming Zhou[1†], Tianxiao Zhang[2†], Huanyu Meng[1†], Dingding Shen[1†], Yao Li[2], Lu He[1], Yining Gao[1], Yizongheng Zhang[1], Xinyun Huang[3], Hongping Meng[3], Biao Li[3], Min Zhang[3*] and Sheng Chen[1,4,5*]

[1]Department of Neurology and Institute of Neurology, Ruijin Hospital, Shanghai Jiao Tong University School of Medicine, Shanghai, China, [2]School of Biomedical Engineering, Shanghai Jiao Tong University, Shanghai, China, [3]Department of Nuclear Medicine, Ruijin Hospital, Shanghai Jiao Tong University School of Medicine, Shanghai, China, [4]Co-innovation Center of Neuroregeneration, Nantong University, Nantong, China, [5]Department of Neurology, Xinrui Hospital, Wuxi, China

Multiple sclerosis (MS) is a chronic inflammatory disease of the central nervous system that is rare in China. At present, there are no widespread quantitative imaging markers associated with disease severity in MS. Despite several previous studies reporting cerebral blood flow (CBF) changes in MS, no consensus has been reached. In this study, we enrolled 30 Eastern MS patients to investigate CBF changes in different brain regions using the arterial spin labeling technique and their relationship with disease severity. The average CBF in MS patients were higher than those in health controls in various brain regions except cerebellum. The results indicated that MS patients with strongly increased CBF showed worse disease severity, including higher Expanded Disability Status Scale (EDSS) scores and serum neurofilament light chain (sNfL) values than those with mildly increased CBF in the parietal lobes, temporal lobes, basal ganglia, and damaged white matter (DWM). From another perspective, MS patients with worse disease severity (higher EDSS score and sNfL values, longer disease duration) showed increased CBF in parietal lobes, temporal lobes, basal ganglia, normal-appearing white matter (NAWM), and DWM. Correlation analysis showed that there was a strong association among CBF, EDSS score and sNfL. MS patients with strongly increased CBF in various brain regions had more ratio in relapsing phase than patients with mildly increased CBF. And relapsing patients showed significantly higher CBF in some regions (temporal lobes, left basal ganglia, right NAWM) compared to remitting patients. In addition, MS patients with cognitive impairment had higher CBF than those without cognitive impairment in the right parietal lobe

and NAWM. However, there were no significant differences in CBF between MS patients with and without other neurologic dysfunctions (e.g., motor impairment, visual disturbance, sensory dysfunction). These findings expand our understanding of CBF in MS and imply that CBF could be a potential quantitative imaging marker associated with disease severity.

KEYWORDS

cerebral blood flow, multiple sclerosis, quantitative imaging marker, disease severity, EDSS, eastern population, neuroimaging

## Introduction

Multiples sclerosis (MS) is a chronic inflammatory disease of the central nervous system characterized by progressive neurologic degeneration, eventually leading to irreversible disability and impaired cognition in around 60% of patients (1). It is known that MS occurs mostly in high latitude regions, such as northern Europe. However, MS is still a rare disease in the Chinese population. The reported age- and sex-adjusted incidence of MS from population surveys in China is 0.235 per 100,000 person-years (2). The mean age at onset in Chinese MS patients is around 30 years, with few cases younger than 20 years (1, 2). Because of the young age of onset and inability to work, the disease burden caused by MS is considered heavy.

Although studies have proposed various imaging measures and laboratory markers as biomarkers for diagnosis and clinical assessment of MS, these biomarkers are not available for widespread clinical use due to their poor correlation with clinical disability (3). Useful biomarkers will likely emerge that will enable us to assess clinical severity and predict and monitor disease progression. At present, magnetic resonance imaging (MRI) is the most important tool for diagnosis and prognosis evaluation of MS. White matter (WM) lesions in MS patients can be visualized by T2W MRI, and acute inflammation can be detected by gadolinium contrast enhancement due to the breach of the blood-brain barrier. Besides damaged white matter (DWM), the widespread and subtle changes occur in normal-appearing white matter (NAWM) and grey matter (GM), which may be accompanied by alterations in vascular function (4). Although growing evidence suggests that vascular aspects play an important role in the disease, brain perfusion changes in MS patients have received little attention (5). Brain perfusion is primarily observed by the measurement of cerebral blood flow (CBF). With the development of imaging technology, researchers can use non-invasive methods to safely and accurately assess intracranial blood flow difference in MS patients. Dynamic susceptibility contrast-enhanced MRI, arterial spin labeling (ASL) technique, computed tomography, and radionuclide imaging can be used to provide cerebral perfusion parameters (6). Despite several studies about brain perfusion changes in MS patients, no consensus has been reached. Some studies reported hypoperfusion in DWM, NAWM, and GM in MS patients (7, 8), while others reported increased CBF in multiple brain regions (9, 10).

Although there is agreement that perfusion changes represent an important component of MS process, the relationship between CBF changes and clinical parameters in MS, such as Expanded Disability Status Scale (EDSS), annualized relapse rate (ARR), motor impairment, and cognitive impairment, is still not clear. Moreover, the CBF distribution in different brain regions in MS patients is varied. It remains unclear if CBF in different brain regions changes with clinical parameters. Thus, correlation analysis between CBF in different brain regions and clinical parameters can provide clues for the evaluation of clinical severity and therapeutic effects. In addition, research on Eastern populations is limited (11). Zhang et al. found that MS patients had reduced CBF in the occipital cortex and increased CBF in the right putamen (11). The potential value of CBF changes in MS remains controversial and poorly understood.

To shed light on these questions, this study evaluated CBF characteristics in a sample of Eastern patients with MS to comprehensively study its association with disease severity and multiple clinical parameters for the first time.

**Abbreviations:** ARR, annualized relapse rate; ASL, arterial spin labeling; Basal_L, left basal ganglia; Basal_R, right basal ganglia; CBF, cerebral blood flow; Cereb_L, left cerebellum; Cereb_R, right cerebellum; DWM, damaged white matter; EDSS, Expanded Disability Status Scale; FA, flip angle; Fron_L, left frontal lobe; Fron_R, right frontal lobe; GM, grey matter; HC, healthy control; MRI, magnetic resonance imaging; MS, multiple sclerosis; NAWM, normal-appearing white matter; NAWM_L, left normal-appearing white matter; NAWM_R, right normal-appearing white matter; Occi_L, left occipital lobe; Occi_R, right occipital lobe; Pari_L, left parietal lobe; Pari_R, right parietal lobe; pASL, pulsed arterial spin labeling; sNfL, serum neurofilament light chain; TE, echo time; Temp_L, left temporal lobe; Temp_R, right temporal lobe; TI, inverse time; TR, repetition time; WM, white matter.

# Methods

## Patients

A total of 30 Eastern MS patients and eight healthy controls (HCs) participated in this study. The inclusion criteria were as follows: 1) being a healthy individual or having a MS diagnosis according to the revised 2017 McDonald criteria and a relapsing-remitting course; 2) between 18–60 years old. The exclusion criteria were: 1) cardiovascular and/or metabolic diseases; 2) psychiatric disorders and/or neurologic disease other than MS; 3) body mass index (weight/height$^2$) higher than 30; or 4) pregnancy. Disability in MS patients was quantified with EDSS administered by an experienced neurologist within two weeks of MRI scan. Cognitive status was assessed using Montreal Cognitive Assessment (MoCA) test and Mini-Mental State Examination (MMSE). Cognitive impairment was defined as both MoCA score < 26 and MMSE score < 25. Motor function was assessed with muscle strength testing based on Medical Research Council (MRC) grades. Patients were classified as motor impaired if they had muscle strength weakness. Follow-up was conducted 18 months after imaging examinations to observe relapse. The study was approved by the Ethics Committee of Ruijin Hospital, and it was performed in accordance with the principles of the Helsinki Declaration. Written informed consent was obtained from all participants.

## MRI protocol and data processing

MRI acquisition was performed using a Biograph mMR system (Siemens, Erlangen, Germany). Single inverse time 2D pulsed arterial spin labeling (pASL) data were acquired with the following parameters: bolus duration = 1675 ms, inverse time (TI) = 1800 ms, repetition time (TR) = 2500 ms, echo time (TE) = 11 ms, flip angle (FA) = 90°, field of view = 192 × 192 mm$^2$, voxel size = 3 × 3 × 5 mm$^3$, slices = 16, measurements = 150, and acquisition time = 6:27 min.

ASL data preprocessing was performed to eliminate systematic and subject-related bias before CBF quantification. First, motion correction was applied on labeled and control images using MCFLIRT tool found in the FMRIB's Software Library (FSL) (12). To reduce intensity inhomogeneity in the coil sensitivity, we implemented the field correction algorithm termed N4ITK in Advanced Normalization Tools (13).

DWM tissue was segmented on MNI space T2-weighted image using a lesion prediction algorithm in the Lesion Segmentation Tool (LST) toolbox (14). For NAWM tissue segmentation, we first performed bias correction algorithm on MNI space T1 images using N4ITK before the WM tissue segmentation (13). A unified segmentation model in Statistical Parametric Mapping (SPM12) software was performed on unbiased 3D T1 images for tissue segmentation (15). WM tissue probabilistic maps could be obtained. Regions where the probabilistic map is greater than 0.95 and is not DWM are defined as NAWM. We checked each segmentation results after the segmentation process.

CBF quantification included the following steps: 1) To eliminated static tissue signal, seventy-five difference images were obtained by subtracting the labeled images from the control image. 2) Perfusion-weighted images were generated by averaging the difference images. 3) Relative CBF images were calculated by general kinetic modelling using the BASIL FSL toolbox (16). 4) Absolute CBF was calibrated by surrogate $M_0$ images calculated from the averaged control images (17).

Quantitative CBF images were registered to MNI space using FMRIB's Linear Image Registration Tool and FMRIB's Nonlinear Image Registration Tool for statistical analysis (18). Firstly, ASL space T1 image was obtained by linear registration of 3D-T1 image into surrogate M0 images calculated from the averaged control ASL images to compensate deviation due to head motion. Secondly, ASL space T1 image was used to generate the deformation field from ASL space to MNI space. Finally, we applied the derived deformation field to ASL space quantitative CBF images, thus obtaining MNI space quantitative CBF images. We double checked the registration results of each step using ITK-SNAP (19). All the MNI space quantitative CBF image were well aligned with MNI template.

## Statistical analysis

Statistical analysis was performed using SPSS 19.0 (IBM, New York, USA). A $p$-value of < 0.05 was considered statically significant. Categorical data were compared using the $\chi^2$ test. Group comparisons were conducted *via* the paired t test or analysis of variance (ANOVA). In cases where the variance between groups was equal ($p > 0.05$) or unequal, the LSD test or Dunnett's $t$-test was performed, respectively. Correlations were assessed using Spearman correlation. The data were presented as the mean ± standard deviation (SD).

# Results

## Demographic and diseases characteristics

A total of 30 MS patients and 8 HCs were enrolled in the study. There were no significant differences in sex or age between MS patients and HCs. The average age was 40.07 ± 11.20 years in MS patients and 34.00 ± 6.55 years in HCs. The MS patients group included 16 males and 14 females, while the HC group included 4 males and 4 females. The longest disease duration was 396 months and the shortest was 23 months. The EDSS score

10.3389/fimmu.2022.1025908

ranged from 1 to 7. The clinical data for MS patients and HCs are shown in Table 1.

## Regional distribution of CBF in MS patients

The lowest CBF in the whole brain was observed in DWM (0.0018 ± 0.0012). CBF in NAWM was significantly higher than that in DWM ($p$ = 0.0024). Among different regions of GM, the highest CBF was in the right temporal lobe (0.0073 ± 0.0039), and the lowest CBF was in the right basal ganglia (0.0036 ± 0.0014) (Figures 1A, B).

Correlation analysis indicated that CBF values in DWM, NAWM, and GM were positively correlated with each other (Figure 1C). In addition, CBF in some GM regions (e.g., bilateral parietal lobes, temporal lobes, and basal ganglia) and NAWM showed a significantly positive correlation with CBF in DWM (Figure 1D). These findings indicate that NAWM and GM in MS patients show insidious changes.

## The comprehensive investigation of CBF changes in MS patients

The patients were divided into different groups respectively (high vs. low EDSS; high vs. low serum neurofilament light chain (sNfL); long vs. short disease duration; high ARR vs. low ARR) based on the median value. We compared CBF among patients with different clinical parameters (high vs. low EDSS; high vs. low sNfL; long vs. short disease duration; in relapsing vs. remitting phase; high ARR vs. low ARR; with vs. without cognitive impairment, motor impairment, visual disturbance, or sensory dysfunction).

TABLE 1 Summary of MS patients and HCs.

| | MS patients | HC |
|---|---|---|
| Number | 30 | 8 |
| Age, year | 40.07 ± 11.20 | 34.00 ± 6.55 |
| Gender (male/female) | 16/14 | 4/4 |
| EDSS | 2.97 ± 1.80 | / |
| EDSS ≤ 3 (n) | 19 | / |
| EDSS > 3 (n) | 11 | / |
| Disease duration (month) | 85.30 ± 90.29 | / |
| Duration ≤ 36 (n) | 14 | / |
| Duration > 36 (n) | 16 | / |
| sNfL (pg/ml) | 20.25 ± 7.10 | / |
| Relapsing phase (n) | 12 | / |
| With new relapsing occurrences | 9 | |
| ARR | 0.54 ± 0.27 | / |
| Cognitive impairment (n) | 8 | / |
| Motor impairment (n) | 11 | / |
| Sensory disturbance (n) | 7 | / |
| Visual impairment (n) | 6 | / |

CBF was higher in the DWM, NAWM, basal ganglia, parietal lobes, and frontal lobes of patients with high EDSS scores (≥ 3, n = 14) compared to those with low EDSS scores (< 3, n = 16) and HCs (Figures 2A, D). However, there were no significant differences in CBF between patients with low EDSS scores and HCs. And MS patients with high sNfL had increased CBF in DWM, bilateral NAWM, GM, bilateral basal ganglia, bilateral temporal lobes, bilateral parietal lobes, and right frontal lobe compared to those with low sNfL (Figures 2B, E).

MS patients with a long disease duration (> 36 months, n = 15) had higher CBF in bilateral parietal lobes (left: $p$ = 0.19, right: $p$ = 0.009), right basal ganglia ($p$ = 0.035), and right frontal lobes ($p$ = 0.020) than those with a short disease duration (≤ 36 months, n = 15) and HCs (Figures 2C, F). However, MS patients with a short disease duration did not show obvious CBF changes compared with HCs.

Except for DWM, CBF values were affected in patients in the relapsing phase. Specifically, the bilateral temporal lobes (left: $p$ = 0.033, right: $p$ = 0011), right NAWM ($p$ = 0.029), and left basal ganglia ($p$ = 0.018) CBF values were significantly increased in relapsing patients compared to remitting patients (Figures 3A–C).

We then tested whether MS patients with different neurologic dysfunctions showed abnormal CBF in multiple brain regions. Relative to MS patients without cognitive disorder (n = 22), MS patients with cognitive disorder (n = 8) had increased CBF in right parietal lobes ($p$ = 0.016) and right NAWM ($p$ = 0.029) (Figure 3D). We compared CBF in MS patients with/without some other neurologic dysfunctions (motor impairment, visual disturbance, sensory dysfunction). However, no significant differences were found in these comparisons. We equally divided MS patients into two groups (high ARR group and low ARR group) according to ARR values. There were no significant differences between two groups in various brain regions.

## Association of CBF data with MS clinical severity

Comparing with HCs, MS patients had significantly increased CBF in right frontal lobe (p = 0.039). Although there were no significant differences, MS patients had slightly higher CBF than HCs in the other brain regions except cerebellum. The 30 MS patients were equally divided into strongly increased CBF (CBF > median, n = 15) and mildly increased CBF (CBF < median, n = 15) groups based on the median CBF in different regions. EDSS scores in MS patients with strongly increased CBF were significantly higher than those in patients with mildly increased CBF in some regions (e.g., bilateral parietal lobes, bilateral temporal lobes, left

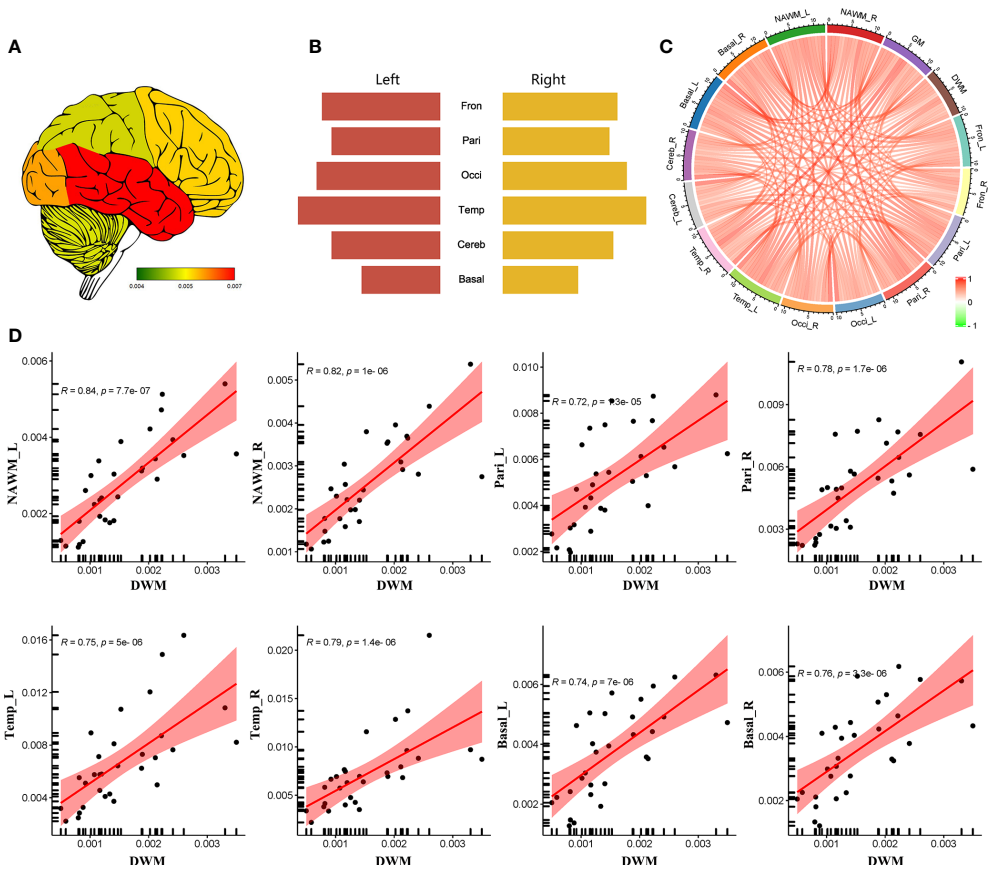


FIGURE 1
The regional distribution of CBF in MS patients. **(A)** CSF heatmap of different brain regions. **(B)** Comparison of CBF in different brain regions. **(C)** Correlation analysis among different regions. **(D)** Significantly positive correlation of CBF between DWM and some brain region (NAWM, parietal lobes, temporal lobes and basal ganglia). (Fron_L, left frontal lobe; Fron_R, right frontal lobe; Pari_L, left parietal lobe; Pari_R, right parietal lobe; Occi_L, left occipital lobe; Occi_R, right occipital lobe; Temp_L, left temporal lobe; Temp_R, right temporal lobe; Cereb_L, left cerebellum; Cereb_R, right cerebellum; Basal_L, left basal ganglia; Basal_R, right basal ganglia; NAWM_L, left normal-appearing white matter; NAWM_R, right normal-appearing white matter; DWM, damaged white matter).

basal ganglia, and DWM) (Figures 4A, 5). In MS patients, elevation in sNfL is linked to worse neurologic function, greater clinical disability, and lower brain volumes (20, 21). Our results showed that MS patients with strongly increased CBF had significantly higher sNfL than patients with mildly increased CBF in some regions, namely the bilateral parietal lobes, bilateral temporal lobes, left basal ganglia, DWM, NAWM, and global GM (Figures 4B, 5).

Next, we used the $\chi^2$ test to compare the ratio of MS patients in the relapsing phase, with cognitive impairment, motor impairment, visual disorder, sensory disturbance, and with new relapsing occurrences in 18-month follow-up between the strongly and mildly increased CBF groups for global GM, DWM, and NAWM. Of 30 MS patients, 12 were in the relapsing phase when they underwent the neuroimaging examination and 18 were in the remitting phase. The strongly increased CBF group had a significantly higher ratio of relapsing MS patients than the mildly increased CBF group in global GM, DWM, and NAWM (Figure 6). At 18-months follow-up after the neuroimaging examination, nine MS patients suffered from relapse. The low GM CBF group had more patients experiencing relapse than the high GM CBF group (Figure 6D). However, there were no significant differences in cognitive impairment, motor impairment, visual disorder, or sensory disturbance (Figure 6). Furthermore, the strongly and mildly increased CBF groups showed no significant differences in ARR for the brain regions.

Correlation analysis revealed that CBF in GM ($R = 0.48$, $p = 0.0074$), bilateral parietal lobes (left: $R = 0.52$, $p = 0.003$, right: $R = 0.57$, $p = 0.0011$), bilateral temporal lobes (left: $R = 0.56$, $p = 0.0013$, right: $R = 0.60$, $p = 0.00052$), bilateral basal ganglia (left: $R = 0.55$, $p = 0.0018$, right: $R = 0.53$, $p = 0.0025$), DWM ($R = 0.55$,

10.3389/fimmu.2022.1025908

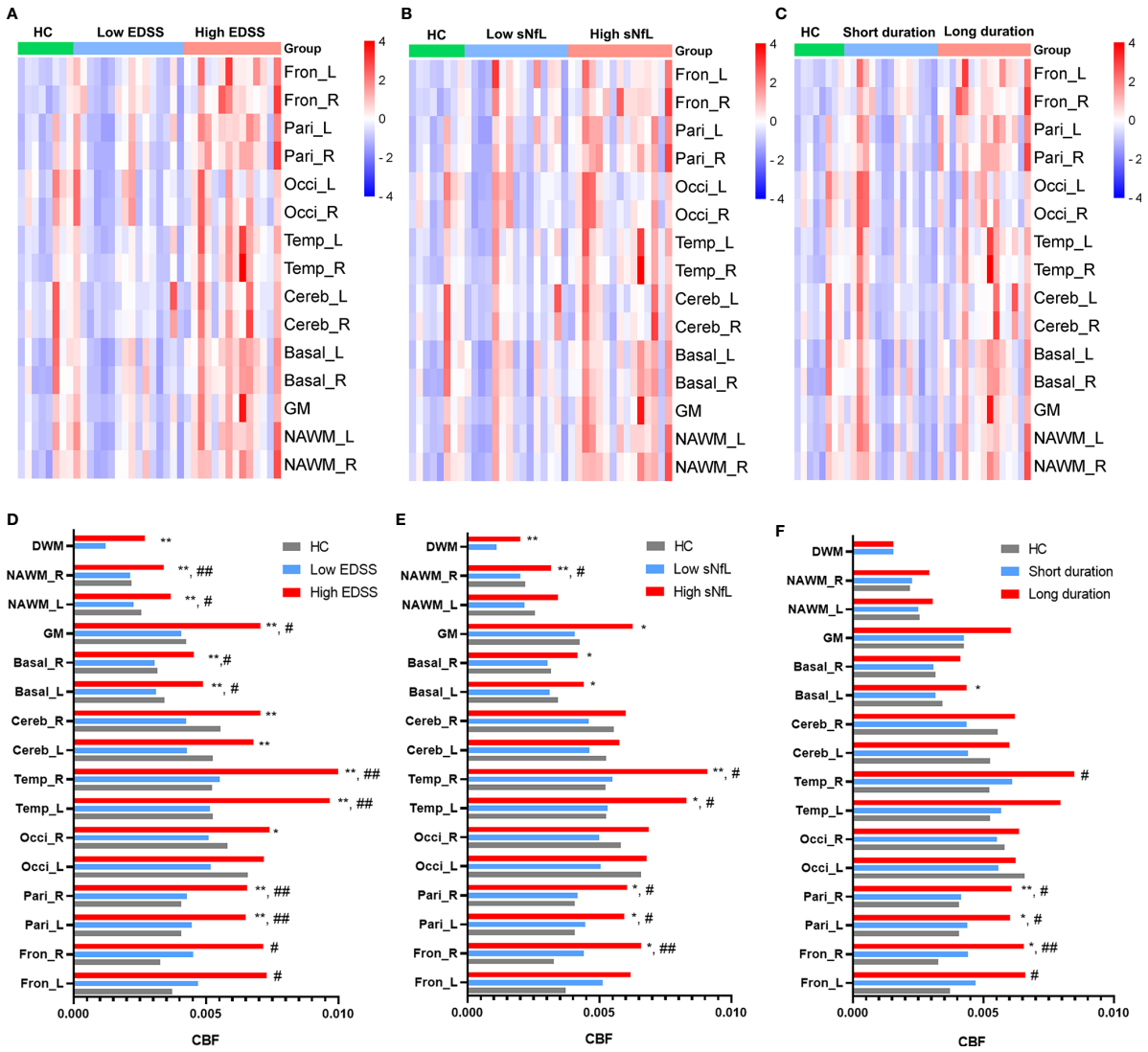


FIGURE 2
Relationship between CBF and clinical parameters. Comparisons of CBF differences in different regions among: **(A)** HCs, MS patients with low EDSS scores, and MS patients with high EDSS scores; **(B)** HCs, MS patients with low sNfL, and MS patients with high sNfL; and **(C)** HCs, MS patients with short disease duration, and MS patients with long disease duration. **(D–F)** Comparison of CBF of different regions according to clinical parameters (EDSS, sNfL, and disease duration). *$p < 0.05$ and **$p < 0.01$ vs. low EDSS group/short duration group/low sNfL group; #$p < 0.05$ and ##$p < 0.01$ vs. HCs.

$p = 0.0018$), and NAWM (left: $R = 0.53$, $p = 0.0023$, right: $R = 0.58$, $p = 0.0007$) were positively correlated with EDSS score (Figure 7), while CBF in GM ($R = 0.52$, $p = 0.003$), bilateral parietal lobes (left: $R = 0.54$, $p = 0.0019$, right: $R = 0.57$, $p = 0.0009$), bilateral temporal lobes (left: $R = 0.58$, $p = 0.00081$, right: $R = 0.63$, $p = 0.00021$), bilateral basal ganglia (left: $R = 0.54$, $p = 0.0023$, right: $R = 0.54$, $p = 0.0021$), bilateral NAWM (left: $R = 0.62$, $p = 0.00025$, right: $R = 0.65$, $p = 0.00011$) and DWM ($R = 0.64$, $p = 0.00013$) were positively correlated with sNfL (Figure 8).

# Discussion

## Limitations of conventional MRI in MS

MS is a chronic disabling disease of the central nervous system characterized by the presence of focal white matter lesions, inflammation, demyelination, and axon loss. The most important method for MS diagnosis is MRI, which can interrogate the entire central nervous system. Conventional MRI (T1WI and T2WI) can help assess lesion load and identify acute

10.3389/fimmu.2022.1025908

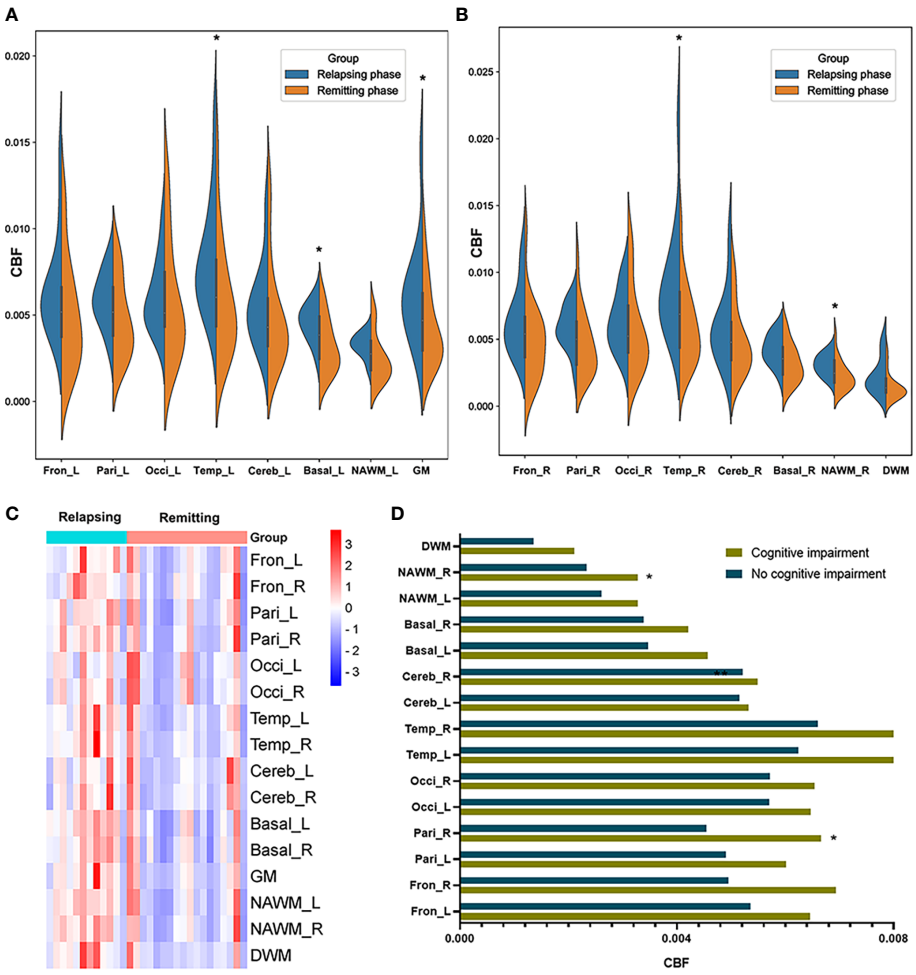


FIGURE 3
CBF differences between MS patients in the relapsing phase and remitting phase, and between MS patients with and without cognitive impairment. **(A, B)** Comparison of CBF between MS patients in the relapsing phase and remitting phase; **(C)** CBF cluster heatmap of different regions in different phases; and **(D)** MS patients with cognitive impairment showed increased CBF in the right parietal lobe and right NAWM compared to those without. *$p < 0.05$ vs. patients in remitting phase/without cognitive impairment.

lesions, thus providing valuable information for diagnosis, assessment of disease severity, and treatment effect. However, it cannot provide quantitative analysis of brain function in MS patients and does not correlate strongly with clinical status (22, 23). Except the pathologic changes in DWM, growing evidence suggests a more widespread and subtle form of disease activity also occurs in NAWM and GM (24, 25), which may have an association with clinical manifestation. Conventional MRI is not sensitive to the pathology affecting CNS tissue outside DWM (i.e., in NAWM and GM).

## Progress in quantitative imaging for MS

Due to the limitations of conventional MRI, some quantitative imaging techniques have been developed, such as positron emission tomography (PET), diffusion tensor imaging (DTI), perfusion MRI, relaxometry, myelin imaging, and magnetization transfer, that could provide better quantification of the extent, type, spatial distribution, and evolution of CNS tissue damage in MS. These methods could contribute to better assessment of disease severity, therapy response, and stratification of disease burden. Furthermore, some quantitative imaging techniques are more sensitive to subtle alterations within or outside lesions compared with conventional MRI. Our previous study demonstrated that dynamic $^{18}$F-florberapir PET is a promising tool for quantitatively monitoring myelin loss and recovery and correlates closely with changes in EDSS (14, 26). DTI can be used to assess CNS tissue integrity and provide information on microstructure changes of DWM and NAWM in MS patients (14). Previous studies have shown that brain perfusion changes

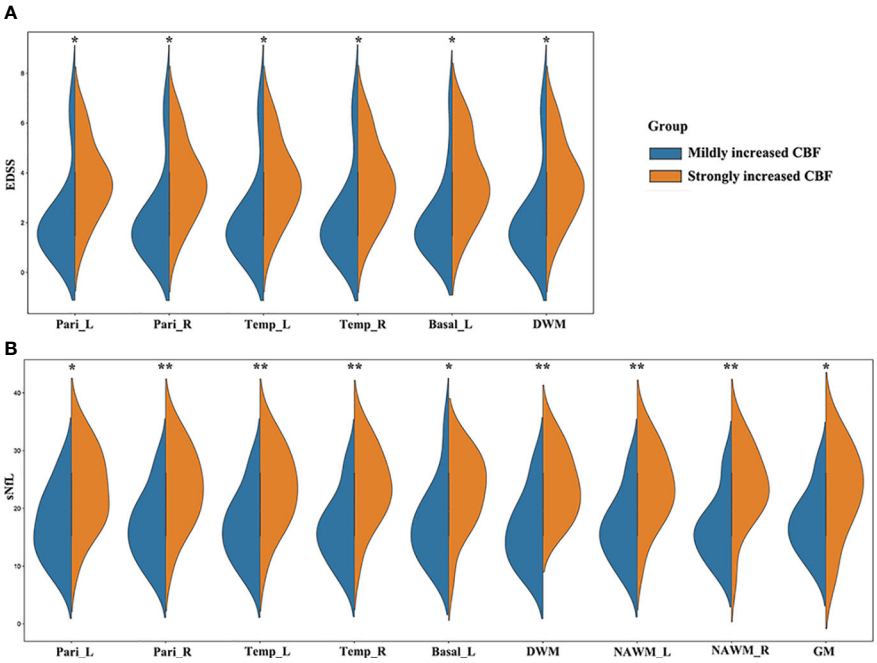


FIGURE 4
MS patients with different CBF values showed different clinical severity. **(A)** EDSS scores in MS patients with strongly increased CBF were significantly higher than those in patients with mildly increased CBF in the bilateral parietal lobes, bilateral temporal lobes, left basal ganglia, and DWM; **(B)** MS patients with strongly increased CBF had significantly higher sNfL than patients with mildly increased CBF in the bilateral parietal lobes, bilateral temporal lobes, left basal ganglia, DWM, bilateral NAWM, and global GM. *$p < 0.05$ and **$p < 0.01$ vs. mildly increased CBF group.

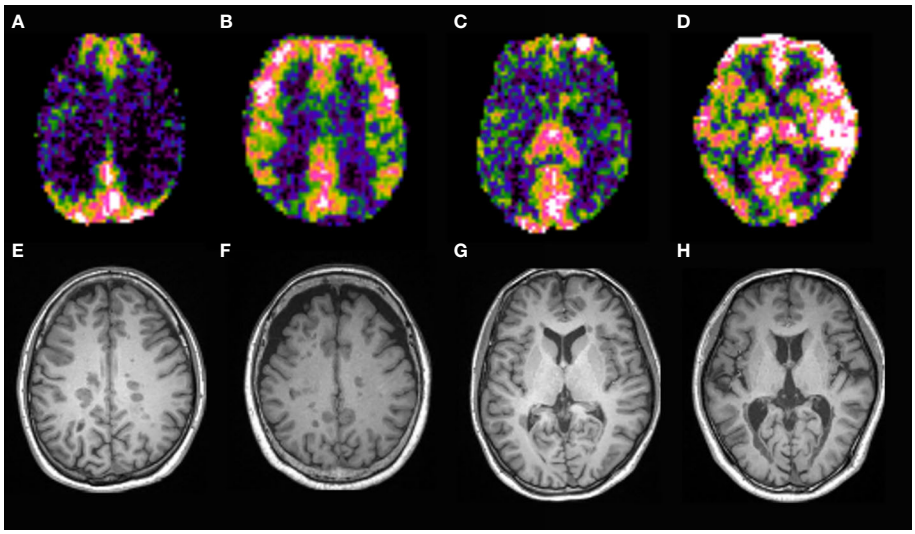


FIGURE 5
CBF map of MS patients. Patients with strongly increased CBF in the parietal lobes **(B, F)** had higher EDSS and sNfL than those with mildly increased CBF **(A, E)**. Patients with strongly increased CBF in the temporal lobes and basal ganglia **(D, H)** had higher EDSS and sNfL than those with mildly increased CBF **(C, G)**.

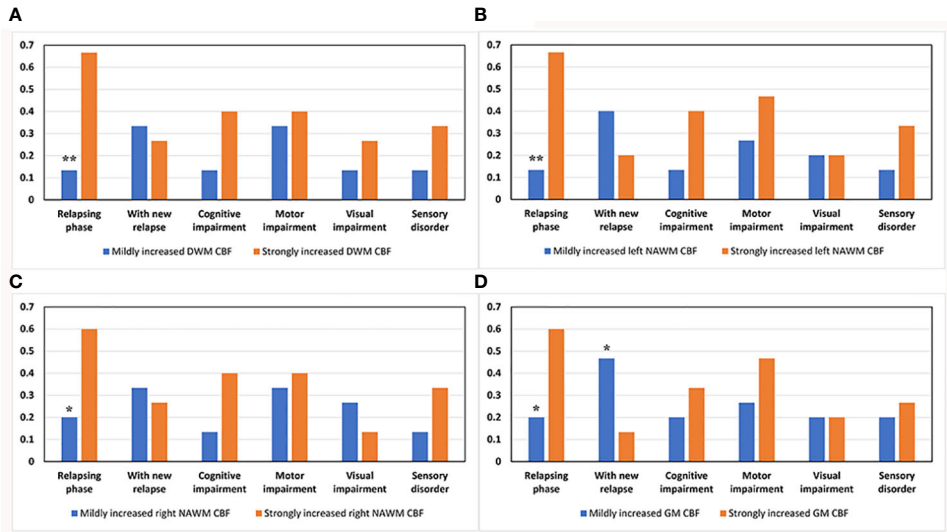


FIGURE 6
Comparison of various clinical parameters between the mildly and strongly increased CBF groups in DWM, NAWM, and GM. The strongly increased CBF group had a higher ratio of patients in the relapsing phase than the mildly increased CBF group in **(A)** DWM ($p$ = 0.003), **(B)** left NAWM ($p$ = 0.003), **(C)** right NAWM ($p$ = 0.025), and **(D)** global GM ($p$ = 0.025). **(D)** The low GM CBF group had a higher ratio of patients experiencing relapse after the neuroimaging examination than the high GM CBF group ($p$ = 0.046). *$p$ < 0.05 and **$p$ < 0.01 vs. strongly increased group.

play an important role in MS pathophysiology and precede the initial blood-brain barrier breakdown and T2-weighted lesion appearance (23, 27). Theoretically, brain perfusion MRI has the ability to quantitatively assess disease status in MS. However, the relationship between brain perfusion and clinical parameters is still controversial (7, 8, 10, 28, 29). As these quantitative imaging techniques have not reached clinical maturity, they are not widely used in clinical practice.

## Characteristics of CBF in an Eastern sample of MS patients and their relationship with clinical parameters

In this study, we first comprehensively investigated CBF changes in Eastern MS patients using the ASL technique. We observed CBF changes in different brain regions, including DWM, NAWM, frontal lobes, parietal lobes, temporal lobes,

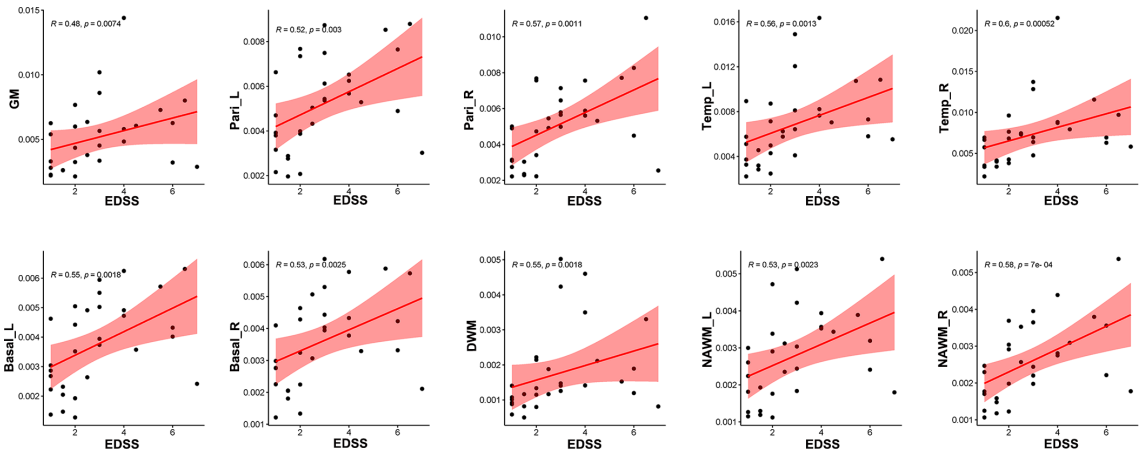


FIGURE 7
Correlation between EDSS scores and CBF in different regions. CBF in global GM, bilateral parietal lobes, bilateral temporal lobes, bilateral basal ganglia, DWM and NAWM were positively related with EDSS sores.

10.3389/fimmu.2022.1025908

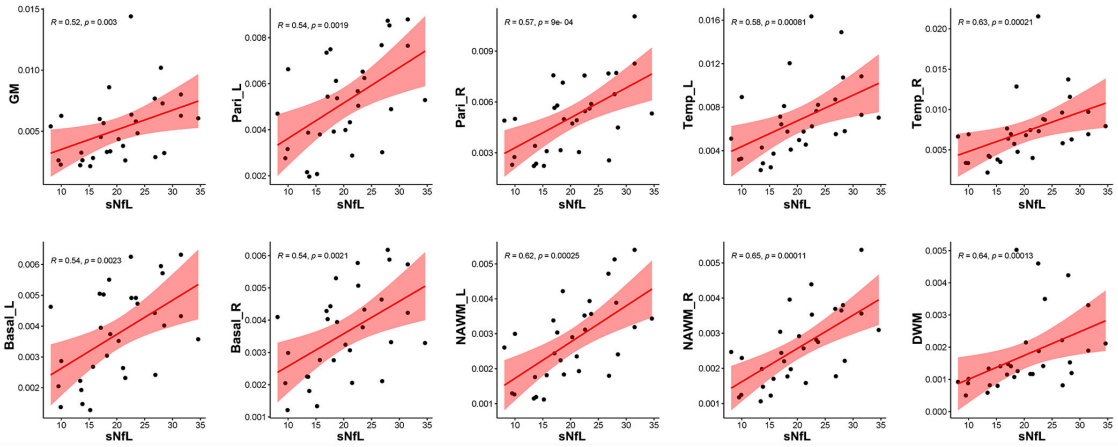


FIGURE 8
Correlation between sNfL and CBF in different regions. CBF values in global GM ($R$ = 0.52, $p$ = 0.0030), bilateral parietal lobes (left: $R$ = 0.54, $p$ = 0.0019, right: $R$ = 0.57, $p$ = 0.0009), bilateral temporal lobes (left: $R$ = 0.58, $p$ = 0.00081, right: $R$ = 0.63, $p$ = 0.00021), bilateral basal ganglia (left: $R$ = 0.54, $p$ = 0.0023, right: $R$ = 0.54, $p$ = 0.0021), NAWM (left: $R$ = 0.62, $p$ = 0.00025, right: $R$ = 0.65, $p$ = 0.00011), and DWM ($R$ = 0.64, $p$ = 0.00013) were positively related to sNfL.

occipital lobes, basal ganglia, and cerebellum. The relationship between CBF changes in various brain regions and multiple clinical parameters (EDSS, sNfL, relapsing/remitting phase, duration, cognitive disorder, ARR, motor impairment, sensory disorder, visual disturbance) was then explored. MS patients with strongly increased CBF in parietal lobes, temporal lobes, and basal ganglia had worse clinical disability (higher EDSS scores and higher sNfL) than those with mildly increased CBF. Increased CBF could represent a physiologic response to an increased demand that was secondary to increased inflammatory, and glial cell activity (6, 30). In an inflammatory environment, the inducible form of NOS (iNOS) is upregulated, producing more nitric oxide (NO) and nitrogen reactive species. NO has the effect of vasodilation and can alter BBB (31).

In addition, the group with strongly increased CBF in DWM, NAWM, and GM had more patients in the relapsing phase compare to the group with mildly increased CBF in these regions, and the ratio of patients experiencing relapse at 18-month follow-up was higher among the group with low GM CBF relative to high GM CBF. At the same time, CBF in patients with serious disability (high EDSS scores and high sNfL) was higher than that in those with mild disability (low EDSS scores and low sNfL) in multiple regions (e.g., DWM, NAWM, parietal lobes, temporal lobes, and basal ganglia). There was a strong correlation between EDSS scores, sNfL values, and CBF changes in these regions.

Furthermore, we found that patients in the relapsing phase, with a long disease duration, or with cognitive impairment had higher CBF in certain brain regions (e.g., parietal lobes, temporal lobes, basal ganglia and NAWM) than those in the remitting phase, with a short disease duration, or without cognitive impairment. In contrast, no significant differences were found in comparisons of other clinical phenotypes (ARR, motor impairment, sensory disorder, visual disturbance). These findings demonstrate that CBF is closely associated with MS clinical severity.

## The potential of CBF as a quantitative imaging marker of disease severity

In MS, the identification of reliable imaging biomarkers will facilitate early diagnosis and monitoring of disease severity (14). Although some imaging biomarkers have been proposed, various challenges limit their widespread adoption in clinical practice (32, 33). For example, brain atrophy is strongly related to disease progression. However, detection of brain atrophy is dependent on complex measuring methods and long-term observation, and it is not suitable for the prediction of early progression (34). Although conventional MRI remains the main imaging technique in MS, quantitative imaging techniques show emerging applications. In the present study, we showed that patients with strongly increased CBF in some regions (e.g., parietal lobes, temporal lobes, basal ganglia, DWM, and NAWM) had worse EDSS scores or higher sNfL than patients with mildly increased CBF, and that patients with high EDSS scores or sNfL had increased CBF compared to those with low EDSS scores or sNfL. Furthermore, strongly increased CBF group had more patients in relapsing phase. Thus, increased CBF suggests a high EDSS score, high sNfL, or acute attack.

Due to the operating complexity and requirements for advanced and expensive hardware or software, some quantitative imaging techniques have poor inter-scanner reproducibility and limited availability. ASL, which does not require intravenous administration of gadolinium-based contrast agents, is simple, noninvasive, and low-cost. As it enables the measurement of CBF with high reproducibility, it has good potential for clinical use. In summary, CBF is a potentially useful quantitative imaging marker associated with MS disease severity.

### Future directions

With pharmaceutical developments, there are increasing drugs available for MS. Therapeutic effects can be assessed by monitoring changes in clinical symptoms and neuroimaging lesions after administration of treatment. It is important that clinicians can predict future response to treatment early after disease onset and choose the most appropriate treatment. Since the present study indicates that CBF measurement could be used to monitor disease severity, it might also be applicable for assessment of treatment effect and aid clinicians in adjusting the treatment dose or treatment type. The identification of imaging markers with prognostic value for disability progression is also of considerable interest. CBF abnormalities may be observed before lesions appear on conventional MRI (23, 27), and our results indicate that relapsing probability might be higher in patients with mildly increased CBF in GM. Thus, CBF measurement has the potential to predict disease progression, prognosis, and treatment response. Due to the relative simplicity and reproducibility of the ASL technique, CBF measurement may have good prospects for clinical application and could be a useful complement to conventional MRI.

### Limitations

This study is subject to several limitations. First, as MS is relatively rare in China, the enrolled sample is not large enough. The sensitivity and effectiveness of CBF as a quantitative imaging marker requires further evaluation larger patient groups. Second, the value of CBF in predicting disease progression was not evaluated due to the lack of long-term follow-up. The longitudinal observation is needed to explore the predictive ability of CBF. Third, because of limited sample size some clinical parameters (e.g., different DMTs, cerebrospinal fluid NfL) were not included in the present study. In the future, we will recruit more MS patients and perform long-term follow-up to deepen our understanding of CBF.

## Conclusion

It is the first study to comprehensively depict the relationship between CBF changes and multiple clinical parameters in Eastern MS patients, enriching the data of CBF in this population. Increased CBF was observed in multiple brain regions, especially NAWM, parietal lobes, temporal lobes, and basal ganglia. Furthermore, there was a strong association between CBF and disease severity. These findings expand our understanding of CBF in MS and suggest that CBF has potential as a quantitative imaging marker associated with disease severity.

## Data availability statement

The original contributions presented in the study are included in the article/supplementary material. Further inquiries can be directed to the corresponding authors.

## Ethics statement

The studies involving human participants were reviewed and approved by Ethics Committee of Ruijin Hospital. The patients/participants provided their written informed consent to participate in this study.

## Author contributions

Conceptualization, SC, MZ and BL. Data curation, QZ, MZ. Formal analysis, QZ, TZ, HYM. Investigation, DS, LH, YG, YZ. Methodology, YL, XH, HPM. Project administration, SC and MZ. Writing – original draft, QZ, DS. Writing - review & editing, SC and MZ.

## Funding

This research was funded by Shanghai Shuguang Plan Project (18SG15), Shanghai outstanding young scholars Project, Shanghai talent development project (2019044), Clinical Research Plan of SHDC (SHDC 2020CR2027B) to SC, and Shanghai Municipal Key Clinical Specialty (shslczdzk03403).

## Conflict of interest

The authors declare that the research was conducted in the absence of any commercial or financial relationships that could be construed as a potential conflict of interest.

## Publisher's note



## References

1. Cheng Q, Cheng XJ, Jiang GX. Multiple sclerosis in China–history and future. *Multiple sclerosis (Houndmills Basingstoke England).* (2009) 15(6):655–60. doi: 10.1177/1352458509102921

2. Tian DC, Zhang C, Yuan M, Yang X, Gu H, Li Z, et al. Incidence of multiple sclerosis in China: A nationwide hospital-based study. *Lancet regional Health Western Pacific.* (2020) 1:100010. doi: 10.1016/j.lanwpc.2020.100010

3. Tavazzi E, Zivadinov R, Dwyer MG, Jakimovski D, Singhal T, Weinstock-Guttman B, et al. MRI Biomarkers of disease progression and conversion to secondary-progressive multiple sclerosis. *Expert Rev neurotherapeutics.* (2020) 20 (8):821–34. doi: 10.1080/14737175.2020.1757435

4. D'Haeseleer M, Cambron M, Vanopdenbosch L, De Keyser J. Vascular aspects of multiple sclerosis. *Lancet Neurology.* (2011) 10(7):657–66. doi: 10.1016/S1474-4422(11)70105-3

5. Pelizzari L, Laganà MM, Baglio F, Bergsland N, Cecconi P, Viotti S, et al. Cerebrovascular reactivity and its correlation with age in patients with multiple sclerosis. *Brain Imaging behavior.* (2020) 14(5):1889–98. doi: 10.1007/s11682-019-00132-5

6. Monti L, Donati D, Menci E, Cioni S, Bellini M, Grazzini I, et al. Cerebral circulation time is prolonged and not correlated with EDSS in multiple sclerosis patients: a study using digital subtracted angiography. *PloS One* (2015) 10(2): e0116681. doi: 10.1371/journal.pone.0116681

7. Inglese M, Adhya S, Johnson G, Babb JS, Miles L, Jaggi H, et al. Perfusion magnetic resonance imaging correlates of neuropsychological impairment in multiple sclerosis. *J Cereb Blood Flow Metab Off J Int Soc Cereb Blood Flow Metab* (2008) 28(1):164–71. doi: 10.1038/sj.jcbfm.9600504

8. Adhya S, Johnson G, Herbert J, Jaggi H, Babb JS, Grossman RI, et al. Pattern of hemodynamic impairment in multiple sclerosis: dynamic susceptibility contrast perfusion MR imaging at 3.0 T. *NeuroImage* (2006) 33(4):1029–35. doi: 10.1016/j.neuroimage.2006.08.008

9. Paling D, Thade Petersen E, Tozer DJ, Altmann DR, Wheeler-Kingshott CA, Kapoor R, et al. Cerebral arterial bolus arrival time is prolonged in multiple sclerosis and associated with disability. *J Cereb Blood Flow Metab Off J Int Soc Cereb Blood Flow Metab* (2014) 34(1):34–42. doi: 10.1038/jcbfm.2013.161

10. Rashid W, Parkes LM, Ingle GT, Chard DT, Toosy AT, Altmann DR, et al. Abnormalities of cerebral perfusion in multiple sclerosis. *J neurology neurosurgery Psychiatry* (2004) 75(9):1288–93. doi: 10.1136/jnnp.2003.026021

11. Zhang X, Guo X, Zhang N, Cai H, Sun J, Wang Q, et al. Cerebral blood flow changes in multiple sclerosis and neuromyelitis optica and their correlations with clinical disability. *Front neurology.* (2018) 9:305. doi: 10.3389/fneur.2018.00305

12. Jenkinson M, Bannister P, Brady M, Smith S. Improved optimization for the robust and accurate linear registration and motion correction of brain images. *NeuroImage.* (2002) 17(2):825–41. doi: 10.1006/nimg.2002.1132

13. Tustison NJ, Avants BB, Cook PA, Zheng Y, Egan A, Yushkevich PA, et al. N4ITK: improved N3 bias correction. *IEEE Trans Med imaging.* (2010) 29 (6):1310–20. doi: 10.1109/TMI.2010.2046908

14. Zhang M, Ni Y, Zhou Q, He L, Meng H, Gao Y, et al. (18)F-florbetapir PET/MRI for quantitatively monitoring myelin loss and recovery in patients with multiple sclerosis: A longitudinal study. *EClinicalMedicine.* (2021) 37:100982. doi: 10.1016/j.eclinm.2021.100982

15. Ashburner J, Friston KJ. Unified segmentation. *NeuroImage.* (2005) 26 (3):839–51. doi: 10.1016/j.neuroimage.2005.02.018

16. Chappell MA, Groves AR, Whitcher B, Woolrich MW. Variational Bayesian inference for a nonlinear forward model. *IEEE Trans Signal Processing.* (2009) 57 (1):223–36. doi: 10.1109/TSP.2008.2005752

17. Testud B, Delacour C, El Ahmadi AA, Brun G, Girard N, Duhamel G, et al. Brain grey matter perfusion in primary progressive multiple sclerosis: Mild decrease over years and regional associations with cognition and hand function. *Eur J neurology.* (2022) 29(6):1741–52. doi: 10.1111/ene.15289

18. Jenkinson M, Beckmann CF, Behrens TE, Woolrich MW, Smith SM. FSL. *NeuroImage.* (2012) 62(2):782–90. doi: 10.1016/j.neuroimage.2011.09.015

19. Yushkevich PA, Yang G, Gerig G. (2016). ITK-SNAP: An interactive tool for semi-automatic segmentation of multi-modality biomedical images, in: *2016 38th Annual International Conference of the IEEE Engineering in Medicine and Biology Society (EMBC)*, Orlando, FL, USA Vol. 2016. pp. 3342–5.

20. Thebault S, Abdoli M, Fereshtehnejad SM, Tessier D, Tabard-Cossa V, Freedman MS. Serum neurofilament light chain predicts long term clinical outcomes in multiple sclerosis. *Sci Rep* (2020) 10(1):10381. doi: 10.1038/s41598-020-67504-6

21. Uphaus T, Steffen F, Muthuraman M, Ripfel N, Fleischer V, Groppa S, et al. NfL predicts relapse-free progression in a longitudinal multiple sclerosis cohort study. *EBioMedicine.* (2021) 72:103590. doi: 10.1016/j.ebiom.2021.103590

22. Reich DS, Lucchinetti CF, Calabresi PA. Multiple sclerosis. *New Engl J Med* (2018) 378(2):169–80. doi: 10.1056/NEJMra1401483

23. Wuerfel J, Bellmann-Strobl J, Brunecker P, Aktas O, McFarland H, Villringer A, et al. Changes in cerebral perfusion precede plaque formation in multiple sclerosis: a longitudinal perfusion MRI study. *Brain J Neurol* (2004) 127 (Pt 1):111–9. doi: 10.1093/brain/awh007

24. Horakova D, Kalincik T, Dusankova JB, Dolezal O. Clinical correlates of grey matter pathology in multiple sclerosis. *BMC neurology.* (2012) 12:10. doi: 10.1186/1471-2377-12-10

25. Cairns J, Vavasour IM, Traboulsee A, Carruthers R, Kolind SH, Li DKB, et al. Diffusely abnormal white matter in multiple sclerosis. *J Neuroimaging Off J Am Soc Neuroimaging.* (2022) 32(1):5–16. doi: 10.1111/jon.12945

26. Zhang M, Liu J, Li B, Chen S. (18)F-florbetapir PET/MRI for quantitatively monitoring demyelination and remyelination in acute disseminated encephalomyelitis. *EJNMMI Res* (2019) 9(1):96. doi: 10.1186/s13550-019-0568-8

27. Bester M, Forkert ND, Stellmann JP, Stürner K, Aly L, Drabik A, et al. Increased perfusion in normal appearing white matter in high inflammatory multiple sclerosis patients. *PloS One* (2015) 10(3):e0119356. doi: 10.1371/journal.pone.0119356

28. Amann M, Achtnichts L, Hirsch JG, Naegelin Y, Gregori J, Weier K, et al. 3D GRASE arterial spin labelling reveals an inverse correlation of cortical perfusion with the white matter lesion volume in MS. *Multiple sclerosis (Houndmills Basingstoke England).* (2012) 18(11):1570–6. doi: 10.1177/1352458512441984

29. Doche E, Lecocq A, Maarouf A, Duhamel G, Soulier E, Confort-Gouny S, et al. Hypoperfusion of the thalamus is associated with disability in relapsing remitting multiple sclerosis. *J neuroradiology = J neuroradiologie.* (2017) 44 (2):158–64. doi: 10.1016/j.neurad.2016.10.001

30. Zeis T, Graumann U, Reynolds R, Schaeren-Wiemers N. Normal-appearing white matter in multiple sclerosis is in a subtle balance between inflammation and neuroprotection. *Brain J Neurol* (2008) 131(Pt 1):288–303. doi: 10.1093/brain/awm291

31. Marshall O, Chawla S, Lu H, Pape L, Ge Y. Cerebral blood flow modulation insufficiency in brain networks in multiple sclerosis: A hypercapnia MRI study. *J Cereb Blood Flow Metab Off J Int Soc Cereb Blood Flow Metab* (2016) 36(12):2087–95. doi: 10.1177/0271678X16654922

32. Ghione E, Bergsland N, Dwyer MG, Hagemeier J, Jakimovski D, Paunkoski I, et al. Brain atrophy is associated with disability progression in patients with MS followed in a clinical routine. *AJNR Am J neuroradiology.* (2018) 39(12):2237–42. doi: 10.3174/ajnr.A5876

33. Zivadinov R, Jakimovski D, Gandhi S, Ahmed R, Dwyer MG, Horakova D, et al. Clinical relevance of brain atrophy assessment in multiple sclerosis. *Implications its Use Clin routine. Expert Rev neurotherapeutics.* (2016) 16 (7):777–93. doi: 10.1080/14737175.2016.1181543

34. Hemond CC, Bakshi R. Magnetic resonance imaging in multiple sclerosis. *Cold Spring Harbor Perspect Med* (2018) 8(5):a028969. doi: 10.1101/cshperspect.a028969

frontiers | Frontiers in Immunology

TYPE Original Research
PUBLISHED 21 October 2022
DOI 10.3389/fimmu.2022.1015372



OPEN ACCESS

EDITED BY
Mei-Ping Ding,
Zhejiang University, China

REVIEWED BY
Marina Kleopatra,
University General Hospital of Thessaloniki, Greece
Claudia Cantoni,
Washington University in St. Louis, United States
Wakiro Sato,
National Center of Neurology and Psychiatry, Japan

*CORRESPONDENCE
Kouichi Ito
itoko@rwjms.rutgers.edu
Suhayl Dhib-Jalbut
jalbutsu@rwjms.rutgers.edu

†PRESENT ADDRESS
John E. Mindur,
Rare Disease Drug Discovery Unit, Takeda Pharmaceuticals USA, Inc., Cambridge, MA, United States
Konstantin E Balashov,
Department of Neurology, Boston University School of Medicine, Boston, MA, United States

‡These authors have contributed equally to this work

SPECIALTY SECTION
This article was submitted to Multiple Sclerosis and Neuroimmunology, a section of the journal Frontiers in Immunology

RECEIVED 09 August 2022
ACCEPTED 04 October 2022
PUBLISHED 21 October 2022

CITATION
Yadav SK, Ito N, Mindur JE, Kumar H, Youssef M, Suresh S, Kulkarni R, Rosario Y, Balashov KE, Dhib-Jalbut S and Ito K (2022) Fecal Lcn-2 level is a sensitive biological indicator for gut dysbiosis and intestinal inflammation in multiple sclerosis.
*Front. Immunol.* 13:1015372.
doi: 10.3389/fimmu.2022.1015372

# Fecal Lcn-2 level is a sensitive biological indicator for gut dysbiosis and intestinal inflammation in multiple sclerosis

Sudhir K. Yadav[1], Naoko Ito[1], John E. Mindur[1†], Hetal Kumar[1], Mysra Youssef[1,2], Shradha Suresh[1], Ratuja Kulkarni[1], Yaritza Rosario[1], Konstantin E. Balashov[1†], Suhayl Dhib-Jalbut[1,3*‡] and Kouichi Ito[1*‡]

[1]Department of Neurology, Rutgers-Robert Wood Johnson Medical School, Piscataway, NJ, United States, [2]Department of Clinical and Chemical Pathology, National Research Centre, Dokki, Egypt, [3]Department of Neurology, Rutgers-New Jersey Medical School, Newark, NJ, United States

Multiple Sclerosis (MS) has been reported to be associated with intestinal inflammation and gut dysbiosis. To elucidate the underlying biology of MS-linked gut inflammation, we investigated gut infiltration of immune cells during the development of spontaneous experimental autoimmune encephalomyelitis (EAE) in humanized transgenic (Tg) mice expressing HLA-DR2a and human T cell receptor (TCR) specific for myelin basic protein peptide (MBP87-99)/HLA-DR2a complexes. Strikingly, we noted the simultaneous development of EAE and colitis, suggesting a link between autoimmune diseases of the central nervous system (CNS) and intestinal inflammation. Examination of the colon in these mice revealed the infiltration of MBP-specific Th17 cells as well as recruitment of neutrophils. Furthermore, we observed that fecal Lipocalin-2 (Lcn-2), a biomarker of intestinal inflammation, was significantly elevated and predominantly produced by the gut-infiltrating neutrophils. We then extended our findings to MS patients and demonstrate that their fecal Lcn-2 levels are significantly elevated compared to healthy donors (HDs). The elevation of fecal Lcn-2 levels correlated with reduced bacterial diversity and increased levels of other intestinal inflammation markers including neutrophil elastase and calprotectin. Of interest, bacteria thought to be beneficial for inflammatory bowel disease (IBD) such as *Anaerobutyricum, Blautia, and Roseburia*, were reduced in fecal Lcn-2-high MS patients. We also observed a decreasing trend in serum acetate (a short-chain fatty acid) levels in MS Lcn-2-high patients compared to HDs. Furthermore, a decrease in the relative abundance of *Blautia massiliensis* was significantly associated with a reduction of acetate in the serum of MS patients. This study suggests that gut infiltration of Th17 cells and recruitment of neutrophils are associated with the development of gut dysbiosis and

10.3389/fimmu.2022.1015372

intestinal inflammation, and that fecal Lcn-2 level is a sensitive biological indicator for gut dysbiosis in multiple sclerosis.

KEYWORDS

multiple sclerosis, gut dysbiosis, colitis, neutrophils, lipocalin-2 (LCN-2), experimental autoimmune encephalomyelitis (EAE), biomarker

## Introduction

Multiple sclerosis (MS) is an immune-mediated neuroinflammatory disease that causes demyelination and axonal loss in the central nervous system (CNS) (1). Recent studies suggest that gut dysbiosis is a risk factor for disease progression (2, 3). For example, a significant decrease in Clostridium clusters XIVa and IV was observed in patients with RRMS (4). Clostridium *clusters* have the potential to induce Foxp3$^+$ T regulatory cells (Tregs), which suppress inflammatory conditions, by metabolizing fiber into short-chain fatty acids (SCFAs) (5–7). Therefore, decreases in the abundance of Clostridium *clusters* may potentially increase susceptibility to relapsing-remitting multiple sclerosis (RRMS) (4). The abundance of other SCFA-producing gut bacteria including *Butyricimonas* and Prevotella *which promote Foxp3+ Treg development*, are also decreased in RRMS patients (8). In contrast, mucin-degrading bacteria *Akkermansia Muciniphila*, Th17-inducing bacteria Streptococcus mitis, and *Methanobrevibacter* are reportedly increased in RRMS patients compared to healthy donors (HDs) (8–10). These studies suggest that gut microbiome imbalance between anti-inflammatory and pro-inflammatory bacteria may increase the risk for autoimmune diseases including MS.

The homeostasis of gut bacteria is regulated in part by the immune system. Under steady state conditions, an excessive activation of immune cells against gut bacteria is suppressed by regulatory immune cells induced by microbial-derived signals (11). However, microbial homeostasis in the alimentary tract can sometimes break under the influence of environmental factors, including diet, infection, antibiotics, and stress, leading to the onset of gut dysbiosis (12). When pathobionts expand in the setting of gut dysbiosis, innate and adaptive immune cells become primed to eliminate them. Neutrophils are a critically important cell subset for responding to pathobionts that favor gut dysbiosis. These innate leukocytes are recruited to the gut in an IL-17A- and CXCR2-dependent manner in response to the IL-17A produced by activated innate and adaptive immune cells in the gut mucosa (11, 13). NOD2 signaling induced by pathobionts also recruits neutrophils (14). The recruited neutrophils eradicate pathobionts by producing antimicrobial proteins, such as elastase and reactive oxygen species (ROS) (15, 16). Neutrophils that have infiltrated the gut mucosa also produce lipocalin-2 (Lcn-2)/neutrophil gelatinase associated lipocalin (NGAL), an innate immune factor that suppresses the proliferation of pathobionts by interacting with bacterial siderophores to limit iron acquisition and subsequent bacterial growth (17, 18). Lcn-2 also enhances phagocytic bacterial clearance in macrophages and promotes antimicrobial activity by preserving myeloperoxidase activity in neutrophils (19, 20). Therefore, Lcn-2 produced by infiltrated neutrophils serves as a biological indicator of gut dysbiosis. In addition, pro-inflammatory cytokines including IFN-γ, TNF-α, IL-17A, IL-6, and IL-1β, which are secreted during gut inflammation, can augment the production of Lcn-2 in an NF-κB-dependent manner in epithelial cells, macrophages, and infiltrated neutrophils (21). Thus, fecal Lcn-2 is a secreted innate factor that appears to serve as both a biomarker of gut dysbiosis and intestinal inflammation (22–24).

While the activation of neutrophils is critical for eliminating expanding pathobionts, neutrophil activation can also function as a double-edged sword by inducing tissue damage in the gut. Activated neutrophils release oxidants and proteases, such as matrix metalloproteases and elastase, that can cause tissue injury (25). Inflammatory bowel disease (IBD) is thought to be triggered by the activation of intestinal immune cells against gut microbes. A hallmark sign of active IBD is neutrophil infiltration in intestinal tissues, although whether infiltrated neutrophils play a harmful or protective role is controversial (26, 27). Of note, MS is reportedly associated with IBD based on epidemiological studies which highlight their reciprocal comorbidity (28–33). Moreover, shared genetic risk factors between MS and IBD have also been described (34). Likewise, recent murine studies revealed that Th17 cells infiltrate the gut during the development of EAE, and that stem-like intestinal Th17 cells, which are maintained by gut microbes, can give rise to pathogenic effector T cells that traffic to the CNS (35–37). The enrichment of Th17 cells in the gut was also previously reported during MS progression (2). Therefore, we hypothesized that IL-17A produced in the gut prior to or during the onset of CNS autoimmunity mediates the infiltration of neutrophils, which contribute to MS-associated gut dysbiosis and intestinal inflammation. To test this hypothesis, we assessed whether the infiltration of neutrophils and production of Lcn-2 are linked to

EAE- and MS-associated gut dysbiosis, intestinal inflammation, and alteration in short-chain fatty acids.

# Materials and methods

## Animals

All experiments were carried out in compliance with the Rutgers Institutional Animal Care and Use Committee guidelines (Protocol number: 999900130). 3A6/DR2a Tg mice were created using a 3A6 T cell clone isolated from an MS patient (38). The development of spontaneous EAE was monitored from the age of 3-weeks-old until 30-weeks-old. Clinical scores were measured as follows: 0: no signs of disease; 1: limp tail; 1.5: paresis of one hindlimb; 2: paresis of both hindlimbs; 2.5: paralysis of one hindlimb; 3.0: paralysis of both hindlimbs; 3.5: paralysis of both hindlimbs and one forelimb paresis; 4: hindlimb paralysis and both forelimb paresis; 5: no mobility/moribund. Fecal samples were collected by placing individual mouse in an empty container for 1-2 hours, and 5-10 fecal pellets were collected for Lcn-2 ELISA and 16S rRNA sequencing.

## Human subjects

Institutional Review Board approval (Approval number: 20160001256) was obtained from Rutgers-Robert Wood Johnson Medical School (RWJMS), and all subjects were provided written informed consent. RRMS subjects as defined by the 2017 revised McDonald Criteria were recruited from the RWJMS Multiple Sclerosis Center (39). Healthy controls were recruited from local New Jersey residents. All patients and controls were recruited from the same geographic region. All enrollees were between the ages of 18 and 60. Exclusion criteria were: use of any antibiotics within 6 months; use of probiotics within 2 months; inflammatory bowel disease; use of probiotics within 2 months before collection of fecal samples. One participant in each of the MS and HD groups were eating a vegetarian diet; other participants were eating a western diet. Participants were provided with a stool collection kit including an airtight container, commode stool collection container, ice packs, and an anerobic sachet. Once the sample is collected in the stool collection container, it is placed in the airtight container with the anerobic sachet and ice pack. Then, samples were brought into the research laboratory within 24 hours of stool collection. Human fecal samples were aliquoted in 2 mL

TABLE 1 Demographics of study subjects.

| Parameters | Healthy donors (n=18) | MS patients (n=14) | P value |
|---|---|---|---|
| **Age (years)** | 36 ± 11.22 | 43.52 ± 9.61 | 0.055 |
| **Gender** | | | 0.721 |
| Male (%) | 7 (39%) | 4 (29%) | |
| Female (%) | 11 (61%) | 10 (71%) | |
| **Race/ethnicity** | | | >0.999 |
| Caucasian | 13 | 10 | |
| African American | 3 | 3 | |
| Hispanic | 2 | 1 | |
| **MS type** | | | |
| RRMS | Not Applicable | 14 | |
| PMS | Not Applicable | 0 | |
| PMS | Not Applicable | 0 | |
| **Disease duration (years)** | Not Applicable | 8.6+/-5.7 | |
| **Symptom when fecal samples were collected** | | | |
| Flare-up | Not Applicable | 0 | |
| Remission | Not Applicable | 14 | |
| **Therapy** | | | |
| Glatiramer acetate | Not Applicable | 4 | |
| Dimethyl fumarate | Not Applicable | 5 | |
| Triflunomide | Not Applicable | 1 | |
| Interferon beta-1a | Not Applicable | 1 | |
| Azilect | Not Applicable | 1 | |
| None | Not Applicable | 2 | |

cryovials in an anaerobic chamber (Sheldon Manufacturing, Cornelius, Oregon) and rapidly frozen using liquid nitrogen. Then, cryovials were kept in -80 °C for long term storage. Demographic information of the study cohort is provided in Table 1.

## Isolation of mouse lamina propria cells from intestines

The small and large intestines were flushed with PBS and cut longitudinally along its length before being cut into smaller pieces. After three washes, intestinal pieces were transferred to a 50 mL tube in 30 mL Hank's balanced salt solution (HBSS) without calcium and magnesium. EDTA (0.5 M) and DTT (1 M) were then added, and the tissue suspension was incubated under gentle shaking at 37°C for 30 min. Epithelial cells and intraepithelial lymphocytes (IEL) were separated by passing supernatant through a 70-micron strainer. The remaining tissue was washed with RPMI media containing 5% FBS and transferred to a new 50 mL tube. 30 mL RPMI media containing 5% FBS was added into the tissue and digested with 100U/mL collagenase IV (Worthington Biochemical Corporation, Lakewood, NJ) and 50 U/mL DNase (Sigma, St.Louis, MO) with shaking at 37°C for 30 min. Lamina propria (LP) cells were isolated from the flowthrough by filtering through a 70-micron strainer, followed by isolation of lamina propria cells using 40% Percoll. Lamina propria cells were obtained as a pellet, which was then washed and suspended in RPMI media containing 10% FBS for further analysis.

## Flow cytometry

Anti-CD4, -CD45, –IFN-γ, and –IL-17 mAbs were all purchased from eBioscience, San Diego, CA. The mAbs against human TCR Vβ5.1 were purchased from Beckman Coulter. Flow cytometry analysis was performed on Gallios and analyzed by Kaluza Software (Beckman Coulter, Brea, CA). Mononuclear cells from the CNS and lamina propria of large and small intestines were stimulated with MBP87-99 (10 μg/mL) and stained with mAbs against CD45, CD4, IFN-γ, IL-17 and human TCR Vβ5.1. $CD45^+$ $Vβ5.1^+$ cells were gated for analysis of Th1 ($CD4^+$ IFN-$γ^+$), and Th17 ($CD4^+$ IL-$17A^+$) cells. To measure the total number of infiltrated cells ($CD4^+$ $Vβ5.1^+$, $CD4^+$ $Vβ5.1^+$ IFN-$γ^+$, and $CD4^+$ $Vβ5.1^+$IL-$17A^+$) in the CNS, mononuclear cells isolated from the brain and spinal cord were counted and then stained with anti-CD45, CD4, Vβ5.1, IFN-γ, and IL-17 A antibodies. The cell number was calculated based on a percentage of $CD45^+CD4^+$ $Vβ5.1^+$, $CD45^+CD4^+$ $Vβ5.1^+$ IFN-$γ^+$, and $CD45^+CD4^+$ $Vβ5.1^+$IL-$17A^+$.

For the migration of MBP-specific Tg T cells into the large intestine, spleen cells isolated from spontaneous EAE mice were labeled with CellTrace Violet (Thermofisher, Waltham, MA) and $1x10^7$ cells were injected into healthy 3A6/DR2a Tg mice. Migration of 3A6 TCR Tg T cells ($Vβ5.1^+CD3^+$) into the spleen, MLN (mesenteric lymph nodes), CLN (cervical lymph nodes), CNS (brain and spinal cord), SI (small intestine), and LI (large intestine) was analyzed by gating CellTrace $Violet^+$ $CD45^+$ cells.

## Immunohistology

Animals were anaesthetized and perfused intracardially with 30 mL ice-cold PBS, followed by 100 mL of 4% paraformaldehyde (PFA). Colon was removed, luminal content was cleaned using PBS, and tissue was kept in 4% paraformaldehyde for 24 hrs. Then, tissue was soaked in 30% sucrose/PBS for 3 days. Cryoblocks of the colon were made by using optimal cutting temperature (O.C.T) (Thermofisher, Waltham, MA) and were cut at a thickness of 10 μm by cryostat and stained with goat anti-Lcn-2 Ab (Abcam, Cambridge, MA) and rat anti-Ly6G Ab (Calbiochem, St. Louis, MO). Donkey anti-goat IgG Rhodamine, and donkey anti-rat IgG Alexa 488 (Jackson Immunoresearch Laboratories, West Grove, PA) were used as secondary antibodies. Cell nuclei were counterstained with DAPI. Digital images of sections were captured by Leica DMi8 fluorescent microscope using LAS X software (Leica, Wetzlar, Germany). Large and small intestines were divided into 4 equal sections and stained. Number of Lcn-$2^+$, $Ly6G^+$ and Lcn-$2^+Ly6G^+$ double positive cells and tissue area for each section were determined using QuPath software (40). The number of infiltrated cells within the section is presented using number of cells/$mm^2$.

## Evaluation of colitis

To evaluate the severity of colitis in 3A6/DR2a mice, H&E staining of colonic sections was prepared at AML Laboratories (Augustine, FL), and colitis severity was scored by Jackson Laboratory pathology service as follows; Normal = 0, Minimal = 1 (generally focal affecting 1-10% of mucosa, or if diffuse then minimal), Mild = 2 (generally focal affecting 11- 25% of mucosa, or if diffuse then mild), Moderate = 3 (26-50% of mucosa affected with areas of gland loss replaced by inflammatory cell infiltrate, milder in remaining areas of mucosa), Marked = 4 (51-75% of mucosa affected with areas of gland loss replaced by inflammatory cell infiltrate, milder in remaining areas of mucosa), Severe = 5 (76-100% of mucosa affected with areas of gland loss replaced by inflammatory cell infiltrate, milder in remaining areas of mucosa) (41).

### Analysis of cytokine production

Human PBMCs were isolated from whole blood by using lymphocyte separation medium (Thermo Fisher Scientific, Waltham, MA). The freshly isolated PBMCs were cultured at

$2 \times 10^6$/ml cell density unstimulated or with LPS (*In vivo*Gen, San Diego, CA) at 5 μg/ml, or CD3/CD28 mAbs (Biolegend, San Diego, CA) at 2 μg/ml for 3 days, and cytokine production was examined by ELISA (Biolegend, San Diego, CA). The remaining cells were frozen and stored in liquid nitrogen.

## ELISA assay for Lcn-2, neutrophil elastase, and calprotectin

To measure the levels of Lcn-2, calprotectin, and elastase, fecal samples (~200 mg) were suspended in 0.5 mL of 0.01% Tween 20 in PBS solution, homogenized using sterile disposable pellet pestles (Fisher Scientific, Waltham, MA), and vortexed. The supernatant was collected by centrifugation at 12000 rpm for 10 min, and Lcn-2 concentration in the fecal supernatants was measured by mouse or human Lipocalin-2/NGAL Quantikine kit (R&D systems, Minneapolis, MN). Human fecal calprotectin was measured using an ELISA kit (Raybiotech, Peachtree Corners, GA). Human fecal neutrophil elastase was measured using an ELISA kit (Immundiagnostik AG, Bensheim, Germany). Total protein of fecal supernatant was measured by the Pierce™ BCA Protein Assay Kit (ThermoFisher, Waltham, MA). Lcn-2, calprotectin, and elastase levels were presented by ng per mg of total fecal protein. Serum endotoxin activity was measured using Human endotoxin (ET) ELISA Kit (MyBioSource, San Diego, CA) according to the manufacturer's recommendation.

## 16S ribosomal RNA sequencing

Fecal DNA was purified by the Fast DNA Stool Mini Kit (QIAGEN, Hilden, Germany) according to the manufacturer's instructions. The concentration of extracted DNA was determined by Nanodrop 1000 (Thermo Scientific, Waltham MA). For human gut microbiota study, 16S rRNA gene sequencing was done by Zymo Research (Irvine, CA) using custom designed primers to provide the best coverage of the V3-V4 region of 16S rRNA gene while maintaining high sensitivity. The final library was sequenced on Illumina® MiSeq™ with a v3 reagent kit (600 cycles). The sequencing was performed with 10% PhiX spike-in. An average of 33811 sequences per sample were obtained (S.D. ± 8876). Unique amplicon sequence (ASV) variants were inferred from raw reads using the DADA2 pipeline (42). Chimeric sequences were also removed with the DADA2 pipeline. Taxonomy assignment was performed using Uclust from QIIME1 (v.1.9.1) with the Zymo Research Database, a 16S database that is internally designed and curated (43), and any unassigned taxa were further identified by NCBI sequence databases. Alpha and beta-diversity analysis was performed based on rarefied abundance matrix. Taxonomy that has significant abundance among different groups were identified by performing statistical tests on relative abundance across groups.

## SCFAs analysis

Fecal and serum SCFAs were measured by microbiomeinsights (Richmond, BC, Canada) and Creative proteomics (Shirley, NY, USA), respectively.

## Statistical analysis

GraphPad Prism Software version 9 (GraphPad Software, Inc., San Diego, CA) and R version 4.0.2 were used for statistical analyses. Spontaneous EAE clinical scores were evaluated by the non-parametric Mann-Whitney U test. Multiple comparisons were performed with one-way ANOVA with Tukey's Multiple Comparison Test or Kruskal Wallis test with Dunn's Multiple Comparison test. Student's *t* test (unpaired) or Mann-Whitney U test was used to assess the differences between two groups. Fisher exact test was used for categorical variables. The Spearman correlation or Pearson correlation test was used to analyze correlation between parameters. All p-values $\leq 0.05$ were considered statistically significant.

# Results

## MBP-specific T cells increase in the large intestine during the development of spontaneous EAE

3A6/DR2a Tg mice harbor T cells expressing the MBP-specific human 3A6 TCR and an MS-linked MHC class II restriction element, HLA-DR2a (38). These mice develop EAE spontaneously during the period of adolescence and young adulthood (44). Since we previously demonstrated that gut dysbiosis was highly associated with spontaneous EAE in 3A6/DR2a Tg animals (44), we analyzed the development and/or infiltration of Th1 and Th17 cells in both the gastrointestinal tract and central nervous system (CNS) in these mice. Expectedly, an enrichment of MBP-specific Th1 and Th17 cells was observed in the CNS upon development of spontaneous EAE (Figures 1A, B). Interestingly, MBP-specific Th1 and Th17 cells were also enriched in the large intestines of these mice (Figures 1C–E). This enrichment was more significantly pronounced in the large intestine compared to the small intestine. To investigate whether MBP-specific T cells can migrate into the large intestine in 3A6/DR2a Tg mice, splenocytes were isolated from animals with spontaneous EAE, labeled with CellTrace Violet, and injected into naive 3A6/DR2a Tg mice. As shown in Figure 1F, MBP-specific $CD4^+$ T cell

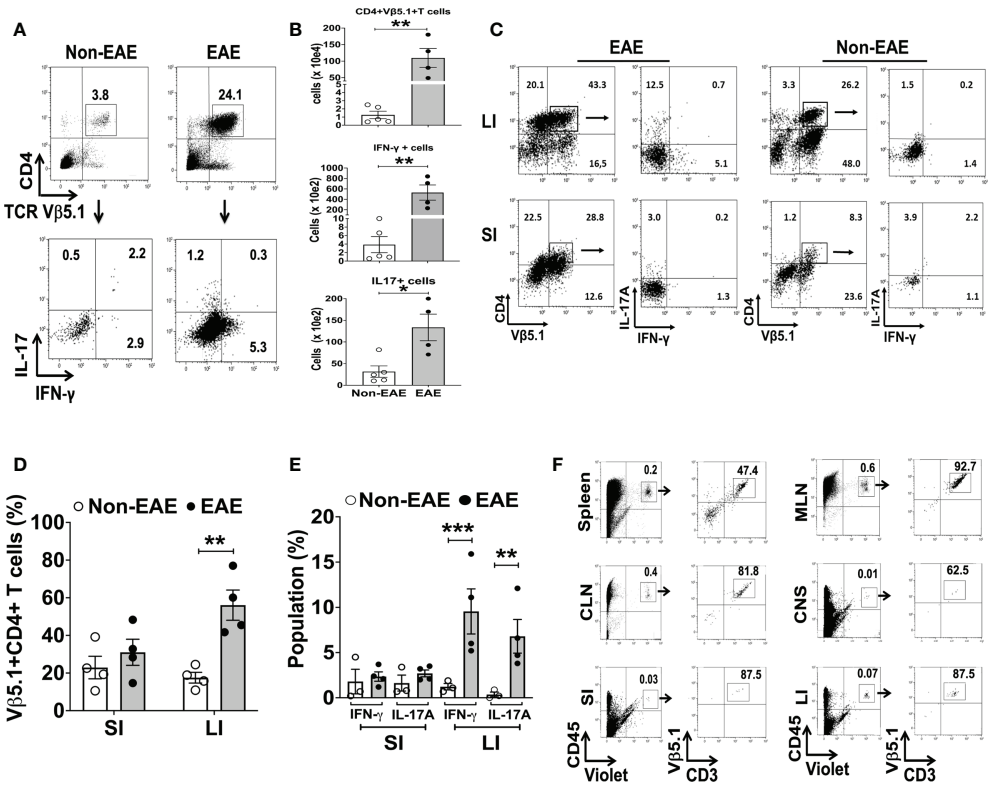


FIGURE 1
Infiltration of MBP-specific T cells in the large intestine during the development of spontaneous EAE in 3A6/DR2a mice. **(A)** Infiltration of $CD4^+$ MBP-TCR $(V\beta5.1)^+$ Tg T cells in the CNS and production of IFN-γ and IL-17A in response to MBP87-99 (10 μg/mL). **(B)** Total number of CNS-infiltrated $CD4^+$ MBP-TCR (Vβ5.1) Tg T cells, Th1 ($CD4^+$ $V\beta5.1^+IFN\text{-}\gamma^+$) cells, and Th17 ($CD4^+$ $V\beta5.1^+Th17A^+$) cells (n = 4-5 in each group). **(C, D)** Enrichment of $CD4^+$ MBP-TCR $(V\beta5.1)^+$ Tg T cells in the large intestine in EAE or non-EAE mice and the percentage of their population within $CD45^+$ leukocytes (n = 4 in each group). **(C, E)** Enrichment of MBP-specific Th1 ($CD4^+$ $IFN\text{-}\gamma^+$) and Th17 ($CD4^+$ $Th17A^+$) cells in the large and small intestines upon development of EAE and their frequency within $CD45^+$ leukocytes (n = 3-4 in each group). **(F)** Migration of MBP-TCR Tg T cells ($V\beta5.1^+CD3^+$) into the large intestine. The spleen cells isolated from spontaneous EAE were labeled with CellTrace Violet and $1x10^7$ cells were injected into healthy 3A6/DR2a Tg mice. Migration of MBP-TCR Tg T cells ($V\beta5.1^+CD3^+$) into the spleen, MLN (mesenteric lymph nodes), CLN (cervical lymph nodes), CNS (brain and spinal cord), small intestine, and large intestine is shown. SI, small intestine; LI, large intestine. Mean ± SEM. *P < 0.05, **P < 0.01, ***P < 0.001.

infiltration into the large intestine was detected based on the CellTrace Violet signal. Taken together, our data suggest that the infiltration and/or proliferation of MBP-specific Th1 and Th17 cells in the large intestine increases during the development of spontaneous EAE in 3A6/DR2a Tg mice.

## Intestinal inflammation is associated with the development of EAE

The expansion of Th17 cells in the gut is observed during intestinal inflammation (45). Hence, we examined the association between EAE and intestinal inflammation in 3A6/DR2a Tg mice. Since fecal Lcn-2 is a sensitive biomarker of intestinal inflammation (23, 24), we assessed levels of fecal Lcn-2 in EAE and non-EAE mice. Notably, an increase in fecal Lcn-2 levels was significantly associated with the development of spontaneous EAE (Figure 2A), and a time course experiment showed that an increase in fecal Lcn-2 levels began one week before symptom onset (Figure 2B). Since Lcn-2 is produced by infiltrated $Ly6G^+$ neutrophils during gut inflammation (46, 47), we examined the gut infiltration of $Ly6G^+$ cells by immunohistology. Of interest, a massive infiltration of $Ly6G^+$ neutrophils were observed in the large intestine of EAE mice (Figures 2C, D), and Lcn-2 was mainly produced by $Ly6G^+$ neutrophils (Figures 2C, E, F). Together, these data indicate that Lcn-$2^+$ neutrophils localize in the large intestines of 3A6/DR2a Tg mice that develop spontaneous EAE.

Since large intestinal neutrophil infiltration is associated with colitis (48, 49), we examined colitis development in EAE mice. The large intestinal epithelium was markedly hyperplastic, which coincided with swelling of the colon tissue, a feature of chronic colitis (Figure 3A). Histopathological examination yielded expanded inflammatory cells in the lamina propria of the large intestine (Figure 3B). Furthermore, higher colitis scores were associated

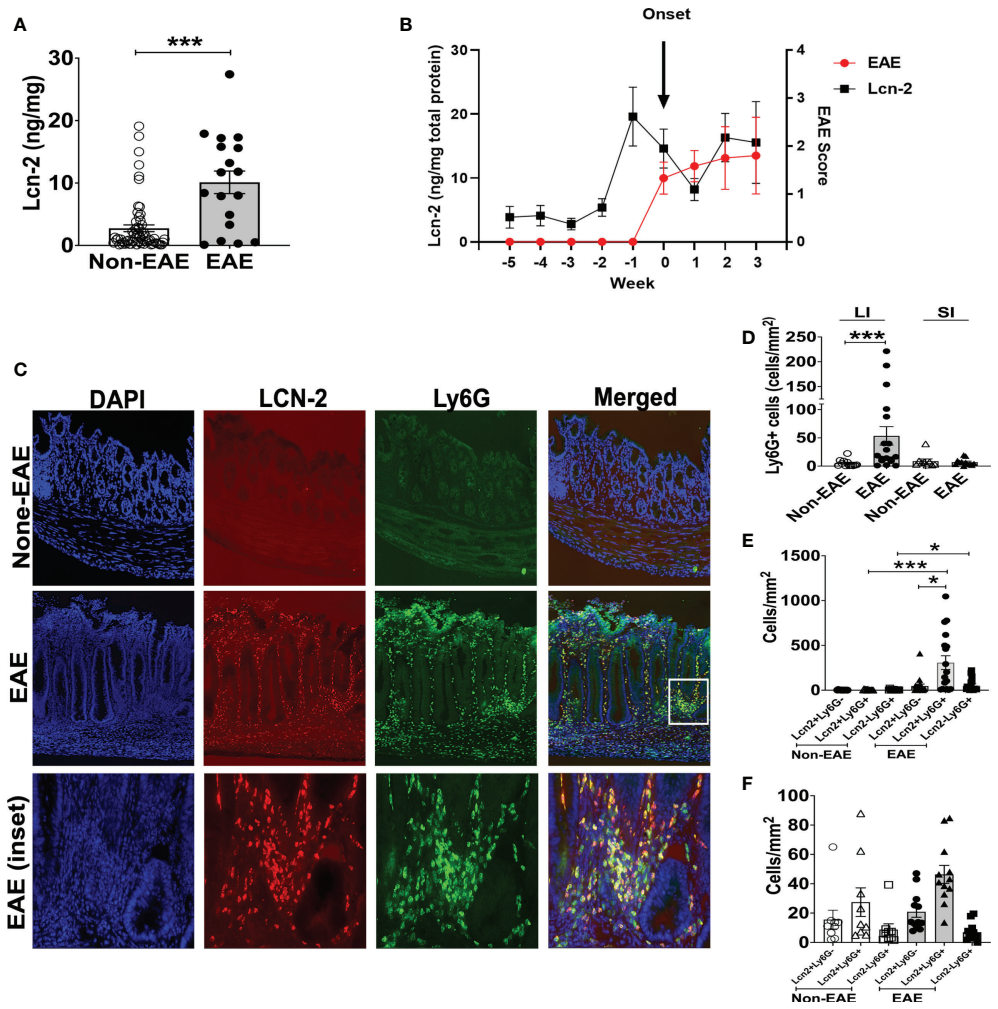


FIGURE 2
Fecal Lcn-2 is a biomarker for the development of spontaneous EAE in 3A6/DR2a mice. **(A)** Association between increase in fecal Lcn-2 levels (ng/mg total protein) and development of spontaneous EAE (Non-EAE; n = 62, EAE; n = 18).**(B)** Time course of development of spontaneous EAE (•) and fecal Lcn-2 levels (■) in 3A6/DR2a Tg mice. Fecal Lcn-2 levels before and after clinical EAE onset are shown. Mean ± SEM (n =6). **(C)** Immunohistopathology showing increase in $Lcn2^+$ $Ly6G^+$ cells in the large intestine upon development of EAE. **(D)** Increase in neutrophil ($Ly6G^+$) cells in the large intestine (LI) upon development of EAE. **(E, F)** Large intestines **(E)** and small intestine **(F)** were stained with anti-Lcn-2 mAb and anti-Ly6G mAb, and number of Lcn-$2^+$(red), $Ly6G^+$ (green), and Lcn-$2^+$ $Ly6G^+$ (yellow) cells were quantified. Mean ± SEM. *P < 0.05, ***P < 0.001.

with the development of EAE in 3A6/DR2a Tg mice (Figure 3C). In sum, these data highlight the coincident development of CNS and gut inflammation in 3A6/DR2a Tg mice. Since fecal Lcn-2 levels were increased before EAE onset (Figure 2B), intestinal inflammation probably preceded the onset of EAE.

## Fecal Lcn-2 levels are increased in patients with RRMS

To examine the association between RRMS and gut dysbiosis, serum and fecal Lcn-2 levels of RRMS patients and healthy donors (HDs) were analyzed. No significant difference in serum Lcn-2 levels was observed between the two groups (Figure 4A). Cytokine secretion assays indicated that the production of pro-inflammatory cytokines, such as IFN-γ, IL-6, and IL-1β, and an anti-inflammatory cytokine, IL-10, in PBMCs was also not significantly different, except for IL-17A which was elevated in the RRMS patients compared to HDs (Supplementary Figure 1). On the other hand, fecal Lcn-2 levels were significantly higher in the RRMS group compared to the HD group (Figures 4B–D), and the increase in fecal Lcn-2 levels significantly correlated with a decrease in microbial alpha diversity (Figures 4E–G). Since we observed fecal Lcn-2-high (>50 ng/mg total protein) and Lcn-2-low groups in

RRMS patients, we examined microbial diversity in HDs, MS Lcn-2-low, and MS Lcn-2-high groups. Alpha diversity (Faith phylogenetic diversity) was reduced in the MS Lcn-2-high group compared to the HD and MS Lcn-2-low groups (Figure 4G right graph), although a significant distance between MS Lcn-2-high and the MS Lcn-2-low/HD groups was not observed by UniFrac distance analysis (Figures 4I, J). Interestingly, serum endotoxin levels were increased in the MS Lcn-2-high group compared to the MS Lcn-2-low group (Figure 4H right graph), suggesting an association between intestinal inflammation and gut permeability. Since fecal calprotectin and neutrophil elastase are other biomarkers of intestinal inflammation (50, 51), we examined their levels in fecal samples. As expected, fecal calprotectin and neutrophil elastase levels were increased in the MS Lcn-2-high group compared to the MS Lcn-2-low and HD groups (Figures 5C, D). Furthermore, fecal calprotectin and neutrophil elastase levels correlated significantly with fecal Lcn-2 levels (Figures 5E, F). We also examined the correlation between alpha diversity and these two biomarkers of intestinal inflammation. As shown in Supplementary Figure 2, the increase in fecal Lcn-2 was mostly significantly correlated with a decrease in alpha diversity among the biomarkers of intestinal inflammation. Collectively, these data suggest that increase in fecal Lcn-2 levels is associated with gut dysbiosis in MS patients.

## Fecal Lcn-2 levels and microbial composition in RRMS

To determine the association between fecal Lcn-2 levels and microbial abundance, we first evaluated microbial abundance in RRMS patients and HDs. 16S rRNA gene sequencing showed a decrease in *Alistipes finegoldii, Alistipes shahii, Bifidobacterium adolescentis*, *Anaerobutyricum* (*Eubacterium*) *hallii, Blautia massiliensis, Coprococcus catus, Ruminococcaceae NA sp 34859 and Ruminococcaceae NA sp 35056*, and an increase in *Blautia brookingsii* in RRMS compared to HDs (Figure 6A). Notably, *Alistipes finegoldii* and *Bifidobacterium adolescentis* have been reported as bacteria that can suppress intestinal inflammation (52, 53), and *Coprococcus catus* and *Anaerobutyricum* (*Eubacterium*) *hallii* are short-chain fatty acid (SCFA)-producing bacteria that are found reduced in IBD patients (54–56). Next, we examined which bacteria are depleted in MS Lcn-2-high patients. While *Alistipes finegoldii, Alistipes shahii*, and *Bifidobacterium adolescentis* were depleted in both MS Lcn-2-low and MS Lcn-2-high patients, we found that *Anaerobutyricum* (*Eubacterium*) *hallii, Blautia massiliensis*, *Clostridium hylemonae*, and *Roseburia sp 32368* were depleted only in MS Lcn-2-high patients (Figure 6B and Supplementary Figure 3). These data suggest that certain types of beneficial bacteria are depleted in RRMS patients and that the additional depletion of *Anaerobutyricum* (*Eubacterium*) *hallii*, *Blautia massiliensis*, *Clostridium hylemonae*, and *Roseburia sp 32368* may favor the development of intestinal inflammation in RRMS patients.

## Decrease in the relative abundance of *Blautia massiliensis* was associated with a reduction in blood SCFA levels

A recent study showed that blood SCFA levels are directly linked to health maintenance during MS and metabolic diseases

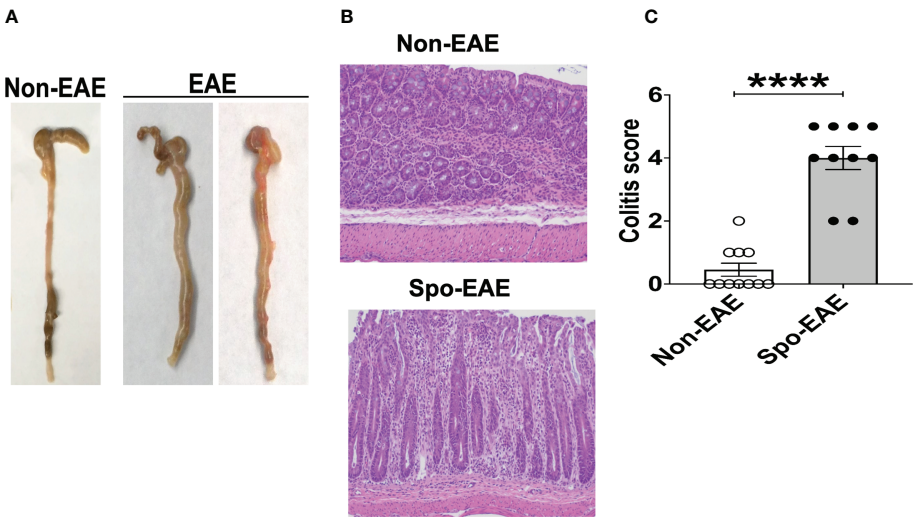


FIGURE 3
Development of colitis in spontaneous EAE mice. **(A)** Swollen colon in spontaneous EAE mice. **(B)** H&E histopathology of swollen colon isolated from spontaneous EAE and non-EAE mice. **(C)** Colitis score was evaluated by immunopathological analysis in non-EAE (n = 11) and EAE mice (n= 10) as described in materials and methods. Mean ± SEM. ****P <0.0001.

(57, 58); therefore, we examined the association between serum SCFA levels and underlying MS-linked intestinal inflammatory activity using Lcn-2 as a readout. Interestingly, we observed a decreasing trend in serum acetate levels in MS Lcn-2-high patients compared to HDs (Figure 7A). Since blood serum SCFA levels are determined based on the initial production of SCFAs by gut microbes and local absorption of SCFAs by the colonic epithelium, fecal SCFA levels were also examined. Interestingly, the level of fecal SCFAs was increased in the MS Lcn-2-high participants (Figure 7B) as observed in metabolic diseases (59, 60). Since intestinal inflammation suppresses the gene expression of SCFA transporters in the intestinal epithelium (61, 62), underlying intestinal inflammation might be actively suppressing SCFA absorption, thereby decreasing the blood circulation of SCFAs. Among MS-associated bacteria, a decrease in the relative abundance of *Blautia massiliensis* was most significantly associated with a reduction in acetic acid in the serum (Figure 8 and Supplementary Figure 4). Since *Blautia massiliensis* is a highly abundant bacterium (relative abundance: 8.3 ± 4.1% in HDs versus 3.7 ± 3.4% in RRMS), its reduced

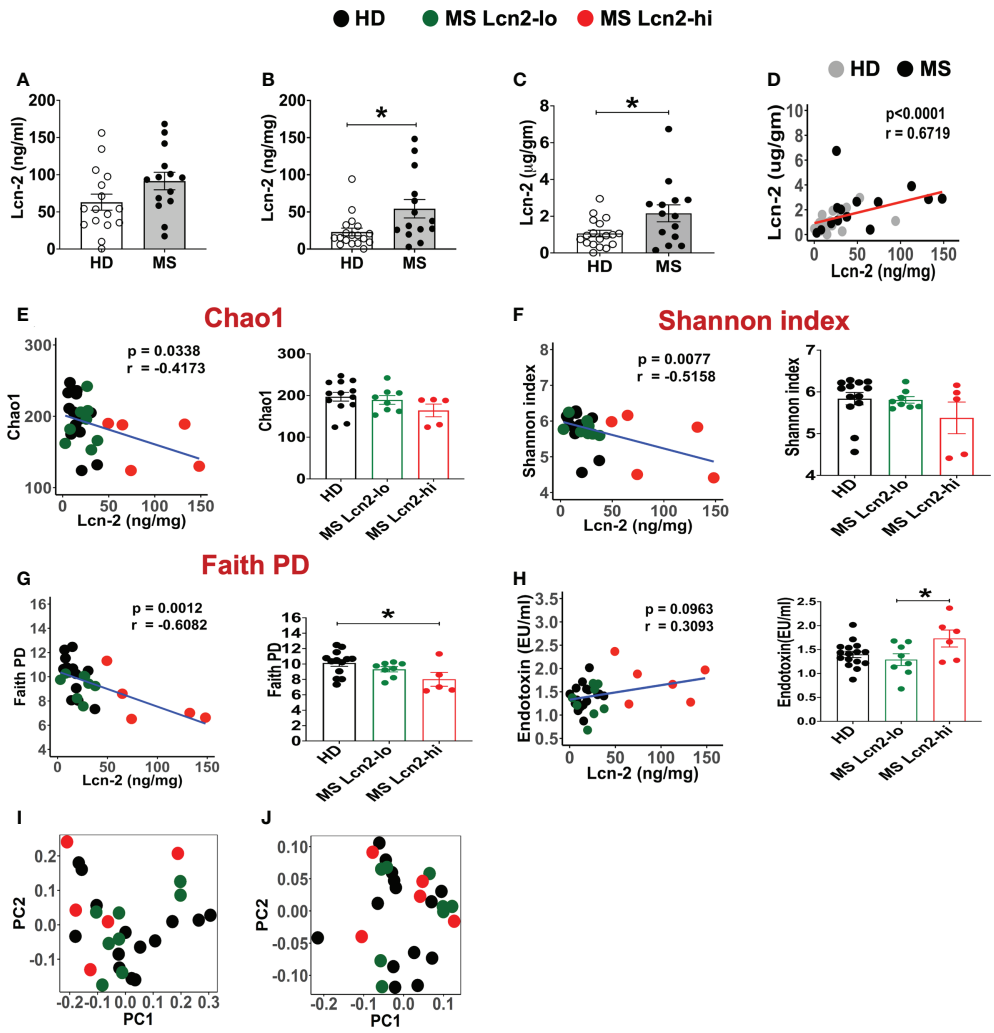


FIGURE 4
Fecal Lcn-2 is a biomarker of gut dysbiosis in RRMS patients. **(A)** Serum Lcn-2 concentration in HDs and RRMS patients. **(B–D)** Fecal Lcn-2 concentration in HDs and RRMS patients. Fecal Lcn-2 levels are shown as ng/mg total protein of fecal extract **(B)** and µg/gm fecal weight **(C)**, and fecal Lcn-2 levels between ng/mg total protein and µg/gm fecal weight are significantly correlated **(D)**. RRMS patients (n = 14) and HDs (n = 18) are shown. (E-G: left graph) Spearman correlations between fecal Lcn-2 levels and alpha diversity based on Chao1 index **(E)**, Shannon index **(F)**, and Faith phylogenetic diversity score **(G)**. (**E–G** right graph) RRMS subjects were divided into Lcn-2-low (<50 ng/mg total protein) and Lcn-2-high (>50 ng/mg total protein) groups, and alpha diversity based on Chao1 index, Shannon index, and Faith phylogenetic diversity score in HDs (n=13), MS Lcn-2-low (n=8), and MS Lcn-2-high (n=5) subjects are shown. **(H)** Spearman's correlation between fecal Lcn-2 and serum endotoxin levels (left graph). Endotoxin levels in the serum of HD (n = 16), Lcn-2-low (n = 8) and Lcn-2-high MS subjects (n = 6) (right graph). **(I, J)** PCoA plot of beta-diversity by Unweighted UniFrac distance analysis **(I)**, and Weighted Unifrac distance analysis **(J)**. Each dot represents an individual subject. Mean ± SEM. *P < 0.05.

abundance in MS may significantly impact the reduction in blood SCFA levels mediated by underlying intestinal inflammation.

## Discussion

In this study, we show that Lcn-2 produced by infiltrated gut neutrophils is a fecal biomarker for EAE- and MS-associated gut dysbiosis. Since peripheral T cells migrate into the gut under steady conditions (63), increases in peripheral pro-inflammatory T cells may lead to increased infiltration of cells into the gut during CNS autoimmune disease. Accordingly, we observed the infiltration and/or expansion of MBP-specific Th17 cells in the large intestine during EAE development in our animal model (Figures 1C–E). This is consistent with earlier studies showing that MOG-specific Th17 cells can migrate into the gut during the development of EAE (35, 36). Interestingly, the enrichment of Th17 cells in the gut was also reported in RRMS patients (2). The augmented production of IL-17A coordinates neutrophil infiltration into the gut (64), and infiltrated neutrophils can eliminate luminal microbes that translocate the epithelium and invade the mucosa. Indeed, we observed that neutrophils infiltrate the large intestines of 3A6/DR2a Tg mice that develop spontaneous EAE. In the setting of MS, similar mechanisms may be involved in the recruitment of neutrophils *via* IL-17A produced by Th17 cells.

Neutrophils mediate pathogenic microorganism removal by phagocytosis, neutrophil extracellular trap (NET) formation, and by the release of reactive oxygen and nitrogen species and antimicrobial factors, such as neutrophil elastase, Lcn-2, and calprotectin (65). Therefore, antimicrobial mediators produced by infiltrated neutrophils could be involved in the induction of gut dysbiosis. Indeed, increased levels of fecal Lcn-2, neutrophil elastase, and calprotectin levels were associated with reduced

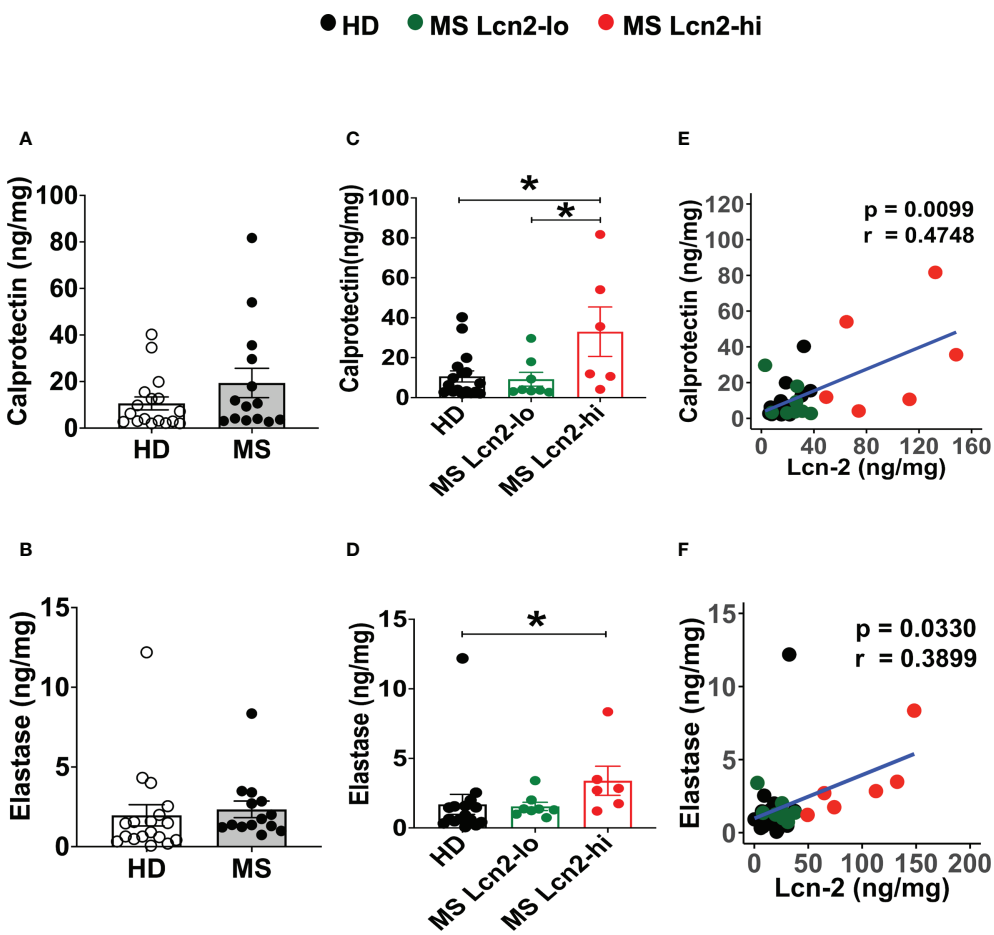


FIGURE 5
Fecal calprotectin and elastase levels in HDs and RRMS patients. **(A, B)** Fecal calprotectin levels **(A)** and fecal elastase levels **(B)** in RRMS (n = 14) and HDs (n = 18) are shown. **(C, D)** The levels of fecal calprotectin **(C)** and fecal elastase **(D)** in HDs, MS Lcn-2-low (<50 ng/mg total protein), and MS Lcn-2-high (>50 ng/mg total protein) subjects are shown. **(E, F)** Spearman correlation between fecal Lcn-2 and fecal calprotectin **(E)** or fecal elastase **(F)** is shown. HDs (n=18), MS Lcn-2-low (n=8), and MS Lcn-2-high (n=6). Mean ± SEM. *P < 0.05.

10.3389/fimmu.2022.1015372

intestinal microbiota diversity in RRMS patients. Among these three mediators, fecal Lcn-2 levels were most significantly associated with MS-linked gut dysbiosis (Supplementary Figure 2). Neutrophils additionally participate in gut inflammation by producing high levels of *reactive oxygen species* (ROS), proteases, and pro-inflammatory factors (IL-8, TNF-α, and leukotriene B4) that damage the epithelial barrier and recruit monocytes into the gut (65). NETs released from neutrophils are also associated with inflammation and are involved in permeabilizing the gut (66–68). Furthermore, elastase released by infiltrated neutrophils has been implicated in the pathogenesis of inflammatory bowel disease (IBD) and reflects disease activity during ulcerative colitis (69–71). Therefore, the coordinated gut infiltration of Th17 cells and neutrophils may be contributing to the pathogenesis of mucosal inflammation in CNS autoimmune diseases.

MS has been reported to be associated with IBD (28–32, 72, 73), and the prevalence of IBD is increased in MS patients compared to the general population (72, 73). Increased prevalence of demyelinating diseases was also observed in IBD patients (31). This linked association suggests a bidirectional comorbidity between MS and IBD. Furthermore, genome-wide association studies involving ulcerative colitis and Crohn's disease have identified shared risk loci between MS and IBD (34), which suggests that common pathological mechanisms affect both conditions. Our observation that 3A6/DR2a Tg mice co-develop EAE and colitis is consistent with observations made in humans (Figure 3). Furthermore, we

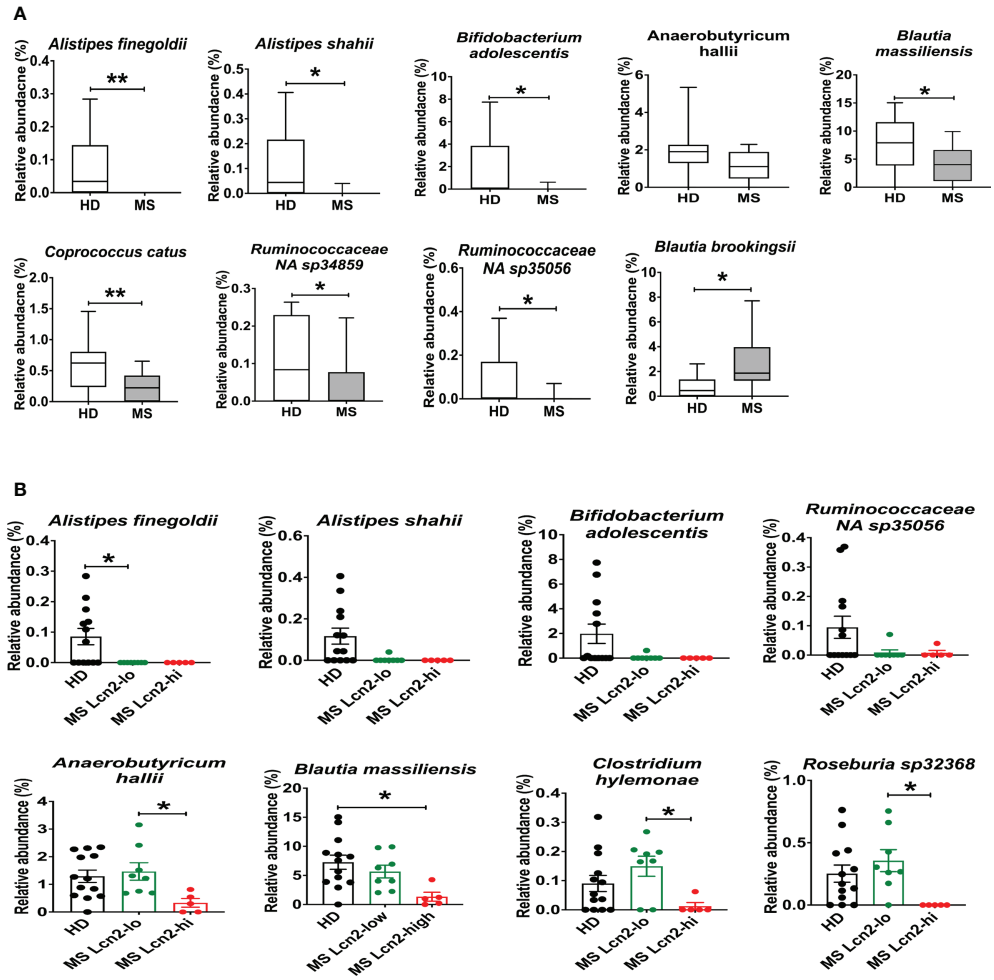


FIGURE 6
Enteric microbial composition in HDs and RRMS patients. **(A)** Enteric microbial composition in HDs and RRMS groups. The list of species exhibits changes in relative abundance of each bacterial taxa between RRMS (n=13) and HDs (n=13) groups. **(B)** Enteric microbial composition in HDs, MS Lcn-2-low and MS Lcn-2-high groups. The list of species exhibits changes in relative abundance of each bacterial taxa between HDs (n=13), MS Lcn-2-low (n=8) and MS Lcn-2-high (n=5) groups. Mean ± SEM. *P < 0.05, **P < 0.01.

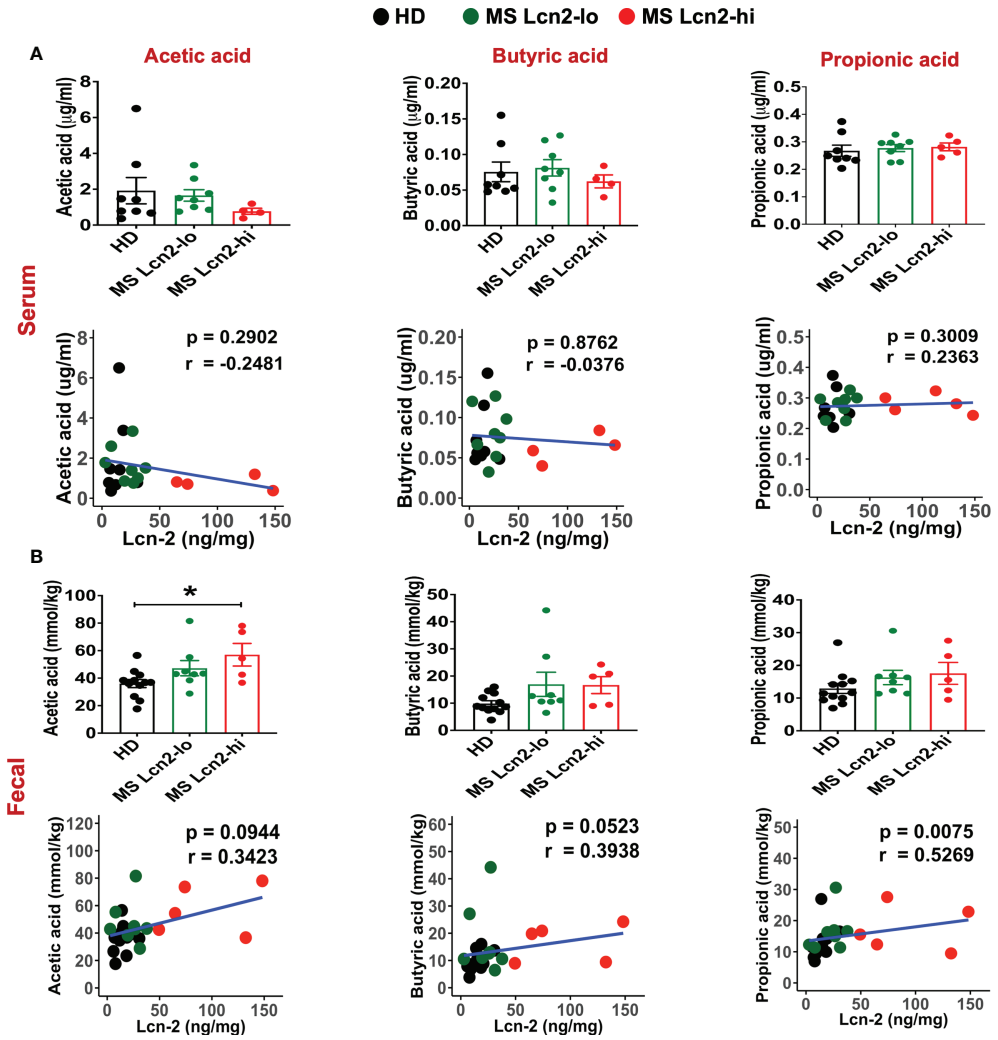


FIGURE 7
SCFAs levels in the serum and fecal samples. SCFAs levels in the serum **(A)** and fecal samples **(B)** isolated from HDs, MS Lcn-2-high, and MS Lcn-2-low groups, and correlation between SCFAs and fecal Lcn-2 levels is shown. HDs (n=8), MS Lcn-2-low (n=8), and MS Lcn-2-high (n=5). *P ≤ 0.05.

previously reported that the expansion of *Bacteroides vulgatus* was significantly associated with spontaneous EAE in 3A6/DR2a Tg mice (44). *B. vulgatus* is a bacterium which localizes in the large intestine and is associated with colitis (74, 75). It is possible that the chronic infiltration of neutrophils and production of pro-inflammatory mediators induced by *B. vulgatus* may trigger colitis in 3A6/DR2a Tg mice. In addition, the expression of MBP in enteric glial cells (76, 77) and 3A6/DR2a Tg animals' partial immunodeficiency stemming from allelic exclusion, which is caused by the expression of a transgenic TCR, may promote the development of colitogenic T cells in 3A6/DR2a Tg mice.

Since Lcn-2 is induced by pro-inflammatory cytokines in a NF-κB-dependent manner, Lcn-2 is suited to be a biomarker of inflammation (21). An increased concentration of Lcn-2 in MS patients' plasma and cerebrospinal fluid suggests a pathological role for Lcn-2 in MS (78). The expression of Lcn-2 in microglia and astrocytes is increased in EAE mice, and disease severity is reduced in Lcn-2 null mice compared to wild-type mice (79). Lcn-2 can also promote the development of Th1 and Th17 cells (79) and M1 microglia (80). In addition, Lcn-2 can suppress remyelination (81) and induce apoptosis in neurons (82). These data suggest that Lcn-2 could play a pathological role in MS. However, the protective and pathological roles of Lcn-2 in colitis are still controversial. Lcn-2 prevents intestinal inflammation and spontaneous colitis in IL-10 null mice by enhancing phagocytic bacterial clearance in macrophages and changing microbial composition, suggesting a protective role in colitis (19, 83). In contrast, Lcn-2 deficiency can protect mice from dextran

sodium sulfate and *Salmonella Typhimurium*-induced colitis, suggesting a pathogenic role of Lcn-2 in colitis (84, 85). Therefore, Lcn-2 may possess a dual function in the pathogenesis of colitis.

We examined serum and fecal Lcn-2 levels in MS patients and HDs. Although we observed an increasing trend of serum Lcn-2 levels in MS patients compared to HDs (Figure 4A), fecal rather than serum Lcn-2 levels were significantly associated with MS (Figures 4B, C). Production of pro- and anti- inflammatory cytokines in PBMCs was also not significantly different except for IL-17A (Supplementary Figure 1). The decreased inflammatory responses in peripheral blood could be attributed to the use of disease-modifying therapies (DMT) in most of the RRMS participants (Table 1). As fecal calprotectin, elastase, and Lcn-2 are well-known biomarkers of intestinal inflammation (23, 51, 86), we examined the levels of these factors in fecal samples collected from RRMS patients and HDs. Fecal Lcn-2 levels were more significantly associated with RRMS than fecal calprotectin and elastase levels (Figures 4B, C, 5A–D). A subset of RRMS patients recorded a higher fecal Lcn-2 concentration ranging between 2.6-6.7 µg/gm (Figure 4C). This range of Lcn-2 levels indicates a mild activity of intestinal inflammation according to previous studies (22, 24). Since fecal Lcn-2 is a sensitive biomarker for intestinal inflammation compared to other biomarkers (24), MS-associated intestinal inflammation and gut dysbiosis can be detected by the fecal Lcn-2 assay. Taxonomy analysis showed that the increase in fecal Lcn-2 levels was associated with a decrease in alpha diversity among intestinal microbiota (Figures 4E–G). Reduced alpha diversity has previously been observed in autoimmune diseases, including MS and IBD (87, 88), and has also been associated with low-grade inflammation (89). Therefore, measuring fecal Lcn-2 levels could be helpful in monitoring MS-related gut dysbiosis and intestinal

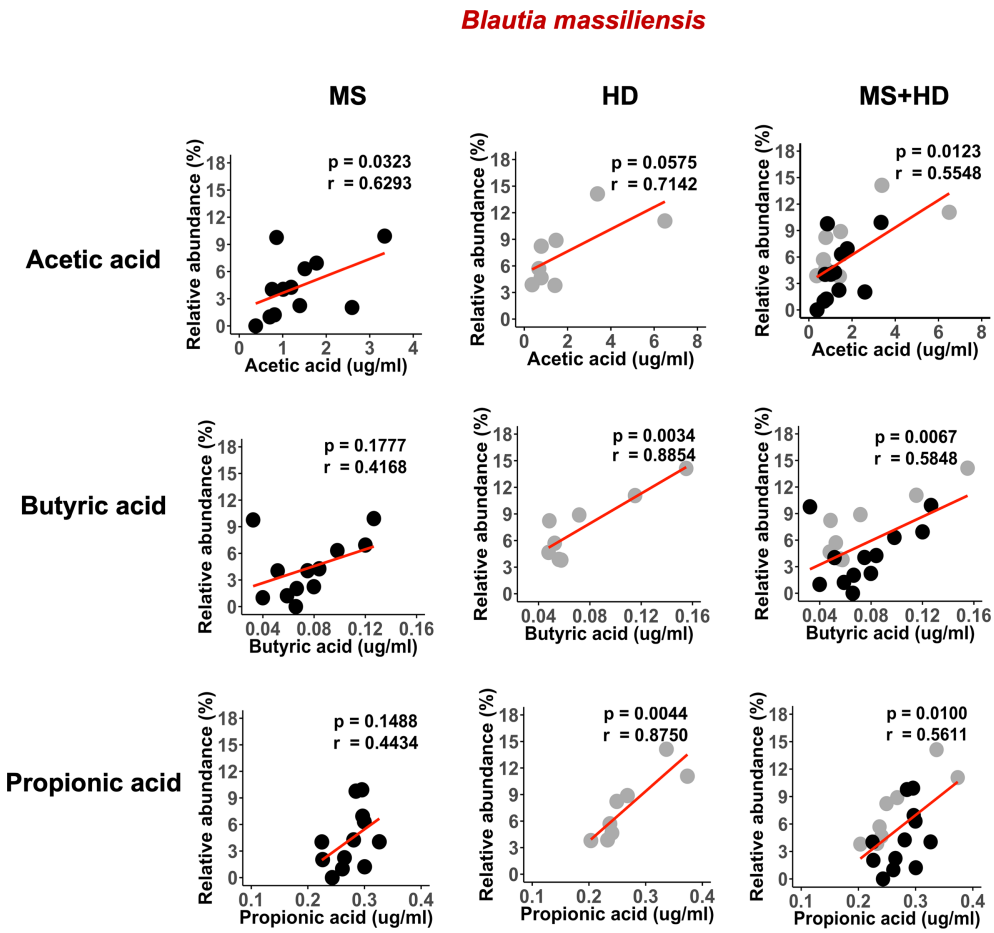


FIGURE 8
*Blautia massiliensis* is associated with serum SCFAs levels. Correlation of *Blautia massiliensis* with serum acetic acid, butyric acid, or propionic acid levels. HDs; n=8, RRMS; n=12.

inflammation. Microbial abundance analysis also showed that *Alistipes finegoldii, Alistipes shahii*, and *Bifidobacterium adolescentis* were depleted in both Lcn-2-low and Lcn-2-high MS patients, whereas *Anaerobutyricum* (*Eubacterium*) *hallii, Blautia massiliensis*, *Clostridium hylemonae*, and *Roseburia sp 32368* were depleted only in MS Lcn-2-high patients (Figure 6B and Supplementary Figure 3). These data suggest that *Anaerobutyricum* (*Eubacterium*) *hallii, Blautia massiliensis*, *Clostridium hylemonae*, and *Roseburia sp 32368* may play a pivotal role in MS-associated intestinal inflammation.

Recent studies have proposed that blood SCFA levels are more directly linked to health maintenance than fecal SCFA levels (57). A decrease in SCFA levels is also associated with an increase in pathogenic immune cells in MS patients (58). Therefore, we examined the effect of gut dysbiosis-mediated intestinal inflammation (fecal Lcn2 levels) on SCFA levels in the blood and feces. Since intestinal inflammation suppresses the expression of SCFA-transporter expressed on the intestinal epithelium (61, 62), intestinal inflammation could suppress the absorption of SCFA and decrease SCFA levels in the blood. We observed a decreasing trend in acetate and butyrate in the blood, while an increasing trend in acetate, butyrate, and propionate in the fecal samples of Lcn-2 high MS patients (Figures 7A, B). Since more than 95% of SCFA produced by intestinal microbiota are absorbed in the gut, the decrease in SCFA absorption by dysbiosis-mediated intestinal inflammation may lead to an increase in SCFA levels in fecal samples. Indeed, recent studies have also shown that increased fecal SCFA levels are associated with gut dysbiosis in metabolic diseases (59, 60). It is worth pointing out that previous studies showed lower fecal SCFA levels in fecal samples collected from MS patients compared to HDs (3, 90). The contrast with our study could be due to differences in dietary habits and genetic background that may affect the growth of SCFA-producing bacteria and expression of the SCFA transporter. A recent study also indicated that fecal and blood SCFA levels in MS patients vary by the disease modifying therapies used (91). Therefore, several factors could contribute to the variations in levels of SCFA in the feces and blood among different studies. We also examined intestinal bacteria that are associated with a decrease in serum SCFA levels and found that depletion of *Blautia massiliensis* was significantly associated with a reduction in serum levels of acetic acid, butyric acid and propionic acid (Figure 8 and Supplementary Figure 4). *Blautia massiliensis* is the third most abundant intestinal bacteria in the participants. Since *Blautia massiliensis* is a newly identified strain (92) and its role in human health is not well understood, further studies are required to explore the involvement of *Blautia massiliensis* in MS-mediated intestinal inflammation/gut dysbiosis and disease activation.

In summary, we demonstrated in a humanized spontaneous EAE model of MS that CNS and gut inflammation can coexist and that they are mechanistically associated with gut-infiltration of pathogenic T cells and recruitment of Lcn-2$^+$ neutrophils. The observations we describe in MS patients support the findings in EAE and indicate that fecal Lcn-2 is a sensitive biological marker for gut dysbiosis in MS. It is often difficult to characterize gut dysbiosis and identify the specific bacteria linked to MS due to a heterogenous microbiome caused by genetic factors, dietary habits, and/or environmental exposures. *Therefore*, analysis of fecal Lcn-2 levels together with taxonomic evaluation could be a useful method to examine intestinal microbial homeostasis in MS. In the future, it is important to explore the association between fecal Lcn-2 levels and clinical parameters including MS relapse rate and disease progression in a larger sample size prospective study.

## Data availability statement

The data presented in the study are deposited in the NCBI repository, accession number: PRJNA875026; https://www.ncbi.nlm.nih.gov/bioproject/PRJNA875026.

## Ethics statement

The studies involving human participants were reviewed and approved by IRB Rutgers University. The patients/participants provided their written informed consent to participate in this study. The animal study was reviewed and approved by IACUC Rutgers University.

## Author contributions

SY, NI, JM, HK, MY, RK, and SS preformed experiments and analyzed the data. SD-J, KB, and YR coordinated the collection of samples from RRMS patients and healthy donors. SY, SD-J, and KI designed research studies. KI and SD-J supervised the research and interpreted the data. SY and KI wrote the manuscript. SD-J and JM reviewed and edited the manuscript. All authors reviewed the manuscript and approved the final version.

## Funding

This study was supported by the National Multiple Sclerosis Society Research grant RG-1901-33077 (to KI and SD-J), NIH R21AI130585 (to KI and SD-J) and the Ruth Dunietz Kushner and Michael Jay Serwitz endowed Chair in Multiple Sclerosis to SD-J.

## Conflict of interest

The authors declare that the research was conducted in the absence of any commercial or financial relationships that could be construed as a potential conflict of interest.

## Publisher's note

All claims expressed in this article are solely those of the authors and do not necessarily represent those of their affiliated organizations, or those of the publisher, the editors and the reviewers. Any product that may be evaluated in this article, or claim that may be made by its manufacturer, is not guaranteed or endorsed by the publisher.

## Supplementary material

The Supplementary Material for this article can be found online at: https://www.frontiersin.org/articles/10.3389/fimmu.2022.1015372/full#supplementary-material

## References


1. Yadav SK, Mindur JE, Ito K, Dhib-Jalbut S. Advances in the immunopathogenesis of multiple sclerosis. *Curr Opin Neurol* (2015) 28(3):206–19. doi: 10.1097/WCO.0000000000000205

2. Cosorich I, Dalla-Costa G, Sorini C, Ferrarese R, Messina MJ, Dolpady J, et al. High frequency of intestinal TH17 cells correlates with microbiota alterations and disease activity in multiple sclerosis. *Sci Adv* (2017) 3(7):e1700492. doi: 10.1126/sciadv.1700492

3. Takewaki D, Suda W, Sato W, Takayasu L, Kumar N, Kimura K, et al. Alterations of the gut ecological and functional microenvironment in different stages of multiple sclerosis. *Proc Natl Acad Sci U.S.A.* (2020) 117(36):22402–12. doi: 10.1073/pnas.2011703117

4. Miyake S, Kim S, Suda W, Oshima K, Nakamura M, Matsuoka T, et al. Dysbiosis in the gut microbiota of patients with multiple sclerosis, with a striking depletion of species belonging to clostridia XIVa and IV clusters. *PloS One* (2015) 10(9):e0137429. doi: 10.1371/journal.pone.0137429

5. Belkaid Y, Hand TW. Role of the microbiota in immunity and inflammation. *Cell* (2014) 157(1):121–41. doi: 10.1016/j.cell.2014.03.011

6. Atarashi K, Tanoue T, Shima T, Imaoka A, Kuwahara T, Momose Y, et al. Induction of colonic regulatory T cells by indigenous clostridium species. *Science* (2011) 331(6015):337–41. doi: 10.1126/science.1198469

7. Atarashi K, Tanoue T, Oshima K, Suda W, Nagano Y, Nishikawa H, et al. Treg induction by a rationally selected mixture of clostridia strains from the human microbiota. *Nature* (2013) 500(7461):232–6. doi: 10.1038/nature12331

8. Jangi S, Gandhi R, Cox LM, Li N, von Glehn F, Yan R, et al. Alterations of the human gut microbiome in multiple sclerosis. *Nat Commun* (2016) 7:12015. doi: 10.1038/ncomms12015

9. Cekanaviciute E, Yoo BB, Runia TF, Debelius JW, Singh S, Nelson CA, et al. Gut bacteria from multiple sclerosis patients modulate human T cells and exacerbate symptoms in mouse models. *Proc Natl Acad Sci U.S.A.* (2017) 114 (40):10713–8. doi: 10.1073/pnas.1711235114

10. Berer K, Gerdes LA, Cekanaviciute E, Jia X, Xiao L, Xia Z, et al. Gut microbiota from multiple sclerosis patients enables spontaneous autoimmune encephalomyelitis in mice. *Proc Natl Acad Sci U.S.A.* (2017) 114(40):10719–24. doi: 10.1073/pnas.1711233114

11. Belkaid Y, Harrison OJ. Homeostatic immunity and the microbiota. *Immunity* (2017) 46(4):562–76. doi: 10.1016/j.immuni.2017.04.008

12. Levy M, Kolodziejczyk AA, Thaiss CA, Elinav E. Dysbiosis and the immune system. *Nat Rev Immunol* (2017) 17(4):219–32. doi: 10.1038/nri.2017.7

13. Flannigan KL, Ngo VL, Geem D, Harusato A, Hirota SA, Parkos CA, et al. IL-17A-mediated neutrophil recruitment limits expansion of segmented filamentous bacteria. *Mucosal Immunol* (2017) 10(3):673–84. doi: 10.1038/mi.2016.80

14. Petnicki-Ocwieja T, Hrncir T, Liu YJ, Biswas A, Hudcovic T, Tlaskalova-Hogenova H, et al. Nod2 is required for the regulation of commensal microbiota in the intestine. *Proc Natl Acad Sci U.S.A.* (2009) 106(37):15813–8. doi: 10.1073/pnas.0907722106

15. Amulic B, Cazalet C, Hayes GL, Metzler KD, Zychlinsky A. Neutrophil function: from mechanisms to disease. *Annu Rev Immunol* (2012) 30:459–89. doi: 10.1146/annurev-immunol-020711-074942

16. Mantovani A, Cassatella MA, Costantini C, Jaillon S. Neutrophils in the activation and regulation of innate and adaptive immunity. *Nat Rev Immunol* (2011) 11(8):519–31. doi: 10.1038/nri3024

17. Kjeldsen L, Cowland JB, Borregaard N. Human neutrophil gelatinase-associated lipocalin and homologous proteins in rat and mouse. *Biochim Biophys Acta* (2000) 1482(1–2):272–83. doi: 10.1016/S0167-4838(00)00152-7

18. Goetz DH, Holmes MA, Borregaard N, Bluhm ME, Raymond KN, Strong RK. The neutrophil lipocalin NGAL is a bacteriostatic agent that interferes with siderophore-mediated iron acquisition. *Mol Cell* (2002) 10(5):1033–43. doi: 10.1016/S1097-2765(02)00708-6

19. Toyonaga T, Matsuura M, Mori K, Honzawa Y, Minami N, Yamada S, et al. Lipocalin 2 prevents intestinal inflammation by enhancing phagocytic bacterial clearance in macrophages. *Sci Rep* (2016) 6:35014. doi: 10.1038/srep35014

20. Singh V, Yeoh BS, Xiao X, Kumar M, Bachman M, Borregaard N, et al. Interplay between enterobactin, myeloperoxidase and lipocalin 2 regulates e. coli survival in the inflamed gut. *Nat Commun* (2015) 6:7113. doi: 10.1038/ncomms8113

21. Zhang Y, Foncea R, Deis JA, Guo H, Bernlohr DA, Chen X. Lipocalin 2 expression and secretion is highly regulated by metabolic stress, cytokines, and nutrients in adipocytes. *PloS One* (2014) 9(5):e96997. doi: 10.1371/journal.pone.0096997

22. Thorsvik S, Damas JK, Granlund AV, Flo TH, Bergh K, Ostvik AE, et al. Fecal neutrophil gelatinase-associated lipocalin as a biomarker for inflammatory bowel disease. *J Gastroenterol Hepatol* (2017) 32(1):128–35. doi: 10.1111/jgh.13598

23. Chassaing B, Srinivasan G, Delgado MA, Young AN, Gewirtz AT, Vijay-Kumar M. Fecal lipocalin 2, a sensitive and broadly dynamic non-invasive biomarker for intestinal inflammation. *PloS One* (2012) 7(9):e44328. doi: 10.1371/journal.pone.0044328

24. Zollner A, Schmiderer A, Reider SJ, Oberhuber G, Pfister A, Texler B, et al. Faecal biomarkers in inflammatory bowel diseases: Calprotectin versus lipocalin-2-a comparative study. *J Crohns Colitis* (2021) 15(1):43–54. doi: 10.1093/ecco-jcc/jjaa124

25. Kruger P, Saffarzadeh M, Weber AN, Rieber N, Radsak M, von Bernuth H, et al. Neutrophils: Between host defence, immune modulation, and tissue injury. *PloS Pathog* (2015) 11(3):e1004651. doi: 10.1371/journal.ppat.1004651

26. Fournier BM, Parkos CA. The role of neutrophils during intestinal inflammation. *Mucosal Immunol* (2012) 5(4):354–66. doi: 10.1038/mi.2012.24

27. Wera O, Lancellotti P, Oury C. The dual role of neutrophils in inflammatory bowel diseases. *J Clin Med 5* (2016) 5(12). doi: 10.3390/jcm5120118

28. Sadovnick AD, Paty DW, Yannakoulias G. Concurrence of multiple sclerosis and inflammatory bowel disease. *N Engl J Med* (1989) 321(11):762–3. doi: 10.1056/NEJM198909143211115

29. Kimura K, Hunter SF, Thollander MS, Loftus EV Jr, Melton LJ 3rd, O'Brien PC, et al. Concurrence of inflammatory bowel disease and multiple sclerosis. *Mayo Clinic Proc Mayo Clinic* (2000) 75(8):802–6. doi: 10.4065/75.8.802

30. Rang EH, Brooke BN, Hermon-Taylor J. Association of ulcerative colitis with multiple sclerosis. *Lancet* (1982) 2(8297):555. doi: 10.1016/S0140-6736(82)90629-8

31. Gupta G, Gelfand JM, Lewis JD. Increased risk for demyelinating diseases in patients with inflammatory bowel disease. *Gastroenterology* (2005) 129(3):819–26. doi: 10.1053/j.gastro.2005.06.022

32. Bernstein CN, Wajda A, Blanchard JF. The clustering of other chronic inflammatory diseases in inflammatory bowel disease: a population-based study. *Gastroenterology* (2005) 129(3):827–36. doi: 10.1053/j.gastro.2005.06.021

33. Kosmidou M, Katsanos AH, Katsanos KH, Kyritsis AP, Tsivgoulis G, Christodoulou D, et al. Multiple sclerosis and inflammatory bowel diseases: a systematic review and meta-analysis. *J Neurol* (2017) 264(2):254–9. doi: 10.1007/s00415-016-8340-8

34. Yang Y, Musco H, Simpson-Yap S, Zhu Z, Wang Y, Lin X, et al. Investigating the shared genetic architecture between multiple sclerosis and inflammatory bowel diseases. *Nat Commun* (2021) 12(1):5641. doi: 10.1038/s41467-021-25768-0

35. Duc D, Vigne S, Bernier-Latmani J, Yersin Y, Ruiz F, Gaia N, et al. Disrupting myelin-specific Th17 cell gut homing confers protection in an adoptive transfer experimental autoimmune encephalomyelitis. *Cell Rep* (2019) 29(2):378–90.e374. doi: 10.1016/j.celrep.2019.09.002

36. Nouri M, Bredberg A, Westrom B, Lavasani S. Intestinal barrier dysfunction develops at the onset of experimental autoimmune encephalomyelitis, and can be induced by adoptive transfer of auto-reactive T cells. *PloS One* (2014) 9(9):e106335. doi: 10.1371/journal.pone.0106335

37. Schnell A, Huang L, Singer M, Singaraju A, Barilla RM, Regan BML, et al. Stem-like intestinal Th17 cells give rise to pathogenic effector T cells during autoimmunity. *Cell* (2021) 184(26):6281–98.e6223. doi: 10.1016/j.cell.2021.11.018

38. Quandt JA, Huh J, Baig M, Yao K, Ito N, Bryant M, et al. Myelin basic protein-specific TCR/HLA-DRB5*01:01 transgenic mice support the etiologic role of DRB5*01:01 in multiple sclerosis. *J Immunol* (2012) 189(6):2897–908. doi: 10.4049/jimmunol.1103087

39. Thompson AJ, Banwell BL, Barkhof F, Carroll WM, Coetzee T, Comi G, et al. Diagnosis of multiple sclerosis: 2017 revisions of the McDonald criteria. *Lancet Neurol* (2018) 17(2):162–73. doi: 10.1016/S1474-4422(17)30470-2

40. Bankhead P, Loughrey MB, Fernandez JA, Dombrowski Y, McArt DG, Dunne PD, et al. QuPath: Open source software for digital pathology image analysis. *Sci Rep* (2017) 7(1):16878. doi: 10.1038/s41598-017-17204-5

41. Erben U, Loddenkemper C, Doerfel K, Spieckermann S, Haller D, Heimesaat MM, et al. A guide to histomorphological evaluation of intestinal inflammation in mouse models. *Int J Clin Exp Pathol* (2014) 7(8):4557–76.

42. Callahan BJ, McMurdie PJ, Rosen MJ, Han AW, Johnson AJ, Holmes SP. DADA2: High-resolution sample inference from illumina amplicon data. *Nat Methods* (2016) 13(7):581–3. doi: 10.1038/nmeth.3869

43. Caporaso JG, Kuczynski J, Stombaugh J, Bittinger K, Bushman FD, Costello EK, et al. QIIME allows analysis of high-throughput community sequencing data. *Nat Methods* (2010) 7(5):335–6. doi: 10.1038/nmeth.f.303

44. Yadav SK, Boppana S, Ito N, Mindur JE, Mathay MT, Patel A, et al. Gut dysbiosis breaks immunological tolerance toward the central nervous system during young adulthood. *Proc Natl Acad Sci U.S.A.* (2017) 114(44):E9318–27. doi: 10.1073/pnas.1615715114

45. Jiang W, Su J, Zhang X, Cheng X, Zhou J, Shi R, et al. Elevated levels of Th17 cells and Th17-related cytokines are associated with disease activity in patients with inflammatory bowel disease. *Inflamm Res* (2014) 63(11):943–50. doi: 10.1007/s00011-014-0768-7

46. Carlson M, Raab Y, Seveus L, Xu S, Hallgren R, Venge P. Human neutrophil lipocalin is a unique marker of neutrophil inflammation in ulcerative colitis and proctitis. *Gut* (2002) 50(4):501–6. doi: 10.1136/gut.50.4.501

47. Singh V, Yeoh BS, Chassaing B, Zhang B, Saha P, Xiao X, et al. Microbiota-inducible innate immune, siderophore binding protein lipocalin 2 is critical for intestinal homeostasis. *Cell Mol Gastroenterol Hepatol* (2016) 2(4):482–98.e486. doi: 10.1016/j.jcmgh.2016.03.007

48. Jarchum I, Liu M, Shi C, Equinda M, Pamer EG. Critical role for MyD88-mediated neutrophil recruitment during clostridium difficile colitis. *Infect Immun* (2012) 80(9):2989–96. doi: 10.1128/IAI.00448-12

49. Kvedaraite E, Lourda M, Idestrom M, Chen P, Olsson-Akefeldt S, Forkel M, et al. Tissue-infiltrating neutrophils represent the main source of IL-23 in the colon of patients with IBD. *Gut* (2016) 65(10):1632–41. doi: 10.1136/gutjnl-2014-309014

50. Walsham NE, Sherwood RA. Fecal calprotectin in inflammatory bowel disease. *Clin Exp Gastroenterol* (2016) 9:21–9. doi: 10.2147/CEG.S51902

51. Barry R, Ruano-Gallego D, Radhakrishnan ST, Lovell S, Yu L, Kotik O, et al. Faecal neutrophil elastase-antiprotease balance reflects colitis severity. *Mucosal Immunol* (2020) 13(2):322–33. doi: 10.1038/s41385-019-0235-4

52. Dziarski R, Park SY, Kashyap DR, Dowd SE, Gupta D. Pglyrp-regulated gut microflora prevotella falsenii, parabacteroides distasonis and bacteroides eggerthii enhance and alistipes finegoldii attenuates colitis in mice. *PloS One* (2016) 11(1):e0146162. doi: 10.1371/journal.pone.0146162

53. Lim SM, Kim DH. Bifidobacterium adolescentis IM38 ameliorates high-fat diet-induced colitis in mice by inhibiting NF-kappaB activation and lipopolysaccharide production by gut microbiota. *Nutr Res* (2017) 41:86–96. doi: 10.1016/j.nutres.2017.04.003

54. Vatn S, Carstens A, Kristoffersen AB, Bergemalm D, Casen C, Moen AEF, et al. Faecal microbiota signatures of IBD and their relation to diagnosis, disease phenotype, inflammation, treatment escalation and anti-TNF response in a European multicentre study (IBD-character). *Scand J Gastroenterol* (2020) 55(10):1146–56. doi: 10.1080/00365521.2020.1803396

55. Pryde SE, Duncan SH, Hold GL, Stewart CS, Flint HJ. The microbiology of butyrate formation in the human colon. *FEMS Microbiol Lett* (2002) 217(2):133–9. doi: 10.1111/j.1574-6968.2002.tb11467.x

56. Engels C, Ruscheweyh HJ, Beerenwinkel N, Lacroix C, Schwab C. The common gut microbe eubacterium hallii also contributes to intestinal propionate formation. *Front Microbiol* (2016) 7:713. doi: 10.3389/fmicb.2016.00713

57. Muller M, Hernandez MAG, Goossens GH, Reijnders D, Holst JJ, Jocken JWE, et al. Circulating but not faecal short-chain fatty acids are related to insulin sensitivity, lipolysis and GLP-1 concentrations in humans. *Sci Rep* (2019) 9(1):12515. doi: 10.1038/s41598-019-48775-0

58. Trend S, Leffler J, Jones AP, Cha L, Gorman S, Brown DA, et al. Associations of serum short-chain fatty acids with circulating immune cells and serum biomarkers in patients with multiple sclerosis. *Sci Rep* (2021) 11(1):5244. doi: 10.1038/s41598-021-84881-8

59. Calderon-Perez L, Gosalbes MJ, Yuste S, Valls RM, Pedret A, Llaurado E, et al. Gut metagenomic and short chain fatty acids signature in hypertension: a cross-sectional study. *Sci Rep* (2020) 10(1):6436. doi: 10.1038/s41598-020-63475-w

60. de la Cuesta-Zuluaga J, Mueller NT, Alvarez-Quintero R, Velasquez-Mejia EP, Sierra JA, Corrales-Agudelo V, et al. Higher fecal short-chain fatty acid levels are associated with gut microbiome dysbiosis, obesity, hypertension and cardiometabolic disease risk factors. *Nutrients* (2018) 11(1):51. doi: 10.3390/nu11010051

61. Sivaprakasam S, Bhutia YD, Yang S, Ganapathy V. Short-chain fatty acid transporters: Role in colonic homeostasis. *Compr Physiol* (2017) 8(1):299–314. doi: 10.1002/cphy.c170014

62. Thibault R, De Coppet P, Daly K, Bourreille A, Cuff M, Bonnet C, et al. Down-regulation of the monocarboxylate transporter 1 is involved in butyrate deficiency during intestinal inflammation. *Gastroenterology* (2007) 133(6):1916–27. doi: 10.1053/j.gastro.2007.08.041

63. Morton AM, Sefik E, Upadhyay R, Weissleder R, Benoist C, Mathis D. Endoscopic photoconversion reveals unexpectedly broad leukocyte trafficking to and from the gut. *Proc Natl Acad Sci U.S.A.* (2014) 111(18):6696–701. doi: 10.1073/pnas.1405634111

64. Pelletier M, Maggi L, Micheletti A, Lazzeri E, Tamassia N, Costantini C, et al. Evidence for a cross-talk between human neutrophils and Th17 cells. *Blood* (2010) 115(2):335–43. doi: 10.1182/blood-2009-04-216085

65. Kolaczkowska E, Kubes P. Neutrophil recruitment and function in health and inflammation. *Nat Rev Immunol* (2013) 13(3):159–75. doi: 10.1038/nri3399

66. Bennike TB, Carlsen TG, Ellingsen T, Bonderup OK, Glerup H, Bogsted M, et al. Neutrophil extracellular traps in ulcerative colitis: A proteome analysis of intestinal biopsies. *Inflamm Bowel Dis* (2015) 21(9):2052–67. doi: 10.1097/MIB.0000000000000460

67. Lin EY, Lai HJ, Cheng YK, Leong KQ, Cheng LC, Chou YC, et al. Neutrophil extracellular traps impair intestinal barrier function during experimental colitis. *Biomedicines* (2020) 8(8):275. doi: 10.20944/preprints202007.0130.v1

68. Dinallo V, Marafini I, Di Fusco D, Laudisi F, Franze E, Di Grazia A, et al. Neutrophil extracellular traps sustain inflammatory signals in ulcerative colitis. *J Crohns Colitis* (2019) 13(6):772–84. doi: 10.1093/ecco-jcc/jjy215

69. Anderson BM, Poole DP, Aurelio L, Ng GZ, Fleischmann M, Kasperkiewicz P, et al. Application of a chemical probe to detect neutrophil elastase activation during inflammatory bowel disease. *Sci Rep* (2019) 9(1):13295. doi: 10.1038/s41598-019-49840-4

70. Adeyemi EO, Hodgson HJ. Faecal elastase reflects disease activity in active ulcerative colitis. *Scand J Gastroenterol* (1992) 27(2):139–42. doi: 10.3109/00365529209165434

71. Morohoshi Y, Matsuoka K, Chinen H, Kamada N, Sato T, Hisamatsu T, et al. Inhibition of neutrophil elastase prevents the development of murine dextran sulfate sodium-induced colitis. *J Gastroenterol* (2006) 41(4):318–24. doi: 10.1007/s00535-005-1768-8

72. Langer-Gould A, Albers KB, Van Den Eeden SK, Nelson LM. Autoimmune diseases prior to the diagnosis of multiple sclerosis: a population-based case-control study. *Mult Scler* (2010) 16(7):855–61. doi: 10.1177/1352458510369146

73. Marrie RA, Reider N, Cohen J, Stuve O, Sorensen PS, Cutter G, et al. A systematic review of the incidence and prevalence of autoimmune disease in multiple sclerosis. *Mult Scler* (2015) 21(3):282–93. doi: 10.1177/1352458514564490

74. Lucke K, Miehlke S, Jacobs E, Schuppler M. Prevalence of bacteroides and prevotella spp. in ulcerative colitis. *J Med Microbiol* (2006) 55(Pt 5):617–24. doi: 10.1099/jmm.0.46198-0

75. Bloom SM, Bijanki VN, Nava GM, Sun L, Malvin NP, Donermeyer DL, et al. Commensal bacteroides species induce colitis in host-genotype-specific fashion in a mouse model of inflammatory bowel disease. *Cell Host Microbe* (2011) 9(5):390–403. doi: 10.1016/j.chom.2011.04.009

76. Rao M, Nelms BD, Dong L, Salinas-Rios V, Rutlin M, Gershon MD, et al. Enteric glia express proteolipid protein 1 and are a transcriptionally unique population of glia in the mammalian nervous system. *Glia* (2015) 63(11):2040–57. doi: 10.1002/glia.22876

77. Wunsch M, Jabari S, Voussen B, Enders M, Srinivasan S, Cossais F, et al. The enteric nervous system is a potential autoimmune target in multiple sclerosis. *Acta Neuropathol* (2017) 134(2):281–95. doi: 10.1007/s00401-017-1742-6

78. Berard JL, Zarruk JG, Arbour N, Prat A, Yong VW, Jacques FH, et al. Lipocalin 2 is a novel immune mediator of experimental autoimmune encephalomyelitis pathogenesis and is modulated in multiple sclerosis. *Glia* (2012) 60(7):1145–59. doi: 10.1002/glia.22342

79. Nam Y, Kim JH, Seo M, Kim JH, Jin M, Jeon S, et al. Lipocalin-2 protein deficiency ameliorates experimental autoimmune encephalomyelitis: the pathogenic role of lipocalin-2 in the central nervous system and peripheral lymphoid tissues. *J Biol Chem* (2014) 289(24):16773–89. doi: 10.1074/jbc.M113.542282

80. Jang E, Lee S, Kim JH, Kim JH, Seo JW, Lee WH, et al. Secreted protein lipocalin-2 promotes microglial M1 polarization. *FASEB J* (2013) 27(3):1176–90. doi: 10.1096/fj.12-222257

81. Al Nimer F, Elliott C, Bergman J, Khademi M, Dring AM, Aeinehband S, et al. Lipocalin-2 is increased in progressive multiple sclerosis and inhibits remyelination. *Neurol Neuroimmunol Neuroinflamm* (2016) 3(1):e191. doi: 10.1212/NXI.0000000000000191

82. Bi F, Huang C, Tong J, Qiu G, Huang B, Wu Q, et al. Reactive astrocytes secrete lcn2 to promote neuron death. *Proc Natl Acad Sci U.S.A.* (2013) 110 (10):4069–74. doi: 10.1073/pnas.1218497110

83. Moschen AR, Gerner RR, Wang J, Klepsch V, Adolph TE, Reider SJ, et al. Lipocalin 2 protects from inflammation and tumorigenesis associated with gut microbiota alterations. *Cell Host Microbe* (2016) 19(4):455–69. doi: 10.1016/j.chom.2016.03.007

84. Liu Z, Cominelli F, Di Martino L, Liu R, Devireddy N, Devireddy LR, et al. Lipocalin 24p3 induction in colitis adversely affects inflammation and contributes to mortality. *Front Immunol* (2019) 10:812. doi: 10.3389/fimmu.2019.00812

85. Kundu P, Ling TW, Korecka A, Li Y, D'Arienzo R, Bunte RM, et al. Absence of intestinal PPARgamma aggravates acute infectious colitis in mice through a lipocalin-2-dependent pathway. *PloS Pathog* (2014) 10(1):e1003887. doi: 10.1371/journal.ppat.1003887

86. Konikoff MR, Denson LA. Role of fecal calprotectin as a biomarker of intestinal inflammation in inflammatory bowel disease. *Inflamm Bowel Dis* (2006) 12(6):524–34. doi: 10.1097/00054725-200606000-00013

87. Manichanh C, Rigottier-Gois L, Bonnaud E, Gloux K, Pelletier E, Frangeul L, et al. Reduced diversity of faecal microbiota in crohn's disease revealed by a metagenomic approach. *Gut* (2006) 55(2):205–11. doi: 10.1136/gut.2005.073817

88. Choileain SN, Kleinewietfeld M, Raddassi K, Hafler DA, Ruff WE, Longbrake EE. CXCR3+ T cells in multiple sclerosis correlate with reduced diversity of the gut microbiome. *J Transl Autoimmun* (2020) 3:100032. doi: 10.1016/j.jtauto.2019.100032

89. Le Chatelier E, Nielsen T, Qin J, Prifti E, Hildebrand F, Falony G, et al. Richness of human gut microbiome correlates with metabolic markers. *Nature* (2013) 500(7464):541–6. doi: 10.1038/nature12506

90. Zeng Q, Junli G, Liu X, Chen C, Sun X, Li H, et al. Gut dysbiosis and lack of short chain fatty acids in a Chinese cohort of patients with multiple sclerosis. *Neurochem Int* (2019) 129:104468. doi: 10.1016/j.neuint.2019.104468

91. iMSMS Consortium Gut microbiome of multiple sclerosis patients and paired household healthy controls reveal associations with disease risk and course. *Cell* (2022) 185(19):3467–3486 e3416 doi: 10.1016/j.cell.2022.08.021

92. Durand GA, Pham T, Ndongo S, Traore SI, Dubourg G, Lagier JC, et al. Blautia massiliensis sp. nov., isolated from a fresh human fecal sample and emended description of the genus blautia. *Anaerobe* (2017) 43:47–55. doi: 10.1016/j.anaerobe.2016.12.001

frontiers | Frontiers in Immunology

TYPE Original Research
PUBLISHED 09 November 2022
DOI 10.3389/fimmu.2022.1027158



OPEN ACCESS

EDITED BY
Mei-Ping Ding,
Zhejiang University, China

REVIEWED BY
Li Du,
Beijing Tiantan Hospital, Capital Medical University, China
Lei Wu,
First Affiliated Hospital of Chinese PLA General Hospital, China

*CORRESPONDENCE
Hongyu Zhou
zhouhy@scu.edu.cn
Mu Yang
mu.yang@uestc.edu

†These authors have contributed equally to this work and share first authorship

SPECIALTY SECTION
This article was submitted to Multiple Sclerosis and Neuroimmunology, a section of the journal Frontiers in Immunology

RECEIVED 24 August 2022
ACCEPTED 21 October 2022
PUBLISHED 09 November 2022

CITATION
Shi Z, Du Q, Wang X, Wang J, Chen H, Lang Y, Kong L, Luo W, Yang M and Zhou H (2022) Granzyme B in circulating CD8+ T cells as a biomarker of immunotherapy effectiveness and disability in neuromyelitis optica spectrum disorders.
*Front. Immunol.* 13:1027158.
doi: 10.3389/fimmu.2022.1027158



# Granzyme B in circulating CD8+ T cells as a biomarker of immunotherapy effectiveness and disability in neuromyelitis optica spectrum disorders

Ziyan Shi[1†], Qin Du[1†], Xiaofei Wang[1], Jianchen Wang[1], Hongxi Chen[1], Yanling Lang[1], Lingyao Kong[1], Wenqin Luo[1], Mu Yang[2,3*] and Hongyu Zhou[1*]

[1]Department of Neurology, West China Hospital, Sichuan University, Chengdu, China, [2]Centre for Translational Research in Cancer, Sichuan Cancer Hospital & Institute, Chengdu, China, [3]School of Medicine, University of Electronic Science and Technology of China, Chengdu, China

**Background and objective:** Neuromyelitis optica spectrum disorders (NMOSD) are chronical inflammatory demyelinating diseases of the central nervous system (CNS) and the underlying mechanism remains unclear. Several recent studies have demonstrated that T cells play a pivotal role in the pathogenesis of NMOSD.In this study, we investigated CD8+ T cell phenotypes and levels of the cytotoxic protein granzyme B (GzmB), as well as their potential clinical application in NMOSD.

**Methods:** In this study, 90 peripheral blood samples were collected from 59 NMOSD patients with seropositive anti-aquaporin-4 (AQP4) antibodies and 31 sex- and age-matched healthy donors (HDs). Flow cytometry was used to detect circulating levels of GzmB and CD8+ T cell subpopulations, including naïve ($T_N$, CCD7+CD45RA+), central memory ($T_{CM}$, CCD7+CD45RA-), effector memory ($T_{EM}$, CCD7-CD45RA-), terminal differentiation effector memory cells ($T_{EMRA}$, CCD7-CD45RA+) in both groups. The associations between GzmB levels in CD8+T cells and clinical characteristics of NMOSD were evaluated.

**Results:** NMOSD patients exhibited significantly decreased proportions of CD8+$T_N$ cells and increased proportions of highly differentiated CD8+T cells ($T_{EMRA}$) compared with HDs. In addition, levels of GzmB in CD8+ T cells were markedly higher in NMOSD patients than in HDs. Moreover, we observed that high proportions of GzmB-expressing CD8+ T cells were more common in patients with a poor response to immunotherapies, and showed a good potential to distinguish poor responders from responders (ACU=0.89). Clinical correlation analysis indicated that high levels of GzmB in CD8+ T cells were not only related to severe disability but also significantly associated with increased serum levels of neurofilament light (NFL) and glial fibrillary acidic protein (GFAP). Multivariate linear regression analyses further suggested that GzmB expression in CD8+ T cells was predominantly associated with disability

and immunotherapy effectiveness in NMOSD, independent of the sex, age, and disease phase. Transcription factor T-bet in CD8+ T cells were also significantly elevated in NMOSD and were associated with increasing number of circulating CD8+$T_{EMRA}$ cells and GzmB-expressing CD8+T cells.

**Conclusions:** Our study support the involvement of GzmB-expressing CD8+ T cells in the inflammatory response in patients with NMOSD and provide a potential biomarker for disease immunotherapy effectiveness and disability progression.

KEYWORDS

**neuromyelitis optica spectrum disorders, NMOSD, granzyme B, GzmB, CD8, T cells, biomarker**

## Introduction

Neuromyelitis optica spectrum disorders (NMOSDs) are inflammatory demyelinating diseases of the central nervous system (CNS) characterized by acute optic neuritis and transverse myelitis (1). Most cases are caused by serum pathogenic anti-aquaporin-4 (AQP4) antibodies that attack astrocytes of the optic nerve and spinal cord. Recurrence and disability rates are high in NMOSD patients, 90% of whom relapse within 3 years, and more than half of patients develop irreversible visual and/or motor disability within 5 years without treatment (2, 3). Numerous studies have shown that conventional immunosuppressants and immunomodulators can reduce the annual relapse rate and risk of disability in NMOSD patients; however, more than one third of patients still experience recurrent attacks and disability progression after immunotherapy (4, 5). Notably, three emerging therapies (eculizumab, satralizumab, and inebilizumab) have been demonstrated to be beneficial in preventing relapse of NMOSD in randomized controlled trials (6). Nevertheless, there is considerable heterogeneity in the response of different individuals to different therapies and a lack of biomarkers for predicting the efficacy of NMOSD drugs. Thus, there is an urgent need to explore the mechanisms underlying the NMOSD and identify new therapeutic targets and biomarkers for predicting disease progression.

T cells play a crucial role in the pathogenesis of NMOSD. Serum autoantibodies against the water channel protein aquaporin-4 (AQP4) are T-cell-dependent antibodies in most NMOSD patients. Autoreactive T cells have been observed in the peripheral blood and within the inflammatory CNS lesions (7–9). Furthermore, animal models have suggested that autoreactive T cells are sufficient to induce NMO-like lesions in the absence of anti-AQP4 antibodies (10), indicating that autoreactive T cells play a pivotal role in NMOSD pathogenesis. Thus, understanding the role of T cells and related cytokines in NMOSD may aid in identifying potential treatment targets and novel biomarkers for predicting disease progression. Previous studies of T cells in NMOSD have mainly focused on CD4+ T cells, while the key role of CD8+ T cells has been largely overlooked. Increasing evidence suggests that cytotoxic CD8+ T cells play an important role in CNS autoimmune diseases including multiple sclerosis (MS), Susac syndrome, and NMOSD (11–13).

In addition to secreting pro-inflammatory cytokines that promote CNS inflammation, cytotoxic CD8+ T cells can also induce target cell death by releasing serine protease granzyme B (GzmB). Previous studies have indicated that cytotoxic CD8+ T cell infiltration in the brain lesions of MS patients mediates axonal injury and neuronal death, and that inhibition of this damage induces neuroprotection *in vitro* and *in vivo* (14, 15). Similarly, researchers have observed that suppression of GzmB expression can effectively reduce inflammatory lesions and disease severity in patients with autoimmune skin diseases (16, 17). These findings support the notion that cytotoxic CD8+T cells expressing GzmB promote autoimmune and neurological processes, highlighting their potential as a therapeutic target and biomarker of disease progression. However, the regulatory mechanisms underlying phenotypic differentiation and functional expression of CD8+ T cells remain unclear.

T-bet is a key transcription factor that regulates CD8+ T-cell activation and differentiation (18). In chronic infection, T-bet promotes CD8+ T cell transfer from central memory ($T_{CM}$) to effector memory ($T_{EM}$) and terminally differentiated effector memory ($T_{EMRA}$) cells and sustains virus-specific CD8+ T cell responses, including increases in the expression of cell lysis-related protein (GzmB) and the pro-inflammatory cytokines interferon γ (IFNγ) and tumor necrosis factor α (TNFα) (19, 20). Although the regulation of CD8+ T phenotypic differentiation

and functional expression by T-bet has been studied in the field of viral infection and cancers, knowledge of its regulatory role in NMOSD remains unknown (21, 22).

Previously, we observed increasing proportions of activated CD8+ T cells in the peripheral blood of NMOSD patients, along with elevated levels of INFγ and TNFα, indicating that CD8+ T cells may be involved in the peripheral inflammation associated with NMOSD (13). In this study, we further investigated the potential clinical value of CD8+ T cell phenotypes and levels of GzmB in NMOSD patients. Our findings indicated that the proportions of CD8+ $T_{EMRA}$ cells in the peripheral blood were significantly increased in NMOSD patients who also exhibited high levels of the cytotoxic protein GzmB. Notably, these increased proportions of GzmB+CD8+ T cells were significantly associated with Expanded Disability Status Scale (EDSS) scores, serum neurofilament light (NFL), serum glial fibrillary acidic protein (GFAP) levels, as well as immunotherapy efficacy in NMOSD patients. In conclusion, our findings suggest GzmB+CD8+ T cells as a potential biomarker treatment effectiveness and disability in NMOSD patients.

# Materials and methods

## Participants

This study was approved by the Medical Ethics Committee of the West China Hospital, Sichuan University and all participants given informed consent prior to their inclusion in this study. Patients diagnosed with NMOSD were recruited from the West China Hospital of Sichuan University between January 2021 and December 2021 (n=59). All patients met the 2015 diagnostic criteria and were seropositive for anti-AQP4 antibodies (EUROIMMUN AG, Luebeck, Germany) (23). Sex- and age-matched healthy donors (HDs) were also enrolled (n=31). EDSS scores were used to assess disability status in each patient with NMOSD (24). The acute phase was defined as within 2 months of onset, while the remission phase was defined as greater than 2 months after attack. Detailed clinical characteristics are summarized in Table 1, including age, sex, disease phases, EDSS scores, and treatments. NMOSD patients were divided into a response group and a poor response group according to their response to immunosuppressive or immunomodulatory therapies (IMT) during remission (treatments lasting for at least 12 months). A response to IMT was defined as relapse free or only 1 mild relapse during treatment, while a poor response to IMT was defined as ≥ 2 relapses or 1 severe relapse (25).

## Flow cytometry

Peripheral blood samples from patients with NMOSD and HDs were prepared as single-cell suspensions and stained for flow cytometry, as previously described (13). Single-cell suspensions were stained with the selected antibodies for 30 min after incubation with Human TruStain FcX™ (BioLegend) at 4°C. Anti-human CD3-APC (OKT3), CD8a-PerCP (RPA-T8), CD45RA-PE (HI100), and CCR7-APC/Cyanine7 (G043H7) (BioLegend) were used to label the surface markers of the CD8+ T cells. Granzyme B-FITC (QA16A02) and Tbet-PE/Cyanine7 (4B10) (BioLegend) were used for intracellular staining after fixation and permeabilization with the Foxp3/Transcription factor staining buffer (Invitrogen). Samples were acquired using an FACS Canto II flow cytometer (BD Biosciences), and the original data analysis was performed

TABLE 1 Demographic and clinical characteristics of participants.

| | HD (n=31) | NMOSD (n=59) | P values |
|---|---|---|---|
| Gender, Female (%) | 26 (84%) | 52 (90%) | 0.745 |
| Age, mean ± SD, years | 42.6 ± 13.29 | 45.87 ± 14.53 | 0.250 |
| EDSS scores, median (range) | | 4 (0-8.5) | |
| Disease phases, n | | | |
| Relapse (≤2 months) | | 27 | |
| Remission (>2months) | | 32 | |
| Treatments, n | | | |
| Untreated | | 12 | |
| Steroids | | 8 | |
| IMT (AZA/MMF/RTX)[a] | | 39 (4/27/8) | |
| Responders (AZA/MMF/RTX) | | 14 (2/11/1) | |
| Poor responders (AZA/MMF/RTX) | | 12 (0/7/5) | |

HD, healthy donors; NMOSD, neuromyelitis optica spectrum disorders; EDSS, Expanded Disability Status Scale; IMT, immunosuppressive or immunomodulatory therapies; AZA, azacytidine, 2mg/kg per day; MMF, mycophenolate mofetil, 20mg/kg per day; RTX, rituximab, 500-1000mg per 6 months. aExclude 8 NMOSD patients with treatment less than 1 year, and 5 NMOSD patients with irregular treatment.

using FlowJo v10 (BD Biosciences).

## Neurofilament light (NFL) and GFAP detection

Serum samples were centrifuged at 2,000 *g* for 10 min at room temperature and stored at -80°C for later use. Serum levels of NFL and GFAP were measured in patients with NMOSD (n=18) using a commercial Simoa Human Neurology 2-Plex B assay (N2PB) kit in accordance with the manufacturer's protocol (serum 1:4 dilution) (26).

## Statistical analysis

Statistical analyses were performed using GraphPad Prism V8.0 (GraphPad Software, San Diego, California, USA) and/or SPSS software V25.0 (IBM Corp., Armonk, NY, USA). Continuous variables are described as mean with standard deviation (SD) and/or median with range. Categorical variables are presented as numbers and percentages. The Mann–Whitney U-test was used to compare continuous variables between two groups, while the Kruskal–Wallis test with Dunn's test for multiple comparisons was used for comparisons among three or more groups. The chi-square test was used to compare categorical variables between groups. Comparisons of CD8+ T cell subpopulations and cytotoxic function between the groups were adjusted for age and sex using linear regression models. Receiver operating characteristic (ROC) curves were performed to evaluate the accuracy of the GzmB-expressing CD8+T cell subsets in distinguishing immunotherapies responders from poor responders. Spearman correlation analysis was used to evaluate the correlation of GzmB levels in CD8+ T cell subsets with EDSS score, serum NFL, and GFAP. Multivariate linear regression analysis was used to estimate the correlation between levels of GzmB in CD8+ T cell subsets and clinical characteristics, including sex, age, EDSS scores, disease phase, and treatments. The level of statistical significance was defined as a two-tailed p value $< 0.05$.

# Results

## Demographic and clinical characteristics of participants

The demographic and clinical characteristics of the participants are summarized in Table 1. A total of 90 peripheral blood samples were collected from 59 patients with NMOSD and 31 HDs. There were no significant differences in sex or age between the NMOSD and HD groups. During sample collection, 12 patients with NMOSD were admitted without any immunotherapy, eight patients were treated with glucocorticoids (GC), and 39 patients were treated with IMT (azacytidine [AZA], n=4; mycophenolate mofetil [MMF], n=27; and rituximab [RTX], n=8). Among the patients who received IMT, 26 received treatment for more than 1 year. These patients were further divided into responder (n=14) and poor responder (n=12) according to their response to IMT.

## Circulating CD8+T cells exhibit high differentiation and increased GzmB expression in patients with NMOSD

We compared the memory and/or effector characteristics of peripheral CD8+ T cells in the NMOSD and HD groups based on the expression of CCR7,CD45RA, and GzmB (27) (Figure 1). Based on the gating strategy of flow cytometry, CD8+ T cells were divided into four subgroups: naïve ($T_N$, CCR7+CD45RA+), central memory ($T_{CM}$, CCR7+CD45RA-), effector memory ($T_{EM}$, CCR7-CD45RA-), and terminally differentiated effector memory ($T_{EMRA}$, CCR7-CD45RA+) cells (Figure 1A). Our results revealed that patients with NMOSD had significantly lower proportions of CD8+ $T_N$ cells than HDs (median, 24.9% vs. 36.5%, P=0.0185) (Figure 1C). In contrast, the highly differentiated CD8+ T cell subpopulation (CD8+ $T_{EMRA}$) was more strongly expressed in patients with NMOSD than in HDs (median: 56.9% vs. 42.3%, P=0.0019) (Figure 1D). However, the subpopulations of $T_{CM}$ and $T_{EM}$ were comparable between patients with NMOSD and HDs (Figures 1B, E). These findings indicate that highly differentiated CD8+ T cells are more common in the blood of patients with NMOSD than in that of HDs.

To explore the cytotoxic function of CD8+ T cells in each group, we further investigated the expression of the cytolytic protein GzmB in CD8+T cells and their effector subsets ($T_{EM}$ and $T_{EMRA}$) (Figure 1F). Compared with HDs, patients with NMOSD exhibited significantly increased proportions of GzmB +CD8+ T cells (50.2% vs. 27.1%, P<0.0001) and GzmB+CD8+ $T_{EMRA}$ cells (64% vs. 49.4%, P=0.0062) (Figures 1G, I). Nevertheless, levels of GzmB+CD8+ $T_{EM}$ cells did not significantly differ between the NMOSD and HD groups (Figure 1H). Our data further demonstrated that CD8+ T cells in the blood of patients with NMOSD are not only highly differentiated but also express a large amount of GzmB, suggesting that CD8+ T cells are involved in the peripheral inflammation associated with NMOSD.

## GzmB-expressing CD8+ T cells as potential biomarkers for predicting the effectiveness of immunotherapies in patients with NMOSD

To assess the effect of immunotherapies on levels of GzmB expression in CD8+ T cells, we divided patients with NMOSD

10.3389/fimmu.2022.1027158

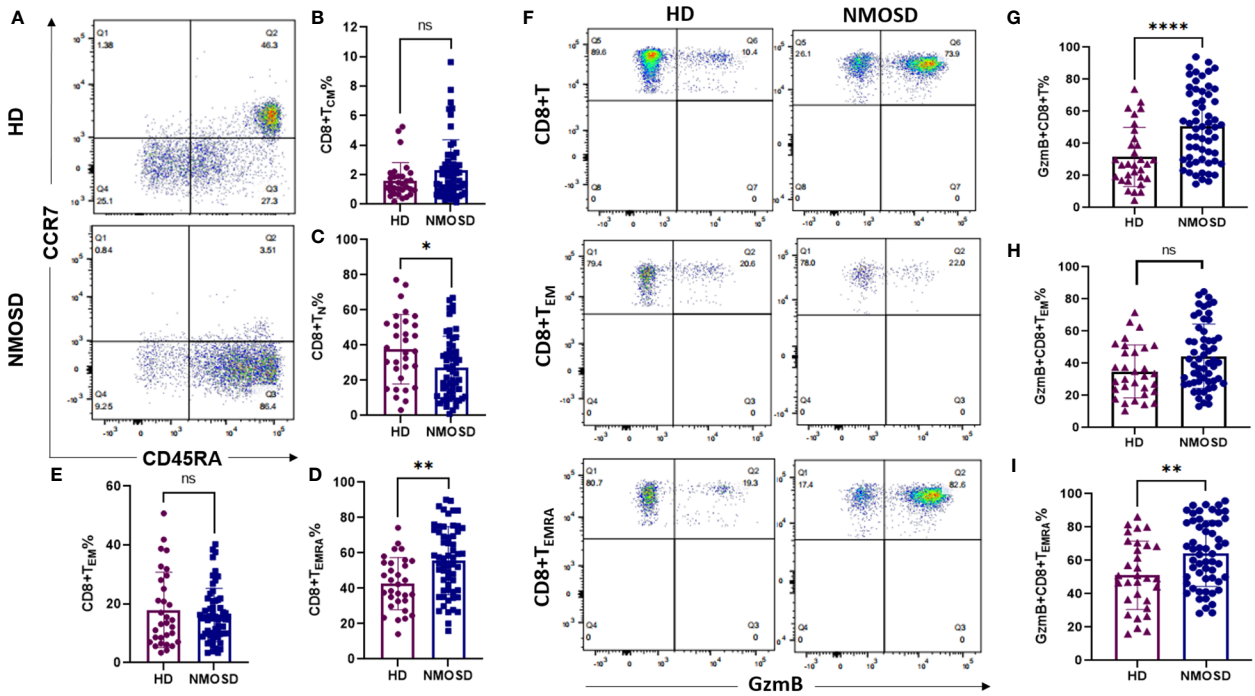


FIGURE 1
Circulating CD8+ T cell subpopulations and GzmB expression in patients with NMOSD and HD. Peripheral blood was collected from healthy donors **(HD)** (n=31) and patients with neuromyelitis optica spectrum disorder (NMOSD) (n=59). **(A)** The flow cytometric gating strategy for CD8+ T cell subpopulations. Central memory ($T_{CM}$, CCD7+CD45RA-), naïve ($T_N$, CCD7+CD45RA+), effector memory ($T_{EM}$, CCD7-CD45RA-), and terminal differentiation effector memory T cells ($T_{EMRA}$, CCD7-CD45RA+). **(B–E)** Comparison of CD8+ T cell subsets between HD and NMOSD. **(F–I)** Proportions of GzmB-expressing CD8+ T, CD8+ $T_{EM}$, and CD8+ $T_{EMRA}$ cells were further measured by flow cytometry. ****P<0.0001, **P < 0.01, *P < 0.05 and ns (not significant) by Mann–Whitney U-test.

into untreated patients (n=12), responders to immunotherapies (n=14), and poor responders to immunotherapies (n=12). The proportions of GzmB+CD8+ T cells in untreated patients and poor responders were comparable, and both were significantly higher than those in responders (P=0.0033 and P=0.0002, respectively) (Figure 2A). Similarly, proportions of GzmB +CD8+ $T_{EMRA}$ cells were also significantly higher in poor responders than in responders, but not those in untreated patients (Figure 2C). No significant differences in the proportions of GzmB+CD8+ $T_{EM}$ cells were observed among the three groups (Figure 2B). In addition, we further compared the proportions of circulating GzmB-expressing CD8+T cells between responders to MMF (n=11) and poor responders to MMF (n=7), and showed that proportions of GzmB+ CD8+T cells were significantly higher in poor responders (P=0.034) (Supplementary Figure 1A). GzmB+CD8+$T_{EM}$ and GzmB +CD8+$T_{EMRA}$ showed the similar trends, although there was no statistically significant difference (Supplementary Figures 1B, C).

Given that GzmB levels in CD8+ T cells significantly differed between patients with good and poor responses to immunotherapies, we next performed a receiver operating characteristic (ROC) curve analysis to assess the percentage of GzmB+CD8+ T cells as a potential biomarker for differentiating the response to immunotherapies. As expected, the percentage of GzmB+CD8+ T cells exhibited good diagnostic potential in distinguishing poor responders from responders (area under the curve [AUC]=0.89, P=0.001), whereas GZMB+CD8+ $T_{EMRA}$ had a relatively lower AUC of 0.86 (P=0.002) (Figure 2D). Subsequently, ROC curve analysis further indicated that the cut-off values for %GzmB+CD8+ T cells and %GZMB+CD8+ $T_{EMRA}$ cells were 49.65% and 71.55%, respectively, and that 75% of the patients above the cut-off value exhibited poor responses to immunotherapies (Figure 2E). Our data suggest that high levels of GzmB in CD8+ T cells are associated with a poor response to immunotherapies in patients with NMOSD, highlighting their potential as a biomarker for predicting the effectiveness of immunotherapies.

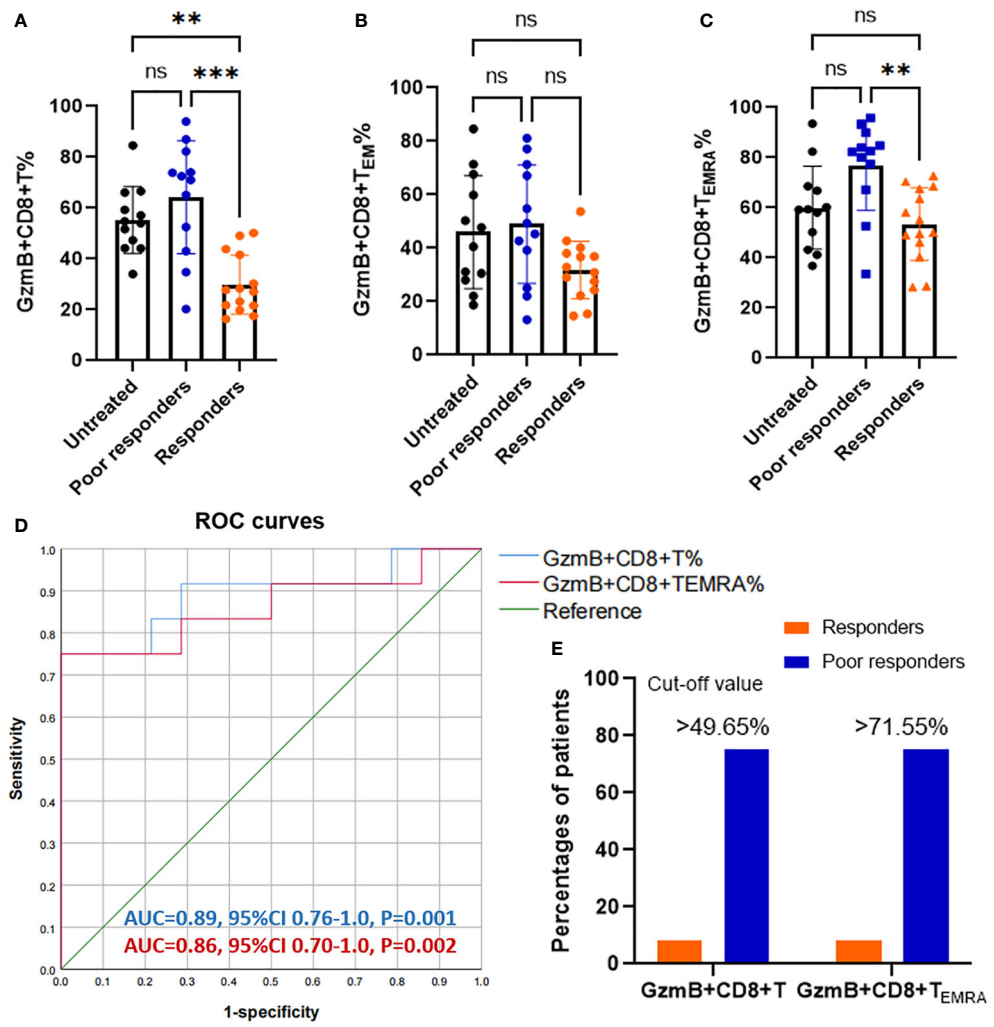


FIGURE 2
Increasing proportions of GzmB-expressing CD8+ T cells in poor responders with NMOSD. **(A–C)** Patients with neuromyelitis optica spectrum disorder (NMOSD) were divided into three groups according to the response to immunotherapies, including untreated (NT) patients (n=12), responders (n=14), and poor responders (n=12). Poor responders exhibited a significant increase in GzmB+CD8+ T% **(A)** and GzmB+CD8+ $T_{EMRA}$% **(C)**, but not in GzmB+CD8+ $T_{EM}$% **(B)**. **(D)** Receiver operating characteristic (ROC) curve for evaluating the diagnostic sensitivity and specificity of GzmB-expressing CD8+ T cells in responders and poor responders. Diagnostic accuracy was assessed based on the area under the curve (AUC). **(E)** Percentages of patients with levels of GzmB-expressing CD8+ T cells over the cut-off value in responders and poor responders. GzmB: granzyme B **P<0.01, ***P<0.001, and ns (not significant) by Kruskal-Wallis test with Dunn's multiple comparisons test.

## High proportions of GzmB-expressing CD8+ T cells are associated with disability in patients with NMOSD

Because GzmB levels in peripheral CD8+ T cells were significantly increased in patients with NMOSD, we explored whether high levels of GzmB play an active role in the disease process. First, we examined the relationship between disability (EDSS scores) and the proportions of GzmB+CD8+ T cell subsets in the NMOSD group (n=59). Spearman correlation analysis indicated that EDSS scores were moderately correlated with the proportions of GzmB+CD8+ T cells in patients with NMOSD (r=0.476, P<0.001)(Figure 3A), and similar relationships were also observed in GzmB+CD8+ $T_{EM}$ and GzmB+CD8+ $T_{EMRA}$ subpopulations (Figures 3B, C). Subsequently, we further explored the correlation between GzmB expressions of CD8+T cells and disability under different treatment conditions (Figure 3D–F). As results, we found a significant association between proportions of GzmB +CD8+ T cells and EDSS scores mainly in the poor-response group (r=0.682, P=0.013), and the same trend was observed in untreated patients, although the difference did not reach statistical significance (r=0.600, P=0.055) (Figure 3D). However, we did not find this association in response group,

10.3389/fimmu.2022.1027158

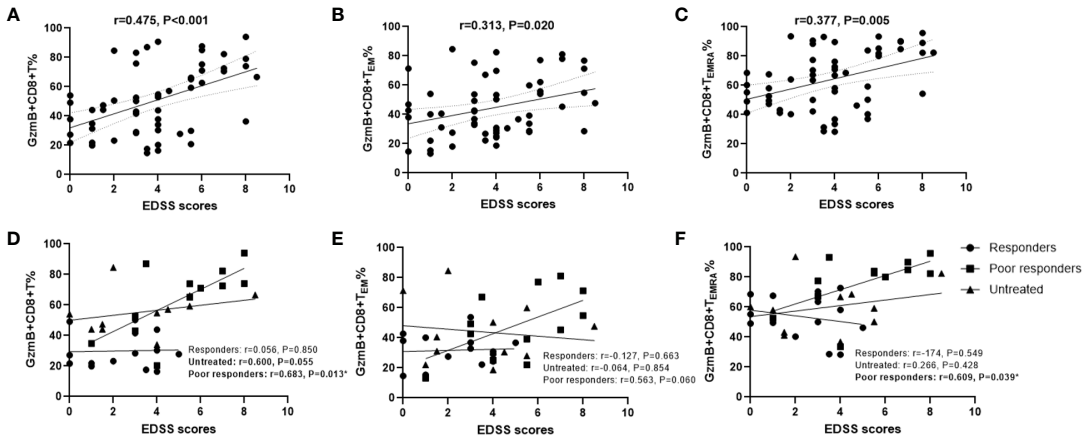


FIGURE 3
High proportions of GzmB-expressing CD8+ T cells are associated with disability in patients with NMOSD. **(A–C)** Correlation between Expanded Disability Status Scale (EDSS) scores and the percentages of GzmB+CD8+ T cells **(A)**, GzmB+CD8+ $T_{EM}$ cells **(B)**, and GzmB+CD8+ $T_{EMRA}$ cells **(C)** (Spearman correlation analysis). **(D–F)** Correlation analysis between EDSS scores and GzmB-expressing CD8+ T cell subpopulations according to the different immunotherapies and response, including responders group (n=14), untreated group (n=12), and poor responders (n=12) (Spearman correlation analysis). GzmB: granzyme **(B)** ns (not significant) by Mann–Whitney U-test. * indicates statistical significance (P<0.05).

suggesting that effective immunotherapy may inhibit GzmB expression in CD8+T cells, thereby eliminating the correlation between GzmB levels and disability in NMOSD.

Next, we evaluated the association between the clinical characteristics of NMOSD and GzmB expression in circulating CD8+ T cells and their effector subsets ($T_{EM}$ and $T_{EMRA}$) using multivariate linear regression models. In the NMOSD cohort, the proportion of GzmB+CD8+ T cells was independently associated with EDSS scores (β=4.47, P=0.005) and treatments (β=-10.01, P=0.010) (Table 2). However, no significant correlations were observed between GzmB+CD8+ T cells and sex, age, or disease stage. In the analysis of GzmB expression levels in effector subsets of CD8+ T cells, we found that the proportion of Gzmb+CD8+ $T_{EMRA}$ cells exhibited a trend of positive correlation with EDSS scores (β=3.23, P=0.056) (Table 2). These results indicate that levels of GzmB expression in CD8+ T cells are not only closely related to disability but are also influenced by immunotherapie.

Increased serum NFL and GFAP concentrations are correlated with CNS damage and have been regarded as biomarkers of disease activity and disability in patients with NMOSD (26). Therefore, serum samples and PBMC were simultaneously collected from 18 patients with NMOSD to evaluate the relationship between GzmB expression in CD8+ T cells and serum levels of NFL and GFAP. The mean concentrations and standard deviation (SD) of serum NFL and

TABLE 2 Associations between GzmB levels in CD8+ T subpopulations and clinical characteristics of NMOSD patients.

| | GzmB+CD8+T | | | GzmB+CD8+$T_{EM}$ | | | GzmB+CD8+$T_{EMRA}$ | | |
|---|---|---|---|---|---|---|---|---|---|
| | β | 95% CI | P values | β | 95% CI | P values | β | 95% CI | P values |
| Sex | | | | | | | | | |
| Male | Reference | | | | | | | | |
| Female | -8.21 | -22.38,5.96 | 0.246 | 0.10 | -16.70,16.90 | 0.991 | -7.74 | -23.34,7.85 | 0.319 |
| Age, years | 0.18 | -0.30,0.66 | 0.443 | -0.07 | -0.64,0.50 | 0.812 | 0.18 | -0.35,0.71 | 0.486 |
| Disease phases | | | | | | | | | |
| Remission | Reference | | | | | | | | |
| Relapse | -5.88 | -18.62,6.85 | 0.354 | 2,72 | -12.37,17.82 | 0.716 | -3.67 | -17.68,10.34 | 0.597 |
| EDSS scores | 4.47 | 1.46,7.48 | **0.005** | 2.25 | -0.1.32,5.81 | 0.209 | 3.23 | -0.08, 6.54 | 0.056 |
| Treatments | -10.01 | -17.40,-2.62 | **0.010** | -5.14 | -13.90,3.62 | 0.240 | -0.83 | -8.96,7.30 | 0.836 |

1=Untreated, 2=Poor responders, 3=Responders

NMOSD, neuromyelitis optica spectrum disorders; EDSS, Expanded Disability Status Scale. The F values and P-values of multivariate linear regression models for GzmB+CD8+T (F=7.26, P<0.001), GzmB+CD8+TEM (F=1.183, P=0.340), and GzmB+CD8+TEMRA (F=2.111, P=0.091). The bold indicates statistical significance (P<0.05).

GFAP were 16.6 ± 14.87 pg/mL and 97.78 ± 31.83 pg/mL, respectively. Correlation analyses revealed that serum NFL levels were positively associated with %GzmB+CD8+ T cells (r=0.515, P=0.029) (Figure 4A), but not with %GzmB+CD8+ $T_{EM}$ cells or %GzmB+CD8+ $T_{EMRA}$ cells (Figures 4B, C). Moreover, serum GFAP levels were positively correlated not only with %GzmB +CD8+ T cells (r=0.505, P=0.033), but also with %GzmB+CD8+ $T_{EMRA}$ cells (r=0.523, P=0.026), although there was no significant correlation with %GzmB+CD8+ $T_{EM}$ cells (Figures 4D–F). These findings further support our hypothesis that high GzmB expression in CD8+ T cells is closely related to disease progression and may be used as a peripheral biomarker of CNS injury in NMOSD.

## Up-regulation of T-bet is associated with increased levels of GzmB in circulating CD8+ T cells

Transcription factor T-bet plays an important role in the activation and functional expression of CD8+ T cells. In this study, we investigated whether high GzmB expression in CD8+ T cells is associated with the un-regulation of the transcription factor T-bet in patients with NMOSD. Flow cytometry analysis was performed to detect the expression of T-bet in CD8+ T cells in patients with NMOSD and HDs (Figure 5A). Compared with HDs, patients with NMOSD exhibited a significant increase in the percentage of T-bet+CD8+ T cells (24.8% vs. 41.25%, P=0.015) (Figure 5B). Furthermore, patients who responded to immunotherapies exhibited significantly lower percentages of T-bet+CD8+ T cells than poor responders (29.12% vs. 56.85%, P=0.005), while no significant difference was observed between untreated patients and poor responders (Figure 5C). Further correlation analysis revealed that T-bet+CD8+ T cell were significantly related to highly differentiated CD8+T cell subpopulations ($T_{EMRA}$) (r=0.744, P<0.0001) (Figure 5D) and GzmB+CD8+ T cells (r=0.765, P<0.0001) (Figure 5E).

These findings suggest that levels of T-bet+CD8+ T cells are increased in the peripheral blood in patients with NMOSD and are associated with hyper differentiation and enhanced cytotoxic function of CD8+ T cells. Thus, inhibiting CD8+ T cell activation and cytotoxicity may reduce peripheral inflammatory responses in patients with NMOSD.

# Discussion

It is widely accepted that autoreactive T cells are activated in the periphery and migrate to the CNS through the blood–brain barrier (BBB) to participate in CNS inflammatory demyelination (28). Although previous studies on CNS autoimmune diseases have mainly focused on CD4+ T cells, histopathological findings from autopsy and biopsy studies suggest that CD8+ T cells are the predominant immune cells infiltrating CNS lesions and exhibit tissue-resident memory and cytotoxicity (29, 30). Our previous study found that circulating CD8+ T cells were

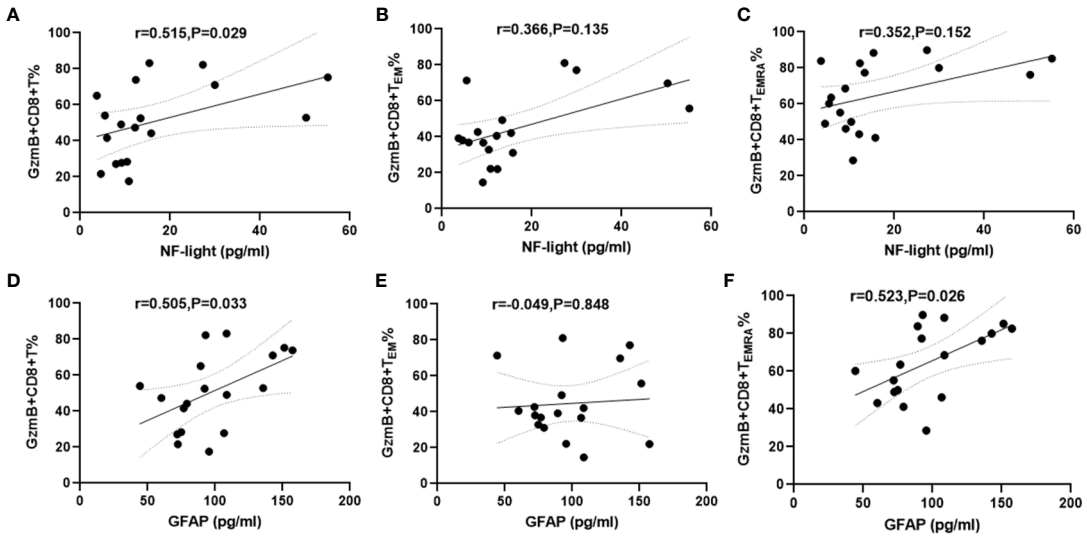


FIGURE 4
Positive correlation between proportions of GzmB+CD8+ T cells and serum NFL and GFAP levels in patients with NMOSD. **(A–C)** Association between the proportion of GzmB-expressing CD8+ T cells and serum NFL (n=18). **(D–F)** Association between the proportion of GzmB-expressing CD8+ T cells and serum GFAP (n=18) by spearman correlation analysis. GzmB, granzyme B; NMOSD, neuromyelitis optica spectrum disorder; NFL, neurofilament light; GFAP, glial fibrillary acidic protein.

abnormally activated in patients with NMOSD and expressed high levels of the pro-inflammatory cytokines IFNγ and TNFα, which may be involved in peripheral inflammatory responses and promote disease progression (13). In the current study, we further demonstrated that CD8+ T cells in the peripheral blood of patients with NMOSD exhibited a highly differentiated phenotype ($T_{EMRA}$) and expressed considerable levels of the cytolytic protein GzmB. Furthermore, the increasing numbers of GzmB-expressing CD8+ T cells were associated with a poor response to immunotherapies and severe disability in the NMOSD group. Levels of the transcription factor T-bet in circulating CD8+ T cells were also significantly elevated in patients with NMOSD and contributed to increasing of terminal differentiation of CD8+ T cells and high expression of GzmB. Our data provide insight into a novel biomarker for predicting the effectiveness of immunotherapies and disability in patients with NMOSD, as well as a potential target for treatments.

Although T cells are considered to be involved in the pathogenesis and development of NMOSD, the key role of CD8+ T cell phenotypes and function in disease progression remains poorly understood. In this study, we observed significantly elevated proportions of CD8+ $T_{EMRA}$ cells and significantly enhanced expression of the neurotoxic mediator GzmB in the peripheral blood of patients with NMOSD. Increasing evidence suggests that cytotoxic CD8+ T cells are involved in the development of multiple autoimmune diseases. Blanco et al. reported a significant increase in CD8+ $T_{EMRA}$ cells expressing high levels of GzmB in the peripheral blood of patients with systemic lupus erythematosus (SLE), which was significantly associated with the clinical activity of the disease (31). In addition, abnormal amplification of cytotoxic CD8+ T cells has been observed in the peripheral blood and brain lesions of patients with Susac syndrome, in whom secreted GzmB adhered to CNS microvessels in different lesion regions, resulting in vascular endothelial cell injury, BBB disruption, and microbleeding (12). Intervention with GzmB significantly improved disease progression in the mouse model of Susac syndrome. Furthermore, Fransen et al. found that increased clustering of CD8+ T cells in the perivascular space correlated with inflammatory lesion activity and demyelinated lesion load in patients with chronic progressive MS (29). These studies imply that activated CD8+ T cells in the peripheral blood may enter the CNS by disrupting the BBB and participating in neuroinflammatory responses and lesion activity. Additionally, evidence from EAE models demonstrates that treatment with a

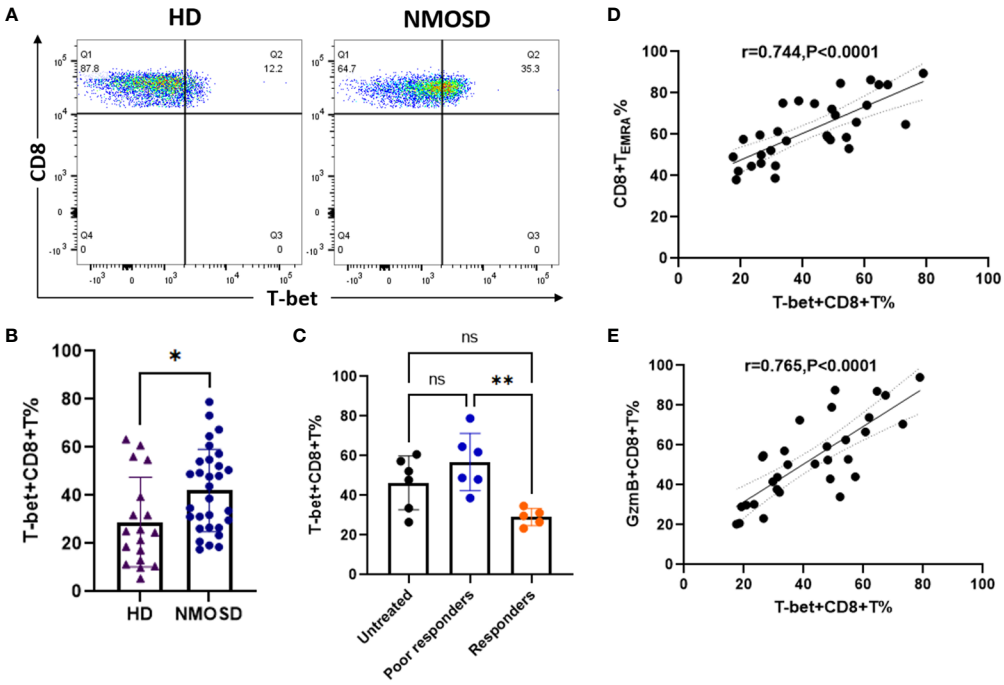


FIGURE 5
Upregulation of the transcription factor T-bet is associated with high expression of GzmB in circulating CD8+ T cells. **(A)** The flow cytometric gating strategy for evaluate levels of T-bet in CD8+ T cells. **(B)** Comparison of T-bet+CD8+ T cells between patients with NMOSD (n=31) and HDs (n=6) (Mann–Whitney U-test). **(C)** Comparison of T-bet+CD8+ T cells among untreated patients (n=6), poor responders (n=6), and responders (n=5) (one-way ANOVA with Tukey's multiple comparison test). **(D,E)** The correlation between T-bet expression and the proportions of CD8+ $T_{EMRA}$ cells **(D)** or GzmB+CD8+ T cells **(E)** in patients with NMOSD. GzmB, granzyme B; NMOSD, neuromyelitis optica spectrum disorder. *P<0.05, **P<0.01, and ns (not significant).

GzmB inhibitor (Serpina3n) can effectively reduce cytotoxic CD8+T cell-mediated axonal and neuronal damage in the CNS, as well as T-cell-mediated neuropathic pain (15). These findings strongly suggest that cytotoxic CD8+ T cells promote inflammatory responses and disease progression in a variety of autoimmune and neurological diseases by secreting GzmB, making GzmB a potential therapeutic target for these diseases and NMOSD.

In addition to GzmB-expressing CD8+T cells, the role of Gzmb-producing B cells has also been widely noticed in autoimmune diseases. GzmB-producing B cells are considered a type of regulatory B cells that have been found to be involved in the pathogenesis of multiple autoimmune diseases. Serval studies have revealed that GzmB-producing regulatory B cells are decreased in peripheral blood of systemic lupus erythematosus (SLE), lupus nephritis, and rheumatoid arthritis (RA), which are closely associated with poor prognosis of these diseases (32–34). On the other hand, a recent study found that circulating Gzmb+CD8+T cells and Gzmb+CD19+ B cells were significantly increased in MS patients during fingolimod and natalizumab treatments (35), suggesting that B cells may exhibit cytotoxic behavior similar to $CD8^+$ T lymphocytes in MS patients under different treatments. These results imply that circulating GzmB-expressing B cells and GzmB-expressing CD8+T cells seem to play different or even opposite roles in the pathogenesis of autoimmune diseases, but whether they interact and how the mechanism is still unknown in NMOSD. We believe that further study of circulating GzmB-releasing from CD8+T cells and B cells in NMOSD is warranted and interesting, which will help us to have a deeper understanding of the mechanism of T cell-B cell interaction in this disease.

Immunotherapies, including AZA, MMF, and RTX, are currently the most used agents for preventing relapse and disability in patients with NMOSD. However, studies have shown that more than 30% of patients still experience frequent relapse and disability progression under the first-line immunotherapies, and there are no biomarkers that can reflect the effectiveness of immunotherapies (4, 5). In this study, we discovered that a high proportion of GzmB-expressing CD8+ T cells was significantly associated with a poor response to immunotherapies and showed good potential for predicting the efficacy of immunotherapies (AUC=0.89). Moreover, our study provides a cut-off value of %GzmB+CD8+ T cells for distinguishing patients who are sensitive to immunotherapies. Based on this cutoff value, 75% of poor responders and only 8% of responders were classified as having high GzmB status. Our study not only confirms that GzmB+CD8+ T cells are involved in NMOSD, but also provides insight into a novel biomarker for predicting the efficacy of first-line immunotherapies, highlighting the need for validation in longitudinal cohort studies. In the future study, it remains necessary to evaluate the role of GzmB-expressing CD8+ T cells in monitoring response to different immunotherapies in NMOSD.

Additionally, our correlation analysis indicated that elevated levels of GzmB in CD8+ T cells were markedly associated with severe disability in patients with NMOSD, independent of sex, age, or disease phase. The significant association between GzmB levels in CD8+ T cells and EDSS scores suggests that GzmB levels in CD8+ T cells are potential biomarkers of disability in NMOSD. Serum levels of NFL and GFAP are widely considered biomarkers of neuroaxonal damage and astrocyte injury, respectively, both of which can reflect disease activity and disability in NMOSD (26). Notably, our study revealed that GzmB levels in CD8+ T cells were positively correlated with serum concentrations of NFL and GFAP, indicating that GzmB expression on peripheral CD8+ T cells may reflect CNS injury in patients with NMOSD. These results support our hypothesis that cytotoxic CD8+ T cells mediate CNS injury by secreting the neurotoxic mediator GzmB and are involved in peripheral and central inflammatory responses in patients with NMOSD.

The differentiation and functional expression of CD8+ T cells are affected by the transcription factor T-bet in the context of chronic infectious disease. Therefore, we further investigated the relationship between T-bet and peripheral CD8+ $T_{EMRA}$ and GzmB+CD8+ T cells in the NMOSD group. Our data revealed that the proportion of T-bet+CD8+ T cells in the peripheral blood was significantly higher in patients with NMOSD than in HDs, whereas it was significantly decreased in patients with a good response to immunotherapies. These findings indicate that levels of T-bet are elevated in the peripheral blood of patients with NMOSD and are regulated by immunotherapy drugs. Importantly, our data further demonstrated that those with high levels of T-bet in CD8+ T cells displayed an increasing proportion of CD8+ $T_{EMRA}$ cells and GzmB expression. In chronic viral infection, T-bet represses the expression of programmed cell death protein 1 (PD-1) and other related inhibitory receptors and sustains functional CD8+ T cell responses (19). Evidence from epigenetic studies and chromatin mapping of human CD8+ T cells *via* ATACT-seq has verified that levels of T-bet and proximity effector genes (Gzmb and Prf1) are upregulated in circulating CD8+ $T_{EMRA}$ cells (27). These data are consistent with our findings, suggesting that T-bet enhances the differentiation and cytotoxic function of CD8+ T cells and promotes disease progression and deterioration in inflammatory CNS diseases such as NMOSD. Taken together, our results suggest that increases in the proportion of CD8+ $T_{EMRA}$ cells and the related effector molecules T-bet and GzmB are associated with poor outcomes in patients with NMOSD. Thus, T-bet and GzmB represent potential therapeutic targets for NMOSD.

Our study was limited by the cross-sectional design and lack of longitudinal follow-up information. Therefore, a prospective

cohort study is required to confirm the prognostic predictive value of cytotoxic CD8+ T cells in patients with NMOSD. In addition, patients receiving immunotherapies were not excluded when detecting serum concentrations of NFL and GFAP in this study, thus the association with circulating GzmB-expressing CD8+T cells might be affected. Therefore, it is necessary to include more untreated patients in the future study to clarify the relationship between GzmB-expressing CD8+T cells and serum NFL and GFAP. Nonetheless, our findings support the involvement of cytotoxic CD8+ T cells in the inflammatory response to NMOSD and provide insight into a potential biomarker for the effectiveness of immunotherapies and disability progression in NMOSD.

## Data availability statement

The original contributions presented in the study are included in the article/Supplementary Material. Further inquiries can be directed to the corresponding authors.

## Ethics statement

The studies involving human participants were reviewed and approved by Medical Ethics Committee of the West China Hospital, Sichuan University. The patients/participants provided their written informed consent to participate in this study.

## Author contributions

Study conception and design: ZS, MY, and HZ. Collection of samples: QD, JW, XW, HC, YL, LYK, and WL. Flow cytometry and data analysis: ZS, QD, and JW. Drafting of manuscript and figures: ZS and QD. Critical revision of the manuscript: HZ. Statistical analysis: ZS, XW, and HC. Obtained funding: ZS and HZ. All authors contributed substantially to this manuscript and approved the final version of the manuscript.

## Funding

This work was funded by the Department of Science and Technology of Sichuan Province (Grant No. 2021YFS0173 and 2022YFS0315), the 1·3·5 project for disciplines of excellence–Clinical Research Incubation Project, West China Hospital, Sichuan University (Grant No. 21HXFH041), and the China Postdoctoral Science Foundation (Grant No. 2021M692295).

## Acknowledgments

The authors thank all the patients and healthy volunteers for their participation.

## Conflict of interest

The authors declare that the research was conducted in the absence of any commercial or financial relationships that could be construed as a potential conflict of interest.

## Publisher's note



## Supplementary material

The Supplementary Material for this article can be found online at: https://www.frontiersin.org/articles/10.3389/fimmu.2022.1027158/full#supplementary-material

## References

1. Jarius S, Paul F, Weinshenker BG, Levy M, Kim HJ, Wildemann B. Neuromyelitis optica. *Nat Rev Dis Primers* (2020) 6:85. doi: 10.1038/s41572-020-0214-9

2. Shi Z, Du Q, Chen H, Zhang Y, Qiu Y, Zhao Z, et al. Effects of immunotherapies and prognostic predictors in neuromyelitis optica spectrum disorder: a prospective cohort study. *J Neurol* (2020) 267:913–24. doi: 10.1007/s00415-019-09649-7

3. Palace J, Lin DY, Zeng D, Majed M, Elsone L, Hamid S, et al. Outcome prediction models in AQP4-IgG positive neuromyelitis optica spectrum disorders. *Brain* (2019) 142:1310–23. doi: 10.1093/brain/awz054

4. Stellmann JP, Krumbholz M, Friede T, Gahlen A, Borisow N, Fischer K, et al. Immunotherapies in neuromyelitis optica spectrum disorder: efficacy and predictors of response. *J Neurol Neurosurg Psychiatry* (2017) 88:639–47. doi: 10.1136/jnnp-2017-315603

5. Mealy MA, Wingerchuk DM, Palace J, Greenberg BM, Levy M. Comparison of relapse and treatment failure rates among patients with neuromyelitis optica: multicenter study of treatment efficacy. *JAMA Neurol* (2014) 71:324–30. doi: 10.1001/jamaneurol.2013.5699

6. Levy M, Fujihara K, Palace J. New therapies for neuromyelitis optica spectrum disorder. *Lancet Neurol* (2021) 20:60–7. doi: 10.1016/S1474-4422(20)30392-6

7. Pohl M, Fischer MT, Mader S, Schanda K, Kitic M, Sharma R, et al. Pathogenic T cell responses against aquaporin 4. *Acta Neuropathol* (2011) 122:21–34. doi: 10.1007/s00401-011-0824-0

8. Varrin-Doyer M, Spencer CM, Schulze-Topphoff U, Nelson PA, Stroud RM, Cree BA, et al. Aquaporin 4-specific T cells in neuromyelitis optica exhibit a Th17 bias and recognize clostridium ABC transporter. *Ann Neurol* (2012) 72:53–64. doi: 10.1002/ana.23651

9. Vaknin-Dembinsky A, Brill L, Kassis I, Petrou P, Ovadia H, Ben-Hur T, et al. T-Cell reactivity against AQP4 in neuromyelitis optica. *Neurology* (2012) 79:945–6. doi: 10.1212/WNL.0b013e318266fc2b

10. Jones MV, Huang H, Calabresi PA, Levy M. Pathogenic aquaporin-4 reactive T cells are sufficient to induce mouse model of neuromyelitis optica. *Acta Neuropathol Commun* (2015) 3:28. doi: 10.1186/s40478-015-0207-1

11. Machado-Santos J, Saji E, Tröscher AR, Paunovic M, Liblau R, Gabriely G, et al. The compartmentalized inflammatory response in the multiple sclerosis brain is composed of tissue-resident CD8+ T lymphocytes and b cells. *Brain* (2018) 141:2066–82. doi: 10.1093/brain/awy151

12. Gross CC, Meyer C, Bhatia U, Yshii L, Kleffner I, Bauer J, et al. CD8+ T cell-mediated endotheliopathy is a targetable mechanism of neuro-inflammation in susac syndrome. *Nat Commun* (2019) 10:5779. doi: 10.1038/s41467-019-13593-5

13. Shi Z, Qiu Y, Zhao Z, Wen D, Chen H, Du Q, et al. CD8+ T cell subpopulations and pro-inflammatory cytokines in neuromyelitis optica spectrum disorder. *Ann Clin Transl Neurol* (2021) 8:43–53. doi: 10.1002/acn3.51241

14. Neumann H, Medana IM, Bauer J, Lassmann H. Cytotoxic T lymphocytes in autoimmune and degenerative CNS diseases. *Trends Neurosci* (2002) 25:313–9. doi: 10.1016/s0166-2236(02)02154-9

15. Haile Y, Carmine-Simmen K, Olechowski C, Kerr B, Bleackley RC, Giuliani F. Granzyme b-inhibitor serpina3n induces neuroprotection *in vitro* and in vivo. *J Neuroinflamm* (2015) 12:157. doi: 10.1186/s12974-015-0376-7

16. Hiroyasu S, Zeglinski MR, Zhao H, Pawluk MA, Turner CT, Kasprick A, et al. Granzyme b inhibition reduces disease severity in autoimmune blistering diseases. *Nat Commun* (2021) 12:302. doi: 10.1038/s41467-020-20604-3

17. Novais FO, Nguyen BT, Scott P. Granzyme b inhibition by tofacitinib blocks the pathology induced by CD8 T cells in cutaneous leishmaniasis. *J Invest Dermatol* (2021) 141:575–85. doi: 10.1016/j.jid.2020.07.011

18. Intlekofer AM, Takemoto N, Wherry EJ, Longworth SA, Northrup JT, Palanivel VR, et al. Effector and memory CD8+ T cell fate coupled by T-bet and eomesodermin. *Nat Immunol* (2005) 6:1236–44. doi: 10.1038/ni1268

19. Kao C, Oestreich KJ, Paley MA, Crawford A, Angelosanto JM, Ali MA, et al. Transcription factor T-bet represses expression of the inhibitory receptor PD-1 and sustains virus-specific CD8+ T cell responses during chronic infection. *Nat Immunol* (2011) 12:663–71. doi: 10.1038/ni.2046

20. Chen Z, Ji Z, Ngiow SF, Manne S, Cai Z, Huang AC, et al. TCF-1-Centered transcriptional network drives an effector versus exhausted CD8 T cell-fate decision. *Immunity* (2019) 51:840–55:e5. doi: 10.1016/j.immuni.2019.09.013

21. Buggert M, Tauriainen J, Yamamoto T, Frederiksen J, Ivarsson MA, Michaëlsson J, et al. T-Bet and eomes are differentially linked to the exhausted phenotype of CD8+ T cells in HIV infection. *PloS Pathog* (2014) 10:e1004251. doi: 10.1371/journal.ppat.1004251

22. Zhu Y, Ju S, Chen E, Dai S, Li C, Morel P, et al. T-Bet and eomesodermin are required for T cell-mediated antitumor immune responses. *J Immunol* (2010) 185:3174–83. doi: 10.4049/jimmunol.1000749

23. Wingerchuk DM, Banwell B, Bennett JL, Cabre P, Carroll W, Chitnis T, et al. International consensus diagnostic criteria for neuromyelitis optica spectrum disorders. *Neurology* (2015) 85:177–89. doi: 10.1212/WNL.0000000000001729

24. Kurtzke JF. Rating neurologic impairment in multiple sclerosis: an expanded disability status scale (EDSS). *Neurology* (1983) 33:1444–52. doi: 10.1212/wnl.33.11.1444

25. Kim SH, Hyun JW, Joung A, Park EY, Joo J, Kim HJ. Predictors of response to first-line immunosuppressive therapy in neuromyelitis optica spectrum disorders. *Mult Scler* (2017) 23:1902–8. doi: 10.1177/1352458516687403

26. Watanabe M, Nakamura Y, Michalak Z, Isobe N, Barro C, Leppert D, et al. Serum GFAP and neurofilament light as biomarkers of disease activity and disability in NMOSD. *Neurology* (2019) 93:e1299–311. doi: 10.1212/WNL.0000000000008160

27. Buggert M, Vella LA, Nguyen S, Wu VH, Chen Z, Sekine T, et al. The identity of human tissue-emigrant CD8+ T cells. *Cell* (2020) 183:1946–61:e15. doi: 10.1016/j.cell.2020.11.019

28. Lindner M, Klotz L, Wiendl H. Mechanisms underlying lesion development and lesion distribution in CNS autoimmunity. *J Neurochem* (2018) 146:122–32. doi: 10.1111/jnc.14339

29. Fransen NL, Hsiao CC, van der Poel M, Engelenburg HJ, Verdaasdonk K, Vincenten MCJ, et al. Tissue-resident memory T cells invade the brain parenchyma in multiple sclerosis white matter lesions. *Brain* (2020) 143:1714–30. doi: 10.1093/brain/awaa117

30. van Nierop GP, van Luijn MM, Michels SS, Melief MJ, Janssen M, Langerak AW, et al. Phenotypic and functional characterization of T cells in white matter lesions of multiple sclerosis patients. *Acta Neuropathol* (2017) 134:383–401. doi: 10.1007/s00401-017-1744-4

31. Blanco P, Pitard V, Viallard JF, Taupin JL, Pellegrin JL, Moreau JF. Increase in activated CD8+ T lymphocytes expressing perforin and granzyme b correlates with disease activity in patients with systemic lupus erythematosus. *Arthritis Rheum* (2005) 52:201–11. doi: 10.1002/art.20745

32. Bai M, Xu L, Zhu H, Xue J, Liu T, Sun F, et al. Impaired granzyme b-producing regulatory b cells in systemic lupus erythematosus. *Mol Immunol* (2021) 140:217–24. doi: 10.1016/j.molimm.2021.09.012

33. Rabani M, Wilde B, Hubbers K, Xu S, Kribben A, Witzke O, et al. IL-21 dependent granzyme b production of b-cells is decreased in patients with lupus nephritis. *Clin Immunol* (2018) 188:45–51. doi: 10.1016/j.clim.2017.12.005

34. Xu L, Liu X, Liu H, Zhu L, Zhu H, Zhang J, et al. Impairment of granzyme b-producing regulatory b cells correlates with exacerbated rheumatoid arthritis. *Front Immunol* (2017) 8:768. doi: 10.3389/fimmu.2017.00768

35. Boldrini VO, Marques AM, Quintiliano R, Moraes AS, Stella C, Longhini A, et al. Cytotoxic b cells in relapsing-remitting multiple sclerosis patients. *Front Immunol* (2022) 13:750660. doi: 10.3389/fimmu.2022.750660

frontiers | Frontiers in Neurology

TYPE Original Research
PUBLISHED 15 November 2022
DOI 10.3389/fneur.2022.1022785



OPEN ACCESS

EDITED BY
Long-Jun Wu,
Mayo Clinic, United States

REVIEWED BY
Honghao Wang,
Guangzhou First People's Hospital, China
Massimiliano Castellazzi,
University of Ferrara, Italy

*CORRESPONDENCE
Yanjie Jia
jiayanjie1971@zzu.edu.cn
Shujie Jiao
529765445@qq.com

SPECIALTY SECTION
This article was submitted to Multiple Sclerosis and Neuroimmunology, a section of the journal Frontiers in Neurology

RECEIVED 18 August 2022
ACCEPTED 02 November 2022
PUBLISHED 15 November 2022

CITATION
Shao Y, Du J, Song Y, Li Y, Jing L, Gong Z, Duan R, Yao Y, Jia Y and Jiao S (2022) Elevated plasma D-dimer levels in patients with anti-N-methyl-D-aspartate receptor encephalitis.
*Front. Neurol.* 13:1022785.
doi: 10.3389/fneur.2022.1022785



# Elevated plasma D-dimer levels in patients with anti-N-methyl-D-aspartate receptor encephalitis

Yingzhe Shao, Juan Du,Yajun Song, Yanfei Li, Lijun Jing, Zhe Gong, Ranran Duan, Yaobing Yao, Yanjie Jia* and Shujie Jiao*

Department of Neurology, The First Affiliated Hospital of Zhengzhou University, Zhengzhou, China

**Purpose:** We aimed to explore the difference in coagulation function between healthy individuals and patients with anti-N-methyl-D-aspartate receptor (anti-NMDAR) encephalitis and its relationship with disease severity.

**Methods:** We retrospectively compared coagulation function in 161 patients with first-attack anti-NMDAR encephalitis and 178 healthy individuals. The association between D-dimer levels and disease severity was analyzed using binary logistic regression. Receiver operating characteristic (ROC) curves were used to analyze the predictive value of D-dimer levels for the severity of anti-NMDAR encephalitis.

**Results:** Compared to control individuals, patients with anti-NMDAR encephalitis had higher D-dimer levels (median 0.14 vs. 0.05 mg/L, $p < 0.001$), blood white blood cell (WBC) count (median 8.54 vs. 5.95 $\times$ $10^9$/L, $p < 0.001$), and neutrophil count (median 6.14 vs. 3.1 $\times$ $10^9$/L, $p < 0.001$). D-dimers (median 0.22 vs. 0.10 mg/L, $p < 0.001$), blood WBC count (median 9.70 vs. 7.70 $\times$ $10^9$/L, $p < 0.001$), neutrophil count (median 7.50 vs. 4.80 $\times$ $10^9$/L, $p < 0.001$), and C-reactive protein (median 2.61 vs. 1.50 mg/l, $p = 0.017$) were higher; however, eosinophils (median 0.02 vs. 0.06 $\times$ $10^9$/L, $p < 0.001$), and blood calcium (median 2.26 vs. 2.31 mmol/L, $p = 0.003$) were lower in patients with severe forms of anti-NMDAR encephalitis than in those with mild to moderate forms, and were associated with initial modified Rankin Scale scores. Multivariate analysis showed that D-dimer levels were significantly associated with severity [odds ratio =2.631, 95% confidence interval (CI) = 1.018–6.802, $p = 0.046$]. The ROC curve was used to analyze the predictive value of D-dimer levels for disease severity. The area under the curve was 0.716 (95% CI = 0.64–0.80, $p < 0.001$), and the best cut-off value was D-dimer = 0.147 mg/L (sensitivity 0.651; specificity, 0.705).

**Conclusion:** Serum D-dimer and neutrophil levels were independent predictors of disease severity in patients with first-attack anti-NMDAR encephalitis.

KEYWORDS

**anti-N-methyl-D-aspartate receptor encephalitis, D-dimer, inflammation, neutrophil, eosinophils, calcium**

# Introduction

Autoimmune encephalitis is a class of encephalitis caused by an immune response to central nervous system antigens mediated by autoimmune mechanisms. Among these, anti-N-methyl-D-aspartate receptor (anti-NMDAR) encephalitis is the most common type, which places a huge economic burden on patients (1). The main clinical symptoms are abnormal (psychiatric) behaviors, cognitive dysfunction, speech disorders, epilepsy, motor disorders, reduced awareness, and autonomic nerve dysfunction, etc. (2). Currently, few biomarkers can felicitously assess the severity of anti-NMDAR encephalitis.

Routine blood and coagulation functions are the most common laboratory indicators in clinics. However, white blood cells (WBC), neutrophils and C-reactive protein (CRP) are also indicators of systemic inflammation. D-dimer is a soluble fibrin degradation product, the expression of which elevated in arterial or venous thrombosis, disseminated vascular coagulation, advanced age, surgery, trauma, tumors, pregnancy, infection, chronic inflammation, liver disease, and kidney disease (3–5). Recent studies have found that D-dimer is associated with disease severity in autoimmune diseases such as lupus (6), rheumatoid arthritis (7), and granulomatosis with polyangiitis (8). In addition, several recent studies have highlighted the importance of activating the coagulation cascade in neuro-inflammation (9–11). Therefore, coagulation tests may be useful in identifying severe cases of anti-NMDAR encephalitis. No clinical research on anti-NMDAR encephalitis and coagulation function has been conducted to date. The aim of the present study was to investigate the differences in coagulation function between healthy people and patients with anti-NMDAR encephalitis and their relationship with disease severity.

# Methods

## Patients

This study was ratified by the Ethics Committee of Zhengzhou University (2019-KY-018). In this retrospective study, we registered 230 patients with first-attack anti-NMDAR encephalitis who were treated at the First Affiliated Hospital of Zhengzhou University between April 2014 and April 2021, all of whom met the standard of diagnosis for anti-NMDAR encephalitis (12) (Chinese expert consensus on the diagnosis and management of autoimmune encephalitis 2017).

The exclusion criteria were as follows: (i) complications with tumors, severe liver and kidney dysfunction, blood system diseases, arteriovenous thrombosis, severe infection, and other diseases affecting coagulation function; (ii) immunotherapy such as plasma exchange, corticosteroids, intravenous immunoglobulin, and immunity inhibitor within 6 months before admission; (iii) anticoagulant thrombolytic therapy within 3 months before admission; (iv) age $>$ 80 years; and (v) missing coagulation function results or inconsistent test reporting units. Gender- and age-matched healthy individuals ($n$ = 178) were comprised in the control group. In total, 161 patients with anti-NMDAR encephalitis and 178 control individuals were included in this study (Figure 1).

## Data collection

Data related to baseline clinical information, demographic characteristics, medical history, clinical symptoms, laboratory test results, and imaging characteristics were collected from the case reports.

Blood samples were collected on an empty stomach during the early hours of the 2nd day after admission. Coagulation function, CRP, and blood calcium were tested and routine blood tests were performed in the biochemical laboratory of the First Affiliated Hospital of Zhengzhou University. Blood WBC count (3.5–9.5 $\times$ $10^9$/L), red blood cell (RBC) count (3.8–5.1 $\times$ $10^{12}$/L), platelet count (125–350 $\times$ $10^9$/L), hemoglobin (115–150 g/L), neutrophil count (1.8–6.3 $\times$ $10^9$/L), lymphocyte count (1.1–3.2 $\times$ $10^9$/L), monocyte count (0.1–0.6 $\times$ $10^9$/L), eosinophil count (0.02–0.52 $\times$ $10^9$/L), basophil count (0–0.06 $\times$ $10^9$/L), prothrombin time (PT; 8.8–13.6 s), activated partial thrombin time (APTT; 26–40 s), fibrinogen (2–4 g/L), thrombin time (TT; 10–18 s), D-dimer (0–0.3 mg/L DDU), CRP (0–10 mg/L), and blood calcium (2.0–2.7 mmol/L) was performed. Blood counts were analyzed using an automated analyzer. PT, APTT, TT, and fibrinogen were coagulation markers, and D-dimer was used for immune turbidimetry. Scatter turbidimetry was used to measure the CRP levels. Calcium ion colorimetry was also performed.

Cerebrospinal fluid analysis and cerebral magnetic resonance imaging (MRI) were performed prior to treatment. Serum and cerebrospinal fluid samples from patients were used to determine their anti-NMDAR status at the Neurology Laboratory of the First Affiliated Hospital of Zhengzhou University using cell-based assays. MRI was performed using a 3.0 T Philips Healthcare (Best, Netherlands).

At least two professional neurologists carefully reviewed the patients' clinical records to calculate the extended modified Rankin Scale (m-RS) scores at admission and discharge. The initial and discharge m-RS scores were recorded, and the former was used to evaluate disease severity. The m-RS scores were converted into categorical variables. Patients with an initial m-RS score of $>$3 at admission were defined as the severe group, and those with an initial m-RS score $\leq$3 were defined as the mild-to-moderate group.

First-line immunotherapy includes plasma exchange, corticosteroids, and intravenous immunoglobulin; second-line immunotherapy includes rituximab and intravenous cyclophosphamide; and long-term immunotherapy includes mycophenolate mofetil and azathioprine.

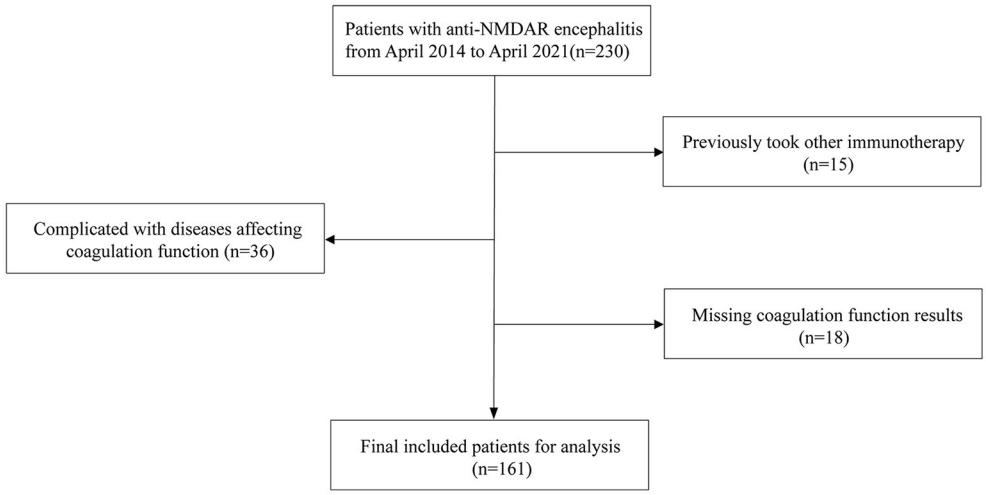


FIGURE 1
Patients selection process. Anti-NMDAR encephalitis, anti-N-methyl-D-aspartate receptor encephalitis.

TABLE 1 Clinical characteristics of the patients with anti-NMDAR encephalitis and healthy controls.

| Clinical characteristics | Anti-NMDAR encephalitis ($n = 161$) | Control ($n = 178$) | $p$ |
|---|---|---|---|
| Age, years, median (IQR) | 25 (16–37) | 27 (17–39.25) | 0.623 |
| Gender, female, *n* (%) | 73 (45.34) | 85 (47.75) | 0.657 |
| Hypertension, *n* (%) | 14 (8.70) | 11 (6.18) | 0.376 |
| Diabetes, *n* (%) | 4 (2.48) | 3 (1.68) | 0.605 |
| PT, median (IQR; s) | 11.0 (10.2–11.6) | 10.5 (10.1–11.1) | <0.001* |
| APTT, median (IQR; s) | 28.8 (26.05–31.45) | 32.1 (29.68–34.50) | <0.001* |
| Fibrinogen, median (IQR; g/L) | 2.78 (2.32–3.35) | 2.45 (2.17–2.89) | <0.001* |
| TT, median (IQR; s) | 14.60 (13.45–16.00) | 14.95 (14.18–16.03) | 0.021* |
| D-dimer, median (IQR; mg/L) | 0.14 (0.07–0.36) | 0.05 (0.038–0.08) | <0.001* |
| WBC, median (IQR; $10^9$/L) | 8.54 (6.60–11.60) | 5.95 (4.96–6.90) | <0.001* |
| RBC, mean ± SD ($10^{12}$/L) | 4.34 ± 0.53 | 4.53 ± 0.48 | 0.001* |
| Hemoglobin, mean ± SD (g/L) | 130.20 ± 16.55 | 135.37 ± 15.00 | 0.001* |
| Platelet, median (IQR; $10^9$/L) | 240 (197–308) | 233 (190.75–282.25) | 0.15 |
| Neutrophil, median (IQR; $10^9$/L) | 6.14 (3.96–8.91) | 3.10 (2.55–4.00) | <0.001* |
| Lymphocyte, median (IQR; $10^9$/L) | 1.56 (1.13–2.46) | 2.02 (1.65–2.46) | <0.001* |
| Monocytes, median (IQR; $10^9$/L) | 0.56 (0.43–0.75) | 0.41 (0.35–0.51) | <0.001* |
| Eosinophils, median (IQR; $10^9$/L) | 0.04 (0.01–0.10) | 0.11 (0.07–0.18) | <0.001* |
| Basophil, median (IQR; $10^9$/L) | 0.03 (0.01–0.04) | 0.03 (0.02–0.04) | 0.026* |

Normally distributed variables were presented as mean ± SD and compared using t-tests. Non-normally distributed variables were presented as median (IQR = 25–75th percentile) and were contrasted using the Mann-Whitney U-test. Categorical variables were described as number (percentage), and the chi-square test or Fisher's exact test was used for comparison between groups.
Anti-NMDAR encephalitis, anti-N-methyl-D-aspartate receptor encephalitis; PT, prothrombin time; APTT, activated partial thrombin time; TT, thrombin time; WBC, white blood cell; RBC, red blood cell.
*$p < 0.05$.

TABLE 2 Clinical characteristics of the patients with anti-NMDAR encephalitis severe group and mild to moderate group.

| Clinical characteristics | Total ($n = 161$) | Mild to moderate group ($n = 78$) | Severe group ($n = 83$) | $p$ |
|---|---|---|---|---|
| Age at onset, years, median (IQR) | 25 (16–37) | 27 (17.75–42) | 24 (15–33) | 0.283 |
| Gender, female, *n* (%) | 73 (45.34) | 29 (37.18) | 44 (53.01) | 0.044* |
| Hospital stays, days, median (IQR) | 26 (18–41) | 24 (17.75–35.25) | 32 (18–48) | 0.025* |
| ICU admission, *n* (%) | 88 (54.66) | 18 (23.08) | 70 (84.34) | <0.001* |
| Hypertension, *n* (%) | 14 (8.70) | 9 (11.54) | 5 (6.02) | 0.215 |
| Diabetes, *n* (%) | 4 (2.48) | 2 (2.56) | 2 (2.41) | 1 |
| Decreased level of consciousness, *n* (%) | 74 (45.96) | 8 (10.26) | 66 (79.52) | <0.001* |
| Abnormal (psychiatric) behavior, *n* (%) | 121 (75.16) | 47 (60.26) | 74 (89.16) | <0.001* |
| Cognitive dysfunction, *n* (%) | 73 (45.34) | 34 (43.59) | 39 (46.99) | 0.665 |
| Speech dysfunction, *n* (%) | 72 (44.72) | 29 (37.18) | 43 (51.81) | 0.062 |
| Movement disorder, *n* (%) | 62 (38.51) | 17 (21.79) | 45 (54.22) | <0.001* |
| Seizures, *n* (%) | 105 (65.22) | 45 (57.69) | 60 (72.29) | 0.052 |
| Autonomic dysfunction, *n* (%) | 48 (29.81) | 15 (19.23) | 33 (39.76) | 0.004* |
| PT, mean ± SD (s) | 11.08 ± 1.16 | 10.84 ± 0.89 | 11.25 ± 1.31 | 0.027* |
| APTT, median (IQR; s) | 28.75 (26.13–31.43) | 29.4 (27.275–32) | 28.1 (25.675–31.325) | 0.068 |
| Fibrinogen, median (IQR; g/L) | 2.85 (2.40–3.41) | 2.88 (2.25–3.51) | 2.85 (2.45–3.25) | 0.266 |
| TT, median (IQR; s) | 14.45 (13.30–15.93) | 14.60 (13.23–16.00) | 14.40 (13.45–15.75) | 0.351 |
| D-dimer, median (IQR; mg/L) | 0.15 (0.08–0.40) | 0.10 (0.05–0.19) | 0.22 (0.12–0.54) | <0.001* |
| WBC, median (IQR; $10^9$/L) | 8.53 (6.60–11.58) | 7.70 (6.05–9.50) | 9.70 (7.32–12.90) | <0.001* |
| RBC, mean ± SD ($10^{12}$/L) | 4.35 ± 0.53 | 4.39 ± 0.54 | 4.31 ± 0.52 | 0.307 |
| Hemoglobin, median (IQR; g/L) | 130.30 (119.03–139.75) | 134.00 (125.15–144.60) | 128.00 (119.00–135.00) | 0.026* |
| Platelet, median (IQR; $10^9$/L) | 239.5 (197–307.75) | 245 (199.5–307.5) | 238 (192–310) | 0.489 |
| Neutrophil, median (IQR; $10^9$/L) | 6.13 (3.98–8.89) | 4.80 (3.59–7.45) | 7.50 (4.70–10.80) | <0.001* |
| Lymphocyte, median (IQR; $10^9$/L) | 1.56 (1.13–2.20) | 1.70 (1.40–2.23) | 1.43 (0.78–2.05) | 0.002* |
| Monocytes, median (IQR; $10^9$/L) | 0.56 (0.43–0.75) | 0.52 (0.42–0.70) | 0.59 (0.45–0.77) | 0.249 |
| Eosinophils, median (IQR; $10^9$/L) | 0.04 (0.01–0.10) | 0.06 (0.03–0.13) | 0.02 (0.01–0.07) | <0.001* |
| Basophil, median (IQR; $10^9$/L) | 0.03 (0.01–0.04) | 0.03 (0.02–0.05) | 0.03 (0.01–0.04) | 0.055 |
| Calcium, median (IQR; mmol/L) | 2.29 (2.21–2.38) | 2.31 (2.26–2.42) | 2.26 (2.17–2.35) | 0.003* |
| CRP, median (IQR; mg/L) | 1.73 (0.79–7.03) | 1.50 (0.50–5.00) | 2.61 (1.00–8.32) | 0.017* |
| Initial m-RS score, median (IQR) | 4 (3–5) | 3 (2–3) | 5 (4–5) | <0.001* |
| Discharge m-RS score, median (IQR) | 2 (1–3) | 1 (1–2) | 2 (1–4) | <0.001* |
| MRI abnormality, *n* (%) | 62 (44.60) | 31 (44.29) | 31 (44.93) | 0.939 |
| First-line immunotherapy, *n* (%) | 156 (96.89) | 75 (96.15) | 81 (97.59) | 0.957 |
| Second-line immunotherapy, *n* (%) | 9 (5.59) | 3 (3.85) | 6 (7.23) | 0.497 |
| Long-time immunotherapy, *n* (%) | 15 (9.32) | 7 (8.97) | 8 (9.64) | 0.885 |

Normally distributed variables were presented as mean ± SD and compared using t-tests. Non-normally distributed variables were presented as medians (IQR = 25–75th percentile) and were contrasted using the Mann-Whitney U-test. Categorical variables were described as number (percentage), and the chi-square test or Fisher's exact test was used for comparison between groups. Severe group, patients with an initial m-RS score of >3 at admission; mild-to-moderate group, patients with an initial m-RS score ≤3.

Anti-NMDAR encephalitis, anti-N-methyl-D-aspartate receptor encephalitis; ICU, intensive care unit; PT, prothrombin time; APTT, activated partial thrombin time; TT, thrombin time; WBC, white blood cell; RBC, red blood cell; CRP, C-reaction protein; m-RS, modified Rankin Scale scores.

*$p < 0.05$.

## Statistical analysis

Data were analyzed using SPSS software (version 26.0; International Business Machines Corporation, Chicago, IL, USA). Graphs were generated by GraphPad Prism 8.3 (GraphPad Inc., Harvey Motulsky, USA).

Normality tests were performed using the Kolmogorov-Smirnov test. If the continuous variables fit a normal distribution, they were expressed as means and standard deviations (SD) and compared using *t*-tests. Non-normally distributed data were presented as medians (interquartile ranges) and were contrasted using the Mann-Whitney

*U*-test. Categorical data were presented as frequency (percentage), and the chi-square test or Fisher's exact test was used for comparison between groups. Spearman's correlation coefficient was calculated to assess the correlations. Univariate and multivariate analyses were used to evaluate the factors potentially related to disease severity in first-attack anti-NMDAR encephalitis patients. The receiver operating characteristic (ROC) curve was used to calculate the predictive value of D-dimer levels for disease severity. All tests were two-sided with a significance level of 0.05.

# Results

## Clinical characteristics of the patients with anti-NMDAR encephalitis and healthy individuals

Seventy-three (45.34%) female patients aged 25 years on average (16–37) were included in the anti-NMDAR encephalitis group ($n = 161$). In the control group ($n = 178$), 85 female patients (47.75%) aged 27 years on average (17–39.25) were included. There were no obvious differences in age or gender between the two groups ($p > 0.05$), indicating comparability. The platelet count and incidence of hypertension and diabetes did not differ significantly between the two groups. Our findings indicated that PT (median 11.0 vs. 10.5 s, $p < 0.001$), fibrinogen (median 2.78 vs. 2.45 g/L, $p < 0.001$), D-dimer (median 0.14 vs. 0.05 mg/L, $p < 0.001$), blood WBC count (median 8.54 vs. 5.95 $\times$ $10^9$/L, $p < 0.001$), neutrophil count (median 6.14 vs. 3.10 $\times$ $10^9$/L, $p < 0.001$), and monocyte count (median 0.56 vs. 0.41 $\times$ $10^9$/L, $p < 0.001$) were higher in patients with anti-NMDAR encephalitis than in healthy individuals. In contrast, the APTT levels (median 32.1 vs. 28.8 s, $p < 0.001$), TT (median 14.95 vs. 14.60 s, $p = 0.021$), RBC count (average 4.53 vs. 4.34 $\times$ $10^{12}$/L, $p < 0.001$), hemoglobin (average 135.37 vs. 130.20 g/L, $p < 0.001$), lymphocyte count (median 2.02 vs. 1.56 $\times$ $10^9$/L, $p < 0.001$), eosinophil count (median 0.11 vs. 0.04 $\times$ $10^9$/L, $p < 0.001$), and basophil count (median 0.03 vs. 0.03 $\times$ $10^9$/L, $p = 0.026$) were significantly higher in healthy controls than in patients with anti-NMDAR encephalitis (Table 1).

## Clinical characteristics of the patients with anti-NMDAR encephalitis with different severity

In the current study, the severe group had a higher proportion of female patients (53.01 vs. 37.18%, $p = 0.044$), intensive care unit admission rates (84.34 vs. 23.08, $p < 0.001$), and longer hospital stays (median 32 vs. 24, $p = 0.025$). Furthermore, patients in the severe group exhibited a significantly higher incidence of decreased consciousness (79.52 vs. 10.26 %, $p < 0.001$), abnormal (psychiatric) behaviors (89.16 vs. 60.26%, $p < 0.001$), movement disorders (54.22 vs. 21.79%, $p < 0.001$), and autonomic dysfunction (39.76 vs. 19.23%, $p = 0.004$) than those in the mild to moderate group. The PT (median 11.25 vs. 10.84 s, $p = 0.027$), D-dimer (median 0.22 vs. 0.10 mg/L, $p < 0.001$), blood WBC count (median 9.70 vs. 7.70 $\times$ $10^9$/L, $p < 0.001$), neutrophil count (median 7.50 vs. 4.80 $\times$ $10^9$/L, $p < 0.001$), and CRP (median 2.61 vs. 1.50 mg/l, $p = 0.017$) in the severe group was higher than that in the mild to moderate group (hemoglobin: median 128.00 vs. 134.00 g/L, $p = 0.026$; lymphocytes: median 1.43 vs. 1.70 $\times$ $10^9$/L, $p = 0.002$; eosinophils: median 0.02 vs. 0.06 $\times$ $10^9$/L, $p < 0.001$, and blood calcium: median 2.26 vs. 2.31 mmol/L, $p = 0.003$). The difference in APTT, fibrinogen, RBC, platelets, monocytes, and basophils between the two groups was insignificant. In addition, significant differences in m-RS between the two groups were present at discharge (median 2 vs. 1, $p < 0.001$), along with insignificant differences in MRI abnormality proportion, and treatment options, as shown in Table 2.

TABLE 3 Spearman correlation analysis between D-dimer and i-mRS in patients with anti-NMDAR encephalitis.

| | i-mRS | |
|---|---|---|
| | *r* | *p* |
| Age at onset | −0.132 | 0.096 |
| Gender | −0.164 | 0.038* |
| PT | 0.160 | 0.042* |
| APTT | −0.115 | 0.148 |
| Fibrinogen | 0.004 | 0.965 |
| TT | −0.037 | 0.644 |
| D-dimer | 0.367 | <0.001* |
| WBC | 0.311 | <0.001* |
| RBC | −0.109 | 0.168 |
| Hemoglobin | −0.188 | 0.017* |
| Platelet | −0.070 | 0.380 |
| Neutrophil | 0.340 | <0.001* |
| Lymphocyte | −0.266 | 0.001* |
| Monocytes | 0.152 | 0.055 |
| Eosinophils | −0.310 | <0.001* |
| Basophil | −0.163 | 0.039* |
| Calcium | −0.268 | 0.001* |
| CRP | 0.206 | 0.016* |

Anti-NMDAR encephalitis, anti-N-methyl-D-aspartate receptor encephalitis; PT, prothrombin time; APTT, activated partial thrombin time; TT, thrombin time; WBC, white blood cell; RBC, red blood cell; CRP, C-reaction protein; i-mRS, initial modified Rankin Scale scores.
*$p < 0.05$.

TABLE 4 Univariate and multivariable logistic regression models of disease severity.

| | Univariate analysis | | Multivariable analysis | |
|---|---|---|---|---|
| | OR (95% CI) | *p* | OR (95% CI) | *p* |
| Age at onset | 0.993 (0.973–1.013) | 0.493 | | |
| Gender | 1.906 (1.015–3.579) | 0.045* | 1.644 (0.80–3.378) | 0.176 |
| Hypertension | 0.491 (0.157–1.537) | 0.222 | | |
| Diabetes | 0.938 (0.129–6.828) | 0.950 | | |
| PT | 1.332 (1.027–1.726) | 0.031* | 1.109 (0.823–1.494) | 0.496 |
| APTT | 0.994 (0.954–1.036) | 0.777 | | |
| Fibrinogen | 1.004 (0.814–1.238) | 0.971 | | |
| TT | 0.967 (0.826–1.131) | 0.672 | | |
| D-dimer | 2.557 (1.116–5.856) | 0.026* | 2.631 (1.018–6.802) | 0.046* |
| WBC | 1.195 (1.084–1.317) | <0.001* | | |
| RBC | 0.733 (0.405–1.328) | 0.306 | | |
| Hemoglobin | 0.987 (0.968–1.006) | 0.170 | | |
| Platelet | 0.999 (0.995–1.003) | 0.627 | | |
| Neutrophil | 1.233 (1.111–1.368) | <0.001* | 1.2 (1.07–1.345) | 0.002* |
| Lymphocyte | 0.865 (0.680–1.100) | 0.236 | | |
| Monocytes | 0.892 (0.623–1.276) | 0.531 | | |
| Eosinophils | 0.003 (0–0.168) | 0.005* | 0.099 (0.002–5.024) | 0.249 |
| Basophil | 0.004 (0–14.446) | 0.189 | | |
| Calcium | 0.098 (0.011–0.901) | 0.040* | 0.328 (0.038–2.799) | 0.308 |
| CRP | 1.018 (0.988–1.049) | 0.249 | | |

WBC were not included in the multivariate analysis because of the strong correlation between WBC and neutrophils (r = 0.933, $p < 0.001$).
CI, confidence interval; PT, prothrombin time; APTT, activated partial thrombin time; TT, thrombin time; WBC, white blood cell; RBC, red blood cell; CRP, C-reaction protein.
*$p < 0.05$.

## Correlations between D-dimer and disease severity in patients with anti-NMDAR encephalitis

Spearman correlation analysis showed that PT ($r = 0.160$, $p = 0.042$) and D-dimer levels ($r = 0.367$, $p < 0.001$), WBC count ($r = 0.311$, $p < 0.001$), hemoglobin ($r = -0.188$, $p = 0.017$), neutrophils ($r = 0.340$, $p < 0.001$), lymphocytes ($r = -0.266$, $p < 0.001$), eosinophils ($r = -0.310$, $p < 0.001$), basophils ($r = -0.163$, $p = 0.039$), calcium ($r = -0.268$, $p = 0.001$), CRP ($r = 0.206$, $p = 0.016$), and the female ratio ($r = -0.164$, $p = 0.038$) were significantly correlated with the initial m-RS score of patients with anti-NMDAR encephalitis. There was no obvious correlation between age at onset, APTT, fibrinogen, TT, RBC count, platelet count, monocyte count, and disease severity ($p > 0.05$; Table 3).

Univariate logistic regression analysis showed that the gender (OR = 1.906, 95% CI = 1.015–3.579, $p = 0.045$), PT (OR = 1.332, 95% CI = 1.027–1.726, $p = 0.031$), D-dimer (OR = 2.557, 95% CI = 1.116–5.856, $p = 0.026$), WBC (OR = 1.195, 95% CI = 1.084–1.317, $p < 0.001$), neutrophils (OR = 1.233, 95% CI = 1.111–1.368, $p < 0.001$), eosinophils (OR = 0.003, 95% CI = 0–0.168, $p = 0.040$), and calcium (OR = 0.098, 95% CI = 0.011–0.901, $p = 0.040$), were significantly correlated with disease severity. However, age, hypertension, diabetes, APTT, fibrinogen, TT, blood RBC, hemoglobin, platelets, lymphocytes, monocytes, basophil count, and CRP level were not significantly correlated with disease severity. In the multivariate model, D-dimer level (OR = 2.631, 95% CI = 1.018–6.802, $p = 0.046$) and neutrophils (OR = 1.2, 95% CI = 1.07–1.345, $p < 0.001$) were independent risk factors for disease severity. WBC were excluded from the multivariate analysis due to the strong correlation between WBC and neutrophils ($r = 0.933$, $p < 0.001$; Table 4).

The ROC curve was used to analyze the predictive value of D-dimer levels for disease severity. The area under the curve was 0.716 (95% CI = 0.64–0.80, $p < 0.001$), the best cut-off value was D-dimer = 0.147, the sensitivity was 0.651, and the specificity was 0.705, showing a good predictive ability for disease severity (Figure 2).

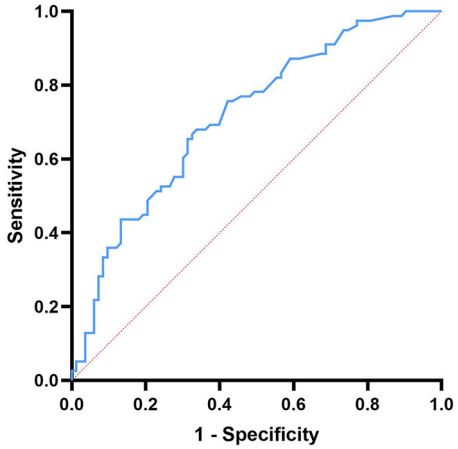


FIGURE 2
Receiver operating characteristic curve showing the predictive ability of D-dimer for disease severity.

TABLE 5 Spearman correlation between D-dimer levels and other Laboratory indicators in patients with anti-NMDAR encephalitis.

| | *r* | *p* |
|---|---|---|
| Age at onset | 0.297 | <0.001* |
| Gender | 0.087 | 0.272 |
| PT | 0.011 | 0.89 |
| APTT | −0.318 | <0.001* |
| Fibrinogen | 0.253 | 0.001* |
| TT | −0.008 | 0.921 |
| WBC | 0.294 | <0.001* |
| RBC | −0.175 | 0.027* |
| Hemoglobin | −0.183 | 0.020* |
| Platelet | −0.110 | 0.163 |
| Neutrophil | 0.301 | <0.001* |
| Lymphocyte | −0.292 | <0.001* |
| Monocytes | 0.065 | 0.416 |
| Eosinophils | −0.109 | 0.165 |
| Basophil | −0.170 | 0.031* |
| Calcium | −0.249 | 0.002* |
| CRP | 0.265 | 0.002* |

Anti-NMDAR encephalitis, anti-N-methyl-D-aspartate receptor encephalitis; PT, prothrombin time; APTT, activated partial thrombin time; TT, thrombin time; WBC, white blood cell; RBC, red blood cell; CRP, C-reaction protein.
*$p < 0.05$.

## Correlation between D-dimer levels and other laboratory indicators in patients with anti-NMDAR encephalitis

Spearman correlation analysis showed that age ($r = 0.297$, $p < 0.001$), APTT levels ($r = -0.318$, $p < 0.001$), fibrinogen ($r = 0.253$, $p = 0.001$), WBC ($r = 0.294$, $p < 0.001$), RBC ($r = -0.175$, $p = 0.027$), hemoglobin ($r = -0.183$, $p = 0.020$), neutrophils ($r = 0.301$, $p < 0.001$), lymphocytes ($r = -0.292$, $p < 0.001$), basophils ($r = -0.170$, $p = 0.031$), calcium ($r = -0.249$, $p = 0.002$), and CRP ($r = 0.265$, $p = 0.002$) were significantly correlated with D-dimer levels in anti-NMDAR encephalitis. There was no obvious correlation between gender and PT, platelets, monocytes, eosinophils, and D-dimer levels ($p > 0.05$; Table 5).

## Discussion

Previous studies have demonstrated the role of D-dimer levels in the severity of immune-related diseases. In this study, we compared the differences in routine blood test results and coagulation function between healthy individuals and patients with anti-NMDAR encephalitis. We evaluated the effect of D-dimer on disease severity in anti-NMDAR encephalitis. We discovered that high D-dimer and neutrophil levels were associated with a more severe disease at onset. D-dimer levels were positively correlated with neutrophils, leukocytes, and CRP and negatively correlated with eosinophil and calcium levels in patients with anti-NMDAR encephalitis. Furthermore, D-dimer levels were found to be an independent predictor of the severity of anti-NMDAR encephalitis.

This study showed that patients with anti-NMDAR encephalitis had shorter APTT and higher D-dimer levels, and the latter was correlated with disease severity. Anti-NMDAR encephalitis is an autoimmune mediated inflammatory disease. Inflammatory phenomena that occur in anti-NMDAR encephalitis are closely associated with a prothrombotic state. Previous studies have shown that systemic inflammation is a potent prethrombotic stimulus and inflammatory mechanisms contribute to activating coagulation factors, reducing natural anticoagulants, and inhibiting fibrinolytic activity (13). Fibrinogen levels increase in inflammation conditions because they promote fibrinogen synthesis, unless consumptive coagulopathy occurs (14). Patients with anti-NMDAR encephalitis had elevated fibrinogen levels in this study, which is consistent with the above results. This may indicate that higher D-dimer levels in patients with anti-NMDAR encephalitis are associated with inflammation rather than thrombosis.

In this study, neutrophil levels were significantly increased in patients with NMDAR encephalitis, which correlated with disease severity and D-dimer levels. Neutrophils, as an important part of innate and adaptive immunity, affect the maturation and function of other leukocytes by secreting cytokines or cell–cell contact, and play an important role in disease occurrence and progression, including infections,

chronic inflammation, tumor and autoimmunity (15, 16). Massberg et al. showed that neutrophils prevent tissue dissemination of pathogens by increasing fibrin formation (17). Studies reported that neutrophil extracellular vesicles and neutrophil extracellular traps (NETs) contribute to thrombosis (18). Kamba et al. demonstrated that neutrophils release tissue factors through NETs, induce thrombin generation, and promote hypercoagulation in vasculitis (19, 20). Recent observations have demonstrated that NETs were blocked by therapeutic-dose low-molecular-weight heparin in coronavirus disease 2019 (21). These findings may provide new therapeutic strategies for the treatment of anti-NMDAR encephalitis.

Inflammatory cytokines induce apoptosis and eosinophil degranulation, causing excessive loss of eosinophils (22). Eosinophils secrete diverse proteins in response to stimuli, including eosinophil cationic protein, which produces endogenous thrombin and promotes thrombus formation (23). In patients with NMDARs, eosinophil levels were lower, which may be associated with hypercoagulability. Eosinophils are the main storage site of tissue factor in blood vessels, and tissue factor is the initiation factor of the extrinsic coagulation pathway (24). Patients in the severe group had lower eosinophil levels and prolonged PT. Eosinophils were consistently negatively correlated with PT in patients with anti-NMDAR encephalitis. Eosinophils can induce the activation of M2 microglia by secreting IL-4 and IL-13 to promote the elimination of inflammation and play the neuroprotective role of microglia (25). This may explain why patients in the severe group had lower eosinophil levels.

Previous studies have shown that the cytokines produced by systemic inflammatory responses can lead to hypocalcemia (26, 27). The hypocalcemia effect may be caused by upregulation of the calcium-sensing receptor by IL-1β and IL-6 (28–30). In this study, patients with severe forms of the disease had higher inflammation levels and lower blood calcium levels than those in the mild-to-moderate group. Calcium is a key component of the coagulation cascade (31). According to our results, serum calcium level was negatively correlated with PT and D-dimer level in patients with anti-NMDAR encephalitis. However, serum calcium levels are closely related to vitamin D and serum albumin levels and are also affected by the concentration of other ions. Thus, its significance in anti-NMDAR encephalitis requires further study.

Our study has some limitations. First, this was a single-center retrospective study. Therefore, our results should be confirmed in a large, multicenter study. In addition, owing to the limitations of retrospective studies, other laboratory indicators such as fibrinogen degradation products and coagulation factor could not be studied in relation to disease severity and inflammatory response. Finally, the exact mechanism underlying the elevation of D-dimer levels in patients with anti-NMDAR encephalitis, particularly whether it is a mere result of inflammation or a part of disease pathogenesis remains unclear. Anticoagulant therapy has been explored in patients with central nervous system autoimmune diseases (32).

## Conclusion

D-dimer and neutrophil levels can be used as predictors of anti-NMDAR encephalitis severity. These factors can help clinicians identify severely ill patients early enough to take appropriate treatment measures. This study indicated that D-dimer may be considered an effective biomarker for anti-NMDAR encephalitis. The mechanism underlying the effect of serum D-dimer levels on disease progression requires further elucidation.

## Data availability statement

The original contributions presented in the study are included in the article/Supplementary material, further inquiries can be directed to the corresponding authors.

## Ethics statement

The studies involving human participants were reviewed and approved by the Ethics Committee of Zhengzhou University. Written informed consent to participate in this study was provided by the participants' legal guardian/next of kin.

## Author contributions

YSh contributed to conception and design of the research and wrote the first draft of the manuscript. JD, YSo, and YL organized the database. LJ, ZG, RD, and YSh performed the statistical analysis. YY, YJ, and SJ undertook the task of revising the manuscript critically. All authors contributed to manuscript revision, read, and approved the submitted version.

## Acknowledgments

We thank the study participants and the clinical staff for their support and contribution to this study and thank Editage (www.editage.cn) for English language editing.

## Conflict of interest

The authors declare that the research was conducted in the absence of any commercial or financial relationships that could be construed as a potential conflict of interest.

## Publisher's note

All claims expressed in this article are solely those of the authors and do not necessarily represent those of their affiliated organizations, or those of the publisher, the editors and the reviewers. Any product that may be evaluated in this article, or claim that may be made by its manufacturer, is not guaranteed or endorsed by the publisher.

## Supplementary material

The Supplementary Material for this article can be found online at: https://www.frontiersin.org/articles/10.3389/fneur.2022.1022785/full#supplementary-material

SUPPLEMENTARY TABLE 1
Anti-NMDAR encephalitis_Data.

SUPPLEMENTARY TABLE 2
Healthy individuals_Date.

## References

1. Li A, Gong X, Guo K, Lin J, Zhou D, Hong Z. Direct economic burden of patients with autoimmune encephalitis in Western China. *Neurol Neuroimmunol Neuroinflamm.* (2020) 7:891. doi: 10.1212/NXI.0000000000000891

2. Graus F, Titulaer MJ, Balu R, Benseler S, Bien CG, Cellucci T, et al. A clinical approach to diagnosis of autoimmune encephalitis. *Lancet Neurol.* (2016) 15:391–404. doi: 10.1016/S1474-4422(15)00401-9

3. Weitz JI, Fredenburgh JC, Eikelboom JW. A test in context: D-dimer. *J Am Coll Cardiol.* (2017) 70:2411–20. doi: 10.1016/j.jacc.2017.09.024

4. Johnson ED, Schell JC, Rodgers GM. The D-dimer assay. *Am J Hematol.* (2019) 94:833–9. doi: 10.1002/ajh.25482

5. Olson JD. D-dimer: an overview of hemostasis and fibrinolysis, assays, and clinical applications. *Adv Clin Chem.* (2015) 69:1–46. doi: 10.1016/bs.acc.2014.12.001

6. Ferreira KS, Cicarini WB, Alves LCV, Loures CMG, Campos FMF, Santos LID, et al. Correlation between active disease and hypercoagulability state in patients with systemic lupus erythematosus. *Clin Chim Acta.* (2019) 490:107–12. doi: 10.1016/j.cca.2018.12.008

7. Xue L, Tao L, Li X, Wang Y, Wang B, Zhang Y, et al. Plasma fibrinogen, D-dimer, and fibrin degradation product as biomarkers of rheumatoid arthritis. *Sci Rep.* (2021) 11:16903. doi: 10.1038/s41598-021-96349-w

8. Borowiec A, Dabrowski R, Kowalik I, Rusinowicz T, Hadzik-Blaszczyk M, Krupa R, et al. Elevated levels of D-dimer are associated with inflammation and disease activity rather than risk of venous thromboembolism in patients with granulomatosis with polyangiitis in long term observation. *Adv Med Sci.* (2020) 65:97–101. doi: 10.1016/j.advms.2019.12.007

9. Ryu JK, Petersen MA, Murray SG, Baeten KM, Meyer-Franke A, Chan JP, et al. Blood coagulation protein fibrinogen promotes autoimmunity and demyelination *via* chemokine release and antigen presentation. *Nat Commun.* (2015) 6:8164. doi: 10.1038/ncomms9164

10. Yates RL, Esiri MM, Palace J, Jacobs B, Perera R, DeLuca GC. Fibrin(Ogen) and neurodegeneration in the progressive multiple sclerosis cortex. *Ann Neurol.* (2017) 82:259–70. doi: 10.1002/ana.24997

11. Schaller-Paule MA, Yalachkov Y, Steinmetz H, Friedauer L, Hattingen E, Miesbach W, et al. Analysis of Csf D-dimer to identify intrathecal fibrin-driven autoimmunity in patients with multiple sclerosis. *Neurol Neuroimmunol Neuroinflamm.* (2022) 9:1150. doi: 10.1212/NXI.0000000000001150

12. Hongzhi G, Wang J. Chinese society of neurology. Chinese expert consensus on the diagnosis and management of autoimmune encephalitis. *Chin J Neurol.* (2017) 50:91–8. doi: 10.3760/cma.j.issn.1006-7876.2017.02.004

13. Ruf W, Ruggeri ZM. Neutrophils release brakes of coagulation. *Nat Med.* (2010) 16:851–2. doi: 10.1038/nm0810-851

14. Haemost JT. Inflammation and thrombosis. *Int Soc Thrombosis Haemostasis.* (2003) 1:1343–8. doi: 10.1046/j.1538-7836.2003.00261.x

15. Jaillon S, Galdiero MR, Del Prete D, Cassatella MA, Garlanda C, Mantovani A. Neutrophils in innate and adaptive immunity. *Semin Immunopathol.* (2013) 35:377–94. doi: 10.1007/s00281-013-0374-8

16. Mantovani A, Cassatella MA, Costantini C, Jaillon S. Neutrophils in the activation and regulation of innate and adaptive immunity. *Nat Rev Immunol.* (2011) 11:519–31. doi: 10.1038/nri3024

17. Massberg S, Grahl L, von Bruehl ML, Manukyan D, Pfeiler S, Goosmann C, et al. Reciprocal coupling of coagulation and innate immunity *via* neutrophil serine proteases. *Nat Med.* (2010) 16:887–96. doi: 10.1038/nm.2184

18. Blanch-Ruiz MA, Ortega-Luna R, Martinez-Cuesta MA, Alvarez A. The neutrophil secretome as a crucial link between inflammation and thrombosis. *Int J Mol Sci.* (2021) 22:84170. doi: 10.3390/ijms22084170

19. Kambas K, Chrysanthopoulou A, Vassilopoulos D, Apostolidou E, Skendros P, Girod A, et al. Tissue factor expression in neutrophil extracellular traps and neutrophil derived microparticles in antineutrophil cytoplasmic antibody associated vasculitis may promote thromboinflammation and the thrombophilic state associated with the disease. *Ann Rheum Dis.* (2014) 73:1854–63. doi: 10.1136/annrheumdis-2013-203430

20. Carminita E, Crescence L, Panicot-Dubois L, Dubois C. Role of neutrophils and nets in animal models of thrombosis. *Int J Mol Sci.* (2022) 23:31411. doi: 10.3390/ijms23031411

21. Petito E, Falcinelli E, Paliani U, Cesari E, Vaudo G, Sebastiano M, et al. Association of neutrophil activation, more than platelet activation, with thrombotic complications in coronavirus disease 2019. *J Infect Dis.* (2021) 223:933–44. doi: 10.1093/infdis/jiaa756

22. Cayrol C, Girard JP. Interleukin-33 (IL-33): a nuclear cytokine from the IL-1 family. *Immunol Rev.* (2018) 281:154–68. doi: 10.1111/imr.12619

23. Uderhardt S, Ackermann JA, Fillep T, Hammond VJ, Willeit J, Santer P, et al. Enzymatic lipid oxidation by eosinophils propagates coagulation, hemostasis, and thrombotic disease. *J Exp Med.* (2017) 214:2121–38. doi: 10.1084/jem.20161070

24. Moosbauer C, Morgenstern E, Cuvelier SL, Manukyan D, Bidzhekov K, Albrecht S, et al. Eosinophils are a major intravascular location for tissue factor storage and exposure. *Blood.* (2007) 109:995–1002. doi: 10.1182/blood-2006-02-004945

25. Guo Z, Hou J, Yu S, Zhang H, Yu S, Wang H, et al. Eosinophils, stroke-associated pneumonia, and outcome after mechanical thrombectomy for acute ischemic stroke. *Front Aging Neurosci.* (2022) 14:830858. doi: 10.3389/fnagi.2022.830858

26. Du X, Zhao D, Wang Y, Sun Z, Yu Q, Jiang H, et al. Low serum calcium concentration in patients with systemic lupus erythematosus accompanied by the enhanced peripheral cellular immunity. *Front Immunol.* (2022) 13:901854. doi: 10.3389/fimmu.2022.901854

27. Qi X, Kong H, Ding W, Wu C, Ji N, Huang M, et al. Abnormal coagulation function of patients with covid-19 is significantly related to hypocalcemia and severe inflammation. *Front Med.* (2021) 8:638194. doi: 10.3389/fmed.2021.638194

28. Canaff L, Zhou X, Hendy GN. The proinflammatory cytokine, interleukin-6, up-regulates calcium-sensing receptor gene transcription *via* Stat1/3 and Sp1/3. *J Biol Chem.* (2008) 283:13586–600. doi: 10.1074/jbc.M708087200

29. Mammadova-Bach E, Nagy M, Heemskerk JWM, Nieswandt B, Braun A. Store-operated calcium entry in thrombosis and thrombo-inflammation. *Cell Calcium*. (2019) 77:39–48. doi: 10.1016/j.ceca.2018.11.005

30. Hendy GN, Canaff L. Calcium-sensing receptor, proinflammatory cytokines and calcium homeostasis. *Semin Cell Dev Biol*. (2016) 49:37–43. doi: 10.1016/j.semcdb.2015.11.006

31. Singh S, Dodt J, Volkers P, Hethershaw E, Philippou H, Ivaskevicius V, et al. Structure functional insights into calcium binding during the activation of coagulation factor XIII A. *Sci Rep*. (2019) 9:11324. doi: 10.1038/s41598-019-47815-z

32. Stolz L, Derouiche A, Devraj K, Weber F, Brunkhorst R, Foerch C. Anticoagulation with warfarin and rivaroxaban ameliorates experimental autoimmune encephalomyelitis. *J Neuroinflammation*. (2017) 14:152. doi: 10.1186/s12974-017-0926-2

frontiers | Frontiers in Immunology

TYPE Original Research
PUBLISHED 08 December 2022
DOI 10.3389/fimmu.2022.1048428



OPEN ACCESS

EDITED BY
Long-Jun Wu,
Mayo Clinic, United States

REVIEWED BY
Jan D. Lünemann,
University of Münster, Germany
Maria Manuela Rosado,
Sapienza University of Rome, Italy

*CORRESPONDENCE
Norio Chihara
chiharan@med.kobe-u.ac.jp
Riki Matsumoto
matsumot@med.kobe-u.ac.jp

SPECIALTY SECTION
This article was submitted to Multiple Sclerosis and Neuroimmunology, a section of the journal Frontiers in Immunology

RECEIVED 19 September 2022
ACCEPTED 31 October 2022
PUBLISHED 08 December 2022

CITATION
Hara A, Chihara N, Akatani R, Nishigori R, Tsuji A, Yoshimura H, Kawamoto M, Otsuka Y, Kageyama Y, Kondo T, Leypoldt F, Wandinger K-P and Matsumoto R (2022) Circulating plasmablasts and follicular helper T-cell subsets are associated with antibody-positive autoimmune epilepsy. *Front. Immunol.* 13:1048428. doi: 10.3389/fimmu.2022.1048428



# Circulating plasmablasts and follicular helper T-cell subsets are associated with antibody-positive autoimmune epilepsy

Atsushi Hara[1], Norio Chihara[1*], Ritsu Akatani[1], Ryusei Nishigori[2], Asato Tsuji[1], Hajime Yoshimura[3], Michi Kawamoto[3], Yoshihisa Otsuka[4], Yasufumi Kageyama[4], Takayuki Kondo[5], Frank Leypoldt[6,7], Klaus-Peter Wandinger[6] and Riki Matsumoto[1*]

[1]Division of Neurology, Kobe University Graduate School of Medicine, Kobe, Japan, [2]Department of Neurology, Kyoto University Graduate School of Medicine, Kyoto, Japan, [3]Department of Neurology, Kobe City Medical Center General Hospital, Kobe, Japan, [4]Department of Neurology, Hyogo Prefectural Amagasaki General Medical Center, Amagasaki, Japan, [5]Department of Neurology, Kansai Medical University Medical Center, Moriguchi, Japan, [6]Neuroimmunology, Institute of Clinical Chemistry, University Hospital Schleswig-Holstein, Kiel, Germany, [7]Department of Neurology, University Hospital Schleswig-Holstein, Kiel, Germany

Autoimmune epilepsy (AE) is an inflammatory disease of the central nervous system with symptoms that have seizures that are refractory to antiepileptic drugs. Since the diagnosis of AE tends to rely on a limited number of anti-neuronal antibody tests, a more comprehensive analysis of the immune background could achieve better diagnostic accuracy. This study aimed to compare the characteristics of anti-neuronal antibody-positive autoimmune epilepsy (AE/Ab(+)) and antibody-negative suspected autoimmune epilepsy (AE/Ab(-)) groups. A total of 23 patients who met the diagnostic criteria for autoimmune encephalitis with seizures and 11 healthy controls (HC) were enrolled. All patients were comprehensively analyzed for anti-neuronal antibodies; 13 patients were identified in the AE/Ab(+) group and 10 in the AE/Ab(-) group. Differences in clinical characteristics, including laboratory and imaging findings, were evaluated between the groups. In addition, the immunophenotype of peripheral blood mononuclear cells (PBMCs) and CSF mononuclear cells, particularly B cells and circulating Tfh (cTfh) subsets, and multiplex assays of serum and CSF were analyzed using flow cytometry. Patients with AE/Ab(+) did not show any differences in clinical parameters compared to patients with AE/Ab(-). However, the frequency of plasmablasts within PBMCs and CSF in patients with AE/Ab(+) was higher than that in patients with AE/Ab(-) and HC, and the frequency of cTfh17 cells and inducible T-cell co-stimulator (ICOS) expressing cTfh17 cells within cTfh subsets was higher than that in patients with AE/Ab(-). Furthermore, the frequency of $ICOS^{high}$cTfh17 cells was positively correlated with that of the unswitched memory B cells. We also found that IL-12, IL-23, IL-6, IL-17A, and IFN-γ levels were elevated in the serum and IL-17A and IL-6 levels were elevated in the CSF of patients with AE/Ab(+). Our findings indicate that patients with AE/Ab(+)

showed increased differentiation of B cells and cTfh subsets associated with antibody production. The elevated frequency of plasmablasts and ICOS expressing cTfh17 shift in PBMCs may be indicative of the presence of antibodies in patients with AE.

KEYWORDS

autoimmune epilepsy, autoimmune encephalitis, plasmablasts, T follicular helper cells, ICOS

# Introduction

Epilepsy is a chronic debilitating disease affecting 0.5–1.0% of the world's population (1). The etiology of epilepsy varies and remains unknown. It has been reported that some cases in which seizures are refractory to antiepileptic drugs can be suppressed by immunotherapy (2). In these cases of patients with autoimmune epilepsy (AE), autoantibodies targeting neuronal surface and intracellular antigens, also called as anti-neuronal antibodies, have been identified. Antibodies against neuronal surface antigens are not only diagnostic markers but also pathogenic factors (3). The incidence of AE is estimated to be approximately 5–7% in adults with epilepsy (4). Diagnosis and treatment tend to be delayed because diagnostic antibody tests depend on a cell-based assay (CBA) that involves a highly sensitive and specific antibody analysis with limited availability.

Recently, APE2 and ACES scores have been reported as diagnostic criteria for autoimmune epilepsy as a predictor of anti-neuronal autoantibodies (5, 6). However, more inclusive criteria for autoimmune encephalitis proposed by Graus et al. in 2016 are widely used to avoid misdiagnosis of treatable autoimmune epilepsy (7). Some cases of epilepsy refractory to antiepileptic drug that meet Graus's criteria for possible autoimmune encephalitis are negative for anti-neuronal antibodies, and even include noninflammatory temporal lobe epilepsy with newly developed seizures or epilepsy that is often difficult to distinguish (8–11). This could lead to a false negative result due to the timing of analysis, other unknown anti-neuronal antibodies, or noninflammatory etiology. In clinical practice, some patients who are negative for anti-neuronal antibody respond to immunotherapy, but the psychological side effects of corticosteroid may make it difficult to accurately determine the effects of treatment (9, 10). Nevertheless, aggressive immunotherapy is necessary, especially when anti-neuronal antibodies against cell surface antigens are positive (11). To decrease the discrepancy between bedside and bench, new biomarkers are required to distinguish the presence of anti-neuronal antibodies in cases of suspected autoimmune epilepsy. However, little is known about the immunopathological background of anti-neuronal antibody-positive autoimmune epilepsy during the active period. It has been reported that anti-neuronal antibodies and other autoantibodies are produced by plasmablasts and long-lived plasma cells with the support of T follicular helper cells (Tfh) (12) Tfh are defined as $CD4^+$ T cells that express C-X-C motif chemokine receptor 5 (CXCR5) in secondary lymphoid tissues (13), and there is considerable clonal overlap between Tfh from lymphoid tissues and circulating T follicular helper cells (cTfh) from peripheral blood mononuclear cells (PBMCs) (14). Generally, cTfh cells are classified into three subsets: cTfh1 (C-X-C motif chemokine receptor 3(CXCR3)+ and C-C chemokine receptor 6(CCR6)–, cTfh2 (CXCR3–CCR6–), and cTfh17 (CXCR3–CCR6+). The cTfh2 and cTfh17 classes switch naive B cells to promote IgG production (15). In several antibody-associated autoimmune diseases, cTfh shift to cTfh17 or cTfh2 (16–20) and increase the cTfh17/cTfh1 cells ratio (21). Notably, the expression of inducible T-cell co-stimulator (ICOS) in cTfh and subset changes in cTfh have been identified as factors that promote B cell differentiation and antibody production (15, 22, 23). Here, we performed comprehensive antibody and lymphocyte subset analyses of B cells and cTfh in 23 patients with suspected autoimmune epilepsy who met Graus's criteria for possible autoimmune encephalitis. The results were compared with clinical evaluations, and diagnostic biomarkers in the active phase of antibody-positive autoimmune epilepsy were discussed.

# Materials and methods

## Patients

This prospective multicenter study was conducted in Japan between January 2016 and May 2022. We recruited patients who visited the Division of Neurology, Kobe University Graduate School of Medicine, Kobe, Japan; Department of Neurology, Kobe City Medical Center and, General Hospital, Kobe, Japan; Department of Neurology, Hyogo Prefectural Amagasaki General Medical Center, Amagasaki City, Japan. Patients who met the following criteria were included in the study:1) had seizures and adequate clinical evaluation to differentiate autoimmune epilepsy, 2) met Graus's criteria for possible autoimmune encephalitis (7), 3) had been comprehensively

analyzed for known anti-neuronal antibodies in cerebrospinal fluid (CSF) or serum, and 4) did not receive oral steroid therapy or immunosuppressive therapy. We recruited age- and sex-matched healthy controls (HC). Patients with active phase epilepsy underwent brain MRI and electroencephalography (EEG), and their peripheral blood and CSF samples were collected before initiating intravenous methylprednisolone therapy. The exclusion criterion was previous intravenous corticosteroid treatment within three months before sampling. MRI abnormalities were defined as hyperintense signals on T2WI or fluid-attenuated inversion recovery in multiple regions, including the medial temporal lobe, gray matter, white matter, or all, reflecting inflammation. EEG abnormalities were defined as focal epileptic or slow-wave activities.

## Anti-neuronal antibody analysis

Anti-neuronal antibodies were analyzed as follows. CSF was analyzed using a CBA for the N-methyl-D-aspartate receptor (NMDAR) antibody (Euroimmun AG, Lübeck, Germany) and leucine-rich glioma-inactivated protein 1 (LGI1) antibody (Cosmic Corporation, Tokyo, Japan). Serum samples were analyzed using a CBA for myelin oligodendrocyte glycoprotein (MOG) antibody (Cosmic Corporation, Tokyo, Japan) and ELISA for GAD antibody (SRL, Tokyo, Japan). If the results were negative, we performed a screen immunohistochemistry using rat brain, as previously reported (24, 25). In brief, fresh rat brains were fixed by 4% paraformaldehyde for 30 min, following dehydrated in 40% sucrose in PBS and keep in 4°C overnight. Then, brains were frozen in liquid nitrogen, and sliced into 7 μm sections on a cryostat, and transferred onto coverslips. The brain slice on coverslips were treated with 0.3% H2O2 in PBS after wash, and blocked with 5% goat serum, followed by incubation with patients' serum at 1:200 or CSF at 1:4 in blocking solution overnight in 4°C. The coverslips were washed and incubated with goat anti-human IgG (H+L) biotinylated antibody (#BA-3000, Vector, CA, USA), followed by staining with the ABC Elite Kit (#PK6100, Vector, CA, USA). The sections were analyzed by at least two conditions blinded experienced investigators using a Zeiss Axioscope (Zeiss, CA, USA).

Samples positive for rat brain screen with immunohistochemistry were further investigated for reactivity against specific neuronal antigens including α-amino-3-hydroxy-5-methyl-4-isoxazole propionic acid receptor (AMPAR), γ-aminobutyric acid type B receptor ($GABA_BR$), contactin-associated protein-like 2 (CASPR2), Delta/Notch-like epidermal growth factor-related receptor (DNER), Zic4, dipeptidyl-peptidase-like protein 6 (DPPX), collapsin response mediator protein 5 (CRMP-5/CV2), Hu, Yo, Ri, Ma, and amphiphysin. To this end, we used standardized commercially available test kits [immunofluorescence tests with tissue, fixed transfected cells, enzyme-linked immunosorbent assay, and immunoblotting appropriately (Euroimmun, Lubeck, Germany)]. We defined patients with antibodies to these known antigens as antibody-positive autoimmune epilepsy: AE/Ab(+), and those with antibodies negative for rat brain immunohistochemistry but who met the inclusion criteria: AE/Ab(-).

## Flow cytometry

PBMCs were separated by density centrifugation using a Ficoll-Paque PLUS (GE Healthcare, Uppsala, Sweden). PBMCs were stained for B cell and cTfh subsets, and CSF samples were stained for B cell subsets using antibodies (Supplementary Table 1). Data were obtained using a FACSVerse or LSRFortessa X-20 (BD Biosciences, Franklin Lakes, NJ, USA). Negative expression was defined as the fluorescence minus one control. All fresh samples were analyzed within 24 h of collection.

Circulating B-cell subsets (plasmablasts, $CD19^{int}CD27^{high}CD38^{high}CD180-$ B cells; naïve B cells, CD19+CD27−IgD+ B cells; unswitched memory B cells, USM, CD19+CD27+IgD+ B cells; switched memory B cells, SWM, CD19+CD27+IgD- B cells; double negative B cells, DN, CD19+CD27−IgD− B cells) circulating Tfh subsets (circulating follicular helper T cells, cTfh, CD3+CD4+CXCR5+ T cells; cTfh1, CXCR3+CCR6−CXCR5+CD4 T cells; cTfh2, CXCR3−CCR6−CXCR5+CD4 T cells; cTfh17, CXCR3−CCR6+CXCR5+CD4 T cells), and their expression rate of ICOS ($ICOS^{high}$cTfh, CD3+CD4+CXCR5+$ICOS^{high}$CD4 T cells; $ICOS^{high}$cTfh1, CXCR3+CCR6−CXCR5+$ICOS^{high}$CD4 T cells; $ICOS^{high}$cTfh2, CXCR3−CCR6−CXCR5+$ICOS^{high}$CD4 T cells; $ICOS^{high}$cTfh17, CXCR3−CCR6+CXCR5+$ICOS^{high}$CD4 T cells) were analyzed. The phenotypes of B cell and cTfh subsets are shown in Supplementary Table 2.

## Serum and CSF cytokine and chemokine levels

Serum and CSF samples were collected during the active phase before intravenous methylprednisolone administration. Both serum and CSF were frozen at −80°C. Cytokine/chemokine production was measured using the LEGENDplex Human Inflammation Panel 1 (BioLegend, San Diego, CA) and BD™ CBA Flex Set System (BD Bioscience) using an LSRFortessa X-20 cell analyzer (BD Biosciences) and BD™ Human Soluble Protein Master Buffer Kit (BD Bioscience) according to the manufacturer's instructions. IFN-γ, IL-6, IL-12p70, IL-17A, and IL-23 levels were analyzed using the LEGENDplex Human Inflammation Panel 1 and IL-4 levels were analyzed using the BD™ CBA Flex Set System.

## Data analysis

Flow cytometry data were analyzed using FlowJo software ver. 10.8.1 (BD Biosciences). Statistical analyses were performed

using GraphPad Prism 9 software (GraphPad Software, San Diego, CA, USA). In addition, the two-sided unpaired *t*-test, two-sided Mann-Whitney *U* test, and Spearman's correlation test were used as appropriate.

## Standard protocol approval, registration, and patient consent

This study was approved by the ethics committee of Kobe University Hospital (Nos.1381 and B190152), and signed informed consent was obtained from all participants.

# Results

## Patient characteristics

We included 23 patients with suspected autoimmune epilepsy and 11 HC. The patient subgroups are summarized in Table 1. Among the 23 patients, 13 (57%) showed the presence and 10 (43%) showed the absence of anti-neuronal antibodies, categorized as the anti-neuronal antibody-positive autoimmune epilepsy (AE/Ab(+)) group and antibody-negative suspected autoimmune epilepsy (AE/Ab(-)) group, respectively. No samples tested positive in rat brains and negative in a CBA. The mean age was 43.8 ± 18.0, 50.2 ± 19.2, and 34.1 ± 6.7 (mean ± SD) for patients with AE/Ab(+), AE/Ab(-), and HC, respectively. Five patients with AE/Ab(+) (38%) were positive for anti-neuronal antibodies against the N-methyl-D-aspartate (NMDA) receptor, four patients (31%) had antibodies against myelin oligodendrocyte glycoprotein (MOG), and four patients (31%) against leucine-rich glioma-inactivated 1 (LGI1). All patients with MOG antibodies had unilateral cortical FLAIR-hyperintense lesions in MOG-associated encephalitis with seizures subtypes of MOG-associated disease (26). There were no differences or bilateral abnormalities on MRI, several CSF abnormalities (cell counts, levels of protein, IgG index, oligoclonal bands), EEG, or tumor comorbidity between the AE/Ab(+) and AE/Ab(-) groups.

## Proportion of plasmablasts was increased in patients with AE/Ab(+)

To elucidate the differences between the two groups, we analyzed the immune phenotype of B cells. The gating strategy

TABLE 1 Characteristics of patients with autoimmune epilepsy and HC.

| | Antibody-positive autoimmune epilepsy (n=13) | Antibody-negative suspected autoimmune epilepsy* (n=10) | HC (n=11) | Antibody-positive autoimmune epilepsy vs. antibody-negative suspected autoimmune epilepsy, p value | Antibody-positive autoimmune epilepsy vs. HC, p value |
|---|---|---|---|---|---|
| Age(y), mean ± SD | 43.8±18.0 | 50.2±19.2 | 34.1±6.7 | 0.44 | 0.15 |
| Sex, female, n (%) | 5 (38) | 3 (30) | 4 (36) | 0.97 | 0.78 |
| Anti neuronal-antibody, n (%) | NMDA 5 (38)<br>MOG 4 (31)<br>LGI1 4 (31) | – | – | – | – |
| Abnormal MRI findings, n(%) | 9 (69) | 10 (100) | – | 0.10 | – |
| Bilateral abnormal MRI findings, n(%) | 4 (31) | 4 (40) | – | 0.66 | – |
| CSF pleocytosis (> 5μl), n (%) | 3 (23) | 1 (10) | – | 0.43 | – |
| Elevated CSF protein (> 40 mg/dl), n (%) | 6 (46) | 5 (50) | – | > 0.99 | – |
| Elevated IgG index > 0.7, n (%) | 1 (8) | 0 (0) | – | > 0.99 | – |
| Oligoclonal banding in CSF, n (%) | 4 (31) | 1 (10) | – | 0.10 | – |
| Abnormal EEG findings, n (%) | 9 (69) | 10 (100) | – | 0.10 | – |
| Tumor association, n (%) | 3 (23) | 2(20) | – | 0.86 | – |

HC, healthy controls; NMDA, N-methyl-D-aspartate; MOG, myelin oligodendrocyte glycoprotein; LGI1, leucine-rich glioma-inactivated protein 1; CSF, cerebrospinal fluid, the two-sided unpaired t-test or Mann-Whitney U test were used for comparisons appropriately.
*Antibody-negative suspected autoimmune epilepsy, patients with antibodies negative for rat brain immunohistochemistry but met inclusion criteria and suspected autoimmune epilepsy.

for the B cell subsets is shown in Supplementary Figure 1. The frequency of plasmablasts in the B cells of PBMCs was higher in patients with AE/Ab(+) than in those with AE/Ab(-) and HC (Figures 1A, B). Next, we compared the AE/Ab(+) group positive for antibodies against the neuronal surface antigen (NSA) (NMDAR or LGI1 antibody-positive group) and MOG antibody-positive group (MOG). The frequency of plasmablasts in the B cells of PBMCs in patients with NSA was higher than that in patients with AE/Ab(-) and HC (Figure 1C). Furthermore, we found that the frequency of B cells and plasmablasts within B cells of the CSF was elevated in patients with AE/Ab(+) compared to that in patients with AE/Ab(-) (Figures 1D, E). There were no differences among patients with AE/Ab(+), AE/Ab(-), and HC with respect to the frequencies of naive B cells, USM, SWM, and DN in the PBMCs (Figure 1F).

## ICOS expressing cTfh and cTfh subsets shifted to cTfh17 were prominent in patients with AE/Ab(+)

Since we found an increase in differentiating B cell subsets in patients with AE/Ab(+), we analyzed cTfh subsets and their ICOS expression in PBMCs (Figure 2A). The gating strategy for the cTfh subsets is shown in Supplementary Figure 1. The frequency of cTfh did not differ between patients with AE/Ab (+), AE/Ab(-) and HC (Figure 2B). In contrast, the frequency of ICOS$^{high}$cTfh in cTfh was higher in patients with AE/Ab(+) than in those with AE/Ab(-) and HC (Figure 2C). In the subset analysis of cTfh, the frequency of cTfh17 in cTfh was higher in patients with AE/Ab(+) than in those with AE/Ab(-) and HC (Figure 2D), and the frequency of ICOS$^{high}$cTfh17 in cTfh was particularly elevated in patients with AE/Ab(+) than in those with AE/Ab(-) and HC (Figure 2E). Furthermore, the cTfh17/cTfh1 cells ratio was higher in patients with AE/Ab(+) than in those with AE/Ab(-) and HC (Figure 2F). The ICOS$^{high}$cTfh17/ICOS$^{high}$cTfh1 cells ratio did not differ between each group (Figure 2G).

## The frequency of USM was associated with that of ICOS$^{high}$cTfh17

We then compared the immune phenotypes of AE/Ab(+) patients with their clinical manifestations. Our data showed an association between plasmablasts in B cells of PBMCs and the modified Rankin Scale (mRS) in patients with AE/Ab(+) on admission (Figure 3A). Furthermore, we analyzed whether the frequency of cTfh subsets was correlated with B cell subsets and found a positive correlation between USM in B cells of PBMCs and ICOS$^{high}$cTfh17 in cTfh of patients with NSA (Figure 3B).

## Proportion of plasmablasts and ICOS$^{high}$cTfh17 was increased in patients with NSA antibody positive autoimmune epilepsy

To assess the consistency of our results in each disease entity with NSA, we compared the phenotypes of B cell and cTfh subsets of patients with NSA. The frequency of plasmablasts in B cells of PBMCs was higher in patients with NMDA antibodies than in those with AE/Ab(-) and HC (Supplemental Figure 2A). Furthermore, the frequency of ICOS$^{high}$cTfh17 in cTfh was higher in patients with NMDA and LGI1 antibodies than HC and was higher in patients with NMDA antibodies than patients with AE/Ab(-) (Supplementary Figure 2B).

## Proinflammatory cytokine levels were elevated in the serum and CSF of patients with AE/Ab(+)

Finally, we measured the proinflammatory cytokine profile in the serum and CSF of patients with AE/Ab(+) and AE/Ab(-). Although the levels of cytokines were heterogeneous in the serum, IL-6, IL-23, IL-17A, IL-12p70, and IFN-γ levels were elevated in patients with AE/Ab(+) compared to those in patients with AE/Ab(-) (Figure 4A). In the CSF, IL-6 and IL-17A levels were elevated in patients with AE/Ab(+) compared to those with AE/Ab(-) (Figure 4B).

# Discussion

Currently, more than 20 anti-neuronal antibodies support the diagnosis of AE. Recent advances in these findings have facilitated recognition of AE cases. AE is a subtype of autoimmune encephalitis with seizure as a clinical symptom. Since anti-neuronal antibody tests are not always available, efforts have been made to diagnose AE without anti-neuronal antibodies testing based on clinical symptoms, imaging, and laboratory testing (5, 6); however, a more comprehensive analysis would be more accurate in preventing misdiagnosis of treatable diseases. Understanding multiple immune cell responses in disease pathogenesis could be a more appropriate strategy to improve the efficacy of AE diagnosis. In this study, we compared antibody-positive and antibody-negative patients with suspected autoimmune epilepsy. We did not observe any differences in clinical parameters, such as MRI findings, CSF markers, EEG findings, and age and sex, between the groups. In contrast, lymphocyte subset analysis of PBMCs showed that plasmablasts were elevated in the antibody-positive group, and

10.3389/fimmu.2022.1048428

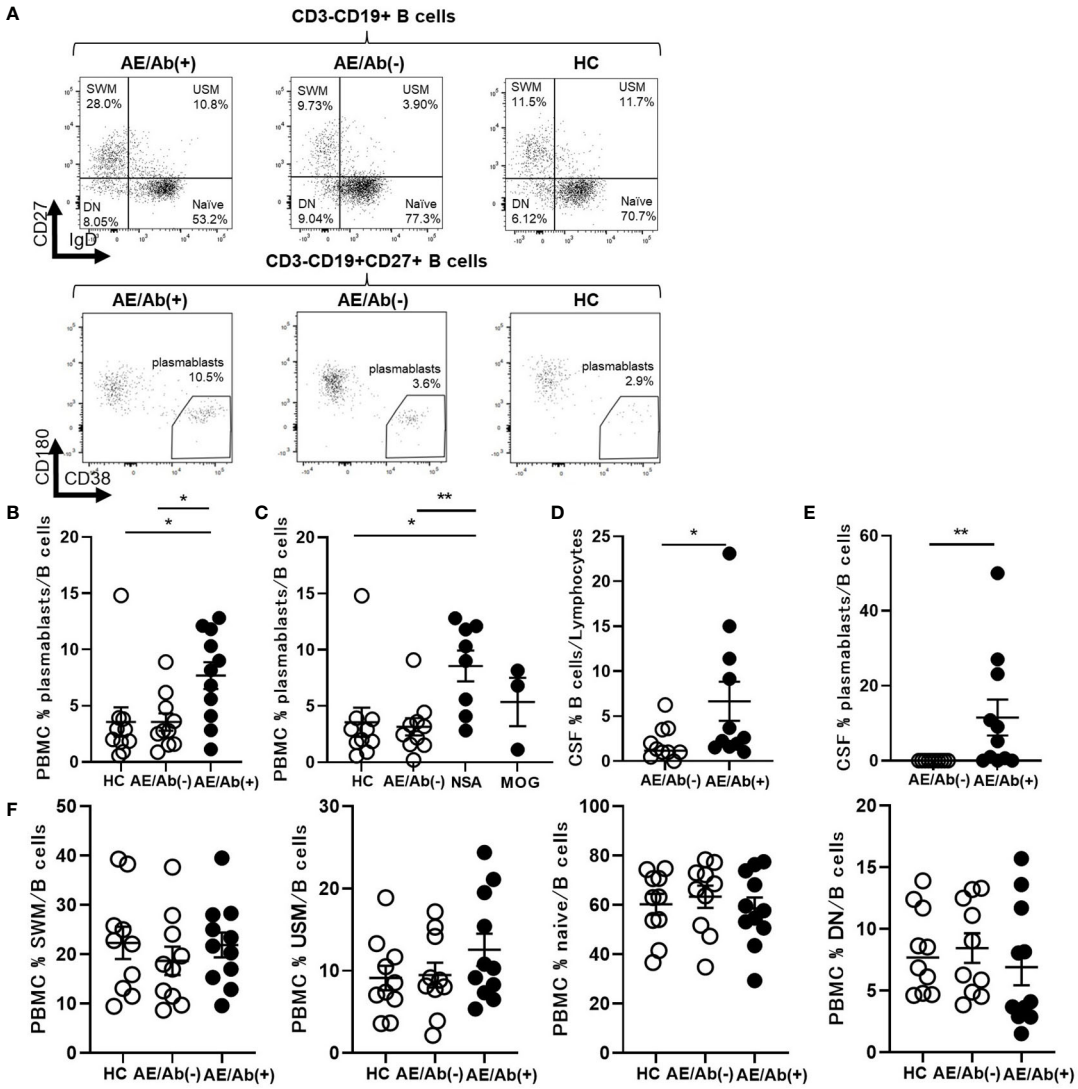


FIGURE 1
Prominent plasmablasts were found in patients with AE/Ab(+). **(A)** Representative flow cytometry analysis of CD19+CD27−IgD+ (naive), CD19+CD27−IgD− (DN), CD19+CD27+IgD+ (USM), CD19+CD27+IgD− (SWM), and $CD19^{int}CD27^{high}CD38^{high}CD180-$ (plasmablasts) in PBMCs of HC, patients with AE/Ab(-) and AE/Ab(+). **(B, C)** The frequency of plasmablasts in B cells of PBMCs of each group. NSA is defined as the patients group of NMDA receptor antibody-positive autoimmune epilepsy and LGI1 antibody associated autoimmune epilepsy. **(D)** The frequency of B cells within lymphocytes in the CSF of patients with AE/Ab(-) and AE/Ab(+). **(E)** The frequency of plasmablasts within B cells in the CSF of patients with AE/Ab(-) and AE/Ab(+). **(F)** The frequency of SWM, USM, naive, and DN within B cells in PBMCs of each group. HC (n=11), AE/Ab(-) (n=10), and AE/Ab(+) (n=11).Values are expressed as the mean ± SEM. *p < 0.05 and **p < 0.01; two-sided unpaired *t*-test or Mann-Whitney *U* test, as appropriate. HC, healthy controls; AE/Ab(-), antibody-negative suspected autoimmune epilepsy; AE/Ab(+), antibody-positive autoimmune epilepsy; SWM, switched memory B cell; USM, unswitched memory B cell; DN, double negative B cell; naive, naive B cell; NSA, neuronal surface antigen; NMDA, N-methyl-D-aspartate; LGI1, leucine-rich glioma-inactivated 1; MOG, myelin oligodendrocyte glycoprotein; PBMCs, peripheral blood mononuclear cells.

the subset of cTfh cells was altered to stimulate B cell antibody production. In a previous study on antibody-positive and antibody-negative cases of autoimmune epilepsy or limbic encephalitis, antibody-positive cases were more likely to show MRI changes in the medial temporal lobes, and antibody-negative cases were more frequent in older men (8, 9). There were no differences in MRI changes, age, or sex between the antibody-positive and antibody-negative groups. These results highlight the difficulty in clinically diagnosing patients with autoimmune epilepsy.

We found that plasmablasts in PBMCs were elevated in patients with AE/Ab(+) compared to those in patients with AE/Ab(-) and HC. Elevated levels of plasmablasts are involved in the pathogenesis of some autoantibody-associated autoimmune

10.3389/fimmu.2022.1048428

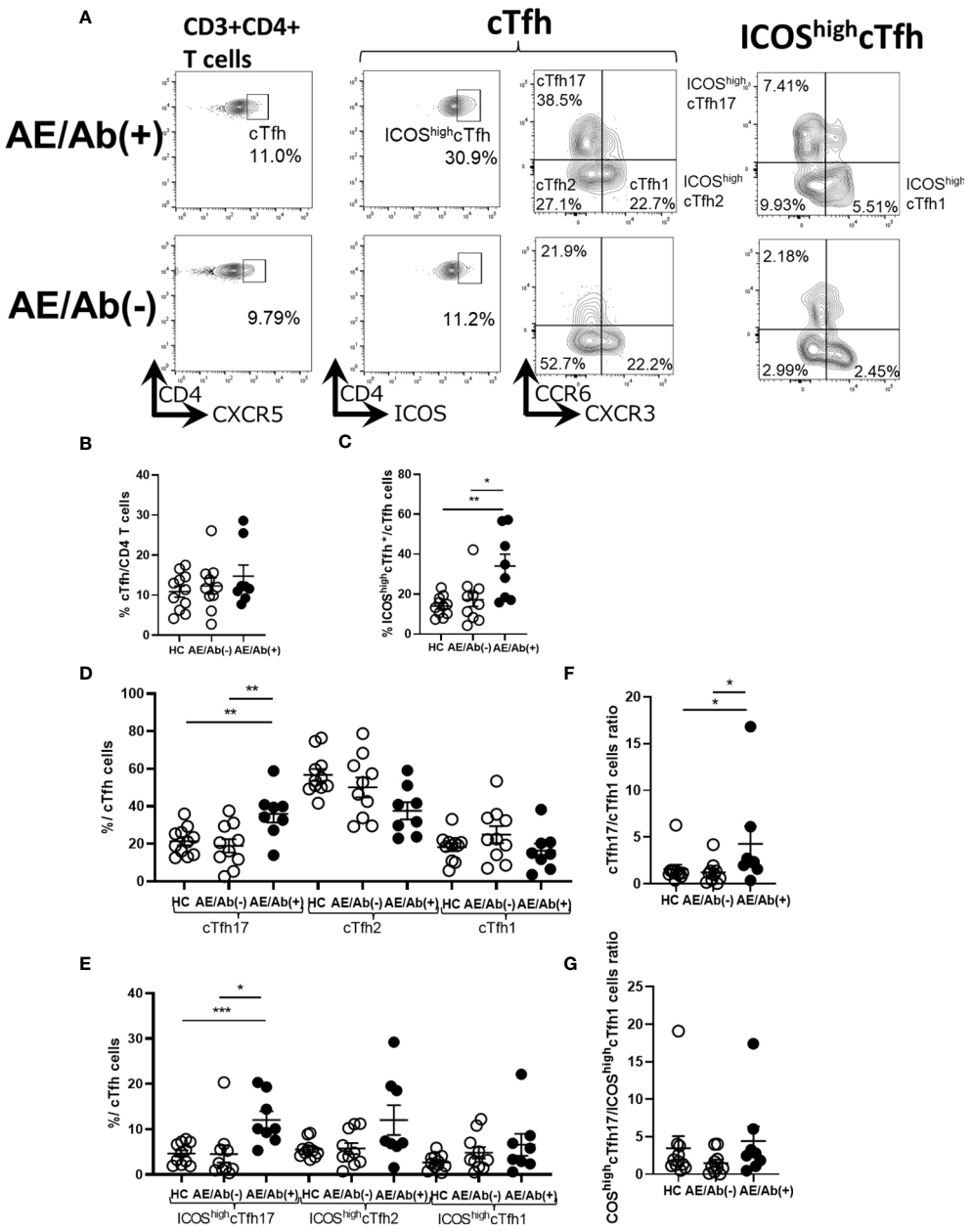


FIGURE 2
cTfh subset shifts to induce B cell differentiation in patients with AE/Ab(+). **(A)** Representative flow cytometry analysis of CD3+CD4+CXCR5+ T cells(cTfh), CD3+CD4+CXCR5+ICOS$^{high}$CD4 T cells (ICOS$^{high}$cTfh), CXCR3+CCR6–CXCR5+CD4 T cells(cTfh1), CXCR3–CCR6–CXCR5+CD4 T cells (cTfh2), CXCR3–CCR6+CXCR5+CD4 T cells (cTfh17), CXCR3+CCR6–CXCR5+ICOS$^{high}$CD4 T cells (ICOS$^{high}$cTfh1), CXCR3–CCR6–CXCR5 +ICOS$^{high}$CD4 T cells (ICOS$^{high}$cTfh2), and CXCR3–CCR6+CXCR5+ICOS$^{high}$CD4 T cells (ICOS$^{high}$cTfh17) in PBMCs. **(B)** The frequency of cTfh within CD4 T cells in HC, patients with AE/Ab(-) and AE/Ab(+). **(C)** The frequency of ICOS$^{high}$cTfh within cTfh in HC and patients with AE/Ab(-), AE/Ab(+). **(D)** The frequency of cTfh17, cTfh2, and cTfh1 within cTfh in HC, patients with AE/Ab(-) and AE/Ab(+). **(E)** The frequency of ICOS$^{high}$cTfh17, ICOS$^{high}$cTfh2, and ICOS$^{high}$cTfh1 of cTfh in HC and patients with AE/Ab(-) and AE/Ab(+). **(F)** cTfh17/cTfh1 cells ratio of cTfh in HC, patients with AE/Ab(-) and AE/Ab(+). **(G)** ICOS$^{high}$cTfh17/ICOS$^{high}$cTfh1 cells ratio in HC, patients with AE/Ab(-) and AE/Ab(+). HC (n=11), AE/Ab(-) (n=10), and AE/Ab(+) (n=8). Values are expressed as the mean ± SEM. *p < 0.05, **p < 0.01 and ***p < 0.001; two-sided unpaired *t*-test or Mann-Whitney *U* test, as appropriate. HC, healthy controls; AE/Ab(-), antibody-negative suspected autoimmune epilepsy; AE/Ab(+), antibody-positive autoimmune epilepsy; cTfh, circulating follicular helper T cell; ICOS, inducible T-cell co-stimulator.

10.3389/fimmu.2022.1048428

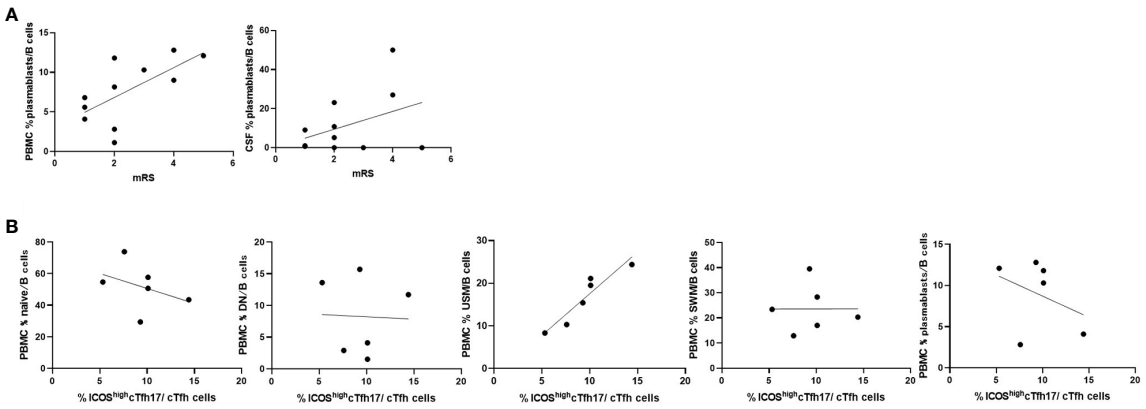


FIGURE 3
Frequencies of B cell subsets were associated with clinical severity and Tfh subsets in patients with AE/Ab(+). **(A)** Scatter plot of the frequency of plasmablasts within B cells in PBMCs or CSF and mRS on admission of patients with AE/Ab(+) (n = 11). The frequency of plasmablasts within B cells in PBMCs were associated with mRS (Spearman correlation coefficient, $r = 0.67$, $p = 0.025$). **(B)** Scatter plot of the frequency of B cell subsets within B cells in PBMCs and the frequency of ICOS$^{high}$cTfh17 within cTfh cells in PBMCs of patients positive for antibodies against NSA (n = 6). The frequency of USM within B cells in PBMCs were associated with the frequency of ICOS$^{high}$cTfh17 (Spearman correlation coefficient, $r = 0.93$, $p = 0.0059$). PBMCs, peripheral blood mononuclear cells; mRS, modified Rankin scale; cTfh, circulating follicular helper T cell; ICOS, inducible T-cell co-stimulator; naive, naive B cell; DN, double negative B cell; USM, unswitched memory B cell; SWM, switched memory B cell.

diseases such as systemic lupus erythematosus (SLE), neuromyelitis optica spectrum disorder (NMOSD), and IgG4-related disorders (27–29). Especially in NMOSD, an autoantibody-associated autoimmune disease of the central nervous system (CNS), plasmablasts are elevated in PBMCs and CSF (27) and produce pathogenic autoantibodies (30, 31). Emerging evidence showing the dynamics of plasmablasts related to disease activity in autoantibody-associated autoimmune diseases highlights the potential of this B cell subset as a representative immune phenotype, which may be called “autoimmune plasmablastosis”. In a study on NMDAR encephalitis, plasmablasts were reported to be elevated in the active phase of the disease in PBMCs and decreased after rituximab administration (32). In another report involving four cases of NMDAR encephalitis, plasma cells in the CSF were elevated in the active phase of the disease and decreased after treatment (33). In line with these previous findings, in our study, patients with AE/Ab(+) showed elevated plasmablasts in PBMCs and CSF, and the former were associated with global physical disability (mRS) upon admission, which may highlight the increase in plasmablasts as an outcome of the immune response of patients with AE/Ab(+). Of note, one patient with AE/Ab(-) and one HC showed a relative increase in plasmablasts in PBMCs, which may reflect heterogeneity of the frequency of plasmablasts in peripheral circulation. Otherwise, other unknown autoantibodies may be present in patients with AE/Ab(-). Further investigation focusing on B cell phenotypes, regardless of anti-neural antibodies, would be worthwhile in future studies.

We further found that cTfh in patients with AE/Ab (+) strongly expressed ICOS. ICOS is preferentially expressed on Tfh; it is required for active regulation of B cell responses by interacting with ICOS ligands on B cells and is involved in IgG production (34, 35). Although ICOS$^{high}$cTfh has been reported to be elevated in myasthenia gravis and idiopathic thrombocytopenic purpura (16, 36), elevated ICOS$^{high}$cTfh levels in autoimmune epilepsy found in this study may reflect a common immunological feature of these diseases. Notably, cTfh was shifted to cTfh17 in the present study. cTfh17 is characterized by the production of the cytokine IL-17 and expression of the transcription factor ROR-γt, which has been shown to have a potent stimulatory effect on plasmablasts that produce IgG in autoimmune diseases, such as dermatomyositis (15). Several reports have shown that cTfh shifts to a subset of cTfh17 or cTfh2 in autoantibody-associated autoimmune diseases (16–19) that is consistent in patients with AE/Ab(+). Moreover, the cTfh17/cTfh1 cells ratio correlates with enhanced humoral immune response (20). In line with this, our data showed that cTfh shifted to cTfh17 in patients with AE/Ab(+), and the cTfh17/cTfh1 ratio increased. Indeed, ICOS$^{high}$cTfh17 within cTfh were elevated in the patients with NMDA and LGI1 antibodies positive autoimmune epilepsy compared with AE/Ab (-) patients or HC. The ICOS$^{high}$cTfh17/ICOS$^{high}$cTfh1 ratio did not differ in each group, but It might be because ICOS is widely expressed among cTfh cell subsets in patients with AE/Ab (+).These results suggest that AE/Ab(+) shares a similar immune background with other autoantibody-associated autoimmune diseases.

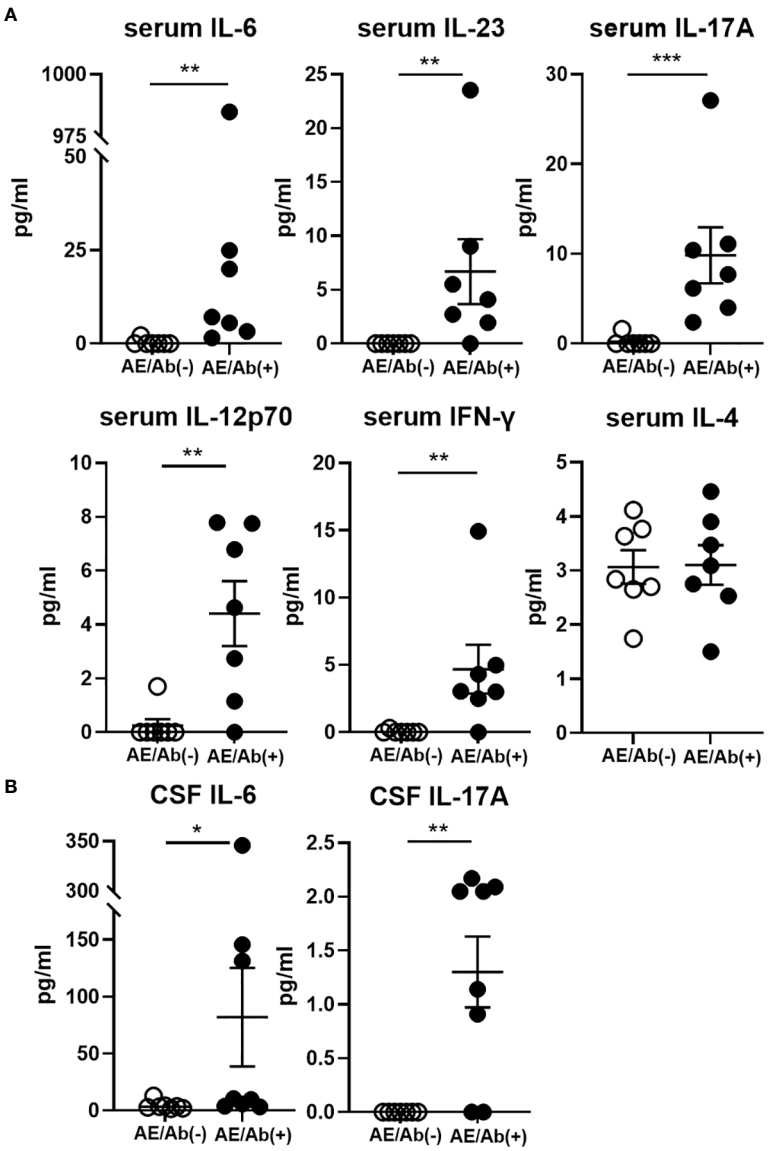


FIGURE 4
Serum and CSF levels of cytokines (pg/ml) in patients with AE/Ab(-) and AE/Ab(+). **(A)** Serum levels of cytokines (pg/ml) in patients with AE/Ab(-) (n=8) and AE/Ab(+) (n=7). **(B)** CSF levels of cytokines (pg/ml) in patients with AE/Ab(-) (n=8) and AE/Ab(+) (n=8). Values are expressed as the mean ± SEM. * $p < 0.05$, **$p < 0.01$, and *** $p < 0.001$; two-sided unpaired *t*-test or Mann-Whitney *U* test, as appropriate. AE/Ab(-), antibody-negative suspected autoimmune epilepsy; AE/Ab(+), antibody-positive autoimmune epilepsy.

In our study, the frequency of $ICOS^{high}$cTfh17 within cTfh cells correlated with USM among the B cell subsets in patients with NSA. USMs are B-cell subsets that enter the germinal center and have the potential for early differentiation into plasmablasts supported by Tfh (37, 38). It has recently been reported that an increase in USM in the peripheral circulation is associated with IgG1/IgM responses to SARS-CoV2 results in earlier COVID-19 recovery (39). Furthermore, a parallel increase in circulating USM with cTfh has been reported in cancer patients who respond well to immune checkpoint therapy (40). Such an immune response in infection and cancer, in turn, potentially suggests an association between USM and cTfh in the autoimmune response in patients with NSA. Notably, this trend was not observed in patients with MOG antibodies, which requires further investigation for the immune background of their autoantibody production. In contrast, USM decreases during the active phase of established disease in SLE and rheumatoid arthritis and is negatively correlated with disease severity (41, 42). Although we did not find a decrease in USM but rather an increase in patients with AE/Ab(+), the differences may reflect that we enrolled patients in

initial disease stages before the establishment of pathologically switched memory B cells.

Next we found IL-12p70, IL-23, IL-6, IL-17A, and IFN-γ levels were elevated in the serum, and IL-6 and IL-17A levels were elevated in the CSF of patients with AE/Ab(+) compared to those of patients with AE/Ab(-). Some studies have reported that cytokine changes in autoimmune encephalitis have focused on the CSF. Elevated levels of IL-6, IL-17A, and CXCL13, which is a ligand of CXCR5 and is a known B-cell-attracting chemokine in CSF, have been reported in NMDAR encephalitis (43, 44). Elevated IL-17A levels in the CSF have also been reported in non-NMDA autoimmune encephalitis (45), suggesting that CSF IL-17A is likely to play an important role in autoimmune encephalitis. In this study, we found elevated IL-6 and IL-17A levels in the CSF, similar to previous reports, and cytokine changes in the serum. IL-12 and IL-23, which are elevated in the serum, activate STAT4 and STAT3, respectively, and promote T-cell differentiation into the Tfh lineage (12, 46). IL-12 also induces Th1 differentiation and IFN-γ production in T cells (47). Elevated levels of IL-12 and IL-23 may induce subset changes in cTfh cells. IL-17 is a pro-inflammatory cytokine produced not only by Th17 cells, but also by Tfh17 (12). IL-17 downregulates tight junction molecules and facilitates leukocyte passage through the blood-brain barrier. IL-6 is also a pro-inflammatory cytokine that is elevated in CNS autoimmune diseases such as NMO, stimulates B cell differentiation (48), promotes plasmablasts survival, and enhances antibody secretion (30). Importantly, the levels of cytokines were less uniform in our AE/Ab(+) cases, which was probably due to the complex immune response in the active phase of AE. Our deeper immune phenotype analysis revealed clearer characteristic cTfh and B cell phenotypes relevant to changes in proinflammatory cytokines.

The shift in cTfh subsets, elevated plasmablasts, and cytokine changes that support their differentiation in peripheral blood suggest that the differentiation of B cells into plasmablasts in AE/Ab(+) takes place outside the CNS. In fact, among autoimmune encephalitis, NMDAR encephalitis does not form lymphatic follicles in brain pathology, but teratomas develop into tertiary lymphatic follicles, and teratoma-derived lymphocytes or the peripherally circulating B cells differentiate into plasmablasts and produce NR1 antibodies specific to NMDAR encephalitis (43, 49, 50). In LGI1 encephalitis, B cells in the CSF and plasmablasts of PBMCs have been reported to be clonally related (51). On the basis of these evidences, Dalmau et al. proposed the pathophysiology of autoimmune encephalitis. Naive B cells experience neuronal antigens in regional lymph nodes outside the CNS and then differentiate into memory B cells and antibody-producing cells *via* Tfh or other pathways. Memory B cells migrate to the CNS and differentiate into antibody-producing cells (52, 53). Our results support these hypotheses and further extend them as there is an alternative pathway for B cell differentiation in peripheral lymphoid organs.

This study had some limitations. First, it was a small-scale study. Although it is the same antibody-related autoimmune disease, the phenotype of each anti-neuronal antibody was difficult to compare due to limited number of available patients would require further evaluation in the future. Moreover, since this study was performed in cross-sectional way, we may need to evaluate patients in multiple points longitudinally to see future immune alteration that did not found in the initial evaluation. Second, the low number of cells in the CSF precluded the comparison of the subset analyses of cTfh in CSF. Third, we were unable to analyze patients with antibodies against intracellular antigens. Hence, a long-term prospective study is needed to determine the phenotype of each antibody in a large number of patients, and to consider the clinical manifestations of cTfh17, ICOS$^{high}$cTfh17, and plasmablasts. Nevertheless, immune phenotype alterations with increased levels of proinflammatory cytokines in the serum highlighted the role of the autoimmune response in the peripheral lymphoid organs during the active phase of patients with AE/Ab(+).

## Conclusion

Given the changes in the subsets of B cells and cTfh cells that promote antibody production observed in the PBMCs of patients with antibody-positive autoimmune epilepsy, our data provide immune-related markers for representing antibody-positive autoimmune epilepsy. In particular, elevated plasmablasts levels and ICOS-expressing cTfh17 shift may provide a new diagnostic and therapeutic indicator for antibody-positive autoimmune epilepsy.

## Data availability statement

The original contributions presented in the study are included in the article/Supplementary material. Further inquiries can be directed to the corresponding authors.

## Ethics statement

The studies involving human participants were reviewed and approved by the ethics committee of Kobe University Hospital (Nos.1381 and B190152). The patients/participants provided their written informed consent to participate in this study.

## Author contributions

Study design and conceptualization: AH and NC. Major role in data acquisition: AH and NC. Analysis or interpretation of the data: AH, NC, RA, RN, AT, HY, MK, YO, YK, TK, FL, K-PW, and RM. Drafting the manuscript for intellectual content: AH and NC. supervision of the entire study: NC and RM. All authors contributed to the article and approved the submitted version.

## Funding

This work was supported by a Grant-in-Aid for Scientific Research from the Japan Society for the Promotion of Science (20H03562), Practical Research Project for Rare/Intractable Diseases by AMED (22ek0109436h0003), Intramural Research Grant for neurological and psychiatric disorders of NCNP, Research grant from the Naito Foundation, a research grant from the Japan Epilepsy Research Foundation (JERF TENKAN 20010), and the Japan Science and Technology Agency (Moonshot R&D) (JPMJMS 2024).

## Acknowledgments

The authors thank their colleagues in the Division of Neurology at Kobe University Graduate School of Medicine, the Department of Neurology at Kobe City Medical Center General Hospital, and the Department of Neurology at Hyogo Prefectural Amagasaki General Medical Center for their help with sample collection.

## Conflict of interest

The authors declare that the research was conducted in the absence of any commercial or financial relationships that could be construed as a potential conflict of interest.

## Publisher's note

All claims expressed in this article are solely those of the authors and do not necessarily represent those of their affiliated organizations, or those of the publisher, the editors and the reviewers. Any product that may be evaluated in this article, or claim that may be made by its manufacturer, is not guaranteed or endorsed by the publisher.

## Supplementary material

The Supplementary Material for this article can be found online at: https://www.frontiersin.org/articles/10.3389/fimmu.2022.1048428/full#supplementary-material

## References

1. Ong MS, Kohane IS, Cai T, Gorman MP, Mandl KD. Population-level evidence for an autoimmune etiology of epilepsy. *JAMA Neurol* (2014) 71 (5):569–74. doi: 10.1001/jamaneurol.2014.188

2. Levite M. Autoimmune epilepsy. *Nat Immunol* (2002) 3(6):500. doi: 10.1038/ni0602-500

3. Quek AM, Britton JW, McKeon A, So E, Lennon VA, Shin C, et al. Autoimmune epilepsy: Clinical characteristics and response to immunotherapy. *Arch Neurol* (2012) 69(5):582–93. doi: 10.1001/archneurol.2011.2985

4. Husari K, Dubey D. Autoimmune epilepsy. *Neuroimmunology* (2021), 189–206. doi: 10.1007/978-3-030-61883-4_13

5. Dubey D, Kothapalli N, McKeon A, Flanagan EP, Lennon VA, Klein CJ, et al. Predictors of neural-specific autoantibodies and immunotherapy response in patients with cognitive dysfunction. *J Neuroimmunol.* (2018) 323:62–72. doi: 10.1016/j.jneuroim.2018.07.009

6. de Bruijn M, Bastiaansen AEM, Mojzisova H, van Sonderen A, Thijs RD, Majoie MJM, et al. Antibodies contributing to focal epilepsy signs and symptoms score. *Ann Neurol* (2021) 89(4):698–710. doi: 10.1002/ana.26013

7. Graus F, Titulaer MJ, Balu R, Benseler S, Bien CG, Cellucci T, et al. A clinical approach to diagnosis of autoimmune encephalitis. *Lancet Neurology.* (2016) 15 (4):391–404. doi: 10.1016/S1474-4422(15)00401-9

8. Ismail FS, Spatola M, Woermann FG, Popkirov S, Jungilligens J, Bien CG, et al. Diagnostic challenges in patients with temporal lobe seizures and features of autoimmune limbic encephalitis. *Eur J Neurol* (2021) 1-8. doi: 10.1111/ene.15026

9. Graus F, Escudero D, Oleaga L, Bruna J, Villarejo-Galende A, Ballabriga J, et al. Syndrome and outcome of antibody-negative limbic encephalitis. *Eur J Neurol* (2018) 25(8):1011–6. doi: 10.1111/ene.13661

10. Jang Y, Kim DW, Yang KI, Byun JI, Seo JG, No YJ, et al. Clinical approach to autoimmune epilepsy. *J Clin Neurol* (2020) 16(4):519–29. doi: 10.3988/jcn.2020.16.4.519

11. Dalmau J, Graus F. Antibody-mediated encephalitis. *N Engl J Med* (2018) 378(9):840–51. doi: 10.1056/NEJMra1708712

12. Schmitt N, Bentebibel SE, Ueno H. Phenotype and functions of memory tfh cells in human blood. *Trends Immunol* (2014) 35(9):436–42. doi: 10.1016/j.it.2014.06.002

13. Ueno H, Banchereau J, Vinuesa CG. Pathophysiology of T follicular helper cells in humans and mice. *Nat Immunol* (2015) 16(2):142–52. doi: 10.1038/ni.3054

14. Brenna E, Davydov AN, Ladell K, McLaren JE, Bonaiuti P, Metsger M, et al. CD4(+) T follicular helper cells in human tonsils and blood are clonally convergent but divergent from non-tfh CD4(+) cells. *Cell Rep* (2020) 30(1):137–52 e5. doi: 10.1016/j.celrep.2019.12.016

15. Morita R, Schmitt N, Bentebibel SE, Ranganathan R, Bourdery L, Zurawski G, et al. Human blood CXCR5(+)CD4(+) T cells are counterparts of T follicular cells and contain specific subsets that differentially support antibody secretion. *Immunity* (2011) 34(1):108–21. doi: 10.1016/j.immuni.2010.12.012

16. Ashida S, Ochi H, Hamatani M, Fujii C, Kimura K, Okada Y, et al. Immune skew of circulating follicular helper T cells associates with myasthenia gravis severity. *Neurol Neuroimmunol Neuroinflamm* (2021) 8(2):e945. doi: 10.1212/NXI.0000000000000945

17. Le Coz C, Joublin A, Pasquali JL, Korganow AS, Dumortier H, Monneaux F. Circulating TFH subset distribution is strongly affected in lupus patients with an active disease. *PloS One* (2013) 8(9):e75319. doi: 10.1371/journal.pone.0075319

18. Bautista-Caro MB, Arroyo-Villa I, Castillo-Gallego C, de Miguel E, Peiteado D, Plasencia-Rodriguez C, et al. Decreased frequencies of circulating follicular helper T cell counterparts and plasmablasts in ankylosing spondylitis patients naive for TNF blockers. *PloS One* (2014) 9(9):e107086. doi: 10.1371/journal.pone.0107086

19. Kurata I, Matsumoto I, Sumida T. T Follicular helper cell subsets: a potential key player in autoimmunity. *Immunol Med* (2021) 44(1):1–9. doi: 10.1080/25785826.2020.1776079

20. Locci M, Havenar-Daughton C, Landais E, Wu J, Kroenke MA, Arlehamn CL, et al. Human circulating PD-1+CXCR3-CXCR5+ memory tfh cells are highly functional and correlate with broadly neutralizing HIV antibody responses. *Immunity* (2013) 39(4):758–69. doi: 10.1016/j.immuni.2013.08.031

21. Li Y, Guptill JT, Russo MA, Howard JFJr., Massey JM, Juel VC, et al. Imbalance in T follicular helper cells producing IL-17 promotes pro-inflammatory responses in MuSK antibody positive myasthenia gravis. *J Neuroimmunol.* (2020) 345:577279. doi: 10.1016/j.jneuroim.2020.577279

22. Nutt SL, Hodgkin PD, Tarlinton DM, Corcoran LM. The generation of antibody-secreting plasma cells. *Nat Rev Immunol* (2015) 15(3):160–71. doi: 10.1038/nri3795

23. Olatunde AC, Hale JS, Lamb TJ. Cytokine-skewed tfh cells: functional consequences for b cell help. *Trends Immunol* (2021) 42(6):536–50. doi: 10.1016/j.it.2021.04.006

24. Dalmau J. NMDA receptor encephalitis and other antibody-mediated disorders of the synapse. *Neurology* (2016) 87(23):2471–82. doi: 10.1212/WNL.0000000000003414

25. Ances BM, Vitaliani R, Taylor RA, Liebeskind DS, Voloschin A, Houghton DJ, et al. Treatment-responsive limbic encephalitis identified by neuropil antibodies: MRI and PET correlates. *Brain* (2005) 128(Pt 8):1764–77. doi: 10.1093/brain/awh526

26. Budhram A, Mirian A, Le C, Hosseini-Moghaddam SM, Sharma M, Nicolle MW. Unilateral cortical FLAIR-hyperintense lesions in anti-MOG-associated encephalitis with seizures (FLAMES): characterization of a distinct clinico-radiographic syndrome. *J Neurol* (2019) 266(10):2481–7. doi: 10.1007/s00415-019-09440-8

27. Chihara N, Aranami T, Oki S, Matsuoka T, Nakamura M, Kishida H, et al. Plasmablasts as migratory IgG-producing cells in the pathogenesis of neuromyelitis optica. *PloS One* (2013) 8(12):e83036. doi: 10.1371/journal.pone.0083036

28. Jacobi AM, Mei H, Hoyer BF, Mumtaz IM, Thiele K, Radbruch A, et al. HLA-DRhigh/CD27high plasmablasts indicate active disease in patients with systemic lupus erythematosus. *Ann Rheum Dis* (2010) 69(1):305–8. doi: 10.1136/ard.2008.096495

29. Mattoo H, Mahajan VS, Della-Torre E, Sekigami Y, Carruthers M, Wallace ZS, et al. *De novo* oligoclonal expansions of circulating plasmablasts in active and relapsing IgG4-related disease. *J Allergy Clin Immunol* (2014) 134(3):679–87. doi: 10.1016/j.jaci.2014.03.034

30. Chihara N, Aranami T, Sato W, Miyazaki Y, Miyake S, Okamoto T, et al. Interleukin 6 signaling promotes anti-aquaporin 4 autoantibody production from plasmablasts in neuromyelitis optica. *Proc Natl Acad Sci USA*. (2011) 108(9):3701–6. doi: 10.1073/pnas.1017385108

31. Bennett JL, Lam C, Kalluri SR, Saikali P, Bautista K, Dupree C, et al. Intrathecal pathogenic anti-aquaporin-4 antibodies in early neuromyelitis optica. *Ann Neurol* (2009) 66(5):617–29. doi: 10.1002/ana.21802

32. Hachiya Y, Uruha A, Kasai-Yoshida E, Shimoda K, Satoh-Shirai I, Kumada S, et al. Rituximab ameliorates anti-N-methyl-D-aspartate receptor encephalitis by removal of short-lived plasmablasts. *J Neuroimmunol.* (2013) 265(1-2):128–30. doi: 10.1016/j.jneuroim.2013.09.017

33. Malviya M, Barman S, Golombeck KS, Planaguma J, Mannara F, Strutz-Seebohm N, et al. NMDAR encephalitis: passive transfer from man to mouse by a recombinant antibody. *Ann Clin Transl Neurol* (2017) 4(11):768–83. doi: 10.1002/acn3.444

34. Wikenheiser DJ, Stumhofer JS. ICOS Co-stimulation: Friend or foe? *Front Immunol* (2016) 7:304. doi: 10.3389/fimmu.2016.00304

35. Mak TW, Shahinian A, Yoshinaga SK, Wakeham A, Boucher LM, Pintilie M, et al. Costimulation through the inducible costimulator ligand is essential for both T helper and b cell functions in T cell-dependent b cell responses. *Nat Immunol* (2003) 4(8):765–72. doi: 10.1038/ni947

36. Xie J, Cui D, Liu Y, Jin J, Tong H, Wang L, et al. Changes in follicular helper T cells in idiopathic thrombocytopenic purpura patients. *Int J Biol Sci* (2015) 11 (2):220–9. doi: 10.7150/ijbs.10178

37. Seifert M, Kuppers R. Molecular footprints of a germinal center derivation of human IgM+(IgD+)CD27+ b cells and the dynamics of memory b cell generation. *J Exp Med* (2009) 206(12):2659–69. doi: 10.1084/jem.20091087

38. Seifert M, Przekopowitz M, Taudien S, Lollies A, Ronge V, Drees B, et al. Functional capacities of human IgM memory b cells in early inflammatory responses and secondary germinal center reactions. *Proc Natl Acad Sci U S A*. (2015) 112(6):E546–55. doi: 10.1073/pnas.1416276112

39. Newell KL, Clemmer DC, Cox JB, Kayode YI, Zoccoli-Rodriguez V, Taylor HE, et al. Switched and unswitched memory b cells detected during SARS-CoV-2 convalescence correlate with limited symptom duration. *PloS One* (2021) 16(1): e0244855. doi: 10.1371/journal.pone.0244855

40. Carril-Ajuria L, Desnoyer A, Meylan M, Dalban C, Naigeon M, Cassard L, et al. Baseline circulating unswitched memory b cells and b-cell related soluble factors are associated with overall survival in patients with clear cell renal cell carcinoma treated with nivolumab within the NIVOREN GETUG-AFU 26 study. *J Immunother Cancer* (2022) 10(5):e004885. doi: 10.1136/jitc-2022-004885

41. Iwata S, Tanaka Y. B-cell subsets, signaling and their roles in secretion of autoantibodies. *Lupus* (2016) 25(8):850–6. doi: 10.1177/0961203316643172

42. Hu F, Zhang W, Shi L, Liu X, Jia Y, Xu L, et al. Impaired CD27(+)IgD(+) b cells with altered gene signature in rheumatoid arthritis. *Front Immunol* (2018) 9:626. doi: 10.3389/fimmu.2018.00626

43. Leypoldt F, Hoftberger R, Titulaer MJ, Armangue T, Gresa-Arribas N, Jahn H, et al. Investigations on CXCL13 in anti-N-methyl-D-aspartate receptor encephalitis: a potential biomarker of treatment response. *JAMA Neurol* (2015) 72(2):180–6. doi: 10.1001/jamaneurol.2014.2956

44. Byun JI, Lee ST, Moon J, Jung KH, Sunwoo JS, Lim JA, et al. Distinct intrathecal interleukin-17/interleukin-6 activation in anti-n-methyl-d-aspartate receptor encephalitis. *J Neuroimmunol.* (2016) 297:141–7. doi: 10.1016/j.jneuroim.2016.05.023

45. Levraut M, Bourg V, Capet N, Delourme A, Honnorat J, Thomas P, et al. Cerebrospinal fluid IL-17A could predict acute disease severity in non-NMDA-Receptor autoimmune encephalitis. *Front Immunol* (2021) 12:673021. doi: 10.3389/fimmu.2021.673021

46. Locci M, Wu JE, Arumemi F, Mikulski Z, Dahlberg C, Miller AT, et al. Activin a programs the differentiation of human TFH cells. *Nat Immunol* (2016) 17 (8):976–84. doi: 10.1038/ni.3494

47. Jacobson NG, Szabo SJ, Weber-Nordt RM, Zhong Z, Schreiber RD, Darnell JEJr., et al. Interleukin 12 signaling in T helper type 1 (Th1) cells involves tyrosine phosphorylation of signal transducer and activator of transcription (Stat)3 and Stat4. *J Exp Med* (1995) 181(5):1755–62. doi: 10.1084/jem.181.5.1755

48. Correale J, Fiol M. Activation of humoral immunity and eosinophils in neuromyelitis optica. *Neurology* (2004) 63(12):2363–70. doi: 10.1212/01.WNL.0000148481.80152.BF

49. Chefdeville A, Treilleux I, Mayeur M-E, Couillault C, Picard G, Bost C, et al. Immunopathological characterization of ovarian teratomas associated with anti-N-methyl-D-aspartate receptor encephalitis. *Acta Neuropathol Commun* (2019) 7 (1):1–11. doi: 10.1186/s40478-019-0693-7

50. Makuch M, Wilson R, Al-Diwani A, Varley J, Kienzler AK, Taylor J, et al. N-methyl-D-aspartate receptor antibody production from germinal center reactions: Therapeutic implications. *Ann Neurol* (2018) 83(3):553–61. doi: 10.1002/ana.25173

51. Lehmann-Horn K, Irani SR, Wang S, Palanichamy A, Jahn S, Greenfield AL, et al. Intrathecal b-cell activation in LGI1 antibody encephalitis. *Neurol Neuroimmunol Neuroinflamm* (2020) 7(2):e669. doi: 10.1212/NXI.0000000000000669

52. Dalmau J, Geis C, Graus F. Autoantibodies to synaptic receptors and neuronal cell surface proteins in autoimmune diseases of the central nervous system. *Physiol Rev* (2017) 97(2):839–87. doi: 10.1152/physrev.00010.2016

53. Dalmau J, Graus F. Antibody-mediated neuropsychiatric disorders. *J Allergy Clin Immunol* (2022) 149(1):37–40. doi: 10.1016/j.jaci.2021.11.008

frontiers | Frontiers in Immunology

TYPE Brief Research Report
PUBLISHED 15 December 2022
DOI 10.3389/fimmu.2022.1069368



OPEN ACCESS

EDITED BY
Shougang Guo,
Shandong Provincial Hospital, China

REVIEWED BY
Jinming Han,
Capital Medical University, China
Soon-Tae Lee,
Seoul National University Hospital, South Korea

*CORRESPONDENCE
Raquel Ruiz-García
rruizg@clinic.cat

SPECIALTY SECTION
This article was submitted to Multiple Sclerosis and Neuroimmunology, a section of the journal Frontiers in Immunology

RECEIVED 13 October 2022
ACCEPTED 25 November 2022
PUBLISHED 15 December 2022

CITATION
Muñoz-Sánchez G, Planagumà J, Naranjo L, Couso R, Sabater L, Guasp M, Martínez-Hernández E, Graus F, Dalmau J and Ruiz-García R (2022) The diagnosis of anti-LGI1 encephalitis varies with the type of immunodetection assay and sample examined. *Front. Immunol.* 13:1069368. doi: 10.3389/fimmu.2022.1069368



# The diagnosis of anti-LGI1 encephalitis varies with the type of immunodetection assay and sample examined

Guillermo Muñoz-Sánchez[1], Jesús Planagumà[2], Laura Naranjo[1], Rocío Couso[1], Lidia Sabater[2], Mar Guasp[2,3,4], Eugenia Martínez-Hernández[2,3], Francesc Graus[2], Josep Dalmau[2,4,5,6] and Raquel Ruiz-García[1,2]*

[1]Immunology Department, Centre Diagnòstic Biomèdic, Hospital Clínic Barcelona, Barcelona, Spain, [2]Neuroimmunology Program, Institut d'Investigacions Biomèdiques August Pi i Sunyer (IDIBAPS), Barcelona, Spain, [3]Neurology Department, Hospital Clínic, and University of Barcelona, Barcelona, Spain, [4]Centro de Investigación Biomédica en Red, Enfermedades Raras (CIBERER), Madrid, Spain, [5]Neurology Department, University of Pennsylvania, Philadelphia, PA, United States, [6]Catalan Institution of Research and Advanced Studies (ICREA), Barcelona, Spain

Detection of Leucine-rich glioma inactivated 1 (LGI1) antibodies in patients with suspected autoimmune encephalitis is important for diagnostic confirmation and prompt implementation of immunomodulatory treatment. However, the clinical laboratory diagnosis can be challenging. Previous reports have suggested that the type of test and patient's sample (serum or CSF) have different clinical performances, however, there are no studies comparing different diagnostic tests on paired serum/CSF samples of patients with anti-LGI1 encephalitis. Here, we assessed the clinical performance of a commercial and an *in house* indirect immunofluorescent cell based assays (IIF-CBA) using paired serum/CSF of 70 patients with suspected anti-LGI1 encephalitis and positive rat brain indirect immunohistochemistry (IIHC). We found that all (100%) patients had CSF antibodies when the *in house* IIF-CBA was used, but only 88 (83%) were positive if the commercial test was used. In contrast, sera positivity rate was higher with the commercial test (94%) than with the *in house* assay (86%). If both serum and CSF were examined with the commercial IIFA-CBA, 69/70 (98.5%) patients were positive in at least one of the samples. These findings are clinically important for centers in which rat brain IIHC and *in house* IIFA-CBA are not available. Moreover, the observation that all patients with anti-LGI1 encephalitis have antibodies in CSF is in line with the concept that these antibodies are pathogenic.

KEYWORDS

**neuronal antibodies, Lgi1, diagnostic test, autoimmune encephalitis (AE), immunofluorescent assay**

## Highlights

All patients with anti-LGI1 encephalitis harbor LGI1 antibodies in CSF. These antibodies are detectable by indirect immunofluorescence cell based assay (IIF-CBA) on cells co-expressing LGI1 and ADAM23.

In patients with suspected autoimmune encephalitis, both serum and CSF should be examined if a commercial IIF-CBA is used for antibody determination.

## Introduction

Autoimmune Encephalitis constitutes a group of inflammatory brain diseases that are characterized by prominent neuropsychiatric symptoms associated with autoantibodies against neuronal cell-surface proteins, ion channels or neurotransmitter receptors (1). Anti-LGI1 associated encephalitis has an estimated annual incidence of 0.83 per 1 million persons, and it represents the most common cause of autoimmune encephalitis of adults older than 40 years (2). Patients usually develop difficulty in forming new memories, confusion, or generalized seizures, often preceded by subtle focal seizures or faciobrachial dystonic seizures (2). Substantial cognitive response to steroids and immunotherapy occur in about 70% of patients at 24 months follow up (3). Despite the good functional status, long-term follow-up shows that 65% patients have mild cognitive impairment (4).

Leucine-rich glioma inactivated 1 (LGI1) is a neuronal secreted synaptic linker protein that interacts with the presynaptic disintegrin and metalloproteinase domain-containing protein 23 (ADAM23) and with the postsynaptic protein ADAM22, that are associated with Kv1.1 voltage-gated potassium channels and AMPA receptors, respectively (5, 6). Anti-LGI1 antibodies prevent the binding of LGI1 to ADAM23 and ADAM22, decreasing the synaptic levels of Kv1.1 and AMPA receptors and promoting neuronal hyperexcitability with increased glutamatergic transmission (6).

Anti-LGI1 antibody detection is important for the diagnosis of the encephalitis and prompt treatment with immunotherapy (7). Most clinical laboratories use the same commercial cell-based indirect immunofluorescence assay on transfected cells with LGI1 anchored to the cell membrane (Autoimmune Encephalitis Mosaic 6 kit; Euroimmun, Lübeck Germany). Several studies have reported that when using CSF, a negative result was found in 37%-47% of patients with anti-LGI1 encephalitis (2, 8, 9). These studies suggested that anti-LGI1 encephalitis, unlike other encephalitis mediated by antibodies against neuronal surface antigens, can occur without antibodies in CSF, and that the sensitivity of antibody detection is superior in serum than CSF. Contrary to this concept, our preliminary experience using more comprehensive techniques suggests that most of these patients have antibodies in CSF, and some do not have antibodies detectable in serum (10). Here, we examined in a large cohort of patients with anti-LGI1 encephalitis the performance of two indirect immunofluorescent cell-based assays (IIF-CBA) in which the LGI1 protein is expressed differently on the cell surface. The findings are important because suggest that current clinical testing misses the diagnosis in some patients.

## Materials and methods

### Patients and samples

We retrospectively examined 70 consecutive patients with available paired serum and CSF known to be LGI1 antibody positive by IIHC in at least one of the samples and a clinical suspicion of autoimmune encephalitis according to Graus et al. (7). All 140 samples were tested by 1) rat brain tissue indirect immunohistochemistry, 2) commercial cell-based IIF (Autoimmune Encephalitis Mosaic 6 kit; Euroimmun, Lübeck Germany) in which cells are only transfected with LGI1 and 3) *in-house* cell-based IIF in which cells are co-transfected with LGI1 and one of its natural synaptic ligands (ADAM23). All studies were examined by two independent observers.

### Rat brain indirect immunohistochemistry

Rat brain tissue indirect immunohistochemistry was performed in all CSF and sera as previously described (11). Briefly, adult Wistar rats were euthanized in a CO2 chamber and the brain was removed without previous tissue perfusion. Brains were sagittally split in two hemispheres, immersed in 4% paraformaldehyde for 1h at 4°C, cryoprotected with 40% sucrose for 48h, and snap frozen in chilled isopentane. Frozen sections were air-dried for 30 min and sequentially treated with hydrogen peroxide 30% in PBS for 15 minutes. Brain sections were blocked with 5% normal goat serum in PBS for 1h at room temperature and incubated with patients' sera (diluted 1:200) or CSF (1:2) overnight at 4°C. Biotinylated goat anti-human IgG (Vector Labs, Burlingame, CA, USA) was added for 2 h, followed by incubation with the avidin–biotin immunoperoxidase complex (Vector Labs, Burlingame, CA, 114 USA) for 1 h. The reaction was developed with 0.05% diaminobenzidine (Sigma, St. Louis, MO, USA). Animal studies were approved in accordance with European (2010/63/UE) and Spanish (RD 53/2013) regulations by the ethics committee of Hospital Clínic of Barcelona.

## Indirect immunofluorescence cell-based assays

All samples were subsequently examined with two types of IIF-CBA: 1) a commercial assay, Autoimmune Encephalitis Mosaic 6 kit (Euroimmun, Lübeck Germany), following manufacturer's instructions and recommended dilutions (undiluted CSF and 1:10 serum), to test IgG antibodies against N-methyl-D-aspartate (NMDA) receptor (GluN1), a-amino-3-hydroxyl-5-methyl-4- isoxazole-propionate (AMPA) receptor (GluA1, GluA2), gamma-aminobutyric (GABA) B receptor (B1 and B2 subunits), contactin-associated protein-like 2 (CASPR2), leucine-rich glioma-inactivated protein 1 (LGI1) and dipeptidyl-peptidase 6 (DPPX), and 2) in-house IIF-CBA in which Human Embryonic Kidney 293 (HEK293) cells were transfected with DNA constructs to express LGI1 together with ADAM23 (12). Briefly, sera and CSF were diluted in PBS-1% BSA (1:2 CSF and 1:10 serum) and incubated with stored pre-fixed transfected cells overnight. Immunodetection was performed using an goat anti-human IgG antibody conjugated with AF488 (A11013, Invitrogen,Waltham, MA, USA) for 1 h. IIF-CBA results were observed in an Axio-Imager 2 microscope (Carl Zeiss, Jena, Germany).

The study was approved by the ethics committee of Hospital Clínic of Barcelona. Patients' samples were coded and clinical information was anonymized prior to analysis.

# Results

## Study cohort

The median age of the patients was 62 years (range, 26-83 years), and 27 (40%) were women (no demographic information available from 3 patients). From the 66 patients with available information, the most common clinical findings were seizures (70%), followed by cognitive impairment (62%), memory loss (59%) and behavioral changes (38%) (Box 1. Representative Case). Brain MRI studies showed abnormalities compatible with limbic encephalitis in 38 out of 49 (78%) patients. EEG was abnormal in 27 out of 38 (71%) patients. CSF pleocytosis was found in 4 out of 41 (10%) patients. One patient had ovarian teratoma and another patient had invasive thymoma. Two patients had concurrent neuronal surface antibodies (one against the $GABA_B$ receptor and another against CASPR2).

## LGI1 antibody detection

Among the 70 sera examined, 69 (98.5%) were positive by brain indirect immunohistochemistry, 66 (94%) by commercial IIF-CBA, and 60 (86%) by *in-house* IIF-CBA. Regarding the 70 paired CSF samples, 68 (97%) were positive by brain indirect immunohistochemistry, 58 (83%) by commercial IIF-CBA, and 70 (100%) by *in-house* IIF-CBA.

47 (67%) patients were positive for LGI1 antibodies in both samples (CSF and serum) with the three indicated techniques, brain immunohistochemistry, commercial IIF, and *in-house* IIF (*concordant patients*). The other 23 (33%) patients showed discordant findings *(discordant patients)* that resulted from the technique employed (commercial vs *in-house* assay) or the sample tested (serum or CSF) (Table 1). A comprehensive analysis of the results from discordant patients showed that the commercial assay missed LGI1 antibodies in CSF more frequently than in serum (12 [52%] vs. 4 [17%]), and one patient was negative in both serum and CSF. In contrast, the *in-house* assay missed LGI1 antibodies in serum more frequently than in CSF (10 [43%] vs. 0 [0%]). All samples negative by one of the assays were positive by the other. No clinical differences were found between concordant and discordant groups of patients (Supplementary Table 1). Patients' samples were negative by IIF-CBA with HEK293 cells expressing only ADAM23 (not shown).

# Discussion

In this study, we show that using an IIF-CBA co-expressing LGI1 and ADAM23 all patients with LGI1 autoimmune encephalitis had LGI1 antibodies in CSF. Thus, the concept that in this type of autoimmune encephalitis the antibodies predominantly occur in serum should be reconsidered. The reason why one IIF-CBA performs better than the other depending on the type of sample (serum or CSF) is unclear. We postulate that the repertoires of antibodies in serum and CSF

Box 1 Representative case.

A 62-year-old woman developed confusion, dizziness and rapid cognitive decline over 3 weeks. Symptoms substantially worsened during the last week and her family described strange behavior and episodes of aggression. Two days before admission to the hospital, she developed faciobrachial dystonic seizures (3-4 per day). At admission, the MRI showed increased FLAIR/T2 signal predominantly involving the left hippocampus, and the EEG showed slow activity. Blood chemistry was normal except for hyponatraemia (128 mEq/L), and the CSF showed mild pleocytosis with 7 leukocytes/$mm^3$. CSF testing using the Autoimmune Encephalitis Mosaic 6 kit (Euroimmun) was negative for all antibodies (NMDA receptor, AMPA receptor, GABA-B receptor, CASPR2, LGI1 and DPPX). Given the suspicion for autoimmune encephalitis, a sample of CSF was sent to our center for further analysis. The CSF sample was tested by rat brain IIHC, showing robust immunostaining of the hippocampus in a pattern highly suggestive of LGI1 antibodies (Figure 1A). However, the same CSF sample was negative in the commercial assay (Figure 1B). Subsequently, CSF and serum were tested by *in-house* IIF-CBA, confirming the presence of LGI1 antibodies in both samples (Figure 1C).

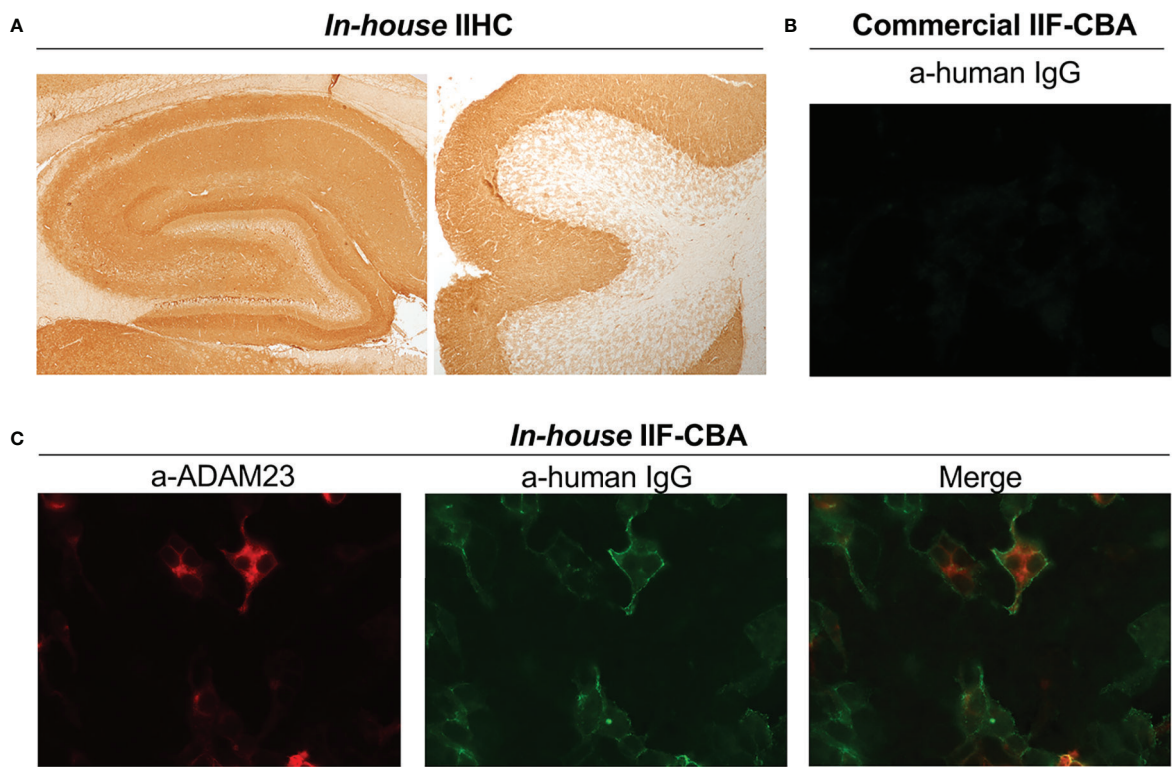


FIGURE 1
LGI1 antibody detection using different tests. **(A)** Patient's CSF showing LGI1 immunoreactivity with rat brain tissue (IIHC), including hippocampus (left) and cerebellum (right). **(B)**Image showing the lack of reactivity of the patient's CSF with HEK293 cells expressing LGI1 (commercial indirect immunofluorescent cell based assay) **(C)** In-house IIF-CBA show the reactivity of the same sample with HEK293 cells co-expressing LGI1 and ADAM23: Left, expression of ADAM23 confirmed with a commercial antibody (a-ADAM23); Middle, reactivity of patient's antibodies with LGI1; Right, merge. Patient's CSF did not react with HEK293 cells expressing only ADAM23 (not shown). IIF-CBA: indirect immunofluorescent cell based assay; ADAM23: disintegrin and metalloproteinase domain-containing protein 23.

are different and that when using CSF, the expression of LGI1 with its natural ligand facilitates the detection of antibodies. Irrespective of these or other unsuspected reasons the findings have important diagnostic implications.

Previous studies suggested that up to 47% of patients with anti-LGI1 encephalitis only have detectable LGI1 antibodies in serum (2, 8, 9) (Table 2). These studies used the IIF-CBA technique that expresses LGI1 anchored to the cell membrane instead of the IIF-CBA that co-expresses LGI1 with ADAM23. In addition, most studies do not use brain immunohistochemistry with CSF, which unambiguously shows intensive immunostaining in a pattern characteristic of LGI1.

The implications of our findings are not only clinical but also pathogenic, challenging the concept that the mechanism of this disease, regarding antibody synthesis, is different from most autoimmune encephalitis in which the prevalence of antibodies is higher in CSF. In autoimmune encephalitis, CSF samples represent better the immune dysregulation that takes places within the CNS than serum samples, and the importance of CSF for antibody detection has been demonstrated in most of these disorders (14). This is well illustrated in anti-NMDA receptor encephalitis where given the risk of false-negative results using serum, most investigators have adopted CSF antibody testing (15, 16). Moreover, in some autoimmune encephalitis, the clinical significance of the detection of antibodies only in serum is unclear; for example, serum $GABA_A$ receptor or glycine receptor antibodies may occur in patients with a wide variety of diseases or symptoms that are not immune-mediated or do not respond to immunotherapy (17, 18).

In the present study we show that screening of any sample (CSF or sera) by IIHC and subsequent confirmation of antibodies in CSF with the IIF-CBA that co-expresses LGI1 with ADAM23 is the best approach to detect LGI1 antibodies. All patients included in our cohort (N=70) were positive with this approach. Although the commercial IIF-CBA with LGI1

TABLE 1 Findings in serum and CSF of patients with anti-LGI1 encephalitis and discordant results in the indicated tests.

| | Brain IIHC | | Commercial IIF-CBA (LGI1 expressed in HEK293 cells) | | *In-House* IIF-CBA (LGI1/ADAM23 expressed in HEK293 cells) | |
|---|---|---|---|---|---|---|
| **Discordant Patient** | **CSF** | **Serum** | **CSF** | **Serum** | **CSF** | **Serum** |
| 1 | + | + | + | + | + | – |
| 2 | + | + | + | + | + | – |
| 3 | + | + | + | + | + | – |
| 4 | + | + | + | + | + | – |
| 5 | + | + | + | + | + | – |
| 6 | + | + | + | + | + | – |
| 7 | + | + | + | + | + | – |
| 8 | + | + | – | + | + | + |
| 9 | + | + | – | + | + | + |
| 10 | + | + | – | + | + | + |
| 11 | + | + | – | + | + | + |
| 12 | + | + | – | + | + | + |
| 13 | + | + | – | + | + | + |
| 14 | + | + | – | + | + | + |
| 15 | + | + | + | – | + | + |
| 16 | + | + | + | – | + | + |
| 17 | + | + | + | – | + | + |
| 18 | + | + | – | + | + | – |
| 19 | + | + | – | + | + | – |
| 20 | – | + | – | + | + | – |
| 21 | – | + | – | + | + | + |
| 22 | + | – | + | + | + | + |
| 23 | + | + | – | – | + | + |

IIHC, Indirect Immunohistochemistry; CSF, Cerebrospinal Fluid; IIF-CBA, immunofluorescence cell-based assay using HEK293 cells expressing LGI1. In the commercial assay LGI1 is expressed on the cell surface with a transmembrane domain, whereas in the in house assay the LGI1 is co-expressed with disintegrin and metalloproteinase domain-containing protein 23 (LGI1/ADAM23).

alone was more sensitive in serum than our IIF-CBA expressing LGI1-ADAM23, the commercial assay performed substantially worse with CSF. Moreover, the diagnosis of 4 patients would have been missed using serum with the commercial IIF-CBA, which is the standard diagnostic test for LGI1 antibodies in most clinical laboratories. In practice, some of these cases are later diagnosed in research laboratories due to the persistence of symptoms and high level of clinical suspicion, but delays in treatment can affect outcome (3, 19, 20). Therefore, clinical laboratories using the commercial IIF-CBA as screening method, should consider including CSF testing if serum is negative and no alternative diagnosis is identified.

TABLE 2 Reported results for LGI1 antibody detection in CSF by IIF-CBA.

| **Study** | **Type of IIF-CBA** | **LGI1 antibodies in CSF (%)** |
|---|---|---|
| van Sonderen A, et al. (2) (Neurology, 2016) | Commercial (LGI1) | 9/17(53%) |
| Gadoth A, et al. (8) (Ann Neurol, 2017) | Commercial (LGI1) | 24/38 (63%) |
| Muñiz-Castrillo S, et al. (13) (Neurol Neuroimm Neuroinfl, 2021) | In-house (LGI1 co-transfected with ADAM22) | 105/134 (78%) |
| McCracken L, et al. (9) (Neurology, 2017) | Commercial (LGI1) | 4/7 (57%) |
| Present Study | Commercial (LGI1)<br>in-house (co-expression of LGI1 and ADAM23) | 58/70 (82%)<br>70/70 (100%) |

In our experience, brain tissue IIHC is a useful complementary test for antibody detection in autoimmune encephalitis. As shown here, this is particularly important for LGI1 antibodies because the brain tissue IIHC with either serum or CSF is highly sensitive and produces a pattern of hippocampus and cerebellum immunostaining that is very suggestive of these antibodies (12).

A task for the future is to determine the repertoire of LGI1 antibody specificities in serum and CSF. We postulate that autorreactive B cells present in CNS are in prolonged contact with the antigen and undergo somatic hypermutation and affinity maturation, facilitating the selection and expansion of auto-reactive B cell clones that specifically recognize LGI1 linked to its natural ligands. Our study suggests heterogeneity among patients' antibodies regarding LGI1 epitope recognition and provides the best strategy to reduce false negative results with tests currently available.

## Data availability statement

The raw data supporting the conclusions of this article will be made available by the authors, without undue reservation.

## Ethics statement

The studies involving human participants were reviewed and approved by the ethics committee of Hospital Clínic of Barcelona. Patients' samples were coded and clinical information was anonymized prior to analysis. Written informed consent for participation was not required for this study in accordance with the national legislation and the institutional requirements. The animal study was reviewed and approved in accordance with European (2010/63/UE) and Spanish (RD 53/2013) regulations by the ethics committee of Hospital Clínic of Barcelona.

## Author contributions

JD, RR-G, EM-H, JP, GM-S and FG designed the study and wrote the manuscript. RR-G, JP, GM-S, LN, LS and RC performed laboratory work and/or data analysis. JP, EM-H and MG collected clinical information from the LGI-1 patients. All authors contributed to the article and approved the submitted version.

## Funding

This study was funded by Instituto de Salud Carlos III - Subdirección General de Evaluación y Formento de la Investigación Sanitaria and co-funded by European Union, FIS (PI21/00255, RR-G); FIS (PI20/00280, JP).

## Acknowledgments

We thank Mrs. M[a] Carmen Anton, Mrs. M[a] Antonia Romera and Mrs. Esther Aguilar for their excellent technical assistance in the immunohistochemistry and IIF-CBA assays.

## Conflict of interest

JD receives royalties from Athena Diagnostics for the use of Ma2 as an autoantibody test and from Euroimmun for the use of NMDA, GABA-B receptor, GABA-A receptor, DPPX and IgLON5 as autoantibody tests. FG receives royalties from Euroimmun for the use of (IgLON5) in an autoantibody test and receives honoraria from MedLink Neurology for his role as an associate editor.

The remaining authors declare that the research was conducted in the absence of any commercial or financial relationships that could be construed as a potential conflict of interest.

## Publisher's note



## Supplementary material

The Supplementary Material for this article can be found online at: https://www.frontiersin.org/articles/10.3389/fimmu.2022.1069368/full#supplementary-material

# References


1. Dalmau J, Geis C, Graus F. Autoantibodies to synaptic receptors and neuronal cell surface proteins in autoimmune diseases of the central nervous system. *Physiol Rev* (2017) 97(2):839–87. doi: 10.1152/physrev.00010.2016

2. van Sonderen A, Thijs RD, Coenders EC, Jiskoot LC, Sanchez E, de Bruijn MAAM, et al. Anti-LGI1 encephalitis. In: *Neurology*, vol. 87. Lippincott Williams and Wilkins (2016) 87:1449–56. doi: 10.1212/WNL.0000000000003173

3. Ariño H, Armangué T, Petit-Pedrol M, Sabater L, Martinez-Hernandez E, Hara M, et al. Anti-LGI1-associated cognitive impairment. In: *Neurology*, vol. 87. Lippincott Williams and Wilkins (2016) 87:759–65. doi: 10.1212/WNL.0000000000003009

4. Sola-Valls N, Ariño H, Escudero D, Solana E, Lladó A, Sánchez-Valle R, et al. Telemedicine assessment of long-term cognitive and functional status in anti-leucine-rich, glioma-inactivated 1 encephalitis. *Neurol Neuroimmunol Neuroinflamm* (2020) 7(2):e652. doi: 10.1212/NXI.0000000000000652

5. Fukata Y, Adesnik H, Iwanaga T, Bredt DS, Nicoll RA, Fukata M. Epilepsy-related Ligand/Receptor complex LGI1 and ADAM22 regulate synaptic transmission. *Sci Sci* (2006) 313(5794):1792–5. doi: 10.1126/science.1129947

6. Petit-Pedrol M, Sell J, Planagumà J, Mannara F, Radosevic M, Haselmann H, et al. LGI1 antibodies alter Kv1.1 and AMPA receptors changing synaptic excitability, plasticity and memory. In: *Brain* Oxford University Press (2018) 141:3092–5. doi: 10.1093/brain/awy253

7. Graus F, Titulaer MJ, Balu R, Benseler S, Bien CG, Cellucci T, et al. A clinical approach to diagnosis of autoimmune encephalitis. In: *The lancet neurology*. Lancet Publishing Group (2016) 15:391–404. doi: 10.1016/S1474-4422(15)00401-9

8. Gadoth A, Pittock SJ, Dubey D, McKeon A, Britton JW, Schmeling JE, et al. Expanded phenotypes and outcomes among 256 LGI1/CASPR2-IgG-positive patients. In: *Annals of neurology* John Wiley and Sons Inc. (2017) 82:79–92. doi: 10.1002/ana.24979

9. McCracken L, Zhang J, Greene M, Crivaro A, Gonzalez J, Kamoun M, et al. Improving the antibody-based evaluation of autoimmune encephalitis. *Neurol Neuroimmunol Neuroinflamm* (2017) 4(6):e404. doi: 10.1212/NXI.0000000000000404

10. Ruiz-García R, Muñoz-Sánchez G, Naranjo L, Guasp M, Sabater L, Saiz A, et al. Limitations of a commercial assay as diagnostic test of autoimmune encephalitis. *Front Immunol Front* (2021) 12:691536. doi: 10.3389/fimmu.2021.691536

11. Lai M, Hughes EG, Peng X, Zhou L, Gleichman AJ, Shu H, et al. AMPA receptor antibodies in limbic encephalitis alter synaptic receptor location. *Ann Neurol Ann Neurol* (2009) 65(4):424–34. doi: 10.1002/ANA.21589

12. Lai M, Huijbers MG, Lancaster E, Graus F, Bataller L, Balice-Gordon R, et al. Investigation of LGI1 as the antigen in limbic encephalitis previously attributed to potassium channels: a case series. *Lancet Neurol* (2010) 9(8):776–85. doi: 10.1016/S1474-4422(10)70137-X

13. Muñiz-Castrillo S, Haesebaert J, Thomas L, Vogrig A, Pinto A-L, Picard G, et al. Clinical and Prognostic Value of Immunogenetic Characteristics in Anti-LGI1 Encephalitis. *Neurol - Neuroimmunol Neuroinflammation* (2021) 8:e974. doi: 10.1212/NXI.0000000000000974

14. Dalmau J, Graus F. Antibodies to neural cell surface antigens. In: *Autoimmune encephalitis and related disorders of the nervous system*. Cambridge University Press (2022). p. 135–66. doi: 10.1017/9781108696722.006

15. Gresa-Arribas N, Titulaer MJ, Torrents A, Aguilar E, McCracken L, Leypoldt F, et al. Antibody titres at diagnosis and during follow-up of anti-NMDA receptor encephalitis: a retrospective study. *Lancet Neurol Lancet Neurol* (2014) 13(2):167–77. doi: 10.1016/S1474-4422(13)70282-5

16. Viaccoz A, Desestret V, Ducray F, Picard G, Cavillon G, Rogemond V, et al. Clinical specificities of adult male patients with NMDA receptor antibodies encephalitis. *Neurology* (2014) 82(7):556–63. doi: 10.1212/WNL.0000000000000126

17. Petit-Pedrol M, Armangue T, Peng X, Bataller L, Cellucci T, Davis R, et al. Encephalitis with refractory seizures, status epilepticus, and antibodies to the GABAA receptor: a case series, characterisation of the antigen, and analysis of the effects of antibodies. In: *The lancet neurology*, vol. 13. Elsevier (2014). p. 276–86. doi: 10.1016/S1474-4422(13)70299-0

18. Martinez-Hernandez E, Sepulveda M, Rostásy K, Höftberger R, Graus F, Harvey R, et al. Antibodies to aquaporin 4, myelin-oligodendrocyte glycoprotein, and the glycine receptor α1 subunit in patients with isolated optic neuritis. *JAMA Neurol* (2015) 72(2):187. doi: 10.1001/jamaneurol.2014.3602

19. Thompson J, Bi M, Murchison AG, Makuch M, Bien CG, Chu K, et al. The importance of early immunotherapy in patients with faciobrachial dystonic seizures. *Brain* (2018) 141(2):348–56. doi: 10.1093/brain/awx323

20. de Bruijn MAAM, van Sonderen A, van Coevorden-Hameete MH, Bastiaansen AEM, Schreurs MWJ, Rouhl RPW, et al. Evaluation of seizure treatment in anti-LGI1, anti-NMDAR, and anti-GABA b r encephalitis. *Neurology* (2019) 92(19):e2185–96. doi: 10.1212/WNL.0000000000007475

frontiers | Frontiers in Immunology

TYPE Original Research
PUBLISHED 05 January 2023
DOI 10.3389/fimmu.2022.1071219



OPEN ACCESS

EDITED BY
Honghao Wang,
Guangzhou First People's Hospital, China

REVIEWED BY
Stefan Blum,
The University of Queensland, Australia
Jinzhou Feng,
First Affiliated Hospital of Chongqing Medical University, China

*CORRESPONDENCE
Shengjun Wang
junwang9999@sina.com
Ling Li
liling5313@sina.com

†These authors have contributed equally to this work and share first authorship

SPECIALTY SECTION
This article was submitted to Multiple Sclerosis and Neuroimmunology, a section of the journal Frontiers in Immunology

RECEIVED 16 October 2022
ACCEPTED 16 December 2022
PUBLISHED 05 January 2023

CITATION
Li J, Li H, Wang Y, Zhao X, Wang S and Li L (2023) CHI3L1 in the CSF is a potential biomarker for anti-leucine-rich glioma inactivated 1 encephalitis. *Front. Immunol.* 13:1071219. doi: 10.3389/fimmu.2022.1071219



# CHI3L1 in the CSF is a potential biomarker for anti-leucine-rich glioma inactivated 1 encephalitis

Jinyi Li[1†], Hongyan Li[2†], Yunhuan Wang[1], Xiuhe Zhao[1], Shengjun Wang[1*] and Ling Li[2*]

[1]Department of Neurology, Qilu Hospital, Cheeloo College of Medicine, Shandong University, Jinan, Shandong, China, [2]Department of Neurology, Qilu Hospital, Cheeloo College of Medicine, Shandong University, Qingdao, Shandong, China

**Objective:** Anti-leucine-rich glioma inactivated 1(LGI1) encephalitis is one rare autoimmune encephalitis which is accompanied by inflammatory responses. (Anti-leucine-rich glioma inactivated 1 (anti-LGI1) encephalitis is an autoimmune disease mediated by inflammatory responses.)This study aimed to investigate the Chitinase 3-like 1(CHI3L1) in anti-LGI1encephalitis patients and evaluate its association with modified Rankin Scale (mRS) score in anti-LGI1 encephalitis at admission and 6 months follow-up.(This study looked into the relationship between Chitinase 3-like 1 (CHI3L1) and the modified Ranking Scale (mRS) score in anti-LGI1 encephalitis patients at admission and 6 months later.)

**Methods:** Thirty-five patients with anti-LGI1 encephalitis and 22 patients with non-inflammatory neurological disease were enrolled in this study. (We enrolled 35 patients with anti-LGI1 encephalitis and 22 patients with non-inflammatory neurological disease.)Cerebrospinal fluid (CSF) and serum levels of CHI3L1 were measured by enzyme-linked immunosorbent assay. (We quantified CHI3L1 in the serum and cerebrospinal fluid (CSF) by performing an enzyme-linked immunosorbent assay.)Patients were evaluated for mRS score at admission and at 6 months follow-up.(We recorded the mRS score of the patients at admission and 6 months later.)

**Results:** CHI3L1 levels in CSF and serum were highly elevated in patients with anti-LGI1 encephalitis at admission compared those with the controls.(At admission, patients with anti-LGI1 encephalitis had elevated CHI3L1 levels in the CSF and serum.) Additionally, patients presenting with cognitive impairment had significantly higher CSF CHI3L1 levels and mRS scores than those without cognitive impairment symptoms. Patients presenting with only faciobrachial dystonic seizures at admission had lower CSF CHI3L1 levels than those with other symptoms. Finally, CSF CHI3L1 levels were positively correlated with CSF lactate levels.

**Conclusion:** CHI3L1 level in CSF is correlated with the severity and prognosis of anti-LGI1 encephalitis. (CSF CHI3L1 levels are correlated with the severity and prognosis of anti-LGI1 encephalitis.)

KEYWORDS

LGI1 encephalitis, cerebrospinal fluid, chitinase 3-like 1, modified rankin scale, prognosis

# Introduction

Anti-leucine-rich glioma inactivated 1 (anti-LGI1) encephalitis is a type of rare autoimmune encephalitis (1). The main clinical manifestations of anti-LGI1 encephalitis are memory loss, seizures, mental behavioral abnormalities and faciobrachial dystonic seizures(FBDS) (2–4). Chitinase-3 like-protein-1 (CHI3L1), a chitinase-like protein, is generated and released by various cells, including macrophages, microglia, including macrophages, microglia, neutrophils, synoviocytes, chondrocytes, fibroblast-like cells, smooth muscle cells, and tumor cells (5–8). CHI3L1 forms a multimeric complex with interleukin-13 receptor α2 and interacts with transmembrane protein 219 (TMEM219), activating the Erk, Akt, and Wnt-linked signaling pathways and suppressing inflammatory cell apoptosis (5, 9, 10). Some studies have shown that patients with anti-N-methyl-d-aspartate receptor (NMDAR) encephalitis have higher CHI3L1 levels in the cerebrospinal fluid (CSF) than viral encephalitis patients or healthy people (11, 12). The study showed thatCSF CHI3L1 levels were positively correlated with the modified Rankin Scale (mRS) score and serum interleukin-6(IL-6) in anti-NMDAR encephalitis (12), suggesting that CSF CHI3L1 level may be positively correlated with the severity of anti-NMDAR encephalitis. However, few studies have documented serum and CSF CHI3L1 levels in patients with anti-LGI1 encephalitis. Thus, we investigated the changes in serum and CSF CHI3L1 levels in anti-LGI1 encephalitis patients and their relationship with severity and prognosis. In parallel, this study analyzed the association between clinical characteristics and mRS score at admission and 6 months later.

# Material and methods

## Patients and controls

We retrospectively studied 35 patients with anti-LGI1 encephalitis. All included patients met the diagnostic criteria for anti-LGI1 encephalitis (13). The control group comprised 22 noninflammatory neurological disorder patients, which included migraine (n = 5), anxiety disorder (n=8), cervical/lumbar disc herniation (n=5), ischemic cerebrovascular disease (n=4). All patients underwent a lumbar puncturewithin 7 days after admission for a cerebrospinal fluidCSF examinationanalysis before starting their immunosuppressants treatment. (Table 1) We assessed the patients' neurological status by recording their mRS score (14) at admission and 6 months after discharge.

The local ethics committee at the Qilu Hospital of Shandong University approved this study, and all participants provided written informed consent.

## Quantification of serum and CSF CHI3L1

CSF and serum samples were centrifuged immediately after collection and then stored at −80°C for testing. Commercially available sandwich ELISA kits were used according to the manufacturer's instructions to quantify CHI3L1 in the CSF and serum. (Elabscience Biotechnology Co. Ltd).

## Statistical analysis

All statistical analyses were performed using SPSS 26. Continuous variables of normally distributed data were presented as the mean ± standard deviation. Non-normally distributed datawere presented as the median and interquartile range (IQR). Groups were compared using Student's t-test. Since CHI3L1 concentrations are non-normally distributed, we compared the anti-LGI1 encephalitis group and the control group using the Mann Whitney U. Spearman's test was used to assess the correlation between CSF CHI3L1 levels and mRS scores. Correlations between the CHI3L1 levels and the clinical data were analyzed by multiple linear regression. Receiver operator characteristic (ROC) curves were used to assess the discriminating power of CHI3L1 levels in anti-LGI1 encephalitis patients. A value of $p < 0.05$ was considered statistically significant.

TABLE 1 Clinical data and laboratory findings of anti-LGI1 encephalitis patients (n=35)and controls (n=22).

| | Anti-LGI1 encephalitis | Control |
|---|---|---|
| Age of onset (years, mean ± SD) | 61.91 ± 11.20 | 59.70 ± 11.73 |
| male/Female | 27/8 | 13/9 |
| CSF samples(%) | 30/35(85.71) | 22/22 (100) |
| Serum samples(%) | 30/35(85.71) | 22/22 (100) |
| Clinical features(%) | | |
| Psychiatric/behavioral problems | 14/35(40.00) | |
| cognitive disturbance | 22/35(62.86) | |
| Seizures | 14/35(40.00) | |
| FBDS | 20/35(57.14) | |
| Initial mRS (median,IQR) | 2 (1–3) | |
| 6-months follow-up mRS (median, IQR) | 1 (1–2) | |
| Abnormal EEG(%) | 23/33(69.70) | |
| Abnormal brain MRI(%) | 15/34(44.12) | |
| CSF WBC count (×106, median, range) | 1.6 (1–4) | 1 (1–2) |
| CSF Protein (g/L, median, IQR) | 0.38(0.27-0.50) | 0.40 ± 0.18 |
| Anti-LGI1 antibodies in CSF(%) | 34/35(97.14) | |
| Anti-LGI1 antibodies in Serum(%) | 32/33(96.97) | |
| Hyponatremia(%) | 20/35(57.14) | |
| CSF CHI3L1 (pg/ml) | 1216.30(511.78-1750.24) | 493.93(354.90-735.98) |
| Serum CHI3L1 (pg/ml) | 919.86(600.09-3110.75) | 610.01(388.66-1355.32) |

CSF, Cerebrospinal fluid; FBDS, faciobrachial dystonic seizures; mRS, modified Rankin Scale scores; IQR, Inter quartile range; EEG, Electroencephalogram; MRI, Magnetic Resonance Imaging; WBC, white blood cell; CHI3L1, Chitinase 3-like 1.

# Results

## Clinical features and demographics

Table 1 lists the clinical features of the included patients. The mean age of the patients with anti-LGI1 encephalitis was 61.91 ± 11.20 years, and that of the control group was 59.70 ± 11.73 years. The male to female ratio of patients recruited with anti-LGI1 encephalitis versus controls was 27/8 and 13/9 respectively. The median mRS score during the onset of anti-LGI1 encephalitis patients was 2 (1–3). The median mRS score during the 6 months follow-up of anti-LGI1 encephalitis patients was1 (1–2). All anti-LGI1 encephalitis patients were treated with methylprednisolone alone or combined with intravenous immunoglobulin during phase of disease, followed by a gradual reduction of the prednisone dose.

## Clinical features related to mRS at admission and 6 months later in anti-LGI1 encephalitis patients

A Simple linear regression analysis revealed that the mRS score at admission was positively associated with hyponatremia(β=0.468, p=0.003) and negatively associated with FBDS (β=-0.426, *p*=0.005). The multiple linear regression analysis also revealed that the mRS score at admission was positively associated with hyponatremia (β=0.364, *p*=0.025) and negatively correlated with FBDS (β=-0.395, *p*=0.016). The mRS score at admission was not associated with serum/CSF LGI1 antibody titers, abnormal brain MRI, CSF protein concentrations, CSF white blood cell count, CSF immunoglobulin G, A, and M titers, and CSF lactate levels.

Meanwhile, the simple linear regression analysis and multiple linear regression analysis revealed that mRS score at

the 6-month follow-up examination was not associated with serum/CSF LGI1 antibody titers, abnormal brain MRI, hyponatremia, FBDS, CSF protein concentrations, CSF white blood cell count, CSF immunoglobulin G, A, and M titers, and CSF lactate levels.

## Increased CSF and serum CHI3L1 levels in anti-LGI1 encephalitis patients

We quantified CHI3L1 in CSF ($n$ =30) and serum samples ($n$ =30) from patients with anti-LGI1 encephalitis ($n$ =35), and controls ($n$ = 22) using an ELISA assay. Patients with anti-LGI1 encephalitis had significantly higher CHI3L1 levels in the serum and CSF than controls. ($p$=0.0026 and $p$=0.0331, respectively; Figures 1A, B).

Next, we evaluated whether CHI3L1 levels could be used to identify anti-LGI1 encephalitis patients using ROC curves. The area under the ROC curve (AUC) of CSF and serum CHI3L1 levels were 0.7377 and 0.6742, respectively (Figures 1C, D). The optimal cut-off values for CSF and serum levels were 868.6 pg/mL and 712.12pg/mL, respectively.

## Anti-LGI1 encephalitis patients with cognitive impairment symptoms had high CSF levels and mRS scores

Patients with anti-LGI1 encephalitis presenting with cognitive impairments (n = 18) had significantly higher CSF CHI3L1 levels than those without cognitive impairment symptoms (n = 12, p = 0.022, Figure 2A), but these two groups had similar serum CHI3L1 levels (Figure 2B). Patients with anti-LGI1 encephalitis who presented with cognitive impairments had significantly higher mRS scores on admission (p < 0.001, Figure 2C) and at the 6-month follow-up examination (p = 0.018, Figure 2D) than those without cognitive impairment symptoms.

Next, patients with other symptoms, such as psychotic behavior abnormalities or seizures, and those without these symptoms had similar CHI3L1 levels. Interestingly, anti-LGI1 encephalitis patients who presented with only FBDS at admission (n = 6) had significantly lower CSF CHI3L1 levels than those without FBDS symptoms (n = 24, p = 0.029; Figure 2E). However, these two groups had similar serum CHI3L1 levels (p = 0.481; Figure 2F).

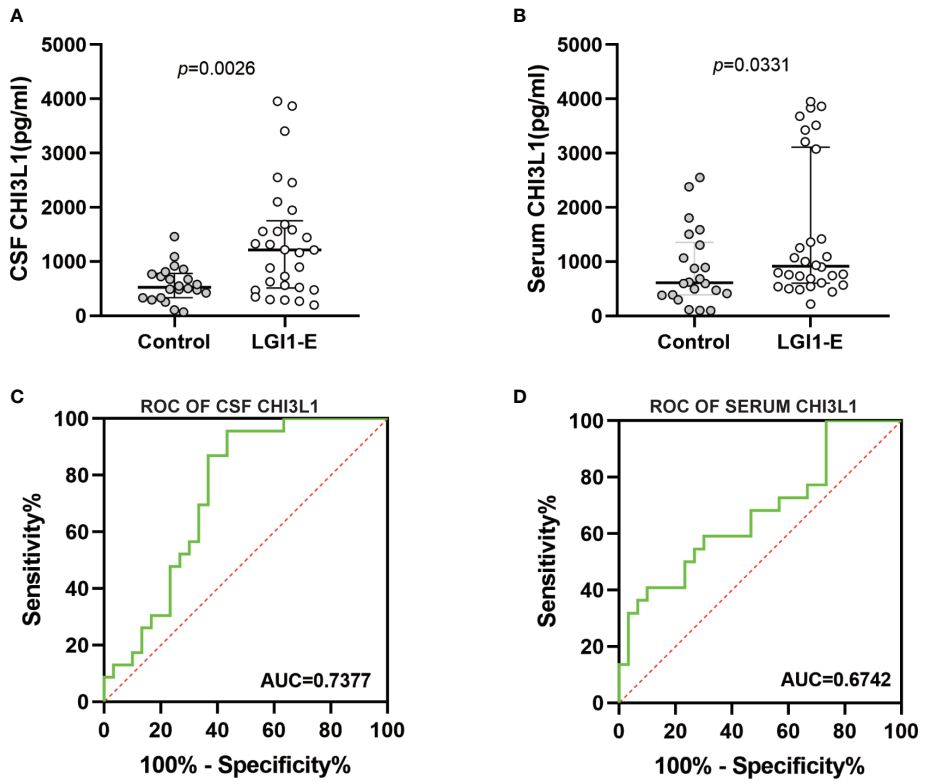


FIGURE 1
Levels of CHI3L1 in cerebrospinal fluid (CSF) and serum. CSF **(A)** and serum **(B)** CHI3L1 levels in patients with anti LGI1 encephalitis and controls; **(C)**, **(D)**Receiver operating characteristic curves for CSF and serum CHI3L1 to discriminate anti-LGI1 encephalitis patients from control patients.

10.3389/fimmu.2022.1071219

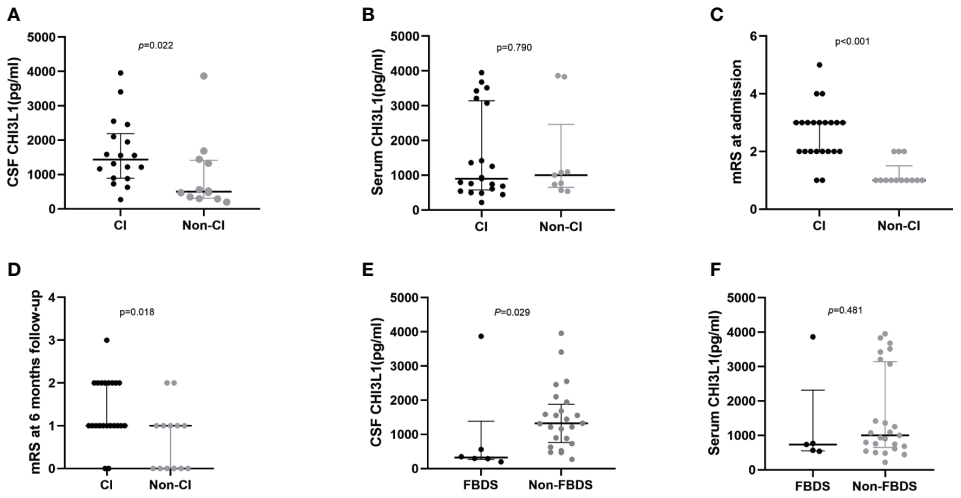


FIGURE 2
CHI3L1 level difference in serum and cerebrospinal fluid of LGI1 patients with different clinical presentations. Cerebrospinal fluid **(A)** and serum **(B)** CHI3L1 levels in anti-LGI1 encephalitis patients with and without cognitive impairment; mRS scores at admission **(C)** and at 6-month follow-up **(D)** of anti-LGI1 antibody encephalitis presenting with cognitive impairment and those without cognitive impairment symptomes; Cerebrospinal fluid **(E)** and serum **(F)** CHI3L1 levels in anti-LGI1 encephalitis patients presenting with only FBDS and other symptoms; CI: Patients presenting with cognitive impairments, Non-CI: Patients presenting without cognitive impairments.

## Clinical features related to increased CSF CHI3L1 concentrations in anti-LGI1 encephalitis patients

The CSF CHI3L1 level were correlated with the patients' mRS scores at admission(r =0.516, $p$= 0.004; Figure 3A) and 6 months later (r=0.552, $p$=0.002; Figure 3B). Meanwhile, serum CHI3L1 concentrations and other clinical features were not associated with the patients' mRS score of the patients at admission (r=0.086, $p$=0.652; Figure 3C) and 6 months later (r=-0.003, $p$=0.988; Figure 3D).

The simple linear regression analysis revealed that CSF CHI3L1 levels were positively correlated with the patients' mRS scores at admission (β=0.448, $p$=0.013), and 6-months later (β=0.450, $p$=0.013) and with the patients' CSF lactate levels (β=0.451, $p$=0.014). The multiple linear regression analysis showed that CSF CHI3L1 levels were positively correlated with the patients' mRS score at the 6-month follow-up examination (β=0.422, $p$=0.011) and the patients' CSF lactate levels (β=0.420, $p$=0.012).

However, the simple linear regression analysis and multiple linear regression analysis revealed no correlation between serum CHI3L1 levels and the mRS score of the patients at onset and 6-months follow-up and other clinical features.

# Discussion

Autoimmune encephalitis is often accompanied by inflammatory cell activation and cytokineproduction during pathogenesis (15, 16). Anti-LGI1 encephalitis patients have elevated neurofilament light chain protein, glial fibrillary acidic protein and chemokine ligand 13 levels and reduced Visinin-like protein 1, Synaptosomal Associated Protein-25 (SNAP-25) and neurogranin levels in the serumand CSF (17–21). However, none of these biomarkers reflect microglia activation. CHI3L1, also has been named YKL-40 in humans, is produced by macrophages, microglial cell and neutrophils (5, 22). As a pro-inflammatory factor, CHI3L1 inhibits inflammatory cell apoptosis and death by inducing PKB/Akt phosphorylation, inhibiting Fas expression (23). Moreover, CHI3L1 promotes the activation and differentiation of immune cells, such as macrophages, dendritic cells and T lymphocytes (24).

Some studies have indicated that elevated CSF CHI3L1 are associated with Alzheimer's disease, multiple sclerosis and Parkinson's disease (22, 25–29). One study has shown that CHI3L1 levels are significantly elevated in the CSF of patients with anti-LGI1 encephalitis. However, that study only included seven patients (21) Patients with anti-NMDAR encephalitis also have elevated CSF CHI3L1 levels (11, 12). Additionally, CSF CHI3L1 levels are associated with the mRS score both at admission and 6 months later (11, 12, 16) An [18F]-DPA714 PET/CT scan study revealed that one patient with recurrent anti-LGI1 encephalitis had activated microglia in the left medial temporal lobe indicating that microglia play a major role in the pathogenesis of anti-LGI1 encephalitis (30). Active microglia might increase CHI3L1 levels in the CSF. Furthermore, CHI3L1 increases T lymphocyte levels, particularly Th2 cells in type 2 inflammatory responses (31). Additionally, neutrophils and endothelial cells also secrete CHI3L1 and may, therefore, contribute to the elevation of CSF CHI3L1 levels in LGI1 patients (32, 33).

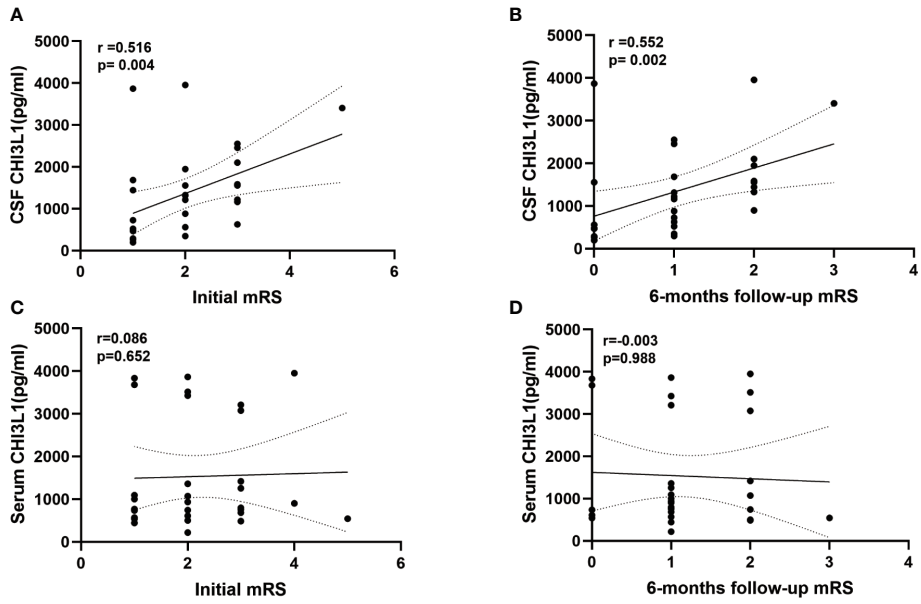


FIGURE 3
Levels of CHI3L1in cerebrospinal fluid (CSF) and serum association with modified Rankin Scale (mRS) at admissiom and 6 months follow-up. **(A, B)** Correlation between CSF CHI3L1 levels andmRS at admissiom and 6 months follow-up in anti-LGI1 encephalitis patients. **(C, D)** Correlation between serum CHI3L1 levels andmRS at admissiom and 6 months follow-up in anti-LGI1 encephalitis patients.

The present study, that patients with anti-LGI1 encephalitis had elevated serum and CSF CHI3L1 levels. CSF CHI3L1 levels were correlated with mRS scores at admission and 6 months later. Moreover, CSF CHI3L1 levels were higher in anti-LGI1 encephalitis patients presenting with cognitive impairment than those without cognitive impairment symptoms. Note-worthily, patients presenting with only FBDS at admission had significantly lower CSF CHI3L1 levels than patients with other symptoms.

These results imply that CSF CHI3L1 levels were associated with severity and outcomes. Most patients presenting with only FBDS at admission did not suffer from serious anti-LGI1 encephalitis. A recent Mayo Clinic study have reported that more than half of patients with anti-LGI1 encephalitis presented with FBDS (34). Those patients with FBDS have no obvious inflammatory responses in the CSF at the early disease stage (35). In these patients, early immunotherapy usually yields good results (36, 37).

Our results revealed that the mRS score at admission was positively correlated with hyponatremia, suggesting that hyponatremia is also related to the severity of the disease. One study demonstrated that the prognosis of anti-LGI1 encephalitis patients with hyponatremia is poor (38). In this study, CSF CHI3L1 levels were correlated with CSF lactate levels. These results suggest that metabolic and inflammatory factors are both involved in the pathogenesis of patients with anti-LGI1 encephalitis.

There are some limitations to our study. First, the patients population remains relatively small. Second, the serum and CSF samples obtained in the follow-up examination were not studied.

## Conclusion

CSF CHI3L1 levels are correlated with the severity and prognosis of anti-LGI1 encephalitis.

## Data availability statement

The raw data supporting the conclusions of this article will be made available by the authors, without undue reservation.

## Ethics statement

The studies involving human participants were reviewed and approved by ethics committee of the Qilu Hospital of Shandong University. The patients/participants provided their written informed consent to participate in this study.

## Author contributions

JL and HL, drafting/revision of the manuscript, data acquisition, study concept and design, and data analysis and

interpretation. YW, major role in sample collection. XZ, SW and LL, revision of the manuscript, study concept and design, and data analysis and interpretation. All authors contributed to the article and approved the submitted version.

## Funding

This work is supported by Qingdao Key Health Discipline Development Fund; Qingdao Clinical Research Center for Rare Diseases of Nervous System(22-3-7-lczx-3-nsh); Clinical New Technology Project of Qilu Hospital of Shandong University (Clinical study on the efficacy of neuromodulation combined with stereotactic electroencephalography in the treatment of intractable epilepsy associated with anxiety and depression).

## Conflict of interest

The authors declare that the research was conducted in the absence of any commercial or financial relationships that could be construed as a potential conflict of interest.

## Publisher's note



## References

1. Uy CE, Binks S, Irani SR. Autoimmune encephalitis: clinical spectrum and management. *Pract Neurol* (2021) 21(5):412–23. doi: 10.1136/practneurol-2020-002567

2. Lai M, Huijbers MG, Lancaster E, Graus F, Bataller L, Balice-Gordon R, et al. Investigation of LGI1 as the antigen in limbic encephalitis previously attributed to potassium channels: a case series. *Lancet Neurol* (2010) 9(8):776–85. doi: 10.1016/s1474-4422(10)70137-x

3. Seery N, Butzkueven H, O'Brien TJ, Monif M. Contemporary advances in antibody-mediated encephalitis: anti-LGI1 and anti-Caspr2 antibody (Ab)-mediated encephalitides. *Autoimmun Rev* (2022) 21(5):103074. doi: 10.1016/j.autrev.2022.103074

4. Sen A, Wang J, Laue-Gizzi H, Lee T, Ghougassian D, Somerville ER. Pathognomonic seizures in limbic encephalitis associated with anti-LGI1 antibodies. *Lancet (London England)* (2014) 383(9933):2018. doi: 10.1016/s0140-6736(14)60684-x

5. Zhao T, Su Z, Li Y, Zhang X, You Q. Chitinase-3 like-protein-1 function and its role in diseases. *Signal Transduct Targeted Ther* (2020) 5(1):201. doi: 10.1038/s41392-020-00303-7

6. Hakala BE, White C, Recklies AD. Human cartilage gp-39, a major secretory product of articular chondrocytes and synovial cells, is a mammalian member of a chitinase protein family. *J Biol Chem* (1993) 268(34):25803–10. doi: 10.1016/S0021-9258(19)74461-5

7. Shackelton LM, Mann DM, Millis AJ. Identification of a 38-kDa heparin-binding glycoprotein (gp38k) in differentiating vascular smooth muscle cells as a member of a group of proteins associated with tissue remodeling. *J Biol Chem* (1995) 270(22):13076–83. doi: 10.1074/jbc.270.22.13076

8. Janelidze S, Mattsson N, Stomrud E, Lindberg O, Palmqvist S, Zetterberg H, et al. CSF biomarkers of neuroinflammation and cerebrovascular dysfunction in early Alzheimer disease. *Neurology* (2018) 91(9):e867–e77. doi: 10.1212/wnl.0000000000006082

9. Kawada M, Seno H, Kanda K, Nakanishi Y, Akitake R, Komekado H, et al. Chitinase 3-like 1 promotes macrophage recruitment and angiogenesis in colorectal cancer. *Oncogene* (2012) 31(26):3111–23. doi: 10.1038/onc.2011.498

10. Edwards LA, Thiessen B, Dragowska WH, Daynard T, Bally MB, Dedhar S. Inhibition of ILK in PTEN-mutant human glioblastomas inhibits PKB/Akt activation, induces apoptosis, and delays tumor growth. *Oncogene* (2005) 24 (22):3596–605. doi: 10.1038/sj.onc.1208427

11. Zhao J, Wang C, Zhang Y, Sun R, Wang H, Li G, et al. Elevated CHI3L1 and OPN levels in patients with anti-n-methyl-d-aspartate receptor encephalitis. *J Neuroimmunol* (2019) 334:577005. doi: 10.1016/j.jneuroim.2019.577005

12. Chen J, Ding Y, Zheng D, Wang Z, Pan S, Ji T, et al. Elevation of YKL-40 in the CSF of anti-NMDAR encephalitis patients is associated with poor prognosis. *Front Neurol* (2018) 9:727. doi: 10.3389/fneur.2018.00727

13. Graus F, Titulaer MJ, Balu R, Benseler S, Bien CG, Cellucci T, et al. A clinical approach to diagnosis of autoimmune encephalitis. *Lancet Neurol* (2016) 15 (4):391–404. doi: 10.1016/S1474-4422(15)00401-9

14. Bamford JM, Sandercock PA, Warlow CP, Slattery J. Interobserver agreement for the assessment of handicap in stroke patients. *Stroke* (1989) 20 (6):828. doi: 10.1161/01.str.20.6.828

15. Hacohen Y, Singh R, Rossi M, Lang B, Hemingway C, Lim M, et al. Clinical relevance of voltage-gated potassium channel–complex antibodies in children. *Neurology* (2015) 85(11):967–75. doi: 10.1212/wnl.0000000000001922

16. Zhang S, Mao C, Li X, Miao W, Teng J. Advances in potential cerebrospinal fluid biomarkers for autoimmune encephalitis: A review. *Front Neurol* (2022) 13:746653. doi: 10.3389/fneur.2022.746653

17. Nissen MS, Ryding M, Nilsson AC, Madsen JS, Olsen DA, Halekoh U, et al. CSF-neurofilament light chain levels in NMDAR and LGI1 encephalitis: A national cohort study. *Front Immunol* (2021) 12:719432. doi: 10.3389/fimmu.2021.719432

18. Kunchok A, McKeon A, Zekeridou A, Flanagan EP, Dubey D, Lennon VA, et al. Autoimmune/Paraneoplastic encephalitis antibody biomarkers: Frequency, age, and sex associations. *Mayo Clin Proc* (2022) 97(3):547–59. doi: 10.1016/j.mayocp.2021.07.023

19. Körtvelyessy P, Goihl A, Guttek K, Schraven B, Prüss H, Reinhold D. Serum and CSF cytokine levels mirror different neuroimmunological mechanisms in patients with LGI1 and Caspr2 encephalitis. *Cytokine* (2020) 135:155226. doi: 10.1016/j.cyto.2020.155226

20. Lin YT, Yang X, Lv JW, Liu XW, Wang SJ. CXCL13 is a biomarker of anti-Leucine-Rich glioma-inactivated protein 1 encephalitis patients. *Neuropsychiatr Dis Treat* (2019) 15:2909–15. doi: 10.2147/ndt.S222258

21. Day GS, Yarbrough MY, Körtvelyessy P, Prüss H, Bucelli RC, Fritzler MJ, et al. Prospective quantification of CSF biomarkers in antibody-mediated encephalitis. *Neurology* (2021) 96(20):e2546–e57. doi: 10.1212/wnl.0000000000011937

22. Lananna BV, McKee CA, King MW, Del-Aguila JL, Dimitry JM, Farias FHG, et al. Chi3l1/YKL-40 is controlled by the astrocyte circadian clock and regulates neuroinflammation and alzheimer's disease pathogenesis. *Sci Trans Med* (2020) 12(574):eax3519. doi: 10.1126/scitranslmed.aax3519

23. Lee CG, Da Silva CA, Dela Cruz CS, Ahangari F, Ma B, Kang MJ, et al. Role of chitin and chitinase/chitinase-like proteins in inflammation, tissue remodeling, and injury. *Annu Rev Physiol* (2011) 73:479–501. doi: 10.1146/annurev-physiol-012110-142250

24. He CH, Lee CG, Dela Cruz CS, Lee CM, Zhou Y, Ahangari F, et al. Chitinase 3-like 1 regulates cellular and tissue responses *via* IL-13 receptor α2. *Cell Rep* (2013) 4(4):830–41. doi: 10.1016/j.celrep.2013.07.032

25. Olsson B, Lautner R, Andreasson U, Öhrfelt A, Portelius E, Bjerke M, et al. CSF and blood biomarkers for the diagnosis of alzheimer's disease: a systematic review and meta-analysis. *Lancet Neurol* (2016) 15(7):673–84. doi: 10.1016/s1474-4422(16)00070-3

26. Molinuevo JL, Ayton S, Batrla R, Bednar MM, Bittner T, Cummings J, et al. Current state of alzheimer's fluid biomarkers. *Acta Neuropathol* (2018) 136(6):821–53. doi: 10.1007/s00401-018-1932-x

27. Wood H. Multiple sclerosis: Biomarkers and genetic variants reflect disease course in multiple sclerosis. *Nat Rev Neurol* (2016) 12(10):553. doi: 10.1038/nrneurol.2016.142

28. Cantó E, Tintoré M, Villar LM, Costa C, Nurtdinov R, Álvarez-Cermeño JC, et al. Chitinase 3-like 1: prognostic biomarker in clinically isolated syndromes. *Brain* (2015) 138(Pt 4):918–31. doi: 10.1093/brain/awv017

29. Magdalinou NK, Paterson RW, Schott JM, Fox NC, Mummery C, Blennow K, et al. A panel of nine cerebrospinal fluid biomarkers may identify patients with atypical parkinsonian syndromes. *J Neurol Neurosurg Psychiatry* (2015) 86(11):1240–7. doi: 10.1136/jnnp-2014-309562

30. Wang J, Jin L, Zhang X, Yu H, Ge J, Deng B, et al. Activated microglia by (18)F-DPA714 PET in a case of anti-LGI1 autoimmune encephalitis. *J Neuroimmunol* (2022) 368:577879. doi: 10.1016/j.jneuroim.2022.577879

31. Shurin MR, Yanamala N, Kisin ER, Tkach AV, Shurin GV, Murray AR, et al. Graphene oxide attenuates Th2-type immune responses, but augments airway remodeling and hyperresponsiveness in a murine model of asthma. *ACS Nano* (2014) 8(6):5585–99. doi: 10.1021/nn406454u

32. Bergmann OJ, Johansen JS, Klausen TW, Mylin AK, Kristensen JS, Kjeldsen E, et al. High serum concentration of YKL-40 is associated with short survival in patients with acute myeloid leukemia. *Clin Cancer Res an Off J Am Assoc Cancer Res* (2005) 11(24 Pt 1):8644–52. doi: 10.1158/1078-0432.Ccr-05-1317

33. Junker N, Johansen JS, Hansen LT, Lund EL, Kristjansen PE. Regulation of YKL-40 expression during genotoxic or microenvironmental stress in human glioblastoma cells. *Cancer Sci* (2005) 96(3):183–90. doi: 10.1111/j.1349-7006.2005.00026.x

34. Rodriguez A, Klein CJ, Sechi E, Alden E, Basso MR, Pudumjee S, et al. LGI1 antibody encephalitis: acute treatment comparisons and outcome. *J Neurol Neurosurg Psychiatry* (2022) 93(3):309–15. doi: 10.1136/jnnp-2021-327302

35. Escudero D, Guasp M, Ariño H, Gaig C, Martínez-Hernández E, Dalmau J, et al. Antibody-associated CNS syndromes without signs of inflammation in the elderly. *Neurology* (2017) 89(14):1471–5. doi: 10.1212/wnl.0000000000004541

36. Thompson J, Bi M, Murchison AG, Makuch M, Bien CG, Chu K, et al. The importance of early immunotherapy in patients with faciobrachial dystonic seizures. *Brain* (2018) 141(2):348–56. doi: 10.1093/brain/awx323

37. Bing-Lei W, Jia-Hua Z, Yan L, Zan Y, Xin B, Jian-Hua S, et al. Three cases of antibody-LGI1 limbic encephalitis and review of literature. *Int J Neurosci* (2019) 129(7):642–8. doi: 10.1080/00207454.2018.1512985

38. Zhao Q, Sun L, Zhao D, Chen Y, Li M, Lu Y, et al. Clinical features of anti-leucine-rich glioma-inactivated 1 encephalitis in northeast China. *Clin Neurol Neurosurg* (2021) 203:106542. doi: 10.1016/j.clineuro.2021.106542

frontiers | Frontiers in Immunology

TYPE Case Report
PUBLISHED 12 January 2023
DOI 10.3389/fimmu.2022.1029294



OPEN ACCESS

EDITED BY
Mei-Ping Ding,
Zhejiang University, China

REVIEWED BY
Weihe Zhang,
China-Japan Friendship Hospital, China
Minjin Wang,
Sichuan University, China

*CORRESPONDENCE
Mei Zhang
hnzhangmei2008@163.com

SPECIALTY SECTION
This article was submitted to Multiple Sclerosis and Neuroimmunology, a section of the journal Frontiers in Immunology

RECEIVED 27 August 2022
ACCEPTED 30 December 2022
PUBLISHED 12 January 2023

CITATION
Li Y, Zhang M, Liu D, Wei M, Sheng J, Wang Z, Xue S, Yu T, Xue W, Zhu B and He J (2023) Case report: Autoimmune encephalitis with multiple auto-antibodies with reversible splenial lesion syndrome and bilateral ovarian teratoma. *Front. Immunol.* 13:1029294. doi: 10.3389/fimmu.2022.1029294



# Case report: Autoimmune encephalitis with multiple auto-antibodies with reversible splenial lesion syndrome and bilateral ovarian teratoma

Yaqiang Li[1,2], Mei Zhang[1]*, Deshun Liu[3], Ming Wei[3], Jun Sheng[3], Zhixin Wang[4], Song Xue[5], Tingting Yu[1], Weimin Xue[1], Beibei Zhu[1] and Jiale He[1]

[1]Department of Neurology, First Affiliated Hospital of Anhui University of Science and Technology (First People's Hospital of Huainan), Huainan, China, [2]Department of Neurology, People's Hospital of Lixin County, Bozhou, China, [3]Department of Radiology, First Affiliated Hospital of Anhui University of Science and Technology (First People's Hospital of Huainan), Huainan, China, [4]Department of Gynecology and Obstetrics, First Affiliated Hospital of Anhui University of Science and Technology (First People's Hospital of Huainan), Huainan, China, [5]Department of Pathology, First Affiliated Hospital of Anhui University of Science and Technology (First People's Hospital of Huainan), Huainan, China

**Background:** Reversible splenial lesion syndrome (RESLES) is a spectrum of disease radiologically characterized by reversible lesions caused by multiple factors, primarily involving the splenium of the corpus callosum (SCC). The most common causes of RESLES include infection, antiepileptic drug use and withdrawal, and severe metabolic disorders. Nevertheless, cases of autoimmune encephalitis (AE) are uncommon.

**Case presentation:** A 26-year-old female computer programming engineer with no previous medical or psychiatric history reported to the psychiatric hospital due to a 3-day episode of irritability, babbling, limb stiffness, sleepwalking, hallucinations, and paroxysmal mania. Brain MRI revealed abnormal signals of the SCC. Lumbar puncture was performed and further testing for auto-antibodies was conducted in both the CSF and serum. CSF of the patient was positive for anti-NMDAR (titer of 1:3.2) antibodies, and serum was also positive for anti-NMDAR (titer of 1:32) as well as mGluR5 (titer of 1:10) antibodies. Enhanced CT of the pelvis showed an enlarged pelvic mass; bilateral ovarian teratomas (mature teratoma and immature teratoma) were evaluated, which were pathologically confirmed after transabdominal left adnexal resection, right ovarian biopsy, and ovarian cystectomy. The patient considerably improved after intravenous administration of steroids, immunoglobulin, oral prednisone, surgical treatment, and chemotherapy. A follow-up MRI revealed completely resolved lesions. During a 3-month follow-up, the patient experienced complete resolution of symptoms without any sign of recurrence and tumors. The titer of the anti-NMDAR antibody decreased to 1:10 in serum.

**Conclusion:** Herein, we report a rare case of AE with overlapping auto-antibodies, along with RESLES and bilateral ovarian teratomas. The current case provides the possibility of the concurrence of mGluR5 antibodies in anti-NMDAR encephalitis. However, the underlying mechanism remains elusive. Furthermore, we provide additional evidence that overlapping antibodies-related pathology may be one of the many causes of RESLES. Nonetheless, caution should be observed in interpreting the observation, considering that this is a single-case study.

KEYWORDS

reversible splenial lesion syndrome, autoimmune encephalitis, ovarian teratomas, anti-N-methyl-D-aspartame receptor (anti-NMDAR) encephalitis, anti-metabotropic glutamate receptor 5 (mGluR5) encephalitis

## Introduction

Anti-N-methyl-D-aspartame receptor (anti-NMDAR) encephalitis is the most commonly known type of autoimmune encephalitis (AE), accounting for 6% to 10% of all encephalitis. It is characterized by severe neuropsychiatric manifestations, particularly psychiatric symptoms (1–3). Unlike other AE, the disease is characterized by the presence of an IgG1 antibody directed against the NR1 subunit of the NMDAR on the neuronal cell surface or synapses in the cerebrospinal fluid (CSF); however, 14.4% to 28.6% of patients have a negative serum antibody test (4, 5). Other auto-antibodies, including anti-alpha-amino-3-hydroxy-5-methyl-4-isoxazolepropionic acid receptor (AMPAR), anti-leucine rich glioma inactivated 1 (LGI1), anti-gamma-aminobutyric-acid B receptor (GABABR), and anti-contactin-associated protein 2 (CASPR2) antibodies are also common (6–9). The occurrence of mGluR5 auto-antibodies was initially reported in 2 young patients with Ophelia syndrome, an encephalitis associated with Hodgkin's lymphoma characterized by psychosis, memory deficits, and a dreamy state (10). Of note, co-existing antibodies may produce an overlap of clinical symptoms in patients with AE, increasing the probability of potential malignancy (11). Literature reports indicate that anti-NMDAR encephalitis occurs mostly in women with an average onset age of approximately 21 years and is frequently related to tumors, especially ovarian teratomas (12–14). A recent systematic review of anti-NMDAR encephalitis found that the most common brain magnetic resonance imaging (MRI) outcome was abnormal temporal lobe signals in the medial temporal lobe with hyperintensity on fluid-attenuated inversion recovery (FLAIR), followed by cortical gray matter changes and subcortical white matter changes. Furthermore, soft meningeal enhancement, followed by cortical enhancement was the most common dynamic contrast-enhanced MRI outcome (15). Reversible splenial lesion syndrome (RESLES) is a clinico-radiological syndrome characterized by reversible lesions in the splenium of corpus callosum (SCC) and commonly caused by infection, antiepileptic drugs use, antiepileptic drugs withdrawal, and severe metabolic disorders (16). Overlapping auto-antibodies and RESLES rarely occur together in AE. Here, we report a rare case of AE with anti-NMDAR as well as anti-mGluR5 antibodies in the serum and anti-NMDAR only in the CSF with RESLES and bilateral ovarian teratomas.

## Case presentation

A 26-year-old female computer programming engineer with no previous medical or psychiatric history visited the psychiatric hospital on December 4, 2021, following a 3-day episode characterized by irritability, babbling, stiffness of the limbs, sleepwalking, hallucinations and paroxysmal mania, all of which had a significant impact on her life. The parents of the patient attributed the episode partially to her recent work stress and breakup. The patient had no history of headache, dizziness, fever, seizures, and dyskinesia, and was diagnosed with schizophrenia by a psychiatrist. During hospitalization, the patient was prescribed olanzapine 5mg twice daily, and sertraline 50mg once daily, but the symptoms were poorly controlled. On the 8th day after initial symptoms, a head computed tomography (CT) scan was performed, and no significant abnormalities were observed. An electroencephalogram (EEG) revealed a diffused slow wave. On the 17th day after initial symptoms, the abnormal signals of the SCC were characterized by slight hypo-intensity on T1-weighted image (T1WI), hyper-intensity on T2-weighted image (T2WI), FLAIR, and diffusion-weighted imaging (DWI) imaging, and hypo-intensity on apparent diffusion coefficient (ADC) map (Figures 1E–I). Despite the treatment, the condition of the patient progressed and was transferred to the department of the neurological department on the 20th day after initial symptoms (Admission Day). Neurological examination showed drowsiness, difficulty with attention, or difficulty with serial 7s. The muscle strength of her limbs was approximately graded 5/5, with normal muscle tone and tendon reflexes; the remaining physical and neurological examination results were not significant. On admission day, a lumbar puncture was performed, showing homogeneous and uniform light red CSF in the anterior and posterior canals, normal opening pressure and glucose levels, increased CSF protein levels (1195.4 mg/L), normal white cell count (4×10^6/L), and high red blood cell count (1.2×10^9/L). After centrifugation, the supernatant of the CSF remained light red, and was positive for an occult blood test; crenocytes could be observed under a light microscope (×800 magnification) (Supplementary Material). No abnormalities were observed in the CSF bacteriological tests, CSF Gram stain, and CSF virus tests (herpes simplex virus, varicella-zoster virus, enterovirus, cytomegalovirus,

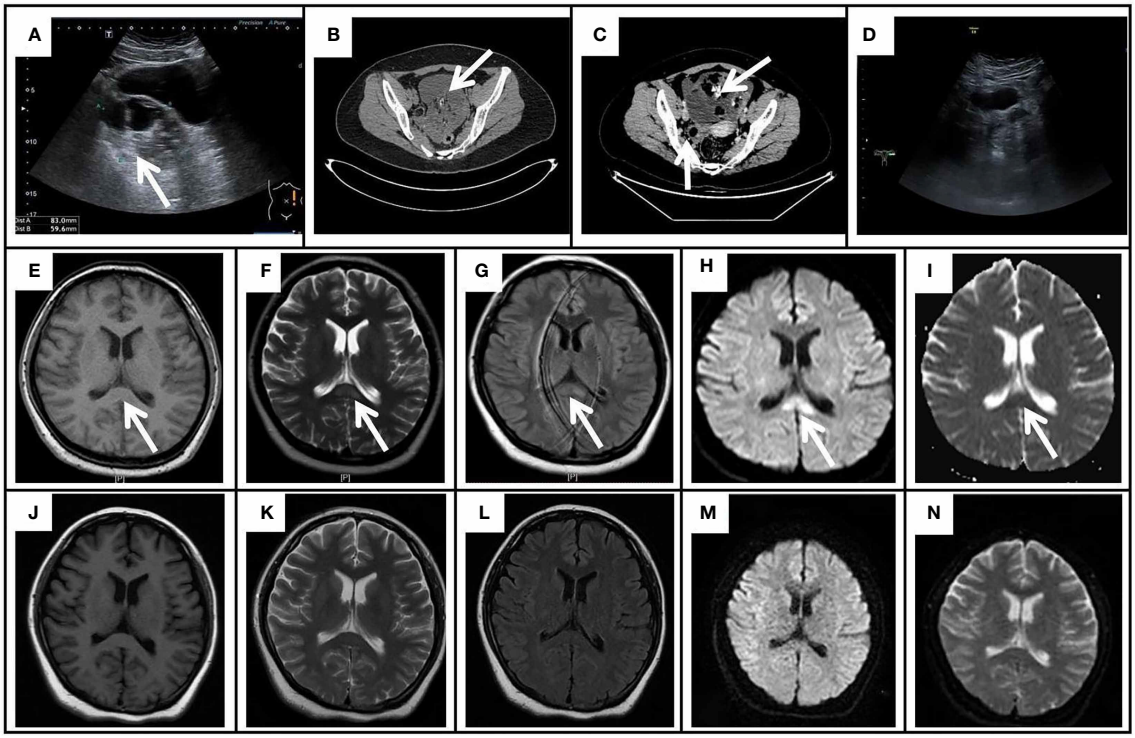


FIGURE 1
The gynecological ultrasound, pelvic CT, and cranial MRI results of the patient. **(A)** The gynecological ultrasound showed a mixed echogenic mass (8.3 cm × 5.9 cm) in the left ovary. **(B)** Pelvic CT showed an irregular cystic mass (10.2 cm × 8.4 cm) with a few calcifications and fatty components in the posterior aspect of the bladder. **(C)** Enhanced CT of the pelvis revealed a large cystic-solid mass in the anterior aspect of the uterus with no enhancement of the cystic component, fat and calcification, and mild enhancement of the solid component; A mass of uneven density on the right side of the uterus with a predominantly solid component, mild enhancement of the solid component and no enhancement of the fatty component. **(D)** The repeated gynecological ultrasound demonstrated no abnormal echogenicity. Initial cranial MRI exhibited an isolated splenium of the corpus callosum (SCC) lesion (arrows) with slight hypointensity on T1WI **(E)**, hyperintensity on T2WI **(F)**, FLAIR **(G)**, and DWI **(H)**, and hypointensity on the ADC map **(I)**. On day 52 after onset, repeated MRI demonstrated the lesion of SCC lesion was completely resolved on T1WI **(J)**, T2WI **(K)**, FLAIR **(L)**, DWI **(M)**, and ADC **(N)**.

rubella virus, and Epstein-Barr virus). Furthermore, we performed additional hospital-related examinations, including a coagulation function test. As a consequence, the mild elevation of D-Dimer was 2.93 mg/L (normal range, 0-0.55 mg/L) and the mild elevation of fibrinogen degradation products was 7.58 mg/L (normal range, 0-5 mg/L). Besides, alanine aminotransferase 56 U/L (normal range, 8-40 U/L), other biochemical indicators, complete blood cell count (including a white blood cell count of 8.5×10^6/L and red blood cell count of 5×10^12/L), routine urine and stool tests, homocysteine, thyroid-stimulating hormone, antithyroglobulin, antithyroperoxidase antibodies, cortisol, vitamin B12, erythrocyte sedimentation rate, and female tumor markers were normal. Serology for syphilis, hepatitis B, mycoplasma, human immunodeficiency virus antibody, herpes simplex virus, hepatitis C virus antibody, varicella, cytomegalovirus, mumps, measles, and Epstein-Barr virus was negative. Moreover, anti-nuclear, anti-SM, anti-SSB, anti-double-stranded DNA, anti-SSA, anti-JO-1, and all other auto-antibody tests were negative. Considering the probability of AE, an antibody test of CSF using a cell-based assay combined with a tissue-based assay (EUROIMMUN Medical Diagnostics company) was also performed on the second day of admission (Figures 2A–F). The anti-NMDAR (titer of 1:3.2) antibody was positive. Serum analysis revealed positive anti-NMDAR (titer of 1:32), and anti-mGluR5 (titer of 1:10) antibodies, but negative anti-AMPA1, anti-AMPA2, anti-GABA-B, anti-LGI 1, anti-GAD65, anti-CASPR2, anti-DPPX, and anti-IgLON5 antibodies. In addition, CNS demyelinating antibodies, including AQP4, MOG, and MBP were also negative. Given the concern for AE, the patient was administered intravenous methylprednisolone (1 g per day, intravenously, for 5 days, 500 mg per day for 3 days, 250 mg per day for 3 days) and intravenous immunoglobulin (0.4 g/kg body weight for 5 days) on the 2nd day after admission. At the same time, olanzapine improved psychiatric symptoms. After 5 days of treatment, the symptoms gradually improved, her mental state improved, and could communicate. One month after the initial symptoms, the patient had not experienced sleepwalking, her mental and behavioral symptoms had largely disappeared, her memory had gradually recovered, and her arithmetic skills had improved significantly unlike before. The Mini-Mental State Examination (MMSE) scores and Montreal Cognitive Assessment (MoCA) scores were 22 and 18, respectively. We further examined for tumor evidence and a gynecological ultrasound revealed a mixed echogenic mass in the left ovary (Figure 1A). Malignancy screening, including a CT of the chest, abdomen, and pelvis was performed to further assess the tumors, which demonstrated an irregular cystic mass (10.2 cm × 8.4 cm) with a few calcifications and fatty components in the posterior region of the bladder; ovarian teratoma was suspected (Figure 1B). Subsequently, a gynecologist recommended surgical removal of the pelvic mass, however, the

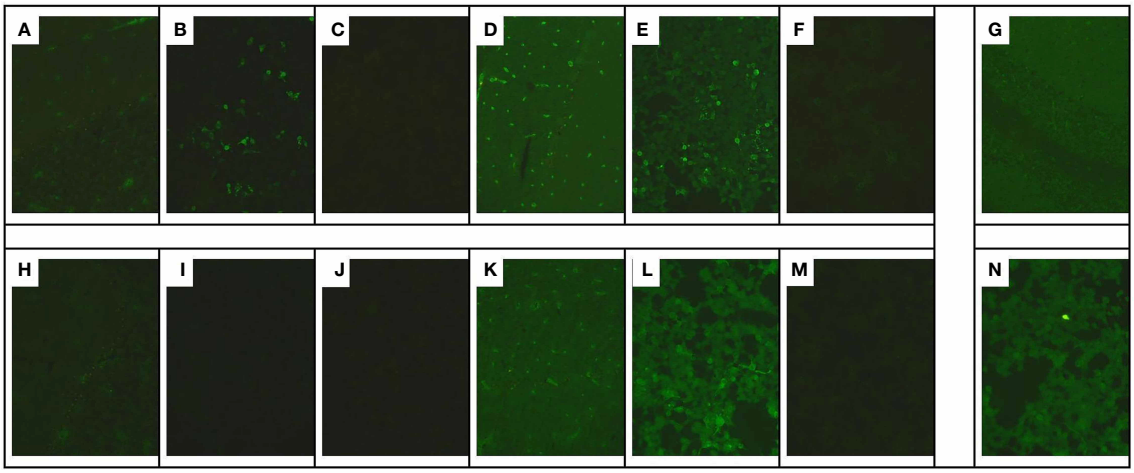


FIGURE 2
Immunofluorescence staining of monkey cerebellar tissues. Cryosections of the monkey cerebellum were incubated with patient serum and CSF in the first step and with FITC-labeled goat anti-human IgG in the second step. Immunofluorescence of anti-NMDAR and anti-mGluR5 antibodies in the CSF and serum of the patient. Anti-mGluR5 and anti-NMDAR antibodies bound on mGluR5 and NMDAR antigens expressed in HEK293 cells, respectively, and visualized by the immunofluorescence of fluorescein on the second antibody. **(A)** Tissue-based indirect immunofluorescence assay of CSF displayed anti-NMDAR antibody presenting as granular fluorescence in monkey cerebellar granular layer cells. ×200 magnification. **(B)** Positive reaction with transfected HEK293 cells expressing NMDAR after incubation with the patient's first CSF **(B)** (titer 1:3.2). ×200 magnification. **(C, I)** Negative reaction with transfected HEK293 cells expressing mGluR5 after incubation with the patient's first CSF **(C)** and the repeated CSF **(I)**. ×200 magnification. **(D, G, J, M)** Tissue-based indirect immunofluorescence assay of the patient's first serum **(D)**, second CSF **(G)**, second serum **(J)**, and third serum **(M)** showed no specific form of fluorescence in the monkey cerebellum. **(E, K, N)** Positive reaction with transfected HEK293 cells expressing NMDAR after incubation with the patient's first serum (titer 1:32) **(E)**, second serum (titer 1:32) **(K)**, and third serum (titer 1:10) **(N)**. **(F)** Positive reaction with transfected HEK293 cells expressing mGluR5 after incubation with the patient's first serum **(F)** (titer 1:10). ×200 magnification. **(H)** Negative reaction with transfected HEK293 cells expressing mGluR5 after incubation with the repeated CSF **(H)**. ×200 magnification. **(L)** Negative reaction with transfected HEK293 cells expressing mGluR5 after incubation with the repeated serum **(L)**. ×200 magnification.

patient temporarily postponed the surgical treatment for personal reasons, and thus was discharged from the hospital on the 19nd day after admission. At this time, the patient had transitioned to prednisone 60 mg, reduced by 5 mg every 2 weeks, with anticipated treatment lasting 6 months. At 1 month follow-up, her mental and behavioral symptoms improved completely, with a score of 30 for both MMSE score and MoCA scores. A follow-up MRI scan (Figures 1J–N) indicated that the lesion in SCC had completely resolved 2 weeks after discharge.

The patient was admitted to our gynecology department on May 16, 2022 (Admission Day), due to intermittent pain in the left lower abdomen for 3 months. A systematic abdominal and neurological examination was performed, revealing abdominal distension, increased abdominal wall tension, and a palpable abdominal mass on the lower abdominal surface; the remaining physical and neurological examination results were not significant. After admission, relevant examinations were performed again. No abnormality was detected by routine blood, urine, and stool tests, biochemical indicators, coagulation, and thyroid functions. Tumor markers were investigated on the 2nd day after admission, and the results revealed alpha-fetoprotein of 51.6 ng/ml (normal range, 0-20 ng/ml) and carbohydrate antigen 125 of 266.8 U/ml (normal range, 0-35 U/ml).

Furthermore, malignancy screening, including the enhanced CT of the abdomen and the pelvic mass was performed to re-evaluate the tumors on the 4nd day after admission. Enhanced CT of the pelvis revealed: a large cystic-solid mass (19 cm × 11 cm) in the anterior region of the uterus with no enhancement of the cystic component, fat and calcification, and mild enhancement of the solid component; A mass (3.3 cm × 2.9 cm) of uneven density on the right side of the uterus with a predominantly solid component, mild enhancement of the solid component and no enhancement of the fatty component (Figure 1C). Transabdominal left adnexal resection, right ovarian biopsy, and ovarian cystectomy were performed under general anesthesia on the 9nd day after admission.

Intraoperatively, irregular tissue of the left adnexa was observed, with a size of approximately 27*21*7 cm (Figure 3A), and the right ovary was slightly enlarged; a papillary bulge was visible on the surface of the ovary, with a size of approximately 1*0.5*0.5 cm (Figures 3I, J). The pathology report showed: immature cystic teratoma (histological grade 2, clinical stage IC) in the left ovary, comprising neuroglia, primitive neural tube, Infantile neural tissue, choroid plexus tissue, naive enamel organ, epidermis, hair follicle and salivary gland tissue (Figures 3B–H); Mature cystic teratoma in the right ovary, consisting of mature neuroglial, mature brain tissue, respiratory epithelium, mature adipose tissue and keratocysts (Figures 3K–N). Surgical intervention was followed by three cycles of a combined chemotherapy regimen of bleomycin + etoposide + cisplatin (BEP) on June 4$^{th}$. The patients achieved complete resolution of abdominal pain without any sign of recurrence and tumors during a 1-month follow-up. Tumor markers revealed CA125 of 22.2 U/ml (normal range, 0-35 U/ml) and AFP of 1.8/μl (normal range, 0-20ng/ml). The gynecological ultrasound demonstrated no abnormal echogenicity (Figure 1D). Anti-mGluR5 antibody in the serum and anti-NMDAR antibody in the CSF were negative, respectively, and the titer of the anti-NMDAR antibody in the serum remained 1:32 (Figures 2G–L). At the 3-month follow-up, although her titer of anti-NMDAR antibodies in serum had decreased to 1:10 (Figures 2M, N),

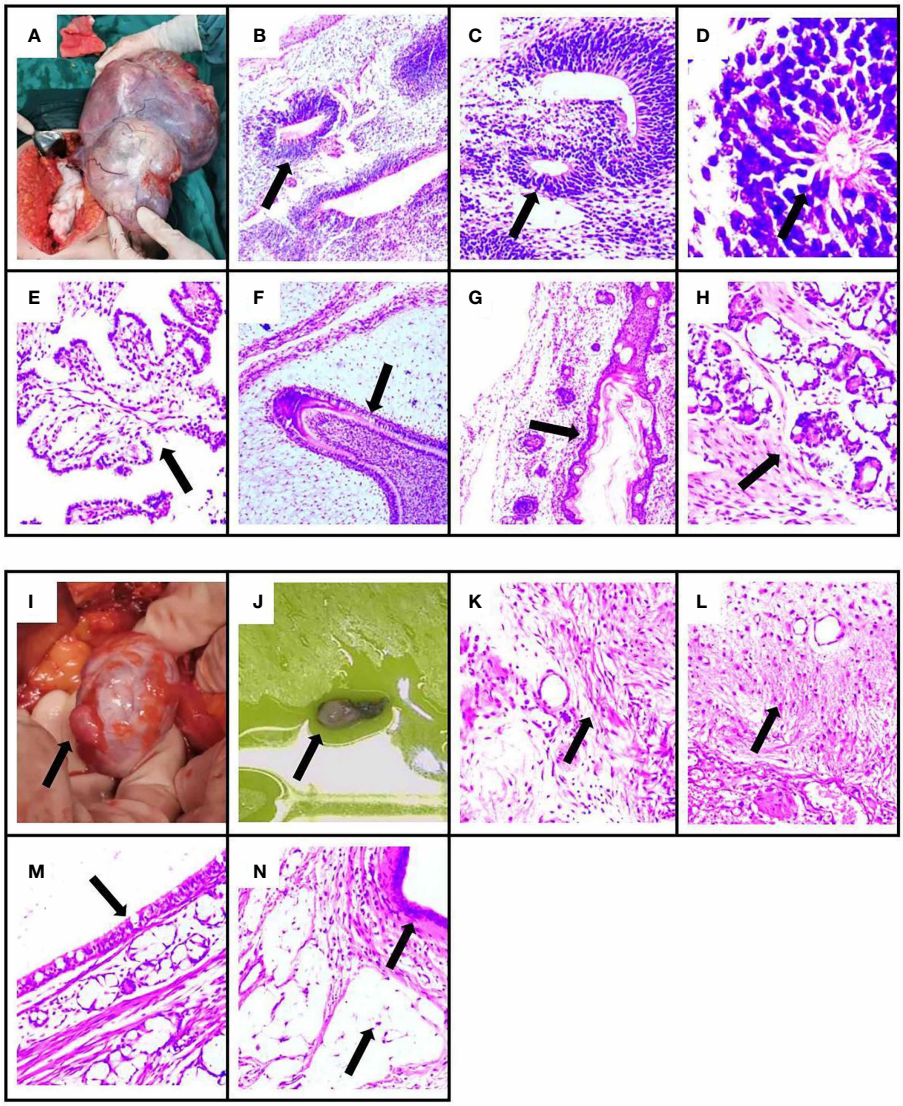


FIGURE 3
The pathology results and surgical specimen of the patient. The specimen showed immature ovarian teratoma, consisting of neuroglia, primitive neural tube, infantile neural tissue, choroid plexus tissue, naive enamel organ, epidermis, hair follicle, and salivary gland tissue by H&E staining. The arrows indicate lesions in **(B–H)**. **(B)** Neuroglia. **(C)** Primitive neural tube. **(D)** Infantile neural tissue. **(E)** Choroid plexus tissue. **(F)** Naive enamel organ. **(G)** Epidermis and hair follicle. **(H)** Salivary gland tissue. **(A)** The immature ovarian teratoma after surgical resection. The specimen showed mature ovarian teratoma, consisting of mature neuroglial, mature brain tissue, respiratory epithelium, mature adipose tissue, and keratocysts by H&E staining. The arrows indicate lesions in **(K–N)**. **(K)** Mature neuroglial. **(L)** Mature brain tissue. **(M)** Respiratory epithelium. **(N)** Mature adipose tissue and keratocysts. **(I, J)** The mature ovarian teratoma after surgical resection.

her daily life was not significantly affected and she resumed work. The entire course of the disease and the therapeutic modalities used have been summarized as a graphical abstract (Figure 4).

## Discussion

For the first time, we report a rare case of a patient diagnosed with overlapping auto-antibody syndromes with RESLES and bilateral ovarian teratoma. The patient was a young woman, with abnormal behavior (hallucinations and agitation) with irritability, followed by speech dysfunction, dyskinesias, and a drop in consciousness level. Based on positive anti-NMDAR antibodies in both CSF and serum, this case satisfied the criteria of definite anti-NMDAR encephalitis (17). So far, few reports exist on mGluR5-associated encephalitis; only 13 cases of mGluR5-associated encephalitis have been reported, with main clinical manifestations comprising abnormal psychiatric behavior, cognitive impairment, sleep disturbance, seizures, decreased level of consciousness, and movement disorder (10, 18–21). In the present case, the clinical manifestations of psychiatric and cognitive disorders could be simultaneously attributed to anti-mGluR5 and anti-NMDAR antibodies. Sleepwalking could be associated with anti-GluR5 antibodies. The presence of mGluR5 in anti-NMDAR encephalitis suggests the possibility of an overlapping autoimmune complex. Thus far, no case report of the simultaneous presence of the anti-mGluR5 and anti-NMDAR antibodies similar to our case has been published in PubMed.

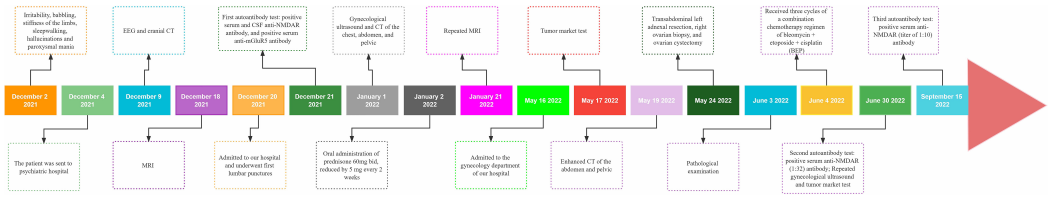


FIGURE 4
Timeline with clinical manifestation, treatment progression, and diagnosis time.

Glutamate is a major excitatory neurotransmitter of the central nervous system and modulates many key neuronal functions (22). However, glutamate overload can cause massive neuronal death and excitatory brain damage due to excessive glutamate receptor activation. Glutamate receptors (GluRs) are primarily classified into ionotropic (iGluRs), which act as glutamate-gated ion channels, and metabotropic (mGluRs), which are G protein-coupled receptors that span seven transmembranes, coupling to G proteins and activating intracellular signaling (23, 24). NMDARs are ligand-gated cation channels that regulate synaptic transmission and plasticity. They are localized in the postsynaptic membrane of neurons and predominantly found in the forebrain and limbic system, specifically the hippocampus. The pathogenesis of anti-NMDAR encephalitis may be attributed to antibody cross-linking and capping and internalization of NMDARs, causing decreased receptor density and reduced synaptic function of neurons (25, 26). mGluR5 is mainly found in the postsynaptic terminals of neurons and microglia. mGluR5 signals through Gq/G11 coupling to activate phospholipase C, leading to calcium mobilization and activation of protein kinase C, mainly expressed in the hippocampus and amygdala. These antibodies cause a decrease in mGluR5 cluster density at both synaptic and extrasynaptic locations, although the exact mechanism by which these antibodies alter receptor density remains unknown (20). Notably, glutamate exerts its important effects through mGluR5s and NMDARs. Antibodies against these two receptors cause anti-NMDA receptor encephalitis and anti-mGluR5 receptor encephalitis, both of which can result in overlapping auto-antibody syndromes.

Autoimmune antibodies can be divided into two types, i.e ., (1) antibodies directed against intracellular proteins (e.g. anti-Hu, Yo, and Ri antibodies) ; (2) antibodies acting on neuronal cell-surface receptors or synaptic proteins (e.g. anti-NMDAR, mGluR5, GABABR, LGI1, and AMPAP antibodies), some of which can occasionally overlap with each other, such as the combination of anti-NMDAR antibodies with anti-GABABR antibodies, anti-NMDAR antibodies with anti-IGI1 antibodies, and anti-NMDAR antibodies with anti-AMPAP antibodies (12, 27, 28). Of note, it is unclear why both antibodies are present in our patient, given their uncommon coexistence. The propensity for overlapping autoantibody syndromes also needs further exploration to elucidate whether either or both antibodies are pathogenic.

The clinical features of overlapping auto-antibody neurological syndromes may be common for each antibody-mediated disease, which individually combine into a single, distinct presentation that is atypical for any one antibody. For example, patients with anti-mGluR5 antibodies combined with positive anti-SOX1 antibodies have symptoms of cerebellar ataxia (20). Hoftberger et al. (27) reported a case of anti-GABABR encephalitis combined with positive anti-NMDAR antibodies, in which the psychiatric symptoms were more pronounced. They reported a similar case but combined with positive anti-GAD65 antibodies accompanied by refractory epilepsy. The titer of anti-mGluR5 antibodies in our case history was low and was only found in serum. It is unlikely that they represented true neurological autoimmunity in this situation. Nevertheless, it may be a marker of increased auto-antibodies produced in response to tumor cell breakdown and antigen release or represents a low titer “false positive” result, as seen in 8% of the general population (29). Since patient serum samples were evaluated three times and the serum anti-NMDAR antibodies remained positive during follow-up with decreasing antibody titers, we hypothesized a relatively low likelihood of a false-positive result for anti-NMDAR antibodies.

The initial brain MRI showed an abnormal signal in the splenium of the corpus callosum (SCC) and repeated MRI revealed complete resolution of the lesion, and the case met the diagnostic criteria for RESLES (16). RESLES commonly occur in children and young adults due to a number of factors, including metabolic disorders, high altitude cerebral edema, infections, and rare causes such as Kawasaki disease, acute poisoning, vitamin B12 deficiency, systemic lupus erythematosus, anorexia nervosa and cerebral venous thrombosis (30–33). Besides, it is commonly reported in patients under antiepileptic drugs, especially after drug withdrawal (16). However, the patient had no previous history of epilepsy, no epileptoid seizure, vomiting, and other symptoms during the onset of the disease, as well as no disorders including hypoglycemia, malnutrition, and liver or kidney failure. Therefore, epilepsy and metabolic disorders (hyponatremia, hypoglycemia, nutritional deficiency, etc.) could not have caused RESLES. Furthermore, the patient had no fever or other signs of infection, and microbiological tests in serum and CSF were negative; therefore, the probability of viral or other pathogenic infection was low. In addition, demyelinating antibodies in the CSF, biochemical indicators, vitamin B12 levels, thyroid function, and rheumatic function tests showed normal metabolic function and no other signs of autoimmune or demyelinating diseases. Repeated MRI revealed complete recovery of the lesion, thus excluding ischemic stroke.

The causative mechanism of RESLES is unclear. It is generally considered to be transient cytotoxic edema of SCC caused by various etiologies, which can be inferred by restricted diffusion on DWI and low ADC values (16). Studies on the relationship between RESLES

and anti-neuronal antibodies are extremely rare. It has only been described previously in cases of anti-NMDAR encephalitis, anti-VGKC encephalitis, anti-GFAP encephalitis, and anti-Yo encephalitis, respectively (34–37). A patient presented with both RESLES and auto-antibodies against voltage-gated potassium channels; the authors suggested a potential causal role for voltage-gated potassium channel autoantibodies, causing changes in potassium concentration within the myelin sheath (37). This may cause hyperpolarization, increased ion concentration, and excitotoxicity, ultimately leading to intramedullary edema manifesting as splenic lesions with diffusion restriction on MRI. A previous study found differences in fractional anisotropy (a measure of diffusion in MRI) in the SCC of patients with systemic lupus, which might be a relationship between more general autoimmune processes and changes detectable by diffusion imaging (38). In addition, the reason why the SCC is a favored site remains unknown. This may be because the enriched vascular supply of SCC, mainly provided by the vertebrobasilar system, could have resulted in increased delivery of auto-antibodies to this region and brought about an inflammatory infiltrate, causing the lesion of SCC (39). A previous case reported RESLES in a patient with anti-NMDAR antibody encephalitis, but the exact mechanism was unknown. In contrast, our case showed overlapping auto-antibodies with RESLES, and repeated CSF anti-NMDAR autoantibodies returned to normal.

The patient in this case had an excellent treatment response. Therefore, her complete recovery from cognitive impairment, the fact that her daily life remained significantly unaffected, and that she resumed normal work constitute a significant strength of this study. Nevertheless, the study has some limitations. First, this is a case study of one individual and therefore no generalizable conclusions or recommendations may be adopted. Secondly, the patients failed to undergo timely surgical treatment for personal reasons, increasing tumor size. Although the patient recovered extremely well, we did not perform a fourth serum anti-NMDAR antibodies test to establish whether the titer of antibodies decreased to normal levels.

In conclusion, this was a rare case of AE with overlapping auto-antibodies, along with RESLES and bilateral ovarian teratomas. The current case hints a possibility of the concurrence of mGluR5 antibodies in anti-NMDAR encephalitis, however, the underlying mechanism remains elusive. We suggest that anti-NMDAR antibodies may be mechanistically linked to the RESLES as described above. Nevertheless, the possibility that anti-mGluR5 autoantibodies might cause RESLES cannot be excluded. Furthermore, we provide additional evidence that overlapping antibodies-related pathology may be one of the many causes of RESLES. However, caution should be observed in interpreting the observation, considering that this is a single-case study. Therefore, additional future studies with a large number of cases may be necessary to improve the understanding of RESLES.

## Data availability statement

The original contributions presented in the study are included in the article/Supplementary Material. Further inquiries can be directed to the corresponding author.

## Ethics statement

Written informed consent was obtained from the individual(s) for the publication of any potentially identifiable images or data included in this article.

## Author contributions

YL wrote the case report under the guidance of MZ. TY and MZ are the Neurologist who treated the patient. ZW is the Gynecologist who treated the patient. MW, DL, and JS from radiology were responsible for the interpretation of images. SX from pathology was responsible for the interpretation of images. All authors contributed to the article and approved the submitted version.

## Acknowledgments

We are indebted to the patient for participation in this project.

## Conflict of interest

The authors declare that the research was conducted in the absence of any commercial or financial relationships that could be construed as a potential conflict of interest.

## Publisher's note



## Supplementary material

The Supplementary Material for this article can be found online at: https://www.frontiersin.org/articles/10.3389/fimmu.2022.1029294/full#supplementary-material

# References


1. Dalmau J, Armangué T, Planagumà J, Radosevic M, Mannara F, Leypoldt F, et al. An update on anti-NMDA receptor encephalitis for neurologists and psychiatrists: mechanisms and models. *Lancet Neurol* (2019) 18:1045–57. doi: 10.1016/S1474-4422(19)30244-3

2. Dalmau J. A probable case of anti-NMDAR encephalitis from 1830. *Neurol Neuroimmunol Neuroinflamm* (2020) 7:e901. doi: 10.1212/NXI.0000000000000901

3. Tozzoli R. Receptor autoimmunity: diagnostic and therapeutic implications. *Auto Immun Highlights* (2020) 11:1. doi: 10.1186/s13317-019-0125-5

4. Guasp M, Módena Y, Armangue T, Dalmau J, Graus F. Clinical features of seronegative,but CSF antibody-positive, anti-NMDA receptor encephalitis. *Neurol Neuroimmunol Neuroinflamm* (2020) 7:e659. doi: 10.1212/NXI.0000000000000659

5. Xu X, Lu Q, Huang Y, Fan S, Zhou L, Yuan J, et al. Anti-NMDAR encephalitis: A single-center, longitudinal study in China. *Neurol Neuroimmunol Neuroinflamm* (2020) 7:e633. doi: 10.1212/NXI.0000000000000633

6. Matthews E, Schmitt B, Passeri M, Mizenko C, Orjuela K, Piquet A. AMPA receptor encephalitis in a patient with metastatic breast cancer receiving palbociclib: A case report. *Neurol Neuroimmunol Neuroinflamm* (2022) 9:e200012. doi: 10.1212/NXI.0000000000200012

7. Zlotnik Y, Gadoth A, Abu-Salameh I, Horev A, Novoa R, Ifergane G. Case report: Anti-LGI1 encephalitis following COVID-19 vaccination. *Front Immunol* (2021) 12:813487. doi: 10.3389/fimmu.2021.813487

8. Saint-Martin M, Pieters A, Déchelotte B, Malleval C, Pinatel D, Pascual O, et al. Impact of anti-CASPR2 autoantibodies from patients with autoimmune encephalitis on CASPR2/TAG-1 interaction and Kv1 expression. *J Autoimmun* (2019) 103:102284. doi: 10.1016/j.jaut.2019.05.012

9. Lin J, Li C, Li A, Liu X, Wang R, Chen C, et al. Encephalitis with antibodies against the GABA b receptor: High mortality and risk factors. *Front Neurol* (2019) 10:1030. doi: 10.3389/fneur.2019.01030

10. Lancaster E, Martinez-Hernandez E, Titulaer MJ, Boulos M, Weaver S, Antoine JC, et al. Antibodies to metabotropic glutamate receptor 5 in the Ophelia syndrome. *Neurology* (2011) 77:1698–701. doi: 10.1212/WNL.0b013e3182364a44

11. Kammeyer R, Piquet al. Multiple co-existing antibodies in autoimmune e ncephalitis: A case and review of the literature. *J Neuroimmunol* (2019) 337:577084. doi: 10.1016/j.jneuroim.2019.577084

12. Yang J, Wu P, Liu X, Xia H, Lai Z. Autoimmune encephalitis with multiple auto-antibodies with concomitant human herpesvirus-7 and ovarian terato ma: A case report. *Front Med (Lausanne)* (2021) 8:759559. doi: 10.3389/fmed.2021.759559

13. Mitra AD, Afify A. Ovarian teratoma associated anti-Nmethyl-D-aspartate receptor encephalitis: a difficult diagnosis with a favorable prognosis. *Autops Case Rep* (2018) 8:e2018019. doi: 10.4322/acr.2018.019

14. Gurrera RJ. Recognizing psychiatric presentations of anti-NMDA receptor encephalitis in children and adolescents: a synthesis of published reports. *Psychiatry Clin Neurosci* (2019) 73:262–8. doi: 10.1111/pcn.12821

15. Bacchi S, Franke K, Wewegama D, Needham E, Patel S, Menon D. Magnetic resonance imaging and positron emission tomography in anti-NMDA receptor encephalitis. *A Syst Rev J Clin Neurosci* (2018) 52:54–9. doi: 10.1016/j.jocn.2018.03.026

16. Garcia-Monco JC, Cortina IE, Ferreira E, Martínez A, Ruiz L, Cabrera A, et al. Reversible splenial lesion syndrome (RESLES): what's in a name? *J Neuroimaging* (2011) 21:e1–14. doi: 10.1111/j.1552-6569.2008.00279.x

17. Graus F, Titulaer MJ, Balu R, Benseler S, Bien CG, Cellucci T, et al. A clinical approach to diagnosis of autoimmune encephalitis. *Lancet Neurol* (2016) 15:391–404. doi: 10.1016/S1474-4422(15)00401-9

18. Mat A, Adler H, Merwick A, Chadwick G, Gullo G, Dalmau JO, et al. Ophelia Syndrome with metabotropic glutamate receptor 5 antibodies in CSF. *Neurology* (2013) 80:1349–50. doi: 10.1212/WNL.0b013e31828ab325

19. Prüss H, Rothkirch M, Kopp U, Hamer HM, Hagge M, Sterzer P, et al. Limbic encephalitis with mGluR5 antibodies and immunotherapy-responsive prosopagnosia. *Neurology* (2014) 83:1384–6. doi: 10.1212/WNL.0000000000000865

20. Spatola M, Sabater L, Planagumà J, Martínez-Hernandez E, Armangué T, Prüss H, et al. Encephalitis with mGluR5 antibodies:symptoms and antibody effects. *Neurology* (2018) 90:el964–1972. doi: 10.1212/WNL.0000000000005614

21. Guevara C, Farias G, Silva-Rosas C, Alarcon P, Abudinen G, Espinoza J, et al. Encephalitis associated to metabotropic glutamate receptor 5 (mGluR5) antibodies in cerebrospinal fluid. *Front Immunol* (2018) 9:2568. doi: 10.3389/fimmu.2018.02568

22. Dalmau J, Geis C, Graus F. Autoantibodies to synaptic receptors and neuronal cell surface proteins in autoimmune diseases of the central nervous system. *Physiol Rev* (2017) 97:839–87. doi: 10.1152/physrev.00010.2016

23. Reiner A, Levitz J. Glutamatergic signaling in the central nervous system: Ionotropic and metabotropic receptors in concert. *Neuron* (2018) 98:1080–98. doi: 10.1016/j.neuron.2018.05.018

24. Chung MK, Ro JY. Peripheral glutamate receptor and transient receptor potential channel mechanisms of craniofacial muscle pain. *Mol Pain* (2020) 16:2068249316. doi: 10.1177/1744806920914204

25. Mikasova L, De Rossi P, Bouchet D, Georges F, Rogemond V, Didelot A, et al. Disrupted surface cross-talk between NMDA and ephrin-B2 receptors in anti-NMDA encephalitis. *Brain* (2012) 135:1606–21. doi: 10.1093/brain/aws092

26. Planagumà J, Leypoldt F, Mannara F, Gutiérrez-Cuesta J, Martín-García E, Aguilar E, et al. Human n-methyl d-aspartate receptor antibodies alter memory and behaviour in mice. *Brain* (2015) 138:94–109. doi: 10.1093/brain/awu310

27. Höftberger R, Titulaer MJ, Sabater L, Dome B, Rózsás A, Hegedus B, et al. Encephalitis and GABAB receptor antibodies: novel findings in a new case series of 20 patients. *Neurology* (2013) 81:1500–6. doi: 10.1212/WNL.0b013e3182a9585f

28. Ji T, Huang Z, Lian Y, Wang C, Zhang Q, Li J. A rare case of anti-LGI1 limbic encephalitis with concomitant positive NMDAR antibodies. *BMC Neurol* (2020) 20:336. doi: 10.1186/s12883-020-01918-7

29. McKeon A, Tracy JA. GAD65 neurological autoimmunity. *Muscle Nerve* (2017) 56:15–27. doi: 10.1002/mus.25565

30. Liu J, Liu D, Yang B, Yan J, Pu Y, Zhang J, et al. Reversible splenial lesion syndrome (RESLES) coinciding with cerebral venous thrombosis: a report of two cases. *Ther Adv Neurol Disord* (2017) 10:375–9. doi: 10.1177/1756285617727978

31. Prilipko 0, Delavelle J, Lazeyras F, Seeck M. Reversible cytotoxic edema in the splenium of the corpus callosum related to antiepileptic treatment: report of two cases and literature review. *Epilepsia* (2005) 46:1633–6. doi: 10.1111/j.l528-1167.2005.00256.x

32. Alakbarova N, Eraslan C, Celebisoy N, Karasoy H, Gonul AS. Mild encephalitis/encephalopathy with a reversible splenial lesion (MERS) development after amanita phalloides intoxication. *Acta Neurol Belg* (2016) 116:211–3. doi: 10.1007/sl3760-015-0525-x

33. Jeong TO, Yoon JC, Lee JB, Jin YH, Hwang SB. Reversible splenial lesion syndrome (RESLES) following glufosinate ammonium poisoning. *J Neuroimaging* (2015) 25:1050–2. doi: 10.1111/jon.12216

34. Kaminski JA, Prüss H. N-methyl-d-aspartate receptor encephalitis with a reversible splenial lesion. *Eur J Neurol* (2019) 26:e68–9. doi: 10.1111/ene.13900

35. Guo K, Lai X, Liu Y, Zhou D, Hong Z. Anti-glial fibrillary acidic proteinantibodies as a cause of reversible splenial lesion syndrome (RESLES): a case report. *Neurol Sci* (2021) . 42:3903–7. doi: 10.1007/s10072-021-05376-y

36. Renard D, Taieb G, Briere C, Bengler C, Castelnovo G. Mild encephalitis/encephalopathy with a reversible splenial, white matter, putaminal, and thalamic lesions following anti-yo rhombencephalitis. *Acta Neurol Belg* (2012) 112:405–7. doi: 10.1007/s13760-012-0080-7

37. Gilder TR, Hawley JS, Theeler BJ. Association of reversible splenial lesion syndrome (RESLES) with anti-VGKC autoantibody syndrome: a case report. *Neurol Sci* (2016) 37:817–9. doi: 10.1007/s10072-015-2464-y

38. Zhang L, Harrison M, Heier LA, Zimmerman RD, Ravdin L, Lockshin M, et al. Diffusion changes in patients with systemic lupus erythematosus. *Magn Reson Imaging* (2007) 25:399–405. doi: 10.1016/j.mri.2006.09.037

39. Shiihara T, Kato M, Hayasaka K. Clinically mild encephalitis/encephalopathy with a reversible splenial lesion. *Neurology* (2005) 63:1854–8. doi: 10.1016/j.surne

frontiers | Frontiers in Immunology

TYPE Original Research
PUBLISHED 16 January 2023
DOI 10.3389/fimmu.2022.1066830



OPEN ACCESS

EDITED BY
Honghao Wang,
Guangzhou First People's Hospital, China

REVIEWED BY
Yuji Tomizawa,
Juntendo University, Japan
Soon-Tae Lee,
Seoul National University Hospital, Republic of Korea

*CORRESPONDENCE
Takahiro Iizuka
takahiro@med.kitasato-u.ac.jp

SPECIALTY SECTION
This article was submitted to Multiple Sclerosis and Neuroimmunology, a section of the journal Frontiers in Immunology

RECEIVED 11 October 2022
ACCEPTED 08 December 2022
PUBLISHED 16 January 2023

CITATION
Nagata N, Kanazawa N, Mitsuhata T, Iizuka M, Nagashima M, Nakamura M, Kaneko J, Kitamura E, Nishiyama K and Iizuka T (2023) Neuronal surface antigen-specific immunostaining pattern on a rat brain immunohistochemistry in autoimmune encephalitis. *Front. Immunol.* 13:1066830. doi: 10.3389/fimmu.2022.1066830



# Neuronal surface antigen-specific immunostaining pattern on a rat brain immunohistochemistry in autoimmune encephalitis

Naomi Nagata, Naomi Kanazawa, Tomomi Mitsuhata, Masaki Iizuka, Makoto Nagashima, Masaaki Nakamura, Juntaro Kaneko, Eiji Kitamura, Kazutoshi Nishiyama and Takahiro Iizuka*

Department of Neurology, Kitasato University School of Medicine, Sagamihara, Japan

A variety of neuronal surface (NS) antibodies (NS-Ab) have been identified in autoimmune encephalitis (AE). Tissue-based assay (TBA) using a rodent brain immunohistochemistry (IHC) is used to screen NS-Ab, while cell-based assay (CBA) to determine NS antigens. Commercial rat brain IHC is currently available but its clinical relevance remains unclear. Immunostaining patterns of NS antigens have not been extensively studied yet. To address these issues, we assessed a predictive value of "neuropil pattern" and "GFAP pattern" on commercial IHC in 261 patients, and characterized an immunostaining pattern of 7 NS antigens (NMDAR, LGI1, GABAaR, GABAbR, AMPAR, Caspr2, GluK2). Sensitivity and specificity of "neuropil pattern" for predicting NS-Ab were 66.0% (95% CI 55.7-75.3), and 98.2% (95% CI 94.8-99.6), respectively. False-positive rate was 1.8% (3/164) while false-negative rate was 34.0% (33/97). In all 3 false-positive patients, neuropil-like staining was attributed to high titers of GAD65-Ab. In 33 false-negative patients, NMDAR was most frequently identified (n=18 [54.5%], 16/18 [88.9%] had low titers [< 1:32]), followed by GABAaR (n=5). Of 261 patients, 25 (9.6%) had either GFAP (n=21) or GFAP-mimicking pattern (n=4). GFAP-Ab were identified in 21 of 31 patients examined with CBA (20 with GFAP pattern, 1 with GFAP-mimicking pattern). Immunostaining pattern of each NS antigen was as follows: 1) NMDAR revealed homogenous reactivity in the dentate gyrus molecular layer (DG-ML) with less intense dot-like reactivity in the cerebellar granular layer (CB-GL); 2) both GABAaR and GluK2 revealed intense dot-like reactivity in the CB-GL, but GABAaR revealed homogenous reactivity in the DG-ML while GluK2 revealed intense reactivity along the inner layer of the DG-ML; and 3) LGI1, Caspr2, GABAbR, and AMPAR revealed intense reactivity in the cerebellar ML (CB-ML) but LGI1 revealed intense reactivity along the middle layer of the DG-ML. Whereas, Caspr2, GABAbR, and AMPAR revealed similar reactivity in the

DG-ML but some difference in other regions. TBA is useful not only for screening NS- or GFAP-Ab but also for estimating NS antigens; however, negative results should be interpreted cautiously because "neuropil pattern" may be missed on commercial IHC when antibody titers are low. Antigen-specific immunoreactivity is a useful biomarker of AE.

KEYWORDS

autoimmune encephalitis, immunohistochemistry, autoantibodies, neuronal surface antigens, tissue-based assay, cell-based assay

# 1 Introduction

Autoimmune encephalitis (AE) is a form of encephalitis that occurs as a result of a brain-specific immune response and usually associates with an antibody against a neuronal or glial, cell surface antigen (1). A variety of neuronal surface (NS) antibodies (NS-Ab) have been identified in patients with AE or related disorder (2). Glial fibrillary acidic protein (GFAP) antibodies (GFAP-Ab) have also been reported concurrently with NMDA receptor (NMDAR) antibodies (NMDAR-Ab) without association with distinct clinico-radiologic features (3). Tissue-based assay (TBA) using a rodent brain immunohistochemistry (IHC) adapted to NS antigens is used to screen NS-Ab, while cell-based assay (CBA) using human embryonic kidney (HEK) 293 cells expressing target antigens on the cell surface membrane is used to determine the NS antigens (4). Live hippocampal neuronal cultures are also used to confirm the presence of NS-Ab. However, these studies are mainly performed at research laboratories (1).

In clinical practice; however, it is difficult to measure all NS-Ab identified to date. A commercial fixed CBA is currently available for many but not for glycine receptor (GlyR), γ-aminobutyric acid A receptor (GABAaR), or glutamate kainate receptor subunit 2 (GluK2), and limitations of the commercial CBA as a diagnostic test of AE have been reported (5). It is an issue which NS antigen should be examined with CBA in the individual cases. Immunostaining patterns highly characteristic of NS antigens have been described (3) but not extensively studied yet. A commercial IHC is also currently available but its clinical relevance remains unclear. If TBA reveals individual NS-antigen-specific immunostaining pattern, it will facilitate identification of the target antigen by choosing appropriate CBA, ultimately leading to early diagnosis and early initiation of appropriate treatment.

To address these issues, we conducted this study to clarify 1) whether the commercial IHC is clinically useful for screening NS- or GFAP-Ab (Part I), and 2) whether TBA reveals an immunostaining pattern highly characteristic of major individual NS antigens (Part II).

# 2 Materials and methods

## 2.1 Patient selection and antibody measurement

First, we retrospectively reviewed the clinical information of 622 patients with suspected AE or related disorder, who underwent a testing for NS-Ab between January 1, 2007 and October 31, 2022. These patients were admitted to Kitasato University Hospital or other hospitals between January 1, 1999 and September 30, 2022 with suspected AE or related disorder; in 7 patients who were admitted to Kitasato University Hospital before January 1, 2007, archived cerebrospinal fluid (CSF)/sera obtained at the onset of disease were used for antibody assays. The CSF/sera obtained from 388 patients (62.4%) of this cohort were referred from other 145 hospitals widely distributed in Japan to Kitasato University to examine NS-Ab. The detailed clinical information was provided from each physician to TI (a primary investigator of the study).

The inclusion criteria of the patients who underwent a testing for NS-Ab are as follows: 1) AE or related neurological disorder is highly suspected based on clinical assessment; 2) detailed clinical information that supports the clinical diagnosis is available for review by TI, including clinical course from the onset of symptoms or prodromal viral-like illness, past history, family history, a habit of smoking or drinking, regular medications, neuropsychological assessment on admission, laboratory test results [blood, CSF, brain or spinal MRIs, body CT, electroencephalography, needle or surface electromyography (when suspected of having stiff-person spectrum disorder, Morvan syndrome, or Isaacs' syndrome)], and subsequent course of the disease when available; and 3) written informed consent is obtained from the patients or their proxies. When all the criteria were fulfilled, we accepted measurement of NS-Ab. However, reasonable exclusion of alternative cause was not considered mandatory at the time of collection of sera/CSF samples. Therefore, we included patients in whom alternative cause had not been completely excluded yet. The sera/CSF samples mainly obtained at the acute phases and kept frozen until antibody testing.

NS-Ab were measured at the laboratory of Josep Dalmau (University of Pennsylvania, Philadelphia, or IDIBAPS Hospital Clínic, Barcelona) with a rat brain in-house IHC adapted to NS antigens and CBA (6–14); they included antibodies against the NMDAR, α-amino-3-hydroxy-5-methyl-4-isoxazolepropionic acid receptor (AMPAR), GABAaR, γ-aminobutyric acid B receptor (GABAbR), metabotropic glutamate receptor 5 (mGluR5), metabotropic glutamate receptor 1 (mGluR1), dipeptidyl peptidase-like protein 6 (DPPX), contactin-associated protein-like 2 (Caspr2), leucine-rich glioma-inactivated 1 (LGI1), neurexin 3, GlyR or GluK2. Both serum and CSF were examined in all patients except 9 (only CSF [n=5] or serum [n=4] was available). These NS antigens were measured with CBA mainly based on the clinical phenotypes of each patient and/or immunostaining pattern on in-house IHC performed at the laboratory of Josep Dalmau.

In addition to NS-Ab, myelin oligodendrocyte glycoprotein (MOG) and aquaporin-4 (AQP4) antibodies were examined with CBA in patients with overlapping encephalitis and demyelinating syndrome (15). GFAP-Ab were also subsequently examined in CSF at the laboratory of Josep Dalmau with established CBA (3) in patients who were clinically suspected of having GFAP-positive meningoencephalomyelitis or when TBA performed at Kitasato University revealed immunoreactivity suggesting GFAP. Autoantibodies against classical paraneoplastic intracellular antigens (CV2/CRMP5, Ma2, Ri, Yo, Hu, amphiphysin) were measured in serum at Kitasato University or referring hospital with immunoblot (Euroimmun AG), when clinically considered necessary. Glutamate decarboxylase (GAD) antibodies (GAD-Ab) were also measured in serum with either radioimmunoassay, enzyme-linked immunosorbent assay (ELISA), or enzyme immunoassay (EIA).

Next, we selected 265 patients (42.6%), whose archived CSF was examined with commercial IHC at Kitasato University between August 1, 2020 and October 31, 2022 to evaluate an immunostaining pattern, irrespective of NS-Ab-positivity. In this study, the results of IHC using sera were not included in the evaluation of immunostaining pattern because it is sometimes difficult to evaluate NS-antigen-specific pattern due to concurrent high background reactivity, intravenous immunoglobulins administered before the collection of the sera, or concurrent antibodies to intracellular antigens, of which clinical relevance in AE is unclear. After exclusion of 4 patients (see Figure 1), 261 (152 female 58.2%), median age at onset 46 years [range, 5-91 years]) were included in Part I. We also performed in-house IHC adapted to NS antigens in 54 patients to compare immunostaining pattern between in-house and commercial IHC.

In Part II, among NS antigens identified in the CSF, we selected 7 major antigens (NMDAR, AMPAR, GABAaR, GABAbR, LGI1, Caspr2, and GluK2). The GlyR was not included because it is difficult to see the reactivity with GlyR on the hippocampus or cerebellum section (1). The DPPX was also not included because no DPPX antibodies were identified in our cohort. After exclusion of 164 NS-Ab-negative patients and 12 NS-Ab-positive patients (5 with antibodies against NS antigen not characterized yet, 5 with antibodies against more than one NS antigen, 2 with GlyR antibodies [GlyR-Ab]), 85 were finally selected for Part II. An immunostaining pattern was evaluated with both in-house and commercial IHC in each group of NS antigen (Figure 1).

## 2.2 In-house and commercial rat brain IHC

In-house IHC was performed at Kitasato University with patients' CSF (diluted 1:2) using a standard technique (16, 17). In brief, Wistar female rats at 10 weeks of age were anesthetized and euthanized by decapitation without tissue perfusion. Brains were removed, fixed in 4% paraformaldehyde for 1 hour at 4°C, cryoprotected in 40% sucrose for 48 hours at 4°C, embedded in freezing media, and snap frozen in isopentane chilled with liquid nitrogen. Ten micron-thick sections were incubated with 0.3% $H_2O_2$ and blocked with 10% goat serum, and then incubated with patient's CSF (diluted 1:2) overnight at 4°C. The sections were incubated with a secondary biotinylated goat anti-human IgG for 1 hour, and the reactivity developed with the avidin-biotin-peroxidase method (Figures 2A–C). The animal study was reviewed and approved by the Animal Experimentation and Ethics Committee of the Kitasato University School of Medicine (2022-031) and were performed in accordance with institutional guidelines for animal experimentation, which are based on the Guidelines for Proper Conduct of Animal Experiments published by the Science Council of Japan.

Commercial IHC was also performed at Kitasato University using a kit (Euroimmun AG, product No: FA 111m-3) following the instruction of the company with indirect immunofluorescent assay (IIFA). The kit consists of 4 biochips per field containing the NMDAR-transfected cells (Figure 2D), control-transfected cells (Figure 2E), cerebellum (Figure 2F), and hippocampus (Figure 2G). IIFA was evaluated with an Olympus BX53 fluorescence microscope (Olympus, Japan). In this study, we evaluated an immunostaining pattern using CSF (diluted 1:2) that was used in in-house IHC.

## 2.3 Evaluation of "neuropil pattern" on commercial rat brain IHC

In Part I, we assessed a predictive value of a pattern of neuropil reactivity ("neuropil pattern") suggesting the presence of NS-Ab. In

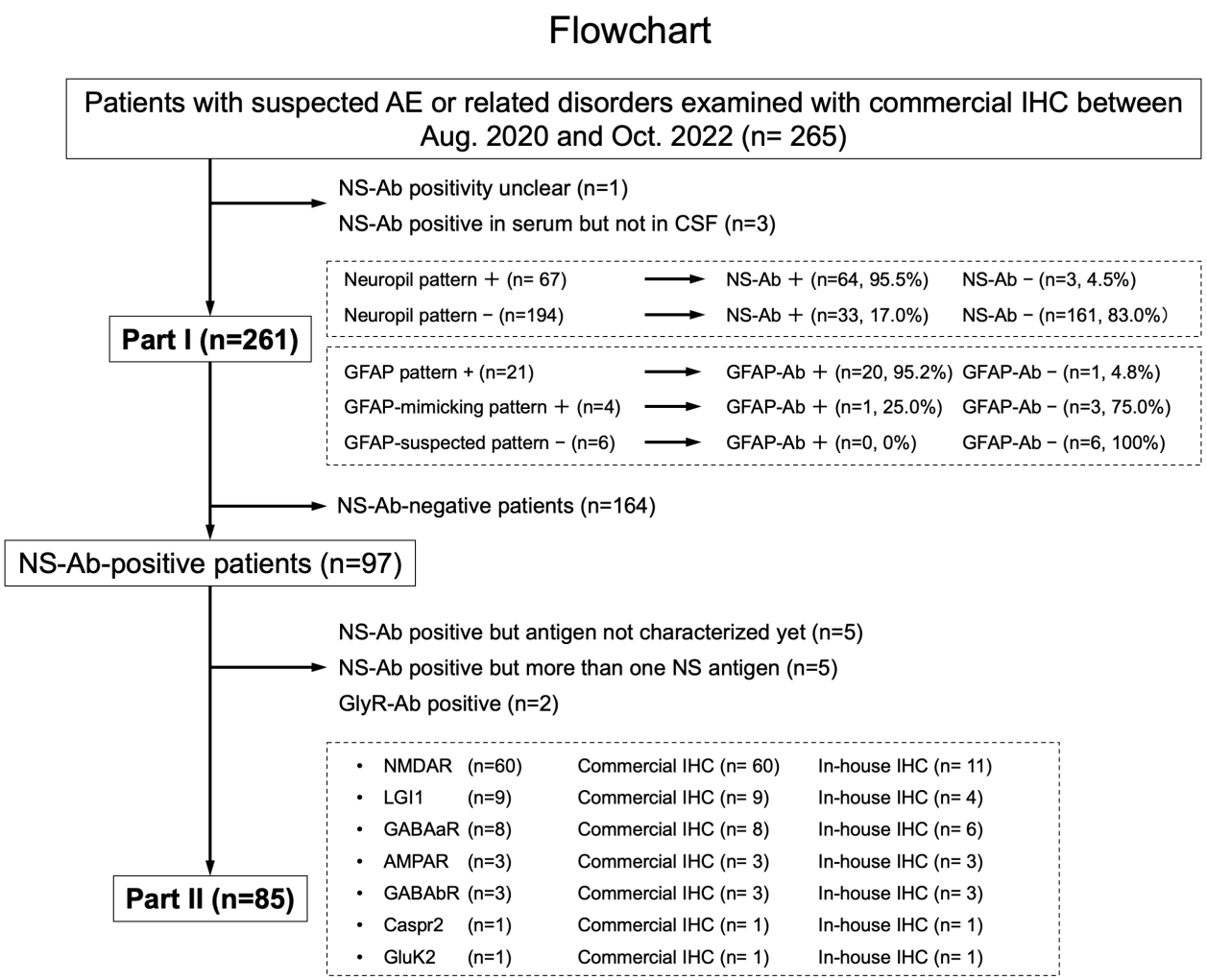


FIGURE 1
This figure shows a diagram of the study conducted including Part I and Part II. In Part I, a predictive value of a "neuropil pattern" suggesting NS-Ab and a pattern suggesting GFAP-Ab were mainly investigated, whereas in Part II, an immunostaining pattern of the pre-selected 7 NS antigens are evaluated based on the subjects listed here. The number of patients is shown in parentheses. AE, autoimmune encephalitis; Ab, antibodies; GFAP, glial fibrillary acidic protein; IHC, immunohistochemistry; NS, neuronal surface.





10.3389/fimmu.2022.1066830

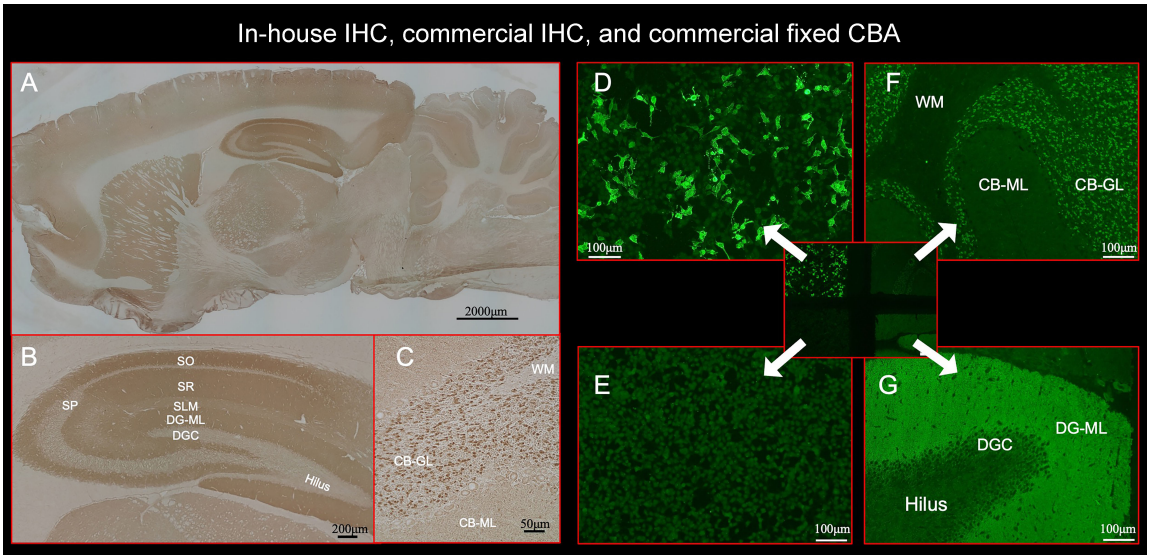


FIGURE 2
This figure shows the results of immunostaining pattern using in-house IHC **(A–C)** and commercial kit, which consists of 4 biochips per field containing the NMDAR-transfected cells **(D)**, control-transfected cells **(E)**, cerebellum **(F)**, and hippocampus **(G)**. Note intense reactivity with NS antigen in the DG-ML **(A, B, G)**, less intense dot-like reactivity in the CB-GL but no apparent reactivity on the CB-ML **(C, F)**. This staining pattern is consistent with NMDAR. **(D)** shows intense staining on NMDAR-transfected cells but not on control-transfected cells **(E)**, confirming the diagnosis of anti-NMDAR encephalitis. Antibody assay was performed using CSF (diluted 1:2) obtained from a patient with anti-NMDAR encephalitis (antibody titer 1:2048), with in-house IHC adapted to NS antigens **(A–C)**, commercial fixed CBA **(D, E)**, and commercial IHC **(F, G)**. See Text. CBA, cell-based assay; CB-GL, cerebellar granular layer; CB-ML, cerebellar molecular layer; DGC, dentate granule cells; DG-ML, dentate gyrus molecular layer; IHC, immunohistochemistry; NMDAR, NMDA receptor; NS, neuronal surface; SLM, stratum lacunosum moleculare; SO, stratum oriens; SP, stratum pyramidale; SR, stratum radiatum; WM, white matter.

this study, the "neuropil pattern" was considered positive when apparent reactivity with NS antigens was visually identified on commercial IHC at the level of hippocampus and cerebellum section. Immunostaining pattern was initially assessed independently by 3 observers (NK, NN, and TI), and only patients whose CSF samples (diluted 1:2) were finally judged to be positive by all of them were considered positive with neuropil pattern. A pattern suggesting reactivity with glial surface antigens (AQP4 or MOG) was not included in the "neuropil pattern". The NS-Ab-positivity or negativity was determined based on the final report from the laboratory of Josep Dalmau. Then, we determined sensitivity and specificity of the "neuropil pattern" for predicting NS-Ab as well as false-negative (NS-Ab positive but "neuropil pattern" negative) or false-positive rate (NS-Ab negative but "neuropil pattern" positive). In Part I, we did not exclude patients with autoantibodies against multiple NS antigens or antigens not characterized yet.

To assess factors potentially associated with false-negative results, we measured antibody titers in CSF using fixed CBA (Euroimmun AG) in patients with NMDAR-Ab because NMDAR was most frequently identified in the false-negative patients. We also performed in-house IHC in some of the patients to evaluate whether in-house IHC can reveal the "neuropil pattern" in the false-negative patients.

## 2.4 Evaluation of "GFAP pattern" on commercial rat brain IHC

In Part I, we also assessed a predictive value of a pattern suggesting the presence of GFAP-Ab. We considered "GFAP-suspected", when either of the following patterns was seen: 1) "GFAP pattern", which is a pattern of GFAP reactivity showing a cactus thorn-like or filamentous reactivity consistent with GFAP (Figure 3E), or 2) "GFAP-mimicking pattern", which is a pattern atypical of GFAP but has liner or reticular reactivity. We also reviewed GFAP pattern on in-house IHC. GFAP-Ab were examined with established CBA at the laboratory of Josep Dalmau, when the patient had either GFAP or GFAP-mimicking pattern, or had clinico-radiologic features (such as radial periventricular enhancement on brain MRI) which were reported in patients with GFAP-positive meningoencephalomyelitis known as autoimmune GFAP astrocytopathy (18).

## 2.5 Evaluation of immunostaining pattern characteristic of individual NS antigens

In Part II, we evaluated an immunostaining pattern in NS-Ab-positive patients (n=85): NMDAR (n=60), LGI1 (n=9),

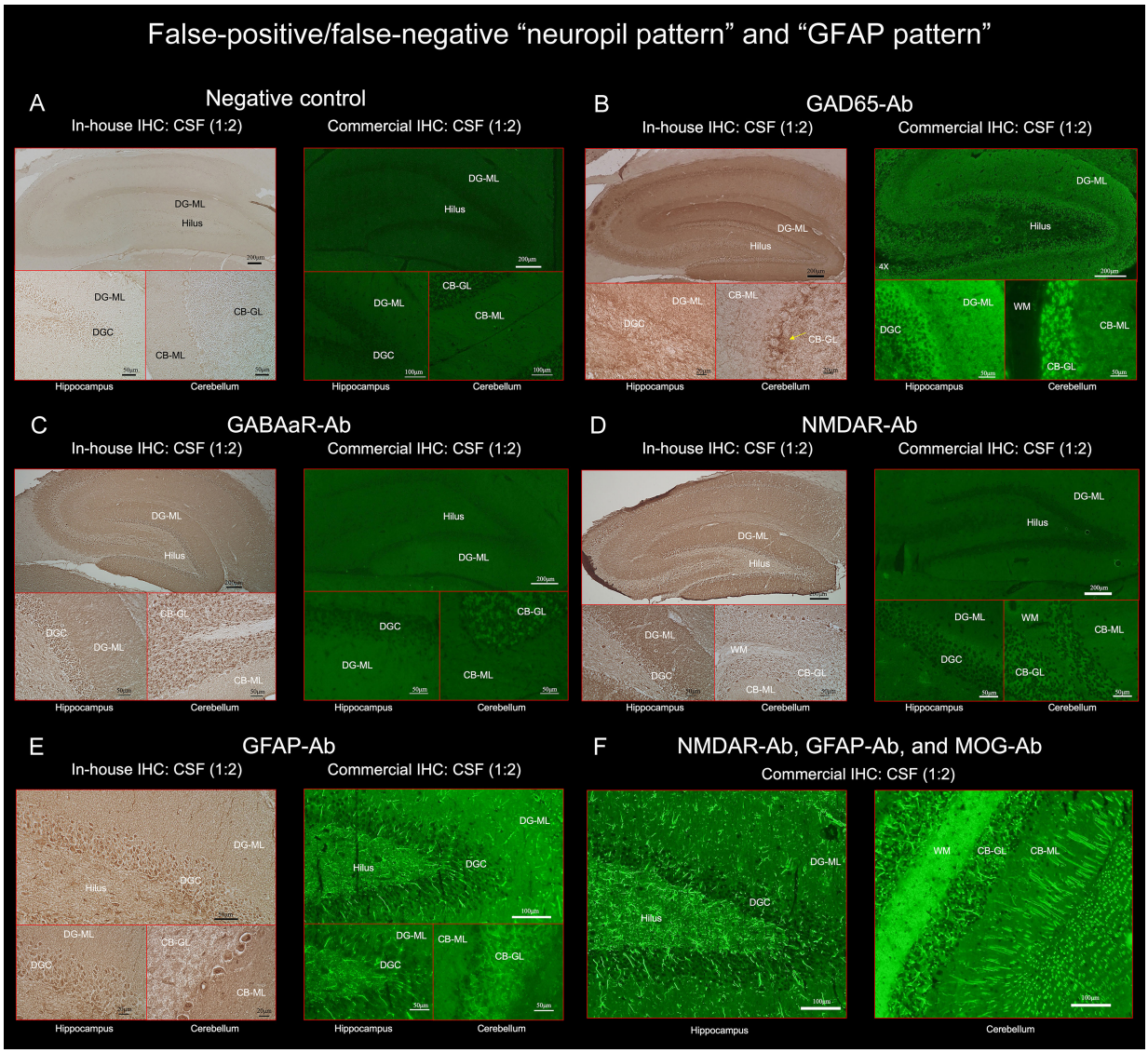


FIGURE 3
**(A)** does not show apparent “neuropil pattern” with negative control, but **(B)** reveals some reactivity mimicking “neuropil pattern” in the middle and outer layers of the DG-ML. Reactivity in the surroundings of the DGC, Purkinje cells, and CB-GL are consistent with a pattern of GAD65 reactivity. **(C, D)** did not reveal apparent “neuropil pattern” on commercial IHC but visually recognizable reactivity on in-house IHC. **(E, F)** reveal a cactus thorn-like or filamentous staining consistent with a pattern of GFAP reactivity. Note that GFAP pattern is more clearly shown on commercial IHC than on in-house IHC **(E)**. **(F)** shows intense reactivity with GFAP and MOG but not apparent “neuropil pattern”. CB-GL, cerebellar granular layer; CB-ML, cerebellar molecular layer; DGC, dentate granule cells; DG-ML, dentate gyrus molecular layer; WM, white matter.

GABAaR (n=8), AMPAR (n=3), GABAbR (n=3), Caspr2 (n=1), and GluK2 (n=1) (Figure 1).

In each pre-selected NS antigen, we characterized the immunostaining pattern at the level of the hippocampus and cerebellum, by focusing on the reactivity with NS antigens expressed on the following regions: dentate gyrus molecular layer (DG-ML), dentate hilus, cerebellar molecular layer (CB-ML), cerebellar granular layer (CB-GL), and cerebellar white matter (CB-WM), all of which are included in the commercial IHC biochips. We also paid attention to antigen-specific laminar reactivity in the DG-ML whether there is difference in intensity along the inner, middle, or outer molecular layers.

The immunostaining pattern characteristic of the individual NS antigens was determined mainly based on the results that showed a robust “neuropil pattern” on both in-house and commercial IHC (Figures 1, 4) while excluding antibody-positive CSF samples with low titer to ensure a more accurate staining pattern. A series of illustrations was finally created by TI

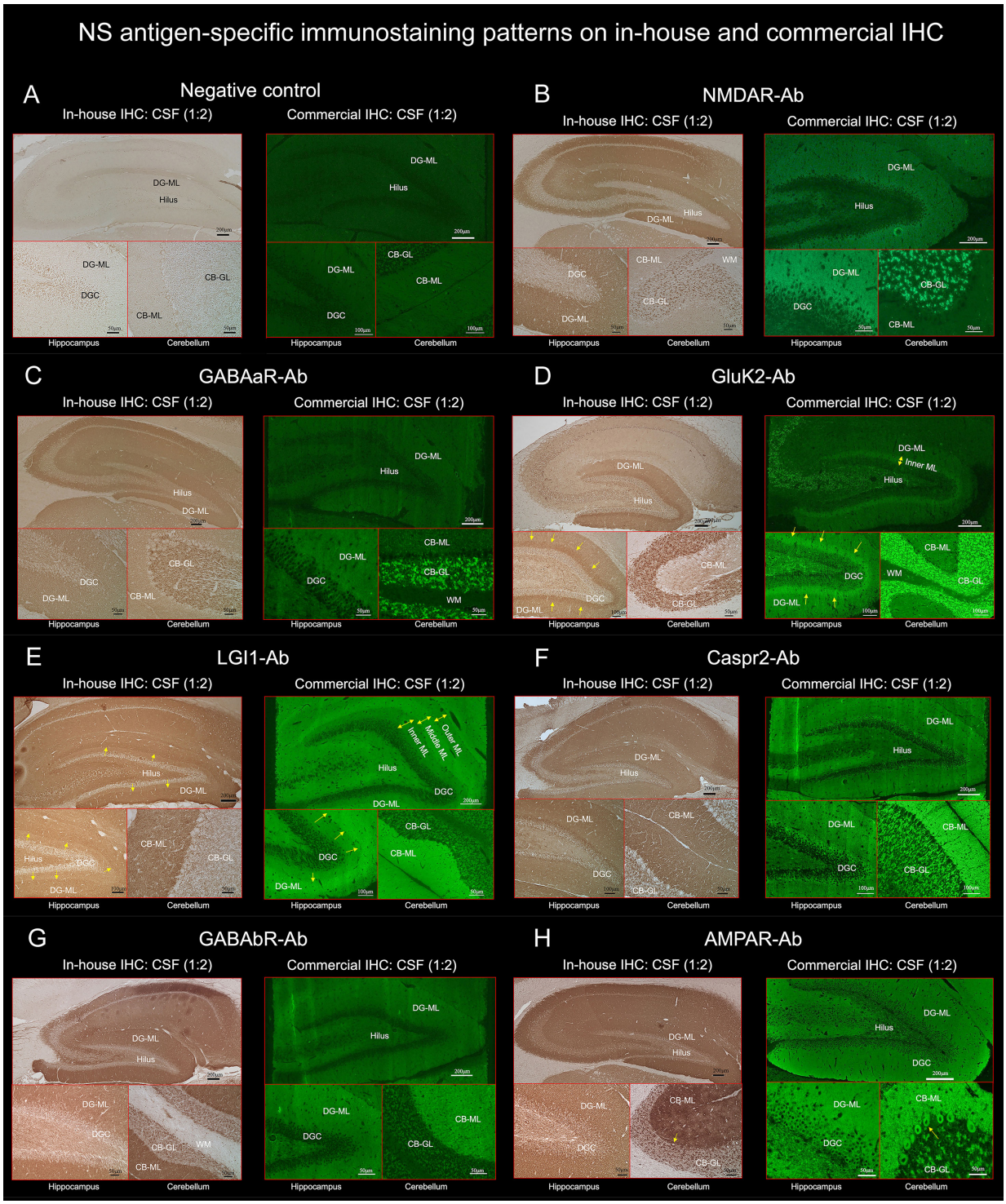


FIGURE 4
TBA reveals an immunostaining pattern highly characteristic of the individual NS antigen. (See Text). These preselected 7 NS antigens reveals intense reactivity with NS antigen "neuropil pattern", among NS antigens, two reveal antigen-specific laminar reactivity, along the inner layer in GluK2 (**D**, arrows) and the middle layer in LGI1 (**E**, arrows). The first 3 NS antigens (NMDAR, GABAaR, GluK2) have dot-like reactivity on the CB-GL **(B–D)**, while the other 4 (LGI1, Caspr2, GABAbR, AMPAR) have homogenous reactivity on the CB-ML with some different immunoreactivity on the hilus, CB-GL, or Purkinje cells (see Text). CB-GL, cerebellar granular layer; CB-ML, cerebellar molecular layer; DGC, dentate granule cells; DG-ML, dentate gyrus molecular layer; ML, molecular layer; WM, white matter.

to make it easy to follow the difference of immunostaining pattern in each NS antigen using Adobe Illustrator (Adobe Inc.).

## 2.6 Standard protocol approvals, registrations, and patient consents

The study was approved by Institutional Review Boards of Kitasato University (B20-280). Written informed consent was obtained from the patients or their proxies. Information on symptoms, CSF, MRI, EEG, and treatments were obtained from the authors or referring physicians.

## 2.7 Statistical analysis

Statistical analyses were performed using JMP, version 14.2.0 (SAS Institute Inc.). The Fisher exact test was performed for comparison of categorical variables, and the Mann-Whitney test was used for continuous variables. The statistical significance was set at $p < 0.05$. The sensitivity and specificity of the commercial IHC were determined with 2-way contingency table analysis using a statistical calculator (MedCalc Software Ltd. https://www.medcalc.org/calc/diagnostic_test.php [Version 20.116]).

# 3 Results

## 3.1 Part I-1. Sensitivity and specificity of "neuropil pattern"

We found "neuropil pattern" in 67 of 261 patients (25.7%), while NS-Ab were identified in 97 patients (37.2%) (Figure 1). NS antigens identified in the CSF included NMDAR (n=62), LGI1 (n=11), GABAaR (n=8), GABAbR (n=5), AMPAR (n=4), GlyR (n=3), Caspr2 (n=2), GluK2 (n=1), and NS antigen not characterized yet (n=7); 5 patients had antibodies against more than one NS antigen. The "neuropil pattern" was seen in 64 of the 97 NS-Ab-positive patients (66.0%) but not in any of the 3 GlyR-Ab-positive patients. The "neuropil pattern" was seen in all 7 pre-selected major NS antigens as follows: GluK2 (1/1, 100%), Caspr2 (1/1, 100%), LGI1 (8/9, 88.9%), NMDAR (42/60, 70.0%), AMPAR (2/3, 66.7%), GABAbR (2/3, 66.7%), and GABAaR (3/8, 37.5%); the 5 patients with multiple NS-Ab were not included in the evaluation of frequency of the "neuropil pattern" in each NS antigen.

NS-Ab were more frequently identified in patients with "neuropil pattern" than those without (64/67 [95.5%] vs 33/194 [17.0%], $p$ <.0001). Sensitivity and specificity of the "neuropil pattern" for predicting NS-Ab were 66.0% (95% CI 55.7-75.3), and 98.2% (95% CI 94.8-99.6), respectively. False-positive rate was 1.8% (3/164) while false-negative rate was 34.0% (33/97).

All 3 false-positive patients had high titers of GAD antibodies in their sera (> 2,000 U/mL, reference < 5), in all of them, the commercial IHC revealed neuropil-like reactivity in the DG-ML, but a pattern of synaptic staining in the CB-ML, CB-GL, and the axon hillocks of Purkinje cells (PC) which are highly characteristic of GAD65 (1) (Figures 3A, B). No NS-Ab were found in either serum or CSF in the 3 patients. We also confirmed the presence of GAD65-Ab in their CSF with GAD65-transfected CBA in the 3 patients. The neuropil-like staining was finally considered attributed to high titers of GAD65 antibodies. High titers of GAD antibodies were also found in the other 5 patients, without apparent "neuropil pattern" but a pattern of GAD65 reactivity was seen in the 5 patients.

Among the identified NS antigens in the false-negative patients (n=33), NMDAR was most frequently found (n=18, 54.5%), followed by GABAaR (n=5), GlyR (n=3, 1 with concurrent GABAbR), GABAbR (n=1), LGI1 (n=1), AMPAR (n=1), and not characterized yet (n=4).

To elucidate the factors potentially related to the false-negative results, we added in-house IHC in 3 false-negative patients with GABAaR-Ab (n=1), LGI1-Ab (n=1), or NMDAR-Ab (n=1). In the all 3 patients, in-house IHC revealed visually recognizable reactivity with corresponding NS antigens (Figures 3C, D). In patients with NMDAR-Ab, the frequency of low antibody titers (< 1:32) was higher in "neuropil-negative" patients than in "neuropil-positive" patients (16/18 [88.9%] vs 1/42 [2.4%]) ($p$ <.0001). It was also noted that false-negative rate was higher in GABAaR than in LGI1 (5/8 [62.5%] vs 1/9 [11.1%]), $p = 0.0498$) but not significantly than in NMDAR (5/8 [62.5%] vs 18/60 [30.0%], $p = 0.1088$). However, antibody titers were not measured in GABAaR because no commercial CBA is available.

## 3.2 Part I-2. Clinical relevance of "GFAP pattern" on commercial IHC

Of 261 patients, 25 (9.6%) had either GFAP (n=21) or GFAP-mimicking pattern (n=4) (Figure 1). GFAP-Ab were examined in 31 patients including 6 who did not have either pattern but clinico-radiologic features reported in GFAP-positive meningoencephalomyelitis, and were identified in 21 patients (67.7%): 20 of the 21 patients (95.2%) with GFAP pattern, 1 of the 4 patients (25.0%) with GFAP-mimicking pattern, but not in any of the other 6 patients. Sensitivity and specificity of "GFAP pattern" for predicting GFAP-Ab were 95.2% (95% CI 76.2-99.9) and 90.0% (95% CI 55.5-99.8), respectively. The GFAP pattern was more clearly seen on commercial IHC than on in-house IHC (Figure 3E). In

addition to GFAP pattern, the commercial IHC revealed intense reactivity along the cerebellar white matter, which was later confirmed due to concurrent MOG antibodies (Figure 3F).

In this cohort, the GFAP-Ab-positive patients were male predominant (13 male [61.9%]), with a median age at onset of 55 years (range, 18-79 years). Their main clinical features consisted of diverse phenotypes, including meningoencephalomyelitis (n=8), meningoencephalitis (n=3, 1 with diffuse sulcus enhancement), encephalitis (n=4, 1 with diffuse white matter MRI abnormalities, 1 with concurrent EBV DNA), myelitis (n=1), ADEM-like syndrome (n=2), stiff-person spectrum disorder-mimicking syndrome (n=1), encephalopathy (n=1), or overlapping anti-NMDAR encephalitis and MOG-positive demyelinating syndrome (n=1).

In one patient, GFAP-Ab were not identified in either serum or CSF despite the presence of apparent "GFAP pattern" on commercial IHC. The patient presented with acute onset of memory and psychobehavioral alterations associated with persistent fever of unknown etiology. CSF examination revealed mild pleocytosis (< 70 white blood cells/μL), without oligoclonal band detection. A brain MRI showed only mildly increased diffusion-weighted image/fluid-attenuated inversion recovery signal in the left insular cortex and ipsilateral fimbria, without abnormal enhancement, and an EEG revealed periodic lateralized epileptiform discharges in the left cerebral hemisphere, but no NS-Ab were identified in either serum or CSF. The clinico-radiologic features were not particularly suggestive of GFAP-Ab; however, GFAP-pattern was seen on commercial IHC (Supplementary Figure 1). In order to clarify whether the filamentous immunoreactivity is consistent with GFAP, we performed double immunolabeling of rat brain IHC using the patient's antibodies and commercial GFAP monoclonal antibody (Clone GA5; Invitrogen), which revealed colocalization of reactivities, indicating that the patient's IgG recognizes GFAP (Supplementary Figure 1).

### 3.3 Part II. Immunostaining patterns of individual NS antigens

TBA revealed an immunostaining pattern highly characteristic of each NS antigen on both commercial and in-house IHC in a similar distribution (Figure 4). TBA did not reveal apparent "neuropil pattern" in NS-Ab-negative CSF (Figure 4A). The immunostaining pattern of each NS antigen was as follows:

NMDAR revealed homogenous reactivity in the DG-ML with less intense dot-like reactivity in the CB-GL (Figure 4B). The regional intensity in the DG-ML was homogenous but more intensely stained in the surroundings of the dentate granule cells compared with the middle or outer molecular layer.

Both GABAaR and GluK2 revealed intense dot-like reactivity in the CB-GL (more densely stained in GluK2 than in GABAaR), but GABAaR revealed homogenous reactivity in the DG-ML (Figure 4C) while GluK2 revealed laminar reactivity in the DG-ML with strongest reactivity along the inner molecular layer (Figure 4D, arrows).

LGI1, Caspr2, GABAbR, and AMPAR revealed intense homogenous reactivity in the CB-ML but LGI1 revealed laminar reactivity in the DG-ML with strongest reactivity along the middle layer, that is highly contrast to a pattern of GluK2 reactivity. Whereas Caspr2, GABAbR, and AMPAR revealed homogenous reactivity in the DG-ML. The dentate hilus was intensely stained in LGI1 but only mildly in Caspr2, GABAbR, and AMPAR (Figures 4E–H). The CB-GL was not apparently stained in LGI1 but mild to moderately as a reticular pattern in Caspr2 and GABAbR, and mild to moderately as a dot-like pattern in AMPAR; there was intense reactivity with cytoplasmic protein in the PC (Figure 4H, arrows) in 1 of the 3 patients with AMPAR antibodies with "neuropil pattern" but no reactivity with the PC in patients with other NS-Ab. Distinctive staining patterns were noted between NS antigens, but Caspr2 and GABAbR revealed much similar staining pattern (Figures 4, 5, and Table 1).

## 4 Discussion

This study reveals that 1) the commercial IHC is useful for screening NS-Ab, but the negative results should be interpreted cautiously because the "neuropil pattern" may be missed in up to one-thirds of the NS-Ab-positive patients particularly when antibody titers are low or due to other reasons, 2) the commercial IHC also provides an easily recognizable "GFAP pattern", and 3) this study confirmed the previous observation that individual NS antigens have antigen-specific immunostaining pattern, which can be used as a biomarker to estimate the target NS antigen.

TBA has been used to identify autoantibodies against not only classical paraneoplastic neuronal (intracellular) antigens but also NS antigens (synaptic receptors or other membrane proteins) (1, 2). However, the brain tissue processing is quite different between intracellular and cell-surface antigens (16, 19, 20). To detect NS-Ab, a tissue processing adapted to cell surface or synaptic proteins is required to preserve the native conformation of the target antigen (1). Tissue perfusion should not be performed before decapitation, and it is recommended that the non-perfused brains are fixed in 4% paraformaldehyde for 1 hour at 4°C (16), as described above. Such IHC has mainly been used at research laboratories. NS-Ab is known to produce "neuropil pattern", but individual staining pattern has not been extensively studied. Therefore, we conducted this study.

Sensitivity and specificity of the "neuropil pattern" identified on commercial IHC for predicting NS-Ab were 66.0% and 98.2%, respectively. All 3 false-positive patients had high titers of GAD65 antibodies, thus, the neuropil-like pattern seen on TBA was considered to reflect abundant GAD65 immunoreactivity in the

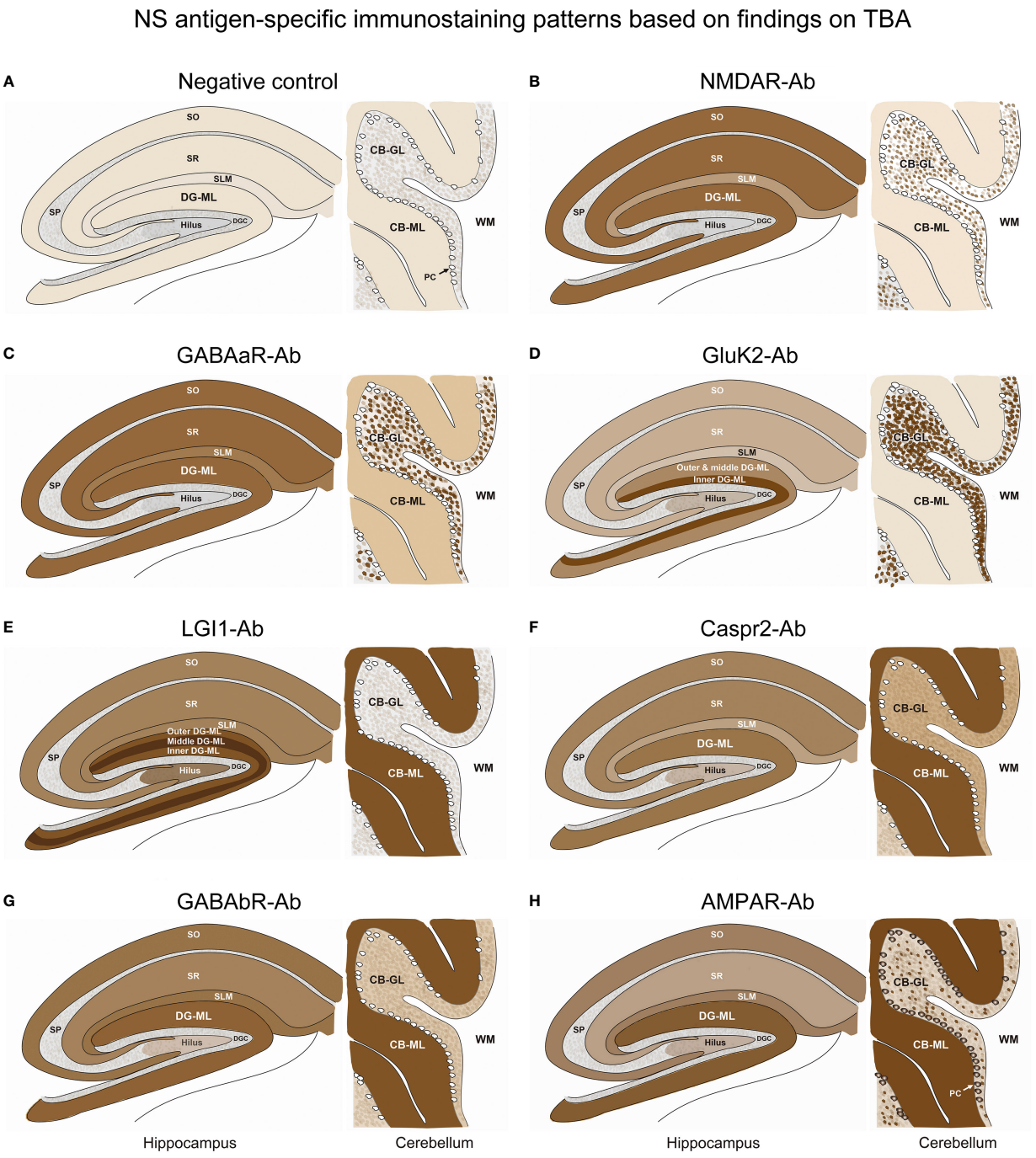


FIGURE 5
A series of illustrations are created as simple as possible to make it easy to follow individual staining pattern at the level of hippocampus and cerebellum. See Text and Figure 4. CB-GL, cerebellar granular layer; CB-ML, cerebellar molecular layer; DGC, dentate granule cells; DG-ML, dentate gyrus molecular layer; PC, Purkinje cells; SLM, stratum lacunosum moleculare; SO, stratum oriens; SP, stratum pyramidale; SR, stratum radiatum; WM, white matter.

axon terminals (21). GAD-Ab are easily examined with ELISA or EIA and show a synaptic pattern characteristic of GAD65. Therefore, such mild reactivity mimicking "neuropil pattern" is less likely to cause confusion in the diagnosis of AE or related disorder. However, relatively high false-negative rate (34.0%) cannot be ignored in clinical practice.

To evaluate factors involved in the false-negative results, we added in-house IHC. In at least 3 false-negative patients, the

10.3389/fimmu.2022.1066830

TABLE 1 Immunostaining pattern highly characteristic of major neuronal surface antigens.

| NS antigen | DG-ML | Dentate hilus | CB-ML | CB-GL | CB-WM | Purkinje cells |
|---|---|---|---|---|---|---|
| NMDAR | Homogenous | None | None | Dot-like, mild | None | None |
| GABAaR | Homogenous | None to mild | Mild | Dot-like, moderate to intense | None | None |
| GluK2 | Laminar: inner layer > middle or outer layer | Mild | Mild | Dot-like, intense | None | None |
| LGI1 | Laminar: middle layer > inner or outer layer | Intense | Intense | Reticular, very mild | None | None |
| Caspr2 | Homogenous | Mild | Intense | Reticular, mild to moderate | None | None |
| GABAbR | Homogenous | Mild | Intense | Reticular, mild to moderate | None | None |
| AMPAR | Homogenous | Mild | Intense | Dot-like, mild to moderate | None | Cytoplasmic but not always |

CB-GL, cerebellar granular layer; CB-ML, cerebellar molecular layer; CB-WM, cerebellar white matter; DG-ML, dentate gyrus molecular layer.

"neuropil pattern" was visually identified on our in-house IHC, suggesting that the "neuropil pattern" may be more clearly shown in our in-house IHC adapted to NS antigen compared with the commercial IHC, of which tissue processing is not available due to industrial secrets, thus we do not know whether the commercial IHC is adapted to NS antigen or not. Further study will be required to determine which one is better in terms of detection of "neuropil pattern".

To address the issue whether antibody titers influence detection rate of "neuropil pattern", we measured antibody titers in 60 patients with anti-NMDAR encephalitis because NMDAR consisted of 54.5% of NS antigens identified in the false-negative patients. As expected, low antibody titers (< 1:32) were more frequently found in false-negative patients compared with "neuropil pattern"-positive patients, suggesting that low antibody titers may be one of the major causes of the false-negative results at least in NMDAR-Ab. Thus, it should be kept in mind that antibody titers may influence the detection rate of the "neuropil pattern" on commercial IHC.

It is also important to note that the detection rate of "neuropil pattern" was different among NS antigens. Although we did not measure antibody titers in NS antigens other than NMDAR, the detection rate may be lower in GABAaR than in other NS antigens. At this point, the cause of higher false-negative results in GABAaR compared with other NS antigen remains speculative. We did not measure antibody titers; thus, we cannot exclude a potential effect of low antibody titers on the higher false-negative results; however, we also concern about a technical difficulty during tissue preparation; we have sometimes faced a difficulty in revealing "neuropil pattern" in GABAaR-Ab-positive samples, even with in-house IHC adapted to NS antigen. It seems to be more difficult to preserve the native conformation of the epitope in GABAaR compared with other NS antigens (such as NMDAR or LGI1). Further studies are required to conclude whether the detection rate is different among NS antigens.

In Part I, we also evaluated a predictive value of "GFAP pattern". When GFAP-Ab are positive, IHC revealed reactivity along the radial glia of Bergmann in the CB-ML and astrocytes in the CB-GL. Although the number of patients examined with CBA is quite small, most of the patients with a pattern of GFAP reactivity were confirmed to have GFAP-Ab in their CSF. Sensitivity and specificity of the "GFAP pattern" were 95.2% and 90.0%, respectively, and a cactus thorn-like or filamentous staining is easily recognizable on commercial IHC. Although "GFAP pattern" highly suggests the presence of GFAP-Ab, IgG GFAP-Ab were not identified with CBA in either serum or CSF in one of the 21 "GFAP pattern"-positive patients.

The reason why GFAP-Ab are not identified with CBA despite the presence of "GFAP pattern" is unclear in the patient, but the discrepancy between commercial IHC and CBA may be explained by difference of GFAP isoform that the patient's IgG antibodies recognize. GFAP is an intermediate filament protein expressed in astrocytes, and has 10 different GFAP isoforms. Among those, GFAP α and δ/ε are the main isoforms (22). After the discovery of GFAP-Ab in 2016 (18), GFAP-α isoform-transfected CBA has been used as a standard test for antibodies against GFAP (23). Therefore, we performed double immunolabeling of rat brain IHC using the patient's antibodies and commercial GFAP monoclonal antibody, which revealed colocalization of reactivities (Supplementary Figure 1). A previous study (24) reported that some of the GFAP-Ab-positive patients may be positive for antibodies against only GFAP δ/ε isoform; therefore, the false-positive results may be due to IgG autoantibodies against GFAP isoform other than GFAP α isoform. Immunoreactivity discrepancies observed between recombinant GFAP proteins and rodent brain tissue has also been reported, and possible explanations have been

discussed, including posttranslational modification of GFAP-α antigenicity or obscuring of a dominant GFAP-α epitope in tissue by 3-dimensional *in situ* interaction between GFAP isoforms and other intermediate filament proteins (18).

Although GFAP-Ab were identified in 21 of 31 examined patients, GFAP is an intracellular autoantigen, thus the IgG GFAP-Ab is unlikely pathogenic (1). GFAP-positive meningoencephalitis is currently presumed to be T-cell mediated (25), and the antibodies can be seen without association of distinct clinical-radiological features (3), but the presence of IgG GFAP-Ab provides a clue supporting immune-mediated disorder as a biomarker of the disease.

In Part II, we characterized NS-antigen-specific immunostaining patterns, and created a series of illustrations by simplifying their staining patterns to make it easy for physicians or observers to recognize antigen-specific pattern (Figure 5). A pattern recognition is important in estimation of NS antigen based on the IHC. Based on the results, we grossly divided the staining pattern into 2 groups; one is a pattern of CB-GL predominant reactivity characterized by a dot-like staining in the CB-GL and the other is a pattern of CB-ML predominant reactivity characterized by homogenous intense staining in the CB-ML as a common characteristic feature. The NMDAR, GABAaR, and GluK2 are included in the former group, while the LGI1, Caspr2, GABAbR, and AMPAR are in the latter one.

The remarkable finding is that this study revealed an antigen-specific laminar reactivity in the DG-ML; strongest reactivity was seen along the middle layer in LGI1 while along the inner layer in GluK2. These patterns are easily recognizable on commercial IHC than on in-house IHC and can be used as a diagnostic marker of NS antigen.

LGI1, Caspr2, GABAbR, and AMPAR show similar intense reactivity in the CB-ML, but there are some different reactivities in the other regions. The dentate hilus is intensely stained in LGI1, but only mildly in Caspr2, GABAaR, GluK2, and GABAbR, or not in NMDAR. Cytoplasmic antigen in the PC may be stained in AMPAR, but not in the other 6 NS antigens. Cytoplasmic staining of the PC may be non-specific and may not be always seen even in AMPAR; however, the cytoplasmic staining of PC has been described (7), and AMPAR subunits are shown to be expressed by the PC (26). Thus, the presence of apparent PC staining sparing the nucleus, with intense reactivity in the CB-ML and sparse but dot-like staining in the CB-GL may suggest AMPAR.

Intensity of the immunoreactivity is more likely to reflect high antibody titers as well as preservation of the native conformation of the epitope, while its distribution is more likely to reflect the location of the target NS antigen expressed in the rodent brain tissue. Although exact distribution of the individual NS antigens has not been well characterized yet in a rodent brain, the intense reactivity along the inner layer of the DG-ML is consistent with expression of GluK2 (27). The dot-like immunoreactivity in the CB-GL seen in NMDAR, GABAaR, GluK2, and AMPAR is presumed due to the reactivity with corresponding NS antigen in the cerebellar glomeruli, which are an intertwined cluster of nerve fibers surrounded by glia where mossy fibers synapse with granule cell axons, where NMDAR, GABAaR, GluK2 and AMPAR are all expressed on cell surface membrane (28–31). Clarification of the distribution of each NS antigen may help identification of novel antibodies against yet unknown antigen.

This study has limitations; no detailed information is available about the brain tissue processing in commercial IHC; antibody titer was determined for NMDAR antibodies with commercial fixed CBA but not with live CBA, and not determined for other NS antigens; the number of patients examined for GFAP-Ab is small; the number of patients examined for immunostaining pattern is also small (1 or 3) in each group of the NS antigen other than NMDAR; immunostaining pattern examined with serum is not taken into account in the analysis for immunostaining pattern; the predictive value of the commercial IHC or in-house IHC is not assessed in a prospective manner; and immunostaining pattern was assessed for preselected 7 major NS antigens, but not for other NS antigens identified to date.

Despite these limitations, this study demonstrates that both in-house and commercial IHC are clinically useful not only for screening NS- and GFAP-Ab, but also for estimating NS antigen. However, the results of the commercial IHC should be interpreted with caution while taking these limitations into consideration when predicting the presence of NS-Ab or estimating NS antigen. The strategy of the diagnosis of AE should be based on both clinical information and immunostaining pattern on TBA. The immunostaining pattern highly characteristic of NS antigens can be used as a biomarker of AE.

## Data availability statement

The original contributions presented in the study are included in article/Supplementary Material. Further inquiries can be directed to the corresponding author.

## Ethics statement

The studies involving human participants were reviewed and approved by Institutional Review Boards of Kitasato University (B20-280). Written informed consent to participate in this study was provided by the participants' legal guardian/next of kin. The animal study was reviewed and approved by the Animal Experimentation and Ethics Committee of the Kitasato University School of Medicine (2022-031).

## Author contributions

NN and NK contributed to the drafting of the manuscript, the acquisition of major data of antibody assay using immunohistochemistry of the rodent brain, and the preparation of the figures. TM, MI, MNag, MNak, JK, EK, and KN contributed to the acquisition of clinical data. TI contributed to analysis of data, the acquisition of clinical data, the drafting of a significant portion of manuscript, the preparation of the figures including illustrations. All translations into English were done by the authors. All authors contributed to the article and approved the submitted version.

## Funding

This study was supported in part by a research support from Astellas Pharma Inc (TI) to measure autoantibodies against neuronal or glial surface antigens.

## Acknowledgments

The authors particularly thank Professor Josep Dalmau in Institut d´Investigació Biomèdica August Pi i Sunyer (IDIBAPS), Barcelona, Spain for examining antibodies against extensive neuronal surface and synaptic proteins, glial surface or GFAP at the laboratory of Josep Dalmau. They also thank Dr. Atsuko Yanagida for contribution to the development of in-house immunohistochemistry at Kitasato University, and they are grateful to all participants and physicians for their contribution to this study.

## Conflict of interest

KN received research supports from Daiichi Sankyo Co., Ltd., Dainippon Sumitomo Pharma Co., Ltd., and Eisai Co., Ltd. TI received a research support from Astellas Pharma Inc.

The remaining authors declare that the research was conducted in the absence of any commercial or financial relationships that could be construed as a potential conflict of interest.

## Publisher's note



## Supplementary material

The Supplementary Material for this article can be found online at: https://www.frontiersin.org/articles/10.3389/fimmu.2022.1066830/full#supplementary-material

## References

1. Dalmau J, Graus F. Autoimmune encephalitis and related disorders of the nervous system. In: *Autoimmune encephalitis and related disorders of the nervous system (pp. I-ii)*. (Cambridge: Cambridge University Press) (2022).

2. Graus F, Titulaer MJ, Balu R, Benseler S, Bien CG, Cellucci T, et al. A clinical approach to diagnosis of autoimmune encephalitis. *Lancet Neurol* (2016) 15 (4):391–404. doi: 10.1016/S1474-4422(15)00401-9

3. Martinez-Hernandez E, Guasp M, García-Serra A, Maudes E, Ariño H, Sepulveda M, et al. Clinical significance of anti-NMDAR concurrent with glial or neuronal surface antibodies. *Neurology* (2020) 94(22):e2302–e10. doi: 10.1212/WNL.0000000000009239

4. Dalmau J. NMDA receptor encephalitis and other antibody-mediated disorders of the synapse: The 2016 cotzias lecture. *Neurology* (2016) 87 (23):2471–82. doi: 10.1212/WNL.0000000000003414

5. Ruiz-García R, Muñoz-Sánchez G, Naranjo L, Guasp M, Sabater L, Saiz A, et al. Limitations of a commercial assay as diagnostic test of autoimmune encephalitis. *Front Immunol* (2021) 12:691536. doi: 10.3389/fimmu.2021.691536

6. Dalmau J, Tüzün E, Wu HY, Masjuan J, Rossi JE, Voloschin A, et al. Paraneoplastic anti-N-methyl-D-aspartate receptor encephalitis associated with ovarian teratoma. *Ann Neurol* (2007) 61(1):25–36. doi: 10.1002/ana.21050

7. Lai M, Hughes EG, Peng X, Zhou L, Gleichman AJ, Shu H, et al. AMPA receptor antibodies in limbic encephalitis alter synaptic receptor location. *Ann Neurol* (2009) 65(4):424–34. doi: 10.1002/ana.21589

8. Lancaster E, Lai M, Peng X, Hughes E, Constantinescu R, Raizer J, et al. Antibodies to the GABA(B) receptor in limbic encephalitis with seizures: Case series and characterisation of the antigen. *Lancet Neurol* (2010) 9(1):67–76. doi: 10.1016/S1474-4422(09)70324-2

9. Lai M, Huijbers MG, Lancaster E, Graus F, Bataller L, Balice-Gordon R, et al. Investigation of LGI1 as the antigen in limbic encephalitis previously attributed to potassium channels: A case series. *Lancet Neurol* (2010) 9(8):776–85. doi: 10.1016/S1474-4422(10)70137-X

10. Lancaster E, Huijbers MG, Bar V, Boronat A, Wong A, Martinez-Hernandez E, et al. Investigations of caspr2, an autoantigen of encephalitis and neuromyotonia. *Ann Neurol* (2011) 69(2):303–11. doi: 10.1002/ana.22297

11. Boronat A, Gelfand JM, Gresa-Arribas N, Jeong HY, Walsh M, Roberts K, et al. Encephalitis and antibodies to dipeptidyl-peptidase-like protein-6, a subunit of Kv4.2 potassium channels. *Ann Neurol* (2013) 73(1):120–8. doi: 10.1002/ana.23756

12. Petit-Pedrol M, Armangue T, Peng X, Bataller L, Cellucci T, Davis R, et al. Encephalitis with refractory seizures, status epilepticus, and antibodies to the GABAA receptor: A case series, characterisation of the antigen, and analysis of the effects of antibodies. *Lancet Neurol* (2014) 13(3):276–86. doi: 10.1016/S1474-4422(13)70299-0

13. Martinez-Hernandez E, Ariño H, McKeon A, Iizuka T, Titulaer MJ, Simabukuro MM, et al. Clinical and immunologic investigations in patients with stiff-person spectrum disorder. *JAMA Neurol* (2016) 73(6):714–20. doi: 10.1001/jamaneurol.2016.0133

14. Landa J, Guasp M, Míguez-Cabello F, Guimarães J, Mishima T, Oda F, et al. Encephalitis with autoantibodies against the glutamate kainate receptors GluK2. *Ann Neurol* (2021) 90(1):101–17. doi: 10.1002/ana.26098

15. Titulaer MJ, Höftberger R, Iizuka T, Leypoldt F, McCracken L, Cellucci T, et al. Overlapping demyelinating syndromes and anti–N-methyl-D-aspartate receptor encephalitis. *Ann Neurol* (2014) 75(3):411–28. doi: 10.1002/ana.24117

16. Gresa-Arribas N, Titulaer MJ, Torrents A, Aguilar E, McCracken L, Leypoldt F, et al. Antibody titres at diagnosis and during follow-up of anti-NMDA receptor encephalitis: A retrospective study. *Lancet Neurol* (2014) 13 (2):167–77. doi: 10.1016/S1474-4422(13)70282-5

17. Suga H, Yanagida A, Kanazawa N, Ohara H, Kitagawa T, Hayashi M, et al. Status epilepticus suspected autoimmune: Neuronal surface antibodies and main clinical features. *Epilepsia* (2021) 62(11):2719–31. doi: 10.1111/epi.17055

18. Fang B, McKeon A, Hinson SR, Kryzer TJ, Pittock SJ, Aksamit AJ, et al. Autoimmune glial fibrillary acidic protein astrocytopathy: A novel meningoencephalomyelitis. *JAMA Neurol* (2016) 73(11):1297–307. doi: 10.1001/jamaneurol.2016.2549

19. Vitaliani R, Mason W, Ances B, Zwerdling T, Jiang Z, Dalmau J. Paraneoplastic encephalitis, psychiatric symptoms, and hypoventilation in ovarian teratoma. *Ann Neurol* (2005) 58(4):594–604. doi: 10.1002/ana.20614

20. Ances BM, Vitaliani R, Taylor RA, Liebeskind DS, Voloschin A, Houghton DJ, et al. Treatment-responsive limbic encephalitis identified by neuropil antibodies: MRI and PET correlates. *Brain* (2005) 128(Pt 8):1764–77. doi: 10.1093/brain/awh526

21. Esclapez M, Tillakaratne NJ, Kaufman DL, Tobin AJ, Houser CR. Comparative localization of two forms of glutamic acid decarboxylase and their mRNAs in rat brain supports the concept of functional differences between the forms. *J Neurosci* (1994) 14(3 Pt 2):1834–55. doi: 10.1523/JNEUROSCI.14-03-01834.1994

22. Moeton M, Stassen OM, Sluijs JA, van der Meer VW, Kluivers LJ, van Hoorn H, et al. GFAP isoforms control intermediate filament network dynamics, cell morphology, and focal adhesions. *Cell Mol Life Sci* (2016) 73(21):4101–20. doi: 10.1007/s00018-016-2239-5

23. Shan F, Long Y, Qiu W. Autoimmune glial fibrillary acidic protein astrocytopathy: A review of the literature. *Front Immunol* (2018) 9:2802. doi: 10.3389/fimmu.2018.02802

24. Long Y, Liang J, Xu H, Huang Q, Yang J, Gao C, et al. Autoimmune glial fibrillary acidic protein astrocytopathy in Chinese patients: A retrospective study. *Eur J Neurol* (2018) 25(3):477–83. doi: 10.1111/ene.13531

25. Yamakawa M, Hogan KO, Leever J, Jassam YN. Autopsy case of meningoencephalomyelitis associated with glial fibrillary acidic protein antibody. *Neurol Neuroimmunol Neuroinflamm* (2021) 8(6):e1081. doi: 10.1212/NXI.0000000000001081

26. Lambolez B, Audinat E, Bochet P, Crépel F, Rossier J. AMPA receptor subunits expressed by single purkinje cells. *Neuron* (1992) 9(2):247–58. doi: 10.1016/0896-6273(92)90164-9

27. Iida I, Konno K, Natsume R, Abe M, Watanabe M, Sakimura K, et al. A comparative analysis of kainate receptor GluK2 and GluK5 knockout mice in a pure genetic background. *Behav Brain Res* (2021) 405:113194. doi: 10.1016/j.bbr.2021.113194

28. Yamada K, Fukaya M, Shimizu H, Sakimura K, Watanabe M. NMDA receptor subunits GluRepsilon1, GluRepsilon3 and GluRzeta1 are enriched at the mossy fibre-granule cell synapse in the adult mouse cerebellum. *Eur J Neurosci* (2001) 13(11):2025–36. doi: 10.1046/j.0953-816x.2001.01580.x

29. Cupello A, Di Braccio M, Gatta E, Grossi G, Nikas P, Pellistri F, et al. GABAA receptors of cerebellar granule cells in culture: Interaction with benzodiazepines. *Neurochem Res* (2013) 38:2453–62. doi: 10.1007/s11064-013-1171-4

30. Straub C, Noam Y, Nomura T, Yamasaki M, Yan D, Fernandes HB, et al. Distinct subunit domains govern synaptic stability and specificity of the kainate receptor. *Cell Rep* (2016) 16(2):531–44. doi: 10.1016/j.celrep.2016.05.093

31. Bats C, Farrant MCull-Candy SG. A role of TARPs in the expression and plasticity of calcium-permeable AMPARs: Evidence from cerebellar neurons and glia. *Neuropharmacology* (2013) 74:76–85. doi: 10.1016/j.neuropharm.2013.03.037

frontiers | Frontiers in Immunology

TYPE Brief Research Report
PUBLISHED 19 January 2023
DOI 10.3389/fimmu.2023.1101087



OPEN ACCESS

EDITED BY
Honghao Wang,
Guangzhou First People's Hospital, China

REVIEWED BY
Jinming Han,
Capital Medical University, China
Zsolt Illes,
University of Southern Denmark, Denmark

*CORRESPONDENCE
Angela M. Kaindl
angela.kaindl@charite.de

†These authors have contributed equally to this work and share first authorship

‡These authors have contributed equally to this work and share last authorship

SPECIALTY SECTION
This article was submitted to Multiple Sclerosis and Neuroimmunology, a section of the journal Frontiers in Immunology

RECEIVED 17 November 2022
ACCEPTED 04 January 2023
PUBLISHED 19 January 2023

CITATION
Bünger I, Makridis KL, Kreye J, Nikolaus M, Sedlin E, Ullrich T, Hoffmann C, Tromm JV, Rasmussen HF, Milovanovic D, Höltje M, Prüss H and Kaindl AM (2023) Maternal synapsin autoantibodies are associated with neurodevelopmental delay. *Front. Immunol.* 14:1101087. doi: 10.3389/fimmu.2023.1101087



# Maternal synapsin autoantibodies are associated with neurodevelopmental delay

Isabel Bünger[1,2†], Konstantin L. Makridis[3,4,5,6†], Jakob Kreye[1,2,3,4,5,7], Marc Nikolaus[3,4,5,7], Eva Sedlin[3,4], Tim Ullrich[3,4], Christian Hoffmann[2], Johannes Vincent Tromm[2], Helle Foverskov Rasmussen[1,2], Dragomir Milovanovic[2], Markus Höltje[8], Harald Prüss[1,2‡] and Angela M. Kaindl[3,4,5,6*‡]

[1]Charité – Universitätsmedizin Berlin, Department of Neurology and Experimental Neurology, Berlin, Germany, [2]German Center for Neurodegenerative Diseases (DZNE) Berlin, Berlin, Germany, [3]Charité – Universitätsmedizin Berlin, Department of Pediatric Neurology, Berlin, Germany, [4]Charité – Universitätsmedizin Berlin, Center for Chronically Sick Children, Berlin, Germany, [5]Charité – Universitätsmedizin Berlin, German Epilepsy Center for Children and Adolescents, Berlin, Germany, [6]Charité – Universitätsmedizin Berlin, Institute of Cell- and Neurobiology, Berlin, Germany, [7]Berlin Institute of Health (BIH), Berlin, Germany, [8]Charité - Universitätsmedizin Berlin, Institute of Integrative Neuroanatomy, Berlin, Germany

Maternal autoantibodies can be transmitted diaplacentally, with potentially deleterious effects on neurodevelopment. Synapsin 1 (SYN1) is a neuronal protein that is important for synaptic communication and neuronal plasticity. While monoallelic loss of function (LoF) variants in the *SYN1* gene result in X-linked intellectual disability (ID), learning disabilities, epilepsy, behavioral problems, and macrocephaly, the effect of SYN1 autoantibodies on neurodevelopment remains unclear. We recruited a clinical cohort of 208 mothers and their children with neurologic abnormalities and analyzed the role of maternal SYN1 autoantibodies. We identified seropositivity in 9.6% of mothers, and seropositivity was associated with an increased risk for ID and behavioral problems. Furthermore, children more frequently had epilepsy, macrocephaly, and developmental delay, in line with the SYN1 LoF phenotype. Whether SYN1 autoantibodies have a direct pathogenic effect on neurodevelopment or serve as biomarkers requires functional experiments.

KEYWORDS

**synapsin 1, antineuronal autoantibodies, transplacental transfer, maternofetal autoimmunity, developmental delay, epilepsy, behavioral problems**

## Introduction

Synapsin 1 (SYN1) is a neuronal phosphoprotein encoded by the *SYN1* gene and plays an important role in neurotransmitter release and neuronal plasticity (1, 2). Patients with loss of function (LoF) variants in the *SYN1* gene have been associated with X-linked phenotypes consisting of epilepsy, learning difficulties, intellectual disability (ID), macrocephaly,

behavioral problems, and autism-spectrum disorders (ASD) (MIM#300491, MIM#300115) (3–5).

In recent years, antineuronal autoantibodies have been increasingly described to cause target-specific autoimmune neurologic disorders, in some cases matching the clinical phenotypes of patient carrying genetic variants of these targets. For example, both patients with variants in $GABA_A$ receptor subunit genes and those with $GABA_A$ receptor autoantibodies display epilepsy as a common phenotype (6–8). Autoantibodies are usually regarded as those generated within an individual; however, they can also be transferred diaplacentally from mother to child (9). As the blood brain barrier is not yet fully matured, these autoantibodies of maternal origin can target the developing brain and thereby potentially affect neurodevelopment (9). There is increasing evidence that maternal immune activation through autoantibodies can influence the occurrence of neurodevelopmental disorders, such as ASD (9). In addition, multiple murine models have demonstrated the direct deleterious effect of various antineuronal autoantibodies in offspring through gestational transfer (10–13).

In previous studies, autoantibodies against SYN1 have been identified in patients with neurologic and psychiatric disorders (14, 15). We have recently shown that SYN1 autoantibodies in pregnant women are associated with abnormalities of fetal development including intrauterine growth retardation (16). However, their role in mothers of children with defined neurologic disorders has not been studied so far. Thus, we assessed the prevalence of SYN1 autoantibodies in mothers of a cohort of 208 pediatric patients with neurological disorders.

# Material and methods

## Cell-based assay

Synapsin 1b (SYN1b) cell-based assay (CBA) was performed using human embryonic kidney (HEK293T) cells which were transfected with human SYN1b. Methanol-fixed cells were then incubated with sera diluted 1:300. IgG AF488-antibody (Dianova, #109-545-003), commercial rabbit SYN1/SYN2 antibody (Synaptic Systems, #106002) and anti-rabbit IgG AF594-antibody (Jackson IR, #111-585-003) were used to detect IgG binding. Two independent investigators scored the CBA using the following semi-quantitative score: 0, no binding; 1, unspecific signal ('background'); 2, positive (intensive binding). Sera were tested on control cells overexpressing the NR1 subunit of the N-methyl-D-aspartate receptor (NMDAR), contactin-associated protein 2 (Caspr2), and SYN1 CBA-positive sera also on untransfected control HEK293T cells to exclude non-specific binding (14, 16).

## Enzyme-linked immunosorbent assay

For the ELISA, 200 ng of recombinant rat Syn1-His-EGFP (17) was diluted in PBS and incubated overnight at 4°C in 96-well high-binding plates. Serum (1:200 diluted in PBS containing 1% BSA, 0.05% Tween) was incubated for one hour at room temperature, on which HRP-coupled anti-human IgG antibody (Dianova, #109-035-003) was added for an additional hour. Ultra TMB substrate solution was added, and reaction terminated after one minute with $H_2SO_4$. Absorbance at 450 nm was measured and corrected with controls (mean of wells without serum and reference absorbance at 630 nm).

## Western blot

SDS-Page and Western blotting were performed as described using cortices from *Syn1/2/3* triple knockout (TKO) mice and wild type (WT) mice (14). Sera of CBA with scores of 1-2 were diluted to 1:200 and used to incubate membranes. A rabbit polyclonal SYN1/2 antibody (Synaptic Systems, #106002) was used as positive control and a mouse monoclonal antibody against glyceraldehyde-3-phosphate dehydrogenase (GAPDH, Merck Millipore, #MAB374) served as loading control.

## Clinical data and statistical analysis

We studied a cohort of 208 mothers of pediatric patients with neurological disorders treated at the Center for Chronically Sick Children, Charité – Universitätsmedizin Berlin, Germany. Healthy mothers of children with unclear developmental disabilities were approached regarding the study by a study team physician at their child's regular treatment appointment. Due to the exploratory approach, no exclusion criteria were specified. Maternal sera were prospectively collected and analyzed. The finding of SYN1 autoantibodies did not influence the treatment of the patients. Patient data were collected retrospectively and blinded to the maternal antibody levels using a standardized data collection sheet. Statistical analysis was performed using R (RStudio version 4.2.1) and the packages *crosstable, ggplot2, UpSetR*, and *psych*. Descriptive statistics were performed to calculate percentages and frequencies. Differences in categorical variables are reported as odds ratio and 95% confidence interval. P values were calculated using the Chi-square test and Fisher's Exact Probability Test, as applicable. Test results with $p<0.05$ were considered statistically significant. The study was approved by the local ethics committee (approval no. #EA2/220/20).

# Results

We screened sera for SYN1 autoantibodies in 208 mothers to assess the relationship with neurodevelopment in children. Due to the explorative approach, no exclusion criteria were set. Mothers gave birth at an average age of 30.93 ± 5.81 years. Children (male n=134, 64.1%) were 6.6 ± 4.14 years old at testing. Developmental delay in the domains speech (n=158, 75.7%) and motor skills (n=153, 73.1%) were the most common findings. Furthermore, 135 patients had intellectual disability (64.4%), and 83 patients had epilepsy (39.9%) (Figure 1). Epilepsy (p=0.049), ASD (p=0.001) and behavioral problems (p=0.008) were more common in male, while microcephaly was more common in female patients (p=0.001).

In a first step, the patients' mothers were screened using the previously described CBA (14). We used a visual scoring system for antibody binding in the CBA, and scores of 2 (intensive binding) were

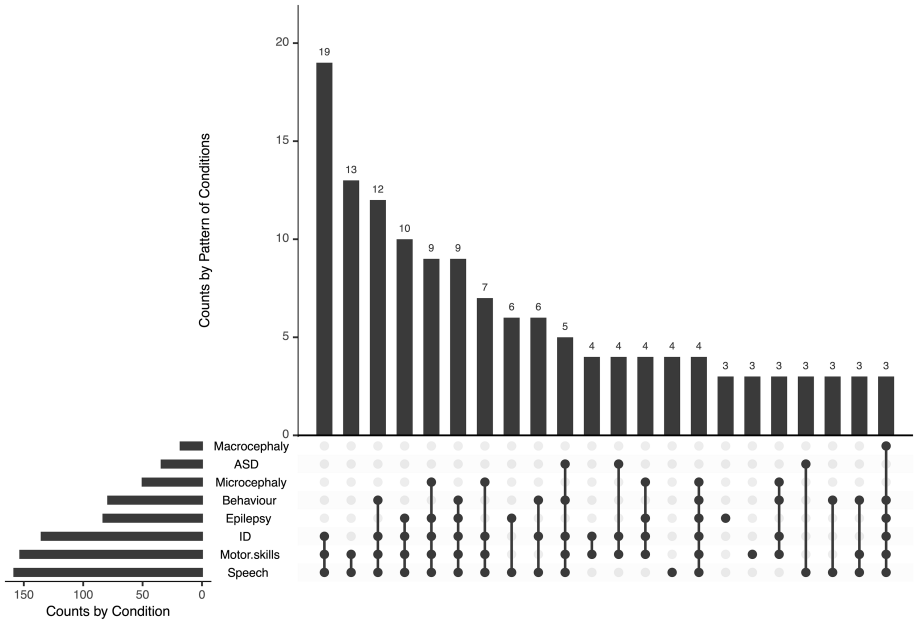


FIGURE 1
Phenotype of children of mothers tested for SYN1 autoantibodies. Developmental delay in the domains speech and motor skills were the most common findings, often associated with intellectual disability and epilepsy. ID, intellectual disability; ASD, autism-spectrum disorder.

considered as positive (Figure 2A). Positive binding was identified in 20 mothers (9.6%). In 30 mothers, unspecific binding was detected while all others (n=158) showed no binding (Figure 2B). We further analyzed the sera of mothers with a SYN1 ELISA. Here, we found only a weak correlation between the CBA and ELISA results (r=0.29, Figure 2C). Possibly, these differing results can be explained by the binding of SYN1 autoantibodies to conformational epitopes that are not detected by ELISA. Therefore, we performed Western blots using the sera and cortex homogenates of wild-type and *SynI/II/III* triple knockout mice. We detected IgG binding to wild-type mouse brain homogenates in four of the 20 CBA-positive sera (Figure 2D). The other sera did not show immunoreactive bands at the expected molecular weight. These results point towards SYN1 IgG autoantibodies binding to linear SYN1 epitopes in only a small group, whereas autoantibodies against conformational synapsin epitopes predominate.

We further analyzed children of mothers with a positive CBA (Table 1). Most commonly the children had ID (n=18, 90%), speech delay (n=17, 85%), motor delay (n=17, 85%), and epilepsy (n=12, 60%). Seven patients had a developmental and epileptic encephalopathy (DEE). Cranial MRI was performed in 15 patients, with abnormalities detected in eight patients (53.3%, Table 1). Genetic testing was carried out in 13 patients, with variants (n=7) and microdeletions (n=1) identified in eight patients (61.5%). Of these seven variants, one was classified as pathogenic (14.3%), three as probably pathogenic (42.9%), and three as variants of unclear significance (42.9%). Identified variants (gene, cDNA, ACMG classification and NM number) are listed in Table 1 for each patient. The four patients with IgG binding to wild-type mouse brain, showed no striking phenotypic differences to patients without binding (Table 1).

We next analyzed the clinical data based on the results of the CBA. While there was no association between CBA and age of mothers, age at birth or children's age, we found an increased risk for specific phenotypes in patients of mothers with positive CBA. A positive CBA was a significant risk factor in their children for the presence of ID (OR: 5.46 [95% CI: 1.52 - 35.01], p = .0134) and behavioral problems (2.71 [1.07 - 7.23], p = .0328). Furthermore, patients showed a tendency for the presence of macrocephaly (3.11 [0.81 - 9.92], p = .0785), epilepsy (2.47 [0.98 - 6.59], p = .0536), ASD (1.32 [0.36 - 3.89], p = .7493), microcephaly (1.40 [0.47 - 3.72], p = .5882), and a developmental delay in the domains speech (1.89 [0.60 - 8.34], p = .4167) and motor skills (2.17 [0.69 - 9.55], p = .2223) (Figures 3A, B).

## Discussion

In this study, we recruited a clinical cohort of 208 mothers and their children and analyzed the prevalence of maternal SYN1 autoantibodies and their association with developmental phenotypes. SYN1 IgG autoantibodies were detected through CBA in 9.6% of mothers with neurologically sick children. Most of the SYN1 CBA positive cases were negative on Western blots under denaturing conditions, suggesting a conformational dependency of their target binding, as similarly observed in other human antineuronal autoantibodies (18). In a study by Höltje et al. that analyzed SYN1 autoantibodies in a cohort of patients with various psychiatric and neurological disorders, binding was detected in immunoblots in about half of all patients (14). It is unclear whether in less denaturing conditions more SYN1 CBA positive cases would be positive. As in this study, we recently reported IgG binding in immunoblots of 263 pregnant women screened for synapsin I

TABLE 1 Phenotype of patients with positive maternal synapsin I (SYN1) autoantibodies.

| no. | sex | age at test (years) | ID | cMRI | Epilepsy; Seizures | Gene name | cDNA position | ACMG | NM number | OMIM | Speech | Motor skills | ASD | Behavior | MIC | MAC |
|---|---|---|---|---|---|---|---|---|---|---|---|---|---|---|---|---|
| 2 | m | 7.84 | + | CM | DEE; focal-onset atonic seizures | *AIFM1* | c.1465G>A | III | 004208.3 | 300169 | + | + | – | + | – | + |
| 7 | m | 2.47 | + | HC | DEE; generalized tonic-clonic seizures | 1,2,3 | | | | | + | + | – | + | – | + |
| 22 | m | 4.24 | + | n.p. | – | 1,2 | | | | | + | + | + | + | – | – |
| 26 | m | 0.72 | + | PCH | DEE; epileptic spasms | n.p. | | | | | + | + | – | + | + | – |
| 41 | m | 1.02 | – | peritrigonal localized dysmyelination | – | *PTEN* | c.441A>T | IV | 000314 | 601728 | + | + | – | – | – | + |
| 42 | f | 0.34 | + | lissencephaly | DEE; focal onset clonic seizures without awareness | microdel. 17p13.3 | | | | 247200, MDLS | + | + | – | – | – | – |
| 46 | m | 1.26 | + | delayed myelination | DEE; epileptic spasms | *1,2,3* | | | | 617057 | + | + | + | – | + | – |
| 60 | m | 4.59 | + | NAD | focal onset seizures without awareness | n.p. | | | | | + | + | – | + | – | – |
| 71 | f | 13.77 | + | NAD | generalized tonic-clonic seizures | 1,2 | | | | | + | – | – | + | – | – |
| 72 | m | 10.07 | + | NAD | DEE; focal onset seizures without awareness | n.p. | | | | | + | + | – | + | + | – |
| 86 | m | 5.06 | + | NAD | – | *DPYD* | c.623G>T | III | 000110 | 612779 | + | + | + | + | – | – |
| 94 | m | 3.92 | + | NAD | – | n.p. | | | | | – | + | + | – | – | – |
| 106 | f | 12.28 | + | n.p. | – | *ANO5* | c.172C>T | IV | 213599.2 | 608662 | + | + | – | + | – | + |
| 146 | f | 15.68 | + | infra- and supratentorial atrophy | DEE; focal onset myoclonic seizures without awareness | *SCN1A* | c.3887T>C | III | 001165963 | 182389, DS | + | + | – | – | + | – |
| 152 | m | 5.06 | + | n.p. | – | *DDB1* | c.637G>A | IV | 001923 | 600045 | + | + | – | – | – | – |
| 158 | m | 4.06 | + | n.p. | – | n.p. | | | | | + | + | – | + | – | – |
| 159 | f | 3.97 | + | SBH | focal onset myoclonic seizures without awareness | *DCX* | c.814C'T | V | 000555 | 300121 | + | + | – | – | + | – |
| 161 | m | 4.62 | + | n.p. | – | 1 | | | | | + | + | – | + | – | – |
| 168 | m | 16.62 | + | NAD | generalized tonic-clonic seizures | n.p. | | | | | – | – | – | + | + | – |
| 208 | m | 6.94 | – | NAD | epilepsy of unknow cause with tonic clonic seizures | n.p. | | | | | – | – | – | – | – | – |

ASD, autism-spectrum disorder; CM, Chiari malformation; DEE, Developmental and epileptic encephalopathy; DS, Dravet syndrome; HC, Hydrocephalus communicans; ID, intellectual disability; MAC, macrocephaly; MIC, microcephaly; MDLS, Miller-Dieker-Lissencephaly syndrome; NAD, no abnormality detected; n.p., not performed; PCH, Pontocerebellar hypoplasia; SBH, subcortical band heterotopia; Genetic analysis: 1, chromosome analysis; 2, microarray-based comparative genomic hybridization (Array-CGH); 3, trio whole-exome analysis.





10.3389/fimmu.2023.1101087

10.3389/fimmu.2023.1101087

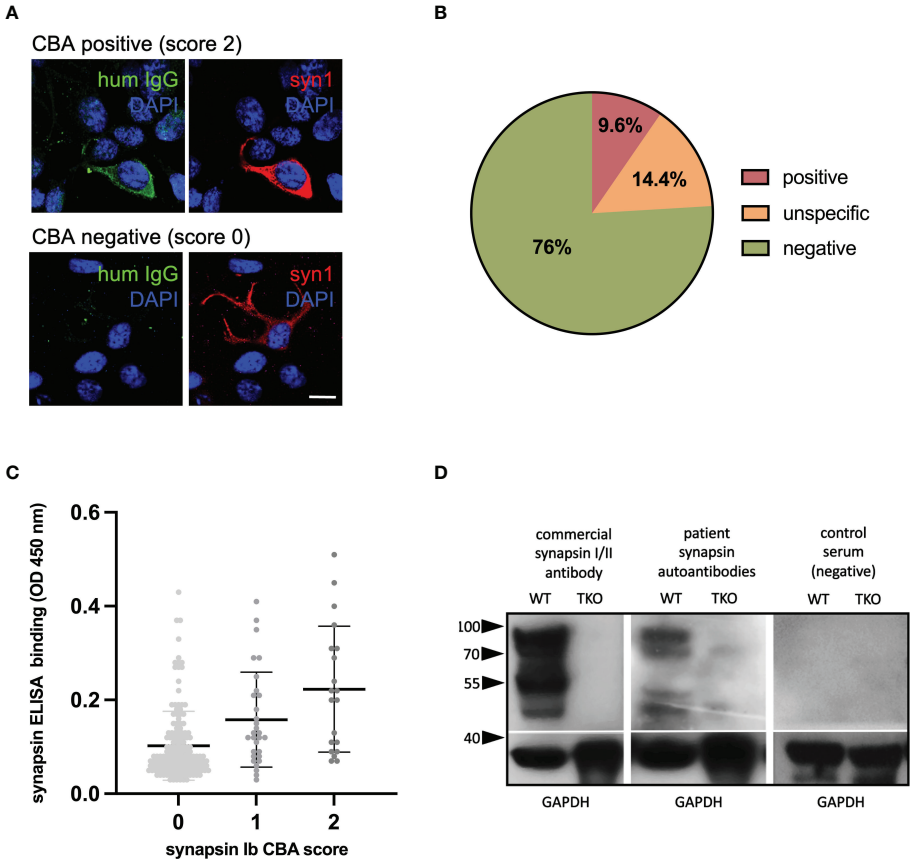


FIGURE 2
Detection of synapsin 1 (SYN1) autoantibodies. **(A)** Examples of immunofluorescence stainings, using human sera at a 1:300 dilution (green) with or without binding to HEK cells overexpressing human SYN1b are shown in the top row and bottom row. Using a commercial SYN1/2 antibody, protein expression is verified (red). DAPI is used to stain the nuclei (blue). Scale bar: 20 µm. **(B)** In 9.6% of mothers SYN1 autoantibodies were detected using a CBA. **(C)** CBA and in-house ELISA correlated weakly, with higher mean serum IgG levels in the CBA-positive group. **(D)** Representative immunoblots of wild type (WT) and Syn1/2/3 triple KO (TKO) mice cortex homogenates with a commercial synapsin 1/2 antibody as positive control, and with sera (1:200 dilution) from a CBA-positive mother and a CBA-negative control. Major bands at 80-90 kDa corresponding to the molecular weight of synapsin 1a/1b and additional bands at 50-55 kDa that could represent the synapsin 2b isoform or breakdown products of synapsin 1 were detected in wild type but not in TKO mouse tissue by both the commercial antibody and the serum of the CBA-positive mother. Detection of GAPDH served as loading control. HEK human embryonic kidney; CBA, cell-based assay; ELISA, enzyme-linked immunosorbent assay, WB, western blot.

autoantibodies in only 22.9% and found no correlation between ELISA and CBA antibody levels (16).

SYN1 is member of the family of synapsins, encoded by the three genes *SYN1*, *SYN2*, and *SYN3* in humans. SYN1 regulates the trafficking of synaptic vessels between the readily releasable pool and reserve pool. Furthermore, Syn1 moderates neuronal development through neurite outgrowth and synaptogenesis (2). *Syn1* mutant mice have severe epilepsy with generalized seizures (19).

In this present study of 208 children with various neurologic disorders, a positive maternal CBA showed a significant association

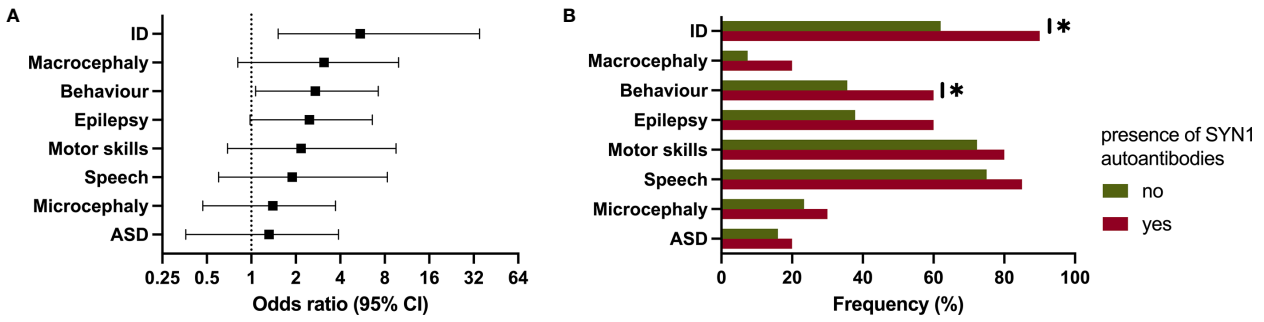


FIGURE 3
Clinical phenotype in patients of mothers with autoantibodies against synapsin 1 (SYN1). **(A, B)** Forest plot and bar chart showing the significantly increased risk for intellectual disability and behavioral problems. ID, intellectual disability; ASD, autism-spectrum disorder. * $p \leq 0.05$.

with ID and behavioral problems, while there was and a trend towards other abnormalities such as macrocephaly and epilepsy. This is intriguing given that patients with LoF variants in *SYN1* display a similar phenotype with epilepsy, ID, ASD, macrocephaly, and behavioral abnormalities (3–5). The lack of a clear association to these phenotypes may relate to the low statistical power of the study and emphasizes to investigate larger cohorts.

When further analyzing the 20 CBA-positive patients, seven had identified genetic variants/microdeletions of which one was considered pathogenic and three as likely pathogenic variants. This raises speculation as to whether genetic alterations in brain proteins may lead to neoantigen formation and increased autoimmunity. Autoantibodies arise from multilayered defects at immune checkpoints due to dysregulated negative selection of B cells which eventually develop into plasma cells or B memory cells (18). These autoantibodies can act through target-specific mechanisms. For example, *in vitro* experiments could show that SYN1 autoantibodies can be internalized through FcγII/III-mediated endocytosis and promote SYN1 aggregation resulting in impairment of synaptic transmission (20). Future experimental models will have to elucidate the functional role of maternal SYN1 autoantibodies and investigate whether they can reach the fetal brain and have a direct pathogenic effect on fetal development *in vivo* or rather represent a clinical biomarker of neuronal cell damage. Synaptic impairment by maternal SYN1 autoantibodies with possible detrimental effects on neurodevelopment may have a similar effect as other maternal antineuronal autoantibodies such as NMDAR, Caspr2, and aquaporin-4 antibodies, for which experimental studies have demonstrated pathogenic effects (10–13). Further, Caspr2 autoantibodies present during pregnancy were associated with ID and developmental disorders (21). However, functional studies on the effects of SYN1 autoantibodies on neurodevelopment are lacking and should be performed using patient-derived monoclonal antibodies (22).

In addition, it is unclear to what extent SYN1 autoantibodies cross the placenta and can be found in CSF. For this, functional experiments are necessary, in which human monoclonal autoantibodies are systemically applied into pregnant mice. It would be further interesting to assess if children of mothers with a positive CBA have SYN1 autoantibodies also in their CSF.

The study has multiple limitations including heterogeneity of the pediatric cohort. Other environmental factors, besides identified genetic variants, can also have an influence on the phenotype of these children. Furthermore, mothers were tested after pregnancy, Thus, it is unclear whether they were also positive during pregnancy which does not allow a direct statement about causality. To assess whether SYN1 autoantibodies have an effect during pregnancy we recently reported on a cohort of 263 pregnant women with seropositivity for SYN1 autoantibodies in 13.3%, matching the prevalence in this cohort (16). Seropositivity was associated with abnormalities of fetal development including intrauterine growth retardation, structural abnormalities and amniotic fluid disorders. The next step is to accurately phenotype these patients to assess the impact of SYN1 during pregnancy on the neurodevelopment of these children. Furthermore, the results of this study need to be validated by larger prospective multicentric studies with age-matched controls of healthy patients to increase power and counteract selection bias.

Despite these limitations, the study indicates a potential influence of maternal SYN1 autoantibodies on neurodevelopment. These results do not currently trigger any direct therapeutic or diagnostic consequences, but could influence standard treatment of pregnant women in the long term and possibly lead to new therapeutic approaches.

## Data availability statement

The original contributions presented in the study are included in the article/supplementary materials. Further inquiries can be directed to the corresponding author.

## Ethics statement

The studies involving human participants were reviewed and approved by Charité - Universitätsmedizin Berlin (approval no. #EA2/220/20). Written informed consent to participate in this study was provided by the participants' legal guardian/next of kin. The animal study was reviewed and approved by Charité - Universitätsmedizin Berlin (approval no. #EA2/220/20).

## Author contributions

Conceptualization: AK and HP. Patient recruitment: IB, KM, TU and ES. CBA and ELISA testing: IB, JK, CH, HR, MH, DM and JT. Western blotting: MH. Data collection, analysis, and visualization: IB and KM. Resources: AK and HP. Writing – original draft: IB, KM. Writing – review & editing: all authors. All authors contributed to the article and approved the submitted version.

## Funding

This work was supported by grants from the German Research Foundation (DFG) (grants FOR3004, PR1274/4-1, PR1274/5-1, PR1274/9-1), by the Helmholtz Association (HIL-A03), the German Federal Ministry of Education and Research (Connect-Generate 01GM1908D), the Einstein Stiftung Fellowship through the Günter Endres Fond, and the Sonnenfeld-Stiftung.

## Acknowledgments

We thank Stefanie Bandura, Matthias Sillmann, Doreen Brandl, Antje Dräger, and Monika Majer for excellent technical assistance and study nurse support. JK and MN are participants in the Berlin Institute of Health (BIH)-Charité Junior Clinician Scientist Program.

## Conflict of interest

The authors declare that the research was conducted in the absence of any commercial or financial relationships that could be construed as a potential conflict of interest.

## Publisher's note



## References

1. Hilfiker S, Benfenati F, Doussau F, Nairn AC, Czernik AJ, Augustine GJ, et al. Structural domains involved in the regulation of transmitter release by synapsins. *J Neurosci* (2005) 25(10):2658–69. doi: 10.1523/jneurosci.4278-04.2005

2. Valtorta F, Benfenati F, Greengard P. Structure and function of the synapsins. *J Biol Chem* (1992) 267(11):7195–8. doi: 10.1016/S0021-9258(18)42501-X

3. Garcia CC, Blair HJ, Seager M, Coulthard A, Tennant S, Buddles M, et al. Identification of a mutation in synapsin I, a synaptic vesicle protein, in a family with epilepsy. *J Med Genet* (2004) 41(3):183–6. doi: 10.1136/jmg.2003.013680

4. Fassio A, Patry L, Congia S, Onofri F, Piton A, Gauthier J, et al. Syn1 loss-of-Function mutations in autism and partial epilepsy cause impaired synaptic function. *Hum Mol Genet* (2011) 20(12):2297–307. doi: 10.1093/hmg/ddr122

5. Giannandrea M, Guarnieri FC, Gehring NH, Monzani E, Benfenati F, Kulozik AE, et al. Nonsense-mediated mrna decay and loss-of-Function of the protein underlie the X-linked epilepsy associated with the W356× mutation in synapsin I. *PloS One* (2013) 8(6): e67724. doi: 10.1371/journal.pone.0067724

6. Kreye J, Wright SK, van Casteren A, Stöffler L, Machule ML, Reincke SM, et al. Encephalitis patient-derived monoclonal gabaa receptor antibodies cause epileptic seizures. *J Exp Med* (2021) 218(11). doi: 10.1084/jem.20210012

7. Noviello CM, Kreye J, Teng J, Prüss H, Hibbs RE. Structural mechanisms of gaba(a) receptor autoimmune encephalitis. *Cell* (2022) 185(14):2469–77.e13. doi: 10.1016/j.cell.2022.06.025

8. Maljevic S, Møller RS, Reid CA, Pérez-Palma E, Lal D, May P, et al. Spectrum of gabaa receptor variants in epilepsy. *Curr Opin Neurol* (2019) 32(2):183–90. doi: 10.1097/wco.0000000000000657

9. Han VX, Patel S, Jones HF, Dale RC. Maternal immune activation and neuroinflammation in human neurodevelopmental disorders. *Nat Rev Neurol* (2021) 17 (9):564–79. doi: 10.1038/s41582-021-00530-8

10. García-Serra A, Radosevic M, Pupak A, Brito V, Ríos J, Aguilar E, et al. Placental transfer of nmdar antibodies causes reversible alterations in mice. *Neurol Neuroimmunol Neuroinflamm* (2021) 8(1). doi: 10.1212/nxi.0000000000000915

11. Mader S, Brimberg L, Vo A, Strohl JJ, Crawford JM, Bonnin A, et al. *In utero* exposure to maternal anti-Aquaporin-4 antibodies alters brain vasculature and neural dynamics in Male mouse offspring. *Sci Transl Med* (2022) 14(641):eabe9726. doi: 10.1126/scitranslmed.abe9726

12. Brimberg L, Mader S, Jeganathan V, Berlin R, Coleman TR, Gregersen PK, et al. Caspr2-reactive antibody cloned from a mother of an asd child mediates an asd-like phenotype in mice. *Mol Psychiatry* (2016) 21(12):1663–71. doi: 10.1038/mp.2016.165

13. Jurek B, Chayka M, Kreye J, Lang K, Kraus L, Fidzinski P, et al. Human gestational n-Methyl-D-Aspartate receptor autoantibodies impair neonatal murine brain function. *Ann Neurol* (2019) 86(5):656–70. doi: 10.1002/ana.25552

14. Höltje M, Mertens R, Schou MB, Saether SG, Kochova E, Jarius S, et al. Synapsin-antibodies in psychiatric and neurological disorders: Prevalence and clinical findings. *Brain Behav Immun* (2017) 66:125–34. doi: 10.1016/j.bbi.2017.07.011

15. Piepgras J, Höltje M, Otto C, Harms H, Satapathy A, Cesca F, et al. Intrathecal immunoglobulin a and G antibodies to synapsin in a patient with limbic encephalitis. *Neurol Neuroimmunol Neuroinflamm* (2015) 2(6):e169. doi: 10.1212/nxi.0000000000000169

16. Bünger I, Kreye J, Makridis K, Höltje M, Rasmussen HF, van Hoof S, et al. Synapsin autoantibodies during pregnancy are associated with fetal abnormalities. *medRxiv* (2022), 2022.09.23.22280284. doi: 10.1101/2022.09.23.22280284

17. Milovanovic D, Wu Y, Bian X, De Camilli P. A liquid phase of synapsin and lipid vesicles. *Science* (2018) 361(6402):604–7. doi: 10.1126/science.aat5671

18. Prüss H. Autoantibodies in neurological disease. *Nat Rev Immunol* (2021) 21 (12):798–813. doi: 10.1038/s41577-021-00543-w

19. Rosahl TW, Spillane D, Missler M, Herz J, Selig DK, Wolff JR, et al. Essential functions of synapsins I and ii in synaptic vesicle regulation. *Nature* (1995) 375 (6531):488–93. doi: 10.1038/375488a0

20. Rocchi A, Sacchetti S, De Fusco A, Giovedi S, Parisi B, Cesca F, et al. Autoantibodies to synapsin I sequestrate synapsin I and alter synaptic function. *Cell Death Dis* (2019) 10(11):1–16. doi: 10.1038/s41419-019-2106-z

21. Coutinho E, Jacobson L, Pedersen MG, Benros ME, Nørgaard-Pedersen B, Mortensen PB, et al. Caspr2 autoantibodies are raised during pregnancy in mothers of children with mental retardation and disorders of psychological development but not autism. *J Neurol Neurosurg Psychiatry* (2017) 88(9):718–21. doi: 10.1136/jnnp-2016-315251

22. Duong SL, Prüss H. Molecular disease mechanisms of human antineuronal monoclonal autoantibodies. *Trends Mol Med* (2022). doi: 10.1016/j.molmed.2022.09.011

frontiers | Frontiers in Immunology

TYPE Systematic Review
PUBLISHED 23 January 2023
DOI 10.3389/fimmu.2022.1064007



OPEN ACCESS

EDITED BY
Long-Jun Wu,
Mayo Clinic, United States

REVIEWED BY
Farinaz Safavi,
National Institutes of Health (NIH), United States
David R. Benavides,
University of Maryland, United States

*CORRESPONDENCE
Minjin Wang
wang.minjin@outlook.com
Yi Xie
xieyi@scu.edu.cn

†These authors have contributed equally to this work

SPECIALTY SECTION
This article was submitted to Multiple Sclerosis and Neuroimmunology, a section of the journal Frontiers in Immunology

RECEIVED 07 October 2022
ACCEPTED 23 December 2022
PUBLISHED 23 January 2023

CITATION
Ma Y, Wang J, Guo S, Meng Z, Ren Y, Xie Y and Wang M (2023) Cytokine/chemokine levels in the CSF and serum of anti-NMDAR encephalitis: A systematic review and meta-analysis.
*Front. Immunol.* 13:1064007.
doi: 10.3389/fimmu.2022.1064007



# Cytokine/chemokine levels in the CSF and serum of anti-NMDAR encephalitis: A systematic review and meta-analysis

Yushan Ma[1,2†], Jierui Wang[3†], Shuo Guo[1†], Zirui Meng[1], Yan Ren[1], Yi Xie[1*†] and Minjin Wang[1,3*†]

[1]Department of Laboratory Medicine, West China Hospital of Sichuan University, Chengdu, China, [2]Department of Laboratory Medicine, The Third Hospital of Mianyang, Sichuan Mental Health Center, Mianyang, China, [3]Department of Neurology, West China Hospital of Sichuan University, Chengdu, China

**Objectives:** To summarize the cytokine/chemokine levels of anti-N-methyl-Daspartate receptor encephalitis (NMDAR-E) and explore the potential role of these molecules and immune cells in the pathogenic mechanism.

**Methods:** The PubMed, Cochrane Library, Embase, and Web of Science databases were searched for various articles that assessed the concentrations of cytokines/chemokines in the unstimulated cerebrospinal fluid (CSF) or serum of patients with NMDAR-E in this systematic review and meta-analysis. The standardized mean difference (SMD) and 95% confidence interval (CI) were calculated by Stata17.0.

**Results:** A total of 19 articles were included in the systematic review from 260 candidate papers, and cytokine/chemokine levels reported in the CSF/serum were examined in each article. This meta-analysis included 17 eligible studies comprising 579 patients with NMDAR-E, 367 patients with noninflammatory neurological disorders, and 42 healthy controls from China, Spain, South Korea, Australia, Czechia, and Sweden. The results indicated that the levels of different cytokines interleukin (IL)-6, tumor necrosis factor (TNF)-α, IL-10, IL-13, IL-1β, IL-12, and IL-17 and chemokine C-X-C motif ligand (CXCL)10 in the CSF were significantly higher in NMDAR-E patients with a large effect size. In addition, B cell activating factor (BAFF), CXCL13, and interferon (IFN)-γ levels in the CSF were higher in NMDAR-E patients with a middle effect size. In contrast, levels of IL-2 and IL-4 in the CSF and CXCL13 and BAFF in the serum did not show a significant difference between cases and controls.

**Conclusions:** These analyses showed that the central immune response in NMDAR-E is a process that involves multiple immune cell interactions mediated by cytokines/chemokines, and T cells play an important role in the pathogenesis of immunity.

**Systematic review registration:** https://www.crd.york.ac.uk/PROSPERO/, identifier (CRD42022342485).

KEYWORDS

cytokine, chemokine, T cell, NMDAR encephalitis, meta-analysis

# 1 Introduction

Anti-N-methyl-D-aspartate receptor encephalitis (NMDAR-E) is one of the most common types of autoimmune neurological disorders, which affects young women more often than it does men (1–3). The clinical manifestations are often variable, including seizures, psychiatric behavior changes, and rapid cognitive decline (2, 4, 5). The majority of NMDAR-E patients have intrathecal antibody synthesis, which can cause a significant decrease in the cell surface and synaptic NMDAR by specific immunoglobulin G (IgG) antibodies against the GluN1 subunit on the neuronal membrane (6). Clinically, it is generally assumed that the progressive deficiency of the receptor function with increased antibody titer can reflect the severity of the disease and/or may be the primary cause of aggravation (7). However, since ongoing intrathecal antibody production does not always signify active encephalitis, this conclusion has certain limitations (8, 9).

Recently, few studies have reported that the key immune pathogenesis of NMDAR-E is often accompanied by immune dysregulation, which is inflammatory in nature. It is usually characterized by massive infiltration of T cells, B cells, and other immune cells into the central nervous system (CNS) (10, 11), triggering substantial neuron damage, demyelination, or neurodegeneration (12, 13). However, although the role of B cells in NMDAR-E has already been demonstrated (7, 14, 15), whether T cells can effectively react against NMDAR and their specific role in disease development remain unclear (16). Moreover, the mechanisms through which they can access the CNS compartment are unclear. Additionally, because T cells are predominantly found in the cerebrospinal fluid (CSF) of affected people while B cells are scarce (17), some prior studies have suggested that NMDAR-E onset could be potentially triggered by the activation of T cells in the periphery and CNS (13). Indeed, current pathological examination and postmortem reports further support the observation that the different effector T helper (Th) cells, such as Th1 and Th17 cells, could extensively be infiltrated in the tissues (11, 13, 14, 18). In particular, previous studies have demonstrated that Th cells can significantly enhance antibody-secreting cell (ASC)-mediated antibody responses, as mice were actively immunized with conformationally stabilized NMDAR protein and both ASCs and CD4+ T cells demonstrated extensive infiltration into the hippocampus (19). This finding indicated that the immune effects of one or several T cells may be important for regulating disease etiology and progression in NMDAR-E patients.

Cytokines/chemokines are low-molecular-weight polypeptides with biological activity mainly derived from the diverse antigen-presenting cells and mononuclear phagocytic cells (20, 21). As important immunoregulatory factors, cytokines/chemokines play a key role in the activation, differentiation, and migration of immune cells (22). In addition, various studies have revealed that dysregulation of the cytokine system plays a key role in neuroinflammatory disorders, and the alteration of cytokine levels has been increasingly linked to NMDAR-E. Interestingly, multiple studies including our own have suggested that CSF cytokine/chemokine signatures, such as elevated levels of interleukin (IL)-17, IL-6, or CXCL10, also suggest the possible involvement of T cells in the etiology of NMDAR-E (23–25). However, there is no broad consensus on these conclusions among the scientific community. This systematic review and meta-analysis focused on analyzing the previous studies related to CSF and serum cytokines and chemokines of NMDAR-E. Our research not only concentrated on the broad range of chemokines and cytokines associated with T-cell activities and examined how their levels were altered during the various clinical courses of NMDAR-E. More importantly, the detailed investigation of these molecules is expected to advance our comprehension of the disease's immune mechanisms.

# 2 Methods

## 2.1 Search strategy

This systematic review and meta-analysis were conducted according to the preferred reporting items for systematic reviews and meta-analyses (PRISMA) criteria recommended for reporting items for systematic reviews and meta-analyses. This meta-analysis has been registered on the PROSPERO (No. CRD42022342485). We searched the PubMed, Web of Science, Embase, and Cochrane Library databases to identify articles published up to 25 June 2022 using a combination of the following keywords: (Anti NMDA Receptor Encephalitis OR anti-N-methyl-d-aspartate receptor encephalitis OR Anti-NMDAR Encephalitis OR N-methyl-d-aspartate antibody encephalitis OR NMDA receptor encephalitis OR anti-N-methyl-d-aspartate receptor antibody encephalitis) AND (cytokine OR interleukin OR interferon OR tumor necrosis factor-alpha OR transforming growth factor OR chemokine). The detailed search strategy used for each database has been described in the *Supplementary Methods*.

## 2.2 Selection criteria

The inclusion criteria were as follows: 1) the types of studies including cross-sectional, case–control, and cohort; 2) the level of anti-NMDAR antibody was found to be positive in the serum or CSF; 3) other autoantibody tests of the specimen were negative; 4) assessed the concentrations of the different cytokines/chemokines in the unstimulated serum or CSF with noninflammatory neurological disorder control or healthy control group.

The exclusion criteria were as follows: 1) reviews, case reports, experiments on animals or cells, conference papers, and editorial materials; 2) incomplete full text or nonconforming data; 3) different studies that mainly used reduplicated data.

## 2.3 Study selection and data extraction

YM and JW, two reviewers, each separately searched the articles, imported them into Endnote X9, and managed the search records. Thereafter, by using the Newcastle–Ottawa Scale (NOS), we also evaluated the quality of the papers that were included. The initial author's name, research period, location, the source of the control

group, sample size, gender, mean/median age, and quality scores were then collected as key data from a few selected studies.

The major results were the variation in the mean levels of inflammatory cytokines and chemokines between each case group and control group. The information about the number of participants, mean levels, and the standard deviation (SD) for cytokines/chemokines of NMDAR-E and control was obtained to calculate the mean difference. If the mean or SD was not stated directly in the articles, we could estimate them from the sample size and the alternative measures, including median, range, and 95% confidence interval (CI) or interquartile range, utilizing Wan and Luo's online data converter (26, 27). If these measures were not available, the data were extracted from the figures and graphs by using an analogy to the approach as described in Saghazadeh and Rezaei (28).

## 2.4 Statistical analysis

In our study, Stata17.0 was used for all data analyses. Meta-analyses were performed when cytokine/chemokine data were extracted from at least three studies. The standardized mean difference (SMD) calculated by Hedges' g was taken to analyze the effect with measurement scale differences across the studies, and its 95% CI was used as the result of the pooled analysis. Then, by using the SMD cutoff points of 0.2, 0.5, and 0.8, effect sizes were also broadly classified as small, medium, and large. We used the random-effects model (DerSimonian–Lard) for each meta-analysis to obtain a satisfactory estimator of heterogeneity variance for the continuous results.

Q statistic test was used to determine whether heterogeneity was presented across the studies of each factor, and tau-squared ($t^2$) was a quantitative measurement of heterogeneity, while the I-squared ($I^2$) was the heterogeneity across the studies from the total heterogeneity. The significance level was considered at $P < 0.1$.

To ensure that the results were robust and reliable, a sensitivity analysis was performed to determine whether the significance of the calculated effect size was sensitive to the effect when every single study was omitted. Thus, to assess the potential publication bias, if there were more than 10 research studies published, we will use a funnel plot and Egger test, where $P < 0.05$ was deemed statistically significant.

# 3 Results

## 3.1 Literature search and selection

A total of 260 candidate articles were initially identified, and 36 studies were considered for further review after in-depth analyses of all of the titles and abstracts. It was found that among these studies, 12 had no interesting data and five had no appropriate control group; 17 studies meeting the inclusion requirements were included in the meta-analysis, and 19 studies were in the quantitative synthesis. The detailed procedure of the selection has been illustrated in Figure 1.

## 3.2 Characteristics of the included studies

Overall, 19 studies met the inclusion and exclusion criteria, and we stipulated that if a certain cytokine or chemokine was measured in more than three studies, then it can be included in the meta-analysis (23, 24, 29–45). cluster of differentiation 146 (CD146) and high-mobility group box protein 1 (HMGB1) concentrations of NMDAR-E were only found in a single study each; these two studies were excluded from the meta-analysis as a result of insufficient data (33, 43). In addition, there were a few studies about the serum cytokine levels in NMDAR-E patients, and in some studies, which only

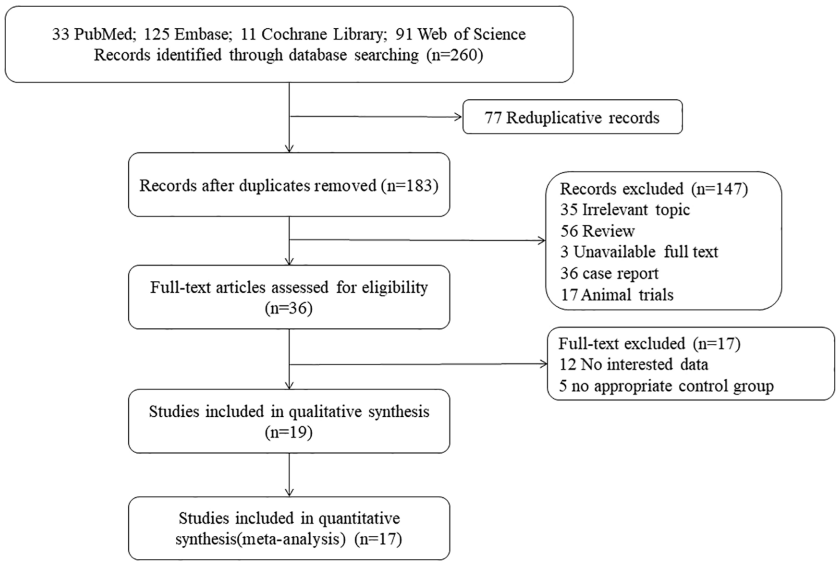


FIGURE 1
The procedures involved in study screening.

measured cytokine levels in the whole autoimmune encephalitis, data about NMDAR-E could not be extracted from the overall data and were also not available from the authors (46, 47). For these reasons, 37 cytokines/chemokines of the CSF and 21 cytokines/chemokines of the serum were not analyzed for having less than three studies, including a proliferation-inducing ligand (APRIL), cluster of differentiation 40 ligand (CD40L), C-C motif ligand(CCL)2 (CCL2), IL-8, granulocyte-macrophage colony-stimulating factor (GM-CSF), CCL17, CCL19, HMGB1, chitinase-3-like protein 1 (YKL-40), NOD-like receptor thermal protein domain associated protein 3 (NLRP3), CD146, osteopontin, etc. (23, 24, 30, 31, 33–35, 38, 40, 42, 43).

Meta-analyses of the different cytokines/chemokines in 13 CSF and two serum studies were performed. The two cytokines found in the CSF with the most studies were IL-17 and IL-6. A total of 579 NMDAR-E patients and 409 controls from China, Spain, South Korea, Australia, Czechia, and Sweden were included. The characteristics of the included subjects are summarized in Supplementary Table S1. The studies selected in the meta-analysis included cross-sectional, cohort ones. Based on the NOS, all of the studies were moderate or high quality, with an average NOS of 7.06. The details have been shown in Supplementary Table S2.

## 3.3 Meta-analysis of cytokines/chemokines

We divided the identified cytokines/chemokines into several groups including the B-cell axis, T-cell axis, and broad spectrum based on the distinct roles of associated lymphocytes in the pathogenesis of NMDAR-E. The outcomes of the meta-analysis showed that the levels of 11 different cytokines/chemokines, BAFF, CXCL13, CXCL10, interferon (IFN)-γ, tumor necrosis factor (TNF)-α, IL-17, IL-6, IL-10, IL-13, IL-1β, and IL-12, in the CSF were significantly higher in NMDAR-E patients compared to those in controls. However, levels of IL-2 and IL-4 in the CSF and CXCL13 and BAFF in the serum showed no significant difference. The details are shown in Table 1 and Figure 2.

Thereafter, for optimal understanding of the results obtained for each cytokine/chemokine, we generalized the key characteristics of our data. Cytokines/chemokines were divided as not statistically significant: the symbol "-" indicated the cytokines/chemokines for which there was no significant evidence ($P \geq 0.05$) . Three asterisks depicted large effect sizes (SMD ≥0.8); two asterisks, medium effect sizes (0.5 ≤ SMD < 0.8); one asterisk, small effect sizes (0.2 ≤ SMD < 0.5). Significantly higher CSF cytokines/chemokines CXCL10, TNF-α, IL-17, IL-6, IL-10, IL-13, IL-1β, and IL-12 were identified in NMDAR-E patients in comparison with those in control subjects associated with the T-cell axis and mononuclear macrophages, dendritic cells, and other immune cells (Table 2).

### 3.3.1 Meta-analysis of B-cell axis cytokines/chemokines

BAFF and CXCL13 can recruit and activate B cells, respectively. NMDAR-E CSF BAFF and CXCL13 levels were found to be significantly higher than those of the control with a middle effect size (BAFF: SMD = 0.75, 95% CI = 0.34–1.17, $P < 0.001$; CXCL13: SMD = 0.64, 95% CI = 0.4–0.89, $P < 0.001$). Moreover, the serum

TABLE 1 Summary of the meta-analysis outcomes for the different cytokines/chemokines.

| | | | | | Main Effect | | | | | Heterogeneity | | | |
|---|---|---|---|---|---|---|---|---|---|---|---|---|---|
| Cytokine/chemokine | | Sample | Study | N(case/control) | SMD | 95%CI | *Z* | *P* | | $\tau^2$ | $I^2$ (%) | df | *P* |
| B cell axis | BAFF | Serum | 3 | 87/50 | 0.26 | -0.10, 0.61 | 1.42 | 0.155 | | <0.01 | <0.01 | 2 | 0.767 |
| | CXCL13 | Serum | 4 | 115/64 | 0.27 | -0.04, 0.58 | 1.69 | 0.090 | | <0.01 | <0.01 | 3 | 0.447 |
| | BAFF | CSF | 3 | 59/48 | 0.75 | 0.34, 1.17 | 3.59 | <0.001 | | <0.01 | <0.01 | 2 | 0.929 |
| | CXCL13 | CSF | 5 | 259/124 | 0.64 | 0.40, 0.89 | 5.16 | <0.001 | | <0.01 | <0.01 | 4 | 0.410 |
| Th1 cell axis | CXCL10 | CSF | 3 | 29/39 | 1.47 | 0.92, 2.03 | 5.19 | <0.001 | | <0.01 | <0.01 | 2 | 0.991 |
| | IFN-γ | CSF | 5 | 97/113 | 0.76 | 0.22, 1.29 | 2.74 | 0.001 | | 0.21 | 58.91 | 4 | 0.119 |
| | TNF-α | CSF | 8 | 159/133 | 1.42 | 1.04, 1.81 | 7.29 | <0.001 | | 0.14 | 48.81 | 7 | 0.057 |
| Th17 cell axis | IL-17 | CSF | 10 | 214/238 | 1.12 | 0.86, 1.37 | 8.45 | <0.001 | | 0.05 | 30.99 | 9 | 0.157 |
| | IL-6 | CSF | 11 | 284/278 | 1.00 | 0.80, 1.21 | 9.58 | <0.001 | | 0.02 | 19.42 | 10 | 0.259 |
| Th2 cell axis | IL-2 | CSF | 3 | 85/90 | 0.46 | -0.15, 1.07 | 1.48 | 0.101 | | 0.18 | 62.97 | 2 | 0.133 |
| | IL-4 | CSF | 3 | 29/43 | 0.07 | -0.42, 0.56 | 0.27 | 0.783 | | <0.01 | <0.01 | 2 | 0.611 |
| | IL-13 | CSF | 3 | 29/43 | 1.08 | 0.15, 2.00 | 2.27 | 0.040 | | 0.43 | 64.65 | 2 | 0.031 |
| Treg cell axis | IL-10 | CSF | 8 | 188/171 | 1.32 | 0.63,2.01 | 3.74 | <0.001 | | 0.83 | 86.41 | 7 | <0.001 |
| Broad spectrum | IL-1β | CSF | 6 | 138/150 | 1.25 | 0.38, 2.11 | 2.82 | 0.005 | | 1.02 | 88.83 | 5 | <0.001 |
| | IL-12 | CSF | 3 | 29/43 | 1.43 | 0.25, 2.61 | 2.37 | 0.018 | | 0.81 | 74.78 | 2 | 0.019 |

SMD, standardized mean difference; Th, T helper; Treg, T regulatory; BAFF, B cell activating factor; CXCL, C-X-C motif ligand; IFN,interferon; TNF, tumor necrosis factor; IL, interleukin.

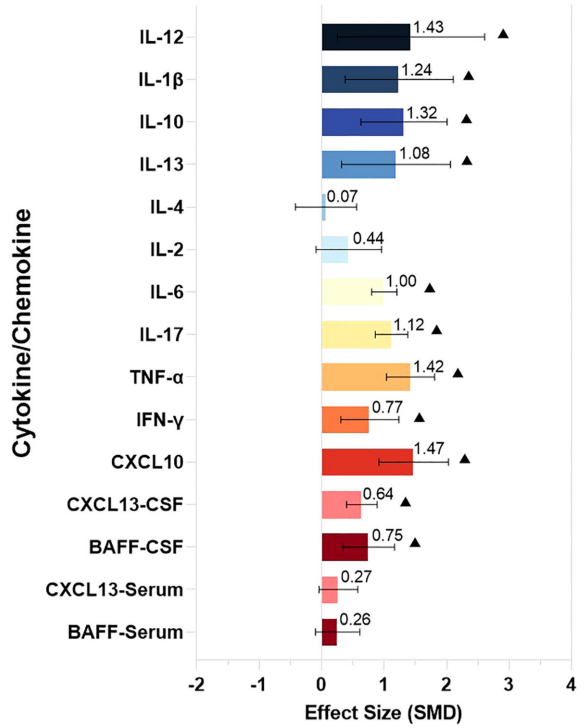


FIGURE 2
The comparison of CSF and serum levels of the cytokines/chemokines in NMDAR-E. Effect size estimates (SMD) and 95% confidence intervals are represented by colored bars and black error bars, ▲ represents $P < 0.05$. SMD, standardized mean difference; Th, T helper; Treg, T regulatory; BAFF, B cell activating factor; CXCL, C-X-C motif ligand; IFN,interferon; TNF, tumor necrosis factor; IL, interleukin.

BAFF and CXCL13 random-effects model meta-analysis indicated that both did not differ significantly from those of the control (BAFF: SMD = 0.26, 95% CI = -0.10 to +0.61, $P = 0.155$; CXCL13: SMD = 0.27, 95% CI = -0.04 to +0.58, $P = 0.090$) (Supplementary Figures S1–S4).

Influence analyses suggested that the effect size for serum CXCL13 was sensitive to the effect of the study reported by Leypoldt et al. (29), and upon omitting this study, the effect size was changed from 0.27 to 0.49, with the 95% CI lower limit changed from -0.04 to 0.08. Thereafter, the case and control groups' outcomes differed in a significant way (SMD = 0.49, 95% CI = 0.08–0.91, $P = 0.02$). The study by Leypoldt et al. contained a larger sample size than the other three studies and played a key role in a meta-analysis of CXCL13 in the CSF (30) (Supplementary Figure S2). The sensitivity analysis of other cytokines and chemokines was robust when omitting either of these articles (Supplementary Figures S1, S3–S15).

### 3.3.2 Meta-analysis of Th1 cell axis cytokines/chemokines

In comparison to those of the control group, it was discovered that the levels of NMDAR-E Th1 axis-related cytokine TNF-α and the chemokine CXCL10 were significantly higher with a large effect size (Figures 3A, B) and IFN-γ with a middle effect size (IFN-γ: SMD = 0.77, 95% CI = 0.31–1.24, $P = 0.001$; TNF-α: SMD = 1.42, 95% CI = 1.04–1.81, $P < 0.001$; CXCL10: SMD = 1.47, 95% CI = 0.92–2.03, $P < 0.001$).

### 3.3.3 Meta-analysis of Th17 cell axis cytokines/chemokines

The levels of Th17 axis-related cytokines IL-17 and IL-6 were found to be significantly increased (Figures 3C, D) (IL-17: SMD = 1.12, 95% CI = 0.86–1.38, $P < 0.001$; IL-6: SMD = 1.00, 95% CI = 0.80–1.21, $P < 0.001$). As there were more than 10 studies related to the cytokines IL-17 and IL-6, we performed publication bias assessment for both IL-6 and IL-17. However, no evidence of publication bias was detected for the meta-analysis of IL-6 ($P = 0.861$, k = 11) and IL-17 ($P = 0.719$, k = 10) by using Egger's regression and the funnel plots (Figure 4).

### 3.3.4 Meta-analysis of Th2 cell axis cytokines/chemokines

The concentrations of IL-13 associated with the Th2 axis increased with a large effect size, but those of IL-2 and IL-4 did not differ significantly (IL-13: SMD = 1.08, 95% CI = 0.05–2.10, $P = 0.040$; IL-2: SMD = 0.44, 95% CI = -0.09 to 0.96, $P = 0.101$; IL-4: SMD = 0.07, 95% CI = -0.42 to 0.56, $P = 0.783$) (Figure 3G). Furthermore, in the IL-13 meta-analysis, included studies were found to be statistically heterogeneous ($I^2 = 71.17\%$), although the random-effects model was used.

### 3.3.5 Meta-analysis of Treg cell axis cytokines/chemokines

T regulatory (Treg) cell axis cytokine IL-10 was also found to be significantly higher in comparison to that of the control with a large effect size (Figure 3E) (SMD = 1.32, 95% CI = 0.63–2.01, $P < 0.001$). The various included studies were statistically heterogeneous ($I^2 = 86.41\%$), although the random-effects model was used.

### 3.3.6 Meta-analysis of the broad-spectrum cytokines/chemokines

We defined IL-1β and IL-12 among the broad-spectrum cytokines, as they are associated with diverse immune cells, and their levels were found to be significantly higher in NMDAR-E compared with those in the control with a large effect size (Figures 3F, H) (IL-1β: SMD = 1.24, 95% CI = 0.38–2.11, $P = 0.005$; IL-12: SMD = 1.43, 95% CI = 0.25–2.61, $P = 0.018$). The various included studies were statistically heterogeneous in IL-1β and IL-12 as determined by the random-effects model (IL-1β: $I^2 = 88.83\%$; IL-12: $I^2 = 74.78\%$).

## 4 Discussion

In our systematic review and meta-analysis, we found that multiple cytokines and chemokines were shown to be significantly higher in NMDAR-E patients, but we specifically focused on those alterations shown in our meta-analysis due to their higher levels of evidence. We observed that the various cytokines IL-6, TNF-α, IL-10, IL-13, IL-1β, IL-12, and IL-17 and chemokine CXCL10 in the CSF were significantly higher in patients with NMDAR-E, and they were associated with T cells and macrophages and other immune cells (48–50). Interestingly, significant heterogeneity was found in the comparisons of IL-10, IL-1β, IL-12, and IL-13. This heterogeneity

10.3389/fimmu.2022.1064007

TABLE 2 Summary of the CSF/serum levels of the cytokines/chemokines in NMDAR-E vs. control subjects.

| Group | Cytokine/ chemokine | Sample | Main Source | Main function | Cytokine/chemokine Levels of NMDAR-E vs. control |
|---|---|---|---|---|---|
| B cell | BAFF | Serum | Mø, DC,T cells | Regulates B-lymphocyte survival and maturation | – |
| | CXCL13 | Serum | Mø, DC | Selective attraction of B cells | – |
| | BAFF | CSF | Mø, DC,T cells | Regulates B-lymphocyte survival and maturation | ** |
| | CXCL13 | CSF | Mø, DC | Selective attraction of B cells | ** |
| Th1 | CXCL10 | CSF | Mø,EC, fibroblasts | Chemotaxis of Mø, NK cells, and DC; promotes T cell adhesion to endothelial cells | *** |
| | IFN-γ | CSF | T cells, natural killers cells | Promotes differentiation of Th0 into Th1;stimulates Mø; increases osteoclastogenesis | ** |
| | TNF-α | CSF | Mø, T cells | Increases PMN migration; up-regulates expression of IL-1β,IL-6, and RANKL | *** |
| Th17 | IL-17 | CSF | Th cells | Stimulates production of TNF-α,IL-6,and IL-1β; increases RANKL expression | *** |
| | IL-6 | CSF | Mø,EC,T cells | Increases inflammatory cell migration; increases osteoclastogenesis | *** |
| Th2 | IL-2 | CSF | T cells | Promotes T cell proliferation and activation; increases NK proliferation | – |
| | IL-4 | CSF | T cells, mast cells | Increases Th0 proliferation; increases IL-10 production; inhibits pro-inflammatory cytokines activity; | – |
| | IL-13 | CSF | Th2 cells | Induces differentiation of monocytes;induces B cell proliferation; Inhibits of inflammation | *** |
| Treg | IL-10 | CSF | Mø, Treg | Inhibits Mø antigen-presenting capacity; activates OPG | *** |
| Broad spectrum | IL-1β | CSF | Mø,EC, fibroblasts,DC | Increases inflammatory cell migration; increases osteoclastogenesis | *** |
| | IL-12 | CSF | Mø,DC | Promotes differentiation of Th0 into Th1; increases NK proliferation | *** |

*** - large (SMD ≥ 0.8) and significant ($p < 0.05$) effect sizes; ** - medium (SMD ≥ 0.5 and SMD < 0.8) and significant ($p < 0.05$) effect sizes; the symbol "-" was used to identify cytokines/chemokines for which no good evidence could be found;MØ, macrophages ;DC, dendritic cells;EC, epithelial cells;SMD, standardized mean difference; NK, natural killer; PMN, polymorphonuclear; RANKL, receptor activator of nuclear factor-kappa B ligand; OPG, Osteoprotegerin.

could be caused by multiple factors, including age, gender, population, and methodology, as well as the inconsistency of the sample collection time and the healthy state of the control group. However, heterogeneity could not be identified from which research or factor due to the small number of studies included in the meta-analysis. These results reinforced the clinical evidence that NMDAR-E is primarily accompanied by an inflammatory response in the CNS with infiltration of T cells and other immune cells in addition to B cells. In this meta-analysis, we did not notice evidence for the involvement of the cytokines IL-2 and IL-4, but it is possible that if there are more studies related to the cytokines found in NMDAR-E patients and a larger sample size can be used in the future, the results of a new meta-analysis might be different. For the same reason, the meta-analysis excluded several cytokines and chemokines that were reported in less than three studies; however, their exclusion does not imply that they are less clinically relevant. The levels of CD40L, chitinase-3-like protein 1 (CHI3L1), OPN, sCD138, and sCD146 were found to be elevated in the CSF of patients with NMDAR-E and may be associated with severity and prognosis, but more studies to validate their roles are still needed (35, 39, 40, 43, 45).

The meta-analysis included 17 studies published between 2015 and 2021, three of which were published between 2015 and 2016, and included patients only with positive anti-NMDAR antibodies in the serum, which also had clinical features consistent with autoimmune encephalitis. It has been established that patients with NMDAR-E who are negative for antibodies in the CSF may have a delayed onset of antibodies or titers of antibodies could be too low to detect. The delayed onset of anti-NMDAR antibody was previously reported in a 2-year-old child with encephalitis presentation; however, the antibody was always negative in the CSF or serum until 1 year later, and the child developed severe neurological sequelae due to untimely immunotherapy (51). Moreover, based on the findings of other reports, we also found that most patients were probably affected with NMDAR-E, as only antibodies were detected in the serum. They were mostly children and young adults, often with cognitive deficits, catatonia, and speech disturbance. It was found that after the administration of immunotherapy, most of these patients were in remission (52, 53). In addition, some cases only with positive anti-NMDAR antibodies in the serum could also be CSF positive at an early stage due to the time interval between the symptom onset and

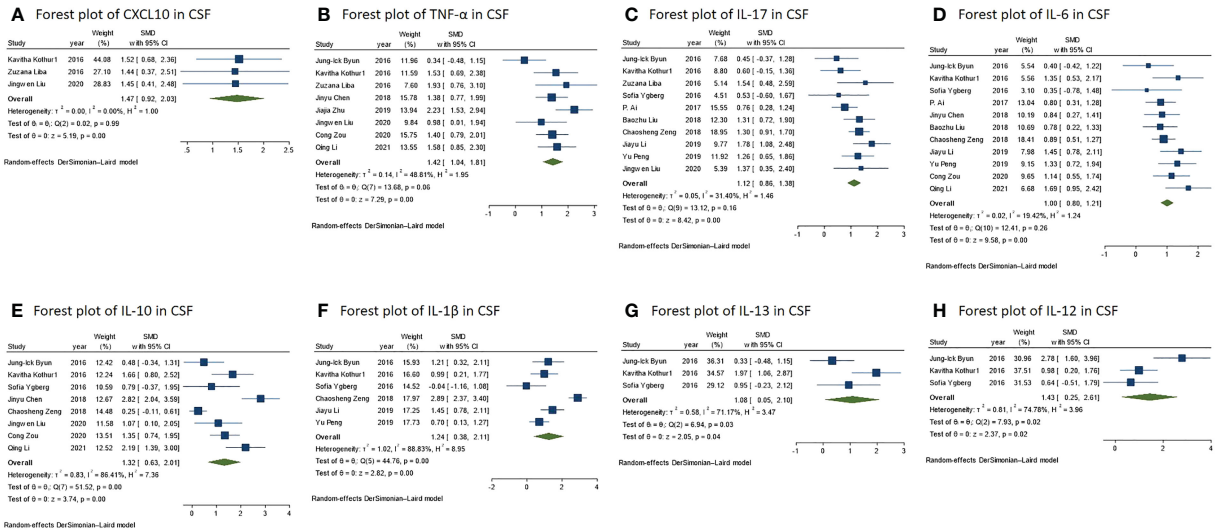


FIGURE 3
**(A)** Forest plot for the meta-analysis of the CXCL10 level in the CSF of NMDAR-E vs. control. **(B)** Forest plot for the meta-analysis of the TNF-α level in the CSF of NMDAR-E vs. control. **(C)** Forest plot for the meta-analysis of the IL-17 level in the CSF of NMDAR-E vs. control. **(D)** Forest plot for the meta-analysis of the IL-12 level in the CSF of NMDAR-E vs. control. **(E)** Forest plot for the meta-analysis of the IL-10 level in the CSF of NMDAR-E vs. control. **(F)** Forest plot for the meta-analysis of the IL-1β level in the CSF of NMDAR-E vs. control. **(G)** Forest plot for the meta-analysis of the IL-13 level in the CSF of NMDAR-E vs. control. **(H)** Forest plot for the meta-analysis of the IL-12 level in the CSF of NMDAR-E vs. control. CSF, cerebrospinal fluid; NMDAR-E, anti-N-methyl-D-aspartate receptor encephalitis, CXCL, C-X-C motif ligand; TNF, tumor necrosis factor; IL, interleukin.

antibody detection (54). Interestingly, in a prior validation study of a commercial diagnostic kit based on indirect immunofluorescence on transfected cells, a false-positive rate of 1.4% has been reported for the application of serum and cell-based assay (55). When autoantibodies are detected only in the serum, confirmatory tests (e.g., *in vivo* neuronal or tissue immunohistochemistry) should be included (2). However, those people might not require immunotherapy. However, in cases of false-positive antibody tests in the serum and delayed presence in the CSF, it could be necessary to perform a CSF antibody screening and tissue-based assay (2). For patients who are antibody negative but probably suffering from autoimmune encephalitis, novel biomarkers should be explored to aid in proper diagnosis.

B-cell responses have been reported to play a crucial role in the establishment of an NMDAR-E mouse model, according to the different previous studies (11, 19, 56), and its pathogenic mechanism cannot be separated from the involvement of selected cytokines/chemokines. CXCL13, also known as B-lymphocyte chemokine, can effectively recruit B cells into the CNS in NMDAR-E (20, 29, 57). Thereafter, IL-6 together with BAFF and APRIL can exert common and complementary functions in promoting survival, differentiation, and secretion of pathogenic IgG autoantibodies (58, 59). The findings of the meta-analysis indicated that high concentrations of CXCL13, BAFF, and IL-6 in the CSF can effectively lead to the enrichment and activation of B cells in the CNS producing more IgG antibodies, which could explain the reported observations about a higher detection rate of antibodies in the CSF in comparison to that in the serum in NMDAR-E (11, 60). Several selected studies have also shown that high concentrations of

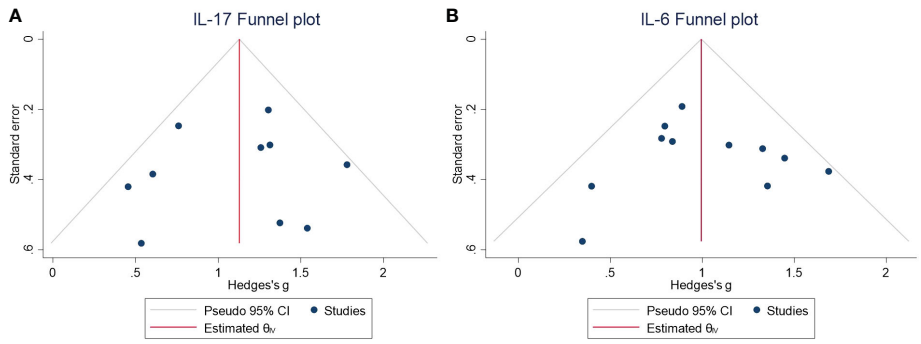


FIGURE 4
**(A)** Funnel plot for the meta-analysis of the IL-17 level in the CSF of NMDAR-E vs. control. **(B)** Funnel plot for the meta-analysis of the IL-6 level in the CSF of NMDAR-E vs. control. CSF, cerebrospinal fluid; NMDAR-E, anti-N-methyl-D-aspartate receptor encephalitis; IL, interleukin; CI, confidence interval.

CXCL13, BAFF, and APRIL in the CSF were related to poor prognosis (29, 32, 61).

The pathological results in mice showed the infiltration of T cells, B cells, and other immune cells into the CNS (11, 62, 63). In NMDAR-E patients, we found that T cells also play a key role in regulating immune pathogenesis by not only assisting B cells to mature and effectively differentiate into plasma cells secreting specific antibodies resulting in specific neuron lesions associated with the extracellular GluN1 subunit but also forming nonspecific inflammatory responses with other immune cells (10, 13). In addition, the various cytokines/chemokines associated with T lymphocytes that were found to be elevated in our meta-analysis also indicated that T cells can play a key role in NMDAR-E. The different immune cells infiltrating into the CNS can stimulate and constrain each other by secreting diverse cytokines/chemokines, thus forming a complex network of action (64, 65).

It has been found that with the help of Th1 and Th2 axis-related cytokines, CD4+ T cells can differentiate into Th1 and Th2, thus maintaining immune regulation homeostasis (66–68). When the Th1/Th2 cell balance is disrupted, Th1 cells can secrete several pro-inflammatory cytokines to further promote inflammation (69, 70). Interestingly, based on the results of our meta-analysis, effect sizes of Th1-related cytokines were significantly higher than those of cytokines that were Th2 cell related, thus indicating that the Th1/Th2 ratio was imbalanced in NMDAR-E patients. The chemokine CXCL10 can recruit Th1 cells to produce IFN-γ and TNF-α, which can further promote the release of varied cytokines/chemokines and enhance the humoral immune response in the CNS, thus increasing the persistence of the immune response in NMDAR-E (41). IL-17 can damage the integrity of the blood–brain barrier by downregulating the tight junction molecules and promoting astrocytes secreting chemokines that can attract neutrophils to the endothelium (63, 71). Moreover, previous studies have reported that Th17 cells and their secreted IL-17 are pathogenic in multiple sclerosis (MS) patients (48). For NMDAR-E, IL-6 and IL-17 can enhance the differentiation and maturation of Th17 cells and B cells, which can release a variety of cytokines to further enhance the immune response and aggravate the inflammatory response, with IL-17 being associated with poor prognosis (30, 36). In addition, further investigations are needed to evolve novel strategies to target Th17 cells and their associated cytokines and to establish whether they can be used for treatment and improve the prognosis. Treg cells are known for reducing immune responses and tissue damage by encouraging macrophages to secrete IL-10 through the release of IL-13 and for phagocytosing apoptotic cells. The study showed that IL-10 was positively related to the modified Rankin scale (mRS) score in NMDAR-E (41, 72, 73).

In the CNS and peripheral blood of NMDAR-E patients, there are also a large number of immune cells that can generate various cytokines and chemokines. Once the inflammatory response is triggered, a series of immune cells such as endothelial cells, astrocytes, and myeloid cells produce different pro-inflammatory cytokines IL-6, IL-17, and TNF-α, which can synergistically aggravate the inflammatory response (74–76). Furthermore, prior studies in mouse models have revealed that autoimmune antibodies can activate both astrocytes and microglia, and then these cells can release cytokines such as IL-1β and IL-12 to promote the epileptic occurrence and enhance the immune effects of Th1 cells (77, 78). In addition, activated follicular helper T cells and follicular dendritic cells can release CXCL13 to promote the immune response (18). These immune cells can facilitate inflammation, especially in the early stages of autoimmune encephalitis (30, 31).

In conclusion, the stimulation of the central immune response in NMDAR-E is primarily a process of immune disorders mediated by multiple immune cells composed of B cells, Th1 cells, Th17 cells, Treg cells, and related cytokines/chemokines. Th1 cells (related to CXCL10, IFN-g, TNF-a) and Th17 cells (related to IL-17, IL-6), which play key roles in promoting inflammation and promoting B-cell differentiation to plasma cells. Further research should aim to explore the immune pathogenesis process and identify novel immunotherapeutic targets to reduce recurrence and improve prognosis.

## 5 Limitations

This meta-analysis has several limitations. First, as the results of only a small number of studies have been included for each cytokine/chemokine, subgroup meta-analyses could not be conducted, and a meta-regression to explain the high heterogeneity of some of the selected cytokines/chemokines was not carried out. Second, for the meta-analysis of several cytokines/chemokines, only three studies were included, and hence, the results lack robustness. Third, since access to the laboratory data and cytokine results for the individual patient was not available, there may have been several cases with negative CSF anti-NMDA antibodies among the included studies in this meta-analysis. In conclusion, we suggest that multicenter approaches may be necessary to analyze the function of different cytokines/chemokines in the pathogenesis of NMDAR-E.

## Data availability statement

The original contributions presented in the study are included in the article/Supplementary Material. Further inquiries can be directed to the corresponding authors.

## Author contributions

YM performed the literature search, analyzed most of the data, and drafted the manuscript. JW analyzed part of the data and wrote the manuscript. SG designed the analyses. ZM analyzed part of the data. YR searched the literature. YX interpreted the results. MW conceived the idea, edited the manuscript, and selected the publication. All authors contributed to the article and approved the submitted version.

## Funding

This work was supported by the Natural Science Foundation of Sichuan Province(Grant Number 2022NSFSC1504).

## Conflict of interest

The authors declare that the research was conducted in the absence of any commercial or financial relationships that could be construed as a potential conflict of interest.

## Publisher's note

All claims expressed in this article are solely those of the authors and do not necessarily represent those of their affiliated organizations, or those of the publisher, the editors and the reviewers. Any product that may be evaluated in this article, or claim that may be made by its manufacturer, is not guaranteed or endorsed by the publisher.

## Supplementary material

The Supplementary Material for this article can be found online at: https://www.frontiersin.org/articles/10.3389/fimmu.2022.1064007/full#supplementary-material

## References


1. Dalmau J, Graus F. Antibody-mediated encephalitis. *New Engl J Med* (2018) 378:840–51. doi: 10.1056/NEJMra1708712

2. Graus F, Titulaer MJ, Balu R, Benseler S, Bien CG, Cellucci T, et al. A clinical approach to diagnosis of autoimmune encephalitis. *Lancet Neurol* (2016) 15:391–404. doi: 10.1016/S1474-4422(15)00401-9

3. Seery N, Butzkueven H, O'Brien TJ, Monif M. Contemporary advances in anti-NMDAR antibody (Ab)-mediated encephalitis. *Autoimmun Rev* (2022) 21:103057. doi: 10.1016/j.autrev.2022.103057

4. Steriade C, Britton J, Dale RC, Gadoth A, Irani SR, Linnoila J, et al. Acute symptomatic seizures secondary to autoimmune encephalitis and autoimmune-associated epilepsy: Conceptual definitions. *Epilepsia* (2020) 61:1341–51. doi: 10.1111/epi.16571

5. Pollak TA, Lennox BR, Müller S, Benros ME, Prüss H, Tebartz van Elst L, et al. Autoimmune psychosis: an international consensus on an approach to the diagnosis and management of psychosis of suspected autoimmune origin. *Lancet Psychiatry* (2020) 7:93–108. doi: 10.1016/S2215-0366(19)30290-1

6. Dalmau J, Tuzun E, Wu HY, Masjuan J, Rossi JE, Voloschin A, et al. Paraneoplastic anti-N-methyl-D-aspartate receptor encephalitis associated with ovarian teratoma. *Ann Neurol* (2007) 61:25–36. doi: 10.1002/ana.21050

7. Dalmau J, Lancaster E, Martinez-Hernandez E, Rosenfeld MR, Balice-Gordon R. Clinical experience and laboratory investigations in patients with anti-NMDAR encephalitis. *Lancet Neurol* (2011) 10:63–74. doi: 10.1016/S1474-4422(10)70253-2

8. Gresa-Arribas N, Titulaer MJ, Torrents A, Aguilar E, McCracken L, Leypoldt F, et al. Antibody titres at diagnosis and during follow-up of anti-NMDA receptor encephalitis: a retrospective study. *Lancet Neurol* (2014) 13:167–77. doi: 10.1016/S1474-4422(13)70282-5

9. Hansen H-C, Klingbeil C, Dalmau J, Li W, Weissbrich B, Wandinger K-P. Persistent intrathecal antibody synthesis 15 years after recovering from anti-N-methyl-D-aspartate receptor encephalitis. *JAMA Neurol* (2013) 70:117–9. doi: 10.1001/jamaneurol.2013.585

10. Martinez-Hernandez E, Horvath J, Shiloh-Malawsky Y, Sangha N, Martinez-Lage M, Dalmau J. Analysis of complement and plasma cells in the brain of patients with anti-NMDAR encephalitis. *Neurology* (2011) 77:589–93. doi: 10.1212/WNL.0b013e318228c136

11. Wagnon I, Helie P, Bardou I, Regnauld C, Lesec L, Leprince J, et al. Autoimmune encephalitis mediated by b-cell response against n-methyl-d-aspartate receptor. *Brain* (2020) 143:2957–72. doi: 10.1093/brain/awaa250

12. Hara M, Martinez-Hernandez E, Ariño H, Armangué T, Spatola M, Petit-Pedrol M, et al. Clinical and pathogenic significance of IgG, IgA, and IgM antibodies against the NMDA receptor. *Neurology* (2018) 90:e1386–94. doi: 10.1212/WNL.0000000000005329

13. Platt MP, Bolding KA, Wayne CR, Chaudhry S, Cutforth T, Franks KM, et al. Th17 lymphocytes drive vascular and neuronal deficits in a mouse model of postinfectious autoimmune encephalitis. *Proc Natl Acad Sci U.S.A.* (2020) 117:6708–16.

14. Tüzün E, Zhou L, Baehring JM, Bannykh S, Rosenfeld MR, Dalmau J. Evidence for antibody-mediated pathogenesis in anti-NMDAR encephalitis associated with ovarian teratoma. *Acta Neuropathol* (2009) 118:737–43. doi: 10.1007/s00401-009-0582-4

15. Hachiya Y, Uruha A, Kasai-Yoshida E, Shimoda K, Satoh-Shirai I, Kumada S, et al. Rituximab ameliorates anti-N-methyl-D-aspartate receptor encephalitis by removal of short-lived plasmablasts. *J neuroimmunol* (2013) 265:128–30. doi: 10.1016/j.jneuroim.2013.09.017

16. Dao LM, Machule ML, Bacher P, Hoffmann J, Ly LT, Wegner F, et al. Decreased inflammatory cytokine production of antigen-specific CD4(+) T cells in NMDA receptor encephalitis. *J Neurol* (2021) 268:2123–31. doi: 10.1007/s00415-020-10371-y

17. de Graaf MT, de Jongste AH, Kraan J, Boonstra JG, Sillevis Smitt PA, Gratama JW. Flow cytometric characterization of cerebrospinal fluid cells. *Cytometry Part B Clin cytometry* (2011) 80:271–81. doi: 10.1002/cyto.b.20603

18. Al-Diwani A, Theorell J, Damato V, Bull J, McGlashan N, Green E, et al. Cervical lymph nodes and ovarian teratomas as germinal centres in NMDA receptor-antibody encephalitis. *Brain* (2022) 145:2742–54. doi: 10.1093/brain/awac088

19. Jones BE, Tovar KR, Goehring A, Jalali-Yazdi F, Okada NJ, Gouaux E, et al. Autoimmune receptor encephalitis in mice induced by active immunization with conformationally stabilized holoreceptors. *Sci Transl Med* (2019) 11(500). doi: 10.1126/scitranslmed.aaw0044

20. Lin YT, Yang X, Lv JW, Liu XW, Wang SJ. CXCL13 is a biomarker of anti-Leucine-Rich glioma-inactivated protein 1 encephalitis patients. *Neuropsychiatr Dis Treat* (2019) 15:2909–15. doi: 10.2147/NDT.S222258

21. Wang R, Li S, Jia H, Si X, Lei Y, Lyu J, et al. Protective effects of cinnamaldehyde on the inflammatory response, oxidative stress, and apoptosis in liver of salmonella typhimurium-challenged mice. *Molecules* (2021) 26(8):2309. doi: 10.3390/molecules26082309

22. Borish LC, Steinke JW. 2. cytokines and chemokines. *J Allergy Clin Immunol* (2003) 111:S460–75. doi: 10.1067/mai.2003.108

23. Byun JI, Lee ST, Moon J, Jung KH, Sunwoo JS, Lim JA, et al. Distinct intrathecal interleukin-17/interleukin-6 activation in anti-n-methyl-d-aspartate receptor encephalitis. *J neuroimmunol* (2016) 297:141–7. doi: 10.1016/j.jneuroim.2016.05.023

24. Liba Z, Kayserova J, Elisak M, Marusic P, Nohejlova H, Hanzalova J, et al. Anti-N-methyl-D-aspartate receptor encephalitis: the clinical course in light of the chemokine and cytokine levels in cerebrospinal fluid. *J Neuroinflamm* (2016) 13:55. doi: 10.1186/s12974-016-0507-9

25. Jiang XY, Lei S, Zhang L, Liu X, Lin MT, Blumcke I, et al. Co-Expression of NMDA-receptor subunits NR1, NR2A, and NR2B in dysplastic neurons of teratomas in patients with paraneoplastic NMDA-receptor-encephalitis: a retrospective clinico-pathology study of 159 patients. *Acta Neuropathol Commun* (2020) 8(1):130. doi: 10.1186/s40478-020-00999-2

26. Wan X, Wang W, Liu J, Tong T. Estimating the sample mean and standard deviation from the sample size, median, range and/or interquartile range. *BMC Med Res Method* (2014) 14:135. doi: 10.1186/1471-2288-14-135

27. Luo D, Wan X, Liu J, Tong T. Optimally estimating the sample mean from the sample size, median, mid-range, and/or mid-quartile range. *Stat Methods Med Res* (2018) 27:1785–805. doi: 10.1177/0962280216669183

28. Saghazadeh A, Rezaei N. Central inflammatory cytokines in tuberculous meningitis: A systematic review and meta-analysis. *J Interferon Cytokine Res* (2022) 42:95–107. doi: 10.1089/jir.2021.0176

29. Leypoldt F, Höftberger R, Titulaer MJ, Armangue T, Gresa-Arribas N, Jahn H, et al. Investigations on CXCL13 in anti-N-methyl-D-aspartate receptor encephalitis: a potential biomarker of treatment response. *JAMA Neurol* (2015) 72:180–6. doi: 10.1001/jamaneurol.2014.2956

30. Kothur K, Wienholt L, Mohammad SS, Tantsis EM, Pillai S, Britton PN, et al. Utility of CSF Cytokine/Chemokines as markers of active intrathecal inflammation: Comparison of demyelinating, anti-NMDAR and enteroviral encephalitis. *PloS One* (2016) 11:e0161656. doi: 10.1371/journal.pone.0161656

31. Ygberg S, Fowler Å., Wickström R. Cytokine and chemokine expression in CSF may differentiate viral and autoimmune NMDAR encephalitis in children. *J Child Neurol* (2016) 31:1450–6. doi: 10.1177/0883073816653780

32. Deng B, Liu XN, Li X, Zhang X, Quan C, Chen XJ. Raised cerebrospinal fluid BAFF and APRIL levels in anti-n-methyl-d-aspartate receptor encephalitis: Correlation with clinical outcome. *J neuroimmunol* (2017) 305:84–91. doi: 10.1016/j.jneuroim.2017.01.012

33. Ai P, Zhang X, Xie Z, Liu G, Liu X, Pan S, et al. The HMGB1 is increased in CSF of patients with an anti-NMDAR encephalitis. *Acta neurol Scandinavica* (2018) 137:277–82. doi: 10.1111/ane.12850

34. Chen J, Ding Y, Zheng D, Wang Z, Pan S, Ji T, et al. Elevation of YKL-40 in the CSF of anti-NMDAR encephalitis patients is associated with poor prognosis. *Front Neurol* (2018) 9. doi: 10.3389/fneur.2018.00727

35. Liu B, Ai P, Zheng D, Jiang Y, Liu X, Pan S, et al. Cerebrospinal fluid pentraxin 3 and CD40 ligand in anti-n-menthyl-d-aspartate receptor encephalitis. *J neuroimmunol* (2018) 315:40–4. doi: 10.1016/j.jneuroim.2017.11.016

36. Zeng C, Chen L, Chen B, Cai Y, Li P, Yan L, et al. Th17 cells were recruited and accumulated in the cerebrospinal fluid and correlated with the poor prognosis of anti-NMDAR encephalitis. *Acta Biochim Biophys Sin* (2018) 50:1266–73. doi: 10.1093/abbs/gmy137

37. Li J, Gu Y, An H, Zhou Z, Zheng D, Wang Z, et al. Cerebrospinal fluid light and heavy neurofilament level increased in anti-n-methyl-d-aspartate receptor encephalitis. *Brain Behav* (2019) 9:e01354. doi: 10.1002/brb3.1354

38. Peng Y, Liu B, Pei S, Zheng D, Wang Z, Ji T, et al. Higher CSF levels of NLRP3 inflammasome is associated with poor prognosis of anti-N-methyl-D-Aspartate receptor encephalitis. *Front Immunol* (2019) 10:905. doi: 10.3389/fimmu.2019.00905

39. Zhao J, Wang C, Zhang Y, Sun R, Wang H, Li G, et al. Elevated CHI3L1 and OPN levels in patients with anti-n-methyl-d-aspartate receptor encephalitis. *J neuroimmunol* (2019) 334:577005. doi: 10.1016/j.jneuroim.2019.577005

40. Zhu J, Li Y, Zheng D, Wang Z, Pan S, Yin J, et al. Elevated serum and cerebrospinal fluid CD138 in patients with anti-N-Methyl-d-Aspartate receptor encephalitis. *Front Mol Neurosci* (2019) 12:116. doi: 10.3389/fnmol.2019.00116

41. Liu J, Liu L, Kang W, Peng G, Yu D, Ma Q, et al. Cytokines/Chemokines: Potential biomarkers for non-paraneoplastic anti-N-Methyl-D-Aspartate receptor encephalitis. *Front Neurol* (2020) 11:582296. doi: 10.3389/fneur.2020.582296

42. Zou C, Pei S, Yan W, Lu Q, Zhong X, Chen Q, et al. Cerebrospinal fluid osteopontin and inflammation-associated cytokines in patients with anti-N-Methyl-D-Aspartate receptor encephalitis. *Front Neurol* (2020) 11:519692. doi: 10.3389/fneur.2020.519692

43. Li Q, Chen J, Yin M, Zhao J, Lu F, Wang Z, et al. High level of soluble CD146 in cerebrospinal fluid might be a biomarker of severity of anti-N-Methyl-D-Aspartate receptor encephalitis. *Front Immunol* (2021) 12:680424. doi: 10.3389/fimmu.2021.680424

44. Liao SH, Li CF, Bi XY, Guo HW, Qian Y, Liu XB, et al. Anti-neuron antibody syndrome: clinical features, cytokines/chemokines and predictors. *J Neuroinflamm* (2021) 18(1):282. doi: 10.1186/s12974-021-02259-z

45. Ma X, Chen C, Fang L, Zhong X, Chang Y, Li R, et al. Dysregulated CD40 and CD40 ligand expression in anti-n-methyl-d-aspartate receptor encephalitis. *J neuroimmunol* (2022) 362:577762. doi: 10.1016/j.jneuroim.2021.577762

46. Kimura A, Yoshikura N, Koumura A, Hayashi Y, Inuzuka T. B-cell-activating factor belonging to the tumor necrosis factor family (BAFF) and a proliferation-inducing ligand (APRIL) levels in cerebrospinal fluid of patients with meningoencephalitis. *J Neurol Sci* (2015) 352:79–83. doi: 10.1016/j.jns.2015.03.036

47. Ulusoy C, Tuzun E, Kurtuncu M, Turkoglu R, Akman-Demir G, Eraksoy M. Comparison of the cytokine profiles of patients with neuronal-Antibody-Associated central nervous system disorders. *Int J Neurosci* (2012) 122:284–9. doi: 10.3109/00207454.2011.648762

48. Kunkl M, Frascolla S, Amormino C, Volpe E, Tuosto L. T Helper cells: The modulators of inflammation in multiple sclerosis. *Cells* (2020) 9(2):482. doi: 10.3390/cells9020482

49. Krishnarajah S, Becher B. $T_H$ Cells and cytokines in encephalitogenic disorders. *Front Immunol* (2022) 13:822919. doi: 10.3389/fimmu.2022.822919

50. Niu Y, Zhou Q. Th17 cells and their related cytokines: vital players in progression of malignant pleural effusion. *Cell Mol Life Sci* (2022) 79:194. doi: 10.1007/s00018-022-04227-z

51. Jan S, Anilkumar AC. Atypical brain MRI findings in a child with delayed diagnosis of anti-N-Methyl-D-Aspartate receptor encephalitis. *Cureus* (2021) 13:e18103. doi: 10.7759/cureus.18103

52. Boesen MS, Born AP, Lydolph MC, Blaabjerg M, Børresen ML. Pediatric autoimmune encephalitis in Denmark during 2011-17: A nationwide multicenter population-based cohort study. *Eur J Paediatr Neurol* (2019) 23:639–52. doi: 10.1016/j.ejpn.2019.03.007

53. Warren N, Flavell J, O'Gorman C, Swayne A, Blum S, Kisely S, et al. Screening for anti-NMDAR encephalitis in psychiatry. *J Psychiatr Res* (2020) 125:28–32. doi: 10.1016/j.jpsychires.2020.03.007

54. Blackman G, Lim MF, Pollak T, Al-Diwani A, Symmonds M, Mazumder A, et al. The clinical relevance of serum versus CSF NMDAR autoantibodies associated exclusively with psychiatric features: a systematic review and meta-analysis of individual patient data. *J Neurol* (2022) 269:5302–11. doi: 10.1007/s00415-022-11224-6

55. Ruiz-García R, Muñoz-Sánchez G, Naranjo L, Guasp M, Sabater L, Saiz A, et al. Limitations of a commercial assay as diagnostic test of autoimmune encephalitis. *Front Immunol* (2021) 12:691536. doi: 10.3389/fimmu.2021.691536

56. Dalmau J, Armangué T, Planagumà J, Radosevic M, Mannara F, Leypoldt F, et al. An update on anti-NMDA receptor encephalitis for neurologists and psychiatrists: mechanisms and models. *Lancet Neurol* (2019) 18:1045–57. doi: 10.1016/S1474-4422(19)30244-3

57. Masouris I, Klein M, Ködel U. The potential for CXCL13 in CSF as a differential diagnostic tool in central nervous system infection. *Expert Rev anti-infective Ther* (2020) 18:875–85. doi: 10.1080/14787210.2020.1770596

58. Mohd Jaya FN, Garcia SG, Borràs FE, Chan GCF, Franquesa M. Paradoxical role of breg-inducing cytokines in autoimmune diseases. *J Trans Autoimmun* (2019) 2:100011. doi: 10.1016/j.jtauto.2019.100011

59. Zidan AA, Al-Hawwas M, Perkins GB, Mourad GM, Stapledon CJM, Bobrovskaya L, et al. Characterization of urine stem cell-derived extracellular vesicles reveals b cell stimulating cargo. *Int J Mol Sci* (2021) 22(1):459. doi: 10.3390/ijms22010459

60. Titulaer MJ, McCracken L, Gabilondo I, Armangué T, Glaser C, Iizuka T, et al. Treatment and prognostic factors for long-term outcome in patients with anti-NMDA receptor encephalitis: an observational cohort study. *Lancet Neurol* (2013) 12:157–65. doi: 10.1016/S1474-4422(12)70310-1

61. Smulski CR, Eibel H. BAFF and BAFF-receptor in b cell selection and survival. *Front Immunol* (2018) 9:2285. doi: 10.3389/fimmu.2018.02285

62. Pan H, Oliveira B, Saher G, Dere E, Tapken D, Mitjans M, et al. Uncoupling the widespread occurrence of anti-NMDAR1 autoantibodies from neuropsychiatric disease in a novel autoimmune model. *Mol Psychiatry* (2019) 24:1489–501. doi: 10.1038/s41380-017-0011-3

63. Borst K, Dumas AA, Prinz M. Microglia: Immune and non-immune functions. *Immunity* (2021) 54:2194–208. doi: 10.1016/j.immuni.2021.09.014

64. Ransohoff RM, Brown MA. Innate immunity in the central nervous system. *J Clin Invest* (2012) 122:1164–71. doi: 10.1172/JCI58644

65. Kenney MJ, Ganta CK. Autonomic nervous system and immune system interactions. *Compr Physiol* (2014) 4:1177–200. doi: 10.1002/cphy.c130051

66. Dong C. Cytokine regulation and function in T cells. *Annu Rev Immunol* (2021) 39:51–76. doi: 10.1146/annurev-immunol-061020-053702

67. Zhu J, Yamane H, Paul WE. Differentiation of effector CD4 T cell populations (*). *Annu Rev Immunol* (2010) 28:445–89. doi: 10.1146/annurev-immunol-030409-101212

68. Kidd P. Th1/Th2 balance: the hypothesis, its limitations, and implications for health and disease. *Altern Med review: J Clin Ther* (2003) 8:223–46.

69. Nath B, Vandna HM, Prasad M, Kumar S. Evaluation of Japanese encephalitis virus e and NS1 proteins immunogenicity using a recombinant Newcastle disease virus in mice. *Vaccine* (2020) 38:1860–8. doi: 10.1016/j.vaccine.2019.11.088

70. Kothur K, Wienholt L, Brilot F, Dale RC. CSF cytokines/chemokines as biomarkers in neuroinflammatory CNS disorders: A systematic review. *Cytokine* (2016) 77:227–37. doi: 10.1016/j.cyto.2015.10.001

71. Huppert J, Closhen D, Croxford A, White R, Kulig P, Pietrowski E, et al. Cellular mechanisms of IL-17-induced blood-brain barrier disruption. *FASEB J* (2010) 24:1023–34. doi: 10.1096/fj.09-141978

72. Rubtsov YP, Rasmussen JP, Chi EY, Fontenot J, Castelli L, Ye X, et al. Regulatory T cell-derived interleukin-10 limits inflammation at environmental interfaces. *Immunity* (2008) 28:546–58. doi: 10.1016/j.immuni.2008.02.017

73. Proto JD, Doran AC, Gusarova G, Yurdagul AJr., Sozen E, Subramanian M, et al. Regulatory T cells promote macrophage efferocytosis during inflammation resolution. *Immunity* (2018) 49:666–677.e6. doi: 10.1016/j.immuni.2018.07.015

74. Campuzano O, Castillo-Ruiz MM, Acarin L, Castellano B, Gonzalez B. Increased levels of proinflammatory cytokines in the aged rat brain attenuate injury-induced cytokine response after excitotoxic damage. *J Neurosci Res* (2009) 87:2484–97. doi: 10.1002/jnr.22074

75. Tsantikos E, Oracki SA, Quilici C, Anderson GP, Tarlinton DM, Hibbs ML. Autoimmune disease in Lyn-deficient mice is dependent on an inflammatory environment established by IL-6. *J Immunol* (2010) 184:1348–60. doi: 10.4049/jimmunol.0901878

76. Pilotto A, Masciocchi S, Volonghi I, De Giuli V, Caprioli F, Mariotto S, et al. Severe acute respiratory syndrome coronavirus 2 (SARS-CoV-2) encephalitis is a cytokine release syndrome: Evidences from cerebrospinal fluid analyses. *Clin Infect Dis* (2021) 73:e3019–26. doi: 10.1093/cid/ciaa1933

77. Taraschenko O, Fox HS, Zekeridou A, Pittock SJ, Eldridge E, Farukhuddin F, et al. Seizures and memory impairment induced by patient-derived anti-N-methyl-D-aspartate receptor antibodies in mice are attenuated by anakinra, an interleukin-1 receptor antagonist. *Epilepsia* (2021) 62:671–82. doi: 10.1111/epi.16838

78. Holz K, Prinz M, Brendecke SM, Hölscher A, Deng F, Mitrücker H-W, et al. Differing outcome of experimental autoimmune encephalitis in Macrophage/Neutrophil- and T cell-specific gp130-deficient mice. *Front Immunol* (2018) 9:836. doi: 10.3389/fimmu.2018.00836

frontiers | Frontiers in Immunology

TYPE Brief Research Report
PUBLISHED 03 March 2023
DOI 10.3389/fimmu.2023.1090548



OPEN ACCESS

EDITED BY
Shougang Guo,
Shandong Provincial Hospital, China

REVIEWED BY
Wioleta Zelek,
Cardiff University, United Kingdom
Yoshiki Takai,
Tohoku University Hospital, Japan

*CORRESPONDENCE
Norimitsu Inoue
inoue-no@wakayama-med.ac.jp

SPECIALTY SECTION
This article was submitted to Multiple Sclerosis and Neuroimmunology, a section of the journal Frontiers in Immunology

RECEIVED 05 November 2022
ACCEPTED 20 February 2023
PUBLISHED 03 March 2023

CITATION
Miyamoto K, Minamino M, Kuwahara M, Tsujimoto H, Ohtani K, Wakamiya N, Katayama K, Inoue N and Ito H (2023) Complement biomarkers reflect the pathological status of neuromyelitis optica spectrum disorders.
*Front. Immunol.* 14:1090548.
doi: 10.3389/fimmu.2023.1090548



# Complement biomarkers reflect the pathological status of neuromyelitis optica spectrum disorders

Katsuichi Miyamoto[1,2], Mai Minamino[1], Motoi Kuwahara[2], Hiroshi Tsujimoto[3], Katsuki Ohtani[4], Nobutaka Wakamiya[5], Kei-ichi Katayama[3], Norimitsu Inoue[3]* and Hidefumi Ito[1]

[1]Department of Neurology, Wakayama Medical University, Wakayama, Japan, [2]Department of Neurology, Kindai University School of Medicine, Osaka-sayama, Japan, [3]Department of Molecular Genetics, Wakayama Medical University, Wakayama, Japan, [4]Department of Clinical Nutrition, Rakuno Gakuen University, Ebetsu, Japan, [5]Department of Medicine and Physiology, Rakuno Gakuen University, Ebetsu, Japan

Complement is involved in the pathogenesis of neuroimmune disease, but the detailed pathological roles of the complement pathway remain incompletely understood. Recently, eculizumab, a humanized anti-C5 monoclonal antibody, has been clinically applied against neuroimmune diseases such as myasthenia gravis and neuromyelitis optica spectrum disorders (NMOSD). Clinical application of eculizumab is also being investigated for another neuroimmune disease, Guillain-Barré syndrome (GBS). However, while the effectiveness of eculizumab for NMOSD is extremely high in many cases, there are some cases of myasthenia gravis and GBS in which eculizumab has little or no efficacy. Development of effective biomarkers that reflect complement activation in these diseases is therefore important. To identify biomarkers that could predict disease status, we retrospectively analyzed serum levels of complement factors in 21 patients with NMOSD and 25 patients with GBS. Ba, an activation marker of the alternative complement pathway, was elevated in the acute phases of both NMOSD and GBS. Meanwhile, sC5b-9, an activation marker generated by the terminal complement pathway, was elevated in NMOSD but not in GBS. Complement factor H (CFH), a complement regulatory factor, was decreased in the acute phase as well as in the remission phase of NMOSD, but not in any phases of GBS. Together, these findings suggest that complement biomarkers, such as Ba, sC5b-9 and CFH in peripheral blood, have potential utility in understanding the pathological status of NMOSD.

KEYWORDS

**neuromyelitis optica spectrum disorders, Guillain-Barré syndrome, complement, alternative pathway, sC5b-9, CFH, Ba**

# Introduction

The complement system plays important roles in the innate immune system, which protects the body from foreign pathogens (1). However, when the regulatory mechanisms of complement activation are disrupted, dysregulated complement activation damages autologous cells and causes diseases such as paroxysmal nocturnal hemoglobinuria (PNH) and atypical hemolytic uremic syndrome (aHUS) (2, 3). Eculizumab, a humanized anti-C5 monoclonal antibody, is effective against PNH and aHUS (3). It specifically inhibits production of anaphylatoxin C5a and subsequent formation of the membrane attack complex (MAC), suppressing pathological complement activation. Its effectivity has been shown against neuroimmune diseases such as myasthenia gravis (MG) and neuromyelitis optica spectrum disorders (NMOSD) (4).

In MG (5) and NMOSD (6, 7), autoantibodies against acetylcholine receptor and aquaporin-4 (AQP4), respectively, activate the complement system, causing neurological symptoms due to destruction of the nervous system by the terminal complement pathway. Eculizumab is effective against these diseases and has been clinically applied (8, 9). Guillain-Barré syndrome (GBS) is also a neuroimmune disease, in which anti-ganglioside autoantibodies are produced after infection with *Campylobacter jejuni* or other organisms, and damage to the myelin sheath causes peripheral neuropathy (10). Clinical application of eculizumab for GBS is currently under investigation (11). Although eculizumab is effective in MG and GBS, some cases are non-responders, and the basis for non-response is unknown (4).

In these diseases, autoantibody titers do not correlate with disease pathology, and accurate biomarkers for complement activation could be useful not only in determining disease severity, but also in determining the potential utility of anti-complement drugs. However, biomarkers that accurately reflect complement activation in the pathogenesis of neurological diseases have not yet been identified. NMOSD and GBS are characterized by activation of the classical complement pathway. In the present retrospective cohort study, however, we measured serum levels of complement-activated markers and complement regulators involved in the alternative or terminal complement pathway in NMOSD and GBS for three reasons. First, eculizumab, which blocks the C5 cleavage involved in the initiation of the terminal complement pathway, is effective in these diseases, so activation of the alternative complement pathway and the formation of MAC in the terminal complement pathway would be expected to cause development of these diseases. Second, although the autoantibodies in NMOSD constantly exist in blood and may always activate the classical complement pathway, symptoms of NMOSD appear suddenly and recurrently, suggesting that the appearance of symptoms requires further complement activation by the alternative complement pathway in addition to the classical complement pathway. Third, in transplant-associated thrombotic microangiopathy (TA-TMA), which is thought to be a disease involving the classical and lectin complement pathways, our group previously demonstrated that abnormally high levels of plasma complement factor Ba fragment (Ba), a biomarker of activation of the alternative pathway, can be used to predict TA-TMA development and non-relapse mortality (12). We examined whether biomarkers that predict activation of the alternative and terminal complement pathways could therefore also be associated with disease pathogenesis, prognosis, and status.

# Methods

## Patients and healthy controls

Patients with NMOSD and GBS treated at Wakayama Medical University Hospital or Kindai University Hospital between 2016 and 2021 were included, and cases with both acute- and remission-paired sera archived were retrospectively selected and enrolled. Medical information was collected from medical charts. Diagnostic criteria were the 2015 international diagnostic criteria for NMOSD (13) and the Asberry diagnostic criteria for GBS (14). Seventy healthy Japanese adults, consisting of 35 males (age, mean ± SD: 45.7± 10.3 years; range: 26-68 years) and 35 females (age, mean ± SD: 44.7± 12.3 years; range: 27-75 years) were enrolled as healthy controls (15).

## Definitions of acute and remission phases of NMOSD

NMOSD relapse was defined based on criteria from previous clinical studies (8). Briefly, new onset or worsening neurologic symptoms must persist >24 hours and should not be attributable to confounding clinical factors. Remission was defined as a period when neurologic symptoms were stable for at least one month, and no new lesions shown on MRI imaging.

## Evaluation of acute and remission phases of GBS

The acute phase of GBS was defined as the peak of symptoms prior to treatment. The stable phase was defined as a time when symptoms became mild and stable following treatment. Disabilities were evaluated using the Hughes functional grade scale (11).

## Measurement of anti-AQP4 and anti-ganglioside antibodies

Anti-AQP4 antibodies titers were analyzed using a cell-based assay with live human embryonic kidney 293 cells stably transfected with the M23 isoform of AQP4. Goat anti-human IgG Fc labelled with DyLight 488 (Thermo Fisher Scientific, Waltham, MA) was used as a secondary antibody after the transfected cells were exposed to the patients' diluted sera. Anti-ganglioside antibodies were examined by ELISA. Serum IgG antibodies to 11 glycolipid

antigens (GM1, GM2, GM3, GD1a, GD1b, GD3, GT1b, GQ1b, GT1a, Gal-C, and GalNAc-GD1a) were analyzed.

## Complement measurement

Serum samples obtained from patients and healthy controls were stocked until analysis at -80°C. Serum levels of sC5b-9 and Ba were measured using MicroVue SC5b-9 Plus EIA and MicroVue Ba EIA, respectively (Quidel, San Diego, CA). Serum levels of complement factor H (CFH) and complement factor I (CFI) were measured using ELISA kits (Abnova, Taipei, Taiwan). Complement data from 70 healthy Japanese volunteers (age: 26–75 years) were used as healthy controls, and reference ranges of complement markers (average levels ± 2 S.D.) in their serum were defined as previously described (15). The normal ranges of serum for sC5b-9 and Ba have been found to be greater than that of EDTA plasma, but the ranges in serum stored at -80 °C until analysis confirmed stability, even after five freeze-thaw cycles. In the present study, we compared the patients data with previous data of 70 healthy Japanese adults as controls.

## Statistical analysis

Statistically significant differences were evaluated between three groups (healthy controls, patients with NMOSD and patients with GBS) using a one-way analysis of variance (ANOVA) and a Tukey-Kramer test as a *post hoc* test, and between two groups (the acute and remission phases) using a paired t-test. $P < 0.05$ (two-tailed) was considered significant for all results. Pearson correlation analysis was performed using JMP pro 16.0 software.

# Results

We retrospectively analyzed 21 patients with NMOSD (19 females and 2 males) and 25 patients with GBS (14 females and 11 males) (Table 1). The mean age at the time of blood collection in the acute phase of NMOSD was 48.0 years, mean duration of illness was 5.1 years, and mean expanded disability status scale (EDSS) was 5.3. Mean EDSS during NMOSD remission was 4.5. The mean age at GBS onset was 50.8 years, and the mean severity of illness was Hughes functional grade scale 3.4. Mean Hughes functional grade scale during the remission phase of GBS (at discharge) was 1.7. Anti-AQP4 and anti-glycolipid autoantibodies were positive in 81% patients with NMOSD and 88% patients with GBS, respectively.

sC5b-9, an activation marker generated by the terminal complement pathway, was significantly higher in the acute phase of NMOSD compared with in the acute phase of GBS (Figure 1A). Activation of the complement system was thus indicated to have progressed to the terminal complement pathway in the acute phase of NMOSD. Serum Ba, an activation marker of the alternative complement pathway, was also higher in the acute phases of both NMOSD and GBS compared with healthy controls (Figure 1A).

Subsequently, we measured complement regulatory protein levels in NMOSD and GBS. CFH was within the reference range but significantly lower in patients with NMOSD than in healthy controls or in patients with GBS (Figure 1A). However, CFI, another complement regulatory protein, was higher in patients with NMOSD and in patients with GBS than in healthy controls.

To determine the correlations of these biomarkers with each other in NMOSD, we performed a correlation analysis (Figure 1B). Ba and sC5b-9 levels (r=0.824, $p<0.00010$), and CFH and CFI levels (r=-0.554, $p=0.0092$) showed positive and

TABLE 1 Patient backgrounds.

| | | NMOSD (n = 21) | GBS (n = 25) | *p*-values |
|---|---|---|---|---|
| Sex (female/male) | | 19/2 | 14/11 | < 0.01 |
| Age, mean ± SD [range] (y) | | 48.0 ± 2.5 [17–74] | 50.8 ± 4.4 [14–77] | NS |
| Disease duration, mean ± SD [range] (y) | | 5.1 ± 1.2 [0–14] | NA | |
| Anti-aquaporin 4 antibody-positive | | 17 (81%) | NA | |
| Anti-glycolipid antibody-positive | | NA | 22 (88%) | |
| Lesions according to MRI findings | Optic nerve | 4 (19.0%) | NA | |
| | Spinal cord | 17 (81.0%) | NA | |
| | Brain | 2 (9.5%) | NA | |
| EDSS, Mean ± SD [range] | Acute phase | 5.3 ± 2.1 [2–8.5] | NA | |
| | Remission | 4.5 ± 2.2 [2–8.0] | NA | |
| Functional grade, Mean ± SD (AU) | Acute phase | NA | 3.4 ± 1.0 | |
| | Remission | NA | 1.7 ± 0.8 | |

NMOSD, neuromyelitis optica spectrum disorders; GBS, Guillain-Barré syndrome; SD, standard deviation; EDSS, expanded disability status scale; MRI, magnetic resonance imaging; NA, not applicable; NS, not significant.

10.3389/fimmu.2023.1090548

negative correlations, respectively. However, no other correlations were detected in samples obtained from patients in the acute phase of NMOSD.

The above-mentioned complement factors examined in the acute phase were also analyzed for changes in the remission phase. The main laboratory data did not change between the acute and remission phases (Table 2). The sC5b-9 and Ba markers, which were elevated in the acute phase of NMOSD, decreased significantly in the remission phase (Figure 2). Although CFH levels were increased in the remission phase of 12 patients with NMOSD, the average levels of CFH still remained lower than the healthy control level during the remission phase as well as during the acute phase. Moreover, in some patients, CFH levels were markedly reduced in the remission phase. The levels of CFI were decreased in 10 patients in the remission phase of NMOSD, but the average levels of CFI were still higher than those of healthy controls during the remission phase. To rule out these changes of complement markers being due to previously-received treatments, we analyzed complement markers in 10 patients that had not received any treatment at the time of the first-episode of NMOSD and obtained similar results (Supplementary Table 1, Supplementary Figures 1, 2). However, in patients with GBS, sC5b-9, Ba, CFH, and CFI did not change between the acute and remission phases, and Ba and CFI in the remission phase remained higher than those in the healthy controls (Figure 2).

We detected no correlations between levels of complement markers and most of the clinical manifestations, disease severity, or cerebrospinal fluid test values in the acute phase of NMOSD. There was, however, a moderate positive correlation between levels of CFI and disease duration (r=0.520) (Supplementary Table 2).

## Discussion

In the present study, we measured serum levels of Ba, sC5b-9, CFH, and CFI in the acute and remission phases of NMOSD and GBS. In NMOSD, we identified that sC5b-9 and Ba levels correlated significantly with clinical stage, suggesting that activation of the alternative and terminal complement pathways contributes to exacerbation of NMOSD. The levels of sC5b-9 and Ba may be influenced by the types of treatments and whether they were obtained at the time of the first-episode or after some treatments, but similar results were also obtained in the 10 patients who had not received any treatment at the time of the first-episode. Furthermore, the increased levels of Ba and sC5b-9 were strongly correlated, suggesting that activation of the classical complement pathway by autoantibodies in the periphery led to activation of the alternative and terminal complement pathway. In addition to increased levels of C5a in cerebrospinal fluid that were previously reported as a biomarker of NMOSD (16), the present findings suggest that sC5b-9 and Ba levels in peripheral blood could be useful markers in determining whether NMOSD is in the active stage. NMOSD is known to be caused by injury to astrocytes which express AQP4 (17). Circulating anti-AQP4 antibodies must destroy the brain-blood barrier (BBB) in order to reach astrocytes. IL-6 (18), anti-glucose-regulated protein 78 autoantibodies (19), and polymorphonuclear leukocytes (20) have been reported to be

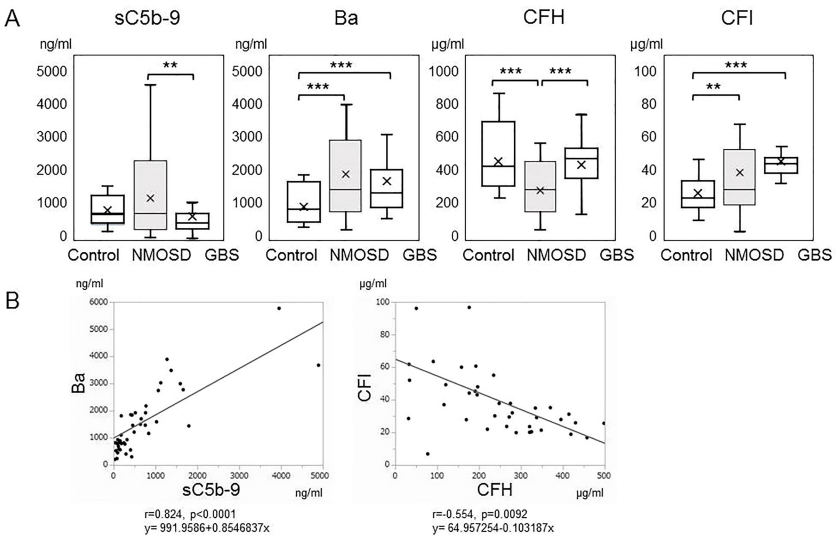


FIGURE 1
**(A)** Serum levels of complement markers in the acute phases of neuromyelitis optica spectrum disorders and Guillain-Barré syndrome. Serum levels of sC5b-9, Ba, complement factor H, and complement factor I in the acute phases of neuromyelitis optica spectrum disorders and Guillain-Barré syndrome, together with those of healthy controls, are shown by box plots. $^{**}p < 0.01$, and $^{***}p < 0.001$, ANOVA and Tukey-Kramer test as a *post hoc* test. **(B)** Correlation analysis of complement markers in the acute phase of neuromyelitis optica spectrum disorders. The relevance of serum levels of sC5b-9, Ba, complement factor H and complement factor I in the acute phase of neuromyelitis optica spectrum disorders were analyzed. Ba and sC5b-9 (r=0.824, $p$<0.00010), and complement factor H and complement factor I (r=-0.554, $p$=0.0092) showed positive and negative correlations, respectively.

10.3389/fimmu.2023.1090548

TABLE 2 Laboratory data and treatments of the patients with NMOSD.

| | Acute phase | Remission | *p*-values |
|---|---|---|---|
| **Blood Tests** | | | |
| White Blood Cells (/μL) | 7223 ± 2187 | 7499 ± 3132 | 0.912 |
| Neutrophils (/μL) | 5138 ± 2169 | 4803 ± 2735 | 0.849 |
| Lymphocytes (/μL) | 1420 ± 639 | 2019 ± 1527 | 0.364 |
| Monocytes (/μL) | 544 ± 354 | 548 ± 253 | 0.983 |
| Albumin (g/dL) | 4.2 ± 0.4 | 3.8 ± 0.6 | 0.807 |
| CRP (mg/dL) | 0.367 ± 0.666 | 0.199 ± 0.485 | 0.410 |
| **Cerebrospinal fluid test** | | | |
| Cell count (/mm$^3$) | 13.7 ± 28.7 | 3.0 ± 3.0 | 0.621 |
| Protein (mg/dL) | 46.8 ± 37.4 | 36.6 ± 20.7 | 0.144 |
| **Treatments at blood collection** | | | |
| None | 10 (47.6%) | 8 (38.1%) | |
| Steroids | 6 (28.6%) | 6 (28.6%) | |
| Immunosuppressants | 1 (4.8%) | 2 (9.5%) | |
| Steroids + Immunosuppressants | 3 (14.3%) | 4 (19.0%) | |
| Plasma exchange | 1 (4.8%) | 1 (4.8%) | |

Data are shown as mean ± standard deviation. CRP, C-reactive protein; NMOSD, neuromyelitis optica spectrum disorders.

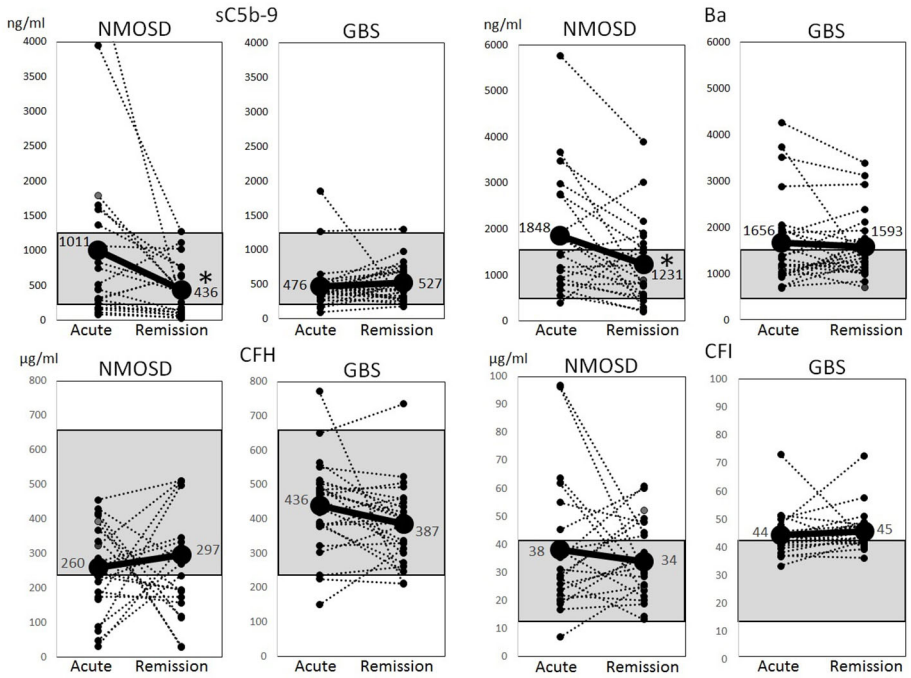


FIGURE 2
Changes of complement markers during the acute and remission phases of neuromyelitis optica spectrum disorders and Guillain-Barré syndrome. Changes of serum levels of sC5b-9, Ba, complement factor H and complement factor I during the acute and remission phases of neuromyelitis optica spectrum disorders and Guillain-Barré syndrome were analyzed. The dotted lines indicate changes in individual cases, and solid lines indicate changes in average levels. The gray shadow indicates reference ranges in healthy Japanese adults (sC5b-9: 181–1266 ng/ml, Ba: 438–1546 ng/ml, complement factor H: 238–663 μg/ml, complement factor I: 11–42 μg/ml) (15). *$p < 0.01$, paired t-test.

involved in the disruption of BBB. Complement activation in the periphery may also contribute to the destruction. The involvement of peripheral complement activation in the pathogenesis of NMOSD using animal models should be clarified in future studies.

CFH was decreased during both acute and remission phases of NMOSD. There are three possible reasons for these decreased levels. First, AQP4 is expressed not only in astrocytes, but also in muscle and renal tubules, and anti-AQP4 antibodies react with them to activate complement in the periphery. CFH may therefore be consumed and reduced in NMOSD to control activation of the complement system. In the present study, CFH levels in 12 patients were increased in the remission phase. A second possible reason for the decreased levels is that NMOSD could be originally caused in individuals with low CFH levels and activation of alternative and terminal complement pathways initiated by anti-AQP4 autoantibodies might not be adequately suppressed by low CFH levels. Eculizumab, which blocks the C5 cleavage involved in the initiation of the terminal complement pathway, is an effective treatment for almost all NMOSD cases with anti-AQP4 autoantibodies (8). In patients with NMOSD, low CFH levels may be a significant cause of complement activation in the periphery. A third possible reason for the decreased levels could be that CFH production may be suppressed by steroid or immunosuppressive therapies. In some patients, remarkably decreased levels of CFH were observed in the remission phase.

In NMOSD, modest increase of CFI levels was also observed, and the levels of CFH and CFI had negative correlation.We detected a moderate positive correlation between CFI levels and disease duration, so CFI may increase by inflammation induced in the acute phase to block activation of the complement system in the periphery.

In GBS, there were no significant differences in sC5b-9, Ba, CFH, or CFI levels between the acute and remission phases. In addition, in the acute phase of GBS, Ba was increased but sC5b-9 was unchanged, suggesting that activation of classical complement pathway by autoantibodies led to activation of the alternative pathway in the periphery, but did not progress to the terminal complement pathway. The levels of CFH and CFI remained high in both acute and remission phases of GBS, suggesting that their regulatory functions would be maintained. Therapies targeting complement pathways other than the terminal complement pathway could therefore be effective in cases of GBS without elevated sC5b-9 levels. Alternatively, anti-C5 antibodies could be effective in cases of GBS with elevated sC5b-9.

Comprehensive measurement of complement biomarkers such as Ba, sC5b-9, and CFH could contribute to delineating the pathogenesis and pathological status of NMOSD. The complement biomarkers in cerebrospinal fluid should also be measured to clarify the contribution to the pathogenesis of NMSD. We will also analyze the complement biomarkers in patients treated with eculizumab in a future study to determine whether these could be predictive biomarkers for response to eculizumab treatment. The present study was performed retrospectively using previously collected serum samples, so the reference ranges were too broad to determine valid cut-off values of Ba and sC5b-9 for prediction of acute and remission phases. However, this study suggests that the results should be validated in a future prospective study using plasma treated with ethylenediaminetetraacetic acid-disodium salt.

## Data availability statement

The raw data supporting the conclusions of this article will be made available by the authors, without undue reservation.

## Ethics statement

The studies involving human participants were reviewed and approved by The study was approved by Research Ethics Committee of Wakayama Medical University (approval number: G154 and 3278) and Kindai University (approval number: 2021-164). Written informed consent for participation was not required for this study in accordance with the national legislation and the institutional requirements.

## Author contributions

KM, NI, and HI contributed to the conception and design of the study. KM, MM, KO, NW, and MK contributed to acquisition and analysis of data. KM, KK and NI contributed to drafting of the text and preparation of the figures. HT contributed to statistical analyses of data. All authors contributed to the article and approved the submitted version.

## Funding

This work was supported by JSPS KAKENHI Grant Numbers JP17H04108, JP20H03580, JP20K07894, and JP22K07498, and a grant on Priority Areas from Wakayama Medical University Research.

## Acknowledgments

We thank the patients for their participation in the study and Kazuko Watase and Fumiko Saito for their technical assistance. We acknowledge proofreading and editing by Benjamin Phillis at the Clinical Study Support Center at Wakayama Medical University.

## Conflict of interest

KM received speaker honoraria from Alexion Pharmaceuticals, Inc., Chugai Pharmaceutical Co. Ltd., Mitsubishi Tanabe Pharma Corporation, and Teijin Pharma Ltd. KO received research support from Asahikasei Pharma. NI received speaker honoraria from Alexion Pharma Corporation, Novartis Pharmaceutical Corporation, UCB Japan Co. Ltd., Sanofi, Chugai Pharmaceutical Co. Ltd. and Japan Blood Products Organization and research support from Alexion Pharmaceuticals, Inc. HI received from Alexion Pharmaceuticals, Inc. and Teijin Pharma Ltd. KO, NW, and NI are councilors of The Japanese Association for Complement Research. NW is a councilor of the International Complement Society.

The remaining authors declare that the research was conducted in the absence of any commercial or financial relationships that could be construed as a potential conflict of interest.

## Publisher's note

All claims expressed in this article are solely those of the authors and do not necessarily represent those of their affiliated organizations, or those of the publisher, the editors and the reviewers. Any product that may be evaluated in this article, or claim that may be made by its manufacturer, is not guaranteed or endorsed by the publisher.

## Supplementary material

The Supplementary Material for this article can be found online at: https://www.frontiersin.org/articles/10.3389/fimmu.2023.1090548/full#supplementary-material

## References


1. Ricklin D, Hajishengallis G, Yang K, Lambris JD. Complement: a key system for immune surveillance and homeostasis. *Nat Immunol* (2010) 11(9):785–97. doi: 10.1038/ni.1923

2. Ricklin D, Reis ES, Lambris JD. Complement in disease: a defence system turning offensive. *Nat Rev Nephrol* (2016) 12(7):383–401. doi: 10.1038/nrneph.2016.70

3. Garred P, Tenner AJ, Mollnes TE. Therapeutic targeting of the complement system: From rare diseases to pandemics. *Pharmacol Rev* (2021) 73(2):792–827. doi: 10.1124/pharmrev.120.000072

4. Dalakas MC, Alexopoulos H, Spaeth PJ. Complement in neurological disorders and emerging complement-targeted therapeutics. *Nat Rev Neurol* (2020) 16(11):601–17. doi: 10.1038/s41582-020-0400-0

5. Masi G, O'Connor KC. Novel pathophysiological insights in autoimmune myasthenia gravis. *Curr Opin Neurol* (2022) 35(5):586–96. doi: 10.1097/WCO.0000000000001088

6. Weinshenker BG, Wingerchuk DM. Neuromyelitis spectrum disorders. *Mayo Clin Proc* (2017) 92(4):663–79. doi: 10.1016/j.mayocp.2016.12.014

7. Pittock SJ, Zekeridou A, Weinshenker BG. Hope for patients with neuromyelitis optica spectrum disorders - from mechanisms to trials. *Nat Rev Neurol* (2021) 17 (12):759–73. doi: 10.1038/s41582-021-00568-8

8. Pittock SJ, Berthele A, Fujihara K, Kim HJ, Levy M, Palace J, et al. Eculizumab in aquaporin-4-Positive neuromyelitis optica spectrum disorder. *N Engl J Med* (2019) 381 (7):614–25. doi: 10.1056/NEJMoa1900866

9. Schneider-Gold C, Gilhus NE. Advances and challenges in the treatment of myasthenia gravis. *Ther Adv Neurol Disord* (2021) 14:17562864211065406. doi: 10.1177/17562864211065406

10. Kusunoki S, Willison HJ, Jacobs BC. Antiglycolipid antibodies in Guillain-barre and Fisher syndromes: discovery, current status and future perspective. *J Neurol Neurosurg Psychiatry* (2021) 92(3):311–8. doi: 10.1136/jnnp-2020-325053

11. Misawa S, Kuwabara S, Sato Y, Yamaguchi N, Nagashima K, Katayama K, et al. Safety and efficacy of eculizumab in Guillain-barre syndrome: a multicentre, double-blind, randomised phase 2 trial. *Lancet Neurol* (2018) 17(6):519–29. doi: 10.1016/S1474-4422(18)30114-5

12. Okamura H, Nakamae H, Shindo T, Ohtani K, Hidaka Y, Ohtsuka Y, et al. Early elevation of complement factor ba is a predictive biomarker for transplant-associated thrombotic microangiopathy. *Front Immunol* (2021) 12:695037. doi: 10.3389/fimmu.2021.695037

13. Wingerchuk DM, Banwell B, Bennett JL, Cabre P, Carroll W, Chitnis T, et al. International consensus diagnostic criteria for neuromyelitis optica spectrum disorders. *Neurology* (2015) 85(2):177–89. doi: 10.1212/WNL.0000000000001729

14. Asbury AK, Cornblath DR. Assessment of current diagnostic criteria for Guillain-barre syndrome. *Ann Neurol* (1990) 27 Suppl:S21–4. doi: 10.1002/ana.410270707

15. Ohtani K, Inoue N, Hidaka Y, Wakamiya N. The analysis of complement factors and activation markers in normal Japanese individuals. *J Jpn Assoc Comple Res* (2019) 56(2):13–22.

16. Piatek P, Domowicz M, Lewkowicz N, Przygodzka P, Matysiak M, Dzitko K, et al. C5a-preactivated neutrophils are critical for autoimmune-induced astrocyte dysregulation in neuromyelitis optica spectrum disorder. *Front Immunol* (2018) 9:1694. doi: 10.3389/fimmu.2018.01694

17. Papadopoulos MC, Verkman AS. Aquaporin 4 and neuromyelitis optica. *Lancet Neurol* (2012) 11(6):535–44. doi: 10.1016/S1474-4422(12)70133-3

18. Takeshita Y, Obermeier B, Cotleur AC, Spampinato SF, Shimizu F, Yamamoto E, et al. Effects of neuromyelitis optica-IgG at the blood-brain barrier. *vitro Neurol Neuroimmunol Neuroinflamm* (2017) 4(1):e311. doi: 10.1212/NXI.0000000000000311

19. Shimizu F, Schaller KL, Owens GP, Cotleur AC, Kellner D, Takeshita Y, et al. Glucose-regulated protein 78 autoantibody associates with blood-brain barrier disruption in neuromyelitis optica. *Sci Transl Med* (2017) 9(397):eaai9111. doi: 10.1126/scitranslmed.aai9111

20. Winkler A, Wrzos C, Haberl M, Weil MT, Gao M, Mobius W, et al. Blood-brain barrier resealing in neuromyelitis optica occurs independently of astrocyte regeneration. *J Clin Invest* (2021) 131(5):e141694. doi: 10.1172/JCI141694

frontiers | Frontiers in Neurology

TYPE Case Report
PUBLISHED 06 March 2023
DOI 10.3389/fneur.2023.1060110



OPEN ACCESS

EDITED BY
Honghao Wang,
Guangzhou First People's Hospital, China

REVIEWED BY
Elanagan Nagarajan,
University of Tennessee at Chattanooga, United States
Hsiuying Wang,
National Yang Ming Chiao Tung University, Taiwan

*CORRESPONDENCE
Shujuan Dai
✉ dssj17@126.com
Qian Wu
✉ qianwu@ydyy.cn

SPECIALTY SECTION
This article was submitted to Multiple Sclerosis and Neuroimmunology, a section of the journal Frontiers in Neurology

RECEIVED 02 October 2022
ACCEPTED 10 February 2023
PUBLISHED 06 March 2023

CITATION
Zhu L, Shang Q, Zhao CW, Dai S and Wu Q (2023) Case report: Anti-neurexin-3α-associated autoimmune encephalitis secondary to contrast-induced encephalopathy. *Front. Neurol.* 14:1060110. doi: 10.3389/fneur.2023.1060110



# Case report: Anti-neurexin-3α-associated autoimmune encephalitis secondary to contrast-induced encephalopathy

Lin Zhu[1], Qunzhu Shang[1], Charlie Weige Zhao[2], Shujuan Dai[1]* and Qian Wu[1]*

[1]Department of Neurology, First Affiliated Hospital, Kunming Medical University, Kunming, Yunnan, China, [2]Department of Internal Medicine, St. Vincent's Medical Center, Bridgeport, CT, United States

A 54-year-old man complained of episodic stinging in his left eye along with weakness and numbness in his right upper and lower extremities for 1 month. The neurological examination was negative. MRI showed bilateral paraventricular demyelination. CTA showed significant stenosis of the left internal carotid (60%) and vertebral arteries (70%). He underwent left internal carotid stenting and was intubated during the procedure. After the procedure, he did not wake up from anesthesia, and he developed flexion and spasticity in the right arm immediately. Thereafter, he was sent to the neurocritical unit (NCU). Anti-seizure treatment was adopted due to recurrent general tonic-clonic seizures. Two days later (day 15 of hospitalization), brain edema and meningitis appeared in MRI, and contrast-induced encephalopathy (CIE) was mainly considered, with the support of CSF results. After 18 days (day 21 of hospitalization), serum anti-neurexin-3α IgG was detected at a dilution of 1:10. Anti-neurexin-3α-associated encephalitis was diagnosed. The patient was fully recovered 7 months after taking immunoglobulin, steroids, mortimycophenate, and cyclophosphamide. Meanwhile, anti-neurexin-3α antibody IgG was negative in both CSF and serum. MRI was also normal. Although scarce evidence clarified the relationship between CIE and anti-neurexin-3α-associated encephalitis, we inferred that the BBB damaged by CIE may result in the anti-neurexin-3α antibody entrance into the CSF from serum, which led to autoimmune encephalitis (AIE).

KEYWORDS

**anti-neurexin-3α-associated autoimmune encephalitis, contrast-induced encephalopathy (CIE), blood brain barrier, neuroimmunology, $Q_{Alb}$ (CSF/serum albumin quotients)**

## Introduction

Contrast-induced encephalopathy (CIE) is a transient and reversible adverse reaction of the nervous system to the use of contrast, characterized by seizures, cortical blindness, global aphasia, focal neurological deficits, and chemical meningitis (1). The risk factors of CIE include large contrast volume (80–400 mL), chronic hypertension, transient ischemic attacks (TIAs), impaired cerebral autoregulation, impaired renal function, vertebral-basilar arteriography, male gender, and previous adverse reactions to contrast (2–4). In 2016, Gresa et al. first reported five patients diagnosed with anti-neurexin-3α-associated autoimmune encephalitis (AIE) (5). Few cases of anti-neurexin-3α-associated AIE have been reported

since then. Herein, we report a patient who was diagnosed and subsequently recovered from anti-neurexin-3$\alpha$-associated AIE secondary to CIE.

## Case report

A 54-year-old man with no significant history complained of episodic stinging pain in his left eye along with weakness and numbness in his right upper and lower extremities for 1 month. The episodes initially lasted for 3–5 min each and occurred only during the daytime but progressively increased in frequency and duration to last up to 10–15 min and occurred during the night. The patient had not gone to the hospital until he developed progressively worsening symptoms. His neurological examination was unremarkable, and the brain MRI showed bilateral paraventricular demyelination.

The episodes were suggestive of TIAs and the patient underwent computed tomography (CT) angiography, which showed significant stenosis of the left internal carotid (60%) and vertebral (70%) arteries. He underwent left internal carotid artery stenting following 200 ml of intravenous contrast administration and was intubated during the procedure. After the procedure, he did not regain consciousness, and half an hour later, he developed flexion and spasticity in the right arm. His temperature was 36.5°C, heart rate was 110/min, blood pressure was 148/106 mmHg, respiratory rate was 22/min, and $SpO_2$ was 98% (on ventilator support). The pupillary diameter was 1.5 mm in ambient light, and the pupillary light reflex was sluggish. On motor examination, he had hypertonia in the extremities and trunk and showed abnormal flexion to pain. His Glasgow Coma Scale score was 4T (E1VTM3). The patient developed recurrent generalized tonic-clonic seizures, lasting from 10 s to several minutes. The lactic acid in his blood was high (12.3 mmol/L).

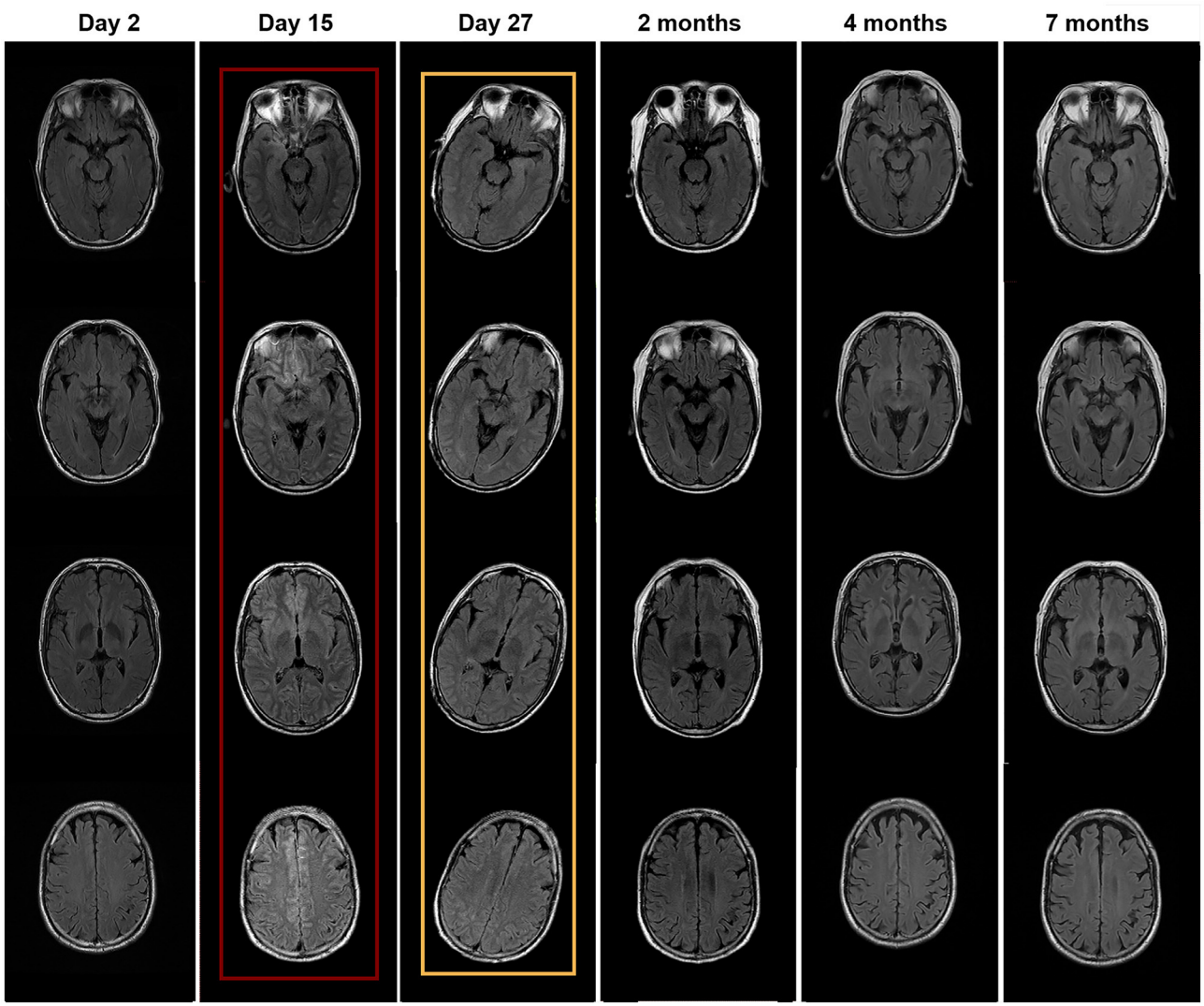


FIGURE 1
Brain MRI performed at different times. MRI with red wireframe was performed 2 days after surgery (day 15 of hospitalization) and showed brain edema and high signal in the meninges. MRI with yellow wireframe was performed on day 27 and showed improvement in abnormal findings.

TABLE 1 Laboratory data.

| Laboratory data | | | | | | | |
|---|---|---|---|---|---|---|---|
| | | Day 17 | Day 21 | Day 29 | 2 months | 4 months | 7 months |
| CSF | Pressure ($mmH_20$) | 230 | 175 | 190 | 155 | 205 | 190 |
| | WBC ($10^6$/L) | 67 | 12 | 4 | 1 | 6 | 1 |
| | RBC ($10^6$/L) | 12 | 2 | 12 | 0 | 2 | 0 |
| | $Cl^-$ (mmol/L) | 138.8 | 130.2 | 131.1 | 129.2 | 129.0 | 136.8 |
| | Glu (mmol/L) | 6.32 | 5.74 | 3.54 | 3.05 | 3.41 | 4.57 |
| | Album (mg/L) | 442.3 | 233.4 | 134.2 | 248.2 | 285.8 | 192.7 |
| | Pro (g/L) | 0.47 | 0.24 | 0.61 | 0.96 | 1 | 0.24 |
| | Anti-neurexin-3$\alpha$ antibody IgG | / | - | - | 1:10 | - | - |
| Blood | Anti-neurexin-3$\alpha$ antibody IgG | / | 1:10 | - | 1:32 | 1:10 | - |
| | Album (mg/L) | 36.5 | 37 | 28.5 | 40.2 | 36.7 | 38.4 |
| | Glu (mmol/L) | 8.9 | 7.5 | 6.8 | 6.5 | / | / |
| | Glu (CSF/Blood) | 0.71 | 0.76 | 0.52 | 0.47 | / | / |
| | $Q_{Alb}$ ($^0/_{00}$) | 12.12 | 6.31 | 4.71 | 6.17 | 7.79 | 5.01 |

He was treated with midazolam and vecuronium. The Richmond Agitation Sedation Scale score was −4. The control of seizures required continuous intravenous infusion of midazolam for 48 h. Subsequently, oral levetiracetam was administered to allow a reduction in the midazolam dose. Several investigations were performed 2 days later (day 15 of hospitalization): His brain MRI showed edema and generalized high signal in the meninges (Figure 1). His electroencephalogram showed low voltage with no epileptiform discharges. The abdomen and testicle ultrasound were normal; the CT chest was normal. Rheumatism immune-related antibodies, including antinuclear antibody (ANA), antineutrophil cytoplasmic antibody (ANCA), anti-ribonucleoprotein antibody (anti-RNP), double-stranded DNA (anti-dsDNA), and Sjögren syndrome-related antigens A and B (anti-SS-A/SS-B), were negative. In addition, the T-cell-based test for tuberculosis infection and the tuberculin skin test were negative. The result of the cerebrospinal fluid (CSF) analysis is presented in Table 1. The patient was empirically treated with the antiviral medication acyclovir.

After 21 days of his hospitalization, serum anti-neurexin-3$\alpha$ IgG came back positive with a ratio of 1:10. The anti-neurexin-3$\alpha$ IgG antibodies were not detected in the CSF. The patient was diagnosed with anti-neurexin-3$\alpha$-associated AIE and treated with a single dose of IV immunoglobulin (0.4 g/kg/day for 5 days). In the following days, the patient developed psychiatric symptoms, including agitation, auditory and visual hallucinations, cognitive dysfunction, and significantly reduced sleep duration. His Bech–Rafaelsen Mania Rating Scale score was 23, indicating severe mania. He was treated with olanzapine to control psychiatric symptoms. On day 28 of hospitalization, CSF analysis was repeated, which was normal, except for raised proteins, and the anti-neurexin-3$\alpha$ antibody was negative in both serum and CSF (Table 1). The brain MRI showed improved both brain edema and high signal in the meninges (Figure 1). Steroids were added to the patient's treatment.

On day 35 of hospitalization, the patient was discharged because of significant improvement and was asked to continue mycophenolate mofetil. The patient presented for follow-up after 2 months and reported significant improvement in the psychotic symptoms, with only mild irritability and agitation. His CSF $Q_{Alb}$ was 6.17, anti-neurexin3$\alpha$ IgG was positive at 1:10, and serum anti-neurexin-3$\alpha$ antibody IgG was 1:32. Therefore, we added cyclophosphamide for 2 months in addition to mycophenolate mofetil. After 4 months, his CSF $Q_{Alb}$ was 7.79, anti-neurexin-3$\alpha$ antibody IgG was negative, serum anti-neurexin-3$\alpha$ antibody IgG was 1:10, and the brain MRI was normal. Thus, the patient was asked to continue mycophenolate mofetil. After 7 months, both the CSF analysis and the brain MRI were normal (Figure 1), the anti-neurexin-3$\alpha$ antibody IgG was negative in CSF and serum, and the patient had a complete recovery and had been back to work for several months. The case timeline was showed in Figure 2.

## Discussion

The major clinical manifestations in our patient were first considered as TIA-like symptoms in the emergency department. He had critical stenosis of the internal carotid artery, for which it was reasonable to perform endovascular treatment. The patient received cerebral angiography due to repeated presentation of TIA-like symptoms although his left internal carotid stenosis was only around 60%. After the surgery, the patient progressed to develop coma, myoclonic jerks, and psychotic symptoms after the surgery. His brain MRI showed high signals in the meninges. The $Q_{Alb}$ [CSF/serum albumin quotients, which is a marker of the blood–brain barrier function with the upper reference limit $8 \times 10^{-3}$ for patients aged <60 years (6)] was increased (Table 1), suggesting BBB damage. Initially, we speculated that the BBB was damaged due to the contrast, which increased the BBB permeability, resulting in coma and myoclonic jerks; therefore, the diagnosis of contrast-induced encephalopathy (CIE) was considered. However, 20 days later, anti-neurexin-3$\alpha$ antibody IgG was detected in serum, and the patient developed extreme agitation, auditory and visual

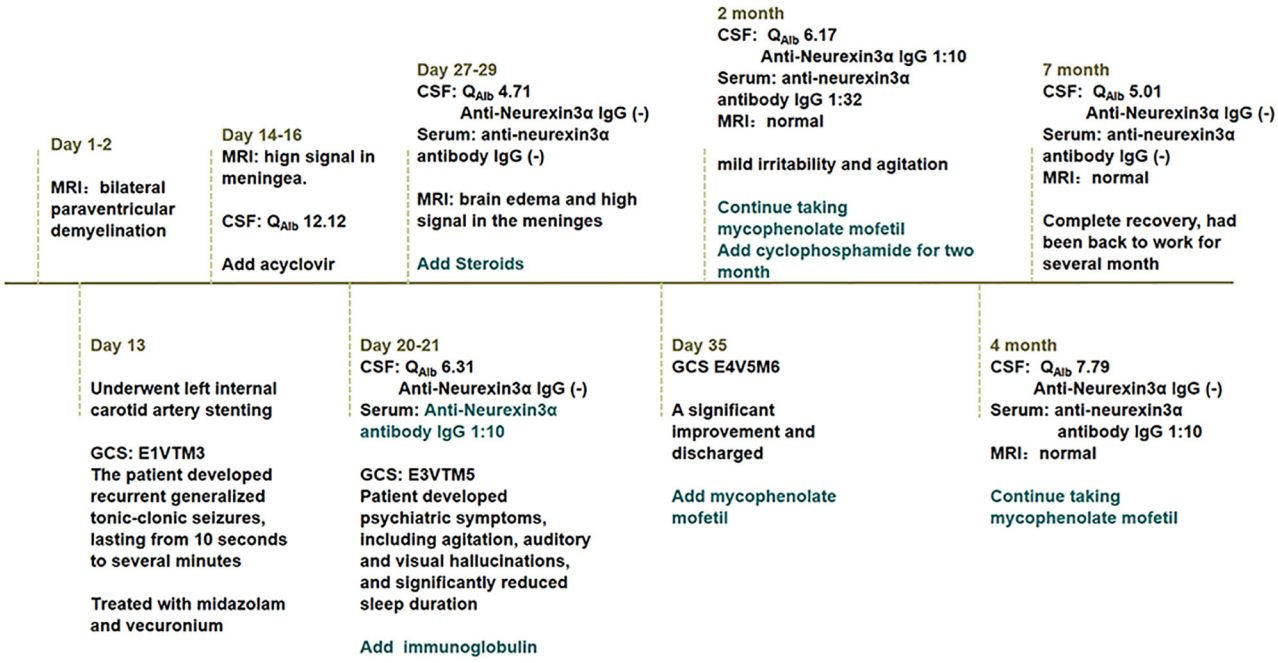


FIGURE 2
Case timeline.

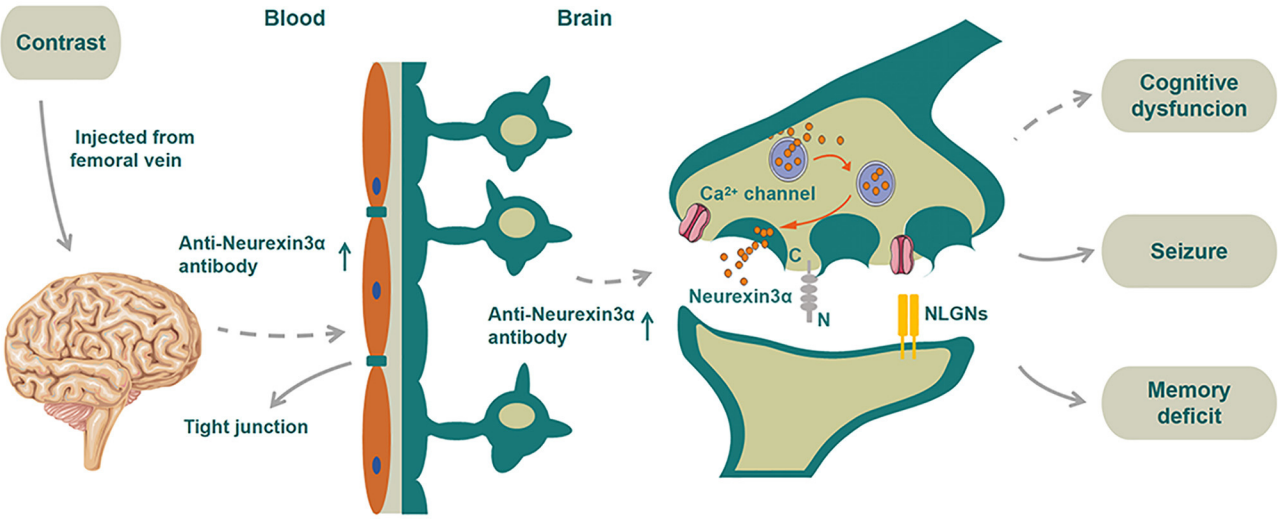


FIGURE 3
Schematic diagram of the proposed mechanism of disease for the patient. We speculated that neurexin-3$\alpha$ may be related to T-Js and the neurexin-3$\alpha$ antibody may promote BBB damage. As a vicious circle, the damaged BBB may allow more entrance of neurexin-3$\alpha$ antibodies to the CSF from serum. Contrast agents that destroyed the BBB would further assist manyfold neurexin-3$\alpha$ antibodies to enter the CSF, thereby disabling the function of neurexin-3$\alpha$ in the presynaptic membrane, impairing the activity of calcium ion channels and eventually leading to a series of neurological symptoms.

hallucinations, and significantly reduced sleep duration; thus, the patient was diagnosed with anti-neurexin-3$\alpha$-associated AIE for which he received immunotherapy. The repeat CSF test also showed positive anti-neurexin-3$\alpha$ antibody IgG. The antibody entered the brain from the blood due to the damaged BBB, which impaired the activity of calcium ion channels and led to several neurological symptoms, including agitation, auditory and visual hallucinations, and significantly reduced sleep duration. To sum up, we inferred that the CIE may have led to BBB damage, which allowed the antibodies to enter the CSF from the serum, eventually leading to anti-neurexin-3$\alpha$-associated AIE (Figure 3).

At present, there are no clear diagnostic criteria for CIE. Chu et al. analyzed a group of patients with CIE and proposed that CIE should be considered if symptoms worsen after endovascular thrombectomy and brain imaging suggest edema and contrast agent residue, especially in patients with renal dysfunction or

previous stroke (7). Similarly, Monforte et al. reported a CIE patient with previous chronic renal dysfunction who developed altered consciousness and myoclonic jerks of the right arm after left internal carotid stenting for critical stenosis (8). To sum up, TIA and endovascular treatment were the risk factors of CIE in the patient. Based on the clinical and MRI findings, we diagnosed CIE.

Currently, the specific mechanism underlying brain injury caused by contrast agents is unclear. Some researchers have proposed that the chemical toxicity of contrast agents can cause the contraction of endothelial cells, destroy the close connection between them, and promote endocytosis and extremes of endothelial cells (9). Wang et al. found that a carotid injection of iohexol damages the BBB in rats and caused dynamic variability in BBB permeability, with progressively increasing permeability, reaching a maximum at 6 h after administration, and then progressively decreasing. The underlying mechanism may be related to the changes in the expression of tight junction (T–J)-related proteins (ZO-1 and occludin) in the BBB (10).

Interestingly, the anti-neurexin-3$\alpha$ antibody was initially detected in the patient's serum and then in the CSF. Neurexins are cell-surface glycoproteins encoded by NRX. Neurexin-3$\alpha$ is the largest and most polymorphic member of the neurexin family. Its C-terminus is involved in the regulation of $Ca^{2+}$ channel function and neurotransmitter release, whereas the N-terminus, which is outside the presynaptic membrane binds to the adhesion protein in the postsynaptic membrane (11, 12) to regulate the formation and function of synapses. In neurexin-$\alpha$ knock-out mice, the lack of function of the presynaptic $Ca^{2+}$ channel (11) leads to severely reduced neurotransmitter release. Some scholars have proposed that the neurexin and neuroligin complex may be related to cognitive diseases, but the underlying mechanism remains to be studied (13).

In 1996, Baumgartner et al. reported that neurexin IV was a new member of the neurexin family located at the septate junctions (S-Js) between the epithelial cells and glial cells; the loss of neurexin IV in S-Js led to BBB destruction (14). The T-Js in vertebrates correspond to the S-Js in invertebrates; thus, we speculated that neurexin-3$\alpha$ may be related to T-Js and the neurexin-3$\alpha$ antibody may promote BBB damage. As a vicious circle, the damaged BBB may allow more entrance of neurexin-3$\alpha$ antibodies to the CSF from serum, thereby disabling the function of neurexin-3$\alpha$ in the presynaptic membrane, impairing the activity of calcium ion channels, and eventually leading to a series of neurological symptoms. In addition, whether the initial TIA-like symptoms might have been focal seizures that induced by AIE were impossible to verify due to absence of immediate EEG and preoperative antibody detection, but this diagnosis should also be taken into consideration. If this assumption was right, contrast agents that destroyed the BBB would further assist manyfold neurexin-3$\alpha$ antibodies to enter the CSF, thereby disabling the function of neurexin-3$\alpha$ in the presynaptic membrane, impairing the activity of calcium ion channels and eventually leading to a series of neurological symptoms (Figure 3).

In conclusion, we should be vigilant against CIE in patients who have a transient and reversible adverse reaction of the nervous system after the use of contrast. In addition, AIE may be secondary to or complicated by a neurological disease, especially in patients with immunosuppression. AIE should be considered when focal neurological episodes presented a comprehensive work-up of MRI; EEG and autoimmune antibody detection are helpful for diagnosis and management. Moreover, this rare case deserves attention and can provide a reference for clinicians.

## Data availability statement

The original contributions presented in the study are included in the article/supplementary material, further inquiries can be directed to the corresponding authors.

## Ethics statement

Written informed consent was obtained from the individual(s) for the publication of any potentially identifiable images or data included in this article.

## Author contributions

LZ drafted the manuscript. QS managed the patient throughout and participated in the discussion of writing the article to provide ideas. CZ provided ideas for writing and language modification. QW and SD guided patient treatment and article writing ideas, and these authors contributed equally to this study and share corresponding authorship. All authors contributed to the article and approved the submitted version.

## Funding

This study was supported by the National Natural Science Foundation of China (82160260), the Yunnan Health Training Project of High-Level Talents (H-2018056), the Yunnan Applied Basic Research Projects (202201AY070001-083), and the Young and Middle-aged and Academic and Technical Leaders Reserve Talents Project of Yunnan Province Science and Technology Department (202205AC160019).

## Conflict of interest

The authors declare that the research was conducted in the absence of any commercial or financial relationships that could be construed as a potential conflict of interest.

## Publisher's note

# References


1. Neilan P, Urbine D. A case of contrast-induced encephalopathy. *BMJ Case Rep.* (2019) 18:540–54. doi: 10.1136/bcr-2019-229717

2. Dattani A, Au L, Tay KH, Davey P. Contrast-induced encephalopathy following coronary angiography with no radiological features: a case report and literature review. *Cardiology.* (2018) 139:197–201. doi: 10.1159/000486636

3. Yu J, Dangas G. Commentary: new insights into the risk factors of contrast-induced encephalopathy. *J Endovasc Ther.* (2011) 18:545–6. doi: 10.1583/11-3476C.1

4. Guimaraens L, Vivas E, Fonnegra A, Sola T, Soler L, Balaguer E et al. Transient encephalopathy from angiographic contrast: a rare complication in neurointerventional procedures. *Cardiovasc Intervent Radiol.* (2010) 33:383–8. doi: 10.1007/s00270-009-9609-4

5. Gresa-Arribas N, Planagumà J, Petit-Pedrol M, Kawachi I, Katada S, Glaser C A et al. Human neurexin-3α antibodies associate with encephalitis and alter synapse development. *Neurology.* (2016) 86:2235–42. doi: 10.1212/WNL.0000000000002775

6. Sindic CJ, Van Antwerpen MP. Goffette S. The intrathecal humoral immune response: laboratory analysis and clinical relevance. *Clin Chem Lab Med.* (2001) 39:333–40. doi: 10.1515/CCLM.2001.052

7. Chu YT, Lee KP. Chen CH, Sung P S, Lin Y H, Lee C W et al. Contrast-induced encephalopathy after endovascular thrombectomy for acute ischemic stroke. *Stroke.* (2020) 51:3756–9. doi: 10.1161/STROKEAHA.120.031518

8. Monforte M, Marca GD, Lozupone E. Contrast-induced encephalopathy. *Neurol India.* (2020) 68:718–9. doi: 10.4103/0028-3886.288986

9. Zhang GL, Wang HY Li T. The role of blood-brain barrier damage in the pathogenesis of contrast-induced encephalopathy. *Arch General Internal Med.* (2018) 24:34–40.

10. Wang H, Li T, Zhao L, Sun M, Jian Y, Liu J et al. Dynamic effects of Ioversol on the permeability of the blood-brain barrier and the expression of ZO-1/Occludin in rats. *J Mol Neurosci.* (2019) 68:295–303. doi: 10.1007/s12031-019-01305-z

11. Zhang W, Rohlmann A, Sargsyan V, Gayane A, Robert E H, Thomas C S et al. Extracellular domains of alpha-neurexins participate in regulating synaptic transmission by selectively affecting N- and P/Q-type Ca2+ channels. *J Neurosci.* (2005) 25:4330–42. doi: 10.1523/JNEUROSCI.0497-05.2005

12. Missler M, Zhang W, Rohlmann A, Kattenstroth G, Hammer R E, Gottmann K et al. Alpha-neurexins couple Ca2+ channels to synaptic vesicle exocytosis. *Nature.* (2003) 423:939–48. doi: 10.1038/nature01755

13. SÜDHOF TC. Neuroligins and neurexins link synaptic function to cognitive disease. *Nature.* (2008) 455:903–11. doi: 10.1038/nature07456

14. Baumgartner S, Littleton JT, Broadie K, Bhat M A, Harbecke R, Lengyel J A et al. A Drosophila neurexin is required for septate junction and blood-nerve barrier formation and function. *Cell.* (1996) 87:1059–68. doi: 10.1016/S0092-8674(00)81800-0

frontiers | Frontiers in Immunology

TYPE Original Research
PUBLISHED 09 March 2023
DOI 10.3389/fimmu.2023.1095966



OPEN ACCESS

EDITED BY
Long-Jun Wu,
Mayo Clinic, United States

REVIEWED BY
Viviana Nociti,
Agostino Gemelli University Polyclinic (IRCCS), Italy
Takeshi Kezuka,
Tokyo Medical University, Japan

*CORRESPONDENCE
Wenjun Zou
wenjunzou2022@163.com
Ke Wang
wangke@jsinm.org

†These authors have contributed equally to this work and share first authorship

SPECIALTY SECTION
This article was submitted to Multiple Sclerosis and Neuroimmunology, a section of the journal Frontiers in Immunology

RECEIVED 11 November 2022
ACCEPTED 27 February 2023
PUBLISHED 09 March 2023

CITATION
Chen X, Cheng L, Pan Y, Chen P, Luo Y, Li S, Zou W and Wang K (2023) Different immunological mechanisms between AQP4 antibody-positive and MOG antibody-positive optic neuritis based on RNA sequencing analysis of whole blood. *Front. Immunol.* 14:1095966. doi: 10.3389/fimmu.2023.1095966



# Different immunological mechanisms between AQP4 antibody-positive and MOG antibody-positive optic neuritis based on RNA sequencing analysis of whole blood

Xuelian Chen[1,2,3†], Libo Cheng[1,2,3,4†], Ying Pan[1,2,3,4], Peng Chen[2,3,4], Yidan Luo[1,2,3], Shiyi Li[2,3,4], Wenjun Zou[1,2,3,4*] and Ke Wang[5,6*]

[1]Department of Ophthalmology, Affiliated Wuxi Clinical College of Nantong University, Wuxi, Jiangsu, China, [2]Department of Ophthalmology, Jiangnan University Medical Center (JUMC), Wuxi, Jiangsu, China, [3]Department of Ophthalmology, Wuxi No.2 People's Hospital, Wuxi, Jiangsu, China, [4]Department of Ophthalmology, The Affiliated Wuxi No.2 People's Hospital of Nanjing Medical University, Wuxi, Jiangsu, China, [5]National Health Commission (NHC) Key Laboratory of Nuclear Medicine, Jiangsu Key Laboratory of Molecular Nuclear Medicine, Jiangsu Institute of Nuclear Medicine, Wuxi, Jiangsu, China, [6]Department of Radiopharmaceuticals, School of Pharmacy, Nanjing Medical University, Nanjing, Jiangsu, China

**Purpose:** To compare the different immunological mechanisms between aquaporin 4 antibody-associated optic neuritis (AQP4-ON) and myelin oligodendrocyte glycoprotein antibody-associated optic neuritis (MOG-ON) based on RNA sequencing (RNA-seq) of whole blood.

**Methods:** Whole blood was collected from seven healthy volunteers, 6 patients with AQP4-ON and 8 patients with MOG-ON, and used for RNA-seq analysis. An examination of immune cell infiltration was performed using the CIBERSORTx algorithm to identify infiltrated immune cells.

**Results:** RNA-seq analysis showed that the inflammatory signaling was mainly activated by *TLR2*, *TLR5*, *TLR8* and *TLR10* in AQP4-ON patients, while which was mainly activated by *TLR1*, *TLR2*, *TLR4*, *TLR5* and *TLR8* in MOG-ON patients. Biological function identification of differentially expressed genes (DEGs) based on Gene Ontology (GO) term and Kyoto encyclopedia of genes and genomes (KEGG) pathway enrichment analysis, as well as Disease Ontology (DO) analysis, showed that the inflammation in AQP4-ON was likely mediated by damage-associated molecular pattern (DAMP), while which in MOG-ON was likely mediated by pathogen-associated molecular pattern (PAMP). Analysis of immune cell infiltration showed that the proportion of immune cell infiltration was related to patients' vision. The infiltration ratios of monocytes (rs=0.69, $P$=0.006) and M0 macrophages (rs=0.66, $P$=0.01) were positively correlated with

the BCVA (LogMAR), and the infiltration ratio of neutrophils was negatively correlated with the BCVA (LogMAR) (rs=0.65, $P$=0.01).

**Conclusion:** This study reveals different immunological mechanisms between AQP4-ON and MOG-ON based on transcriptomics analysis of patients' whole blood, which may expand the current knowledge regarding optic neuritis.

KEYWORDS

optic neuritis, aquaporin 4, myelin oligodendrocyte glycoprotein, RNA-Seq, toll-like receptors

# 1 Introduction

Optic neuritis (ON) is an inflammatory demyelinating disease that mainly affects young people, and its prevalence rate is about 1 to 6 per 100,000 population (1). In patients with non-infectious ON, 12% were aquaporin 4-immunoglobulin G (AQP4-IgG) positive and 10% were myelin oligodendrocyte glycoprotein-IgG (MOG-IgG) positive (2). Patients with AQP4-IgG related ON (AQP4-ON) have worse vision and usually develop blindness, while patients with MOG-ON have a higher recurrence rate (3, 4).

AQP4, the target protein attacked by AQP4-IgG, is responsible for maintaining water homeostasis and solute transfer, and can provide a fast water transport channel for astrocytes (5). Meanwhile, MOG, the target antigen recognized by MOG-IgG, is involved in myelin sheath adhesion and maintaining the integrity of the myelin sheath (6). Due to the distinct functions of AQP4 and MOG, the clinical features and pathological lesions caused by AQP4-IgG and MOG-IgG are different (7, 8). Besides, the co-existence of MOG-IgG and AQP4-IgG is highly uncommon (rate of 0.06%), indicating that AQP4-ON and MOG-ON may be developed through different immunological mechanisms (9, 10). However, to date, there have been no reports on the difference between the two types of immune-mediated ON.

We investigated the molecular mechanisms and therapeutic targets of AQP4-ON and MOG-ON by bioinformatic analysis. Whole blood samples from patients with AQP4-ON and MOG-ON as well as healthy control (HC) subjects were subjected to RNA sequencing (RNA-seq) analysis. The key differentially expressed genes (DEGs) in AQP4-ON and MOG-ON patients were comprehensively analyzed, and on this basis, the immune cell infiltration rates in all patients were analyzed.

# 2 Materials and methods

## 2.1 Subjects and samples

All subjects were recruited at the Affiliated Wuxi Clinical College of Nantong University from November 2020 to August 2022. The diagnosis of ON was made following the guidelines of the Optic Neuritis Treatment Trial (ONTT) study (11). The inclusion criteria were (1): serum AQP4-IgG or MOG-IgG was positive (2), the first attack of ON and in the stage of acute attack and (3) no treatment with glucocorticoid and other drugs. Exclusion criteria were (1) neurological disease such as encephalitis and myelitis (2), other eye diseases except cataract, such as glaucoma、uveitis and ischemic optic neuropathy. For high sensitivity and absolute specificity, the AQP4-IgG was measured using an enzyme-linked immunosorbent assay (ELISA) kit (RSR Ltd., Cardiff, UK) according to the previous study (12) and results 3.0 u/mL were considered as positive. The MOG-IgG was measured by indirect immunofluorescence testing (IIFT) using a cell-based assay (CBA), and the normal value was negative. For statistical analysis, the Snellen best-corrected visual acuity (BCVA) was transformed to logarithm of minimum angle of resolution (LogMAR) units (13). The ethics committee of the Affiliated Wuxi Clinical College of Nantong University approved the use of blood samples for scientific research purposes (certificate No.2021 Y-33), and all participants signed written informed consent.

## 2.2 RNA extraction and library preparation

Peripheral venous whole blood was collected from patients and HC subjects in vacuum tubes containing EDTA as an anticoagulant. After blood collection, 4 mL of TRIzol reagent (Beyotime, Nantong, China) was added to each blood sample and stored at −80°C for subsequent RNA extraction. Subsequently, after collecting all the samples, total RNA was extracted from each sample using the TRIzol extraction method, following the manufacturer's instructions. After verifying its integrity, the total RNA was reverse transcribed into cDNA, and then the cDNA was size selected to 250-300 bp using AMPure XP beads (Beckman Coulter Inc., Brea, CA, USA). Following polymerase chain reaction (PCR) amplification, the PCR product was once more purified using AMPure XP beads to prepare the cDNA library. The quality of the library was assessed using the Agilent 2100 bioanalyzer (Agilent Technologies Inc., Santa Clara, CA, USA), and then sequenced using the Illumina NovaSeq 6000 platform (Illumina Inc., San Diego, CA, USA).

## 2.3 Data quality control and quantification

Cleaned data were obtained by filtering the original data, and the cleaned reads were compared with the reference genome using the HISAT2 v2.0.5 software (http://daehwankimlab.github.io/hisat2/). The new genes were predicted by the StringTie (1.3.3b) software, and the gene expression level was quantified by feature counts (1.5.0-P3). The raw data have been submitted to GEO database (GEO accession numbers: GSE217410).

## 2.4 DEGs analysis

The DESeq (1.20.0) software was used to analyze the DEGs (relative to HC group) between the two groups of patients (http://www.bioinformatics.babraham.ac.uk/pro-jects/trim_galore/). The Benjamini and Hochberg method was used to adjust the *P* value and the false discovery rate for multiple comparisons. The genes with *P* value ≤ 0.05 adjusted by DESeq2 were considered to be differentially expressed.

## 2.5 Enrichment analysis of DEGs

Gene Ontology (GO) enrichment analysis (as implemented in the cluster Profiler R package (3.8.1)), was performed on DEGs, in which gene length bias was corrected. The ClusterProfiler (3.8.1) software package in the R platform was used to perform the Kyoto encyclopedia of genes and genomes (KEGG) pathway enrichment analysis of DEGs. The Disease Ontology (DO) is a knowledge database related to human diseases that describes the association of human genes to diseases.

## 2.6 Protein-protein interaction network analysis

The STRING software was used to predict the differential protein-protein interaction (PPI) network from the interaction relationship in the STRING protein interaction database, and then Cytoscape V3.9.1 was used to visually edit it to find the module network and prioritize the genes (14).

## 2.7 Immunocyte infiltration analysis

Cell-type identification by estimating relative subsets of RNA transcripts (CIBERSORTx) (https://cibersortx.stanford.edu) is a method to characterize the cell composition of complex tissues from gene expression profiles (GEPs). The CIBERSORTx algorithm was used to analyze 22 immune cell subsets significantly differentially expressed in all patients and control subjects. Then, the Immune Cell Abundance Identifier (ImmuCellAI) gene set signature-based method (http://bioinfo.life.hust.edu.cn/ImmuCellAI#!/) was used to estimate the proportion of infiltrated immune cell types.

## 2.8 Statistical analysis

Statistical analysis was performed using the IBM SPSS statistical 26.0. software for macOS (IBM Corporation, Armonk, NY, USA). For statistics, Snellen visual acuity was converted to logarithm of the minimum angle of resolution (logMAR). Counting fingers vision was converted to a value of 2.0 logMAR, hand motion vision was converted to a value of 2.5 logMAR, light perception vision was converted to a value of 3.0 logMAR and no light perception vision was converted to a value of 3.5 logMAR (15). Fisher's exact test was used for comparison of clinical characteristics among the groups. One-way analysis of variance (ANOVA) was used to compare normally distributed data, and the Kruskal-Wallis test was used for non-normally distributed data. Spearman correlation analysis was used to evaluate the relationship between data and vision. Data are expressed as the mean ± standard deviation (SD) or median, $P < 0.05$ was considered statistically significant. Graphs were plotted using the GraphPad Prism 9 software (GraphPad Software Inc., San Diego, CA, USA).

# 3 Results

## 3.1 Clinical features of included individuals

A flow chart of this study was shown in Figure 1. The clinical manifestations in 6 AQP4-ON patients, 8 MOG-ON patients and 7 HC subjects were shown in Table 1. The mean age was 37.83 ± 20.48 years for the AQP4-ON group, 38.25 ± 17.21 years for the MOG-ON group, and 41.42 ± 3.99 years for HC group. At the beginning of the disease, the BCVA (LogMAR) of the AQP4-ON group (2.13 ± 0.97) was slightly worse than which of the MOG-ON group (1.20 ±

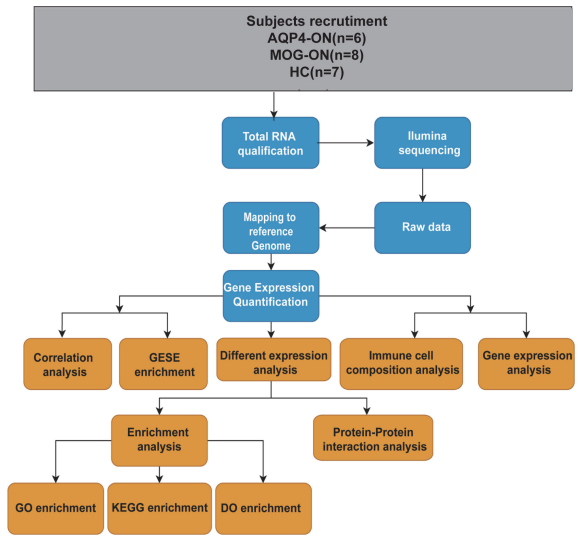


FIGURE 1
A workflow of this study. Age (years): age at the time of blood sample collection. Antibody titers: anti-AQP4 antibody titers detected by ELISA and the anti-MOG antibody titers detected by a CBA before blood samples were collected.

TABLE 1 Demographic data of AQP4-ON and MOG-ON patients and healthy controls (HCs).

| | AQP4-ON | MOG-ON | HC | *P* value |
|---|---|---|---|---|
| Number | 6 | 8 | 7 | – |
| Sex (female/male) | 6/0 | 5/3 | 5/2 | 0.36 |
| Age(years) | 37.83±20.48 | 38.25±17.21 | 41.42±3.99 | 0.90 |
| IOP(mmHg) | 15.75±5.74 | 16.15±3.67 | NA | 0.88 |
| BCVA at diagnosis | 2.13±0.97 | 1.20±0.71 | NA | 0.06 |
| BCVA at the last follow-up | 0.78±1.34 | 0.27±0.29 | NA | 0.31 |
| AQP4 antibody titers | 50.98±29.35 | – | NA | – |
| MOG antibody titers | – | 46.50±44.92 | NA | – |

Age: years at diagnosis; IOP, Intra-Ocular Pressure; BCVA: Snellen visual acuity was converted to logarithm of the minimum angle of resolution (logMAR). Counting fingers vision was converted to a value of 2.0 logMAR, hand motion vision was converted to a value of 2.5 logMAR, light perception vision was converted to a value of 3.0 logMAR and no light perception vision was converted to a value of 3.5 logMAR. NA, Not applicable.

0.71). The mean titer of anti-AQP4-IgG was 50.98 ± 29.35, and which of anti-MOG-IgG was 1:46.50 ± 44.92. In patients with AQP4-ON or MOG-ON, the thickness of the ganglion cell complex (GCC) and retinal nerve fiber layer (RNFL) became thinner as different degrees (Figure 2). In addition, one AQP4-ON patient and one MOG-ON patient were positive for antinuclear antibodies (ANA), and one MOG-ON patient had hypothyroidism.

## 3.2 Overview of RNA-Seq data and differential gene expression profiles

The gene expression matrices of AQP4-ON and MOG-ON patients and HC subjects were standardized, and the principal component analysis (PCA) plot was drawn (Figure 3A). The PCA results revealed (PC1 = 30.95%) that there was no significant difference among the three groups. Venn diagram showed that there were five co-expressed genes among the three groups, 517 unique genes in the AQP4-ON group and 1,198 unique genes in the MOG-ON group (Figure 3B). Heatmap analysis showed that there were significant differences in gene expression among the three groups (Figure 3C). For all DEGs, see Supplementary Document 1. Further analysis of the DEGs among the three groups was conducted (Figure 4). In the AQP4-ON group, the expressions of *AC099489.1*, *ADAMTS2*, *REM2*, *CXCL1* and *CACNA1E* were significantly increased, while the expressions of *DDX3Y*, *EEF1A1P6*, *PRKY*, *RPL2P4* and *RPL13AP25* were significantly decreased, compared to the HC group. In MOG-ON group, the expressions of *SULT1B1*, *FNIP1*, *RAB5B*, *NECAB2*, *HBP1* were significantly increased, and the expressions of *EEF1A1P6*,

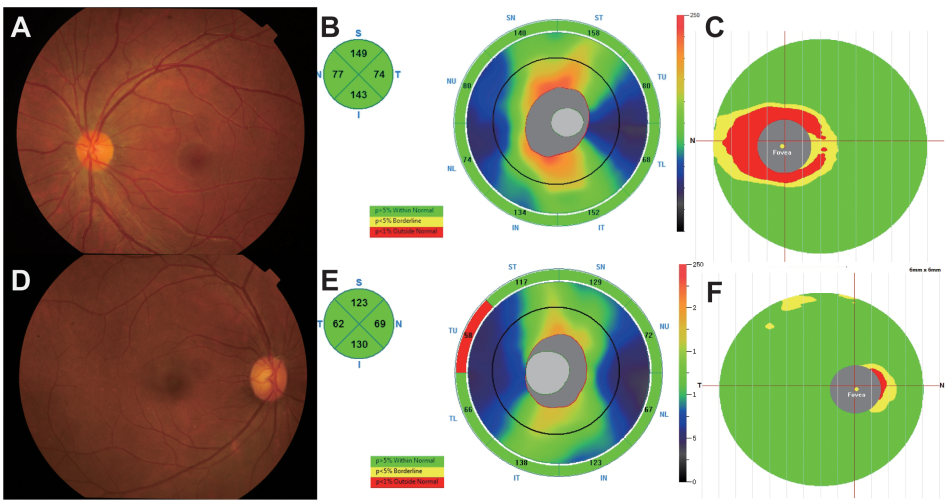


FIGURE 2
**(A–C)** A 25-year-old female complained of blurred vision in her left eye for 1 day. The BCVA (LogMAR) on presentation was 0.1 OD (Oculus Dexter) and 2 OS (Oculus Sinister). Fundus examination **(A)** showed a mildly edematous optic disc on OS, and optical coherence tomography (OCT) showed slight thickening of the retinal nerve fiber layer (RNFL) and thinning of the ganglion cell complex (GCC) at 1 month **(B, C)**. The anti-AQP4 antibody titer in this patient was 79.9 u/ml. **(D–F)** A 39-year-old female presented to our hospital with blurred vision in both eyes for 1 month, and the BCVA (logMAR) was 0 OU (oculus uterque). According to fundus photographs **(D)**, the optic disc of the right eye was almost normal, and the thicknesses of the RNFL and GCC were within the normal range **(E, F)**. The titer of the anti-MOG antibody in this patient was 1:10.

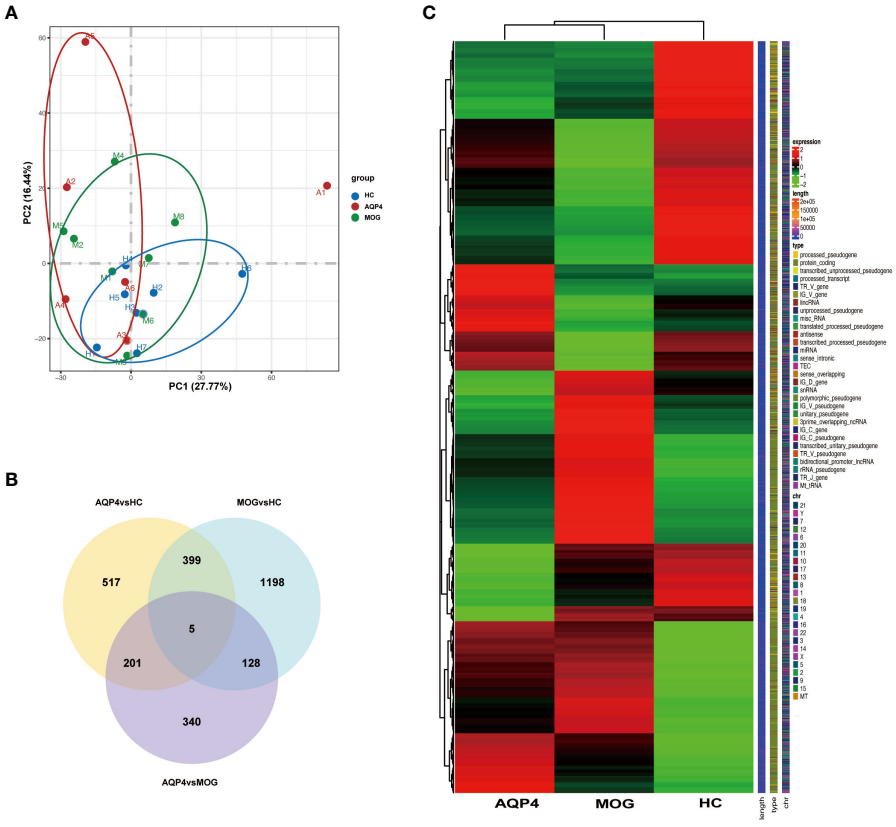


FIGURE 3
**(A)** Principal component analysis (PCA). The green, red and blue dots represent the HC, AQP4-ON, and MOG-ON groups, respectively. **(B)** Co-expression Venn diagram. **(C)** Cluster map of FPKM value of DEGs. The abscissa is the group name, and the ordinate is the gene name. The redder the color, the higher the expression level, and the greener the color, the lower the expression level.

*MARCO*, *HNRNP1AP48*, *MALAT1* and *HNRNP1AP10* were significantly decreased, compared to the HC group. Furthermore, due to the important roles in innate immunity and adaptive immunity, the expression of toll-like receptors (TLRs) was compared among the three groups. Compared to the HC group, *TLR2*, *TLR5*, *TLR8* and *TLR10* were up-regulated in the AQP4-ON group, and *TLR1*, *TLR2*, *TLR4*, *TLR5* and *TLR8* were up-regulated in the MOG-ON group. In addition, it was also found that the expression of *NLRP6* in AQP4-ON was increased and the expression of *TLR7* in MOG-ON was decreased. The differential expression of TLRs and NODs might indicate the different immunological mechanism involved in the pathogenesis of AQP4-ON and MOG-ON (Figure 4C).

## 3.3 Biological significance of DEGs

For the biological functional analysis of DEGs, GO term enrichment analysis, KEGG pathway enrichment analysis and DO enrichment analysis were used to identify enriched GO functional categories (Biological Process (BP)), KEGG pathways and human diseases for DEGs. According to the GO term enrichment analysis of DEGs associated with the 10 most significant GO terms (Figure 5), the DEGs in AQP4-ON were likely associated with damage-associated molecular pattern (DAMP)-mediated inflammation, including neutrophil degranulation, neutrophil activation involved in immune response and neutrophil mediated immunity, and the DEGs in MOG-ON were likely associated with pathogen-associated molecular pattern (PAMP)-mediated inflammation, including activation of innate immune response, regulation of innate immune response and other biological functions. According to KEGG pathway enrichment analysis of the DEGs in AQP4-ON, they were mainly related to acquired immunity, including IL-17 signaling pathway, TNF signaling pathway and Th1 and Th2 cell differentiation. The corresponding KEGG enrichment analysis of the DEGs in MOG-ON revealed that MOG-ON signaling pathways mainly involved Influenza A, Kaposi sarcoma-associated herpesvirus infection, Herpes simplex infection and Toll-like receptor signaling pathway. According to DO enrichment analysis, the AQP4-ON group was mainly associated with atherosclerosis, arteriosclerotic cardiovascular disease and arteriosclerosis, while the MOG-ON group was associated with Alzheimer's disease, hypersensitivity reaction type II disease and rheumatoid arthritis. The prediction of the interaction between proteins performed by PPI analysis in the AQP4-ON group using the STRING database revealed that *TSPO* and *MAPK14* were the

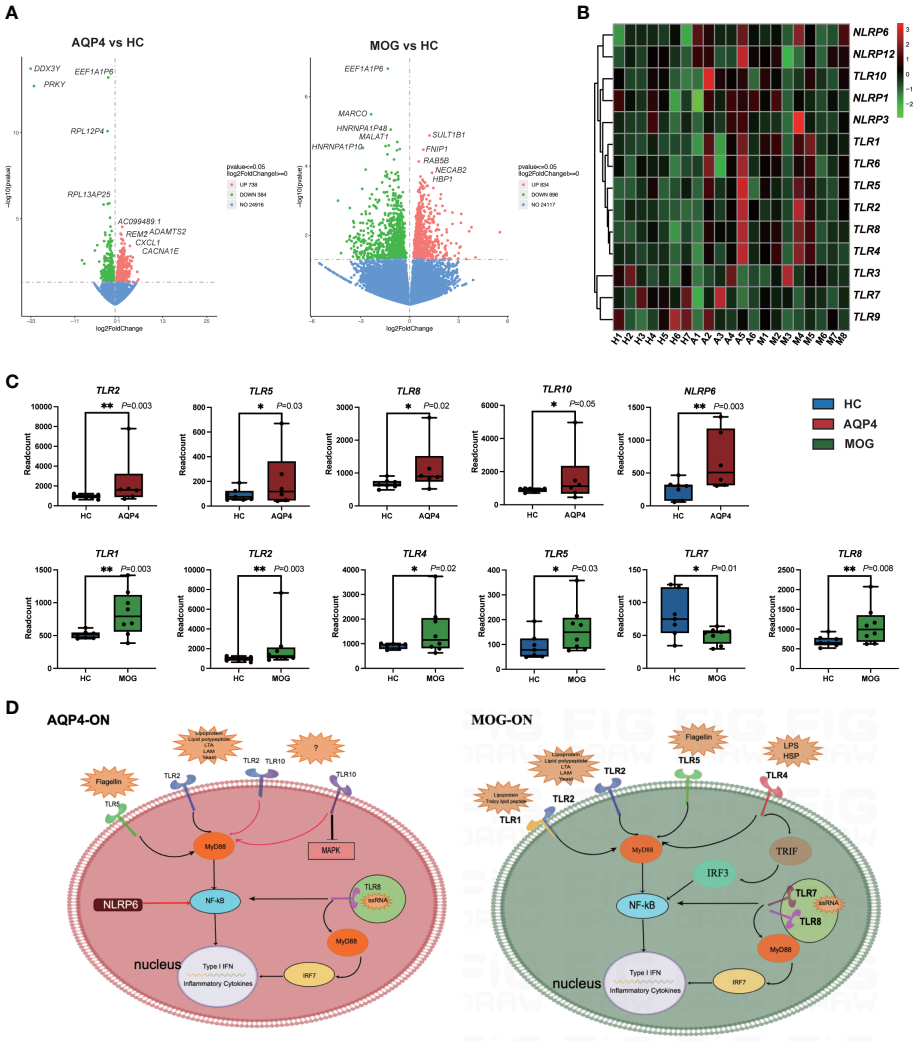


FIGURE 4
**(A)** Volcano plots showing the DEGs in the AQP4-ON group and MOG-ON group. The left panel is the volcanic map of AQP4-ON group vs HC group, and the right is the volcanic map of the MOG-ON group vs HC group. Red and green dots represent up-regulated and down-regulated genes, respectively. **(B)** is the cluster map of FPKM value of the TLR genes. **(C)** The box plot of the TLRs and NLRs of the AQP4-ON and MOG-ON groups according to the result of the statistical analysis of DEGs. The symbol * indicates that the p-value is less than 0.05, and the symbol ** indicates that the p-value is less than 0.01. **(D)** was according to the DEG analysis, GO term enrichment analysis and KEGG pathway enrichment analysis, AQP4-ON and MOG-ON activate the NF-κB pathway through the promotion of the expression of different TLRs and NLRs. The mechanism plot was drawn using the online tool Figdraw (www.figdraw.com). Red arrows indicate inhibition and black arrows indicate promotion.

core genes (Figure 5B). Translocator protein (TSPO) has been found to be up-regulated in inflammation diseases of central nervous system, and according our results, TSPO may be an important target for AQP4-ON (16). *MAPK14* is an important player in a variety of nervous system diseases, and contributes to the control of cerebrovascular and blood-brain barrier. The disruption of the blood-brain barrier in AQP4-ON may be related to the activation of *MAPK14* (17). Meanwhile the PPI analysis in the MOG-ON group identified *UBB* and *MAPK14* as the most significant targets. *UBB* is an important gene encoding ubiquitin, and ubiquitination plays an important role in biological functions such as antigen presentation, immune response and inflammation, and according our results, UBB may be an important target for MOG-ON (18).

## 3.4 Cell type analysis based on gene expression signature

The proportion of immune cells in the three groups showed individual differences (Supplementary Table 1). The 22 types of immune cells analyzed by CIBERSORTx showed no Macrophages M1, mast cells activated and eosinophils infiltration in any subject, and T cells CD4 naïve was only found in one healthy control. Neutrophils were the largest subset of cells in the subjects (22.6%~80.1%). B cells memory infiltration was found only in A2, A4 and M5, T cells CD4 memory resting was found only in A1, A2 and a healthy control, T cells gamma delta was found only in A4, and Macrophages M2 was found only in A2 and A5. Finally, we found that Dendritic cells resting and Dendritic cells activated existed almost in ON patients. Then, the PCA

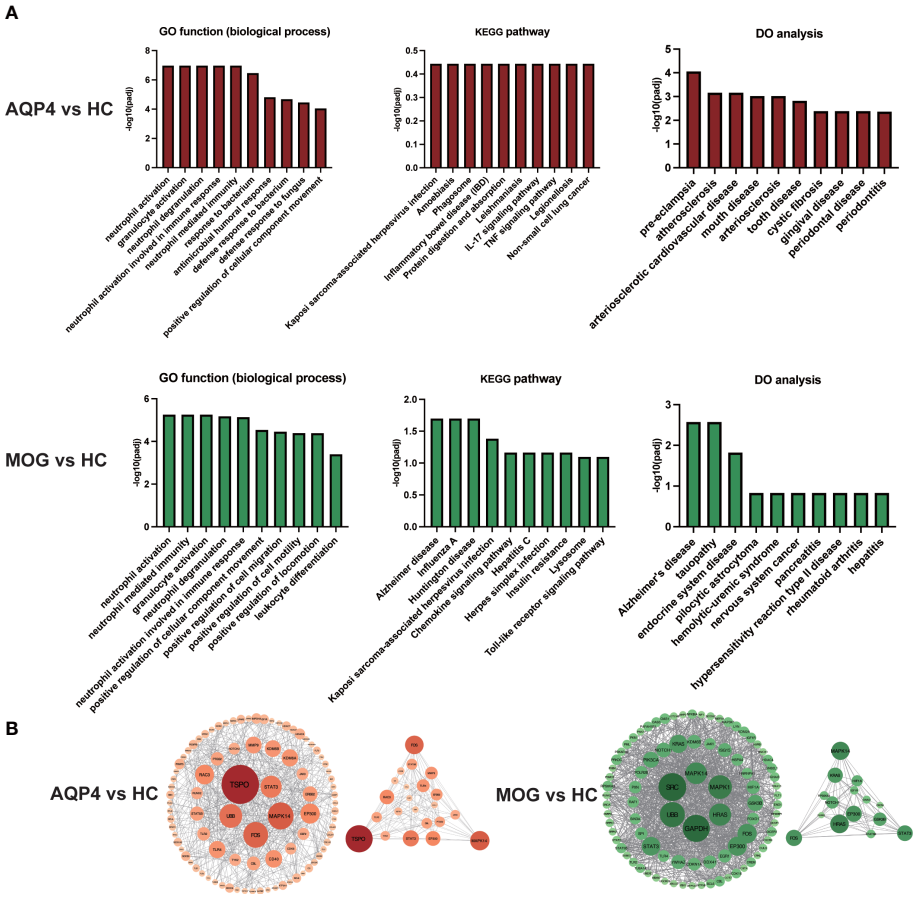


FIGURE 5
**(A)** GO functional enrichment analysis, KEGG pathway enrichment analysis and DO enrichment analysis of DEGs in the AQP4-ON group and MOG-ON group. **(B)** PPI analysis of DEGs in the AQP4-ON group and MOG-ON group.

based on the results of the CIBERSORTx analysis revealed that except for the sample from patient A1, the other samples showed obvious intra group clustering and inter group differences (Figure 6A). (Figure 6B, C) showed that there are differences in the proportion of immune cells among the three groups

## 3.5 Correlation between immune cell infiltration and clinical outcomes

The results of the ImmuCellAI analysis (Figure 7A) for AQP4-ON, MOG-ON and HC group revealed that although there were differences between the two methods in the classification of immune cells, the proportion of infiltrated immune cell types was roughly similar to that of CIBERSORTx. Thus, we analyzed the correlation between the proportion of infiltrated immune cell types and the clinical results of patients. A total of 14 patients were included in this study, and the therapeutic regimen as well as the BCVA(LogMAR) at the last follow up were shown in Table 2. The patient A4 refused to be treated, and the BCVA (LogMAR) of the Oculus Dexter (OD) recovered to normal levels in about 2 months after the onset, and no recurrence has occurred to date. The data in Figure 5B revealed that there was almost no B cell infiltration in the peripheral blood, which might explain the good prognosis of this patient. The AQP4-IgG titer of patient A2 was only 10.37 u/ml; however, despite the IVMP and oral prednisolone treatment, her vision was still very poor. It showed that the proportion of neutrophil infiltration accounted for the largest proportion of all subjects, which might indicate that her severe inflammatory rection was the cause of irreversible damage of her vision. The Spearman correlation analysis of the relationship between the 22 kinds of immune cells and patients' BCVA (LogMAR) at diagnosis (Figure 7) showed that the infiltration ratios of monocytes (rs=0.69, $P$=0.006) and M0 macrophages (rs=0.66, $P$=0.01) were positively correlated with the BCVA (LogMAR). Moreover, the infiltration ratio of neutrophils was negatively correlated with the BCVA (LogMAR) (rs=0.65, $P$=0.01). No significant correlation was found among the other 18 immune cell subtypes (data not shown).

# 4 Discussion

Currently, most researchers in the field believe that although MOG-ON is similar to AQP4-ON in clinical manifestations, unlike

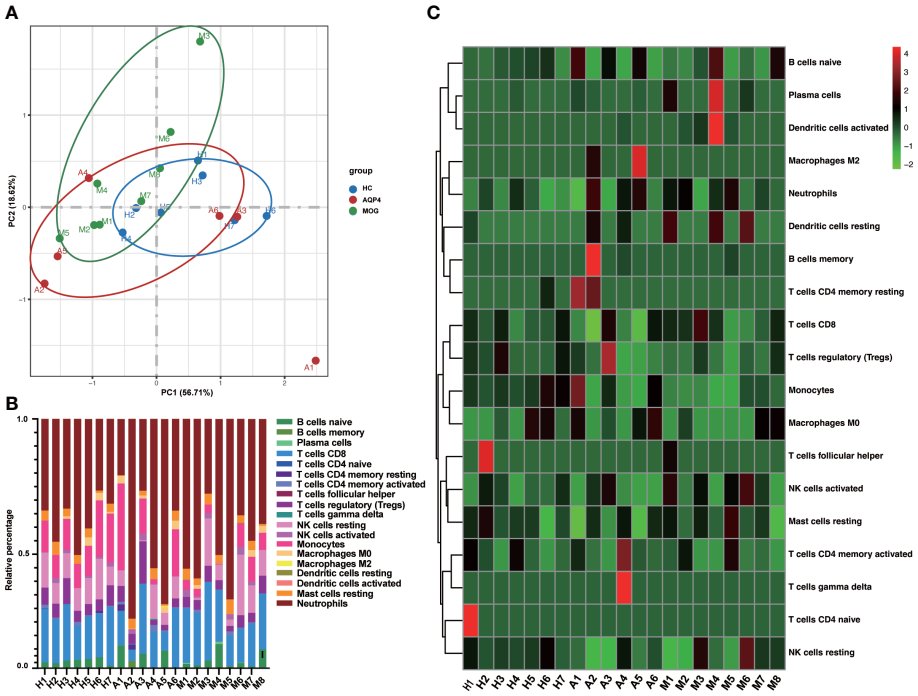


FIGURE 6
**(A)** PCA based on CIBERSORTx results. **(B)** The cumulative histogram of the proportion of 22 immune cell subtypes in each sample, and the total proportion of the 22 immune cell subtypes is equal to 100%. **(C)** The specific heat map analysis of the 22 immune cell subtypes in each sample.

AQP4-ON, MOG-ON is not an immune subtype of neuromyelitis optica spectrum disorder (NMOSD), but a subtype of MOG antibody-related diseases (MOGAD) (19). Moreover, magnetic resonance imaging (MRI) reveals obvious differences between the cortical grey/juxtacortical white matter lesions on the brain of patients with MOGAD and those of patients with AQP4-IgG seropositive NMOSD (20). This finding indicates that the immunological mechanism of AQP4-ON and MOG-ON may be different. In this study, the RNA-seq analysis of whole blood from AQP4-ON and MOG-ON patients and HC subjects revealed that there were significant differences in gene expression and cell function among the three groups. In particular, the results suggested that the AQP4-ON patients likely presented PAMP-induced inflammation, and MOG-ON patients likely presented DAMP-induced inflammation. In addition, cell type analysis based on gene expression signature showed that the proportion of immune cells was similar in the HC group, but was significantly different between the AQP4-ON group and MOG-ON group.

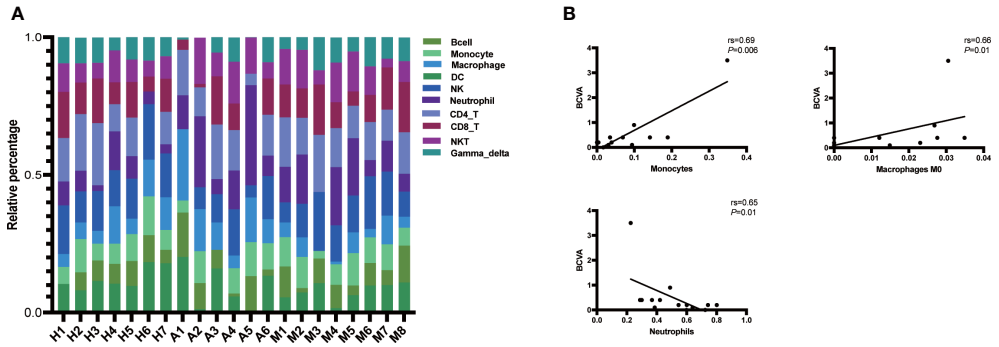


FIGURE 7
**(A)** Immune cell abundance analysis was performed on all patients and subjects using the ImmuCellAI software. Histogram of the proportions of the 24 immune cells in the AQP4-ON group, MOG-ON group and HC group. X-axis: ID of each subject; Y-axis: percentage of immune cell types. Gamma_delta: γδ T cell, NKT, natural killer T cell; CD8_T, CD8 + T cell; CD4_T, CD4 + T cell; NK, natural killer T cell; DC, dendritic cell. **(B)** Spearman correlation analysis of the relationship be-tween immune cells and BCVA (LogMAR) at diagnosis. rs is the Spearman correlation coefficient, negative number represents negative correlation and positive number represents positive correlation. $P < 0.05$ indicates statistical significance.

10.3389/fimmu.2023.1095966

TABLE 2 Treatment and prognosis of patients.

| Patient ID | Age (years) | Sex | Antibody titer | Affected eyes | Therapeutic methods | BCVA at diagnosis | Last follow-up BCVA |
|---|---|---|---|---|---|---|---|
| A1 | 71 | Female | AQP4-IgG:>80u/ml | Right | IVMP and oral prednisolone | 3.5 | 3.5 |
| A2 | 45 | Female | AQP4-IgG:10.37u/ml | Left | Oral prednisolone | 1.7 | 2 |
| A3 | 11 | Female | AQP4-IgG:67.90u/ml | Right | IVMP and oral prednisolone | 2 | 0.4 |
| A4 | 43 | Female | AQP4-IgG:40.83u/ml | Right | None | 0.6 | 0 |
| A5 | 32 | Female | AQP4-IgG:>80u/ml | Right | IVMP and oral prednisolone | 2.5 | 0.2 |
| A6 | 25 | Female | AQP4-IgG:26.8u/ml | Left | IVMP and oral prednisolone | 2.5 | 0.4 |
| M1 | 18 | Male | MOG-IgG:1:10 | Left | IVMP and oral prednisolone | 0.4 | 0.2 |
| M2 | 32 | Female | MOG-IgG:1:10 | Left | IVMP and oral prednisolone | 0.5 | 0.1 |
| M3 | 57 | Female | MOG-IgG:1:10 | Left | IVMP and oral prednisolone | 1.1 | 0.4 |
| M4 | 24 | Female | MOG-IgG:1:100 | Left | IVMP and oral prednisolone | 1.1 | 0.2 |
| M5 | 39 | Female | MOG-IgG:1:10 | Right | IVMP and oral prednisolone | 2 | 0 |
| M6 | 70 | Female | MOG-IgG:1:100 | Left | IVMP and oral prednisolone | 2 | 0.1 |
| M7 | 35 | Male | MOG-IgG:1:32 | Right | IVMP and oral prednisolone | 2 | 0.9 |
| M8 | 31 | Male | MOG-IgG:1:100 | Right | IVMP and oral prednisolone | 0.5 | 0.2 |

Age: years at diagnosis; IVMP, intravenous pulses of methylprednisolone. BCVA: Snellen visual acuity was converted to logarithm of the minimum angle of resolution (logMAR). Counting fingers vision was converted to a value of 2.0 logMAR, hand motion vision was converted to a value of 2.5 logMAR, light perception vision was converted to a value of 3.0 logMAR and no light perception vision was converted to a value of 3.5 logMAR.

DAMPs are endogenous molecules released from the cell, which serve as potent activators of the immune system (21). Cellular stressors, including physical (trauma, radiation), chemical (toxins, osmolarity), metabolic (ischemia/reperfusion), and infectious (viruses, bacteria, protozoa) factors, can trigger DAMP release (21). DAMPs are systemically and locally up-regulated in autoimmune diseases, such as rheumatoid arthritis. PAMPs are derived from microorganisms and recognized by pattern recognition receptor (PRR)-bearing cells of the innate immune system (22). However, the roles of DAMPs and PAMPs in AQP4-ON and MOG-ON have never been reported. Biological function analysis of DEGs revealed that DEGs in AQP4-ON patients were mainly involved in the regulation of inflammatory cells, such as regulation of granular chemotaxis, positive regulation of leucocyte chemotaxis, regulation of leucocyte chemotaxis. and these over-represented terms are closely related to DAMP-induced adaptive immunity. The analysis also revealed that DEGs in MOG-ON patients were mainly involved in the activation of inflammatory cells, such as neutrophil activation, granulocyte activation, neutrophil activation involved in immune responses, and the reaction to bacteria and viruses, such as response to bacteria, defense response to bacterium, response to LPS, and these enriched terms fully indicate that MOG-ON is closely related to PAMP-induced innate immunity. Currently, PAMPs and DAMPs are known to bind to the receptors of TLRs to modulate their activation and promote the synthesis of cytokines. TLRs are type I transmembrane pattern recognition receptors which can recognize molecules present on the surface of pathogen cells (23). Ten types of TLRs have been identified in human, with different ligands. TLRs are widely distributed on the surface of macrophages, dendritic cells and epithelial cells. It has been found that the percentage of peripheral $CD4^+$ T cells expressing TLR2, TLR4 and TLR9 in NMOSD samples was significantly higher than that in healthy subjects (24). According to our DEGs analysis, the expression of TLRs was clearly different between the AQP4-ON and MOG-ON groups. Specifically, *TLR2*, *TLR5*, *TLR8* and *TLR10* were significantly up-regulated in the AQP4-ON group, while *TLR1*, *TLR2*, *TLR4*, *TLR5* and *TLR8* were significantly up-regulated in the MOG-ON group. Both the *TLR2* and *TLR5* are only expressed on the cell surface of myeloid cells, such as monocytes and macrophages, while *TLR7* is found in intracellular vesicles, where it is involved in identifying the nucleic acid

components of microorganisms, and all of them can activate NF-κB. TLR10 is the most recently identified human TLR, and its function and ligand are still unclear. TLR10 can inhibit other TLRs by competing with dimers of TLR1, TLR2 and TLR6, which can induce PI3K/AKT signaling, but other studies have reported that TLR10 may stimulate and amplify the activity of TLR2 when it forms an isomeric dimer with TLR2 (25). However, the detailed functions of TLR10 in AQP4-ON need to be further investigated in animal models. TLR4 is the main receptor of LPS, an important PAMP. The binding of LPS to TLR4 activates signal transduction pathways in two ways, namely through toll-interleukin-1 receptor domain containing adaptor protein (TIRAP) and MyD88. TLR2/TLR4 have emerged as targets for treating a wide array of autoimmune disorders. Liu et al. reported that blocking TLR2/TLR4 in the experimental autoimmune encephalomyelitis (EAE) model of multiple sclerosis prevents the production of proinflammatory factors, which is consistent with our clinical data (26). In addition to TLRs, Nod-like receptors (NLRs) are also important PRRs for identifying PAMP and DAMP. Our results showed that NLRP6 was significantly up-regulated in AQP4-ON, which is different from other pro-inflammatory mechanisms initiated by NLRs (27).

At present, it has been confirmed that T, NK and B cells play important roles in the pathogenesis of AQP4-ON and MOG-ON. The B cell-mediated humoral immune response by autoreactive IgG antibodies against AQP4 or MOG is considered to be the driver of NMOSD. Recently, other immune cells, such as T cells, have also attracted the attention of researchers. However, their detailed functions remain unclear. A previous study by Zhou et al. analyzed non-coding RNAs in peripheral blood mononuclear cells (PBMCs) from NMOSD patients using the online web tool xCell, and found that the immune scores of CD8+ T cells, M1 macrophages and plasma cells in the NMOSD group were increased, while that of M2 macrophages was decreased (28). The traditional method uses immunohistochemistry to infer immune subsets of cells to evaluate immune cell tissue invasion, but such a method is often useful for solid tumors (29). At present, flow cytometry is widely used for counting mixed cells, which is an alternative method for quantitating immune infiltration that can simultaneously measure multiple parameters (30). However, this method requires processing samples in a timely and precise manner, which may lead to loss of some cell types and distortion of GEPs. Unlike flow cytometry, which relies on cell surface marker antibodies as the basis for cell classification, our study applied CIBERSORTx to quantify cell fractions from GEPs using a deconvolution algorithm based on peripheral blood RNA-seq data, and then accurately estimated the proportion of infiltrated immune cells. CIBERSORTx immune cell infiltration results were verified by fluorescent activated cell classification, and have been widely used in a variety of tumors and immune diseases. Our analysis of the correlation between the proportion of 22 types of immune cells and BCVA (LogMAR) of patients at the last follow-up showed that the ratio of monocytes or M0 macrophages was negatively correlated with BCVA (LogMAR), while the ratio neutrophils was positively correlated with BCVA (LogMAR). In other words, the infiltration ratio of monocytes or M0 macrophages was negatively correlated with the prognosis of the visual acuity of patients, and the infiltration ratio of neutrophils was positively correlated with the prognosis of the visual acuity of patients. Therefore, our study revealed that monocytes, M0 macrophages and neutrophils might serve as indicators of the visual prognosis of patients.

Over all, this study revealed different immunological mechanisms between AQP4-ON and MOG-ON patients based on transcriptomics analysis of patients' whole blood, and found the proportion of immune cell infiltration was closely related to patients' vision. However, there are still some limitations to this study. First, the sample size is still small, which may lead to the deviation of the results, and it needs to expand the sample size in the further study. Then, future research is warranted to investigate the detailed pathological mechanism responsible for AQP4-ON and MOG-ON using *in vitro* and *in vivo* models based on transcriptomics data; however, this is beyond the scope of the current study.

## 5 Conclusion

In conclusion, our study shows that AQP4-ON and MOG-ON differ in the immune mechanism of activation of different TLR-related pathways as well as the infiltration of different immune cells, which not only provides novel insights into the pathogenic mechanism of AQP4-ON and MOG-ON, but also clues for the development of new therapeutic approaches for these diseases.

## Data availability statement

The datasets presented in this study can be found in online repositories. The names of the repository/repositories and accession number(s) can be found below: GSE226808 (GEO).

## Ethics statement

The studies involving human participants were reviewed and approved by The ethics committee of the Affiliated Wuxi Clinical College of Nantong University. Written informed consent to participate in this study was provided by the participants' legal guardian/next of kin. Written informed consent was obtained from the [individual(s) AND/OR minor(s)' legal guardian/next of kin] for the publication of any potentially identifiable images or data included in this article.

## Author contributions

Study conception and design: WZ, and KW. Collection of samples: XC, LC, YP, PC, YL, and SL. Data analysis: XC and LC.

Drafting of manuscript and figures: XC and LC. Critical revision of the manuscript: WZ and KW. Statistical analysis: YP and PC. Obtained funding: WZ. All authors contributed to the article and approved the submitted version.

## Funding

This research was financially supported by Major project of Wuxi Commission of Health (Z202014), Young and middle-aged top medical and health talents project of Wuxi Commission of Health (BJ2020031) and Postdoctoral Science Foundation funded project of Jiangsu Province (2021K196B). The funding organization played no role in the study design or its conduct.

## Acknowledgments

The authors thank all the patients and healthy volunteers for their participation.

## Conflict of interest

The authors declare that the research was conducted in the absence of any commercial or financial relationships that could be construed as a potential conflict of interest.

## Publisher's note



## Supplementary material

The Supplementary Material for this article can be found online at: https://www.frontiersin.org/articles/10.3389/fimmu.2023.1095966/full#supplementary-material

## References

1. Levin MH. Demyelinating optic neuritis and its subtypes. *Int Ophthalmol Clin* (2019) 59:23–37. doi: 10.1097/IIO.0000000000000278

2. Ishikawa H, Kezuka T, Shikishima K, Yamagami A, Hiraoka M, Chuman H, et al. Epidemiologic and clinical characteristics of optic neuritis in Japan. *Ophthalmology* (2019) 126:1385–98. doi: 10.1016/j.ophtha.2019.04.042

3. Toosy AT, Mason DF, Miller DH. Optic neuritis. *Lancet Neurol* (2014) 13:83–99. doi: 10.1016/S1474-4422(13)70259-X

4. Kitley J, Waters P, Woodhall M, Leite MI, Murchison A, George J, et al. Neuromyelitis optica spectrum disorders with aquaporin-4 and myelin-oligodendrocyte glycoprotein antibodies: A comparative study. *JAMA Neurol* (2014) 71:276–83. doi: 10.1001/jamaneurol.2013.5857

5. Nielsen S, Nagelhus EA, Amiry-Moghaddam M, Bourque C, Agre P, Ottersen OP. Specialized membrane domains for water transport in gial cells: high-resolution immunogold cytochemistry of aquaporin-4 in rat brain. *J Neurosci* (1997) 17(1):171–80. doi: 10.1523/JNEUROSCI.17-01-00171.1997

6. Marignier R, Hacohen Y, Cobo-Calvo A, Pröbstel A-K, Aktas O, Alexopoulos H, et al. Myelin-oligodendrocyte glycoprotein antibody-associated disease. *Lancet Neurol* (2021) 20:762–72. doi: 10.1016/S1474-4422(21)00218-0

7. Filippatou AG, Mukharesh L, Saidha S, Calabresi PA, Sotirchos ES. AQP4-IgG and MOG-IgG related optic neuritis–prevalence, optical coherence tomography findings, and visual outcomes: A systematic review and meta-analysis. *Front Neurol* (2020) 11:540156. doi: 10.3389/fneur.2020.540156

8. Reindl M, Waters P. Myelin oligodendrocyte glycoprotein antibodies in neurological disease. *Nat Rev Neurol* (2019) 15:89–102. doi: 10.1038/s41582-018-0112-x

9. Sotirchos ES, Filippatou A, Fitzgerald KC, Salama S, Pardo S, Wang J, et al. Aquaporin-4 IgG seropositivity is associated with worse visual outcomes after optic neuritis than MOG-IgG seropositivity and multiple sclerosis, independent of macular ganglion cell layer thinning. *Mult Scler* (2020) 26:1360–71. doi: 10.1177/1352458519864928

10. Kunchok A, Chen JJ, McKeon A, Mills JR, Flanagan EP, Pittock SJ. Coexistence of myelin oligodendrocyte glycoprotein and aquaporin-4 antibodies in adult and pediatric patients. *JAMA Neurol* (2020) 77:257–9. doi: 10.1001/jamaneurol.2019.3656

11. Beck RW, Cleary PA, Anderson MM, Keltner JL, Shults WT, Kaufman DI, et al. A randomized, controlled trial of corticosteroids in the treatment of acute optic neuritis. *N Engl J Med* (1992) 326:581–8. doi: 10.1056/NEJM199202273260901

12. Tampoia M, Abbracciavento L, Barberio G, Fabris M, Bizzaro N. A new M23-based ELISA assay for anti-aquaporin 4 autoantibodies: diagnostic accuracy and clinical correlation. *Auto Immun Highlights* (2019) 10:5. doi: 10.1186/s13317-019-0115-7

13. Lee JWY, Lai JSM, Yick DWF, Tse RKK. Retrospective case series on the long-term visual and intraocular pressure outcomes of phacomorphic glaucoma. *Eye* (2010) 24:1675–80. doi: 10.1038/eye.2010.108

14. Szklarczyk D, Franceschini A, Kuhn M, Simonovic M, Roth A, Minguez P, et al. The STRING database in 2011: Functional interaction networks of proteins, globally integrated and scored. *Nucleic Acids Res* (2011) 39:D561–8. doi: 10.1093/nar/gkq973

15. Schulze-Bonsel K, Feltgen N, Burau H, Hansen L, Bach M. Visual acuities "Hand motion" and "Counting fingers" can be quantified with the freiburg visual acuity test. *Invest Ophthalmol Vis Sci* (2006) 47:1236. doi: 10.1167/iovs.05-0981

16. Tournier BB, Tsartsalis S, Ceyzériat K, Garibotto V, Millet P. *In vivo* TSPO signal and neuroinflammation in alzheimer's disease. *Cells* (2020) 9:1941. doi: 10.3390/cells9091941

17. Asih PR, Prikas E, Stefanoska K, Tan ARP, Ahel HI, Ittner A. Functions of p38 MAP kinases in the central nervous system. *Front Mol Neurosci* (2020) 13:570586. doi: 10.3389/fnmol.2020.570586

18. Banasiak K, Szulc NA, Pokrzywa W. The dose-dependent pleiotropic effects of the UBB+1 ubiquitin mutant. *Front Mol Biosci* (2021) 8:650730. doi: 10.3389/fmolb.2021.650730

19. Jarius S, Paul F, Aktas O, Asgari N, Dale RC, de Seze J, et al. MOG encephalomyelitis: international recommendations on diagnosis and antibody testing. *J Neuroinflamm* (2018) 15:134. doi: 10.1186/s12974-018-1144-2

20. Salama S, Khan M, Shanechi A, Levy M, Izbudak I. MRI Differences between MOG antibody disease and AQP4 NMOSD. *Mult Scler* (2020) 26:1854–65. doi: 10.1177/1352458519893093

21. Gong T, Liu L, Jiang W, Zhou R. DAMP-sensing receptors in sterile inflammation and inflammatory diseases. *Nat Rev Immunol* (2020) 20:95–112. doi: 10.1038/s41577-019-0215-7

22. Rai DV, Agrawal DK. The role of DAMPs and PAMPs in inflammation-mediated vulnerability of atherosclerotic plaques. *Can J Physiol Pharmacol* (2017) 95 (10):1245–53. doi: 10.1139/cjpp-2016-0664

23. Akira S, Takeda K. Toll-like receptor signalling. *Nat Rev Immunol* (2004) 4:499–511. doi: 10.1038/nri1391

24. Jiménez-Dalmaroni MJ, Gerswhin ME, Adamopoulos IE. The critical role of toll-like receptors — from microbial recognition to autoimmunity: A comprehensive review. *Autoimmun Rev* (2016) 15:1–8. doi: 10.1016/j.autrev.2015.08.009

25. Lai N, Qian Y, Wu Y, Jiang X, Sun H, Luo Z, et al. Toll-like receptor 10 expression in b cells is negatively correlated with the progression of primary sjögren's disease. *Clin Immunol* (2022) 237:108989. doi: 10.1016/j.clim.2022.108989

26. Liu X, Zhang X, Niu X, Zhang P, Wang Q, Xue X, et al. Mdivi-1 modulates Macrophage/Microglial polarization in mice with EAE *via* the inhibition of the TLR2/4-GSK3β-NF-κB inflammatory signaling axis. *Mol Neurobiol* (2022) 59:1–16. doi: 10.1007/s12035-021-02552-1

27. Anand PK, Malireddi RKS, Lukens JR, Vogel P, Bertin J, Lamkanfi M, et al. NLRP6 negatively regulates innate immunity and host defence against bacterial pathogens. *Nature* (2012) 488:389–93. doi: 10.1038/nature11250

28. Zhou Y, Song S, Han Y, Liu J, Yin B, Yuan C, et al. Altered non-coding RNA profiles and potential disease marker identification in peripheral blood mononuclear cells of patients with NMOSD. *Int Immunopharmacol* (2022) 109:108899. doi: 10.1016/j.intimp.2022.108899

29. Sukswai N, Khoury JD. Immunohistochemistry innovations for diagnosis and tissue-based biomarker detection. *Curr Hematol Malig Rep* (2019) 14:368–75. doi: 10.1007/s11899-019-00533-9

30. Saeys Y, Van Gassen S, Lambrecht BN. Computational flow cytometry: helping to make sense of high-dimensional immunology data. *Nat Rev Immunol* (2016) 16:449–62. doi: 10.1038/nri.2016.56

frontiers | Frontiers in Neurology

TYPE Original Research
PUBLISHED 09 March 2023
DOI 10.3389/fneur.2023.1090631



OPEN ACCESS

EDITED BY
Honghao Wang,
Guangzhou First People's Hospital, China

REVIEWED BY
Yongchang Li,
Xinjiang Agricultural University, China
Candice Brinkmeyer-Langford,
Texas A&M University, United States

*CORRESPONDENCE
Majid Motovali-Bashi
✉ mbashi@sci.ui.ac.ir
Mostafa Ghaderi-Zefrehei
✉ mghaderi@yu.ac.ir;
✉ mosmos741@yahoo.com

†These authors have contributed equally to this work and share first authorship

SPECIALTY SECTION
This article was submitted to Multiple Sclerosis and Neuroimmunology, a section of the journal Frontiers in Neurology

RECEIVED 05 November 2022
ACCEPTED 10 February 2023
PUBLISHED 09 March 2023

CITATION
Karimi N, Motovali-Bashi M and Ghaderi-Zefrehei M (2023) Gene network reveals *LASP1*, *TUBA1C*, and *S100A6* are likely playing regulatory roles in multiple sclerosis. *Front. Neurol.* 14:1090631. doi: 10.3389/fneur.2023.1090631



# Gene network reveals *LASP1*, *TUBA1C*, and *S100A6* are likely playing regulatory roles in multiple sclerosis

Nafiseh Karimi[1†], Majid Motovali-Bashi[1*†] and Mostafa Ghaderi-Zefrehei[2*†]

[1]Department of Cell and Molecular Biology and Microbiology, Faculty of Biological Science and Technology, University of Isfahan, Isfahan, Iran, [2]Department of Animal Genetics, Yasouj University, Yasuj, Iran

**Introduction:** Multiple sclerosis (MS), a non-contagious and chronic disease of the central nervous system, is an unpredictable and indirectly inherited disease affecting different people in different ways. Using Omics platforms genomics, transcriptomics, proteomics, epigenomics, interactomics, and metabolomics database, it is now possible to construct sound systems biology models to extract full knowledge of the MS and recognize the pathway to uncover the personalized therapeutic tools.

**Methods:** In this study, we used several Bayesian Networks in order to find the transcriptional gene regulation networks that drive MS disease. We used a set of BN algorithms using the R add-on package bnlearn. The BN results underwent further downstream analysis and were validated using a wide range of Cytoscape algorithms, web based computational tools and qPCR amplification of blood samples from 56 MS patients and 44 healthy controls. The results were semantically integrated to improve understanding of the complex molecular architecture underlying MS, distinguishing distinct metabolic pathways and providing a valuable foundation for the discovery of involved genes and possibly new treatments.

**Results:** Results show that the *LASP1*, *TUBA1C*, and *S100A6* genes were most likely playing a biological role in MS development. Results from qPCR showed a significant increase ($P < 0.05$) in *LASP1* and *S100A6* gene expression levels in MS patients compared to that in controls. However, a significant down regulation of *TUBA1C* gene was observed in the same comparison.

**Conclusion:** This study provides potential diagnostic and therapeutic biomarkers for enhanced understanding of gene regulation underlying MS.

KEYWORDS

**multiple sclerosis (MS), Bayesian network, transcriptome, Cytoscape, qPCR**

## 1. Introduction

Multiple sclerosis (MS) is a multifocal inflammatory autoimmune disease (1). Even though MS is usually considered a white matter disease, but several studies have demonstrated the involvement of gray matter impairment in conjunction with cortical and deep (2–6) leading to progressive neuronal damage in genetically sensitive hosts (1). MS is a complex multicomponent demyelinating disease and its pathophysiology consist of redox, autoimmune, vascular, and neurodegenerative systems, to name a few. The clear-cut

mechanisms of MS triggering, its development, and progression are still obscure. In MS, impairing of the myelin sheath of neural axons in the Central Nervous System (CNS) is observed (7, 8). MS shows a long range of symptoms e.g., from pathological processes to severe physical disabling. Gender preferences, genetical factors, and geographical differences have been reported for people suffering from MS. Over outburst of MS, monocytes, which are a preserved subset of white blood cells, are activated by interferon-β (IFN-β) (7). MS study is quite vivid, using Omics data, many authors have used gene networks to get some insight into molecular mechanisms of MS (9–19). The integration of information gleaned from a variety of resources encompassing transcriptomics, genomics, proteomics and patient clinical data could boost our understanding of the mechanism(s) underpinning the reason for this disease (20). In this regard, we can explore the signaling pathways involved in MS (21), apply logical networks to model signaling pathways in MS (22) and use networks to combine information on transcriptome-interactome data from MS studies (17). We can also apply theory of biochemical systems for improving therapeutic drugs in re-myelination (15), create molecular networks based on transcription factors and genes expressed in mononuclear cells in MS patients (23), and design reactive networks between distinct miRNA and target genes in T cells (23). This approach will help explain the molecular mechanisms of the MS disease (12). Supplementary Table 1 shows some examples of network-based studies used with different MS biological data. As one can see, Bayesian Network (BN) modeling paradigms have rarely been applied in this setting. BN uses probability theory to reason under uncertainty. BN as a graphical scheme (directed acyclic graph) consists of a qualitative part (structural model) and a quantitative part (local probability distributions), which allow for a different kind of probabilistic inference, and quantitatively measures even the smallest impact of a variable or set of variables on others. This sort of modeling is of great importance in transcriptomic studies, since it can reveal both qualitative and quantitative elements of learned gene networks. BN has previously been used in several transcriptomic studies (10, 24, 25).

Many existing categories of gene networks identify groups of related genes as gene sets, making experimental follow-up a formidable task. With BN, it is possible to determine whether a gene is a driving source of changes in its gene network or not, since both in-degree and out-degrees of connectivity of each gene can be readily verified. The more out-degree gene has, the higher likelihood of being a possible regulator one. This would be a crucial characteristic for example when looking for potential drug targets. However, it is likely that a specific transcription factor defining a particular cell type that drives pathology, may not have a large number of out-degrees while still being crucial. To this end, if a particular gene is expressed across different cell types, for example like *S100A6*, then it may be correlated with different genes, but this may be a spurious correlation. Therefore, to leave off possible artifacts, we should use extra source of information when interpreting the results. Today, MS research is increasingly data-driven—a trend that arguably shall continue at a much higher rate in times to come. To tackle these large amounts of heterogeneous data, and to derive insight into MS disease, many interdisciplinary scientists have started using a variety of computational tools. In this study, we aim to gain much insight into the regulatory transcriptional gene network underlying MS using systems biology approaches in the context of BN, that may yield mechanistically interpretable results.

Abbreviations: BIC, Bayesian information criterion; BN, Bayesian Network; CNS, central nervous system; DEGs, differentially expressed genes; DAG, diacylglycerol; ER, endoplasmic reticulum; GEO, gene expression omnibus; GWAS, genome-wide association study; IP3, inositol-1,4,5-triphosphate; *LASP1*, The *LIM* and *SH3* protein 1; MS, multiple sclerosis; NLS, nuclear localization signal; NFATc3, nuclear factor of activated T cells 3; NF-κB, nuclear factor-kappa B; PLC, phospholipase C; PPI, protein-protein interaction; RIN, RNA integrity number; RRMS, relapsing-remitting MS; SPMS, secondary progressive MS; TFs, transcription factors; TCR, T cell receptor; YY1, Yi and Yang 1.

# 2. Methods

## 2.1. Network analysis

In this study, the Gene Expression Omnibus (GEO) database (https://www.ncbi.nlm.nih.gov/geo/) was scanned using a combination of several simple key words, and resulting DNA microarray experiments related to MS, that fulfilled our criteria. In the end, based on our criteria for choosing a suitable GEO data set, the microarray series with accession number GSE17048 was downloaded from GEO using the GEO query package (26). This accession was seen to have the highest number of arrays per probe—a fact that would help minimize the rate of false positives while training the regulatory gene BN. The GSE17048 contained 56 blood samples from MS group [44 patients were in the RRMS phase (relapsing-remitting) and 12 patients were in the SPMS phase (progressive-secondary)]. The control population was 44 healthy people without any symptoms. The average age of the patients was 39.5 years old and the control group was 39.23 years old, and in terms of gender, the MS included 29 women and 15 men (higher prevalence of the disease in women) and 23 men and 21 women were studied in the control group. In order to remove noise from the data, probes with the highest variance were obtained and used as an input to train the gene regulatory BN using bnlearn, an R add-on package (27, 28). The following codes were used to filter the probes with highest variances: *qt <- quantile[t(data1); probs = c(0.0002,0.99)]; rows1 <- apply[t(data1), function(x) any(x < qt | x > qt)]; data2 <- t(data1)[, rows1]*. We obtained the best fitted BN model on our data using Bayesian information criterion (BIC) and its adjacency matrix, with the help of the *Cytoscape*-based *aMatReader* plugin, with the *Cytoscape* (29) environment used for further downstream scrutiny.

## 2.2. Downstream analysis

This was accomplished with the following *Cytoscape* add-on packages. The *jActiveModules* were used to explore the

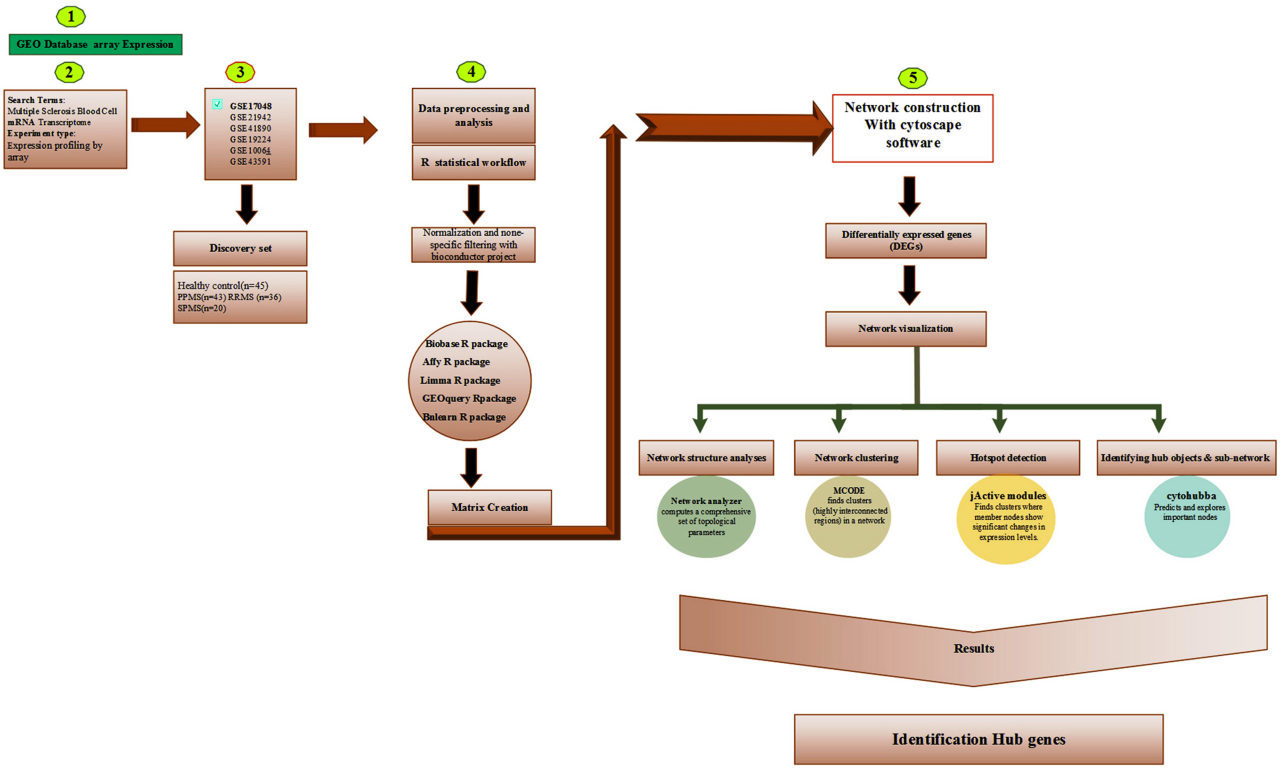


FIGURE 1
The analysis pipeline used in this study[1,2,3,4].

concept of gene modules and find sub-networks (30); *MCODE* to identify putative complexes by finding regions of significant local density (31); *CytoHubba* to explore the protein-protein interaction (PPI) network of hub genes using eleven different methods (32). The *NetworkAnalyzer* was used to determine the hub genes, taking into account the degree of topological criteria (e.g., the number of nodes, edges, and connected components, along with the network diameter, radius, density, centralization, heterogeneity, clustering coefficient, the characteristic path length, the distributions of node degrees, neighborhood connectivity, average clustering coefficients, and shortest path lengths) (33). The *iRegulon* was used to detect targets / motifs/paths from a set of genes; and the *CyTargetLinker* to integrate regulatory reactions in network analysis. In addition, we used *Metascape* (34) to annotate the multiple gene lists in our study. Even though transcriptomic statistical analysis is generally based on probe level data, the probe names were converted to their corresponding gene names using g:Profiler (https://biit.cs.ut.ee/gprofiler/gost) to get better insight into the data. Results from the aforementioned software were combined. Figure 1 shows the analysis used in this study.

1 https://www.ncbi.nlm.nih.gov/geo/.

2 https://www.r-project.org/ (2022).

3 https://www.bioconductor.org/ (2003–2022).

4 https://cytoscape.org/ National Institute of General Medical Sciences (NIGMS).

## 2.3. Validation of *LASP1*, *TUBA1C*, and *S100A6* genes using quantitative real-time PCR

### 2.3.1. Ethics statement

Following the bioinformatics analysis, validation of significant differentially expressed genes (DEGs) (*LASP1, TUBA1C,* and *S100A6*) was carried out using QRT-PCR. A total of 100 whole blood samples (56 MS cases, mean age: 39.5 years and 44 controls, mean age: 39.5 years), obtained from MS Research Center and Al-Zahra Hospital in Isfahan (http://alzahra.mui.ac.ir) were used. All procedures were approved and carried out in accordance with Medical Research Ethics Committee of Iran under code IR.UI.REC.1399.076.

### 2.3.2. RNA extraction

Total RNA was extracted from each sample according to the standard TRIzol protocol (Bio BASIC, Canada) according to manufacturer's instructions. RNA concentration and quality were determined using both Nanodrop (Thermo Scientific Tm Nano Drope One C model) and gel electrophoresis. The existence of two sharp bands representing 18S and 28S ribosomal RNA on a 1% (w/v) ethidium bromide stained agarose gel during electrophoresis through TAE buffer (40 mM Tris-acetate, 1 mM EDTA, pH 8.0) at 100 V for 30 min confirmed the quality of the extracted RNAs.

Those RNA samples with a RNA integrity Number (RIN) < 1.8 were excluded from further analysis. For all the RNA work DEPC-Treated Water was used. High quality extracted total RNA was stored at −70°C until cDNA synthesis.

### 2.3.3. cDNA synthesis

Initially, DNAse I (Fermentase Cat # ENO 521) treatment was used to remove genomic DNA before cDNA synthesis. Next, cDNA synthesis was carried out using a commercial kit provided by Yektatajhiz Company (Cat No.: YT4500) according to manufacturer's instructions. This involved keeping the samples on ice under sterile conditions at 70°C for 5 mins, 37°C for 60 mins, 70°C for 5 mins, and finally storing all synthesized cDNAs at −20°C.

### 2.3.4. Quantitative real time PCR analysis

To enable the validation of our candidate genes (*LASP1, TUBA1C,* and *S100A6*), SYBR Green -based QRT-PCR was performed using a LightCycler® 96 (BioRad, Germany). The sequence of all primers used are listed in the Table 1. These were designed using the PRIMER3 program (http://frodo.wi.mit.edu). QRT-PCR reactions were performed in duplicate and the values of average cycle threshold (Ct) were determined for each sample. The conditions of QRT-PCR amplification were: 1 cycle at 95°C for 2 min, 40 cycles at 95°C for 50 s, 60°C for 30 s. The *human beta-actin* gene (*ACTB_HUMAN*) was used as the internal control. Hence, all calculated concentrations are relative to the concentration of the standard, expressed in arbitrary units and the quantification cycle values were automatically calculated with Rotor-Gene software version 6.1.

The results were analyzed using the $2^{-\Delta\Delta Ct}$ method (35). In this study, beta-actin gene (as a reference gene) and *S100A6*, *TUBA1C*, and *LASP1* genes [as target genes (TRG)] and CT data from real-time expression of *TUBA1C*, *LASP1*, and *S100A6* were statistically analyzed ($P < 0.05$) by REST 2009 software. After checking the normality of data, using the Kolmogorov Smirnov test and the unpaired *t*-test in GraphPad Prism 8 software, a significant difference in the expression levels of genes *LASP1*, *TUBA1C,* and *S100A6* was observed between patients and healthy individuals.

TABLE 1 Primers designed for QRT-PCR.

| No. | Gene | Name | Seq.(5-3) | TM |
|---|---|---|---|---|
| 1 | *H-TUBA1C* | F | TTCCACCCTGAGCAACTC | 60 |
| | | R | AACCAAGAAGCCCTGAAG | |
| 2 | *H-S100A6* | F | AGCACACCCTGAGCAAGA | 60 |
| | | R | TCACCTCCTGGTCCTTGT | |
| 3 | *H-LASP1* | F | GAGCAGCAGCCTCACCAC | 64 |
| | | R | TACCGCTTCCCGCCAC | |
| 4 | *β-actin* | F | TGGAGGTACCACCATGTACC | 60 |
| | | R | CACATCTGCTGGAAGGTGGA | |

## 3. Results

The fundamental idea behind this analysis was to shed some light into gene-gene interactions underpinning MS disease with regard to cause and effect (36). In this study, we reused GSE17048 experiment data which contained the profiled mRNA expression for all known genes in whole blood from 144 health individuals, 99 with MS (43 PPMS, 36 RRMS, and 20 SPMS). As meta-data of GSE17048 shows in the Gene Expression Omnibus–NCBI, in the conducting the experimental design, whole blood mRNA expression was compared between different types of MS and age-matched healthy control. The nature of probability distribution induced by a gene regulatory BN will allow diverse probabilistic gene queries to be answered in linear time. This makes BN to be practically appealing. The results of comparison of the network structures determined from various algorithms, including Hill Climbing, Tabu Search, Max-Min Hill Climbing, and Restricted Maximize algorithms with different scoring functions, are shown in Table 2. Some key properties of BN are fundamental in judging estimated results.

Figure 2 shows some properties of trained BN gene networks.

Topological parameters can characterize the location of genes in a gene network (37). Using *NetworkAnalyzer*, the following network topological parameters were calculated in our data. This was based on clustering coefficient (0.003), number of nodes (1,707), connected components (857), network diameter (26), network radius (1), shortest paths (192,463), characteristics path (8.313), the average number of neighbors (1.992), network density (0.0), isolated nodes (854), number of self-loops (0), multi-edge node pairs (0), and analysis times (1.467). The nature of probability distribution induced by a gene regulatory BN allowed diverse probabilistic gene queries to be answered in linear time. However, many structural BN parameters may be important. One of the key parameters (shown in Table 2) is the branching factor. This parameter plays a significant role in development of the gene network. Each Node (gene) will have its own branching measure, which will determine the out degree of that gene. If the branching factor value is not uniform in the network, an average branching factor can generally be calculated. This value turned out to be different depending on the type of algorithm used. Max-Min Hill Climbing returned a higher average than Restricted Maximize. In terms of system level understanding of research, the higher the branching factor, the more frequently gene regulators can be identified in the network. Biological networks have a modular architecture (38). *MCODE* can find connected and dense areas of the gene network based on network topology measures. In our analysis, 12 different modules were detected using *MCODE*, among which, 7 modules had 3 nodes; 3 edges with different interaction modes; 3 modules had 6 nodes and 7 edges; 1 module 15 nodes and 17 edges and finally 1 module had 6 nodes and 6 edges (Supplementary Figure 1). The active subnetworks were obtained using *jActiveModules*. The *jActiveModules* comprised 5 modules, where ILLMN_1742167 (*TUBA1C*), ILLMN_1665909 (*LASP1),* and ILLMN_1713636 (*S100A6*) were seen to be enriched modules (Figure 3). The number of modules detected by this method was different than those identified with the *MCODE* based method.

TABLE 2 Estimation of structural Bayesian network parameters with different algorithms.

| Parameters | Score based algorithm | | Hybrid algorithm | |
|---|---|---|---|---|
| | Hill climbing | Tabu search | Max-min hill climbing | Restricted maximize |
| No. of Nodes | 1,707 | 1,707 | 1,707 | 1,707 |
| No. of Arcs | 1,700 | 1,500 | 2,485 | 2,188 |
| Undirected arcs | 0 | 0 | 0 | 0 |
| Directed arcs | 1,700 | 1,500 | 2,485 | 2,188 |
| Markov blanket | 3.32 | 2.69 | 4.64 | 3.93 |
| Neighborhood size | 1.99 | 1.76 | 2.91 | 2.56 |
| Branching factor | 1 | 0.88 | 1.46 | 1.28 |
| No. of tests | 4,354,565 | 413,365 | 9,721,786 | 7,228,057 |
| loglik-g | −1,308,146 | −1,308,146 | −1,318,282 | −1,313,436 |
| AIC-g | −1,312,560 | −1,312,560 | −1,323,884 | −1,319,335 |
| BIC-g | −1,319,115 | −1,319,115 | −1,332,202 | −1,328,094 |

loglik-g, The multivariate Gaussian log-likelihood (loglik-g) score; AIC-g, Akaike Information Criterion score; BIC-g, Bayesian Information Criterion score.

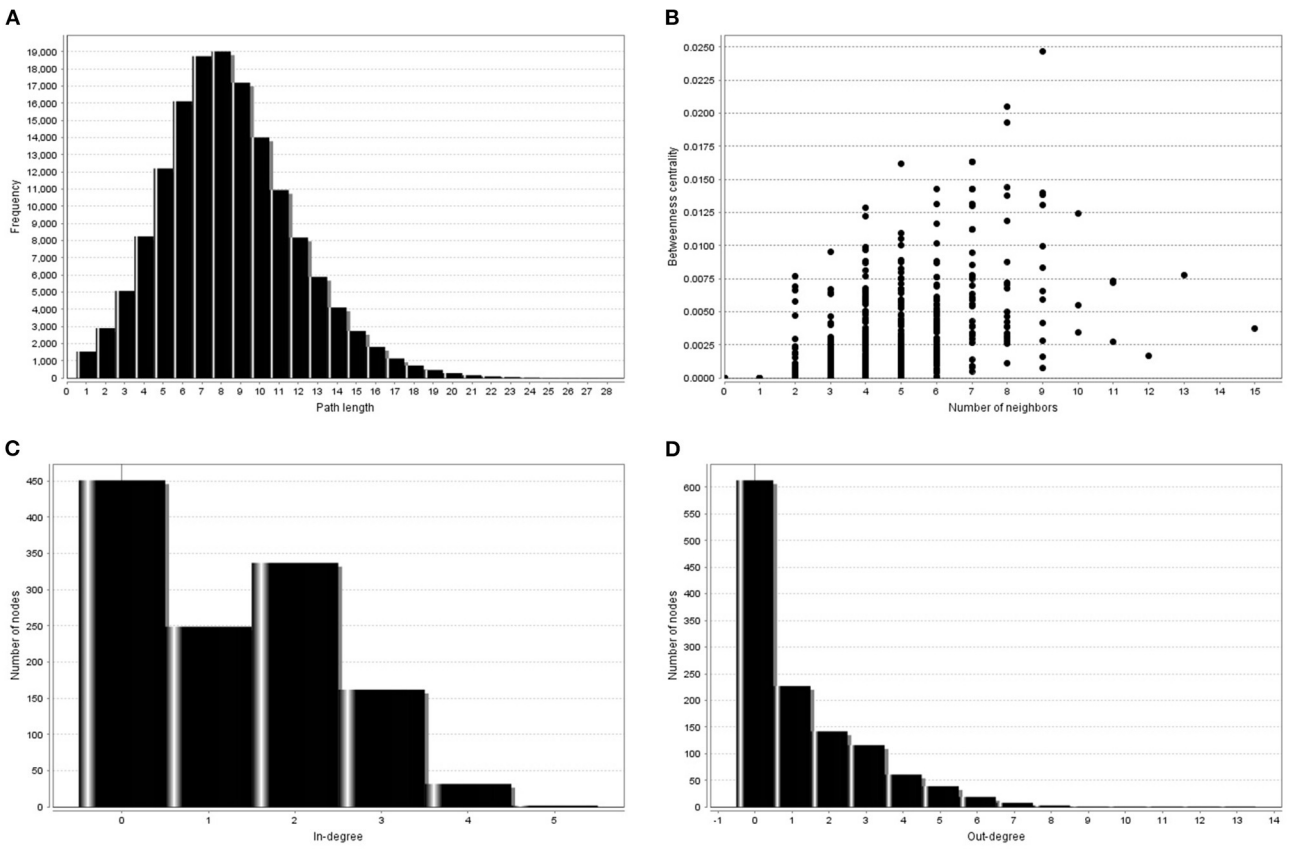


FIGURE 2
Some topological measures of trained gene regulatory BN visualized by *NetworkAnalyzer*. **(A)** Shortest path length distribution. The path length is the number of edges along the path. The distance $d_{ij}$ between a pair of different nodes i and j is the length of the shortest path connection. **(B)** Between-ness centrality. The Between-ness centrality of a node reflects the amount of control that this node exerts over the interaction of other nodes in the network. **(C)** Distribution of in-degree gene connectivity measure. **(D)** Distribution of out-degree gene connectivity measure.

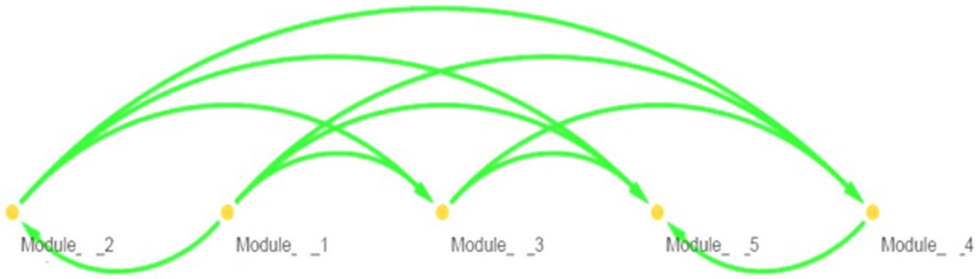


FIGURE 3
Extracted molecular modules using jActiveModules.

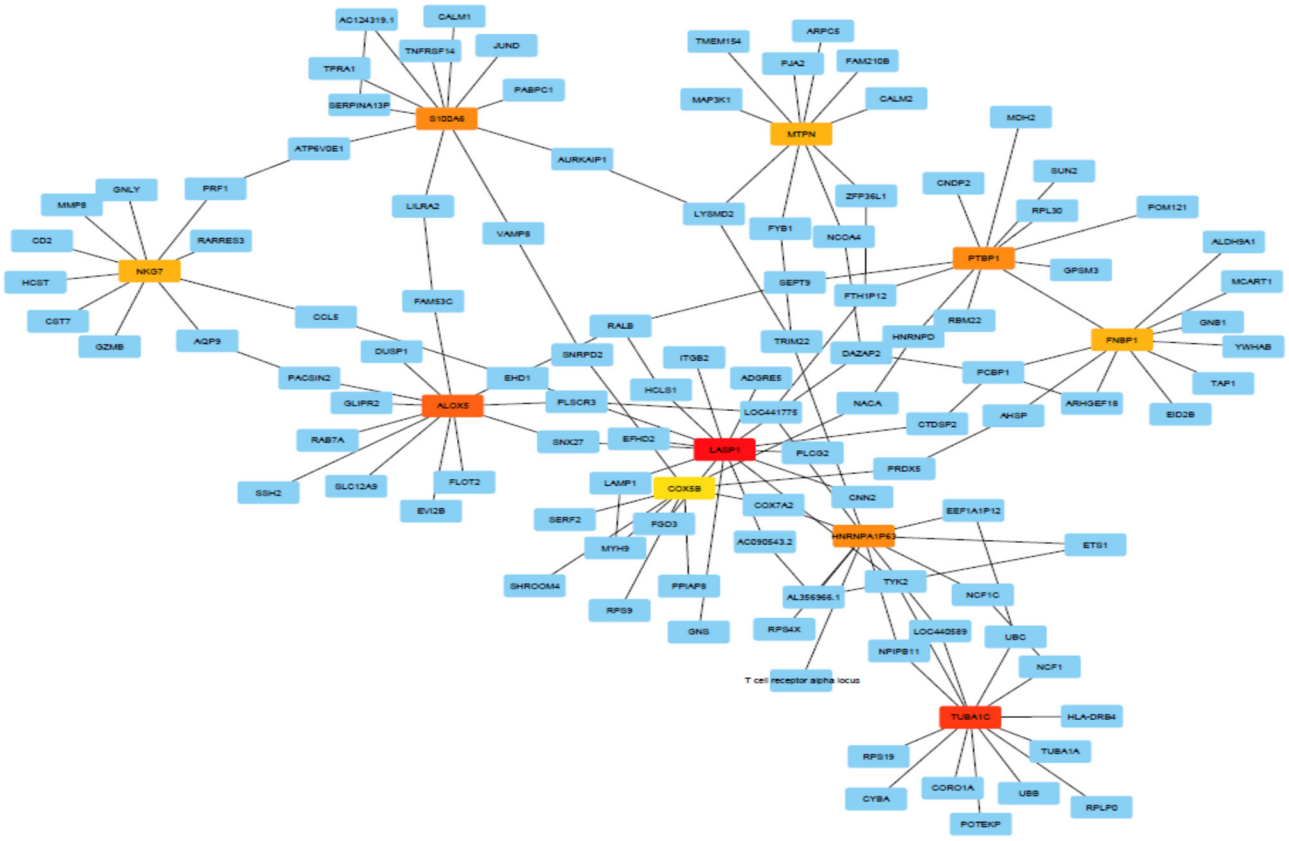


FIGURE 4
The MCC method captures essential genes in the top ranked list.

Figure 3 shows predicted modules in different modes of interaction. Module-level analysis explores the organization of biological systems and reconstructs module networks [A network module is a group of nodes (hub genes) that work together. Node or Vertex is a connection point or a branch point or an end point in a connection. And the path that connects the nodes to each other is called edge]. Figure 3 shows a module-level view of our gene regulatory BN network that denotes a high-level representation of the regulatory machinery of the MS gene network topology. Dense module searching of two MS Genome-Wide Association Study (GWAS) datasets identified several genes (*GRB2*, *HDAC1*, *IL2RA*, *JAK2*, *KEAP1*, *MAPK1*, *RELA*, and *STAT3*). These genes were enriched for glial cell differentiation (14). *CytoHubba* provides a user-friendly interface for discovering important nodes in biological networks (32). *CytoHubba* considers the shortest path between groups of nodes. Among the 11 proposed algorithms, MCC fitted better than the others. In Figure 4 and Table 3, we present the top 10 identified probes. Many of the genes, such as *TUBA1C, LASP1,* and *S100A6* shown in Figure 4, are close to the hub genes and were actually identified as hub genes by other algorithms such as *CyTargetLinker*. *The iRegulon* software then allowed us to identify regulons using

TABLE 3 The 10 top genes/probes identified by the MCC method.

| Probe ID | Transcript ID | Gene Name |
|---|---|---|
| ILMN_2180682 | ENSG00000105887 | "MTPN", myotrophin |
| ILMN_1797342 | ENSG00000187239 | "FNBP1", formin binding protein 1 |
| ILMN_1713636 | ENSG00000197956 | "S100A6", S100 calcium binding protein A6 |
| ILMN_1663512 | ENSG00000135940 | "COX5B", cytochrome c oxidase subunit 5B |
| ILMN_2333319 | ENSG00000011304 | "PTBP1", polypyrimidine tract binding protein 1 |
| ILMN_1792150 | ENSG00000012779" | "ALOX5", arachidonate 5-lipoxygenase |
| ILMN_1682993 | ENSG00000105374 | "NKG7", natural killer cell granule protein 7 |
| ILMN_1665909 | ENSG00000002834 | "*LASP1*", *LIM* and *SH3* protein 1 |
| ILMN_1742167 | ENSG00000167553 | "*TUBA1C*", tubulin alpha 1c |
| ILMN_1691611 | ENSG00000227453 | "*HNRNPA1P63*", heterogeneous nuclear ribonucleoprotein A1 pseudogene 63 |

TABLE 4 The top 10 transcription factors (TFs) estimated to affect hub genes.

| Transcription factors (TF) | NES* | AUC** | Target genes |
|---|---|---|---|
| *STAT5A* | 3.017 | 0.043 | *LASP1, TUBA1C* |
| *NFATC1* | 3.12 | 0.044 | |
| *MTA3* | 3.193 | 0.044 | |
| *NFKB1* | 4.005 | 0.037 | |
| *ZNF362* | 3.381 | 0.026 | |
| *SPI1* | 6.961 | 0.037 | *LASP1, S100A6* |
| *GABPB1* | 4.865 | 0.03 | |
| *DLX1* | 3.354 | 0.046 | *TUBAC, S100A6* |
| *YY1* | 6.592 | 0.036 | *LASP1, TUBA1C, S100A6* |
| *NFATC3* | 5.383 | 0.032 | |

*Normalized enrichment score (NES). **Area under the cumulative recover.

motif discovery in a set of regulated genes. Identified transcription factors affecting the hub genes are listed in Supplementary Table 2 and Supplementary Figure 2 and their common factors identified are given in Table 4. The most significant, the STAT5A protein, mediates the responses of many cell ligands, such as IL2, IL3 and different growth hormones. In this study, the gene identifiers were uploaded to Metascape and used in conjunction with KEGG pathways, GO biological processes, Reactome gene complexes, canonical and CORUM pathways (39). The results of the enrichment analysis, including descriptions, function, ontology, expression, etc. are shown in Table 5, Supplementary Table 3, and Supplementary Figure 3.

Genes were ranked from top to bottom based on degree, closeness and betweenness [higher degree (hub), higher betweenness (throat) and higher closeness centrality (shortest distance with other genes in the network)]. In terms of these parameters, three genes (*LASP1, TUBA1C,* and *S100A6*) showed a significant correlation with MS disease. These were thus identified as hub genes (Supplementary Table 4). In this study, probes ILLMN_1665909, ILLMN_1742167, and ILLMN_1713636 had high degrees of 15, 13, and 11, respectively and were identified as hub probes. In total of 850 probes had zero input edges, 200 probes had 1 in-degree. ILLMN_1665909, with the highest out-degree (13 out-degree) and 2 in-degree (mapped to human *LASP1*) plays an important role in regulating activity. Its encoded cytoplasmic protein binds focal adhesion proteins and plays a role in cell signaling, migration, and proliferation. ILLMN_1742167, with 12 out-degree and 1 in-degree mapped to the *human tubulin* gene (*TUBA1C*), and ILLMN_1713636 with 9 out-degree and 2 in-degree mapped to the *S100A6* gene (Figure 2).

## 3.1. Real-time reverse transcription polymerase chain reaction

As given in the Material and Methods section, we used RT-PCR to validate the results of Bayesian gene network. RT-PCR, that actually reflects product accumulation, is a routine lab-based method to validate array based transcriptomic results. In this study, the *LASP1, TUBA1C,* and *S100A6* genes turned out to be playing regulatory roles in MS. In validating aforementioned genes, using RT-PCR experiment, it was indicated that the patterns of relative gene expression for these genes (*LASP1, TUBA1C,* and *S100A6*) were significant between MS cases and controls ($P < 0.05$). The calculations based on the formula $-\Delta\Delta$ct shown the amount of mRNA transcripts of *LASP1* and *S100A6* genes, increased (5.491 and 36.556 times respectively) in patients though a decrease (0.166 times) in *TUBA1C* gene expression was seen in MS patients ($P < 0.05$) (Table 6 and Figure 5).

The results after studying the normality of the distribution of variables using the one sample Kolmogorov–Smirnov test and unpaired *t*-test in GraphPad Prism 8 software show a significant difference in expression levels of *LASP1*, *TUBA1C,* and *S100A6* genes between patients and healthy controls. *P*-values were: TUBA1C $< 0.0001$, S100A6 $< 0.0001$, LASP1 $< 0.003$. Mean expression of *TUBA1C*, *LASP1,* and *S100A6* genes in patient samples was 7.4, 5.6, and 2.9 respectively and 4.9, 8.1, and 8.0, respectively in healthy individuals. Results from statistical analysis also showed a decrease in *TUBA1C* gene expression and an increase in *LASP1* and *S100A6* gene expression in MS patients compared to the control group (Figure 6).

# 4. Discussion

At present, the cause of MS is not fully understood, but knowledge of the genetic factors involved is essential for effective diagnosis and identification of the most appropriate MS therapeutic interventions. In this study, three genes (*LASP1*, *TUBA1c,* and *S100A6*) with high degree, high closeness centrality and high betweenness measures were highlighted as potential MS candidate regulator markers. These three genes (*LASP1*, *TUBA1c,* and *S100A6)* seem to be the most significant in the MS disease

TABLE 5 Metascape results *LASP1*, *TUBA1C*, and *S100A6* genes.

| Input ID | Gene ID | Tax ID | Gene symbol | Description | Biological process (GO) | Subcellular location (Protein atlas) |
|---|---|---|---|---|---|---|
| *LASP1* | 3927 | H. sapiens | *LASP1* | LIM and SH3 protein 1 | GO: 0034220 ion transmembrane transport; GO: 0009967 positive regulation of signal transduction; GO: 0023056 positive regulation of signaling | Cytosol; Plasma membrane (Supported) Focal adhesion sites (Approved) |
| *TUBA1C* | 84790 | H. sapiens | *TUBA1C* | tubulin alpha 1c | GO: 0030705 cytoskeleton-dependent intracellular transport; GO: 0000226 microtubule cytoskeleton organization; GO: 0051301 cell division | Microtubules (Supported) |
| *S100A6* | 6277 | H. sapiens | *S100A6* | S100 calcium binding protein A6 | GO: 0048146 positive regulation of fibroblast proliferation; GO: 0048145 regulation of fibroblast proliferation; GO: 0007409 axonogenesis | Cytosol; Plasma membrane (Enhanced) |

TABLE 6 REST software data compared *LASP1*, *TUBA1c*, and *S100A6* genes in MS patient and control groups.

| Gene | Type | Reaction efficiency | Expression | Std. error | 95% C.I. | P(H1) | Result |
|---|---|---|---|---|---|---|---|
| *ACTB* | REF | 1.0 | 1.000 | | | | |
| *LASP1* | TRG | 1.0 | 5.491 | 1.183–32.843 | 0.335–266.871 | <0.001 | UP |
| *TUBA1C* | TRG | 1.0 | 0.166 | 0.058–0.523 | 0.027–1.417 | <0.001 | DOWN |
| *S100A6* | TRG | 1.0 | 36.556 | 9.630–140.562 | 2.367–416.452 | <0.001 | UP |

P(H1), Probability of alternate hypothesis that difference between sample and control groups is due only to chance; TRG, Target; REF, Reference; Interpretation: LASP1 is UP-regulated in sample group (in comparison to control group) by a mean factor of 5.491 (S.E. range is 1.183–32.843); LASP1 sample group is different to control group. P(H1) = 0.000. TUBA1c is DOWN-regulated in sample group (in comparison to control group) by a mean factor of 0.166 (S.E. range is 0.058–0.523). TUBA1c sample group is different to control group. P(H1) = 0.000. S100a6 is UP-regulated in sample group (in comparison to control group) by a mean factor of 36.556 (S.E. range is 9.630–140.562). S100A6 sample group is different to control group. P(H1) = 0.000.

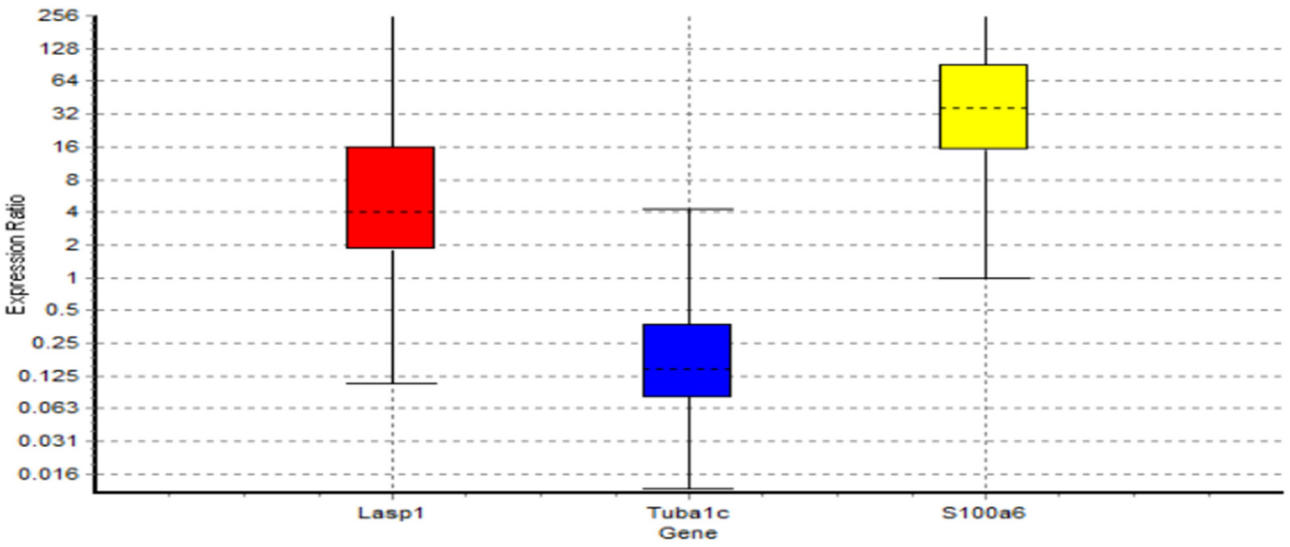


FIGURE 5
Boxes represent the interquartile range, or the middle 50% of observations. The dotted line represents the median gene expression. Whiskers represent the minimum and maximum observations.

process. S100A6 functions in a wide range of cell types as a member of the S100 family and this family expression in MS patients could be considered as a diagnostic biomarker for MS. Its inhibition of demyelinating nerve cells suggests that S100 proteins could act as a candidate therapeutic target in MS (40). Komatsu et al. reported increased expression of S100A6 (Calcyclin), a calcium-bound protein of the S100 family, in human colorectal adenocarcinoma (41). Peterova et al. reported an overexpression of S100 protein-encoding mRNA in both colorectal cancer cell lines and surgically resected specimens of colorectal cancer (42). A study by Bartkowska et al. (43) showed that in response to different stress conditions, the level of *S100A6* decreased in several brain structures, indicating that *S100A6* may modulate stress responses. The genome-wide methylation array has identified

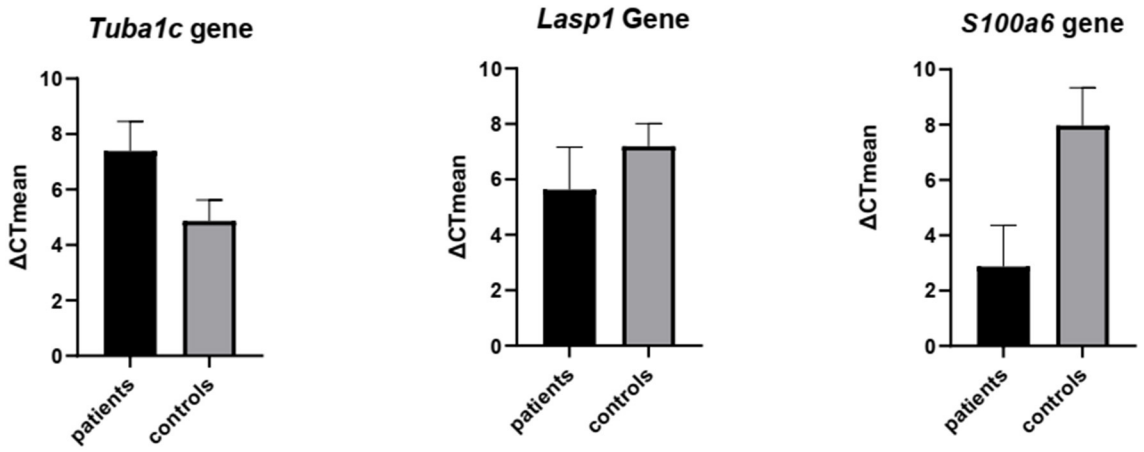


FIGURE 6
Validation of the expression of *TUBA1C*, *LASP1*, and *S100A6* genes by real-time PCR. Unpaired *t*-test was used to detect differences in gene expression between 2 groups patients & controls using the Graph Pad Prism 8 software. Significance: *P*-value TUBA1C $< 0.0001$, *P*-value S100A6 $< 0.0001$, *P*-value LASP1 $< 0.003$.

a few hypomethylated immune-related genes, amongst them *S100A6* which shows up-regulation in autoimmune encephalitis patients (44). Even though *S100A6* is involved in many biological phenomena, its biological activity is still unknown (45). At the transcriptional level, upstream stimulatory factor and Nuclear factor-kappa B (NF-κB) activates the *S100A6* gene promoter, although p53 might act indirectly to suppress transcription of the *S100A6* gene (46). *TUBA1C* is a member of Microtubules which are vulnerable to degradation and disorganization in a variety of neurodegenerative diseases (47–49). Malfunction of microtubules (e.g., *TUBA1C*) is also considered as the central physiopathological mechanism of neurodegenerative diseases. The abnormalities in the regulatory pathways of microtubules disrupt the properties and functions of microtubules, leading to nerve damage (50). A decreased expression of the *TUBA1C* gene in Parkinson's disease has already been demonstrated by quantitative analysis of gene expression (51). *LASP1*)*The LIM and SH3 protein 1*), a focal adhesion adaptor protein, is an actin-binding, signaling pathway-regulated phosphoprotein which localizes within multiple sites of dynamic actin assembly. It has the potential to interact with various molecules, and is highly expressed in the adult CNS. Microarray data has revealed that alterations in LASP1 proteins affect cell migration, adhesion, and cytoskeletal organization (52). *LASP1*, significantly expressed by CNS neurons, is localized at synaptic sites (53).

A couple of significant transcription factors (TFs) that interact with these hub genes were identified in this study. The YY1 TF (Yi and Yang 1) is a multifactorial protein that, depending on the cell tissue, can activate or suppress gene expression (54). It is expressed in the nervous system. The YY1 promoter lacks the usual TATA box but has a rich GC sequence and therefore resembles a large subset of housekeeping and growth regulator genes. These features suggest that it may play an important role in development. In the CNS, myelination is performed by oligodendrocytes. YY1 function in oligodendrocytes was first reported by Berndt et al. (55). YY1 activates the promoter of myelin lipids and has been identified as an important player in myelination of the central nervous system during growth. In multiple neurodegenerative diseases, YY1 function is degraded through distinct mechanisms, including protein utilization, protein degradation, and ectopic nuclear/cytoplasmic shuttle (N/C). These disorders inhibit YY1 transcriptional activity and lead to gene transcriptional abnormalities that contribute to disease pathogenesis. A future goal in YY1 research is to discover other potential mechanisms that lead to YY1 dysfunction in neurodegenerative diseases, such as ectopic changes after translation (56). The other TF identified in study was Nuclear Factor of Activated T Cells 3 (NFATc3), a member of NFAT family. NFATc3 acts as signal integrators because their function is to bind STAT3, c-Jun, CREB, and ATF3 factors at specific DNA binding sites. NFATc3 cannot be regulated alone and act as calcium-dependent transcription factors. The antigen-mediated T cell receptor (TCR) mediates multiple signaling cascades, including phospholipase C (PLC) -dependent pathways that are secondary messengers of inositol-1,4,5-triphosphate (IP3) and diacylglycerol (DAG). IP3 binds to the IP3 receptor in the endoplasmic reticulum (ER) and releases $Ca^{2+}$ ions into the cytoplasm (57). In this way, NFATc1-4, activates intracellular calcium *via* dephosphorylation (35). The findings show that NFATc3 is defined as a marker of a specific subset of astrocytes that are activated in response to lesions, as well as some degree of heterogeneity among astrocytes that may have consequences for cells in the nervous system (58). Preliminary findings in neuroblast cells have shown that various treatments that alter tubulin polymerization, such as reducing the mineral zinc, prevent the transfer of NFATc3 to the nucleus. In agreement with a functional relationship between NFAT and microtubules, it has been observed that the degradation of several proteins that control the proper organization of the microtubule network, and the actin-cytoskeletal linker, disrupts the nucleus and transcriptional activity of NFAT. Overall, it indicates the involvement of microtubules in NFAT nuclear stimulation (59). The *LASP1* gene enhances NFAT2 nuclear translocation by activating the nuclear factor Akt (60).

NFAT can affect processes such as axon growth, synaptogenesis, Schwann cell differentiation, and myelination (58). In general, it can be concluded that increase of the expression of *LASP1* and *S100A6* genes and decrease the expression of the *TUBA1C* gene in multiple sclerosis disrupts NFAT transcriptional activity. Although the role of NFAT in regulating the immune system is well established, our knowledge of NFAT in human disease is limited. The function of NFAT in other aspects of human immune or inflammatory diseases is also largely unknown (61).

The involvement of hub genes identified in this study in other disorders have been reported as well. Patients with MS are known to suffer from a number of digestive problems (62) and studies have shown that *LASP1* (63) and *S100A6* genes have high expression in the digestive system. A link can therefore be established between the expression of these genes, MS, gastrointestinal problems and possibly other types of human cancers (64). Also, *LASP1* plays a crucial role in the growth and metastasis of gastric cancer and other cancers (52, 63, 65–68). For example, *LASP1* can cause the progression and metastasis of colorectal cancer (CRC), but its mechanism is still unclear (69). A connection between *LASP1* and *S100A* has reported underpinning *LASP1* binds to the calcium-binding protein family (*S100A*) and increases its expression in colon cancer (Kappa = 0.347, $P < 0.01$) (70). On this basis, the present study confirmed the importance of three gene expression patterns (*LASP1, S100A6,* and *TUBA1C*) for understanding the transcriptome complexity of MS. This leads us to conclude that upregulation of *LASP1* and *S100A6* genes along with down-regulation of *TUBA1C* is central to MS pathology. To our knowledge, this is the first report to evaluate the level of expression of the above genes for discovery of a transcriptomic signature for MS disease. These findings provide a potential mechanism for some significant biomarkers responsible for the pathogenesis of MS. However, we still have a long way to go to understand the larger transcriptomic profile for this disease. This study provides initial data to further investigate the possible role of these genes in the pathogenesis of MS.

## 5. Conclusions

Results of the present study indicate that the analysis of gene expression data based on gene-gene interaction networks can provide opportunities to determine the genes involved in MS. The importance of three candidate marker genes in this disease were highlighted. These candidate marker genes, *LASP1*, *TUBA1C*, and *S100A6*, identified by the biological systems approach, have been further confirmed in the laboratory. The significant difference in the expression of these three genes in patients with MS will help further research on this disease and its treatment. This useful tool can serve as a good starting point for identifying new therapies and understanding the basic mechanisms controlling normal cellular processes and disease pathologies. It is crucial to point out here that for learning Bayesian gene network in this study, we did not separate sets of possible signaling protein molecules and transactional factors beforehand in our data, and consider them to be parents (causatives) in the learned network. By doing so, the learned Bayesian gene network probably would be biologically much more appealing. We aim to do this in a due course in the future.

## Data availability statement

The data presented in the study are deposited in the https://www.ncbi.nlm.nih.gov/geo/query/acc.cgi?acc=GSE17048 repository, accession number GSE17048.

## Ethics statement

All procedures were approved and carried out in accordance with Medical Research Ethics Committee in Iran under code IR.UI.REC.1399.076. The patients/participants provided their written informed consent to participate in this study.

## Author contributions

NK and MG-Z developed the theoretical formalism, designed the model and the computational framework, and analyzed the data. NK performed experimental lab the analytic calculations. MM-B conducted the backbone of the experiment and contributed to the final version of the manuscript. All authors have read and agreed to the published version of the manuscript.

## Funding

This study was funded with the budget of the University of Isfahan (use of laboratory equipment and purchase of materials) and the Biotechnology Development Headquarters (grant for purchase of laboratory materials).

## Acknowledgments

The authors thank all the patients, their families, and caregivers. The authors thank all the clinicians for their involvement and contribution to the study. This work was supported by Jacqueline Smith from The University of Edinburgh, Easter Bush, Midlothian, EH25 9RG, UK for writing—review and editing.

## Conflict of interest

The authors declare that the research was conducted in the absence of any commercial or financial relationships that could be construed as a potential conflict of interest.

## Publisher's note

All claims expressed in this article are solely those of the authors and do not necessarily represent those of

their affiliated organizations, or those of the publisher, the editors and the reviewers. Any product that may be evaluated in this article, or claim that may be made by its manufacturer, is not guaranteed or endorsed by the publisher.

## Supplementary material

The Supplementary Material for this article can be found online at: https://www.frontiersin.org/articles/10.3389/fneur.2023.1090631/full#supplementary-material

## References


1. Hernandez AL, O'Connor KC, Hafler DA. Chapter 52 - Multiple Sclerosis. In: Rose NR, Mackay IR, editors. *The Autoimmune Diseases (Fifth Edition)*. Boston: Academic Press (2014). p. 735–56. doi: 10.1016/B978-0-12-384929-8.00052-6

2. Anderson VM, Fisniku LK, Altmann DR, Thompson AJ, Miller DH. MRI Measures show significant cerebellar gray matter volume loss in multiple sclerosis and are associated with cerebellar dysfunction. *Multiple Sclerosis.* (2009) 15:811–7. doi: 10.1177/1352458508101934

3. Daniel O, Praneeta C, Kedar R M, Douglas L A, Michael G D, Susan A G, et al. The North American imaging in multiple sclerosis cooperative (NAIMS), deep grey matter injury in multiple sclerosis. a NAIMS consensus statement. *Brain.* (2021) 144:1974–84. doi: 10.1093/brain/awab132

4. Enzinger C FF. Measuring gray matter and white matter damage in MS: why this is not enough. *Front Neurol.* (2015) 6:56. doi: 10.3389/fneur.2015.00056

5. Messina S PF. Gray matters in multiple sclerosis: cognitive impairment and structural MRI. *Mult Scler Int.* (2014) 2014:609694. doi: 10.1155/2014/609694

6. Raz E CM, Sbardella E, Totaro P, Pozzilli C, et al. Gray- and White-Matter Changes 1 Year after First Clinical Episode of Multiple Sclerosis: Mr Imaging. *Radiology.* (2010) 257:448–54. doi: 10.1148/radiol.10100626

7. Almsned F, Lipsky RH, Jafri MS. Transcriptomic analysis of multiple sclerosis patient-derived monocytes by RNA-sequencing for candidate gene discovery. *Inform Med Unlocked.* (2021) 23:100563. doi: 10.1016/j.imu.2021.100563

8. Miljković D SI. Multiple sclerosis: molecular mechanisms and therapeutic opportunities. *Antioxid Redox Signal.* (2013) 18:2286–334. doi: 10.1089/ars.2012.5068

9. Brosch T, Yoo Y, Li DKB, Traboulsee A, Tam R. Modeling the variability in brain morphology and lesion distribution in multiple sclerosis by deep learning. *Med Image Comput Comput Assist Interv MICCAI.* (2014) 17:462–9. doi: 10.1007/978-3-319-10470-6_58

10. Cervantes-Gracia K, Husi H. Integrative analysis of multiple sclerosis using a systems biology approach. *Sci Rep.* (2018) 8:5633. doi: 10.1038/s41598-018-24032-8

11. Freiesleben S, Hecker M, Zettl UK, Fuellen G, Taher L. Analysis of microrna and gene expression profiles in multiple sclerosis: integrating interaction data to uncover regulatory mechanisms. *Sci Rep.* (2016) 6:34512. doi: 10.1038/srep34512

12. Liu M, Hou X, Zhang P, Hao Y, Yang Y, Wu X, et al. Microarray gene expression profiling analysis combined with bioinformatics in multiple sclerosis. *Mol Biol Rep.* (2013) 40:3731–7. doi: 10.1007/s11033-012-2449-3

13. Luo D, Fu J. Identifying characteristic mirnas-genes and risk pathways of multiple sclerosis based on bioinformatics analysis. *Oncotarget.* (2018) 9:5287–300. doi: 10.18632/oncotarget.23866

14. Manuel AM Dai Y, Freeman LA, Jia P, Zhao Z. Dense module searching for gene networks associated with multiple sclerosis. *BMC Med Genomics.* (2020) 13:48. doi: 10.1186/s12920-020-0674-5

15. McGuinness MJ. *A mathematical model of Remyelination in multiple sclerosis.* Undergraduate Honors Theses (2017).

16. Navaderi M, Rajaei S, Rahimirad S, Jafari Harandi A, Ghaleh Z, Falahati K, et al. Identification of multiple sclerosis key genetic factors through multi-staged data mining. *Multiple Scler Rel Diso.* (2020) 39:101446. doi: 10.1016/j.msard.2019.101446

17. Safari-Alighiarloo N, Rezaei-Tavirani M, Taghizadeh M, Tabatabaei SM, Namaki S. Network-based analysis of differentially expressed genes in cerebrospinal fluid (CSF) and blood reveals new candidate genes for multiple sclerosis. *PeerJ.* (2016) 4:e2775. doi: 10.7717/peerj.2775

18. Shang Z, Sun W, Zhang M, Xu L, Jia X, Zhang R, et al. Identification of key genes associated with multiple sclerosis based on gene expression data from peripheral blood mononuclear cells. *PeerJ.* (2020) 8:e8357. doi: 10.7717/peerj.8357

19. Yang Q, Pan W, Qian L. Identification of the MIRNA–MRNA regulatory network in multiple sclerosis. *Neurol Res.* (2017) 39:142–51. doi: 10.1080/01616412.2016.1250857

20. Hanafy KA, Sloane JA. Regulation of remyelination in multiple sclerosis. *FEBS Lett.* (2011) 585:3821–8. doi: 10.1016/j.febslet.2011.03.048

21. Han MH, Steinman L. Systems biology for identification of molecular networks in multiple sclerosis. *Multiple Sclerosis J.* (2009) 15:529–30. doi: 10.1177/1352458509103318

22. Kotelnikova E, Bernardo-Faura M, Silberberg G, Kiani NA, Messinis D, Melas IN, et al. Signaling networks in MS: a systems-based approach to developing new pharmacological therapies. *Multiple Sclerosis J.* (2014) 21:138–46. doi: 10.1177/1352458514543339

23. Muñoz-San Martín M, Reverter G, Robles-Cedeño R, Buxò M, Ortega FJ, Gómez I, et al. Analysis of MIRNA signatures in CSF identifies upregulation of Mir-21 and Mir-146a/B in patients with multiple sclerosis and active lesions. *J Neuroinflam.* (2019) 16:220. doi: 10.1186/s12974-019-1590-5

24. Diaz-Beltran L, Cano C, Wall DP, Esteban FJ. Systems biology as a comparative approach to understand complex gene expression in neurological diseases. *Behavioral Sciences.* (2013) 3:253–72. doi: 10.3390/bs3020253

25. Friedman N, Linial M, Nachman I, Pe'er D. Using Bayesian Networks to analyze expression data. In: *Proceedings of the Fourth Annual International Conference on Computational Molecular Biology*. (2000). p. 127–35. doi: 10.1145/332306.332355

26. Davis S MP. A Bridge between the gene expression omnibus (GEO) and bioconductor. *Bioinf.* (2007) 14:1846–7. doi: 10.1093/bioinformatics/btm254

27. Scutari M. Bayesian Network constraint-based structure learning algorithms: parallel and optimised implementations in the Bnlearn R package. arXiv preprint *arXiv:14067648* (2014).

28. Hao C. *Learning Bayesian Network structure from data.* Doctoral dissertation, thesis submitted for the degree of MSc in Mathematics. Institute of Mathematics Eötvös Loránd University. (2018).

29. Assenov Y, Albrecht M, Lengauer T. *Topological analysis of biological networks.* Doctoral dissertation, Max Planck Institute for Informatics. (2006).

30. Su G, Morris JH, Demchak B, Bader GD. Biological Network Exploration with Cytoscape 3. *Curr Protoc Bioinform.* (2014) 47:8.13.1–8.0.24. doi: 10.1002/0471250953.bi0813s47

31. Cline MS, Smoot M, Cerami E, Kuchinsky A, Landys N, Workman C, et al. Integration of biological networks and gene expression data using cytoscape. *Nat Protoc.* (2007) 2:2366–82. doi: 10.1038/nprot.2007.324

32. Chin C-H, Chen S-H, Wu H-H, Ho C-W, Ko M-T, Lin C-Y. Cytohubba: Identifying hub objects and sub-networks from complex interactome. *BMC Syst Biol.* (2014) 8:S11–S. doi: 10.1186/1752-0509-8-S4-S11

33. Assenov Y, Ramírez F, Schelhorn S-E, Lengauer T, Albrecht M. Computing topological parameters of biological networks. *Bioinformatics.* (2007) 24:282–4. doi: 10.1093/bioinformatics/btm554

34. Zhou Y, Zhou B, Pache L, Chang M, Khodabakhshi AH, Tanaseichuk O, et al. Metascape provides a biologist-oriented resource for the analysis of systems-level datasets. *Nat Communic.* (2019) 10:1523. doi: 10.1038/s41467-019-09234-6

35. Giaimo BD, Oswald F, Borggrefe T. Dynamic chromatin regulation at notch target genes. *Transcription.* (2017) 8:61–6. doi: 10.1080/21541264.2016.1265702

36. Detanico T, Virgen-Slane R, Steen-Fuentes S, Lin WW, Rhode-Kurnow A, Chappell E, et al. Co-expression networks identify DHX15 RNA helicase as a B Cell regulatory factor. *Front Immunol.* (2019) 10:2903. doi: 10.3389/fimmu.2019.02903

37. Newman MEJ. The structure and function of complex networks. *SIAM Review.* (2003) 45:167–256. doi: 10.1137/S003614450342480

38. Barabási A-L, Gulbahce N, Loscalzo J. Network medicine: a network-based approach to human disease. *Nat Rev Genet.* (2010) 12:56. doi: 10.1038/nrg2918

39. Giurgiu M, Reinhard J, Brauner B, Dunger-Kaltenbach I, Fobo G, Frishman G, et al. CORUM: the comprehensive resource of mammalian protein complexes-—2019. *Nucleic Acids Res.* (2019) 47:D559–63. doi: 10.1093/nar/gky973

40. Barateiro A, Afonso V, Santos G, Cerqueira JJ, Brites D, van Horssen J, et al. S100b as a potential biomarker and therapeutic target in multiple sclerosis. *Mol Neurobiol.* (2016) 53:3976–91. doi: 10.1007/s12035-015-9336-6

41. Komatsu K, Andoh A, Ishiguro S, Suzuki N, Hunai H, Kobune-Fujiwara Y, et al. Increased expression of S100a6 (Calcyclin), a calcium-binding protein of the S100 family, in human colorectal adenocarcinomas. *Clin Cancer Res.* (2000) 6:172–7.

42. Peterova E, Bures J, Moravkova P, Kohoutova D. Tissue MRNA for S100a4, S100a6, S100a8, S100a9, S100a11, and S100p proteins in colorectal neoplasia: A pilot study. *Molecules.* (2021) 26:402. doi: 10.3390/molecules26020402

43. Bartkowska K, Swiatek I, Aniszewska A, Jurewicz E, Turlejski K, Filipek A, et al. Stress-dependent changes in the Cacybp/Sip interacting protein S100a6 in the mouse brain. *PLoS ONE.* (2017) 12:e0169760. doi: 10.1371/journal.pone.0169760

44. Tsai M-H, Lin C-H, Tsai K-W, Lin M-H, Ho C-J, Lu Y-T, et al. S100a6 Promotes B lymphocyte penetration through the blood–brain barrier in autoimmune encephalitis. *Front Genet.* (2019) 10:1188. doi: 10.3389/fgene.2019.01188

45. Donato R, Cannon BR, Sorci G, Riuzzi F, Hsu K, Weber DJ, et al. Functions of S100 Proteins. *Curr Mol Med.* (2013) 13:24–57. doi: 10.2174/156652413804486214

46. Leśniak. W, Słomnicki Ł P, Filipek A. S100a6 - New Facts and Features. *Biochem Biophys Res Commun.* (2009) 390:1087–92. doi: 10.1016/j.bbrc.2009.10.150

47. Dubey J, Ratnakaran N, Koushika SP. Neurodegeneration and microtubule dynamics: death by a thousand cuts. *Front Cell Neurosci.* (2015) 9:343. doi: 10.3389/fncel.2015.00343

48. Aiken J, Buscaglia G, Bates EA, Moore JK. The A-tubulin gene tuba1a in brain development: a key ingredient in the neuronal isotype blend. *J Dev Biol.* (2017) 5:8. doi: 10.3390/jdb5030008

49. Matamoros AJ, Baas PW. Microtubules in health and degenerative disease of the nervous system. *Brain Res Bull.* (2016) 126:217–25. doi: 10.1016/j.brainresbull.2016.06.016

50. Sferra A, Nicita F, Bertini E. Microtubule dysfunction: a common feature of neurodegenerative diseases. *Int J Mol Sci.* (2020) 21:7354. doi: 10.3390/ijms21197354

51. Kim JM, Lee KH, Jeon YJ, Oh JH, Jeong SY, Song IS, et al. Identification of genes related to Parkinson's disease using expressed sequence tags. *DNA Res.* (2006) 13:275–86. doi: 10.1093/dnares/dsl016

52. Zhang H, Chen X, Bollag WB, Bollag RJ, Sheehan DJ, Chew CS. Lasp1 gene disruption is linked to enhanced cell migration and tumor formation. *Physiol Genomics.* (2009) 38:372–85. doi: 10.1152/physiolgenomics.00048.2009

53. Phillips GR, Anderson TR, Florens L, Gudas C, Magda G, Yates JR, et al. Actin-binding proteins in a postsynaptic preparation: lasp-1 is a component of central nervous system synapses and dendritic spines. *J Neurosci Res.* (2004) 78:38–48. doi: 10.1002/jnr.20224

54. He Y, Casaccia-Bonnefil P. The Yin and Yang of Yy1 in the nervous system. *J Neurochem.* (2008) 106:1493–502. doi: 10.1111/j.1471-4159.2008.05486.x

55. Berndt JA, Kim JG, Tosic M, Kim C, Hudson LD. The transcriptional regulator Yin Yang 1 activates the myelin PLP gene. *J Neurochem.* (2001) 77:935–42. doi: 10.1046/j.1471-4159.2001.00307.x

56. Chen ZS, Chan HYE. Transcriptional dysregulation in neurodegenerative diseases: who tipped the balance of Yin Yang 1 in the brain? *Neural Regener Res.* (2019) 14:1148–51. doi: 10.4103/1673-5374.251193

57. Lee J-U, Kim L-K, Choi J-M. Revisiting the concept of targeting Nfat to control T cell immunity and autoimmune diseases. *Front Immunol.* (2018) 9:2747. doi: 10.3389/fimmu.2018.02747

58. Serrano-Pérez MC, Martín ED, Vaquero CF, Azcoitia I, Calvo S, Cano E, et al. Response of transcription factor Nfatc3 to excitotoxic and traumatic brain insults: identification of a subpopulation of reactive astrocytes. *Glia.* (2011) 59:94–107. doi: 10.1002/glia.21079

59. Mastrogiovanni M, Juzans M, Alcover A, Di Bartolo V. Coordinating cytoskeleton and molecular traffic in T cell migration, activation, and effector functions. *Front Cell Developm Biol.* (2020) 8:1138. doi: 10.3389/fcell.2020.591348

60. Wu L, Lin W, Liao Q, Wang H, Lin C, Tang L, et al. Calcium channel blocker nifedipine suppresses colorectal cancer progression and immune escape by preventing Nfat2 nuclear translocation. *Cell Rep.* (2020) 33:108327. doi: 10.1016/j.celrep.2020.108327

61. Pan MG, Xiong Y, Chen F. Nfat gene family in inflammation and cancer. *Curr Mol Med.* (2013) 13:543–54. doi: 10.2174/15665240113130 40007

62. Gulick E, Namey M. Bowel dysfunction in persons with multiple sclerosis. In: *Constipation–Causes, Diagnosis And Treatment* (2012).

63. Orth MF, Cazes A, Butt E, Grunewald TGP. An update on the LIM and Sh3 domain protein 1 (Lasp1): A versatile structural, signaling, and biomarker protein. *Oncotarget.* (2015) 6:26. doi: 10.18632/oncotarget.3083

64. Wang XH, Du H, Li L, Shao DF, Zhong XY, Hu Y, et al. Increased expression of S100a6 promotes cell proliferation in gastric cancer cells. *Oncol Lett.* (2017) 13:222–30. doi: 10.3892/ol.2016.5419

65. Butt E, Raman D. New frontiers for the cytoskeletal protein Lasp1. *Front Oncol.* (2018) 8:391. doi: 10.3389/fonc.2018.00391

66. Li Z, Chen Y, Wang X, Zhang H, Zhang Y, Gao Y, et al. Lasp-1 induces proliferation, metastasis and cell cycle arrest at the G2/M phase in gallbladder cancer by down-regulating S100p Via the Pi3k/Akt pathway. *Cancer Lett.* (2016) 372:239–50. doi: 10.1016/j.canlet.2016.01.008

67. Grunewald TG, Butt E. The LIM and SH3 domain protein family: structural proteins or signal transducers or both? *Molec Cancer.* (2008) 7:31. doi: 10.1186/1476-4598-7-31

68. Zheng J, Yu S, Qiao Y, Zhang H, Liang S, Wang H, et al. Lasp-1 promotes tumor proliferation and metastasis and is an independent unfavorable prognostic factor in gastric cancer. *J Cancer Res Clin Oncol.* (2014) 140:1891–9. doi: 10.1007/s00432-014-1759-3

69. Zhao L, Wang H, Liu C, Liu Y, Wang X, Wang S, et al. Promotion of colorectal cancer growth and metastasis by the LIM and SH3 domain protein1. *Gut.* (2010) 59:1226–35. doi: 10.1136/gut.2009.202739

70. Niu Y, Shao Z, Wang H, Yang J, Zhang F, Luo Y, et al. Lasp1-S100a11 axis promotes colorectal cancer aggressiveness by modulating Tgfβ/Smad signaling. *Sci Rep.* (2016) 6:26112. doi: 10.1038/srep26112

frontiers | Frontiers in Immunology

TYPE Original Research
PUBLISHED 05 April 2023
DOI 10.3389/fimmu.2023.1084883



OPEN ACCESS

EDITED BY
Mei-Ping Ding,
Zhejiang University, China

REVIEWED BY
Yuji Tomizawa,
Juntendo University, Japan
Li Feng,
Central South University, China
Weihong Lin,
First Affiliated Hospital of Jilin University, China
Xuewu Liu,
Shandong University, China

*CORRESPONDENCE
Qun Wang
wangq@ccmu.edu.cn

†These authors have contributed equally to this work

SPECIALTY SECTION
This article was submitted to Multiple Sclerosis and Neuroimmunology, a section of the journal Frontiers in Immunology

RECEIVED 31 October 2022
ACCEPTED 21 March 2023
PUBLISHED 05 April 2023

CITATION
Sun Y, Qin X, Huang D, Zhou Z, Zhang Y and Wang Q (2023) Anti-amphiphysin encephalitis: Expanding the clinical spectrum.
*Front. Immunol.* 14:1084883.
doi: 10.3389/fimmu.2023.1084883



# Anti-amphiphysin encephalitis: Expanding the clinical spectrum

Yueqian Sun[1†], Xiaoxiao Qin[1†], Danxia Huang[2], Ziqi Zhou[1], Yudi Zhang[1] and Qun Wang[1,3,4*]

[1]Department of Neurology, Beijing Tiantan Hospital, Capital Medical University, Beijing, China, [2]Department of Neurology, Fujian Medical University Affiliated First Quanzhou hospital, Quanzhou, China, [3]National Center for Clinical Medicine of Neurological Diseases, Beijing, China, [4]Beijing Institute of Brain Disorders, Collaborative Innovation Center for Brain Disorders, Capital Medical University, Beijing, China

**Objective:** An analysis of the clinical features of autoimmune encephalitis accompanied by anti-amphiphysin antibodies.

**Methods:** The data of encephalitis patients with anti-amphiphysin antibodies were retrospectively evaluated, including demographics, neurological and laboratory findings, imaging, treatment, and prognostic predictions.

**Results:** Ten patients aged between 29 and 78 years (median age 52 years) were included. The male: female ratio was 4:6. Limbic encephalitis was found in nine patients while epileptic seizures were present in seven patients. All patients showed anti-amphiphysin antibody positivity in sera while one ninth was positive for CSF antibody. The EEG findings were abnormal, including reductions in background activity, and the presence of diffuse slow waves, sharp waves, and spikes and waves. Five patients showed signs of increased T2 signals in the medial temporal lobe on MRI while PET showed either hyper- or hypo-metabolic changes in several brain regions, including the temporal lobe, hippocampus, basal ganglia, frontal and parietal cortices. Nine of ten patients were treated with immunotherapy, with improvements of varying degrees. There was a significant reduction in seizure frequency, and all patients were seizure-free at last follow-up.

**Conclusion:** Autoimmune encephalitis with anti-amphiphysin antibodies has a variety of clinical manifestations. The most common symptom is limbic encephalitis. Although relief from seizures can be achieved relatively easily, many patients suffer psychiatric, cognitive, and sleep sequelae. The disease was found to be associated with a lower incidence of cancer than has been previously reported for paraneoplastic neurologic syndromes.

KEYWORDS

**amphiphysin, autoimmune encephalitis, clinical features, treatment, prognosis**

# Introduction

Autoimmune encephalitis (AE) is a form of encephalitis resulting from autoimmune reactions (1). It is generally acute or subacute and has an annual incidence of approximately 0.8/100,000 (2). The typical presentation includes behavioral disorders, psychiatric symptoms, cognitive impairment, seizures, and impaired consciousness (1, 3). Since the first description of AE, characterized as anti-*N*-methyl-d-aspartate receptor (NMDAR) antibodies in 2007 (4), a variety of encephalitis-associated autoantibodies directed against components of the neuron have been discovered. These include antibodies against leucine-rich glioma-inactivated 1 protein (LGI1), contactin-associated protein-like 2 (CASPR2), γ-aminobutyric acid B receptor ($GABA_BR$), α-amino-3-hydroxy-5-methyl-4-isoxazole-propionic acid receptor (AMPAR), glycine receptor (GlyR), and so on.

Amphiphysin is a Bin/Amphiphysin/Rvs (BAR) domain containing protein that is involved in clathrin-dependent endocytosis during inhibitory neurotransmission (5). Its SH3 domain acts as a binding site during the formation of clathrin-coated intermediates (6). Amphiphysin has been associated with paraneoplastic neurological syndromes (PNS) in breast or small-cell lung cancers (7). The presence of anti-amphiphysin autoantibodies is most commonly associated with limbic encephalitis (LE) and stiff-person syndrome (8–10). Apart from the above, a number of case reports and small case series have reported a link between anti-amphiphysin antibodies and brainstem encephalitis (11), myelopathy (12, 13), peripheral neuropathy (11, 14), and cerebellar dysfunction (11). Anti-amphiphysin encephalitis is usually treated in the same way as other AE. First-line therapies are corticosteroids, intravenous gamma globulin (IVIG), and plasmapheresis (PLEX) and second-line treatment involves the addition of rituximab or cyclophosphamide in patients unresponsive to first-line therapy (15). Immunotherapy is effective for treating encephalitis patients with anti-amphiphysin antibodies, especially those without tumors (15). Treatment of tumors should be performed without delay to improve outcomes (1).

However, an in-depth understanding of amphiphysin-IgG-associated encephalitis is lacking. Here, we describe the clinical features of 10 anti-amphiphysin encephalitis patients and their outcomes after immunotherapy. A literature review of amphiphysin-antibody-associated neuropathy was also performed.

# Materials and methods

Patients with anti-amphiphysin antibody positivity in serum or cerebrospinal fluid (CSF) admitted to the Beijing Tiantan Hospital between 2018 and 2022 were reviewed. Ten patients fitting the criteria of autoimmune encephalitis updated in 2016 were retrospectively enrolled (1).

## Laboratory tests

Antibody testing of the sera and/or CSF of all patients with suspected autoimmune encephalitis was performed. The spectrum of antibodies tested included all known neuronal autoantibodies (NMDAR, LGI1, CASPR2, GABABR, AMPAR, and glutamic acid decarboxylase 65 [GAD65]) and classical paraneoplastic antibodies (Hu, Yo, Ri, Ma2, CV2, and amphiphysin). Samples were analyzed semi-quantitatively by cell-based assays (Euroimmun, Lübeck, Germany) and immunohistochemistry was performed by the Neuroimmunology Laboratory of the Peking Union Medical College Hospital (Beijing, China).

## EEG and imaging

Routine long-term video-electroencephalography (EEG) recording was performed with standard 10-20 system electrodes. Magnetic resonance imaging (MRI) was performed on each patient with a 3T MRI system (Signa HD xt *3T* Volume, *GE*, *GE* Healthcare, USA) while $^{18}$F-FDG positron emission tomography (PET) scans were done using a PET/CT scanner in all except two patients due to concerns of radiation exposure (Elite Discovery, GE HealthCare, Fairfield, CT, USA).

## Functional assessment and evaluation of outcomes

For most patients (except Patients #4, #9, #10), the Montreal Cognitive Assessment (MOCA) and the Mini-Mental State Examination (MMSE) were used to evaluate cognition. The modified Rankin Scale (mRS) was used for the assessment of clinical outcomes at discharge and follow-up.

## Literature review

A comprehensive literature search for articles published between January 2002 and October 2022 was conducted in the PubMed database using the search terms “Amphiphysin” and “encephalitis”. All results of the literature search were reviewed and relevant information was extracted and summarized. This search yielded 42 publications, from which 13 papers were included in the final review.

# Results

## Clinical characteristics

The ratio of males to females was 4:6 and the median onset age was 52 years old (range 29-78 years old). Most patients did not experience prodromal symptoms, with only one having fever and headache (Patient #9). The details of the clinical presentations are summarized in Table 1. Additionally, Patient #1 had a history of invasive ductal carcinoma in the right breast that was completely resected before the onset of encephalitis.

In this study, limbic encephalitis was the most common symptom. Seven patients suffered from epileptic seizures, with four having more

TABLE 1 Clinical manifestation of anti-amphiphysin encephalitis.

| Patient | Gender | Age | LE | | | Stiffness | Pain | Limb weakness/ numbness | Paresthesia | Ataxia | Sleep disorder | Dysautonomia |
|---|---|---|---|---|---|---|---|---|---|---|---|---|
| | | | Seizure | Cognitive disorder | Mental and behavior disorder | | | | | | | |
| 1 | F | 42 | | + (MMSE=28/ MOCA=25) | | + | + | + | + | | + (DIS) | + (hidrosis) |
| 2[a] | M | 54 | | + (MMSE=22/ MOCA=13) | + (apathy) | | | | | | | |
| 3 | M | 69 | + | + (MMSE=29/ MOCA=24) | | | | | | | + (RBD) | |
| 4 | M | 77 | + | + | + (irritable) | | | | | + | | |
| 5 | F | 42 | + | + (MMSE=30/ MOCA=20) | | | | | | | | |
| 6 | M | 59 | + | (MMSE=29/MOCA=29) | | | | | | | | |
| 7 | F | 42 | + | + (MMSE=26/ MOCA=21) | + (anxiety, depression) | | | + | + | + | | |
| 8 | F | 78 | + | + (MMSE=27) | | | | | | | + (DMS) | |
| 9 | F | 29 | | | | | + | + | | + | | |
| 10 | F | 50 | + | + | | | | | | | | |

DIS, difficulty initiating sleep; DMS, difficulty maintaining sleep; LE, limbic encephalitis; MMSE, Mini-Mental State Examination; MoCA, Montreal Cognitive Assessment; RBD, rapid-eye-movement sleep behavior disorder. a, anti-AMPAR and anti-CV2 antibodies were positive in serum. ; +, positive.



10.3389/fimmu.2023.1084883

than one type of seizure. Four patients experienced focal and bilateral tonic-clonic seizures, preceded by focal impaired awareness. One patient had myoclonic seizures involving both arms (Patient #1). Three of the seven patients suffered status epilepticus (Patients #4, #7, and #10). One patient was admitted to the Intensive Care Unit (ICU) due to hypoxemia during a seizure attack (Patient #10). In addition, 8 patients had cognitive disorder, of which 6 mentioned mild memory loss. Mental and behavioral disorders were infrequently observed, with only three patients reporting apathy, irritability, and anxiety-depression, respectively. In addition, sleep disorders were reported by patients #1, #3, and #8, which presented as difficulty initiating sleep (DIS), rapid-eye-movement sleep behavior disorder (RBD), and difficulty maintaining sleep (DMS).

None of the patients showed rigidity or spasm involving the axial muscles, described as stiff-person syndrome (16). Only one (Patient #1) showed episodic left upper limb extension with wrist adducent stiffness, induced by massage and lasting 1-2 minutes each time, always accompanied by sweating. Weakness and pain were present when lifting the upper right limb during the attack.

Sensory neuronopathy was found in two patients. In one patient (Patient #1), pruritus was easily induced by touching, usually on the upper limbs, shoulder, and back. Another patient (Patient #7) experienced soreness, numbness, and hyperalgesia in the right limbs. Furthermore, one (Patient #9) experienced numbness of the extremities, which was later confirmed by spinal cord MRI to be myelitis. She also showed impaired vision in the right eye and the visual acuities were 20/25 OD and 20/20 OS.

Cerebellar ataxia occurred in three patients (Patients #4, #7, and #9). All showed unstable walking, with one showing right limbs ataxia on physical examination, while no dysarthria or postural ataxia was observed.

## Auxiliary examinations

Nine patients had both serum and CSF samples tested, with one (Patient #8) not undergoing CSF testing due to rejection of the lumbar puncture. All showed anti-amphiphysin antibody positivity in the sera while positivity was only found in the CSF in one patient. Anti-AMPAR and anti-CV2 antibodies were also present in the serum of Patient #2. Detailed results of the laboratory tests are shown in Table 2.

The CSF results showed evidence of central nervous system (CNS) inflammation and abnormalities of the immune system. Two of nine patients had elevated white blood cell (WBC) counts (>10 n/μL) while five of nine patients had protein concentrations exceeding 45 mg/dL; the ranges of the WBC counts and protein levels were 1-40 n/μl and 17.26-92.24 mg/dL, respectively. CSF-specific oligoclonal bands were detected in most patients (7/8) and eight of the 10 patients showed abnormal levels of tumor markers (Table 2). One of these patients showed highly elevated PROGrp (4297 pg/mL, normal range 0-65.7 pg/mL), indicating a high likelihood of lung cancer, which was confirmed to be small-cell lung cancer by subsequent PET-CT.

Five patients showed involvement of the hippocampus on MRI (four unilateral, one bilateral). In Patient #4, to our surprise, the structure of the bilateral thalamus was blurred, with T2 high-signal lesions in the right thalamus (Figure 1). In addition, evidence of

TABLE 2 Laboratory and neuroimaging data of anti-amphiphysin encephalitis.

| Patient | CSF | | | Tumor marker | MRI | EEG | PET-CT | |
|---|---|---|---|---|---|---|---|---|
| | WBC (n/μL) | Protein (mg/dL) | SOB | | | | Brain/spinal | Whole body |
| 1 | 4 | 50.2↑ | + | Normal | Increased T2 signal in right MTL | NA | Right MTL hypermetabolism | Normal |
| 2 | 8 | 26.64 | + | NSE 65.5 ng/mL, Cyfra21-1 6.9 ng/mL, PROGrp 4297 pg/mL | Normal | NA | Right PL, bilateral FL hypometabolism, bilateral BG hypermetabolism | Lung and mediastinal mass with hypermetabolism |
| 3 | 4 | 49.42↑ | + | CA19-9 27.22 U/mL, NSE 20.72 ng/mL, TPSA 4.31 ng/mL | Increased T2 signal in left MTL | Sharp waves in left MTL | Left MTL hypometabolism | Normal |
| 4 | 6 | 46.7↑ | + | CA19-9 3.64 ng/mL, TPSA 6.52 ng/mL | DWI showed diffusion restriction in bilateral thalamus with blurred structure | NA | Bilateral central cortex, left fronto-parietal para-sagittal, BG, right thalamus hypermetabolism | Normal |
| 5 | 1 | 17.26 | – | AFP 11.2 ng/mL | Decreased volume of left hippocampus | Sharp waves in right MTL | Right MTL hypometabolism | Normal |
| 6 | 34 | 22.85 | + | CA72-4 11.97 U/mL | Increased T2 signal in the left MTL | Normal | Left MTL hypometabolism | Normal |

*(Continued)*

TABLE 2 Continued

| Patient | CSF | | | Tumor marker | MRI | EEG | PET-CT | |
|---|---|---|---|---|---|---|---|---|
| | WBC (n/μL) | Protein (mg/dL) | SOB | | | | Brain/spinal | Whole body |
| 7 | 2 | 17.62 | + | NSE 21.2 ng/mL | Normal | Continuous sharp waves in the left central-parietal area | Left MTL hypermetabolism | NA |
| 8 | NA | NA | NA | Normal | Normal | NA | NA | NA |
| 9 | 40 | 92.24↑ | + | CA19-9 28.42 U/mL | Increased T2 signal and enhancement in posterior horn of the spinal cord (C2-7) | NA | Spinal cord hypermetabolism | Normal |
| 10 | 9 | 58.3↑ | NA | Normal | Increased T2 signal in bilateral MTL | Normal | NA | NA |

AFP, alpha-fetoprotein; BG, basal ganglia; CA, carbohydrate antigen; CSF, cerebrospinal fluid; Cyfra21-1, cytokeratin 19 fragment antigen2 -1;EEG, electroencephalogram; FL, frontal lobe; MTL, medial temporal lobe; MRI, magnetic resonance imaging; NA, not applicable; NSE, neuron-specific enolase; PET-CT, positron emission tomography-computed tomography; PL, parietal lobe; PROGrp, Progastrin-releasing peptide; TPSA, total prostate specific antigen; SOB, CSF-specific oligoclonal bands; WBC, white blood cell; +, positive; -, negative.

non-specific lacunar infarctions and white-matter lesions were common in our older patients, although these were not AE-related. Brain PET-CT revealed either hyper- or hypo-metabolic changes in several brain regions including the temporal lobe, hippocampus, basal ganglia, and the frontal and parietal cortices (Figure 2). EEG was performed on a total of five patients, with abnormal findings in 3/5 (60%), including diffuse slow waves and sharp waves (Figure 3).

Furthermore, Holter electrocardiogram (ECG) examinations revealed asymptomatic bradycardia in one patient (Patient #6). Two patients received breast ultrasound examinations and were found to have benign hyperplastic nodules (Patients #7 and #9).

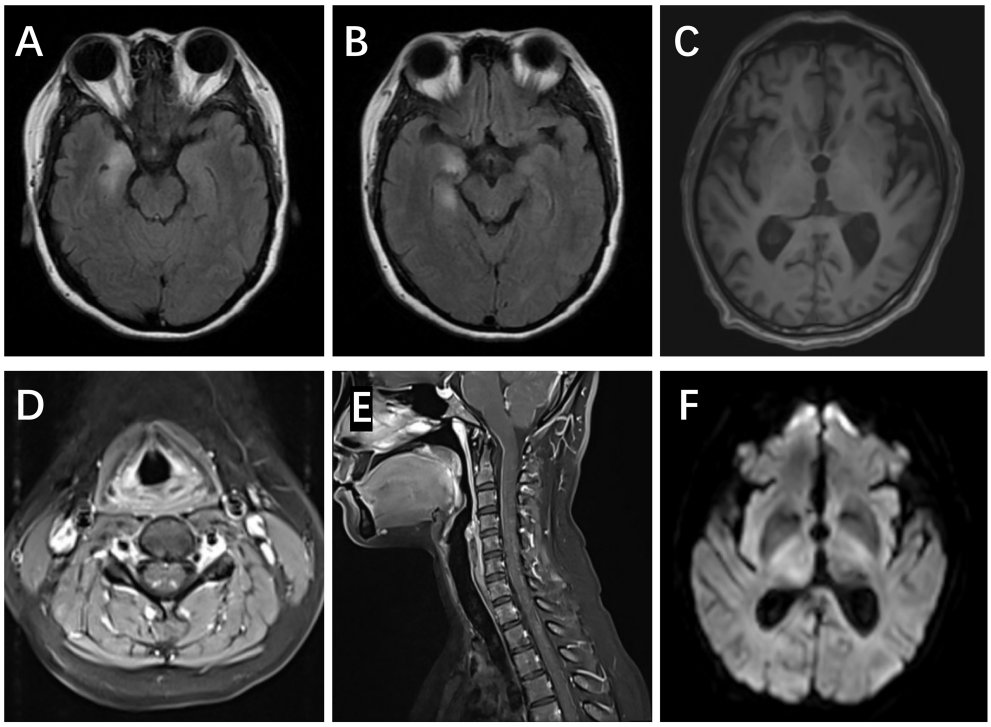


FIGURE 1
MRI scans in anti-amphiphysin encephalitis. **(A, B)** Right FLAIR hyperintensities in the medial temporal lobes, including both the amygdala and hippocampus (Patient #1). **(C)** The blurred structure of the bilateral thalamus (Patient #4). **(D, E)** Increased T2 signal and enhancement in posterior horn of the spinal cord (C2-7) (Patient #9). **(F)** Restriction of DWI in the right thalamus (Patient #4).

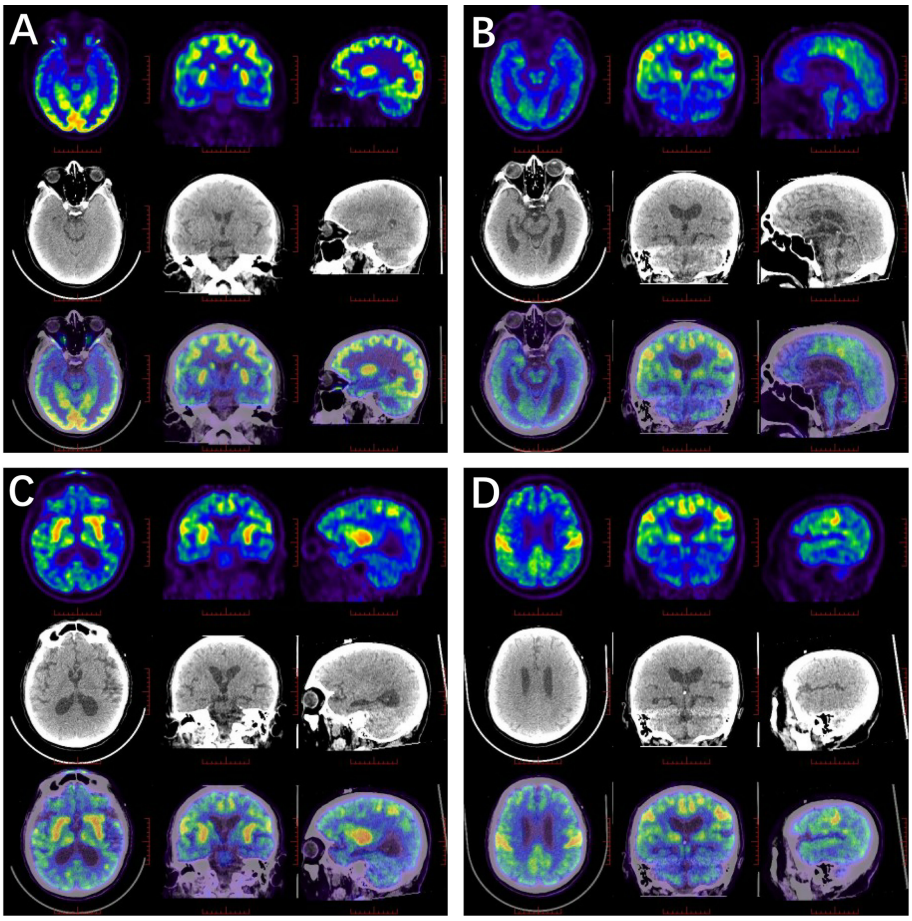


FIGURE 2
$^{18}$F-FDG PET/CT scan in anti-amphiphysin encephalitis. **(A)** Glucose metabolism decreased in the right hippocampus (Patient #1). **(B–D)** High FDG uptake in the bilateral central cortex, left fronto-parietal para-sagittal, bilateral caudate heads, putamen and right thalamus, while the remaining brain cortex was diffusely and slightly decreased (Patient #4).

## Treatment and prognosis

Nine patients were given first-line treatment, while one refused immunotherapy due to concern about side effects (Patient #8). Of the treated patients, five received IVIG administration only, three were treated with IVIG combined with steroids, and one was treated only with corticosteroids. In addition, patients received anti-seizure medications (ASMs), including sodium valproate (VPA), oxcarbazepine (OXC), levetiracetam (LEV), lacosamide (LCM), and lamotrigine (LTG).

All patients were followed up for at least three months after discharge, and the sequelae are summarized in Table 3. Patients #5, #7, #9, and #10 undertook sequential oral corticosteroids after discharge. None of the ten patients undertook second cycle of IVIG or corticosteroids treatment. A comparison of the mRS scores before and after treatment indicated the effectiveness of treatment, as the scores of 7 patients had decreased by at least one point. The seizure frequency was significantly reduced after treatment and all patients retrieved seizure free at last follow-up. However, sleep disorders, cognitive impairment and emotional disorders persisted on follow-up.

# Discussion

We retrospectively enrolled 10 patients diagnosed with amphiphysin-antibody-related encephalitis. The male: female ratio was 4:6, which is consistent with previous studies showing a greater frequency among female patients (17–19). The age of onset was during middle or old age, consistent with previously published data (17–19).

Anti-amphiphysin encephalitis has a variety of clinical manifestations, including limbic encephalitis, stiffness, limb weakness/numbness, paresthesia, ataxia, sleep disorders, and dysautonomia, amongst others. Of these, limbic encephalitis is the most common symptom. Notably, patients who conform to the AE criteria should be suspected of having anti-amphiphysin antibodies when presenting with stiffness or paresthesia, even though it is rare.

Stiff-person syndrome (SPS) is a characteristic manifestation in amphiphysin-antibody-positive cases, although it did not appear as frequently as expected in our cohort (18–20). Amphiphysin-antibody-related SPS involves neck and arm instead of axial muscles of trunk and thus usually confused clinicians (18). One patient in our study presented unilateral upper limb stiffness,

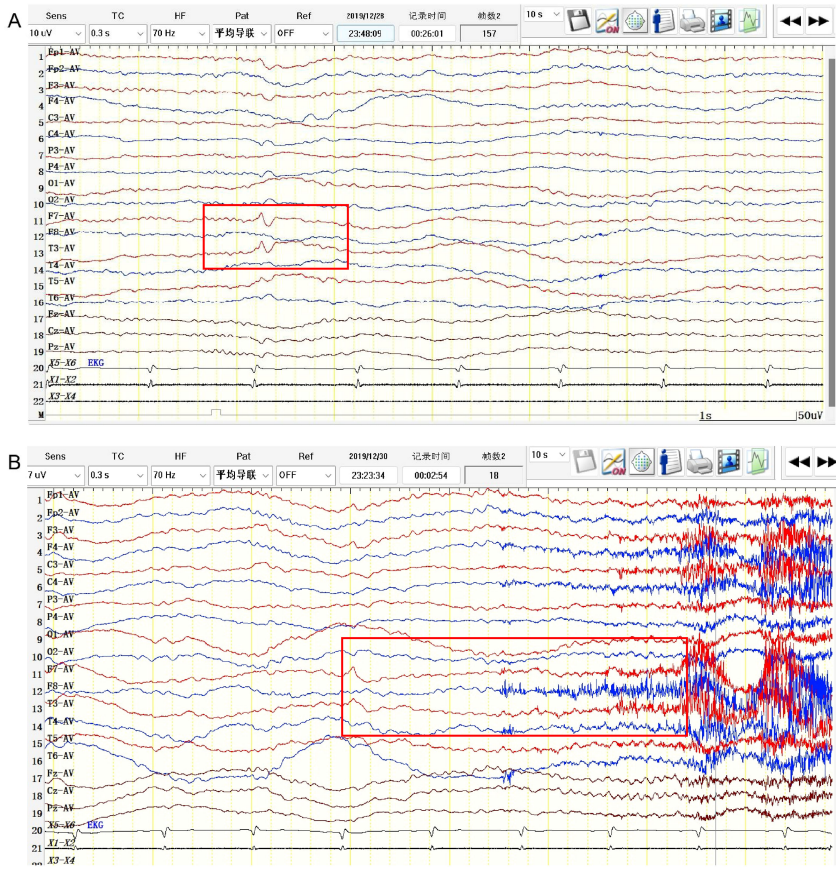


FIGURE 3
EEG pattern in anti-amphiphysin encephalitis. (Patient #3). **(A)** Interictal EEG showed sharp and waves in the left anterior temporal region (F7, T3). **(B)** Ictal EEG showed low-amplitude fast rhythmic activity with evolution originating from left temporal region.

TABLE 3 Treatment and prognosis of anti-amphiphysin encephalitis.

| Patient | Treatment | | Prognosis | | |
|---|---|---|---|---|---|
| | Immunotherapy | ASMs | Symptoms left at last follow-up | mRS at discharge | mRS in 3 months |
| 1 | IVIG; chemotherapy | (-) | Right upper limb numbness, painful, and pruritus; lower limbs weakness; sleep disorder (15 m) | 4 | 4 |
| 2 | IVIG; chemotherapy | (-) | Hallucination, irritable, hyperhidrosis, urinary retention, and constipation (14 m) | 3 | 1 |
| 3 | IVIG | OXC | Sleep disorder, anxiety-depression (33 m) | 1 | 1 |
| 4 | IVIG | LEV | Numbness of extremities, walking instable, anxiety-depression (10 m) | 3 | 2 |
| 5 | Corticosteroids | LCM | Anxiety-depression, anorexic; sleep disorder (restless sleep) (3 m) | 2 | 1 |
| 6 | IVIG | LEV | Memory loss (4 m) | 2 | 1 |
| 7 | IVIG + corticosteroids | OXC, LEV, LTG | Weakness of right limbs, walking instable (5 m) | 3 | 2 |
| 8 | (-) | LCM | Memory loss, sleep disorder (3 m) | 1 | 1 |
| 9 | IVIG + corticosteroids | (-) | Headache, back numbness (10 m) | 2 | 1 |
| 10 | IVIG + corticosteroids | LEV, VPA | Memory loss (17 m) | 4 | 1 |

ASMs, anti-seizure medications; IVIG, intravenous immune globulin; LCM, lacosamide; LEV, levetiracetam; LTG, lamotrigine; m, month; mRS, modified Rankin Scale; OXC, oxcarbazepine; RBD, rapid-eye-movement sleep behavior disorder; VPA, valproic acid; (-), none; +, plus.

accompanied by paresthesia and dysautonomia. She fitted the diagnosis of progressive encephalomyelitis with rigidity and myoclonus (PERM), a severe immunophenotype of stiff-person spectrum disorder (SPSD) (21). This patient showed strong anti-amphiphysin antibody positivity in her serum, much higher than that seen in the other patients, suggesting a potential link between higher antibody titers and SPS severity. However, the relationship between antibody titers and the severity of clinical manifestation is still not clear in AE and requires future in-depth research.

Patients also demonstrated symptoms of myelitis. In Patient #9, the MRI showed the presence of a lesion in the posterior horn (C2-7). Similarly, Galassi et al. reported longitudinally extensive transverse myelitis (LETM) in a 40-year-old woman with amphiphysin antibody positivity (22). A study also demonstrated post-mortem histopathological evidence of the presence of CD8+ T cell-mediated immune responses in the spinal cord and dorsal root ganglia (17), confirming the involvement of the spinal cord.

Sensory neuronopathy has been found to be closely related to the presence of amphiphysin antibodies by previous studies (23). Our two patients, however, despite their complaints of paresthesia, did not meet the criteria of sensory neuronopathy (24). Besides, it had been considered that involvement of motor nerve or CSF inflammatory may indicate a paraneoplastic origin (25).

Amphiphysin is an intraneuronal protein that is targeted in 5-10% of PNS cases, and the presence of anti-amphiphysin antibodies has been listed as a significant risk factor for tumor occurrence (>80%) (23). Amphiphysin antibodies are widely known to be associated with both breast and small-cell lung cancers. Associations with other cancers have also been reported, including angiosarcoma and thyroid adenoma (Supplementary Table 1). Nevertheless, a much lower rate of cancer (2/10) was found in this study (19). No new neoplasms were diagnosed after discharge in our patient cohort. It is possible that insufficient follow-up may partially account for our low detection rate. Repeated screening every four or six months for two years is recommended (23). Accordingly, the necessity of cancer screening must be emphasized, and systemic tumor screening requires whole-body PET-CT as the first choice.

Amphiphysin antibodies are usually detected by immunoblotting, the gold standard for the identification of intracellular antibodies. Previous studies have reported the co-existence of amphiphysin antibodies with anti-neuronal nuclear antibody type 1 (ANNA1) and CRMP5 antibodies (17, 19). Here, we observed a co-occurrence of amphiphysin antibodies with CV2 and AMPAR antibodies. This overlap between amphiphysin antibodies and other subtypes of autoantibodies suggests that AE has both a complex etiology and mechanism. Furthermore, although not included in the present study, we have noticed amphiphysin antibody positivity in some AD (Alzheimer's disease) and PD (Parkinson's disease) patients. Although cognitive impairment may be a common manifestation, the progressive course of the disease suggests neurodegeneration rather than encephalitis. Thus, amphiphysin antibodies could be either causative agents or nonpathogenic bystanders caused by other CNS diseases. In terms of clinical diagnosis, the identification of this disease should thus be based on a thorough understanding of amphiphysin antibody pathology as well as clinical experience.

Patients with anti-amphiphysin encephalitis did not show distinctive features on either EEG or brain MRI. Involvement of the mesial temporal lobe was most common, which may mimic other subtypes of AE. Furthermore, involvement of the thalamus was found in one patient, consistent with the findings of a previous report (10). PET-CT revealed evidence of abnormal metabolism in several brain regions, although these were not specific. With the development of imaging analyses, more attention focusing on characteristic structural and functional imaging patterns is needed.

In our study, most patients received IVIG or corticosteroids along with ASMs, and their mRS scores reduced at follow-up. In animal experiments, animals exposed to purified amphiphysin antibodies showed symptom relief after plasmapheresis (26, 27). Clinically, a combination of immunotherapy and tumor treating is required (28). Besides, responses to high-dose benzodiazepine have also been noted (18). Follow-ups of the patients showed that the duration of symptoms varied under standard therapy. Although the seizure frequencies were observed to be reduced during follow-ups of 1 to 33 months, there was minimal improvement in cognitive impairment, sleep disturbances, or psychotic mood disorders. By tracking for 13 years, Taube et al. observed a similar outcome in a patient who was treated promptly with immunotherapy (29). As in other forms of AE, anti-amphiphysin encephalitis presenting with acute symptomatic seizures has a lower risk of subsequent unprovoked seizure development, which perhaps explains the disappearance of seizures in most patients.

There are some limitations in this study. Firstly, the sample size may have been too small. Secondly, immunoblotting is a semi-quantitative assay that does not show the exact titers of antibodies and may be subject to false-positive or false-negative results. In addition, in some cases, the absence of important examination findings such as electromyography and polysomnography hampered physician awareness of the disease and its treatment. In the future, the sample size should be expanded for more in-depth research.

## Conclusion

Amphiphysin-antibody-related encephalitis is a rare type of autoimmune encephalitis. The most common manifestation was limbic encephalitis and a lower association with cancer was observed compared with that reported in other PNS cohorts. Although seizure frequencies declined in response to immunotherapy, psychiatric and cognitive symptoms, as well as sleep disturbances, often remained. The awareness of the clinical features of amphiphysin antibody-related encephalitis provides valuable information for a better understanding of the disease and may help to facilitate its early diagnosis, treatment strategy, and prognosis prediction.

## Data availability statement

The original contributions presented in the study are included in the article/Supplementary Material. Further inquiries can be directed to the corresponding authos.

## Ethics statement

The studies involving human participants were reviewed and approved by KY2021-088-03. The patients/participants provided their written informed consent to participate in this study. Written informed consent was obtained from the individual(s) for the publication of any potentially identifiable images or data included in this article.

## Author contributions

QW and YS concepted, designed, and supervised the study. YS, XQ and DH acquired the data. YS and XQ analyzed and interpreted the data, provided statistical analysis, had full access to all of the data in the study, and are responsible for the integrity of the data and the accuracy of the data analysis. YS and XQ drafted the manuscript. ZZ, YZ and QW critically revised the manuscript for important intellectual content. All authors contributed to the article and approved the submitted version.

## Funding

The study was financially supported by the National Key R&D Program of China grant (2022YFC2503800 and 2017YFC1307500), the Capital Health Research and Development of Special grants (2016-1-2011 and 2020-1-2013), the Beijing-Tianjin-Hebei Cooperative Basic Research Program (H2018206435), and the Beijing Natural Science Foundation (Z200024).

## Conflict of interest

The authors declare that the research was conducted in the absence of any commercial or financial relationships that could be construed as a potential conflict of interest.

## Publisher's note

All claims expressed in this article are solely those of the authors and do not necessarily represent those of their affiliated organizations, or those of the publisher, the editors and the reviewers. Any product that may be evaluated in this article, or claim that may be made by its manufacturer, is not guaranteed or endorsed by the publisher.

## Supplementary material

The Supplementary Material for this article can be found online at: https://www.frontiersin.org/articles/10.3389/fimmu.2023.1084883/full#supplementary-material

## References

1. Graus F, Titulaer MJ, Balu R, Benseler S, Bien CG, Cellucci T, et al. A clinical approach to diagnosis of autoimmune encephalitis. *Lancet Neurol* (2016) 15:391–404. doi: 10.1016/s1474-4422(15)00401-9

2. Dubey D, Pittock SJ, Kelly CR, Mckeon A, Lopez-Chiriboga AS, Lennon VA, et al. Autoimmune encephalitis epidemiology and a comparison to infectious encephalitis. *Ann Neurol* (2018) 83:166–77. doi: 10.1002/ana.25131

3. Broadley J, Seneviratne U, Beech P, Buzzard K, Butzkueven H, O'brien T, et al. Prognosticating autoimmune encephalitis: A systematic review. *J Autoimmun* (2019) 96:24–34. doi: 10.1016/j.jaut.2018.10.014

4. Dalmau J, Tüzün E, Wu HY, Masjuan J, Rossi JE, Voloschin A, et al. Paraneoplastic anti-N-methyl-D-aspartate receptor encephalitis associated with ovarian teratoma. *Ann Neurol* (2007) 61:25–36. doi: 10.1002/ana.21050

5. Pruss H, Kirmse K. Pathogenic role of autoantibodies against inhibitory synapses. *Brain Res* (2018) 1701:146–52. doi: 10.1016/j.brainres.2018.09.009

6. Evergren E, Marcucci M, Tomilin N, Low P, Slepnev V, Andersson F, et al. Amphiphysin is a component of clathrin coats formed during synaptic vesicle recycling at the lamprey giant synapse. *Traffic.* (2004) 5:514–28. doi: 10.1111/j.1398-9219.2004.00198.x

7. McCracken L, Zhang J, Greene M, Crivaro A, Gonzalez J, Kamoun M, et al. Improving the antibody-based evaluation of autoimmune encephalitis. *Neurol Neuroimmunol Neuroinflamm.* (2017) 4:e404. doi: 10.1212/nxi.0000000000000404

8. Saiz A, Dalmau J, Butler MH, Chen Q, Delattre JY, De Camilli P, et al. Anti-amphiphysin I antibodies in patients with paraneoplastic neurological disorders associated with small cell lung carcinoma. *J Neurol Neurosurg Psychiatry* (1999) 66:214–7. doi: 10.1136/jnnp.66.2.214

9. Krishna VR, Knievel K, Ladha S, Sivakumar K. Lower extremity predominant stiff-person syndrome and limbic encephalitis with amphiphysin antibodies in breast cancer. *J Clin Neuromuscul Dis* (2012) 14:72–4. doi: 10.1097/CND.0b013e31826f0d99

10. Moon J, Lee ST, Shin JW, Byun JI, Lim JA, Shin YW, et al. Non-stiff anti-amphiphysin syndrome: Clinical manifestations and outcome after immunotherapy. *J Neuroimmunol.* (2014) 274:209–14. doi: 10.1016/j.jneuroim.2014.07.011

11. Coppens T, Van Den Bergh P, Duprez TJ, Jeanjean A, De Ridder F, Sindic CJ. Paraneoplastic rhombencephalitis and brachial plexopathy in two cases of amphiphysin auto-immunity. *Eur Neurol* (2006) 55:80–3. doi: 10.1159/000092307

12. Chamard L, Magnin E, Berger E, Hagenkötter B, Rumbach L, Bataillard M. Stiff leg syndrome and myelitis with anti-amphiphysin antibodies: A common physiopathology? *Eur Neurol* (2011) 66:253–5. doi: 10.1159/000331592

13. Flanagan EP, Mckeon A, Lennon VA, Kearns J, Weinshenker BG, Krecke KN, et al. Paraneoplastic isolated myelopathy: clinical course and neuroimaging clues. *Neurology.* (2011) 76:2089–95. doi: 10.1212/WNL.0b013e31821f468f

14. Perego L, Previtali SC, Nemni R, Longhi R, Carandente O, Saibene A, et al. Autoantibodies to amphiphysin I and amphiphysin II in a patient with sensory-motor neuropathy. *Eur Neurol* (2002) 47:196–200. doi: 10.1159/000057898

15. Wesselingh R, Butzkueven H, Buzzard K, Tarlinton D, O'brien TJ, Monif M. Innate immunity in the central nervous system: A missing piece of the autoimmune encephalitis puzzle? *Front Immunol* (2019) 10:2066. doi: 10.3389/fimmu.2019.02066

16. Shaw PJ. Stiff-man syndrome and its variants. *Lancet.* (1999) 353:86–7. doi: 10.1016/S0140-6736(05)76151-1

17. Pittock SJ, Lucchinetti CF, Parisi JE, Benarroch EE, Mokri B, Stephan CL, et al. Amphiphysin autoimmunity: Paraneoplastic accompaniments. *Ann Neurol* (2005) 58:96–107. doi: 10.1002/ana.20529

18. Murinson BB, Guarnaccia JB. Stiff-person syndrome with amphiphysin antibodies: distinctive features of a rare disease. *Neurology.* (2008) 71:1955–8. doi: 10.1212/01.wnl.0000327342.58936.e0

19. Dubey D, Jitprapaikulsan J, Bi H, Do Campo RV, Mckeon A, Pittock SJ, et al. Amphiphysin-IgG autoimmune neuropathy: A recognizable clinicopathologic syndrome. *Neurology.* (2019) 93:e1873–80. doi: 10.1212/WNL.0000000000008472

20. Xie YY, Meng HM, Zhang FX, Maimaiti B, Jiang T, Yang Y. Involuntary movement in stiff-person syndrome with amphiphysin antibodies: A case report. *Med (Baltimore).* (2021) 100:e24312. doi: 10.1097/MD.0000000000024312

21. Martinez-Hernandez E, Arino H, Mckeon A, Iizuka T, Titulaer MJ, Simabukuro MM, et al. Clinical and immunologic investigations in patients with stiff-person spectrum disorder. *JAMA Neurol* (2016) 73:714–20. doi: 10.1001/jamaneurol.2016.0133

22. Galassi G, Ariatti A, Rovati R, Genovese M, Rivasi F. Longitudinally extensive transverse myelitis associated with amphiphysin autoimmunity and breast cancer: a paraneoplastic accompaniment. *Acta Neurol Belg.* (2016) 116:395–7. doi: 10.1007/s13760-015-0534-9

23. Graus F, Vogrig A, Muniz-Castrillo S, Antoine JG, Desestret V, Dubey D, et al. Updated diagnostic criteria for paraneoplastic neurologic syndromes. *Neurol Neuroimmunol Neuroinflamm.* (2021) 8(4):e1014. doi: 10.1212/NXI.0000000000001014

24. Camdessanche JP, Jousserand G, Ferraud K, Vial C, Petiot P, Honnorat J, et al. The pattern and diagnostic criteria of sensory neuronopathy: a case-control study. *Brain.* (2009) 132:1723–33. doi: 10.1093/brain/awp136

25. Camdessanche JP, Jousserand G, Franques J, Pouget J, Delmont E, Creange A, et al. A clinical pattern-based etiological diagnostic strategy for sensory neuronopathies: a French collaborative study. *J Peripher Nerv Syst* (2012) 17:331–40. doi: 10.1111/j.1529-8027.2012.00411.x

26. Sommer C, Weishaupt A, Brinkhoff J, Biko L, Wessig C, Gold R, et al. Paraneoplastic stiff-person syndrome: Passive transfer to rats by means of IgG antibodies to amphiphysin. *Lancet* (2005) 365:1406–11. doi: 10.1016/s0140-6736(05)66376-3

27. Baizabal-Carvallo JF. The neurological syndromes associated with glutamic acid decarboxylase antibodies. *J Autoimmun* (2019) 101:35–47. doi: 10.1016/j.jaut.2019.04.007

28. Schmierer K, Valdueza JM, Bender A, Decamilli P, David C, Solimena M, et al. Atypical stiff-person syndrome with spinal MRI findings, amphiphysin autoantibodies, and immunosuppression. *Neurology.* (1998) 51:250–2. doi: 10.1212/wnl.51.1.250

29. Taube J, Witt JA, Baumgartner T, Helmstaedter C. All's well that ends well? long-term course of a patient with anti-amphiphysin associated limbic encephalitis. *Epilepsy Behav Rep* (2022) 18:100534. doi: 10.1016/j.ebr.2022.100534

frontiers | Frontiers in Immunology

TYPE Review
PUBLISHED 05 April 2023
DOI 10.3389/fimmu.2023.1111719



OPEN ACCESS

EDITED BY
Honghao Wang,
Guangzhou First People's Hospital, China

REVIEWED BY
Youming Long,
The Second Affiliated Hospital of Guangzhou Medical University, China
Jia Geng,
Affiliated Hospital and Clinical Medical College of Chengdu University, China

*CORRESPONDENCE
Chao Zhang
chaozhang@tmu.edu.cn

SPECIALTY SECTION
This article was submitted to Multiple Sclerosis and Neuroimmunology, a section of the journal Frontiers in Immunology

RECEIVED 30 November 2022
ACCEPTED 16 March 2023
PUBLISHED 05 April 2023

CITATION
Zhang F, Gao X, Liu J and Zhang C (2023) Biomarkers in autoimmune diseases of the central nervous system. *Front. Immunol.* 14:1111719. doi: 10.3389/fimmu.2023.1111719



# Biomarkers in autoimmune diseases of the central nervous system

Fenghe Zhang[1], Xue Gao[1], Jia Liu[1] and Chao Zhang[1,2]*

[1]Department of Neurology and Institute of Neuroimmunology, Tianjin Medical University General Hospital, Tianjin, China, [2]Centers of Neuroimmunology and Neurological Diseases, China National Clinical Research Center for Neurological Diseases, Beijing Tiantan Hospital, Capital Medical University, Beijing, China

The autoimmune diseases of the central nervous system (CNS) represent individual heterogeneity with different disease entities. Although clinical and imaging features make it possible to characterize larger patient cohorts, they may not provide sufficient evidence to detect disease activity and response to disease modifying drugs. Biomarkers are becoming a powerful tool due to their objectivity and easy access. Biomarkers may indicate various aspects of biological processes in healthy and/or pathological states, or as a response to drug therapy. According to the clinical features described, biomarkers are usually classified into predictive, diagnostic, monitoring and safety biomarkers. Some nerve injury markers, humoral markers, cytokines and immune cells in serum or cerebrospinal fluid have potential roles in disease severity and prognosis in autoimmune diseases occurring in the CNS, which provides a promising approach for clinicians to early intervention and prevention of future disability. Therefore, this review mainly summarizes the potential biomarkers indicated in autoimmune disorders of the CNS.

KEYWORDS

**autoimmune diseases, biomarkers, neurofilament light chain, glial fibrillary acidic protein, Kappa free light chain, cytokines, CNS**

## Introduction

With the deep investigation on the pathogenic mechanisms of the CNS, the study of biomarkers has become a particularly active research field because of its potential application in clinical practice in disease diagnosis and prognosis evaluation. They are easy to quantify and can well characterize the autoimmune diseases. Molecular biomarkers combined with imaging tools largely contribute to the diagnosis, evaluation of the efficacy of disease modifying drugs (DMDs), and prediction of disability in clinical practice. At present, Biomarkers with clinical significance and prospects from blood and cerebrospinal fluid (CSF) have been proposed one after another. Therefore, this review collates the biomarkers related to CNS autoimmune diseases and potential clinical significance.

## Neurofilament light chain (NfL)

Neurofilament is the cytoskeleton component of neurons, which is especially rich in axons and plays a structural role in maintaining axon morphology. Neurofilament consists of three subunits, namely, neurofilament light chain (NfL), neurofilament medium chain and neurofilament heavy chain. NfL refers to the neurofilament chain with molecular weight less than 68 kDa, which is the most widely studied component of neurofilament. When axonal or neuronal damage occurs, NfL could be released and can be detected in the CSF and blood (1). Previous studies have found that CSF NfL is associated with disease disability, disease activity, and the time since the last relapse in patients with relapsing and remitting multiple sclerosis (RRMS) (1–7). However, the previous study could only accurately quantify NfL in CSF samples, because the sensitivity of the detection technique is not accurate enough to quantify the level of serum NfL (sNfL) (1). Because lumbar puncture is an invasive operation, it is more suitable for clinical diagnosis and treatment for the study of sNfL. At present, single molecular array (SIMOA) is generally used to determine NfL. Current studies have shown that there is a close correlation between sNfL levels and multiple sclerosis (MS). SNfL is related to disease activity, treatment response, disease and disability progression, and can be combined with magnetic resonance imaging (MRI) to assist in disease diagnosis and treatment (Table 1). However, NfL can be increased in any status that leads to axonal damage, including normal aging. Therefore, despite its high sensitivity, it is not an ideal biomarker for a single diagnostic test (8).

As a biomarker of disease activity, NfL can be used to provide a quick overview of disease activity. A large nested case-control study

TABLE 1 Overview of the biomarkers described in this review.

| Biomarkers | Common Related Diseases | Function |
|---|---|---|
| CNS Injury Markers | | |
| NfL | MS, NMOSD | To monitor disease activity,<br>To monitor drug treatment response,<br>To predict disability progression,<br>To aid imaging diagnosis |
| GFAP | NMOSD | To monitor disease activity and disability progression,<br>To monitor drug treatment response,<br>To aid differential diagnosis |
| CNTN-1 | MS | To monitor disease activity,<br>To monitor drug treatment response |
| CHI3L1 | MS | To predict disability progression |
| Humoral Markers | | |
| KFLC | MS | Diagnostic and prognostic markers,<br>To monitor disease changes and efficacy |
| KFLC Index | MS | To aid diagnosis and differential diagnosis<br>Prognostic markers |
| AQP4-IgG | NMOSD | Diagnostic markers |
| MOG-IgG | MOGAD | Prognostic markers |
| Autoimmune encephalitis associated antibody | AE | Diagnostic markers |
| Cytokines | | |
| IL-6 | NMOSD, MS | Prognostic markers |
| IL-17A | AE | To evaluate short-term severity |
| CXCL13 | MS, NMDAR encephalitis | Diagnostic and prognostic markers,<br>To monitor drug treatment response, |
| OPN | MS | To monitor disease activity and progression,<br>Diagnostic and prognostic markers |
| Cell Markers | | |
| Memory B cells and plasma cells | NMOSD, MS | To monitor drug treatment response |
| Eomes+ Th cells | MS | To monitor disease progression,<br>Prognostic markers |

CNS, central nervous system; NfL, neurofilament light chain; GFAP, glial fibrillary acid protein; CNTN-1, Contactin-1; CHI3L1, chitinase3-like protein1; KFLC, kappa free light chain; AQP4-IgG, aquaporin-4-IgG; MOG-IgG, myelin oligodendrocyte glycoprotein-IgG; IL-6, interleukin-6; IL-17A, Interleukin-17A; CXCL13, chemokine (C-X-C motif) ligand 13; OPN, osteopontin; MS, multiple sclerosis; NMOSD, neuromyelitis optica spectrum disorders; MOGAD, myelin oligodendrocyte glycoprotein-IgG associated disease; AE, autoimmune encephalitis; NMDAR, N-methyl D-aspartate receptor.

on patients with MS found that the elevation of sNfL was usually several years earlier than the clinical onset of MS. The level of sNfL increased close to the clinical attack and the onset itself was related to the significant increase of sNfL. The inherent increase of sNfL level before symptoms was related to the high risk of MS, suggesting that MS may have a prodromal period lasting for several years, during which axonal damage has occurred (9). Another study showed that patients with higher sNfL levels had a higher risk of relapse than patients with lower levels (10). In addition, sNfL also has a prognostic value in patients with clinical isolation syndrome (CIS) in the conversion to clinically defined MS (10).

As a marker of subsequent attacks, sNfL can also be used as an index to monitor treatment response. It was found that DMD treatment was an independent factor related to sNfL levels. The sNfL level of patients treated with DMD was lower compared with untreated patients, and sNfL level decreased significantly during follow-ups (11, 12). Compared with other treatments, high-efficiency therapies may lead to a greater decline in sNfL levels over time (10). After excluding the influence of confounding factors such as age and body mass index on sNfL measurement, Benkert and his colleagues established a reference database by using the statistical methods of percentile and Z score (13). The results showed that sNfL can be used as a biomarker to predict the individual therapeutic effect and course of MS. In addition, sNfL could be used as an additional measure of disease activity and sNfL concentration could also be used to quantitatively compare the long-term effectiveness of disease modification therapy (DMT) (13). This study showed that in all patients with MS and patients with no evidence of disease activity, a sNfL Z score greater than 1.5 was associated with an increased risk of future clinical or MRI disease activity. And Z score was more accurate compared to the absolute value of sNfL (13).

In addition, the level of sNfL was independently correlated with the score of Expanded Disability Status Score (EDSS) (14, 15), and could be used as a predictor of the long-term course of disability in MS. Several studies found that baseline sNfL levels were significantly correlated with EDSS scores, MS clinical phenotype and treatment response (10). Another study also indicated that as baseline sNfL levels increased (equal to or higher 7.3 pg/ml), the risk of disability progression as measured by relapse-free EDSS-progression also increased, and patients with lower sNfL levels than 7.3 pg/ml were significantly less likely to experience disability progression (16). Patients with secondary progressive MS (SPMS) transition were more likely to show higher sNfL levels during follow-up compared to baseline. The results showed that sNfL measurement could predict disability progress and could distinguish SPMS patients, thus promoting the early diagnosis of patients at risk (16). In addition, some studies have also found that sNfL was related to the EDSS score and seizure severity of myelin oligodendrocyte glycoprotein-IgG associated disease (MOGAD), and may predict the long-term prognosis of MOGAD (17). In a prospective study, the relationship between sNfL levels and disease severity and prognostic indicators of neuromyelitis optica spectrum disorders (NMOSD) was evaluated. The results also showed that sNfL level was positively correlated with EDSS score. Therefore, sNfL may be a biomarker of disease activity and disability in MS, MOGAD and NMOSD (18).

The increase of sNfL level is also related to the loss of brain and cervical spinal cord volume in MS patients (15), and the baseline sNfL level is a predictor of brain atrophy (19). A large observation cohort with a 12-year follow-up in a single center showed that sNfL level was correlated with brain atrophy (10). In a recent study, baseline sNfL predicted brain atrophy in the following 12 and 24 months, with the latter baring the stronger correlation (19). In a group of newly diagnosed CIS and RRMS patients, it was found that the sNfL level at the diagnosis time point was significantly correlated with the baseline T2 lesion volume (20). Besides, a higher baseline sNfL level can predict brain atrophy in the next 2 years (20). After 2 years, the brain volume of patients with higher baseline sNfL decreased faster, and the volume of T2 lesions increased faster (20). Furthermore, higher CSF and sNfL levels in MS patients are associated with more severe gray matter atrophy (21, 22), and CSF NfL concentration is an independent predictor of gray matter volume in CIS (22).

High NfL concentration in serum and CSF is related to Gd enhancement and the number of new/enlarged lesions on MRI, which is not limited to RRMS, but also in patients with progressive MS (8, 15). sNfL level was positively correlated with the existence and number of Gd+ lesions which indicating acute inflammatory neuron injury (20). Within 3 months after Gd+ injury, sNfL level increased (23). In addition, sNfL seems to have the potential to distinguish clinical recurrence with Gd+ lesions from clinical recurrence without Gd+ lesions (23). Therefore, sNfL measurement can be used as a tool in clinical practice to decide when a patient needs MRI enhancement evaluation (20).

## Glial fibrillary acid protein (GFAP)

GFAP is the main intermediate filament that makes up the cytoskeleton of astrocytes, which maintains the integrity of cell structure. It also plays a role in cell mitosis, astrocyte-neuron communication and glial scar formation. The detection of GFAP in CSF or serum reflects the damage of astrocytes (24, 25). There is a close correlation between CSF and serum GFAP (sGFAP) levels in patients with demyelinating diseases (26, 27).

Recently, a large number of studies have investigated the potential of GFAP as an indicator of disability progression, diagnosis and early disease activity in MS (24). One study established a positive correlation between sGFAP and EDSS score or recent attacks, but no therapeutic effect was detected in RRMS. In RRMS, sGFAP levels were associated with the maximum EDSS score indicating disease progression during the most recent attack, but not with the remission between recent attack. In addition, the study analyzed sera samples from 32 RRMS patients in remission and found that the GFAP levels were not higher compared to previous studies. The value of sGFAP to predict subsequent attack in MS warrants further study (26). In addition, CSF GFAP is more likely to be related to progressive MS compared to RRMS (28). Therefore, GFAP may be not sufficient to be an appropriate

biomarker for MS diagnosis and disease activity assessment alone, and more biomarkers and imaging evidence are needed to distinguish MS from other neurological diseases.

It was found that in patients with aquaporin-4 (AQP4)-IgG+ NMOSD, sGFAP was also significantly correlated with clinical disability parameters. sGFAP has a potential role as a biomarker of disease severity and future disease activity in patients with AQP4-IgG+NMOSD in clinical remission (29). In addition, sGFAP is not only correlated with disease activity, but also with inebilizumab-treatment response in NMOSD (30). In contrast, no association between sGFAP and clinical disability parameters was observed in patients with MOGAD (29). However, the correlation between sNfL and clinical disability parameters and future disease activity in AQP4-IgG+ patients is to be determined. The potential correlation between sGFAP as a biomarker of disease severity and prognosis of AQP4-IgG+NMOSD deserves further study in an independent cohort of AQP4-IgG+NMOSD patients (29). Another study found a strong correlation between sGFAP levels and EDSS scores and recent attack rates, suggesting that sGFAP levels are biomarkers of disability and disease activity in NMOSD, regardless of age or sex (26). The level of sNfL in NMOSD was higher in patients with higher EDSS score and older patients. sGFAP is associated with recent myelitis attack, but not with clinical disease activity from other anatomical attacks. The results showed that sGFAP and sNfL may be good biomarkers of disease activity and disability, while sGFAP/sNfL quotient at attacks may be a potential diagnostic marker for NMOSD. Higher sGFAP/SNfL quotient at attacks has a sensitivity of 73.0% and specificity of 75.8% to distinguish NMOSD from MS (26). When the disease relapsed, the level of sNfL in NMOSD and MS groups decreased with time, but the decline rate in NMOSD group was slower compared with MS patients. It seems that not sNfL but the combination of sGFAP and sNfL helps distinguish NMOSD from MS (25).

SNfL and sGFAP can also be used as biomarkers of therapeutic effect in NMOSD (31). A recent study showed, tocilizumab and rituximab (RTX) significantly decreased the levels of sNfL and sGFAP at the end of follow-up compared to corticosteroids (32).

## Contactin-1 (CNTN-1)

Contact proteins are a group of cell adhesion molecules, which are mainly expressed in the brain and are indispensable in axon domain organization, axon orientation, neurogenesis, neuron development, synaptic formation and plasticity, axon-glial cell interaction and nerve regeneration. At present, enzyme-linked immunosorbent assays (ELISAs) is generally used to detect the concentration of CNTN-1 in CSF. A previous study showed that the decrease of CSF CNTN-1 level in patients with MS was associated with disease progression, suggesting that CNTN-1 can be used as a new marker of axonal injury (33). Compared with healthy controls, the levels of CNTN-1 and CNTN-2 in RRMS and SPMS decreased at most by 1.4 times, while in patients with CIS, CNTN-1 tended to increase compared with controls. Baseline CNTN-2 levels also play a vital role in predicting longitudinal decline in cortical volume. CSF CNTN-1 levels in SPMS patients were positively correlated with MRI standardized brain volume, but negatively correlated with T2 lesion load. As for RRMS and primary progressive multiple sclerosis (PPMS), there was no correlation between CNTN-1 and CNTN-2 and standardized brain volume or T2 lesion load (34). A recent study has shown that serum CNTN-1 (sCNTN-1) can be used as a biomarker of long-term disease progression in MS. According to a 3-year prospective study, median sCNTN-1 levels were significantly lower in RRMS patients with natalizumab-treated compared with healthy controls. It also found that sCNTN-1 levels in RRMS patients with disability progression decreased significantly before and 12 months after treatment compared with non-progressive patients (35). Therefore, CNTN-1 can be used as a sensitive biomarker of disease activity and also as a biomarker of therapeutic response (Table 1). It can complement MRI and clinical evaluation in the process of diagnosis, but more studies are needed to verify the pathogenesis of CNTN-1 and its role in MS pathology.

## Chitinase-3-like protein 1 (CHI3L1)

Chitinase3-like protein1 (CHI3L1), a secretory glycoprotein, is one of the newly discovered markers of inflammation in recent years, which can mediate inflammation, macrophage polarization, apoptosis and carcinogenesis. But its physiological and pathophysiological role in the development of cancer and neurodegenerative diseases is still unclear. In human, CHI3L1 is also called chitin protein-40 (chitinaseprotein-40, YKL-40), based on its three N-terminal amino acids, tyrosine (Y), lysine (K) and leucine (L) (36). The relative molecular weight is about 40 kDa. It is a chitin-binding lectin and belongs to the glycosyl hydrolase family 18 (36). In CNS disorders, CHI3L1 is expressed in astrocytes and microglia/macrophages, mainly in active demyelinating areas. Levels of CHI3L1 in the CSF were reported to be increased during acute inflammation of demyelinating disease (37). Patients with SPMS and PPMS had significantly higher levels of CHI3L1 compared to RRMS and CIS in CSF and blood samples. Patients with RRMS were more likely to show high NfL with low CHI3L1 levels (38, 39). However, the expression of CHI3L1 in peripheral blood was affected by many factors, and the specificity for CNS disorders was lower compared to CHI3L1 in CSF. A number of studies have shown that CHI3L1 in CSF is helpful to distinguish the progressive MS and RRMS (38–40). The elevated level of CHI3L1 is a characteristic of progressive disease. In patients with RRMS, high level of CHI3L1 in CSF is an independent predictor of the deterioration of neurological dysfunction and the progression of the disease to SPMS. Therefore, CHI3L1 in CSF may predict the progression of RRMS (37–40). In addition, CHI3L1 has a good prognostic effect in the early MS and has the potential to become a therapeutic target in MS (38, 41).

## Kappa free light chain (KFLC)

Kappa chain (κ chain) is a kind of Ig molecular light chain (L chain), which is mainly produced in the sheath in the CNS. The light chain of Ig includes Kappa chain (κ chain) and Lambda chain (λ chain) (42). FLC in serum is mainly cleared by kidney, but this process does not exist in CSF. Thus quantitative detection of FLC

combined with blood-brain barrier function can reflect the synthesis of intrathecal Ig, which can be used in the diagnosis and prognosis of CSF inflammatory and infectious diseases (43). Electrophoresis is generally used to detect KLFC in CSF. Compared with oligoclonal band (OCB), CSF KFLC has higher sensitivity in the diagnosis of MS/CIS, and there is no significant loss of specificity. Studies have shown that the determination of CSF KFLC is a valuable quantitative substitute or supplement for the qualitative evaluation of OCB (43, 44). The total amount of intrathecal KFLC synthesis can distinguish MS myelitis from NMOSD myelitis. KFLC IF (intrathecal fraction) > 78% can distinguish myelitis caused by MS and NMOSD, with a sensitivity of 88.5% and a specificity of 88.9% (45). In addition, KFLC has high stability and has additional advantages over OCB, such as objectivity, easier standardization, faster speed, lower cost and so on (43, 44). However, steroids have a significant effect on KFLC levels (46), and further studies are needed to determine how much steroid treatment affects KFLC levels.

## KFLC index

KFLC index is a method for measuring the production of KFLC in the sheath. The index is obtained by linear modeling to calculate the concentration of KFLC in serum and CSF. The formula of KFLC index is: FLC index = $Q_{FLC}/Q_{alb}$ with $Q_{FLC}$ = CSF FLC/serum FLC and $Q_{alb}$ = CSF albumin/serum albumin (47). Similar to CSF KFLC, KFLC index is better than OCB in the diagnosis of MS and differentiation of MS and other inflammatory CNS disorders (44, 47, 48), so KFLC index may replace OCB as a first-line biomarker of MS in clinical practice. The early initiation of DMDs in MS is important to slow down progression in disability and cognitive impairment. KFLC index predicted the second clinical attack in patients with CIS in both space and time (47), and high KFLC index was an independent risk factor for early further attacks. In a prospective cohort study, a 10% increase in the KFLC index indicates an increase in the risk of a second clinical attack of about 13%. Patients with a high KFLC index (> 100) are twice as likely to have a second clinical attack within 12 months as those with a low KFLC index (49). Compared to OCB, KFLC index has methodological advantages in the diagnosis of MS and is independent of subjective interpretation (48). KFLC index may be not affected by DMT, demographic factors, clinical demyelination event types or MS phenotypes (47, 48). Young age, female sex and evidence of disease activity are independent factors associated with high KFLC index of MS (47). Current evidence suggests that the KFLC index is a reliable prognostic biomarker that may replace the OCB assay and bring us closer to the tailored drugs of MS.

## Anti-AQP4-Antibody (AQP4-IgG)

AQP4 is a widely expressed water channel mainly expressed in astrocytes of the CNS, especially in astrocytes involved in the formation of the blood-brain barrier (50). AQP4-IgG positive NMOSD is marked by the destruction of astrocytes (51). Current studies have shown that clinical, pathological and preclinical evidence consistently support the pathogenic role of AQP4-IgG in NMOSD. AQP4-IgG exists in up to 70% ~ 90% of NMOSD patients and is highly specific for the disease (52, 53).The titer of AQP4-IgG in serum is more than 500 times higher than that in CSF, so only patients with negative serum should be considered for CSF detection to improve sensitivity. The detection of AQP4-IgG in serum is necessary in the diagnostic criteria of the international expert group of NMOSD in 2015 (52). The laboratory method with the highest sensitivity and specificity for detecting AQP4-IgG is cell-based array (CBA) detection (54), with a sensitivity and specificity of 76% and 99%, respectively. However, limited evidence indicate that AQP4-IgG serum status cannot be used as a biomarker to predict disease activity and immunosuppressive drug response (52).

## Anti-MOG-Antibody (MOG-IgG)

Myelin oligodendrocyte glycoprotein (MOG) is usually found on the surface of mature oligodendrocyte and the myelin sheath of the CNS, and its expression begins in the late stage of myelin formation (53). It may play a structural role in microtubule stability, myelin fiber adhesion and response to inflammation. MOG-IgG usually belongs to IgG1 subclass. It can activate the complement cascade and determine the disorder of the cytoskeleton of oligodendrocytes, resulting in demyelination (52). At present, the best method to detect MOG-IgG is CBA. In the past 40 years, the pathogenicity of autoimmune response to MOG has been well confirmed (55). Acute disseminated encephalomyelitis (ADEM) is the most common clinical manifestation associated with anti-MOG antibodies. Anti-MOG antibody was only briefly observed in monophasic diseases such as ADEM, and its decrease was associated with a good prognosis, but persisted in polyphasic ADEM, NMOSD, relapsing optic neuritis or myelitis (56). The titer of MOG-IgG fluctuates during the clinical course of the disease and the level is higher in the acute attacks (57). However, the titer of MOG-IgG was not related to the risk of relapses or the final clinical outcome (58). In early studies, the lack of disease specificity was revealed by testing MOG-IgG at low titers in MS patients or other neurological diseases or even in healthy individuals (59). These observations suggest that MOG-IgG in the serum may bind to MOG and produce non-specific positive signals, or these antibodies may belong to the natural antibody class that is relatively common at low levels and will not be deleted by the B cell tolerance mechanism, but do not cause disease (59). Some studies have shown that MOG-IgG is associated with AQP4-IgG seronegative NMOSD. Compared with AQP4-IgG seropositive patients, MOG-IgG seropositive patients have a lower risk of further relapses and a better visual field prognosis (54). MOG-IgG is associated with clinical manifestations and younger age of onset of human inflammatory demyelinating diseases, with the highest incidence in pediatric patients (56, 59). The available evidence shows that MOG-IgG can be used as a prognostic biomarker of MOGAD (54).

## Autoimmune encephalitis associated antibody

Autoimmune encephalitis (AE) is characterized by the existence of autoantibodies that directly attack the protein in or on the surface of neurons, so the detection of protein-specific antibodies in CNS has changed our understanding of AE and our ability to make an accurate diagnosis (60). At present, the best method to detect these antibodies is CBA. These antibodies target important brain proteins, including neurotransmitter receptors, ion channels and related membrane proteins (60). They are specific for a definite diagonis of AE. For example, the only specific diagnostic test against N-methyl D-aspartate receptor (NMDAR) encephalitis is to prove the IgG autoantibodies targeting the GluN1 subunit of the NMDAR in CSF of patients (61). The antibody of anti-LGI1 encephalitis is IgG antibody targeting leucine-rich glioma-inactivated 1 (LGI1) protein (an extracellular component of the voltage-gated Kv1 potassium channel-complex) (62). This study has confirmed that IgG4 is the major subclass of LGI1-IgG, and a higher LGI1-IgG specific CSF index, that is, the index of intrathecal antibody synthesis, is related to the poor prognosis of patients with anti-LGI1 encephalitis (62). Autoimmune GFAP astrocytopathy is a meningoencephalitis associated with GFAP-specific IgG (63). GFAP-specific IgG can be used as a biomarker of recurrent autoimmune meningoencephalitis that responds to immunotherapy (64). Positive sGFAP specific IgG can distinguish autoimmune GFAP meningoencephalitis from other diseases (64). One of the types of AE that is difficult to diagnose is antibody-negative AE, because there is no definite antibody or known AE syndrome to explain this manifestation (65). In a cohort of children, antibody-negative AE was associated with poor cognitive outcomes compared with NMDAR encephalitis (66). The diagnosis of AE without antibody recognition is usually made without alternative diagnosis, such as neuroimaging, CSF analysis and electroencephalogram (EEG) (65). Recognition of the characteristic examinations in the limbic system of AE is an important clue to guide the diagnosis (67). Brain MRI may be normal, non-specific, or show multifocal T2/FLAIR high signal changes (68). EEG has no specific pattern association with most AE subtypes, except for the extreme delta brush pattern found in NMDAR encephalitis (69). EEG may help to distinguish organic and mental pathology (70). EEG may also serve as a biomarker of disease severity to guide treatment decisionmaking (70). CSF detection is very important because classical CSF analysis provides more timely information, such as CSF leukocyte count, total protein and OCB of CSF, which may support the diagnosis of AE (71). The presence of specific CSF and serum autoantibodies is extremely important for the final diagnosis of AE. CSF antibody detection is more sensitive and specific, so it is better than serum antibody detection (72).

## Cytokines

Cytokines and chemokines have multiple effects on many inflammatory cells, most of which have unique characteristics and are elevated in many neuroimmune diseases of the CNS. Therefore, cytokines and chemokines can be used as biomarkers for diagnosis of autoimmune disease and detection of intrathecal inflammation, which can be used to evaluate disease activity and to predict disease progression (73). Chemokine is a secretory protein that controls the transport and localization of leukocytes to the target organ (74). At present, ELISA is generally used to detect these biomarkers. Soluble inflammatory mediators have long been studied as appropriate biomarkers that can predict the process of MS (75). Some of these soluble markers are not disease specific, and the challenge of biomarker research is still lack of repeatability and sensitivity. However, some candidate biomarkers have been studied and need to be verified, and" omics "technology is developing rapidly, providing a basis for future research (76).

### IL-6

Interleukin-6 (IL-6) is considered to be an important cytokine in inflammatory diseases of the CNS. It has multiple functions and mediates many biological activities. It participates in acute inflammation by inducing the synthesis of acute phase proteins, so the increased concentration of IL-6 in CSF may represent a non-specific marker of inflammation in the CNS (77). In addition, IL-6 is also one of the B cell stimulating factors, which differentiate B cells into plasma cells and lead to the production of immunoglobulin (78). IL-6 is significantly increased in serum and CSF of NMOSD patients, which may play a variety of roles in the pathophysiology of NMOSD by promoting plasma cell survival, stimulating the production of anti-AQP4 antibody, destroying the integrity and function of blood-brain barrier and enhancing the differentiation and activation of pro-inflammatory T lymphocytes (79). Blocking IL-6 signal transduction with anti-IL-6 receptor monoclonal antibody tocilizumab is very effective for refractory NMOSD patients (80). The increased CSF IL-6 level at diagnosis is associated with increased recurrence and disability in RRMS patients during the 3-year follow-up (77). In addition, the ratio of IL2:IL6 in CSF may be a prognostic biomarker of early MS and may be helpful to predict the early relapsing activity of MS (81). CSF IL-6 can also be used as a biomarker to distinguish NMO from MS (82). Besides, the increase of serum IL-6 level in AE patients may indicate the persistent proinflammatory state of AE and may lead to poor prognosis (83). In anti-NMDAR encephalitis, with the increase of cytokines including IL-6, the clinical symptoms are aggravated (84). Therefore, IL-6 may be a new biomarker of anti-NMDAR encephalitis.

### IL-17A

Interleukin-17A (IL-17A) is an effective proinflammatory cytokine produced by Th17 cells and IL-17-secreting CD8+T cells (85). It promotes the pathophysiology of autoimmune diseases and may mediate delayed inflammation by inducing neutrophils and monocytes to recruit chemokines at inflammatory sites (85). A recent study has shown that IL-17 impairs myelin regeneration and promotes myelin damage through oligodendrocyte/myelin injury mediated by increasing voltage-gated K+ channel 1 (86). Some

researchers speculate that the level of IL-17A may increase in the early stage of MS inflammation, and the level of IL-17A will gradually decrease with the remission of inflammation, but this speculation still needs further study (87). IL-17A may regulate inflammatory immune response in NMOSD through PI3K-m TOR signaling pathway, and promote disease progression (88). The high expression of IL-17A in peripheral blood of patients with relapsing NMOSD suggests that it may be related to relapse (88). The concentration of pro-inflammatory IL-17A in CSF of AE patients increased and correlated with the severity of the disease at the time of onset (89). Therefore, IL-17A in CSF can be used to evaluate the short-term severity of AE patients and can lead to early immunosuppressive therapy (89).

### CXCL13

Chemokine (C-X-C motif) ligand 13 (CXCL13) is an effective B cell chemical attractor, which is essential for B cell migration and the development of B cell follicles and secondary lymphoid structures (73). CXCL13 is increased in patients with autoimmune diseases and is related to the disease severity, activity and prognosis (90). A meta-analysis shows that CSF CXCL13 and blood IL-23 levels in patients with MS are always different from those in healthy controls, and they may be used for diagnostic purposes (91). Increased concentration of CXCL13 was detected in blood, CSF and active demyelinating brain lesions in patients with MS (90). Notably, in patients with RRMS, CSF CXCL13 levels were associated with increased relapsing rates and disease severity measured by the EDSS (90). The level of CSF CXCL13 in MS patients decreased significantly after treatment (91). Therefore, CSF CXCL13 may be used in the diagnosis of MS in clinical practice, and may also become a biomarker of drug treatment response and disease progression of MS (91). Further research is needed to verify this. Besides, CXCL13 may also be a promising biomarker for the course of AE (82). For example, it has been shown that the increase of CSF CXCL13 in 70% of patients with early anti-NMDAR encephalitis is associated with intrathecal NMDAR antibody synthesis (82).

### Osteopontin

Osteopontin (OPN), also known as secreted phosphoprotein-1 (SPP1), is mainly released by endothelial cells, microglia, macrophages and dendritic cells in the brain (92). OPN mainly reflects the activation of innate immune system and promotes inflammation by increasing the production of IL-12, IL-17 and interferon-γ (IFN-γ) and inhibiting the expression of IL-10 (93). OPN tends to induce proinflammatory cytokines in NMOSD and MS (94). Plasma OPN levels in patients with NMOSD were higher than healthy controls, especially in the cases with attacks and severe disability (95). High levels of OPN can be detected in CSF, serum or plasma in patients with MS, indicating that the protein may be used as a biomarker for monitoring disease activity and progression (95). A meta-analysis showed that OPN levels in CSF and blood in patients with MS were significantly elevated, and OPN levels in CSF in active MS patients were significantly compared to non-active patients (93). OPN may play a harmful role in the development of MS (92) and is closely related to disease activity (92, 96). The levels of tumor necrosis factor and OPN in CSF of patients with early RRMS after dimethyl fumarate treatment are related to disease activity (96). Therefore, the combined detection with OPN and other markers can help clinicians make personalized treatment strategies. Moreover, OPN in CSF can predict the development of lesions and microstructural abnormalities within 10 years (97). The increase of OPN concentration in CSF indicates the enlargement of lateral and inferior ventricles in progressive MS, accompanied by changes in cortical and subcortical gray matter and white matter volume (94). Higher OPN levels in CSF indicate poor prognosis and long-term disease progression and are associated with the deterioration of the disease (94, 98). More and more evidence shows that OPN can be used as a biomarker for clinical diagnosis or prediction and prognosis.

### Combined detection of cytokines

The combined detection of these cytokines may be more helpful to the prediction and evaluation of diseases. Moreover, CSF CXCL13, CXCL8 and IL-12p40 can be used as biomarkers to predict the progression from CIS to MS (74). Increased concentrations of IL-6, IL-17 and CXCL13 are considered to be key factors in inducing the formation of NMO lesions (82). These molecules have been shown to be associated with the severity of NMO disease and EDSS scores (82). IL6, IL-17A, CXCL10 and CXCL13 in CSF can be used to detect inflammation in acute stage of AE (99). The elevated levels of cytokines such as CXCL-13, CXCL-10, IL-6 and IL-17A are related to the clinical severity of anti-NMDAR encephalitis (100). The levels of IFN- γ, IL-17, IL-12 and IL-23 in the CSF of AE patients with positive autoantibodies to cell surface protein are higher than those of AE patients with positive autoantibodies to intracellular antigens (101).

## Cell markers

### Memory B cells and plasma cells

The antigen presentation process not only activates autoreactive T cells, but also induces the proliferation of presenting B cells and their subsequent differentiation into memory B cells and antibody-producing plasma cells (102). At present, flow cytomety is generally used to detect cell markers. Memory B cells (CD19+/CD27+), as part of the secondary immune response, can rapidly produce immunoglobulins. Many studies indicate that CD19+/CD27+ memory B cells can be used as biomarkers for RTX treatment monitoring and retreatment in patients with NMOSD. Class-switched memory B-cells (CD19+/CD27+/IgM-/IgD-, SMB), an early regenerated memory B cell subset, may also be a sensitive biomarker of disease recurrence risk (103). By monitoring the memory B cells or SMB cells in peripheral blood mononuclear

cells, individualized RTX administration regimens for NMOSD patients can be made without losing the efficacy while reducing the cumulative dose and medical expenses of RTX (103–105). Plasma cells (PCs) represent the terminal differentiation from mature B cells and play a key role in effective short- and long-term humoral immunity by producing a large number of antigen-specific antibodies (106). A recent study shows that CSF plasmablasts can distinguish MS from other neurological diseases (107).

### Eomes+ Th cells

Recent studies found that cytotoxic CD4+T cells expressing Eomes (Eomes+ Th cells) may play an important role in the pathogenesis of SPMS and have the potential value of distinguishing biomarkers between SPMS and RRMS patients (Table 1) (108). Eomes+ Th cells from experimental autoimmune encephalomyelitis lesions and the blood of SPMS patients can release cytotoxic granzyme B and IFN- γ and up-regulate CD107a (also known as lysosomal associated membrane protein 1) (109, 110). Granzyme B released by Eomes+ Th cells binds and activates protease-activated receptor-1 on the surface of neurons and leads to neurodegeneration (109). Compared with healthy subjects and RRMS patients, Eomes+ Th cells in peripheral blood and CSF were significantly increased in SPMS patients (109). The detection of Eomes+ Th cells is of great value for SPMS diagnosis and prognosis monitoring. The accuracy of Eomes+ Th cell level as a biomarker to predict the risk of disease progression in SPMS patients was more than 80% (108). In addition, Eomes+ Th cells may also be a potential therapeutic target for SPMS patients (109).

## Conclusion

We have systematically reviewed the potential biomarkers of CNS autoimmune diseases. With the improvement of diagnostic methods, neurologists can make faster and more accurate diagnosis of CNS autoimmune diseases, so as to significantly improve the treatment response of patients and reduce the rate of disability. However, at present, many biomarkers cannot be used as independent markers in the clinical diagnosis and treatment of diseases, so the joint detection of biomarkers can better achieve the purpose of detection. Although the current research on biomarkers of CNS autoimmune diseases is very extensive, it is still not perfect and more in-depth research is needed.

## Author contributions

FZ and CZ contributed to the conception and design of the study. XG, JL, and CZ contributed to the supervision of the manuscript. XG and CZ edited the paper scientifically. All authors contributed to the article and approved the submitted version.

## Funding

The study was supported by the National Natural Science Foundation of China (grant no. 82171777 to CZ) and the Natural Science Foundation of Tianjin Province (grant no. 20JCJQJC00280 to CZ).

## Conflict of interest

The authors declare that the research was conducted in the absence of any commercial or financial relationships that could be construed as a potential conflict of interest.

## Publisher's note



## References

1. Khalil M, Teunissen CE, Otto M, Piehl F, Sormani MP, Gattringer T, et al. Neurofilaments as biomarkers in neurological disorders. *Nat Rev Neurol* (2018) 14:577–89. doi: 10.1038/s41582-018-0058-z

2. Rosengren LE, Karlsson JE, Karlsson JO, Persson LI, Wikkelso C. Patients with amyotrophic lateral sclerosis and other neurodegenerative diseases have increased levels of neurofilament protein in CSF. *J Neurochem* (1996) 67:2013–18. doi: 10.1046/j.1471-4159.1996.67052013.x

3. Lycke JN, Karlsson JE, Andersen O, Rosengren LE. Neurofilament protein in cerebrospinal fluid: A potential marker of activity in multiple sclerosis. *J Neurol Neurosurg Psychiatry* (1998) 64:402–04. doi: 10.1136/jnnp.64.3.402

4. Norgren N, Sundstrom P, Svenningsson A, Rosengren L, Stigbrand T, Gunnarsson M. Neurofilament and glial fibrillary acidic protein in multiple sclerosis. *Neurology* (2004) 63:1586–90. doi: 10.1212/01.wnl.0000142988.49341.d1

5. Teunissen CE, Iacobaeus E, Khademi M, Brundin L, Norgren N, Koel-Simmelink MJ, et al. Combination of CSF n-acetylaspartate and neurofilaments in multiple sclerosis. *Neurology* (2009) 72:1322–29. doi: 10.1212/WNL.0b013e3181a0fe3f

6. Khalil M, Enzinger C, Langkammer C, Ropele S, Mader A, Trentini A, et al. CSF neurofilament and n-acetylaspartate related brain changes in clinically isolated syndrome. *Mult Scler* (2013) 19:436–42. doi: 10.1177/1352458512458010

7. Arrambide G, Espejo C, Eixarch H, Villar LM, Alvarez-Cermeno JC, Picon C, et al. Neurofilament light chain level is a weak risk factor for the development of MS. *Neurology* (2016) 87:1076–84. doi: 10.1212/WNL.0000000000003085

8. Novakova L, Zetterberg H, Sundstrom P, Axelsson M, Khademi M, Gunnarsson M, et al. Monitoring disease activity in multiple sclerosis using serum neurofilament light protein. *Neurology* (2017) 89:2230–37. doi: 10.1212/WNL.0000000000004683

9. Bjornevik K, Munger KL, Cortese M, Barro C, Healy BC, Niebuhr DW, et al. Serum neurofilament light chain levels in patients with presymptomatic multiple sclerosis. *JAMA Neurol* (2020) 77:58–64. doi: 10.1001/jamaneurol.2019.3238

10. Canto E, Barro C, Zhao C, Caillier SJ, Michalak Z, Bove R, et al. Association between serum neurofilament light chain levels and long-term disease course among patients with multiple sclerosis followed up for 12 years. *JAMA Neurol* (2019) 76:1359–66. doi: 10.1001/jamaneurol.2019.2137

11. Salzer J, Svenningsson A, Sundstrom P. Neurofilament light as a prognostic marker in multiple sclerosis. *Mult Scler* (2010) 16:287–92. doi: 10.1177/1352458509359725

12. Dalla CG, Martinelli V, Sangalli F, Moiola L, Colombo B, Radaelli M, et al. Prognostic value of serum neurofilaments in patients with clinically isolated syndromes. *Neurology* (2019) 92:e733–41. doi: 10.1212/WNL.0000000000006902

13. Benkert P, Meier S, Schaedelin S, Manouchehrinia A, Yaldizli O, Maceski A, et al. Serum neurofilament light chain for individual prognostication of disease activity in people with multiple sclerosis: A retrospective modelling and validation study. *Lancet Neurol* (2022) 21:246–57. doi: 10.1016/S1474-4422(22)00009-6

14. Kaneko K, Sato DK, Nakashima I, Ogawa R, Akaishi T, Takai Y, et al. CSF cytokine profile in MOG-IgG+ neurological disease is similar to AQP4-IgG+ NMOSD but distinct from MS: A cross-sectional study and potential therapeutic implications. *J Neurol Neurosurg Psychiatry* (2018) 89:927–36. doi: 10.1136/jnnp-2018-317969

15. Barro C, Benkert P, Disanto G, Tsagkas C, Amann M, Naegelin Y, et al. Serum neurofilament as a predictor of disease worsening and brain and spinal cord atrophy in multiple sclerosis. *Brain* (2018) 141:2382–91. doi: 10.1093/brain/awy154

16. Uphaus T, Steffen F, Muthuraman M, Ripfel N, Fleischer V, Groppa S, et al. NfL predicts relapse-free progression in a longitudinal multiple sclerosis cohort study. *Ebiomedicine* (2021) 72:103590. doi: 10.1016/j.ebiom.2021.103590

17. Mariotto S, Ferrari S, Gastaldi M, Franciotta D, Sechi E, Capra R, et al. Neurofilament light chain serum levels reflect disease severity in MOG-ab associated disorders. *J Neurol Neurosurg Psychiatry* (2019) 90:1293–96. doi: 10.1136/jnnp-2018-320287

18. Wang J, Cui C, Lu Y, Chang Y, Wang Y, Li R, et al. Therapeutic response and possible biomarkers in acute attacks of neuromyelitis optica spectrum disorders: A prospective observational study. *Front Immunol* (2021) 12:720907. doi: 10.3389/fimmu.2021.720907

19. Disanto G, Barro C, Benkert P, Naegelin Y, Schädelin S, Giardiello A, et al. Serum neurofilament light: A biomarker of neuronal damage in multiple sclerosis. *Ann Neurol* (2017) 81:857–70. doi: 10.1002/ana.24954

20. Siller N, Kuhle J, Muthuraman M, Barro C, Uphaus T, Groppa S, et al. Serum neurofilament light chain is a biomarker of acute and chronic neuronal damage in early multiple sclerosis. *Mult Scler* (2019) 25:678–86. doi: 10.1177/1352458518765666

21. Jakimovski D, Kuhle J, Ramanathan M, Barro C, Tomic D, Hagemeier J, et al. Serum neurofilament light chain levels associations with gray matter pathology: a 5-year longitudinal study. *Ann Clin Transl Neurol* (2019) 6:1757–70. doi: 10.1002/acn3.50872

22. Tortorella C, Direnzo V, Ruggieri M, Zoccolella S, Mastrapasqua M, D'Onghia M, et al. Cerebrospinal fluid neurofilament light levels mark grey matter volume in clinically isolated syndrome suggestive of multiple sclerosis. *Mult Scler* (2018) 24:1039–45. doi: 10.1177/1352458517711774

23. Rosso M, Gonzalez CT, Healy BC, Saxena S, Paul A, Bjornevik K, et al. Temporal association of sNfL and gad-enhancing lesions in multiple sclerosis. *Ann Clin Transl Neurol* (2020) 7:945–55. doi: 10.1002/acn3.51060

24. Kaisey M, Lashgari G, Fert-Bober J, Ontaneda D, Solomon AJ, Sicotte NL. An update on diagnostic laboratory biomarkers for multiple sclerosis. *Curr Neurol Neurosci Rep* (2022) 22:675–88. doi: 10.1007/s11910-022-01227-1

25. Wang J, Liu J, Li R, Wang C. Research and progress on biomarkers of neuromyelitis optica spectrum disorders. *J Recept Signal Transduct Res* (2021) 41:417–24. doi: 10.1080/10799893.2020.1830109

26. Watanabe M, Nakamura Y, Michalak Z, Isobe N, Barro C, Leppert D, et al. Serum GFAP and neurofilament light as biomarkers of disease activity and disability in NMOSD. *Neurology* (2019) 93:e1299–311. doi: 10.1212/WNL.0000000000008160

27. Kuhle J, Maceski AM, Meinert R, Ludwig I, Hack T, Kappos L, et al. Data from: Plasma Neurofilament Light Chain and Glial Fibrillary Acidic Protein Levels Are Prognostic of Disability Worsening: A Biosignature That Helps Differentiating Active From Non-active SPMS (2580). (2021) Available at: https://n.neurology.org/content/96/15_Supplement/2580.

28. Sun M, Liu N, Xie Q, Li X, Sun J, Wang H, et al. A candidate biomarker of glial fibrillary acidic protein in CSF and blood in differentiating multiple sclerosis and its subtypes: A systematic review and meta-analysis. *Mult Scler Relat Disord* (2021) 51:102870. doi: 10.1016/j.msard.2021.102870

29. Schindler P, Grittner U, Oechtering J, Leppert D, Siebert N, Duchow AS, et al. Serum GFAP and NfL as disease severity and prognostic biomarkers in patients with aquaporin-4 antibody-positive neuromyelitis optica spectrum disorder. *J Neuroinflamm* (2021) 18. doi: 10.1186/s12974-021-02138-7

30. Aktas O, Smith MA, Rees WA, Bennett JL, She D, Katz E, et al. Serum glial fibrillary acidic protein: A neuromyelitis optica spectrum disorder biomarker. *Ann Neurol* (2021) 89:895–910. doi: 10.1002/ana.26067

31. Zhang TX, Chen JS, Du C, Zeng P, Zhang H, Wang X, et al. Longitudinal treatment responsiveness on plasma neurofilament light chain and glial fibrillary acidic protein levels in neuromyelitis optica spectrum disorder. *Ther Adv Neurol Disord* (2021) 14:91631256. doi: 10.1177/17562864211054952

32. Yang S, Zhang C, Zhang TX, Feng B, Jia D, Han S, et al. A real-world study of interleukin-6 receptor blockade in patients with neuromyelitis optica spectrum disorder. *J Neurol* (2022) 270:348–356. doi: 10.1007/s00415-022-11364-9

33. Chatterjee M, Schild D, Teunissen CE. Contactins in the central nervous system: role in health and disease. *Neural Regener Res* (2019) 14:206–16. doi: 10.4103/1673-5374.244776

34. Chatterjee M, Koel-Simmelink MJ, Verberk IM, Killestein J, Vrenken H, Enzinger C, et al. Contactin-1 and contactin-2 in cerebrospinal fluid as potential biomarkers for axonal domain dysfunction in multiple sclerosis. *Mult Scler J Exp Transl Clin* (2018) 4:1841727793. doi: 10.1177/2055217318819535

35. van Lierop ZY, Wieske L, Koel-Simmelink MJ, Chatterjee M, Dekker I, Leurs CE, et al. Serum contactin-1 as a biomarker of long-term disease progression in natalizumab-treated multiple sclerosis. *Mult Scler* (2022) 28:102–10. doi: 10.1177/13524585211010097

36. Mazur M, Zielinska A, Grzybowski MM, Olczak J, Fichna J. Chitinases and chitinase-like proteins as therapeutic targets in inflammatory diseases, with a special focus on inflammatory bowel diseases. *Int J Mol Sci* (2021) 22. doi: 10.3390/ijms22136966

37. Cubas-Nunez L, Gil-Perotin S, Castillo-Villalba J, Lopez V, Solis TL, Gasque-Rubio R, et al. Potential role of CHI3L1+ astrocytes in progression in MS. *Neurol Neuroimmunol Neuroinflamm* (2021) 8. doi: 10.1212/NXI.0000000000000972

38. Pinteac R, Montalban X, Comabella M. Chitinases and chitinase-like proteins as biomarkers in neurologic disorders. *Neurol Neuroimmunol Neuroinflamm* (2021) 8. doi: 10.1212/NXI.0000000000000921

39. Gil-Perotin S, Castillo-Villalba J, Cubas-Nunez L, Gasque R, Hervas D, Gomez-Mateu J, et al. Combined cerebrospinal fluid neurofilament light chain protein and chitinase-3 like-1 levels in defining disease course and prognosis in multiple sclerosis. *Front Neurol* (2019) 10:1008. doi: 10.3389/fneur.2019.01008

40. Schneider R, Bellenberg B, Gisevius B, Hirschberg S, Sankowski R, Prinz M, et al. Chitinase 3-like 1 and neurofilament light chain in CSF and CNS atrophy in MS. *Neurol Neuroimmunol Neuroinflamm* (2021) 8. doi: 10.1212/NXI.0000000000000906

41. Lucchini M, De Arcangelis V, Piro G, Nociti V, Bianco A, De Fino C, et al. CSF CXCL13 and chitinase 3-like-1 levels predict disease course in relapsing multiple sclerosis. *Mol Neurobiol* (2022) 60:36–50. doi: 10.1007/s12035-022-03060-6

42. Kaplan B, Livneh A, Sela BA. Immunoglobulin free light chain dimers in human diseases. *ScientificWorldJournal* (2011) 11:726–35. doi: 10.1100/tsw.2011.65

43. Saadeh RS, Ramos PA, Algeciras-Schimnich A, Flanagan EP, Pittock SJ, Willrich MA. An update on laboratory-based diagnostic biomarkers for multiple sclerosis and beyond. *Clin Chem* (2022) 68:1134–50. doi: 10.1093/clinchem/hvac061

44. Duell F, Evertsson B, Al NF, Sandin A, Olsson D, Olsson T, et al. Diagnostic accuracy of intrathecal kappa free light chains compared with OCBs in MS. *Neurol Neuroimmunol Neuroinflamm* (2020) 7. doi: 10.1212/NXI.0000000000000775

45. Susse M, Feistner F, Grothe M, Nauck M, Dressel A, Hannich MJ. Free light chains kappa can differentiate between myelitis and noninflammatory myelopathy. *Neurol Neuroimmunol Neuroinflamm* (2020) 7. doi: 10.1212/NXI.0000000000000892

46. Konen FF, Wurster U, Witte T, Jendretzky KF, Gingele S, Tumani H, et al. The impact of immunomodulatory treatment on kappa free light chains as biomarker in neuroinflammation. *Cells* (2020) 9. doi: 10.3390/cells9040842

47. Levraut M, Laurent-Chabalier S, Ayrignac X, Bigaut K, Rival M, Squalli S, et al. Kappa free light chain biomarkers are efficient for the diagnosis of multiple sclerosis: A Large multicenter cohort study. *Neurol Neuroimmunol Neuroinflamm* (2023) 10. doi: 10.1212/NXI.0000000000200049

48. Rosenstein I, Rasch S, Axelsson M, Novakova L, Blennow K, Zetterberg H, et al. Kappa free light chain index as a diagnostic biomarker in multiple sclerosis: A real-world investigation. *J Neurochem* (2021) 159:618–28. doi: 10.1111/jnc.15500

49. Berek K, Bsteh G, Auer M, Di Pauli F, Grams A, Milosavljevic D, et al. Kappa-free light chains in CSF predict early multiple sclerosis disease activity. *Neurol Neuroimmunol Neuroinflamm* (2021) 8. doi: 10.1212/NXI.0000000000001005

50. Weber MS, Derfuss T, Metz I, Bruck W. Defining distinct features of anti-MOG antibody associated central nervous system demyelination. *Ther Adv Neurol Disord* (2018) 11:1276983651. doi: 10.1177/1756286418762083

51. Bruscolini A, Sacchetti M, La Cava M, Gharbiya M, Ralli M, Lambiase A, et al. Diagnosis and management of neuromyelitis optica spectrum disorders - an update. *Autoimmun Rev* (2018) 17:195–200. doi: 10.1016/j.autrev.2018.01.001

52. Rocca MA, Cacciaguerra L, Filippi M. Moving beyond anti-aquaporin-4 antibodies: emerging biomarkers in the spectrum of neuromyelitis optica. *Expert Rev Neurother* (2020) 20:601–18. doi: 10.1080/14737175.2020.1764352

53. Fiala C, Rotstein D, Pasic MD. Pathobiology, diagnosis, and current biomarkers in neuromyelitis optica spectrum disorders. *J Appl Lab Med* (2022) 7:305–10. doi: 10.1093/jalm/jfab150

54. Boziki M, Sintila S, Ioannidis P, Grigoriadis N. Biomarkers in rare demyelinating disease of the central nervous system. *Int J Mol Sci* (2020) 21:8409. doi: 10.3390/ijms21218409

55. Marignier R, Hacohen Y, Cobo-Calvo A, Probstel AK, Aktas O, Alexopoulos H, et al. Myelin-oligodendrocyte glycoprotein antibody-associated disease. *Lancet Neurol* (2021) 20:762–72. doi: 10.1016/S1474-4422(21)00218-0

56. Peschl P, Bradl M, Hoftberger R, Berger T, Reindl M. Myelin oligodendrocyte glycoprotein: Deciphering a target in inflammatory demyelinating diseases. *Front Immunol* (2017) 8:529. doi: 10.3389/fimmu.2017.00529

57. Tea F, Lopez JA, Ramanathan S, Merheb V, Lee FXZ, Zou A, et al. Characterization of the human myelin oligodendrocyte glycoprotein antibody response in demyelination. *Acta Neuropathol Commun* (2019) 7. doi: 10.1186/s40478-019-0786-3

58. Cobo-Calvo A, Sepúlveda M D, Indy H, Armangué T, Ruiz A, Maillart E, et al. Usefulness of MOG-antibody titres at first episode to predict the future clinical course in adults. *J Neurol* (2019) 266:806–15. doi: 10.1007/s00415-018-9160-9

59. Reindl M, Waters P. Myelin oligodendrocyte glycoprotein antibodies in neurological disease. *Nat Rev Neurol* (2019) 15:89–102. doi: 10.1038/s41582-018-0112-x

60. Lancaster E. Autoantibody encephalitis: Presentation, diagnosis, and management. *J Clin Neurol* (2022) 18:373–90. doi: 10.3988/jcn.2022.18.4.373

61. Dalmau J, Armangué T, Planagumà J, Radosevic M, Mannara F, Leypoldt F, et al. An update on anti-NMDA receptor encephalitis for neurologists and psychiatrists: mechanisms and models. *Lancet Neurol* (2019) 18:1045–57. doi: 10.1016/S1474-4422(19)30244-3

62. Gadoth A, Zekeridou A, Klein CJ, Thoreson CJ, Majed M, Dubey D, et al. Elevated LGI1-IgG CSF index predicts worse neurological outcome. *Ann Clin Transl Neurol* (2018) 5:646–50. doi: 10.1002/acn3.561

63. Shan F, Long Y, Qiu W. Autoimmune glial fibrillary acidic protein astrocytopathy: A review of the literature. *Front Immunol* (2018) 9:2802. doi: 10.3389/fimmu.2018.02802

64. Fang B, McKeon A, Hinson SR, Kryzer TJ, Pittock SJ, Aksamit AJ, et al. Autoimmune glial fibrillary acidic protein astrocytopathy: A novel meningoencephalomyelitis. *JAMA Neurol* (2016) 73:1297–307. doi: 10.1001/jamaneurol.2016.2549

65. Hardy D. Autoimmune encephalitis in children. *Pediatr Neurol* (2022) 132:56–66. doi: 10.1016/j.pediatrneurol.2022.05.004

66. Gadian J, Eyre M, Konstantoulaki E, Almoyan A, Absoud M, Garrood I, et al. Neurological and cognitive outcomes after antibody-negative autoimmune encephalitis in children. *Dev Med Child Neurol* (2022) 64:649–53. doi: 10.1111/dmcn.15101

67. Kelley BP, Patel SC, Marin HL, Corrigan JJ, Mitsias PD, Griffith B. Autoimmune encephalitis: Pathophysiology and imaging review of an overlooked diagnosis. *Ajnr Am J Neuroradiol* (2017) 38:1070–78. doi: 10.3174/ajnr.A5086

68. Wu H, Yu H, Joseph J, Jaiswal S, Pasham SR, Sriwastava S. Neuroimaging and CSF findings in patients with autoimmune encephalitis: A report of eight cases in a single academic center. *Neurol Int* (2022) 14:176–85. doi: 10.3390/neurolint14010014

69. Moise AM, Karakis I, Herlopian A, Dhakar M, Hirsch LJ, Cotsonis G, et al. Continuous EEG findings in autoimmune encephalitis. *J Clin Neurophysiol* (2021) 38:124–29. doi: 10.1097/WNP.0000000000000654

70. Gillinder L, Warren N, Hartel G, Dionisio S, O'Gorman C. EEG Findings in NMDA encephalitis - a systematic review. *Seizure* (2019) 65:20–4. doi: 10.1016/j.seizure.2018.12.015

71. Blinder T, Lewerenz J. Cerebrospinal fluid findings in patients with autoimmune encephalitis-a systematic analysis. *Front Neurol* (2019) 10:804. doi: 10.3389/fneur.2019.00804

72. Liang C, Chu E, Kuoy E, Soun JE. Autoimmune-mediated encephalitis and mimics: A neuroimaging review. *J Neuroimaging* (2023) 33:19–34. doi: 10.1111/jon.13060

73. Barizzone N, Leone M, Pizzino A, Kockum I, Martinelli-Boneschi F, D'Alfonso S. A scoping review on body fluid biomarkers for prognosis and disease activity in patients with multiple sclerosis. *J Pers Med* (2022) 12. doi: 10.3390/jpm12091430

74. Pranzatelli MR. Advances in biomarker-guided therapy for pediatric- and adult-onset neuroinflammatory disorders: Targeting Chemokines/Cytokines. *Front Immunol* (2018) 9:557. doi: 10.3389/fimmu.2018.00557

75. Stampanoni BM, Iezzi E, Landi D, Monteleone F, Gilio L, Simonelli I, et al. Delayed treatment of MS is associated with high CSF levels of IL-6 and IL-8 and worse future disease course. *J Neurol* (2018) 265:2540–47. doi: 10.1007/s00415-018-8994-5

76. Nociti V, Romozzi M, Mirabella M. Update on multiple sclerosis molecular biomarkers to monitor treatment effects. *J Pers Med* (2022) 12. doi: 10.3390/jpm12040549

77. Stampanoni BM, Iezzi E, Drulovic J, Pekmezovic T, Gilio L, Furlan R, et al. IL-6 in the cerebrospinal fluid signals disease activity in multiple sclerosis. *Front Cell Neurosci* (2020) 14:120. doi: 10.3389/fncel.2020.00120

78. Ashtari F, Madanian R, Shaygannejad V, Zarkesh SH, Ghadimi K. Serum levels of IL-6 and IL-17 in multiple sclerosis, neuromyelitis optica patients and healthy subjects. *Int J Physiol Pathophysiol Pharmacol* (2019) 11:267–73.

79. Fujihara K, Bennett JL, de Seze J, Haramura M, Kleiter I, Weinshenker BG, et al. Interleukin-6 in neuromyelitis optica spectrum disorder pathophysiology. *Neurol Neuroimmunol Neuroinflamm* (2020) 7. doi: 10.1212/NXI.0000000000000841

80. Yamamura T, Araki M. [Use of tocilizumab, an antibody against interleukin-6 receptor, for the treatment of neuromyelitis optica]. *Brain Nerve* (2014) 66:1159–65. doi: 10.11477/mf.1416200004

81. Petržalka M, Meluzínová E, Libertínová J, Mojžišová H, Hanzalová J, Ročková P, et al. IL-2, IL-6 and chitinase 3-like 2 might predict early relapse activity in multiple sclerosis. *PloS One* (2022) 17:e270607. doi: 10.1371/journal.pone.0270607

82. Kothur K, Wienholt L, Brilot F, Dale RC. CSF cytokines/chemokines as biomarkers in neuroinflammatory CNS disorders: A systematic review. *Cytokine* (2016) 77:227–37. doi: 10.1016/j.cyto.2015.10.001

83. Wesselingh R, Griffith S, Broadley J, Tarlinton D, Buzzard K, Seneviratne U, et al. Peripheral monocytes and soluble biomarkers in autoimmune encephalitis. *J Autoimmun* (2023) 135:103000. doi: 10.1016/j.jaut.2023.103000

84. Liu J, Liu L, Kang W, Peng G, Yu D, Ma Q, et al. Cytokines/Chemokines: Potential biomarkers for non-paraneoplastic anti-N-Methyl-D-Aspartate receptor encephalitis. *Front Neurol* (2020) 11:582296. doi: 10.3389/fneur.2020.582296

85. Maciak K, Pietrasik S, Dziedzic A, Redlicka J, Saluk-Bijak J, Bijak M, et al. Th17-related cytokines as potential discriminatory markers between neuromyelitis optica (Devic's disease) and multiple sclerosis-a review. *Int J Mol Sci* (2021) 22. doi: 10.3390/ijms22168946

86. Liu H, Yang X, Yang J, Yuan Y, Wang Y, Zhang R, et al. IL-17 inhibits oligodendrocyte progenitor cell proliferation and differentiation by increasing k(+) channel Kv1.3. *Front Cell Neurosci* (2021) 15:679413. doi: 10.3389/fncel.2021.679413

87. Li M, Chen H, Yin P, Song J, Jiang F, Tang Z, et al. Identification and clinical validation of key extracellular proteins as the potential biomarkers in relapsing-remitting multiple sclerosis. *Front Immunol* (2021) 12:753929. doi: 10.3389/fimmu.2021.753929

88. Guo HL, Shen XR, Liang XT, Li LZ. The role of autophagy-related proteins in the pathogenesis of neuromyelitis optica spectrum disorders. *Bioengineered* (2022) 13:14329–38. doi: 10.1080/21655979.2022.2084273

89. Levraut M, Bourg V, Capet N, Delourme A, Honnorat J, Thomas P, et al. Cerebrospinal fluid IL-17A could predict acute disease severity in non-NMDA-Receptor autoimmune encephalitis. *Front Immunol* (2021) 12:673021. doi: 10.3389/fimmu.2021.673021

90. Pan Z, Zhu T, Liu Y, Zhang N. Role of the CXCL13/CXCR5 axis in autoimmune diseases. *Front Immunol* (2022) 13:850998. doi: 10.3389/fimmu.2022.850998

91. Bai Z, Chen D, Wang L, Zhao Y, Liu T, Yu Y, et al. Cerebrospinal fluid and blood cytokines as biomarkers for multiple sclerosis: A systematic review and meta-analysis of 226 studies with 13,526 multiple sclerosis patients. *Front Neurosci* (2019) 13:1026. doi: 10.3389/fnins.2019.01026

92. Marastoni D, Magliozzi R, Bolzan A, Pisani AI, Rossi S, Crescenzo F, et al. CSF levels of CXCL12 and osteopontin as early markers of primary progressive multiple sclerosis. *Neurol Neuroimmunol Neuroinflamm* (2021) 8. doi: 10.1212/NXI.0000000000001083

93. Agah E, Zardoui A, Saghazadeh A, Ahmadi M, Tafakhori A, Rezaei N. Osteopontin (OPN) as a CSF and blood biomarker for multiple sclerosis: A systematic review and meta-analysis. *PloS One* (2018) 13:e190252. doi: 10.1371/journal.pone.0190252

94. Orsi G, Hayden Z, Cseh T, Berki T, Illes Z. Osteopontin levels are associated with late-time lower regional brain volumes in multiple sclerosis. *Sci Rep* (2021) 11. doi: 10.1038/s41598-021-03173-3

95. Cappellano G, Vecchio D, Magistrelli L, Clemente N, Raineri D, Barbero MC, et al. The yin-yang of osteopontin in nervous system diseases: damage versus repair. *Neural Regener Res* (2021) 16:1131–37. doi: 10.4103/1673-5374.300328

96. Marastoni D, Pisani AI, Schiavi G, Mazziotti V, Castellaro M, Tamanti A, et al. CSF TNF and osteopontin levels correlate with the response to dimethyl fumarate in early multiple sclerosis. *Ther Adv Neurol Disord* (2022) 15:81594084. doi: 10.1177/17562864221092124

97. Orsi G, Cseh T, Hayden Z, Perlaki G, Nagy SA, Giyab O, et al. Microstructural and functional brain abnormalities in multiple sclerosis predicted by osteopontin and neurofilament light. *Mult Scler Relat Disord* (2021) 51:102923. doi: 10.1016/j.msard.2021.102923

98. Yim A, Smith C, Brown AM. Osteopontin/secreted phosphoprotein-1 harnesses glial-, immune-, and neuronal cell ligand-receptor interactions to sense and regulate acute and chronic neuroinflammation. *Immunol Rev* (2022) 311:224–33. doi: 10.1111/imr.13081

99. Zhang S, Mao C, Li X, Miao W, Teng J. Advances in potential cerebrospinal fluid biomarkers for autoimmune encephalitis: A review. *Front Neurol* (2022) 13:746653. doi: 10.3389/fneur.2022.746653

100. Ciano-Petersen NL, Cabezudo-García P, Muñiz-Castrillo S, Honnorat J, Serrano-Castro PJ, Oliver-Martos B. Current status of biomarkers in anti-N-Methyl-D-Aspartate receptor encephalitis. *Int J Mol Sci* (2021) 22. doi: 10.3390/ijms222313127

101. Soltani KA, Pahlevan-Fallahy MT, Shobeiri P, Teixeira AL, Rezaei N. Cytokines and chemokines profile in encephalitis patients: A meta-analysis. *PloS One* (2022) 17:e273920. doi: 10.1371/journal.pone.0273920

102. Häusser-Kinzel S, Weber MS. The role of b cells and antibodies in multiple sclerosis, neuromyelitis optica, and related disorders. *Front Immunol* (2019) 10:201. doi: 10.3389/fimmu.2019.00201

103. Trewin BP, Adelstein S, Spies JM, Beadnall HN, Barton J, Ho N, et al. Precision therapy for neuromyelitis optica spectrum disorder: A retrospective analysis of the use of class-switched memory b-cells for individualised rituximab dosing schedules. *Mult Scler Relat Disord* (2020) 43:102175. doi: 10.1016/j.msard.2020.102175

104. Cohen M, Romero G, Bas J, Ticchioni M, Rosenthal M, Lacroix R, et al. Monitoring CD27+ memory b-cells in neuromyelitis optica spectrum disorders patients treated with rituximab: Results from a bicentric study. *J Neurol Sci* (2017) 373:335–38. doi: 10.1016/j.jns.2017.01.025

105. Lebrun C, Cohen M, Rosenthal-Allieri MA, Bresch S, Benzaken S, Marignier R, et al. Only follow-up of memory b cells helps monitor rituximab administration to patients with neuromyelitis optica spectrum disorders. *Neurol Ther* (2018) 7:373–83. doi: 10.1007/s40120-018-0101-4

106. Wang AA, Gommerman JL, Rojas OL. Plasma cells: From cytokine production to regulation in experimental autoimmune encephalomyelitis. *J Mol Biol* (2021) 433:166655. doi: 10.1016/j.jmb.2020.09.014

107. Kister I, Lotan I, Wallach A, Bacon T, Cutter G, Arbini A. CSF plasmablasts differentiate MS from other neurologic disorders. *Mult Scler Relat Disord* (2021) 48:102719. doi: 10.1016/j.msard.2020.102719

108. Raveney B, Sato W, Takewaki D, Zhang C, Kanazawa T, Lin Y, et al. Involvement of cytotoxic eomes-expressing CD4(+) T cells in secondary progressive multiple sclerosis. *Proc Natl Acad Sci U S* (2021) 118. doi: 10.1073/pnas.2021818118

109. Raveney BJ, Oki S, Hohjoh H, Nakamura M, Sato W, Murata M, et al. Eomesodermin-expressing T-helper cells are essential for chronic neuroinflammation. *Nat Commun* (2015) 6:8437. doi: 10.1038/ncomms9437

110. Oki S. Eomes-expressing T-helper cells as potential target of therapy in chronic neuroinflammation. *Neurochem Int* (2019) 130:104348. doi: 10.1016/j.neuint.2018.11.023

frontiers | Frontiers in Immunology

TYPE Original Research
PUBLISHED 04 May 2023
DOI 10.3389/fimmu.2023.1110672



OPEN ACCESS

EDITED BY
Honghao Wang,
Guangzhou First People's Hospital, China

REVIEWED BY
Sheng Chen,
Shanghai Jiao Tong University, China
Jinzhou Feng,
First Affiliated Hospital of Chongqing Medical University, China

*CORRESPONDENCE
Guang-Zhi Liu
guangzhi2002@hotmail.com

†These authors have contributed equally to this work

RECEIVED 29 November 2022
ACCEPTED 24 April 2023
PUBLISHED 04 May 2023

CITATION
Liu P-J, Yang T-T, Fan Z-X, Yuan G-B, Ma L, Wang Z-Y, Lu J-F, Yuan B-Y, Zou W-L, Zhang X-H and Liu G-Z (2023) Characterization of antigen-specific CD8+ memory T cell subsets in peripheral blood of patients with multiple sclerosis. *Front. Immunol.* 14:1110672. doi: 10.3389/fimmu.2023.1110672



# Characterization of antigen-specific CD8+ memory T cell subsets in peripheral blood of patients with multiple sclerosis

Pen-Ju Liu[1†], Ting-Ting Yang[1†], Ze-Xin Fan[1], Guo-Bin Yuan[1], Lin Ma[1], Ze-Yi Wang[1], Jian-Feng Lu[1], Bo-Yi Yuan[1], Wen-Long Zou[1], Xing-Hu Zhang[2] and Guang-Zhi Liu[1*]

[1]Department of Neurology, Beijing Anzhen Hospital, Capital Medical University,, Beijing, China, [2]Department of Neurology, Beijing Tiantan Hospital, Capital Medical University, Beijing, China

**Background:** Increasing evidence indicates the importance of $CD8^+$ T cells in autoimmune attack against CNS myelin and axon in multiple sclerosis (MS). Previous research has also discovered that myelin-reactive T cells have memory phenotype functions in MS patients. However, limited evidence is available regarding the role of $CD8^+$ memory T cell subsets in MS. This study aimed to explore potential antigen-specific memory T cell-related biomarkers and their association with disease activity.

**Methods:** The myelin oligodendrocyte glycoprotein (MOG)-specific $CD8^+$ memory T cell subsets and their related cytokines (perforin, granzyme B, interferon (IFN)-γ) and negative co-stimulatory molecules (programmed cell death protein 1 (PD-1), T- cell Ig and mucin domain 3 (Tim-3)) were analyzed by flow cytometry and real-time PCR in peripheral blood of patients with relapsing-remitting MS.

**Results:** We found that MS patients had elevated frequency of MOG-specific $CD8^+$ T cells, MOG-specific central memory T cells ($T_{CM}$), MOG-specific $CD8^+$ effector memory T cells ($T_{EM}$), and MOG-specific $CD8^+$ terminally differentiated cells ($T_{EMRA}$); elevated granzyme B expression on MOG-specific $CD8^+$ $T_{CM}$; and, on MOG-specific $CD8^+$ $T_{EM}$, elevated granzyme B and reduced PD-1 expression. The Expanded Disability Status Scale score (EDSS) in MS patients was correlated with the frequency of MOG-specific $CD8^+$ $T_{CM}$, granzyme B expression in $CD8^+$ $T_{CM}$, and granzyme B and perforin expression on $CD8^+$ $T_{EM}$, but with reduced PD-1 expression on $CD8^+$ $T_{EM}$.

**Conclusion:** The dysregulation of antigen-specific $CD8^+$ memory T cell subsets, along with the abnormal expression of their related cytokines and negative co-stimulatory molecules, may reflect an excessive or persistent inflammatory response induced during early stages of the illness. Our findings strongly suggest positive regulatory roles for memory T cell populations in MS pathogenesis, probably *via* molecular mimicry to trigger or promote abnormal peripheral immune responses. Furthermore, downregulated PD-1 expression may stimulate a positive feedback effect, promoting MS-related inflammatory

10.3389/fimmu.2023.1110672

responses *via* the interaction of PD-1 ligands. Therefore, these parameters are potential serological biomarkers for predicting disease development in MS.

KEYWORDS

multiple sclerosis, peripheral blood mononuclear cells, memory T cells, oligodendrocyte glycoprotein, pentamer

# Introduction

Multiple sclerosis (MS) is a chronic inflammatory demyelinating disease of the central nervous system (CNS). The disease frequently has a relapsing-remitting course and, in the later phases, tends to cause irreparable and severe neurological disability. Although its etiology remains uncertain, it is widely speculated that autoreactive T cell responses directed against CNS myelin are responsible for its pathogenesis (1). Importantly, several studies have found that MS patients have different memory phenotypes of myelin-reactive T cells.

Conventional $CD4^+$ and $CD8^+$ memory T cells can be divided into $CCR7^+CD45RA^-$ central memory T cells ($T_{CM}$), $CCR7^-CD45RA^-$ effector memory T cells ($T_{EM}$), and $CD45RA^+CCR7^-$ terminally differentiated cells ($T_{EMRA}$), with district homing and effector properties (2–4). $T_{CM}$ and naïve cells home to secondary lymphoid tissues in physiological circumstances, whereas $T_{EM}$ and $T_{EMRA}$ traffick to non-lymphoid organs that are inflamed and exert effects such as stimulating interferon (IFN)-γ secretion and causing potent cytotoxicities. $T_{CM}$, in contrast, are longer-lived with a greater proliferative capacity (5, 6).

Mounting evidence indicates that $CD8^+$ T cells have a significant role in autoimmune CNS attack in MS. $CD8^+$ T cells are accumulated in white matter lesions. These cells frequently outnumber $CD4^+$ T cells at this location, and are in a quiet neibourhood close to oligodendrocytes and demyelinated CNS axons (7–9), the latter of which are believed to produce early neurological symptoms (10). $CD8^+$ T cells are present in immune cell infiltrates in the early phases of MS cortical demyelinating lesions (11). Strikingly, $CD8^+$ T cells with an effector-memory phenotype have been found to accumulate in the MS lesions, exhibiting inflammatory and cytotoxic potential due to enhanced expression of granzyme B and interferon (IFN)-γ (12, 13). In parallel with these findings, we previously reported that MS patients display elevated $CD8^+CCR7^+CD45RA^-$ $T_{CM}$, which tends to decrease after treatment with the immunomodulatory agent IFN-β1α (14). Together, these findings strongly suggest that a skewed distribution of autoreactive $CD8^+$ memory T-cell subsets is involved in the disease pathogenesis, given that an increased frequency of circulating $CD4^+$ $T_{EM}$ has been demonstrated in MS patients after specific antigen-driven stimulation. Notably, human leucocyte antigen (HLA)-A*03:01 is associated with about a two-fold increase in risk of developing MS—independent of HLA-DR2 (15–17).

However, further research is still required to understand the distribution of memory T-cell subsets in the illness and the potential contribution of abnormal T-cell homeostasis to the pathophysiology of inflammation. Thus, we analyzed circulating antigen-specific memory T-cell subsets using the pentamer, HLA-A*03:01-RVVHLYRNGK (myelin oligodendrocyte glycoprotein $(MOG)_{46\text{-}55}$ peptide) and its related cytokines, to determine if these cell populations are correlated with disease activity.

**Abbreviations:** AUC, area under the receiver operating characteristic curve; CNS, central nervous system; EDSS, Expanded Disability Status Scale; HC, healthy controls; IFN, interferon; MOG, myelin oligodendrocyte glycoprotein; MS, multiple sclerosis; OND, other neurological disease; PBMC, peripheral blood mononuclear cells; PD-1, programmed cell death protein 1; PCR, polymerase chain reaction; ROC, receiver operating characteristic; RRMS, relapsing-remitting multiple sclerosis; $T_{CM}$, central memory T cells; $T_{EM}$, effector memory T cells; $T_{EMRA}$, terminally differentiated cells; Tim-3, T- cell Ig and mucin domain 3.

# Patients and methods

## Subjects

Twenty-four patients with definite MS (five men and 19 women; mean age 35.2 ± 5.3 years) were included. All patients experienced relapsing-remitting MS (RRMS) and had never been using immunosuppressive medications, including glucocorticosteroids, for more than 6 months prior to the study. Five of these RRMS patients were chosen for serial examination while receiving treatment with teriflunomide (Aubagio®, Sanofi, Paris, France). Patients underwent clinical neurological examination including expanded disability status scale (EDSS), blood sampling before and after 2 and 4 weeks of treatment (18).

Twenty-three patients with atherothrombotic stroke (6 men and 17 women; mean age 36.7 ± 5.9 years) were recruited as "other neurological diseases" (OND) controls. Twenty-four healthy individuals participated as the healthy controls ("HC", six men and 18 women; mean age 35.0 ± 6.5 years). All participating subjects were Han Chinese and tested positive for the A3 allele *via* HLA-A genotyping using polymerase chain reaction (PCR) sequence-specific primers (PCR-SSP). At the Department of Clinical Chemistry, whole blood cell counts and leucocyte differential analysis, were measured for patients and HC.

## Sample collection

Blood samples that had been heparinized were gathered between 9 and 12 AM. Blood samples from teriflunomide-treated individuals were taken before, and after 2 and 4 weeks of therapy as part of a serial trial.

## FACS-isolation of antigen-specific CD8$^+$ memory T-cell subsets

To examine the expression of multiple cytokines (perforin, granzyme B, IFN-γ) and checkpoint receptor members ((programmed cell death protein 1 (PD-1) and T-cell Ig and mucin domain 3 (Tim-3)) in the antigen-specific CD8$^+$ memory T-cell subsets, PBMCs were isolated by density gradient centrifugation and resuspended in phosphate buffer saline (PBS) containing 2% fetal calf serum. Thereafter, CD8$^+$ $T_{CM}$, $T_{EM}$, and $T_{EMRA}$ were isolated with allophycocyanin (APC)-labelled Pro5MHC Pentamer [HLA-A*03:01 $MOG_{46-55}$ pentamers-RVVHLYRNGK] (Proimmune, Oxford, UK), phycoerythrin (PE)-cy7-labelled anti-CCR7 (eBioscience, San Diego, CA), APC-cy7-labelled anti-CD8 (BD Pharmingen, San Diego, CA, USA), and peridinin chlorophyll protein (PerCP)-Cy5.5-labelled-anti-CD45RA (Tonbo Biosciences, San Diego, CA) monoclonal antibody (MoAb) *via* a flow sorter (Becton Dickinson, San Jose, CA, USA).

## Flow cytometry

Antigen-specific CD8$^+$ memory T-cell subsets were characterized in peripheral blood mononuclear cells (PBMCs) of the patients and controls by assessing PD-1 and Tim-3 expression *via* four-color direct fluorescence staining and flow cytometry using a FACScan (BD Biosciences, San Jose, CA, USA). After washing with PBS (0.5% BSA, pH 7.2), the cells were resuspended in PBS, to a final concentration of $1 \times 10^6$ cells/mL. The following MoAb were added to $1 \times 10^6$ cells following the manufacturer's instructions: APC-cy7-labelled CD8; APC-labelled Pro5 MHC Pentamer [HLA-A*03:01 $MOG_{46-55}$ pentamers-RVVHLYRNGK]; PE-cy7-labelled anti-CCR7; PerCP-Cyanine5.5-labelled-anti-CD45RA, Super Bright (SB)645-labelled anti-PD-1 (Thermo Fisher Scientific, Waltham, MA, USA); SB600-labelled anti-Tim-3 (Thermo Fisher Scientific). After 30-min incubation at room temperature, the cells were washed with PBS, fixed with 1% paraformaldehyde, and finally analyzed using a FACScan.

To perform intracellular cytokine staining, $1 \times 10^6$ cells were incubated with the Cell Stimulation Cocktail (Tonbo Bioscience) for 4–5 h at 37°C in complete RPMI. Intracellular staining with eFluor 450-labelled anti-perforin (Thermo Fisher Scientific), Brilliant Violet (BV)510-labelled anti-granzyme B (BD Biosciences), and BV711-labelled anti-IFN-γ (BD Biosciences) MoAbs was completed following fixation/permeabilization according the manufacturer's instructions (Cytofix/Cytoperm, BD Biosciences).

## RNA preparation and cDNA synthesis

RNA isolation was performed using RNeasy® Mini Kit (Qiagen, Hilden, Germany), according to standard protocol. Reverse transcription was conducted with HiScript III 1st Strand cDNA Synthesis Kit (Nanjing Vazyme Biotech Co. Nanjing, China) using random hexamers and primer containing 50 μM oligio (dt). The process was carried out at 25°C for 10 min, 48°C for 30 min, and 95°C for 5 min on a T100 PCR system (Bio-Rad Laboratories, Hercules, CA, USA).

## Real-time PCR

Perforin, granzyme B, IFN-γ, PD-1, and Tim-3 mRNA were quantified using cDNA-specific primers (Sangon Biotec, Shanghai, China) as described elsewhere (Table 1) (19, 20). Twenty-five nanograms of cDNA and 200 nM forward and reverse primers were added to the PCR reactions using the AceQ Universal SYBR qPCR Master Mix (Nanjing Vazyme Biotech, Nanjing, China). β-Actin was chosen as the endogenous control. Real-time PCR was conducted using an ABI PRISM 7500 sequencing detector (Applied Biosystems, Foster City, CA, USA). Perforin, granzyme B, IFN- γ, PD-1, Tim-3, and 18 S PCR conditions were: hold at 50°C for 90 s, then 95°C for 10 min, followed by 40 cycles at 95°C for 15 s, 60°C for 1 min, and 72°C for 45 s.

## Statistics

Age, disease course, EDSS, and blood leukocyte count data are shown as means ± standard deviation. Memory T-cell subsets, surface and intracellular expression of cytokines, PD-1, and Tim-

TABLE 1 Primers used in the study.

| Gene | Sense primer (5′-3′) | Antisense primer (5′-3′) |
|---|---|---|
| Perforin | GCAATGTGCATGTGTCTGTG | TTACCCAGGCTGAGTACTGCT |
| Interferon-γ | GCATCGTTTTGGGTTCTCTTGGCTGTTACTGC | CTCCTTTTTCGCTTCCCTGTTTTAGCTGCTGG |
| Granzyme B | GGGGAAGCTCCATAAATGTCACCT | TACACACAAGAAGGCCTCCAGAGT |
| PD-1 | CAGGATGGTTCTTAGACTC | TACCAGTTTAGCACGAAG |
| Tim-3 | CAGATACTGGCTAAATGGG | CTTGGCTGGTTTGATGAC |
| β-actin | ATCTGGCACCACACCTTCTACATTGAGCTGCG | CGTCATACTCCTGCTTGCTGATCCACATCTGC |

3 mRNA data are shown as medians with range. Categorical variables (sex) are expressed as percentages. Normal distribution data were analyzed using one-way ANOVA or a Pearson correlation test. Non-normal distribution data were analyzed using Kruskal-Wallis analysis or a Spearman correlation test. Categorical variables were analyzed utilizing a chi-square test. Receiver operating characteristic (ROC) curve analysis was conducted for quantitative MOG-specific $CD8^+$ $T_{CM}$, MOG-specific $CD8^+$granzyme-$B^+$ $T_{CM}$ or $T_{EM}$, MOG-specific $CD8^+$perforin$^+$ $T_{EM}$, and MOG-specific $CD8^+$ PD-$1^+$ $T_{EM}$ frequency, followed by the calculation of area under the ROC curve (AUC). $P < 0.05$ was deemed statistically significant.

# Results

## Clinical and laboratory data

Table 2 shows the clinical and laboratory data gathered from patients during blood sampling. There were no remarkable differences among the three groups.

## Memory T-cell subsets

Table 3 shows the comparison of MOG-specific CD8+ T cells, naïve T cells and memory T cell subsets in peripheral blood between patients with MS,OND and HC.

MS Patients had an increased proportion of MOG-specific $CD8^+$ T cells, MOG-specific $CD8^+$ $T_{CM}$ (HLA-A*03:01/$MOG_{46-55}$ pentamers$^+$$CCR7^+$$CD45RA^-$), MOG-specific $CD8^+$ $T_{EM}$ (HLA-A*03:01/$MOG_{46-55}$ pentamers$^+$$CCR7^-$$CD45RA^-$), and MOG-specific $CD8^+$ $T_{EMRA}$ (HLA-A*03:01/$MOG_{46-55}$ pentamers$^+$$CCR7^-$$CD45RA^+$) compared to OND patients and HC *via* FACScan (Figure 1). In contrast, MS patients had a lower proportion of MOG-specific naive $CD8^+$ T cells either OND patients or HC. After 2 and 4 weeks of therapy, five MS patients showed a tendency for a gradual decrease in MOG-specific $CD8^+$ $T_{CM}$ and $T_{EM}$ (Figures 2B, C), while the remaining cell subsets displayed minor or irregular alternations (Figures 2A, D).

## Intracellular expression of perforin, granzyme B and IFN-γ, and surface expression of PD-1 and Tim-3

MS patients demonstrated elevated expression of granzyme B, and reduced expression of PD-1, on MOG-specific $CD8^+$ $T_{EM}$, compared to HC (Figures 3A, D), as well as increased expression of granzyme B on MOG-specific $CD8^+$ $T_{CM}$, when compared with HC (Figure 3F). Although there was a slight increase in perforin expression, no marked differences were found between these three groups (Figures 3C, H). OND patients demonstrated slightly higher expression of Tim-3 on MOG-specific $CD8^+$ $T_{EM}$ and $CD8^+$ $T_{CM}$ than HC, but did not reach statistical significance (Figures 3E, J). However, we did not measure the above cytokines or PD-1 and Tim-3 on $CD8^+$ $T_{EMRA}$, owing to the extremely low proportion of this cell population in peripheral blood. Five MS patients treated with teriflunomide exhibited a continuous increase in PD-1 expression on MOG-specific $CD8^+$ $T_{EM}$ after 2- and 4-weeks therapy (Figure 4D), while the expression of the remaining cytokines or co-stimulatory molecules presented slight or irregular changes (Figures 4A-C, E-J).

## Quantification of perforin, granzyme B, IFN-γ, PD-1, and Tim-3 mRNA expression

Of the isolated $CD8^+$ memory T cell subsets, MOG-specific $CD8^+$ $T_{EM}$ exhibited lower PD-1 and Tim-3 mRNA expression in

TABLE 2 Baseline characteristics of patients with multiple sclerosis (MS), other neurological disease (OND), and healthy controls (HC).

| | MS (n=24) | OND (n=23) | HC (n=24) | *P* value |
|---|---|---|---|---|
| Age (years) | 35.2 ± 5.3 | 36.7 ± 5.9 | 35.0 ± 6.5 | 0.533 |
| Sex (male / female) | 15/19 | 16/17 | 16/18 | 0.904 |
| Disease course (years) | 2.5 ± 1.3 | – | – | – |
| EDSS | 1.9 ± 1.4 | – | – | – |
| HLA-A*03:01 [n (%)] | 24 (100%) | 23 (100%) | 24 (100%) | 0.999 |
| Leukocyte (× $10^3$/μl) | 5.70 ± 1.75 | 6.72 ± 1.62 | 6.53 ± 1.56 | 0.086 |
| Neutrophils (× $10^3$/μl) | 3.76 ± 1.28 | 4.39 ± 1.08 | 4.36 ± 1.44 | 0.162 |
| Lymphocytes (× $10^3$/μl) | 1.63 ± 0.54 | 1.62 ± 0.61 | 1.84 ± 0.48 | 0.298 |
| Monocytes (× $10^3$/μl) | 0.35 ± 0.08 | 0.41 ± 0.11 | 0.39 ± 0.13 | 0.101 |
| Eosinophils (× $10^3$/μl) | 0.07 ± 0.51 | 0.18 ± 0.14 | 0.11 ± 0.08 | 0.201 |
| Basophils (× $10^3$/μl) | 0.02 ± 0.01 | 0.03 ± 0.01 | 0.02 ± 0.01 | 0.092 |

Data are mean ± SD. EDSS, The Expanded Disability Status Scale.

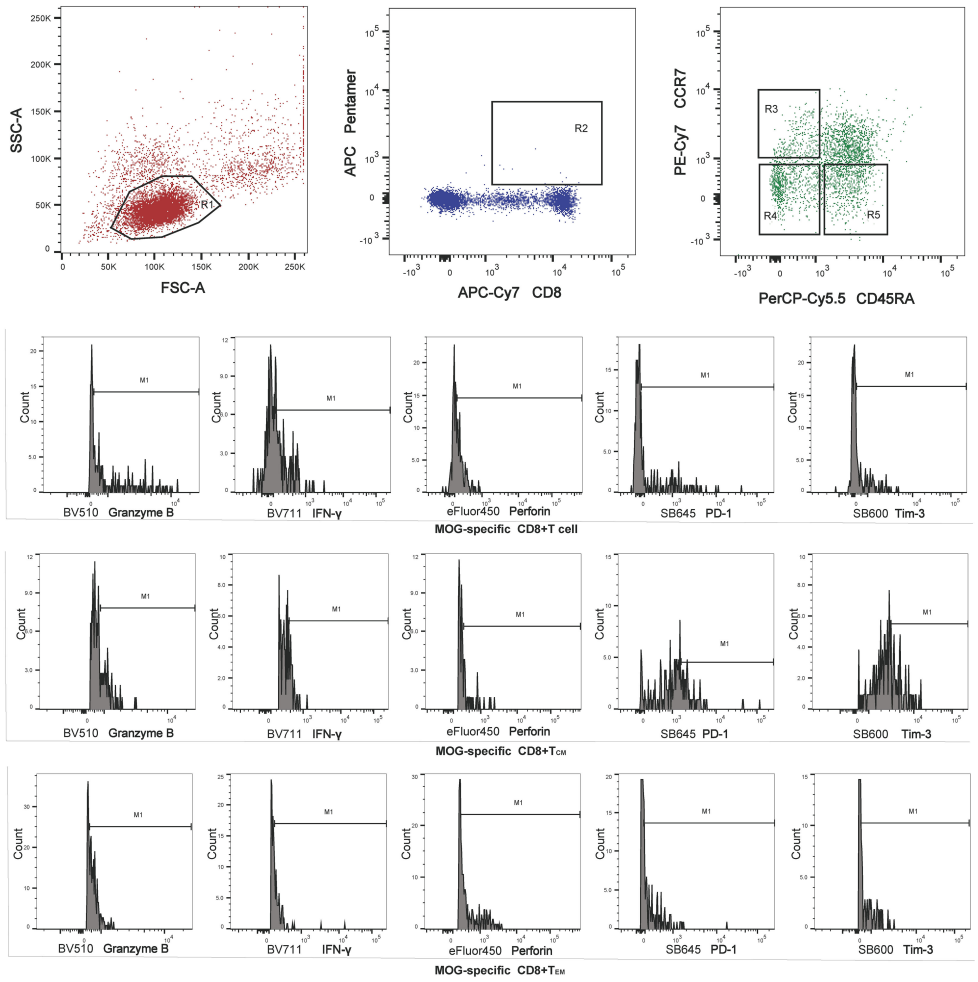


FIGURE 1
Region 1 (R1) was selected to set the mononuclear cell gate according to the forward light scatter (FSC) and side light scatter (SSC) properties. Region 2 (R2) was used to set the second gate, to separate MOG-specific $CD8^+$ T cells for analysis of memory T cell subsets. Regions 3, 4, and 5 (R3–R5) were selected to set the central memory T cell ($T_{CM}$), effector memory T cell ($T_{EM}$) and terminally differentiated cell ($T_{EMRA}$) gates, respectively, for perforin, granzyme B, interferon (IFN)-γ, programmed cell death protein 1 (PD-1), and T- cell Ig and mucin domain 3 (Tim-3) analysis.

MS patients than in HC, while PD-1 expression did not differ significantly between MS and OND patients (Figures 5D, E). MS patients displayed significantly higher mRNA expression of granzyme B in MOG-specific $CD8^+$ $T_{CM}$ than OND patients and HC (Figure 5F). However, no significant difference in above proinflammatory cytokines or PD-1 and Tim-3 mRNA expression in $T_{EMRA}$ were found between MS patients and control groups.

## ROC of selected MOG-specific $CD8^+$ T-cell subsets as well as their expression of cytokines and PD-1

ROC curves were generated to calculate the AUC on the basis of the optimal cut-off value, as well as maximum sensitivity and specificity. For the MOG-specific $CD8^+$ $T_{CM}$ proportion, AUC was 0.9089 (optimal threshold cutoff, 6.65%; sensitivity, 91.67%; and specificity, 75%); for MOG-specific $CD8^+$granzyme-$B^+$ $T_{CM}$, AUC was 0.6528 (optimal threshold cutoff, 7.605%; sensitivity, 66.67%; specificity, 75%); for MOG-specific $CD8^+$granzyme-$B^+$ $T_{EM}$, AUC was 0.691 (optimal threshold cut-off, 4.364%; sensitivity, 100%; specificity, 29.17%); for MOG-specific $CD8^+$perforin$^+$ $T_{EM}$, AUC was 0.678% (optimal threshold cutoff, 0.5885%; sensitivity, 58.33%; specificity, 87.5%); for MOG-specific $CD8^+$ PD-$1^+$ $T_{EM}$, AUC was 0.6918 (optimal threshold cutoff, 0.0415%, sensitivity 75%, specificity, 70.83%) (Figure 6).

## Correlation analysis

In MS patients, EDSS score before treatment was correlated with the frequency of MOG-specific $CD8^+$ $T_{CM}$ ($r$ = 0.421, $P$ = 0.041); granzyme B expression in $CD8^+$ $T_{CM}$ ($r$ = 0.507, $P$ = 0.012); and, for $CD8^+$ $T_{EM}$, the expression of granzyme B ($r$ = 0.512, $P$ = 0.01), perforin ($r$ = 0.446, $P$ = 0.029), and PD-1 ($r$ = −0.520, $P$ = 0.009). EDSS score after treatment of teriflunomide was correlated

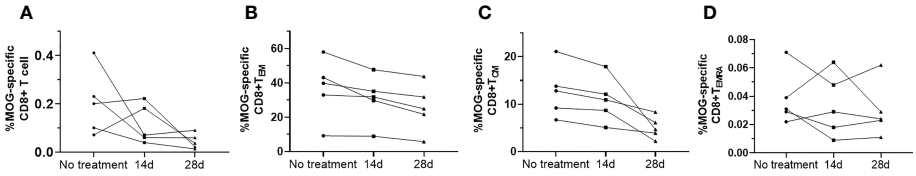


FIGURE 2
Serial study of the MOG-specific memory T-cell subsets **(A–D)** in the peripheral blood from five patients with multiple sclerosis (MS) before and after 14 d and 28 d of treatment with teriflunomide.

with the frequency of MOG-specific CD8$^+$ $T_{EM}$ ($r$ = 0.975, $P$ = 0.033). Moreover, EDSS score after 4 weeks of treatment with teriflunomide was correlated with the granzyme B expression in MOG-specific CD8$^+$ $T_{EM}$ ($r$ = 0.975, $P$ = 0.033).

## Discussion

To the best of our knowledge, this is the first human-based research utilizing MHC pentamers to identify myelin antigen-specific CD8$^+$ T cells and their memory T cell subsets in MS patients. As a result, MS patients had higher frequency of MOG-specific CD8$^+$ T cells, MOG-specific CD8$^+$ $T_{CM}$, MOG-specific CD8$^+$ $T_{EM}$, and MOG-specific CD8$^+$ $T_{EMRA}$, in contrast to a lower frequency of MOG-specific naïve CD8+ T cells; elevated granzyme B expression on MOG-specific CD8$^+$ $T_{CM}$; and, on MOG-specific CD8$^+$ $T_{EM}$, elevated granzyme B and reduced PD-1 expression. In MS patients, EDSS was correlated with the frequency of MOG-specific CD8$^+$ $T_{CM}$, granzyme B expression in CD8$^+$ $T_{CM}$, and granzyme-B and perforin expression on CD8$^+$ $T_{EM}$, but with reduced PD-1 expression on CD8$^+$ $T_{EM}$.

Our results indicate that MS patients have a skewed distribution of antigen-specific CD8$^+$ memory T cell subsets, with more $T_{CM}$, $T_{EM}$, and $T_{EMRA}$, and fewer naive CD8$^+$ T cells, than HC. These findings validate the derangement of these cell populations during the inflammatory process in MS. Together with our previous report revealing elevated IL-15 release into circulation (14), our current findings suggest that the differentiation of naïve cells is what causes the rise in CD8$^+$ TCM and TEM because IL-15 is generally considered a central regulator of primary and memory antigen-specific CD8$^+$ T cell production (21, 22). Interestingly, patients with atherosclerotic stroke and HC do not differ in the frequency of antigen-specific CD8$^+$ T cells and their memory T cell subsets, since the former category of patients exhibits CD4$^+$ memory T cells and CD8$^+$ T cells in the atherosclerotic tissue from their carotid arteries (23). Hence, further research is required to elucidate this.

Several sphingosine 1-phosphate (S1P1) receptor antagonists, such as fingolimod (FTY720), have been commonly used for the treatment of RRMS; these antagonists selectively retain CCR7$^+$ naïve T cells and $T_{CM}$, and particularly autoreactive Th17 cells, within the secondary lymphoid organs (24–26). Nonetheless, the exact role of CD8$^+$ T cell subsets such as $T_{CM}$ and $T_{EM}$ in MS remains elusive. However, in our recently published pilot study, adoptive transfer of autoreactive CD8$^+$ $T_{CM}$ into Rag-1−/− mice failed to induce EAE symptoms or EAE-related pathology (27). Notably, a lower proportion of memory CD8$^+$ T cell subsets (particularly effector memory and $T_{EMRA}$) has been observed in patients with untreated RRMS than in HC, probably due to inherent

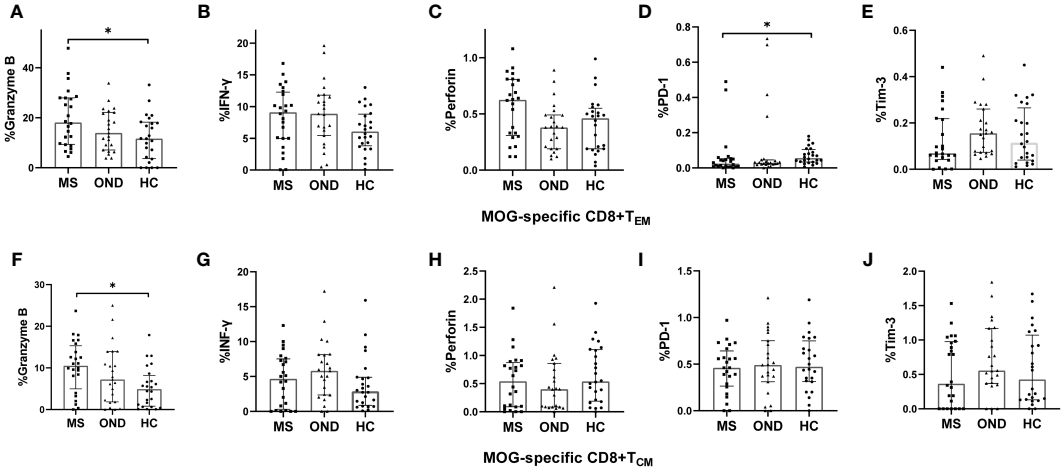


FIGURE 3
Peripheral blood expression of perforin, granzyme B, interferon (IFN)-γ, programmed cell death protein 1 (PD-1), and T- cell Ig and mucin domain 3 (Tim-3) on MOG-specific CD8+ effector memory T cells (TEM) **(A–E)** and CD8+ central memory T cells (TCM) **(F–J)**, in patients with multiple sclerosis (MS), those with other neurological disease (OND), and healthy controls (HC). Horizontal lines: medians. * P < 0.05, ** P < 0.01.

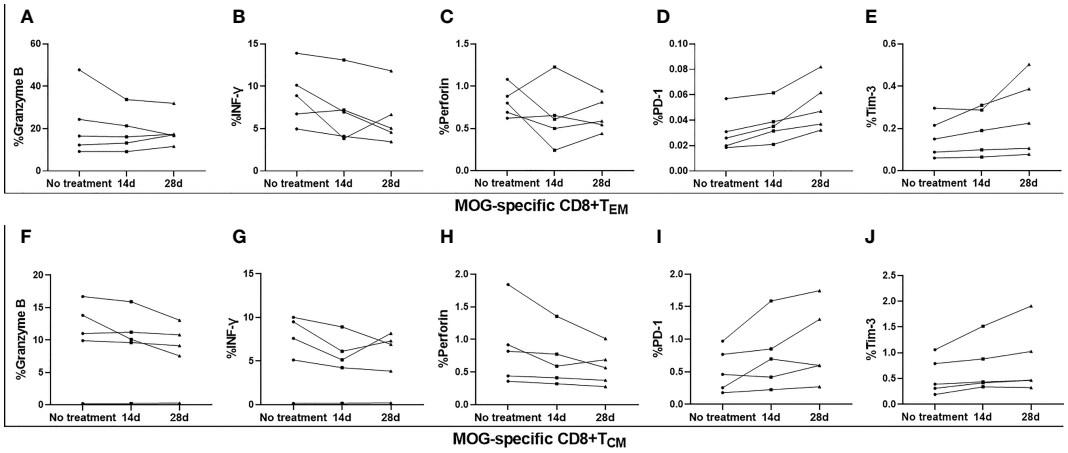


FIGURE 4
Serial analysis of perforin, granzyme B, interferon (IFN)-γ, programmed cell death protein 1 (PD-1), and T- cell Ig and mucin domain 3 (Tim-3) on MOG-specific CD8+ central memory T cells (TCM) and CD8+ effector memory T cells (TEM) in the peripheral blood of five patients with multiple sclerosis (MS) before and after 14 d and 28 d of treatment with teriflunomide **(A–J)**.

(i.e., genetically determined) defects rather than a pathophysiological effect of MS (28, 29). In our experiments, despite an irregular change in total MOG-specific $CD8^+$ T cells in MS patients, MOG-specific $CD8^+$ $T_{CM}$ and $CD8^+$ $T_{EM}$ exhibited a decreasing trend at 14 and 28 d post-treatment with teriflunomide, a well-known immunosuppressant agent (30). Together with a recent MS study revealing markedly lower IFN-γ and tumor necrosis factor-α levels on $T_{EMRA}$ and $T_{EM}$ following 12 months of teriflunomide use (31), our results indicate that these cell populations play a positive regulatory role in disease pathogenesis, presumably *via* a mechanism of molecular mimicry to trigger or promote abnormal peripheral immune responses and,

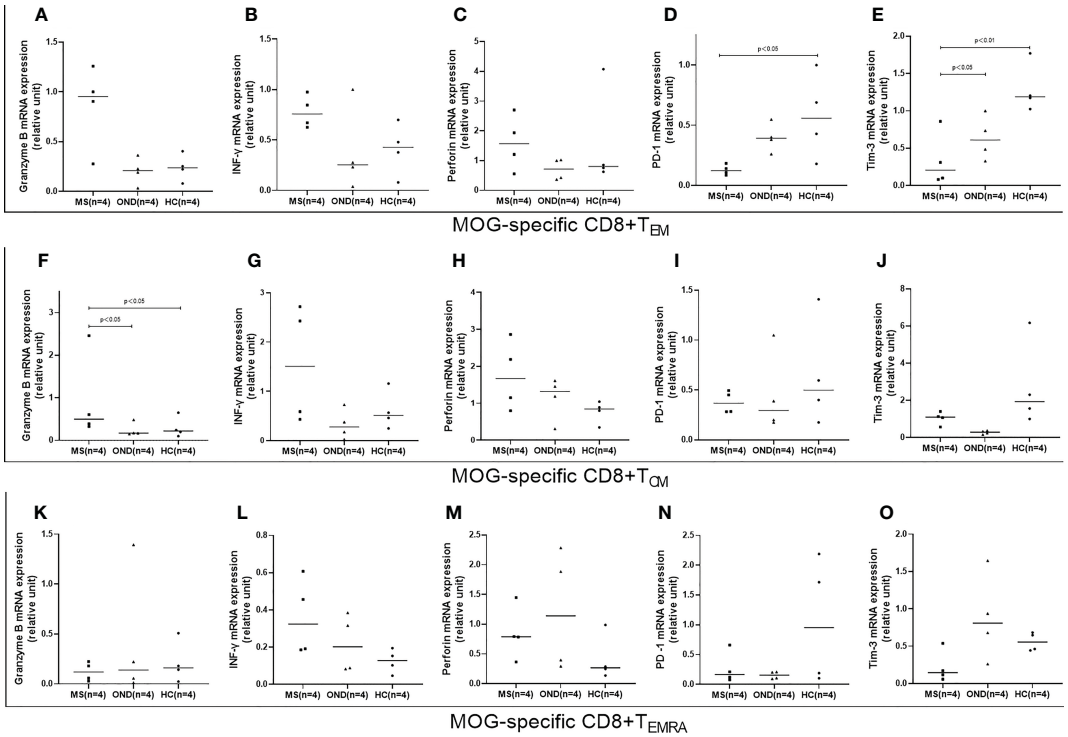


FIGURE 5
Peripheral blood mRNA expression of granzyme B, interferon (IFN)-γ, perforin, PD1, and TIM3 on CD8+ effector memory T cells (TEM) **(A–E)**, CD8+ central memory T cells (TCM) **(F–J)**, and terminally differentiated cells (TEMRA) **(K–O)**, in patients with multiple sclerosis (MS), those with other neurological disease (OND), and healthy controls (HC). Horizontal lines: medians.

10.3389/fimmu.2023.1110672

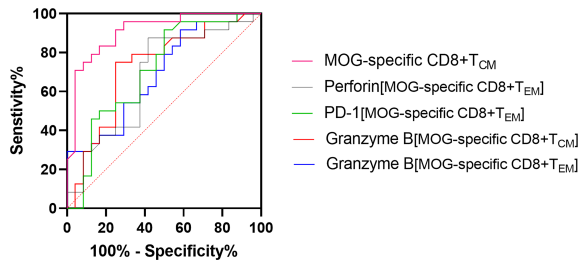


FIGURE 6
Receiver operating characteristic (ROC) curve analysis, in patients with multiple sclerosis (MS), of the frequency of MOG-specific $CD8^+$ central memory T cells ($T_{CM}$), MOG-specific $CD8^+$granzyme-$B^+$ $T_{CM}$ or effector memory T cells ($T_{EM}$), MOG-specific $CD8^+$perforin$^+$ $T_{EM}$, and MOG-specific $CD8^+$ PD-$1^+$ $T_{EM}$.

consequently, aggravate neuroinflammation, and myelin and axonal damage in the brain. The positive correlations that we observed here between disease severity and the frequencies of MOG-specific $CD8^+$ $T_{CM}$ and MOG-specific $CD8^+$ granzyme $B^+$ $T_{CM}$ or $T_{EM}$ further support this view. More importantly, these markers are potentially valuable in defining RRMS and secondary progressive MS (SPMS), because growing evidence suggests the involvement of distinct memory T cell subsets in different forms of MS and/or at different disease stages (29, 32, 33).

As negative co-stimulatory molecules, Tim-3 and PD-1 are expressed on the cell surface and negatively modulate the immune response; their signaling impairs functional activities of $CD8^+$ T cell, eventually leading to $CD8^+$ T cell exhaustion, particularly in chronic viral infection and tumors (34, 35). Co-expression of Tim-3 and PD-1 are characteristic of the most severely exhausted $CD8^+$ T cell subset (36, 37). Blockade of Tim-3 and PD-1 pathway can reverse this exhaustion and rescue the T-cell function (38, 39). However, it is difficult to determine their function on $CD8^+$ T cells, since TIM-3 is implicated in both T cell exhaustion and activation (35, 40–44). Here, MS patients showed a significant reduction in PD-1 and slight reduction in Tim-3 surface expression on MOG-specific $CD8^+$ $T_{EM}$, compared to HC. This suggests that the molecule dysregulation in $CD8^+$ memory T cells might be more prevalent in $CD8^+$ $T_{EM}$ than in $CD8^+$ $T_{CM}$. However, these results should be interpreted with caution, because the expression of PD-1 and Tim-3 are insufficient to define the function of $CD8^+$ T cells in the absence of their ligands. Nevertheless, more efforts are needed to explore their expression as well as the effects of these two costimulatory pathways on $CD8^+$ T cells in our future study.

The reduced PD-1 and Tim-3 mRNA expression in MOG-specific $CD8^+$ $T_{EM}$ that we observed in MS patients further substantiates our findings. Consistent with our results, a previous study (45) reported that $CD4^+$ and $CD8^+$ T cells stimulated by myelin basic protein demonstrated significantly higher PD-1-positive cell frequency in stable than in acute MS. Tim-3 activation, on the other hand, stimulates the formation of effector T cells as evidenced by the acquisition of an activated effector phenotype, elevated cytokine secretion, higher proliferative activities, and a transcription program linked with the differentiation of human antigen-specific CD8 T cells (42). Indeed, there was a trend towards increased expression of PD-1 on $CD8^+$ $T_{EM}$ during 4 weeks of treatment with teriflunomide. Taken together, these findings for MS suggest aberrant PD-1 and Tim-3 co-stimulation in $CD8^+$ $T_{EM}$ rather than in $CD8^+$ $T_{CM}$. PD-1 may reduce the inflammation caused by local cell–cell interactions, by halting co-stimulation of the host immune cells such as lymphocytes, or by suppressing apoptotic signaling *via* interaction with PD-1 ligands (40, 46). Tim-3 may exert complex regulatory effects on the immunoactivity of $CD8^+$ memory T cell subsets in different stages of MS. Together with our ROC analysis of abnormal antigen-specific memory T cell subsets, our findings strongly suggest that dysregulated PD-1 and Tim-3 co-stimulation are implicated in MS pathogenesis, and may therefore be useful for assessing disease severity.

## Conclusion

In conclusion, in MS patients, we observed remarkable upregulation of antigen-specific $CD8^+$ $T_{EM}$, $T_{EMRA}$ and $T_{CM}$, with elevated intracellular expression of granzyme B and reduced expression of PD-1 in MOG-specific $CD8^+$ $T_{EM}$. This may implicate a persistent chronic $CD8^+$ memory T cell-mediated inflammatory response, potentially induced in the early stages of this disorder. More strikingly, MS severity was at least partially reflected in the elevated MOG-specific $CD8^+$ $T_{CM}$ frequency and granzyme B and perforin expression, and reduced PD-1 expression. These are therefore potential serological biomarkers

TABLE 3 Comparison of MOG-specific $CD8^+$ T cells and memory T cell subsets in peripheral blood between patients with multiple sclerosis (MS), other neurological disease (OND) and healthy controls (HC).

| | Total $CD8^+$ (%) | Naïve (%) | $T_{CM}$ (%) | $T_{EM}$ (%) | $T_{EMRA}$ (%) |
|---|---|---|---|---|---|
| MS (n=24) | 0.21 (0.12,0.37) $^{**\Delta\Delta}$ | 16.7(5.46,35.30)$^{*\Delta}$ | 11.95 (9.38,13.88) $^{**\Delta\Delta}$ | 37.0 (25.33,44.98) $^{**\Delta\Delta}$ | 0.25 (0,4.22) $^{**\Delta\Delta}$ |
| OND (n=23) | 0.09 (0.03,0.11) | 32.40(25.0,46.60) | 3.14 (1.63,4.81) | 12.30 (7.60, 28.60) | 0 (0,0) |
| HC (n=24) | 0.04 (0,0.1) | 30.15(21.18,48.35) | 4.65 (3.40,7.65) | 10.90 (4.48,21.38) | 0 (0,0) |
| *P* value | <0.0001 | 0.0184 | <0.0001 | <0.0001 | 0.0018 |

Data are median with range. $^{**}p < 0.01$ or $^{*}p < 0.05$ for post hoc comparison with HC; $^{\Delta\Delta}p < 0.01$ or $^{\Delta}p < 0.05$ for post hoc comparison with OND group. $T_{CM}$, central memory T cells; $T_{EM}$, effector memory T cells; $T_{EMRA}$, terminally differentiated cells.

for predicting the development of MS. Nevertheless, further studies, such as those with a prospective cohort design, are required. Given that other disorders (e.g., oncological malignancies) also demonstrate dysregulated $CD8^+$ memory T cells, it is necessary to evaluate their specificity, sensitivity, cytotoxicity, and negative co-stimulation to demonstrate whether these markers might be specific for MS. Other issues should be addressed, such as their prognostic vs. non-prognostic value in predicting acute episodes in patients diagnosed as clinically isolated syndrome (CIS). Our findings strongly suggest positive regulatory roles for memory T cell populations in MS pathogenesis, probably *via* molecular mimicry to trigger or promote abnormal peripheral immune responses. Furthermore, downregulated PD-1 expression may stimulate a positive feedback effect, promoting MS-related inflammatory responses *via* the interaction of its ligands (PDL1), although the expression of PD-1 is not sufficient to define the function of $CD8^+$ T cells in the absence of its ligand. Our discovery of antigen-specific $CD8^+$ T cell subsets and PD-1 expression in MS paves the way for identifying potential MS biomarkers and, more importantly, for exploring a novel treatment approach against this disease through intervention in the PD-1–PDL1 pathway.

## Data availability statement

The raw data supporting the conclusions of this article will be made available by the authors, without undue reservation.

## Ethics statement

The studies involving human participants were reviewed and approved by Ethics Committee of Beijing Anzhen Hospital, Capital Medical University. The patients/participants provided their written informed consent to participate in this study.

## Author contributions

P-JL and G-ZL wrote the article. G-ZL designed the research. P-JL and T-TY performed the research. Z-XF and Z-YW analyzed the data. G-BY, LM, W-LZ, J-FL, X-HZ, and B-YY contributed new reagents/analytical tools. All authors contributed to the article and approved the submitted version.

## Funding

The National Natural Science Foundation secured assistance for this research (NSF 81870951 and 82071342).

## Acknowledgments

The authors would like to express their tremendous gratitude to all participants.

## Conflict of interest

The authors declare that the research was conducted in the absence of any commercial or financial relationships that could be construed as a potential conflict of interest.

## Publisher's note



## References

1. Rodríguez Murúa S, Farez MF, Quintana FJ. The immune response in multiple sclerosis. *Annu Rev Pathol* (2022) 17:121–39. doi: 10.1146/annurev-pathol-052920-040318

2. Sallusto F, Lenig D, Förster R, Lipp M, Lanzavecchia A. Two subsets of memory T lymphocytes with distinct homing potentials and effector functions. *Nature(1999)* (6754) 401:708–12. doi: 10.1038/44385

3. Sani MM, Ashari NSM, Abdullah B, Wong KK, Musa KI, Mohamud R, et al. Reduced CD4+ terminally differentiated effector memory T cells in moderate-severe house dust mites sensitized allergic rhinitis patients. *Asian Pac J Allergy Immunol* (2019) 37(3):138–46. doi: 10.12932/AP-191217-0220

4. Delgobo M, Heinrichs M, Hapke N, Ashour D, Appel M, Srivastava M, et al. Terminally differentiated CD4+ T cells promote myocardial inflammaging. *Front Immunol* (2021) 12:584538. doi: 10.3389/fimmu.2021.584538

5. Mahnke YD, Brodie TM, Sallusto F, Roederer M, Lugli E. The who's who of T-cell differentiation: human memory T-cell subsets. *Eur J Immunol* (2013) 43(11):2797–809. doi: 10.1002/eji.201343751

6. Sallusto F, Geginat J, Lanzavecchia A. Central memory and effector memory T cell subsets: function, generation, and maintenance. *Annu Rev Immunol* (2004) 22:745–63. doi: 10.1146/annurev.immunol.22.012703.104702

7. Frischer JM, Bramow S, Dal-Bianco A, Lucchinetti CF, Rauschka H, Schmidbauer M, et al. The relation between inflammation and neurodegeneration in multiple sclerosis brains. *Brain* (2009) 132:1175–89. doi: 10.1093/brain/awp070

8. Liblau RS, Wong FS, Mars LT, Santamaria P. Autoreactive CD8 T cells in organ-specific autoimmunity: emerging targets for therapeutic intervention. *Immunity* (2002) 17:1–6. doi: 10.1016/s1074-7613(02)00338-2

9. Neumann H, Medana IM, Bauer J, Lassmann H. Cytotoxic T lymphocytes in autoimmune and degenerative CNS diseases. *Trends Neurosci* (2002) 25:313–9. doi: 10.1016/s0166-2236(02)02154-9

10. Kipp M, Victor M, Martino G, Franklin RJ. Endogeneous remyelination: findings in human studies. *CNS Neurol Disord Drug Targets* (2012) 11(5):598–609. doi: 10.2174/187152712801661257

11. Lucchinetti CF, Popescu BFG, Bunyan RF, Moll NM, Roemer SF, Lassmann H, et al. Inflammatory cortical demyelination in early multiple sclerosis. *N Engl J Med* (2011) 365:2188–97. doi: 10.1056/NEJMoa1100648

12. Ifergan I, Kebir H, Terouz S, Alvarez JI, Lécuyer M-A, Gendron S, et al. Role of ninjurin-1 in the migration of myeloid cells to central nervous system inflammatory lesions. *Ann Neurol* (2011) 70:751–63. doi: 10.1002/ana.22519

13. Van Nierop GP, Van Luijn MM, Michels SS, Melief M-J, Janssen M, Langerak AW, et al. Phenotypic and functional characterization of T cells in white matter lesions of multiple sclerosis patients. *Acta Neuropathol* (2017) 134:383–401. doi: 10.1007/s00401-017-1744-4

14. Liu G-Z, Fang L-B, Hjelmström P, Gao X-G. Increased CD8+ central memory T cells in patients with multiple sclerosis. *Mult Scler* (2007) 13(2):149–55. doi: 10.1177/1352458506069246

15. Burfoot RK, Jensen CJ, Field J, Stankovich J, Varney MD, Johnson LJ, et al. SNP mapping and candidate gene sequencing in the class I region of the HLA complex: searching for multiple sclerosis susceptibility genes in tasmanians. *Tissue Antigens* (2008) 71(1):42–50. doi: 10.1111/j.1399-0039.2007.00962.x

16. Fogdell-Hahn A, Ligers A, Grønning M, Hillert J, Olerup O. Multiple sclerosis: a modifying influence of HLA class I genes in an HLA class II associated autoimmune disease. *Tissue Antigens* (2000) 55(2):140–8. doi: 10.1034/j.1399-0039.2000.550205.x

17. Harbo HF, Lie BA, Sawcer S, Celius EG, Dai K-Z, Oturai A, et al. Genes in the HLA class I region may contribute to the HLA class II-associated genetic susceptibility to multiple sclerosis. *Tissue Antigens* (2004) 63(3):237–47. doi: 10.1111/j.0001-2815.2004.00173.x

18. Kurtzke JF. Rating neurologic impairment in multiple sclerosis: an expanded disability status scale (EDSS). *Neurology* (1983) 33:444–52. doi: 10.1212/wnl.33.11.1444

19. Sawayama T, Sakaguchi K, Senoh T, Ohta T, Nishimura M, Takaki A, et al. Effects of pulsing procedure of interleukin-12 in combination with interleukin-2 on the activation of peripheral blood lymphocytes derived from patients with hepatocellular carcinoma. *Acta Med Okayama* (2003) 57(6):285–92. doi: 10.18926/AMO/32813

20. Mahmoudian RA, Mozhgani S, Abbaszadegan MR, Mokhlessi L, Montazer M, Gholamin M. Correlation between the immune checkpoints and EMT genes proposes potential prognostic and therapeutic targets in ESCC. *J Mol Histol.* (2021) 52(3):597–609. doi: 10.1007/s10735-021-09971-3

21. Weninger W, Crowley MA, Manjunath N, von Andrian UH. Migratory properties of naive, effector,and memory CD8(+) T cells. *J Exp Med* (2001) 194:953–66. doi: 10.1084/jem.194.7.953

22. Schluns KS, Williams K, Ma A, Zheng XX, Lefrançois L. Cutting edge: requirement for IL-15 in the generation of primary and memory antigen-specific CD8 T cells. *J Immunol* (2002) 168(10):4827–31. doi: 10.4049/jimmunol.168.10.4827

23. Gao J, Shi L, Gu J, Zhang D, Wang W, Zhu X, et al. Difference of immune cell infiltration between stable and unstable carotid artery atherosclerosis. *J Cell Mol Med* (2021) 25(23):10973–9. doi: 10.1111/jcmm.17018

24. Gräler MH, Goetzl EJ. The immunosuppressant FTY720 down-regulates sphingosine 1-phosphate G-proteincoupled receptors. *FASEB J* (2004) 18(3):551–3. doi: 10.1096/fj.03-0910fje

25. Matloubian M, Lo CG, Cinamon G, Lesneski MJ, Xu Y, Brinkmann V, et al. Lymphocyte egress from thymus and peripheral lymphoid organs is dependent on S1P receptor 1. *Nature* (2004) 427(6972):355–60. doi: 10.1038/nature02284

26. Gholamnezhadjafari R, Falak R, Tajik N, Aflatoonian R, Ali Keshtkar A, Rezaei A. Effect of FTY720 (fingolimod) on graft survival in renal transplant recipients: a systematic review protocol. *BMJ Open* (2016) 6(4):e010114. doi: 10.1136/bmjopen-2015-010114

27. Ting-Ting Y, Hong J, Ya-Juan X, Yang H, Pen-Ju L, He Y, et al. Priliminary study on pathogenic role of autoreactive CD8+ central memory T cells in experimental autoimmune encephalomyelitis. *Chin Neuroimmunol Neurol* (2021) 28(2):93–102. doi: 10.3969/j.jssn.1006-2963

28. Pender MP, Csurhes PA, Pfluger CMM, Burrows SR. Deficiency of CD8 +Effector memory T cells is an early and persistent feature of multiple sclerosis. *Mult Scler J* (2014) 20(14):1825–32. doi: 10.1177/1352458514536252

29. Canto-Gomes J, Silva CS, Rb-Silva R, Boleixa D, da Silva AM, Cheynier R, et al. Low memory T cells blood counts and high naïve regulatory T cells percentage at relapsing remitting multiple sclerosis diagnosis. *Front Immunol* (2022) 13:901165. doi: 10.3389/fimmu.2022.901165

30. Bar-Or A, Pachner A, Menguy-Vacheron F, Kaplan J, Wiendl H. Teriflunomide and its mechanism of action in multiple sclerosis. *Drugs* (2014) 74(6):659–74. doi: 10.1007/s40265-014-0212-x

31. Tilly G, Cadoux M, Garcia A, Morille J, Wiertlewski S, Pecqueur C, et al. Teriflunomide treatment of multiple sclerosis selectively modulates CD8 memory T cells. *Front Immunol* (2021) 12:730342. doi: 10.3389/fimmu.2021.730342

32. Nielsen BR, Ratzer R, Börnsen L, von Essen MR, Christensen JR, Sellebjerg F. Characterization of naïve, memory and effector T cells in progressive multiple sclerosis. *J Neuroimmunol* (2017) 310:17–25. doi: 10.1016/j.jneuroim.2017.06.001

33. Canto-Gomes J, Da Silva-Ferreira S, Silva CS, Boleixa D, Martins da Silva A, González-Suárez I, et al. People with primary progressive multiple sclerosis have a lower number of central memory T cells and HLA-DR+ tregs. *Cells* (2023) 12(3):439. doi: 10.3390/cells12030439

34. Takano S, Saito H, Ikeguchi M. An increased number of PD-1+ and Tim-3+ CD8+ T cells is involved in immune evasion in gastric cancer. *Surg Today* (2016) 46:1341–7. doi: 10.1007/s00595-016-1305-9

35. Fourcade J, Sun Z, Benallaoua M, Guillaume P, Luescher IF, Sander C, et al. Upregulation of Tim-3 and PD-1 expression is associated with tumor antigen-specifc CD8+ T cell dysfunction in melanoma patients. *J Exp Med* (2010) 207:2175–86. doi: 10.1084/jem.20100637

36. Wherry EJ. T Cell exhaustion. *Nat Immunol* (2011) 12:492–9. doi: 10.1038/ni.2035

37. Xu YY, Wang SC, Lin YK, Li DJ, DU MR. Tim-3 and PD-1 regulate CD8+ T cell function to maintain early pregnancy in mice. *J Reprod Dev* (2017) 63(3):289–94. doi: 10.1262/jrd.2016-177

38. Kim JE, Patel MA, Mangraviti A, Kim ES, Theodros D, Velarde E, et al. Combination therapy with anti-PD-1, antiTIM-3, and focal radiation results in regression of murine gliomas. *Clin Cancer Res* (2017) 23:124–36. doi: 10.1158/1078-0432

39. Liu J, Zhang S, Hu Y, Yang Z, Li J, Liu X, et al. Targeting PD-1 and Tim-3 pathways to reverse CD8 T-cell exhaustion and enhance ex vivo T-cell responses to autologous Dendritic/Tumor vaccines. *J Immunother* (2016) 39:171–80. doi: 10.1097/CJI.0000000000000122

40. Verdon DJ, Mulazzani M, Jenkins MR. Cellular and molecular mechanisms of CD8+ T cell differentiation, dysfunction and exhaustion. *Int J Mol Sci* (2020) 21 (19):7357. doi: 10.3390/ijms21197357

41. Gorman JV, Starbeck-Miller G, Pham NL, Traver GL, Rothman PB, Harty JT, et al. Tim-3 directly enhances CD8 T cell responses to acute listeria monocytogenes infection. *J Immunol* (2014) 192:3133–42. doi: 10.4049/jimmunol.1302290

42. Sabins NC, Harman BC, Barone LR, Shen S, Santulli-Marotto S. Differential expression of immune checkpoint modulators on *in vitro* primed CD4(+) and CD8(+) T cells. *Front Immunol* (2016) 7:221. doi: 10.3389/fimmu.2016.00221

43. Qiu Y, Chen J, Liao H, Zhang Y, Wang H, Li S, et al. Tim-3-expressing CD4+ and CD8+ T cells in human tuberculosis (TB) exhibit polarized effector memory phenotypes and stronger anti-TB effector functions. *PloS Pathog* (2012) 8(11): e1002984. doi: 10.1371/journal.ppat.1002984

44. Jin HT, Anderson AC, Tan WG, West EE, Ha SJ, Araki K, et al. Cooperation of Tim-3 and PD-1 in CD8 T-cell exhaustion during chronic viral infection. *Proc Natl Acad Sci USA* (2010) 107:14733–8. doi: 10.1073/pnas.1009731107

45. Trabattoni D, Saresella M, Pacei M, Marventano I, Mendozzi L, Rovaris M, et al. Costimulatory pathways in multiple sclerosis: distinctive expression of PD-1 and PD-L1 in patients with different patterns of disease. *J Immunol* (2009) 183(8):4984–93. doi: 10.4049/jimmunol.0901038

46. Odorizzi PM, Pauken KE, Paley MA, Sharpe A, Wherry EJ. Genetic absence of PD-1 promotes accumulation of terminally differentiated exhausted CD8+ T cells. *J Exp Med* (2015) 212(7):1125–37. doi: 10.1084/jem.20142237

frontiers | Frontiers in Neurology

TYPE Original Research
PUBLISHED 25 May 2023
DOI 10.3389/fneur.2023.1111063



OPEN ACCESS

EDITED BY
Mei-Ping Ding,
Zhejiang University, China

REVIEWED BY
Maria Pia Giannoccaro,
University of Bologna, Italy
Mireya Fernandez-Fournier,
University Hospital La Paz, Spain

*CORRESPONDENCE
Pilar Martinez-Martinez
✉ p.martinez@maastrichtuniversity.nl

†These authors have contributed equally to this work

RECEIVED 29 November 2022
ACCEPTED 10 May 2023
PUBLISHED 25 May 2023

CITATION
Zong S, Vinke AM, Du P, Hoffmann C, Mané-Damas M, Molenaar PC, Damoiseaux JGMC, Losen M, Rouhl RPW and Martinez-Martinez P (2023) Anti-GAD65 autoantibody levels measured by ELISA and alternative types of immunoassays in relation to neuropsychiatric diseases versus diabetes mellitus type 1.
*Front. Neurol.* 14:1111063.
doi: 10.3389/fneur.2023.1111063



# Anti-GAD65 autoantibody levels measured by ELISA and alternative types of immunoassays in relation to neuropsychiatric diseases versus diabetes mellitus type 1

Shenghua Zong[1], Anita M. Vinke[2†], Peng Du[1†], Carolin Hoffmann[1,3], Marina Mané-Damas[1], Peter C. Molenaar[1], Jan G. M. C. Damoiseaux[4], Mario Losen[1], Rob P. W. Rouhl[1,2,5] and Pilar Martinez-Martinez[1*]

[1]Department of Psychiatry and Neuropsychology, School for Mental Health and Neuroscience (MHeNS), Maastricht University, Maastricht, Netherlands, [2]Department of Neurology, Maastricht University Medical Center (MUMC +), Maastricht, Netherlands, [3]Algarve Biomedical Center, Algarve Biomedical Center Research Institute, Faro, Portugal, [4]Central Diagnostic Laboratory, MUMC+, Maastricht, Netherlands, [5]Academic Centre for Epileptology Kempenhaeghe/MUMC+, Maastricht, Netherlands

**Background:** Anti-GAD65 autoantibodies (GAD65-Abs) may occur in patients with epilepsy and other neurological disorders, but the clinical significance is not clear-cut. Whereas high levels of GAD65-Abs are considered pathogenic in neuropsychiatric disorders, low or moderate levels are only considered as mere bystanders in, e.g., diabetes mellitus type 1 (DM1). The value of cell-based assays (CBA) and immunohistochemistry (IHC) for GAD65-Abs detection has not been clearly evaluated in this context.

**Objective:** To re-evaluate the assumption that high levels of GAD65-Abs are related to neuropsychiatric disorders and lower levels only to DM1 and to compare ELISA results with CBA and IHC to determine the additional value of these tests.

**Methods:** 111 sera previously assessed for GAD65-Abs by ELISA in routine clinical practice were studied. Clinical indications for testing were, e.g., suspected autoimmune encephalitis or epilepsy (neuropsychiatric cohort; $n=71$, 7 cases were initially tested positive for GAD65-Abs by ELISA), and DM1 or latent autoimmune diabetes in adults (DM1/LADA cohort ($n=40$, all were initially tested positive)). Sera were re-tested for GAD65-Abs by ELISA, CBA, and IHC. Also, we examined the possible presence of GAD67-Abs by CBA and of other neuronal autoantibodies by IHC. Samples that showed IHC patterns different from GAD65 were further tested by selected CBAs.

**Results:** ELISA retested GAD65-Abs level in patients with neuropsychiatric diseases was higher than in patients with DM1/LADA (only retested positive samples were compared; 6 vs. 38; median 47,092U/mL vs. 581U/mL; $p=0.02$). GAD-Abs showed positive both by CBA and IHC only if antibody levels were above 10,000U/mL, without a difference in prevalence between the studied cohorts. We found other neuronal antibodies in one patient with epilepsy (mGluR1-Abs, GAD-Abs negative), and in a patient with encephalitis, and two patients with LADA.

**Conclusion:** GAD65-Abs levels are significantly higher in patients with neuropsychiatric disease than in patients with DM1/LADA, however, positivity in

CBA and IHC only correlates with high levels of GAD65-Abs, and not with the underlying diseases.

KEYWORDS

GAD65 autoantibodies, autoimmune encephalitis, epilepsy, diabetes type 1, neuronal autoantibodies, ELISA, immunohistochemistry, cell-based assay

# Introduction

Glutamate decarboxylase 65 (GAD65) is an intracellular enzyme responsible for the synthesis of the inhibitory neurotransmitter γ-aminobutyric acid (GABA), which is present in neurons and also in the beta-cells in the pancreas (1, 2). As such, autoantibodies against GAD65 (GAD65-Abs) have been associated with not only several neuropsychiatric conditions, including stiff-person syndrome (SPS), epilepsy, limbic encephalitis, cerebellar ataxia, and paraneoplastic neurological syndromes (3), but also with type-1 diabetes mellitus (DM1) and latent autoimmune diabetes in adults (LADA), in which the presence of GAD65-Abs suggests autoimmune-induced destruction of the insulin-producing beta-cells in the pancreas.

GAD65-Abs levels are usually found to be much higher in the mentioned neurological disorders than in DM1 (1, 4, 5). Recently, a study suggested that GAD65-Abs levels higher than 10,000 U/mL could be used as a cut-off for immunotherapy in neurological disorders (6). Such levels are derived from the comparison among enzyme-linked immunosorbent assay (ELISA), cell-based assay (CBA), and rat brain-based immunohistochemistry (IHC) with sera from patients who initially tested positive for GAD65-Abs by ELISA, while ELISA negatives were not included (7). Considering the fact that CBA, or IHC, is able to identify autoantibodies that bind exclusively to antigens that are expressed in their natural conformation in their resident membranes, ELISA negative cases, in theory, have the chance of being positive by CBA or IHC.

It should be borne in mind, however, because of its intracellular location, that GAD65 as a pathogenic autoimmune target might be doubtful; GAD65-Abs could in fact be harmless bystander immunoglobulins, while other, genuinely pathogenic, but unknown, autoantibodies could be present in the same individual, causing an autoimmune disease (8, 9). These yet unidentified autoantibodies can be detected based on the sera staining on rat brain-based immunohistochemistry (IHC) (9). Besides, it has been reported that some cases had autoantibodies against GAD67, another isoform of GAD, even in the absence of GAD65-Ab (10–12).

In this study, we compared the sera reactivity to GAD65-Abs by CBA, IHC, and ELISA in a previously described neuropsychiatric cohort including ELISA positive and negative cases (13), with an additional diabetes cohort as disease control. We aimed to re-evaluate the background of the assumption that high GAD65-Abs levels are related to neurological disorders and lower levels are related to diabetes. To exclude other immunoreactivity and to evaluate the value of these tests in this clinical situation, we also tested for autoantibodies against conformational epitopes on GAD65, or solely against GAD67 by CBA, and neuronal autoantibodies that were not routinely tested in the clinic after positive findings in IHC.

# Methods

## Cohort

We retrospectively included all patients from whom a GAD65-Abs test was ordered at Maastricht University Medical Centre (MUMC+) and Kempenhaeghe Epilepsy Centre between 2010 and 2014 (as reported previously) (13). In the initial study, in total, the cohort consisted of 117 patients with DM1/LADA and 119 patients with (possible) neuropsychiatric disorders (mostly epilepsy and/or encephalitis) who were tested for GAD antibodies during this period (13). For the current retrospective study, samples of the patients were selected in a process as shown in Figure 1. In brief, 40 GAD65-Abs positive sera from DM1/LADA patients were retrieved when available. Seventy six samples from patients with suspected autoimmune encephalitis/epilepsy were retrieved including 10 positives for GAD65-Abs, and 66 negatives for GAD65-Abs. We also took the results of previous tests for other anti-neuronal antibodies (from routine clinical practice) into account. We excluded three of these patients with positive results in these tests because they had the typical clinical presentation associated with the detected autoantibodies (one with anti-Hu and GAD65-Abs, and 2 cases negative for GAD65 but with anti-VGKC, and anti-NMDAR antibodies respectively). One patient with anti-VGKC and GAD65-Abs was not excluded, because the clinical syndrome was considered linked to the GAD65-Abs (and not to the anti-VGKC). In 2 patients the GAD65-Abs were not deemed to be related to the neuropsychiatric disease based on the initial and the follow-up evaluations (reassessed by AMV and RPWR), which were also excluded. This led to a final inclusion of 7 cases with GAD65-Abs and 64 cases negative for GAD65-Abs in the neuropsychiatric cohort (NP cohort) (Figure 1).

We retrieved the clinical symptoms at presentation, comorbidities, and previous history from the electronic patient files [as previously described in (13)]. The data are shown in Table 1. Ethical approval was obtained from the medical ethical committees of the two participating centers, MUMC+ and Kempenhaeghe (METC 15-4-002).

## Autoantibody detection methods

### ELISA

As mentioned in our previous study, during routine clinical diagnosis, an ELISA for GAD65-Abs detection was performed at different national reference laboratories (all accredited according to national standards) using commercial ELISA kits following manufacturers' instructions (13). Due to possible inter-laboratory differences, it is impossible to compare the levels of the used tests. To be able to compare the levels of the GAD65-Abs, we retested all

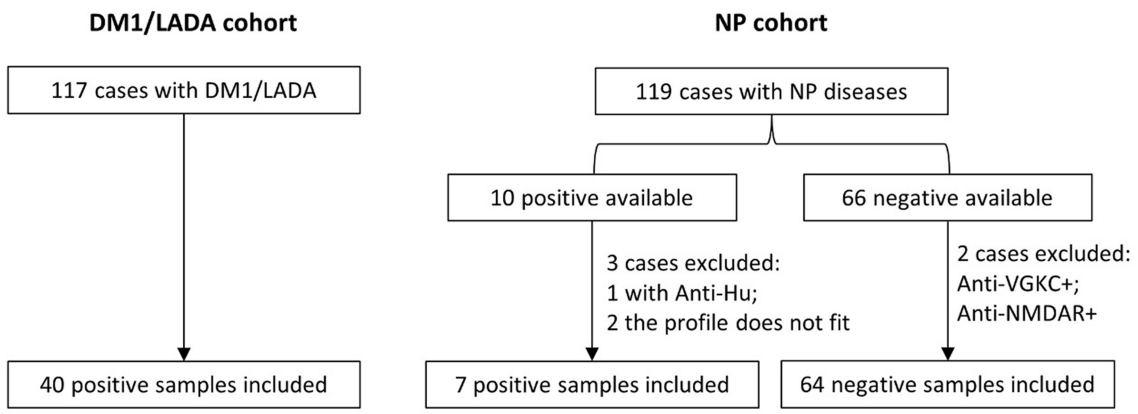


FIGURE 1
Procedure of the selection of blood samples and the basic subgroups for 3 different aims: (1) Comparison of the GAD-65 levels between positive samples of DM1/LADA and NP by ELISA (re-evaluation); (2) Comparison of the GAD-65-Abs detection methods between ELISA, CBA and IHC using both positive and negative cohorts. (3) Detection of GAD67-Abs by CBA and of other neuronal autoantibodies by CBA and IHC in all the mentioned groups.

TABLE 1 Demographic and clinical characteristics of patients.

| Main parameters | DM1/LADA | Neuropsychiatric cohort | | *p*-value |
|---|---|---|---|---|
| Previous GAD65-Abs ELISA result | 40 positive | 9 positive | 64 negative | |
| Age (mean/range) | 38/4–68 | 33/15–64 | 40/1–83 | NS |
| **Sex** | | | | |
| Female | 18 (55%) | 5 (55.6%) | 32 (50%) | NS |
| Male | 22 (45%) | 4 (44.4%) | 32 (50%) | NS |
| children (<18 years) | 9 (22.5%) | 1 (11.1%) | 8 (12.5%) | NS |
| **Indication for GAD65-Abs test request of the neuropsychiatric patients*** | | | | |
| Refractory epilepsy | | 6 (66.7%) | 28 (43.8%) | NS |
| Other neuropsychiatric disorders (encephalitis, movement disorders, psychotic disorders) | | 3 (33.3%) | 36 (56.2%) | NS |
| Comorbid with DM1/LADA | | 6 (66.7%) | 1 (1.6%) | 0.0001 |
| Tumor | | 0 | 4 (6.3%) | NS |
| Clinically diagnosed as GAD-Abs related neuropsychiatric disease | | 7 (77.8%) | | |
| Treated with immunotherapy | | 4 | | |
| Response to immunotherapy | | 4 | | |

GAD65-Ab, glutamate decarboxylase 65 autoantibodies; DM1/LADA, diabetes mellitus type 1 or latent autoimmune diabetes in adults; NS, no significant difference.

samples using the commercial ELISA kit (RSR Limited, Cardiff, UK) in our laboratory following the same guidelines as above. Samples with levels above 2000 U/mL were further diluted 1 in 100 with phosphate-buffered saline (PBS) for a second test, and if still out of range further diluted 1 in 100 in PBS (1/10,000). Levels were expressed in units/mL (U/mL), levels below 5 U/mL were considered negative.

## Cell-based assay for GAD65/67-Abs

Antigen-specific screening for autoantibodies against GAD65 and GAD67 was performed, respectively, using CBA as described in our previous study (14, 15). Basically, HEK293 cells were plated on coverslips coated with poly-D-lysine (#P7280, Sigma, St. Louis, United States) in 60 mm-culture plates (#628160, Greiner Bio-One, Alphen aan den Rijn, NL) in Dulbecco's Modified Eagle Medium with 10% fetal calf serum, 4 mM L-glutamine and 100 U/mL penicillin-streptomycin and incubated overnight to attach. Cells were transfected with polyethyleneimine (#23966, Polysciences Inc. Warrington, PA, United States) and 4 µg expression vectors encoding the according antigen (plasmids pCMV6-XL5 containing human GAD65 or GAD67, a kind gift of Dr. Francesc Graus) and expression allowed for 22–26 h. Cells were fixed in 3.5% formaldehyde (#87837.180, VWR, Amsterdam, NL) for 10 min and permeabilized with 0.3% Triton-X-100 for 10 min. After blocking with 1% bovine serum albumin (BSA) for 1 h, cells were incubated with 40 µL human sera (diluted 1:40 in 1% BSA) for 1 h at room temperature. After that, secondary antibodies goat-anti-human-IgG-Alexa488 (1:1,000, # A11013, Invitrogen, Waltham, United States) were used for probing the autoantibody staining. Lastly, cover glasses were mounted with7 µL DAPI mounting

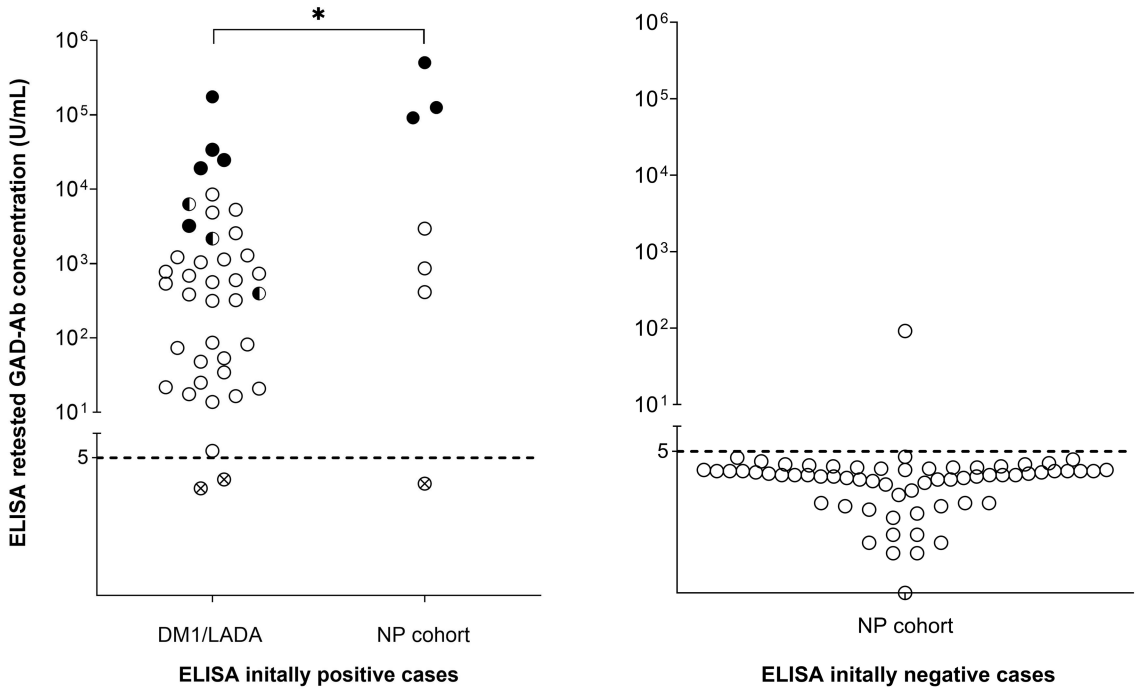


FIGURE 2
Analysis of GAD65-Ab by ELISA, CBA, and IHC in sera of patients with DM1/LADA and patients with neuropsychiatric disease. Every circle indicates an individual sample. Samples with GAD65-Abs levels above 5U/mL were considered positive by ELISA. Half-black symbols indicate samples that were also positive by CBA (CBA+), and full-black symbols indicate cases positive by both CBA and IHC. Circles with cross symbols indicate samples that were retested negative in the ELISA initially tested positive cases. All samples with GAD65-Ab levels ≥10,000U/mL were positive for both CBA and IHC, and patients with positive CBA and IHC were found in both DM1/LADA and NP groups. The difference in GAD65-Ab levels between patients with GAD-related neuropsychiatric disease and patients with DM1/LADA was significant ($p$=0.02, Mann–Whitney $U$ test).

medium (#H-1200, vector laboratories, CA, United States) and the results were evaluated with a BX51 Olympus microscope by two observers of which one was blinded of the sample's information. A serum sample with antibodies both positive to GAD65 and GAD67 from a refractory epilepsy patient was used as positive control. The positivity had been initially tested by CBA using transfected cells and co-stained with antibodies from immunized rabbits specifically targeting GAD65 or GAD67, respectively. The two antibodies were rabbit anti-human GAD65 (1:1,000, 7309LB) and GAD67 (1:1,000, 10266/20B), a kind gift from Christiane Hampe (University of Washington). Additionally, a serum sample from a healthy individual was used as negative control (Supplementary Figure S1). Results were graded as strong positive, positive, weak positive and negative. All samples were tested once and positive samples were repeated at least once more for verification.

## Immunohistochemistry (IHC) on rat brain

Neuronal autoantibodies were identified by IHC on rat brain tissue following standard procedures as described in our previous studies (14, 15). Different from those reported by other groups that focus mainly on cerebellum staining pattern (16), for the GAD65-Abs detection by IHC, the hippocampus staining pattern was focused since the cerebellum molecular layer staining is not specific for GAD65, and not all the hillock area of the Purkinje cells would be revealed clearly in each section. In our hands, the hippocampus staining pattern gave specific results compared to the negative control as shown in our previous study (15). In brief, rat brains were fixed for 1 h in 4% paraformaldehyde and cryoprotected by incubating in 30% sucrose solution. Frozen brains were cut into 7-µm thick tissue sections using a Leica CM3050S cryostat and stored at −80°C. Sections were subsequently blocked with 0.3% $H_2O_2$ for 15 min followed by washing with PBS 3 times and blocking with 5% goat serum for 1 h at room temperature. Next, sections were incubated with 200 µL diluted human serum (1:200 in 5% goat serum) overnight at 4°C, followed by incubation with 200 µL biotinylated goat anti-human IgG (1:1,000, 109-066-008, Jackson laboratory) for 2 h at room temperature, followed by incubation with the same amount of ABC mixture (1:800 in TBS, # PK 6100 vector laboratories, CA, United States), for 1 h at room temperature and the reactivity developed using diaminobenzidine. A negative control from a healthy individual and a positive control serum for GAD65-Ab (serum from an autoimmune GAD65-Ab encephalitis patient, which was tested GAD65 and GAD67-Ab positive by CBA and gave a typical pattern on rat brain as compared to previous studies (15, 17)) and also our rabbit- anti-GAD65 antibody, see Figure 2. Images were taken by the VENTANA iScan HT slide scanner (20× objectives) and graded by 2 experienced observers separately (S. Zong, C. Hoffmann, or M. Damas) using the Ventana Image Viewer. Hippocampal reactivity of sera was ranked as negative (0), borderline (1), weak positive (2), strong positive (3), based on the intensity and contrast of the staining. Staining was repeated and only if repeatedly found positive with the same pattern by 2 observers, a final decision of positivity was made.

TABLE 2 Comparison of ELISA, CBA, and IHC results.

| | ELISA initially positive cases | | ELISA initially negative cases | |
|---|---|---|---|---|
| | DM1/LADA ($n$=40) | NP ($N$=7) | NP ($n$=64) | |
| ELISA retested GAD65-Abs+* | 38 (95%) | 6 (85.7%) | 1 (1.6%) | |
| CBA GAD65-Abs+ | 8 (20%) | 3 (42.9%) | 0 | |
| IHC GAD65-Abs+ | 5 (12.5%) | 3 (42.9) | 0 | |
| IHC positive for other Abs | 2 (5%) | 0 | 2 (3.1%) | |
| | CBA GAD65-Abs+ | | CBA GAD65-Abs−** | |
| | DM1/LADA ($n$ = 8) | NP ($N$ = 3) | DM1/LADA ($n$ = 32) | NP ($N$ = 4) |
| CBA GAD67-Abs+*** | 6 (75%) | 3 (100%) | 0 | 0 |
| IHC GAD65-Abs+ | 5 (62.5%) | 3 (100%) | 0 | 0 |

*GAD65-Abs+: Positive for GAD65 autoantibodies;
**GAD65-Abs−: Negative for GAD65 autoantibodies
***GAD67-Abs+: Positive for GAD67 autoantibodies.

# Results

## GAD-Abs levels are higher in patients with neuropsychiatric disease than in patients with diabetes

To evaluate if the GAD65-Abs levels are substantially different between diabetes and GAD-related neurological disease, we compared results from the newly performed ELISA tests. We found that 38 out of 40 samples (95%) from the DM1/LADA cohort, and 6 out of 7 samples (85.7%) from the NP cohort were confirmed positive, whereas 63 out of 64 samples (98.4%) were confirmed negative in our hands (Figure 2; Table 2). In the neuropsychiatric group with confirmed positive ELISA results, 6 patients had a clinical diagnosis of GAD65-Abs related neuropsychiatric disease (epilepsy or encephalitis). The GAD65-Abs level in patients diagnosed with GAD-related neuropsychiatric disease ($n$ = 6) was higher than in patients with DM1/LADA ($n$ = 38), with statistical significance: median 47,092 U/mL vs. 581 U/mL; $p$ = 0.02, Mann-Whitney $U$ test (Figure 2).

## Only samples with high levels of GAD65-Abs by ELISA are positive by CBA and IHC

To assess a possible added value of CBA and IHC for the detection of GAD65-Abs, all samples were further tested by these 2 methods; the results were compared to the ELISA results between the two studied cohorts (Figures 2, 3; Table 2). 42.9% (3 out of 7) of the ELISA positive samples from NP patients were positive for both CBA and IHC (GAD65 Abs levels between 91,238 U/mL and 503,001 U/mL), whereas 20% (8 out of 40) of ELISA positive samples from DM1/LADA patients had positive CBA(the lowest GAD65 Abs level was 396 U/mL), 5 of which were also positive by IHC (the lowest GAD65 Abs level was 3,219 U/mL), with no significant prevalence difference between the 2 cohorts. Notably, all samples ($n$ = 7) with antibody levels above 10,000 U/mL were positive by CBA and IHC, regardless of cohorts difference (Figure 2). All ($n$ = 64) ELISA negative samples were negative in IHC and CBA (Table 2).

## Besides GAD65-Abs, other neuronal autoantibodies are present in both patient groups

To test for the presence of other neuronal autoantibodies, all samples were tested for GAD67-Abs by CBA and other neuronal autoantibodies by IHC. Nine samples tested positive for GAD67-Abs; all were also positive for GAD65-Abs by CBA (six were from the DM1/LADA cohort and three from the NP cohort, Table 2).

Samples from four cases gave staining patterns different from typical GAD65-Abs by IHC (Table 2; Figures 3D–G). Two cases were patients with LADA (GAD65-Ab levels were 779 U/mL and 1,136 U/mL, respectively). One of these patients had an anxiety disorder, and by IHC there was mainly staining in the molecular layer of the dentate gyrus (DG) and the subiculum regions; the other patient did not have any neuropsychiatric symptoms and showed diffuse staining over the hippocampus (Figures 3D,E; Table 3 case 1 and case 2, respectively).

Also, in the GAD65-Abs negative patients with the neuropsychiatric disease, we could identify cases with reactivity in IHC. In case 3, there was strong reactivity in the CA3 and DG area of the hippocampus and the molecular layer of the cerebellum (different from the 2 patterns found in the LADA cases mentioned above, seen in Figure 3F; Table 3 case 3). This patient had epilepsy. The staining pattern was similar to anti-mGluR1 as previously reported (18) and we confirmed this by mGluR1 CBA. The details of this case can be found in our recently published case report (19). In case 4, the patient had encephalitis, and the sample showed a staining pattern similar to case 1 (Table 3).

# Discussion

We found that patients with neuropsychiatric disease tend to have higher levels of GAD65-Abs in their serum than DM1/LADA patients, though there is a substantial overlap. This suggests that the antibody levels may be a discriminative factor between the two clinical groups. However, neither the results of IHC nor CBA assays show a significant difference between the two groups.

Previously, studies showed that GAD65-Abs levels in patients with confirmed GAD65-Abs related neuropsychiatric diseases were higher

than those in patients with DM1. Baekkeskov et al. in 1990 firstly described that the level of the GAD65-Abs in stiff person syndrome was 10–200 times higher than in DM1 patients on the basis of an immunoprecipitation method, and later Honnorat et al. in 2001 found similar results in patients with cerebellar ataxia compared to patients with DM1 using RIA and IHC (with the staining pattern of GAD65-Abs on rat cerebellum) (1, 20). In both studies, however, the confirmation of the GAD65-Abs was done with two methods in patients with neuropsychiatric disease, but only with one for patients with DM1.

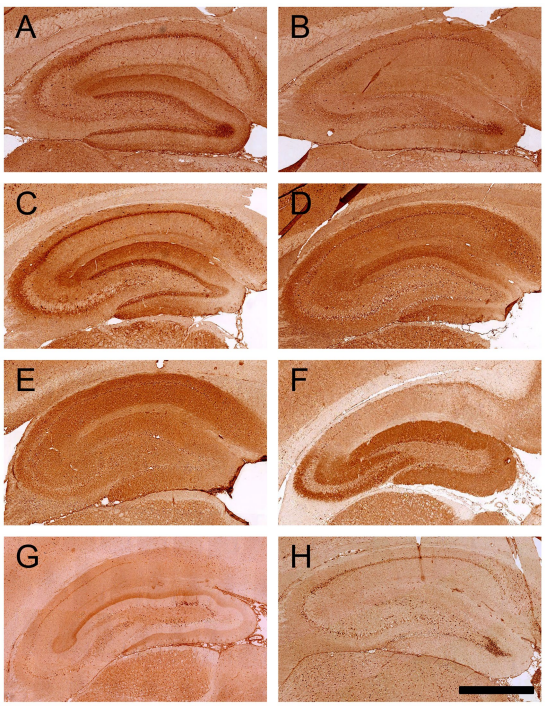


FIGURE 3
IHC staining patterns on rat brain hippocampus given by sera of patients with DM1/LADA and neuropsychiatric disease. Commercial antibodies to GAD65 or GAD67, or human sera were incubated on rat brain slices, followed by biotinylated secondary antibodies, ABC kit, and DAB to develop the color reaction. **(A)** Commercial antibodies specific to GAD65 showed intracellular granular staining in the hippocampus and neuropil staining in the outer layer of the DG region. **(B)** The commercial antibody directed against GAD67 did not give strong staining in the hippocampus region. **(C)** Positive serum with high GAD65-Abs levels by ELISA (>10,000U/mL) gave the same pattern as the commercial GAD65-Abs. **(D–G)** Two samples from DM1/LADA patients (Case 1 and Case 2) and 2 samples with neuropsychiatric disease (Case 3 and Case 4) gave strong neuropil staining in the hippocampus (**G** represents staining performed at another time point; therefore, the background staining is different). **(H)** Negative control serum from a healthy individual showed overall background staining (scale bar=500μm).

GAD-65 analysis in neuropsychiatric cohorts, e.g., epilepsy or autoimmune encephalitis were tested but the quantification of the results contradicted each other (4, 5). Since there are no clear criteria to diagnose and define GAD-related neuropsychiatric disorders, the selection procedures in these studies were different, which may have contributed to the conflicting results. Within the inclusion cohort in the present study, our findings tend to support that the cut-off value of autoantibody levels (GAD65-Abs levels) for clinical significance in patients with neuropsychiatric disease cannot be as strict as claimed in earlier studies (7). The limitation of applying this cut-off is that patients from DM1/LADA with high GAD65-Abs titers, if combining with neurological or psychiatric disorders, might be suspicions, while this is not supported by the current study because only 2 of the 5 DM1/LADA patients with high titers GAD65 antibodies (positive for all the assays) had psychiatric disorders. Furthermore, considering the relatively high comorbidity of DM1 in patients with epilepsy (21), the clinical relevance of GAD65-Abs for the neuropsychiatric disease (mainly epilepsy in this case) in these patients remains doubtful.

Measurements of GAD65-Abs in cerebrospinal fluid (CSF) and serum, as well as analysis of intrathecal synthesis were proposed to be important to identify GAD associated autoimmunity (16), Based on the dynamic turnover rate of immunoglobulin G (IgG) between serum and CSF, around 1% of the serum levels of these antibodies would enter the CSF (18, 22). In case of disruption of the blood–brain barrier, the CSF antibody levels would be higher. According to this theory, diabetes patients with high antibody levels would also show positive results in CSF. On the other hand, intrathecal synthesized antibodies would leak to serum as well and lead to a relatively low but positive serum antibody levels. Thus, as long as measurements of GAD65-Abs in serum is the starting point in the clinical practice, a positive result should always lead to further investigation, while the level should not be used as an absolute marker for diagnosis. This is partially supported when comparing the clinical features and treatment response between the triple positive patients and the ELISA only patients, of which no obvious correlation with the titers (Supplementary file, Supplementary Tables S1, S2).

TABLE 3 Four Clinical characteristics of four cases with other neuronal autoantibodies identified by IHC.

| | Sex | Age | ELISA GAD65-Ab | CBA GAD65/67-Ab | IHC | Diagnosis | Comorbidity | Treatment | Response to treatment |
|---|---|---|---|---|---|---|---|---|---|
| Case 1 | M | 50 | 779.1 | Negative | Weak positive to unknown antigens | LADA | Anxiety | n/a | n/a |
| Case 2 | M | 65 | 1136.5 | Negative | Weak positive to unknown antigens | LADA | No | n/a | n/a |
| Case 3 | F | 51 | 3.4 | Negative | Anti-mGluR1 | Refractory epilepsy (anti-mGluR1 encephalitis)* | No | Valproic acid (IVIG)* | Seizure reduction; (further reduction)* |
| Case 4 | M | 83 | 0.3 | Negative | Weak positive to unknown antigens | Encephalitis | No | Fenytoin, Levetiracetam | Seizure reduction |

GAD65/67-Abs, glutamate decarboxylase 65/67 autoantibodies; ELISA, enzyme-linked immunosorbent assay; CBA, cell-based assay; IHC, immunohistochemistry; Anti-Hu, anti-Hu autoantibodies; Anti-mGluR1, autoantibodies against metabotropic glutamate receptor 1; LADA, Latent Autoimmune Diabetes in Adults; n/a, not applicable.
*Anti-mGluR1 encephalitis was the final diagnosis of case 3 after the IHC results confirmed by CBA, thus the patient was treated further.

Another point is the possibility that in the different related disorders the GAD65-Abs are directed against different antigenic regions of GAD65 (8, 23). However, until now literature has not provided a practical method to identify antibodies targeting different antigen binding sites for a clear-cut diagnosis of GAD65-related diseases. Here, we limit our discussion to the comparison of the current clinical methods: CBA, and in some laboratories also IHC, are used frequently in the detection of neuronal autoantibodies. We found positive results only by CBA and IHC when the concentrations of GAD65-Abs are high, and there was no additional value in the use of IHC or CBA to distinguish the 2 clinical groups. Apparently, the latter assays seem to be less sensitive for GAD65-Abs.

Whether other co-existing autoantibodies might be more relevant contributors to the disease than GAD65 should be assessed case by case. The clinical relevance of neuronal autoantibodies, like anti-NMDAr, anti-LGI1, and anti-GABAbr, is mostly clear, whereas neuronal autoantibodies with only weak reactivity to the brain (in IHC) might be common and only related to aging (14, 24). In our study, 2 cases with unknown IHC patterns had LADA and one of these also suffered from anxiety. In these cases, further studies analyzing a possible correlation between the unknown neuronal autoantibodies and the anxiety symptoms in LADA are needed, because also clinically, diabetes and anxiety disorders have high co-occurrence (25, 26).

Our study has some limitations: Firstly, the matched CSF samples were not available for testing. Secondly, the rate of false positive IHC results for detecting novel neuronal autoantibodies is unknown. Thus, the autoantibodies found positive only by IHC would always need further confirmation with more specific methods. Furthermore, we were dependent on the availability of sera in the archives of the participating centers, which led to a relatively small sample size of patients with neurological GAD65-Abs related diseases leading to a somewhat skewed comparison between the groups. Even though the rarity of this disease makes it difficult to have substantial number of patient samples, a larger sample size would increase the statistical power.

In conclusion, we reconfirmed a marked difference between GAD65-Abs levels between patients with neuropsychiatric disease and patients with DM1/LADA, whereas positive results in CBA and IHC overlap in both groups. Consequently, the clinical significance of the identification of GAD65-Abs in patients with neuropsychiatric disease remains unclear, even in patients with high levels of antibodies. We also recommend a strict correlation to the clinical symptoms and the demonstration of absence of other neuronal antibodies by practical methods such as CBA and/or IHC.

## Data availability statement

The raw data supporting the conclusions of this article will be made available by the authors, without undue reservation.

## Ethics statement

Ethical approval was obtained from the medical ethical committees of the two participating centers, MUMC+ and Kempenhaeghe (METC 15-4-002). Written informed consent from the participants' legal guardian/next of kin was not required to participate in this study in accordance with the national legislation and the institutional requirements.

## Author contributions

SZ contributed to the study design, acquisition, analysis and interpretation of the data, and manuscript drafting and revision. AV contributed to the acquisition, analysis and interpretation of the data (especially to the clinical information collection and analysis), and revision. PD contributed to the analysis and interpretation of the data, and revision (specifically focusing on the additional experiments' performance and results analysis during this stage). CH contributed to the study design, acquisition, analysis and interpretation of the data and the revision. MM-D contributed to the study design, acquisition, analysis and interpretation of the data. PM contributed to the interpretation of the data and the revision. JD contributed to the study design, acquisition and interpretation of the data (especially on the sample collection), and revision. ML contributed to the study design, interpretation of the data, and manuscript revision. RR contributed to the study design, analysis and interpretation of the data, and critical revision of the manuscript. PM-M contributed to the study design, acquisition, analysis, and interpretation of the data, manuscript and revision, and has access to the data in the study and takes responsibility for the integrity and data analysis. All the authors contributed to the critical revision of the manuscript for important intellectual content.

## Funding

The authors are thankful for the financial support received from the following funding organizations: PM-M was supported by an Aspasia/NWO grant (015.011.033), and SZ received CSC scholarship (201507720015) and Kootstra Talent Fellowship (Fall, 2019), which support his research in Maastricht University. CH and MM-D were supported by Kootstra Talent Fellowships.

## Conflict of interest

The authors declare that the research was conducted in the absence of any commercial or financial relationships that could be construed as a potential conflict of interest.

## Publisher's note



## Supplementary material

The Supplementary material for this article can be found online at: https://www.frontiersin.org/articles/10.3389/fneur.2023.1111063/full#supplementary-material

# References


1. Baekkeskov S, Aanstoot HJ, Christgai S, Reetz A, Solimena M, Cascalho M, et al. Identification of the 64K autoantigen in insulin-dependent diabetes as the GABA-synthesizing enzyme glutamic acid decarboxylase. *Nature*. (1990) 347:151–6. doi: 10.1038/347151a0

2. Legay F, Henry S, Tappaz M. Evidence for two distinct forms of native glutamic acid decarboxylase in rat brain soluble extract: an immunoblotting study. *J Neurochem*. (1987) 48:1022–6. doi: 10.1111/j.1471-4159.1987.tb05620.x

3. Saiz A, Blanco Y, Sabater L, González F, Bataller L, Casamitjana R, et al. Spectrum of neurological syndromes associated with glutamic acid decarboxylase antibodies: diagnostic clues for this association. *Brain*. (2008) 131:2553–63. doi: 10.1093/brain/awn183

4. T1D Exchange BiobankLiimatainen S, Honnorat J, Pittock SJ, McKeon A, Manto M, et al. GAD65 autoantibody characteristics in patients with co-occurring type 1 diabetes and epilepsy may help identify underlying epilepsy etiologies. *Orphanet J Rare Dis*. (2018) 13:55. doi: 10.1186/s13023-018-0787-5

5. Gresa-Arribas N, Ariño H, Martínez-Hernández E, Petit-Pedrol M, Sabater L, Saiz A, et al. Antibodies to inhibitory synaptic proteins in neurological syndromes associated with glutamic acid decarboxylase autoimmunity. *PLoS One*. (2015) 10:e0121364. doi: 10.1371/journal.pone.0121364

6. Muñoz-Lopetegi A, de Bruijn MAAM, Boukhrissi S, Bastiaansen AEM, Nagtzaam MMP, Hulsenboom ESP, et al. Neurologic syndromes related to anti-GAD65: clinical and serologic response to treatment. *Neurol Neuroimmunol Neuroinflam*. (2020) 7:e696. doi: 10.1212/NXI.0000000000000696

7. Muñoz-Lopetegi A, de Bruijn MAAM, Boukhrissi S, Bastiaansen AEM, Nagtzaam MMP, Hulsenboom ESP, et al. Neurologic syndromes related to anti-GAD65. *Clin Serol Res Treatm*. (2020) 7:e696. doi: 10.1212/NXI.0000000000000696

8. Fouka P, Alexopoulos H, Akrivou S, Trohatou O, Politis PK, Dalakas MC. GAD65 epitope mapping and search for novel autoantibodies in GAD-associated neurological disorders. *J Neuroimmunol*. (2015) 281:73–7. doi: 10.1016/j.jneuroim.2015.03.009

9. Chang T, Alexopoulos H, McMenamin M, Carvajal-González A, Alexander SK, Deacon R, et al. Neuronal surface and glutamic acid decarboxylase autoantibodies in nonparaneoplastic stiff person syndrome. *JAMA Neurol*. (2013) 70:1140–9. doi: 10.1001/jamaneurol.2013.3499

10. Meinck H-M, Faber L, Morgenthaler N, Seissler J, Maile S, Butler M, et al. Antibodies against glutamic acid decarboxylase: prevalence in neurological diseases. *J Neurol Psychiatry*. (2001) 71:100–3. doi: 10.1136/jnnp.71.1.100

11. Jayakrishnan B, Hoke DE, Langendorf CG, Buckle AM, Rowley MJ. An analysis of the cross-reactivity of autoantibodies to GAD65 and GAD67 in diabetes. *PLoS One*. (2011) 6:e18411. doi: 10.1371/journal.pone.0018411

12. Guasp M, Solà-Valls N, Martínez-Hernández E, Gil MP, González C, Brieva L, et al. Cerebellar ataxia and autoantibodies restricted to glutamic acid decarboxylase 67 (GAD67). *J Neuroimmunol*. (2016) 300:15–7. doi: 10.1016/j.jneuroim.2016.09.019

13. Vinke AM, Schaper FLWVJ, Vlooswijk MCG, Nicolai J, Majoie MHJM, Martinez Martinez P, et al. Anti-GAD antibodies in a cohort of neuropsychiatric patients. *Epilepsy Behav*. (2018) 82:25–8. doi: 10.1016/j.yebeh.2018.03.004

14. Zong S, Correia-Hoffmann C, Mané-Damas M, Kappelmann N, Molenaar PC, van Grootheest G, et al. Novel neuronal surface autoantibodies in plasma of patients with depression and anxiety. *Transl Psychiatry*. (2020) 10:404. doi: 10.1038/s41398-020-01083-y

15. Hoffmann C, Zong S, Mané-Damas M, Stevens J, Malyavantham K, Küçükali Cİ, et al. The search for an autoimmune origin of psychotic disorders: prevalence of autoantibodies against hippocampus antigens, glutamic acid decarboxylase and nuclear antigens. *Schizophr Res*. (2021) 228:462–71. doi: 10.1016/j.schres.2020.12.038

16. Graus F, Saiz A, Dalmau J. GAD antibodies in neurological disorders — insights and challenges. *Nat Rev Neurol*. (2020) 16:353–65. doi: 10.1038/s41582-020-0359-x

17. Niehusmann P, Dalmau J, Rudlowski C, Vincent A, Elger CE, Rossi JE, et al. Diagnostic value of N-methyl-D-aspartate receptor antibodies in women with new-onset epilepsy. *Arch Neurol*. (2009) 66:458–64. doi: 10.1001/archneurol.2009.5

18. Cutler RW, Watters GV, Hammerstad JP. The origin and turnover rates of cerebrospinal fluid albumin and gamma-globulin in man. *J Neurol Sci*. (1970) 10:259–68. doi: 10.1016/0022-510X(70)90154-1

19. Vinke AM, Zong S, Janssen JH, Correia-Hoffmann C, Mané-Damas M, Damoiseaux JGMC, et al. Autoimmune encephalitis with mGluR1 antibodies presenting with epilepsy, but without cerebellar signs. *Case Rep*. (2022) 9:e1171. doi: 10.1212/NXI.0000000000001171

20. Honnorat J, Saiz A, Giometto B, Vincent A, Brieva L, de Andres C, et al. Cerebellar Ataxia with anti–glutamic acid decarboxylase antibodies: study of 14 patients. *Arch Neurol*. (2001) 58:225–30. doi: 10.1001/archneur.58.2.225

21. Chou IC, Wang CH, Lin WD, Tsai FJ, Lin CC, Kao CH. Risk of epilepsy in type 1 diabetes mellitus: a population-based cohort study. *Diabetologia*. (2016) 59:1196–203. doi: 10.1007/s00125-016-3929-0

22. Hoffmann C, Zong S, Mané-Damas M, Molenaar P, Losen M, Martinez-Martinez P. Autoantibodies in neuropsychiatric disorders. *Antibodies (Basel)*. (2016) 5:2. doi: 10.3390/antib5020009

23. Tsiortou P, Alexopoulos H, Dalakas MC. GAD antibody-spectrum disorders: progress in clinical phenotypes, immunopathogenesis and therapeutic interventions. *Ther Adv Neurol Disord*. (2021) 14:17562864211003486. doi: 10.1177/17562864211003486

24. Candore G, di Lorenzo G, Mansueto P, Melluso M, Fradà G, Li Vecchi M, et al. Prevalence of organ-specific and non organ-specific autoantibodies in healthy centenarians. *Mech Ageing Dev*. (1997) 94:183–90. doi: 10.1016/S0047-6374(96)01845-3

25. Grigsby AB, Anderson RJ, Freedland KE, Clouse RE, Lustman PJ. Prevalence of anxiety in adults with diabetes: a systematic review. *J Psychosom Res*. (2002) 53:1053–60. doi: 10.1016/S0022-3999(02)00417-8

26. Roy T, Lloyd CE. Epidemiology of depression and diabetes: a systematic review. *J Affect Disord*. (2012) 142:S8–S21. doi: 10.1016/S0165-0327(12)70004-6

# Frontiers in Immunology

**Explores novel approaches and diagnoses to treat immune disorders.**

The official journal of the International Union of Immunological Societies (IUIS) and the most cited in its field, leading the way for research across basic, translational and clinical immunology.

## Discover the latest Research Topics

See more →


**Frontiers**

Avenue du Tribunal-Fédéral 34
1005 Lausanne, Switzerland
frontiersin.org

**Contact us**

+41 (0)21 510 17 00
frontiersin.org/about/contact